Biological control capabilities of plant growth promoting bacteria against plant parasitic nematodes and their potential for oilseed rape bioremediation, assessed by nematode bioindicators

A thesis submitted by

Aoife A. Egan B.Sc. (Hons.)

To the Higher Education and Training Awards Council (HETAC)

In fulfilment of the Requirements for the

Degree of Doctor of Philosophy

Department of Science and Health

Institute of Technology Carlow

Kilkenny Road, Carlow

Ireland

Supervisor: Dr Thomais Kakouli-Duarte

External examiner: Dr Gerard Korthals

Internal examiner: Dr Rosemary O'Hara

Submitted to the Institute of Technology Carlow

June 2019

Declaration of Authorship

I, Aoife Egan, declare that this thesis titled, "Biological control capabilities of plant growth promoting bacteria, against plant parasitic nematodes, and their potential for oilseed rape bioremediation, assessed by nematode bioindicators" and the work presented in it are my own. I confirm that:

- This work was done wholly while in candidature for a research degree at the Institute of Technology Carlow.
- Where I have consulted the published work of others, this is always clearly attributed.
- Where I have quoted from the work of others, the source is always given. With the exception of such quotations, this thesis is entirely my own work.
- I have acknowledged all main sources of help.

Signed:

Date:

Abstract

The global population is increasing and the availability of land suitable for food production is in decline. Growing bioenergy crops on contaminated land is an innovative approach to alleviate this land shortage, which in turn has the potential to help meet global food demands. Bioenergy plants like oilseed rape (*Brassica napus*) can be grown on these contaminated brownfield sites with an aim to phytoremediate the soil. Beneficial bacteria such as *Pseudomonas fluorescens*, colonising the rhizosphere and bioenergy plants, have the capacity to increase plant growth and aid bioremediation. On the other hand, there is considerable crop loss globally due to pests and diseases, such as those caused by phytoparasitic nematode infections each year. With the current use of chemical pesticides and nematicides heavily regulated, there is huge potential for the development of a low-cost, natural and sustainable bio-based solutions. Three different capabilities of *P. fluorescens* were explored in the present study: biocontrol, plant growth promotion and bioremediation. Susceptibility of free-living bacterial feeding and plant parasitic nematodes to these bacterial strains was investigated. The plant-parasitic nematode biocontrol properties of the *P. fluorescens* strains was further explored in *in planta* with *Meloidogyne javanica*. The plant growth promotion capacity of *P. fluorescens* strains was determined in both tomato (*Solanum lycopersicum*) and oilseed rape plants. The nickel bioremediation capacity of the bacterial strains in oilseed rape was also evaluated. Nematode assemblages were utilised as bioindicators of the bioremediation process. It was found that the bacterial strains investigated in the current study, were producing compounds associated with plant growth promotion and biocontrol of root pathogens, including nematicidal and antimicrobial properties, as assessed by gas chromatography-mass spectrometry analysis. Oilseed rape nickel bioremediation determined by atomic absorption spectroscopy and nematode assemblage bioindicator analysis was not successful, although the bacterial strain L321 was found to have the potential for nickel biosorption. Tomato and oilseed rape plant biomass treated with the bacterial strains L124 and L321, respectively, was increased. Treatment with the bacterial strain L321 resulted in high plant-parasitic nematode mortality and delayed *M. javanica* infection in tomato plants. In addition, Fourier transform - infrared spectroscopy was assessed as a successful novel method for nematode characterisation, in particular for *M. javanica*. The results in relation to these two key bacterial strains contribute to the toolkit of sustainable agricultural practices that can be utilised as effective alternatives to chemical applications for phytoparasitic nematode management and plant growth promotion reducing the use of mineral fertilisers. Nickel biosorption is also an

additional beneficial property they acquire that enhances soil remediation.

Dissemination of Work

- Egan, A. A. and Kakouli-Duarte, T. (2012). Use of nematodes to evaluate the bioremediating ability of bacterial endophytes in bioenergy crops. Paper presented at 2^{nd} International Symposium on Nematodes as Environmental Bioindicators, Ghent, Belgium.
- Egan, A. A. and Kakouli-Duarte, T. (2015). Evaluation of the bioremediating ability of bacterial endophytes using nematodes as bioindicators in a bioenergy crop. Paper presented at Rhizosphere 4, Maastricht, the Netherlands.
- Egan, A. A. and Kakouli-Duarte, T. (2016). An investigation into plant parasitic nematodes and endophytic bacterial interactions. Paper presented at Environ 2016, Limerick, Ireland.
- Egan, A. A. and Kakouli-Duarte, T. (2016). Plant parasitic nematode and endophytic bacterial interactions. Paper presented at 32^{nd} Symposium of the European Society of Nematologists, Braga, Portugal.
- Egan, A. A. and Kakouli-Duarte, T. (2016). Nematodes as environmental bioindicators-Use of nematodes to evaluate the bioremediating ability of bacterial endophytes in a bioenergy crop. Paper presented at 32^{nd} Symposium of the European Society of Nematologists, Braga, Portugal.
- Egan, A. A. and Kakouli-Duarte, T. (2017). Classical and novel approaches in using nematodes as bioindicators of endophytic bacterial bioremediation in an oilseed rape crop. Paper presented at 3^{rd} International Symposium on Nematodes as Environmental Bioindicators, Carlow, Ireland.
- Egan, A. A. and Kakouli-Duarte, T. (2019). Estimating the potential of Fourier transform infrared spectroscopy as a novel tool for nematode characterisation. Paper presented at Environ 2019, Carlow, Ireland.
- Egan, A. A. and Kakouli-Duarte, T. (2019). Plant growth promoting bacteria biocontrol of the plant parasitic nematode *Meloidogyne javanica*. Paper presented at Environ 2019, Carlow, Ireland.

Acknowledgements

A special thank you to my supervisor Dr Thomae Kakouli-Duarte for giving me the opportunity to undertake this research, your encouragement, patience and advice were invaluable. As you have said to me numerous times, a PhD is a marathon, not a sprint - finally we have crossed the finish line.

Department of Science and Health staff, Dr Dina Brazil for re-introducing me to the fundamentals of microbiology. Mr Bob Stacey, Dr Guiomar Garcia-Cabellos, Mr Dick Farrell and Ms Gillian O'Brien for all your help, support and encouragement. The ladies in the science office Ms Sarah Clark and Ms Aisling Linnane for always pointing me in the right direction. IT crew for any technical issues, in particular Mr Ray Dermody for going above and beyond to ensure I had SPSS, I really appreciate your efforts.

Postgraduate colleagues in the Dargan Centre, past and present, for your friendship and assistance in the lab. My interns over the years, especially Ms Aimee Brownrigg for your dedication and help in the lab. Dr Mary Jo, you have been my rock and my council through out this whole experience, both academically and personally so a huge thank you for your friendship. That train journey in Portugal is an experience I will never forget. Dr Eileen, thank you for your support and kindness, for all the lifts in your car and the chats. Dr John C, for imparting your knowledge of GC-MS, for not giving up on finding 2,4-DAPG and for proof reading Chapter 2. Dr Richie, for keeping us all going, the craic and for Snapchat Friday- the highlight of our week. Dr John B, for sharing your knowledge on FT-IR and for proof reading Chapter 5. Seán, the 'go to guy' for any technical issues, your expertise on EndNote was invaluable. Dr Sérgio, for sharing your knowledge on molecular biology. Dr Emma for the chats and the laugh. Sam, for your witty humour and for keeping us entertained on our extended lunch breaks.

My parents Kevin and Aveen, thank you for your endless love, support and encouragement. Mam, this PhD would not have happened without you being there for me, for holding off on your dreams so I could follow mine. I will never forget all that you have done for me. My sister Aisling for her positivity, kindness and for always being there for me. Paul for your optimism and for never mentioning that dreaded question, 'Are you nearly finished?'.

My little man Ruadhán, for making the commute home more bearable knowing I was coming home to you, for your endearing curiosity of the world, and for always making me smile. You were my reminder of why I was doing this.

Contents

List of Figures

List of Tables

List of Abbreviations

Symbols

©	Copyright
°C	Degree Celsius
λ_{max}	lambda max
μg	micro gram
μl	micro litre
μm	micro meter

Organisms

B. napus	*Brassica napus*
C. elegans	*Caenorhabditis elegans*
E. coli	*Escherichia coli*
G. mellonella	*Galleria mellonella*
G. pallida	*Globodera pallida*
H. bacteriophora	*Heterohabditis bacteriophora*
M. javanica	*Meloidogyne javanica*
P. agglomerans	*Pantoea agglomerans*
P. pacificus	*Pristionchus pacificus*
P. fluorescens	*Pseudomonas fluorescens*
S. carpocapsae	*Steinernema carpocapsae*
S. feltiae	*Steinernema feltiae*

Abbreviations

2,4-DAPG	2,4-Diacetylphloroglucanol
AAS	Atomic absorption spectroscopy
AHC	Agglomerative hierarchical clustering
AMDIS	Automated mass spectral deconvolution and identification system
ANOVA	Analysis of variance
AU	Arbitrary units
b	Basal
BI	Basal index
bp	Base pair
c	Channel

CFU	Colony forming units
Cd	Cadmium
CMRs	Carcinogenic, mutagenic or toxic for reproduction
CI	Channel index
cm	Centimetre
c-p	Coloniser-persister
Cr	Chromium
Cu	Copper
DESS	DMSO/ EDTA/ NaCl saturated
DGGE	Denaturing gradient gel electrophoresis
dH_2O	Deionised water
ddH_2O	Double deionised water
DMSO	Dimethyl sulphoxide
DNA	Deoxyribonucleic Acid
EDTA	Ethylenediaminetetraacetic acid
EEA	European environment agency
e	Enrichment
EI	Enrichment index
EPN	Entomopathogenic nematode
FLBFN	Free living bacterial feeding nematode
FT-IR	Fourier transform infrared spectroscopy
GC-MS	Gas chromatography mass spectrometry
GFP	Green fluorescent protein
H’	Shannon Wiener diversity index
HEAR	High euric acid rape
Hg	Mercury
HO	High oleic
HSP	Heat shock proteins
H_2O	Water
IJ	Infective juvenile
IPM	Integrated pest management
IR	Infrared
J	Juvenile
J’	Pielous evenness index
kDa	Kilo Daltons
l	Litre
L	Larval
LB	Lysogeny broth
LL	Low linolenic
m	Meter
MDS	Multi dimensional scaling
MF	Match factor
mg	Milligram
MI	Maturity index
ml	Millilitre
m/z	Mass per charge
NA	Nutrient agar
NaCl	Sodium chloride
NCR	Nematode channel ratio

NB	Nutrient broth
NGM	Nematode growth medium
Ni	Nickel
NIST	National Institute of Standards and Technology
nm	Nano meters
OD	Optical density
OSR	Oilseed rape
RT	Retention time
Pb	Lead
PBTs	Persistent bio-accumulative and toxic substances
PCA	Principal component analysis
PCN	Potato cyst nematodes
PCR	Polymerase chain reaction
PGP	Plant growth promotion
PGPR	Plant growth promoting rhizobacteria
POPs	Persistent organic pollutants
PPI	Plant parasitic index
PPN	Plant parasitic nematode
ppm	Parts per million
RFU	Relative fluorescent units
RKN	Root knot nematodes
ROI	Region of interest
RPM	Revolutions per minute
s	Structure
SDS	Sodium dodecyl sulfate
S_j	Pielous evenness index
spp.	Species
SEM	Standard error of the mean
SGA	Sucrose glutamic acid
SI	Structure index
SPW	Soil pore water
TEMED	Tetramethylethylenediamide
UN	United Nations
UPGMA	Unweighted pair-group method with arithmetic means
UV	Ultra violet
V	Volts
W	Andrassays equation
Zi	Zinc

Chapter 1

General Introduction

1.1 Introduction

According to the European Environment Agency (EEA), there are potentially 2.5 million contaminated sites across Europe (EEA, 2018). Of these polluted sites, 14%, which is the equivalent of 340, 000 sites, are so heavily contaminated that they will require remediation. Currently, 15% of these polluted sites have been remediated through mechanical methods, by removing contaminated soil, applying chemical treatments or by incineration in a different location. Environmental contamination such as that from heavy metals can cause major health problems in humans and animals due to their cytotoxicity, mutagenicity and carcinogenicity (Ma *et al.*, 2011b). Phytoremediation has become a major focus regarding these problems. The phytoremediation processes are dependent on the plants' ability to hyperaccumulate heavy metals in their appendages while tolerating large doses of heavy metals in the soil, with an aim of producing a large biomass (Ma *et al.*, 2011a). The use of nematodes as bioindicators are a non-invasive approach to monitoring such process.

Beneficial plant growth promoting (PGP) bacteria, such as rhizospheric or bacterial endophytes can colonise plant roots, or inhabit the interior of leaves, stems and branches, without causing any harm to the host plant (Siddiqui and Shaukat, 2003). These close interactions are favourable for both, as the plants provide nutrients and a safe niche to live, in exchange for improved plant growth and health. Bacterial plant colonisation can occur via transmission on plant seeds, vegetation and planting material from the surrounding environment. However, it is mostly accepted that the rhizosphere soil, is the initial source of colonisation (Siddiqui and Shaukat, 2003). Weyens *et al.* (2009) suggest that bacterial endophytes enter the plant through the roots; once they are inside the plant, they either reside in specific plant tissues, such as the root cortex or the xylem, or they can colonise the plants' vascular system or

apoplast. There are two types of factors that can aid plant colonisation: abiotic, such as rainfall and UV radiation, and biotic factors, including interactions between microorganisms, such as other bacteria, fungi and nematodes, and infection particles such as viruses (Ortíz-Castro *et al.*, 2009). These interactions include competition, antibiosis, niche exclusion, symbiosis and mutualism (Ortíz-Castro *et al.*, 2009; Siddiqui and Shaukat, 2003).

These PGP bacteria have an important role in protecting host plants from infection, adding in plant growth promotion (Goudaa *et al.*, 2018; Leveau and Lindow, 2005; Vejan *et al.*, 2016) and in biocontrol (Aravind *et al.*, 2010; Shahid *et al.*, 2017; Singh and Siddiqui, 2010) against plant pathogens. It has been suggested by Siddiqui and Shaukat (2003) that endophytic bacteria may be better at inducing plant defence compared to rhizobacteria, as they develop a closer relationship with the plants, over a longer period. They are also associated with bioremediation, enhancing host plants' capacity of cleaning contaminated soils (Ma *et al.*, 2011b; Montalbán *et al.*, 2016, 2017). There is a broad range of bacteria classified as endophytes, including *Pseudomonas* spp, *Bacillus* spp., *Enterobacter* spp. *Pantoea* spp. and *Streptomyces* spp. (Aravind *et al*. 2010). Bioenergy crops inoculated with beneficial bacteria, including, endophytic bacteria for bioremediation of contaminated soil is a current approach of interest and has great potential, both economically and environmentally.

Bioenergy crops, such as oilseed rape (OSR; *Brassica napus*), are becoming more popular as demands for the supply of fuel and alternative energy sources increases. In order to meet such demands, arable and grassland must be used for bioenergy crop production, thus reducing land available for food production (Vasile *et al.*, 2016). Growing bioenergy crops in heavily contaminated lands known as brown field sites (Andersson-Sköld *et al.*, 2014), has been suggested as a means of dealing with the land shortage issue. Certain bioenergy crops have the capacity to decontaminate and remediate such land in an environmentally friendly process called phytoremediation. However, the environmental impact of this practice must be thoroughly assessed per site, including the handing and disposal of residues (Anderson-Sköld et al., 2014). In addition, the plant biomass and by-products must be economically profitable (Cheng *et al.*, 2015). A means of non-invasive monitoring of such process is the utilisation of nematodes as bioindicators.

Nematodes are multicellular vermiform organisms, they are the most numerous metazoa in soil and can be found in abundance in most environments, such as marine, soil and fresh water (Dodds and Whiles, 2010). They occur in all land types and conditions, including polar regions and deserts (Murfin *et al.*, 2012) and can be found in hot springs (Dodds and Whiles, 2010), high up on mountains and in the deepest oceans (Guilini *et al.*, 2011). Free-living nematodes are extremely abundant in soils and sediments, where they feed on organic material, bacteria, fungi, and other nematodes (Majdi and Traunspurger, 2015). Some nematodes are plant parasites (PPN) and may cause disease in economically important crops (Degenkolb and Vilcinskas, 2016), while other nematodes live part or most of their life cycles as insect

parasites (Lacey and Georgis, 2012). Nematodes play an important role in the soil, as they inhabit the middle of the food web (Figure 1.3) and are therefore an important food source for many higher level predatory organisms, bacteria and fungi (Bongers and Bongers, 1998). They are also associated with decomposition, energy flows (Sochová *et al.*, 2006), and nutrient cycling, such as mineralizing, or releasing nutrients in plant-available forms (Wang and McSorley, 2018).

Nematodes are actively involved with the distribution of bacteria and fungi in a soil system, by transporting live and dormant microbes on their cuticle and in their digestive tracts. When nematode densities are low in a soil system, feeding nematodes can stimulate the growth rate of prey populations and plant-feeding nematodes can stimulate plant growth. At high nematode densities, nematodes can reduce the population of their prey, resulting in decreased plant productivity and reduced decomposition and immobilization rates by bacteria and fungi. Therefore, predatory nematodes may regulate populations of bacterial and fungal feeding nematodes, and ultimately prevent over-grazing by those groups. Likewise, nematode grazing may control the balance between bacteria and fungi, and the species composition of the microbial community. Nematodes are highly valuable organisms in an ecosystem and their potential as bioindicators of physical, biological or chemical fluctuations in the soil environment, in particular, to soil contamination (Sochová *et al.*, 2006), is an important area of research interest.

Further developments in exploiting beneficial bacteria characteristics for parasitic nematode biocontrol, plant growth promotion and bioremediation, coupled with the use of bioenergy crops for phytoremediation of contaminated land, may become economically worthwhile. The use of nematodes as bioindicators of this process has good and promising potential, due to their sensitive nature to disruptions in the soil ecosystem through irrigation, drainage, agrochemicals and monoculture. They respond very quickly to disturbances or changes in soil composition, including the addition of contaminants and this sensitivity makes the use of nematodes as bioindicators a very suitable tool in monitoring soil health. This study investigated the potential of beneficial bacteria biocontrol of plant parasitic nematodes, the efficiency of PGP bacteria at increasing OSR and tomato plant growth, and the nickel (Ni) bioremediation potential of PGP bacteria inoculated OSR. The efficiency of nematode assemblages as bioindicators of this bioremediation was also explored. In addition, the suitability of Fourier transform infrared microspectroscopy (FT-IR) for nematode characterisation was assessed.

1.2 Research Aims and Objectives

1.2.1 Overall Aims

The overall aims of this project were to (1) explore beneficial bacteria PGP, Ni bioremediation, and PPN biocontrol potential, (2) assess the suitability of nematodes as bioindicators of Ni bioremediation, and (3) develop the potential of FTIR microspectroscopy for nematode characterisation.

1.2.2 Project Objectives

The main objectives of this study included:

Chapter 2

- Conducting bioassays to investigate free-living bacterial feeding (FLBF) nematodes and PPN susceptibility to beneficial bacteria *Pseudomonas fluorescens* and *Pantoea agglomerans* strains and to bacterial metabolites at different life stages, to determine the nematode mortality.
- Assessing the effects of the antibiotic 2,4-diacetylphloroglucanol (2,4-DAPG) on FLBF nematodes and PPN via toxicity assays.
- Identifying secondary metabolites produced by the *P. fluorescens* strains L124, L228, L321, S118 and *P. agglomerans* strain S222 via gas chromatography–mass spectrometry (GC-MS) analysis.
- Exploring the effect of beneficial bacterial metabolites and 2,4-DAPG on *Meloidogyne javanica* and *Globodera pallida* egg hatch and juvenile recovery.

Chapter 3

- Assessing the attraction of the nematodes *Caenorhabditis elegans*, *M. javanica* and *G. pallida* to *P. fluorescens* F113, L124 and L321, to *P. agglomerans* L222, and to 2,4-DAPG via a directional response assay and by determining the chemotaxis index.
- Conducting plant trials to investigate *M. javanica* development in tomato plants inoculated with PGP bacteria or treated with 2,4-DAPG, over three time points.
- Comparing two plant trials, inoculated with PGP bacteria or treated with 2,4-DAPG, to induce a systemic response (ISR) in *M. javanica* infected tomato plants.

Chapters 3 and 4

- Evaluating PGP potential of beneficial bacteria inoculated tomato (after 20, 30, 50, and 70 days) and OSR plants (after 3 and 6 months).

Chapter 4

- Determining the capacity of PGP bacteria inoculated OSR to bioremediate Ni spiked soil, by (1) assessing the bacteria viability in the rhizosphere, root and phyllosphere of the plants, by (2) conducting a nematode assemblage characterisation via morphological nematode identification and via a molecular assessment of the nematode assemblage through DGGE analysis.
- Investigating the suitability of maturity, diversity and ecological indices to indicate the success of PGP bacteria bioremediation in OSR.
- Evaluating transgenic *C. elegans* as a biosensor of Ni bioremediation.

Chapter 5

- Investigating the suitability of FT-IR microspectroscopy for nematode characterisation of both lab reared nematodes and nematodes extracted from soil.

1.3 Literature Review

1.3.1 Beneficial Bacteria Plant Growth Promotion Traits

Plant growth promoting rhizobacteria (PGPR), including bacterial endophytes, have considerable potential for enhancing sustainable agriculture and increasing the production potential of biofuels (Lally *et al.*, 2017). There are two modes that PGPR can enhance plant growth: either directly or indirectly. The bacteria directly affect plant growth by increasing the availability of nutrients to the plants by nitrogen fixation, such as the action of *Azorhizobium* in wheat, *Herbaspirillum* in rice and *Rhizobia* in legumes (Vejan *et al.*, 2016). Other direct mechanisms include mineral solubilisation, such as phosphorous by *P. fluorescens* (Otieno *et al.*, 2015), or by increasing iron up-take capacity through the production of siderophores under iron-limiting conditions by *Pseudomonas* spp. (Goudaa *et al.*, 2018). Production of phytohormones, are another direct means, such as indole-3-acetic acid (IAA), which is associated with root elongation and increased root production. Increased plant growth can also be attributed to the production of 1-aminocyclopropane-1-carboxylate (ACC) deaminase that is related to regulating the plant stress hormone ethylene, caused by abiotic stress conditions (Leveau and Lindow, 2005). Beneficial bacteria, such as bacterial endophytes indirectly affect plant growth by preventing the colonisation, growth and activity of plant pathogens by niche exclusion on or within the plant, therefore competing with them for space and nutrients (Montalbán *et al.*, 2016) and inducing plant defence systems (Weyens *et al.*, 2009). The production of antibiotics, such as 2,4-DAPG (Meyer *et al.*, 2016) and pyoluteorin, synthesised by some species of *Pseudomonas* (Huang *et al.*, 2008) can also contribute to increased plant growth. In a phytoremediation capacity (further discussed in Section 1.3.2.3), the adsorption of metals by plant-associated bacteria results in reduced metal uptake and translocation inside the plant, therefore improving plant growth by decreasing phytotoxicity (Montalbán *et al.*, 2016).

1.3.2 Bioremediation Potential of Beneficial Bacteria

1.3.2.1 Nickel in Irish Soils

Trace metals are represented by numerous elements present in the soil at low concentrations, which are beneficial to both plants and animals that ingest them. They are, however, when present in excessive amounts, known as heavy metals that can have negative effects. Examples of such trace elements include cadmium (Cd), copper (Cu), mercury (Hg), Ni, lead (Pb) and Zinc (Zn; McGrath and Fleming, 2007).

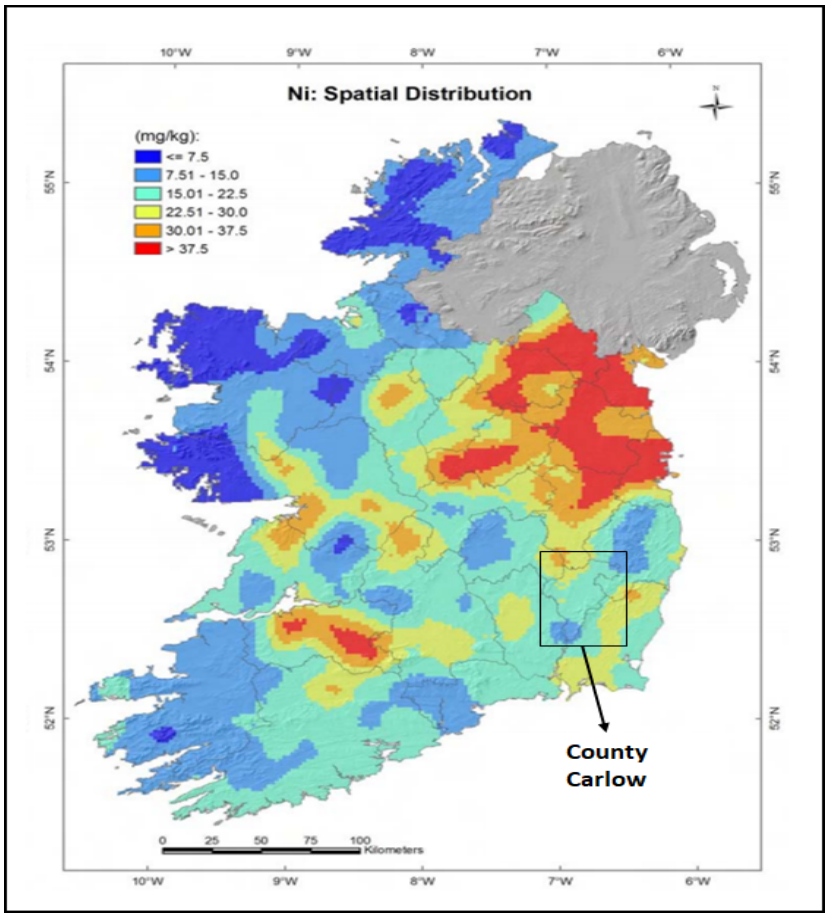

FIGURE 1.1: Spatial distribution of the trace element Ni in Irish soil, specifically in County Carlow (Fay *et al.*, 2007).

The trace element Ni, which is the heavy metal of interest in this study, is present naturally in most soils, with a typical range of 0.5 - 100 ppm in uncontaminated soil (ibid.). It occurs as a result of the combustion of fossil fuels, application of sewage sludge and emissions from industrial activities using or producing the metal. Nickel is also utilised in the production of alloys, jewellery, paint, ceramics and rechargeable batteries (Fay *et al.*, 2007). The National Soil Database (EPA, 2017) consists of a collection of soil samples, taken across Ireland, assessed for major nutrients and elements, essential trace elements, and trace elements of special interest, which were mapped to indicate spatial distribution (Figure 1.1) throughout Ireland. The results indicate that, due to the application of sewage sludge to the land, the level of Ni in the soil exceeded the threshold value of 30 ppm by 23% (McGrath and Fleming, 2007). North Carlow, where the soil samples for this study were acquired, has limestone soil which is associated with elevated levels of Ni. In this area, Ni levels are above the limit set by the EU Directive (McGrath and Fleming, 2007).

1.3.2.2 Phytoremediation of Contaminated Media

Remediation of soil, sludges, sediments or water contaminated with organic and inorganic pollutants by plants is known as phytoremediation. It works by removing, detoxifying or immobilising environmental contaminants from a growth medium, by plant, chemical, biological or physical activity. The ability of the plant roots to absorb and metabolise such contaminants, transport and store them in stems and leaves, is what makes them an ideal organism for organic remediation (Tangahu *et al.*, 2011). Phytoremediation can be used as an alternative to mechanical or chemical remediation technologies, such as soil washing, solvent treatments or vaporization (Voijant Tangahu *et al.*, 2011). These harsh methods destroy the biological composition of the soil, including nutrients and minerals present, drastically altering the soil chemical and physical properties. After the growth period, the plants are harvested, processed and disposed of. This disposal includes processes such as direct disposal, ashing and liquid extraction. However, incineration or smelting are suggested to be the most effective and efficient methods, both environmentally and economically (Sas-Nowosielska *et al.*, 2004). Phytoremediation is suitable for low to moderate levels of contamination (Lone *et al.*, 2008), such as metals, pesticides, polyaromatic hydrocarbons, and landfill leachates.

1.3.2.3 Phytoremediation using Oilseed Rape

Oilseed rape is an annual plant with branched stems, that grows up to 1.5 meters, has yellow flowers and is well suited to the Irish climate. Varieties of OSR are classified according to their seed production (conventional or hybrid), the seed fatty acid profile (double low, high erucic acid rape (HEAR), high oleic (HO), low linolenic (LL) fatty acid profile) and canopy structure (Zahoor and Forristal, 2000). The double low (oil content of 43-44%) varieties are typically grown in Ireland as high protein meal for animals. High erucic acid rape varieties are non-food crops and are grown for bio-fuel and fuel additives, such as lubricants among others. The other varieties, HO and LL are grown for oil production suitable for human consumption. There are two types of rape grown in Ireland, Winter oilseed rape (WOSR) and Spring oilseed rape (SOSR). The yield of WOSR is much greater than the Spring varieties, with up to 5.0 tonnes per hectare recorded, compared to 3.3 tonnes per hectare recorded for SOSR. There were over 7500 hectares of OSR grown in Ireland in 2015 with crop market price of €380 per tonne in 2017 (Phelan, 2017). It is an excellent break crop, particularly from the soil fungus *Gaeumannomyces graminis* var. tritici, that causes take-all disease in wheat crops (Angus *et al.*, 2015). It has been reported that wheat yields after sowing OSR can increase between 0.5 and 1.5 tonnes per hectare (Zahoor and Forristal, 2000), depending on the severity of fungal infection in the previous year.

Oilseed rape plants are also known as hyperaccumulators and several reports have been published on the resilience of *Brassica* spp. to toxic heavy metals (Mourato *et al.*, 2015).

Hernández-Allica *et al.* (2008) discovered that *Brassica* spp. have a high tolerance to Zn but a lesser tolerance to Pb and Cd, and is more effective at removing Zn from soil compared to Cu (Ebbs and Kochian, 1997). Accumulator species traits were reported in Mourato *et al.* (2015), whereby the accumulation of heavy metals Cd, Cr, Cu, Ni, lead and Zn were found to be highest in shoots compared to roots in *B. napus*, confirming its hyperaccumulator potential. Typically, hyperaccumulating plants are solely utilised for their phytoremediation potential. However, Park *et al.* (2012) investigated the possibility of using *B. napus* for the remediation of heavy metals in soils, whilst also utilising the oil for energy consumption. Growing this crop, therefore, could be more profitable and could become more economically important. Although *B. napus* has proven to be a successful hyperaccumulator, research suggests it is not the most effective at accumulating Ni (Purakayastha *et al.*, 2008).

A logical question arising is whether the interactions between PGP bacteria and hyperaccumulating plants, such as *B. napus* could increase the plants' potential for Ni accumulation (this was explored in Chapter 4). The efficiency of phytoremediation may be increased due to the colonisation of beneficial bacteria internally and externally on the plants. This occurs by increasing (1) biomass, due to enhanced plant growth (discussed in Section 1.3.1), (2) metal up-take from the growth medium, via the excretion of organic acids, thus lowering the pH of the rhizosphere or by producing siderophores that increase the mobility of Fe(III) and (3) plant tolerance to the toxic metals due to metal-resistant bacteria colonising the plant and aiding in metal detoxification (Montalbán *et al.*, 2017). There have been many incidents where beneficial bacteria, such as endophytic bacteria, have been reported to increase phytoremediation. Montalbán *et al.* (2016) described endophytic bacteria, isolated from Zn contaminated soil, increasing *B. napus* root length and plant height in *Helianthus tuberosus* when grown in vertical agar plates containing toxic concentrations of Cd and Zn. Ma *et al.* (2011b) report that the isolation of *Pseudomonas* spp. from the roots of *Alyssum serpyllifolium* displayed high levels of colonisation in the internal tissues of roots and shoots of *B. juncea* and also increased Ni content in *A. serpyllifolium*. The results from these reports suggest that these types of bacteria are beneficial, not only for the host plants that they are isolated from but also for plants from different families that are not related to the initial host plant.

1.3.3 Nematodes as Bioindicators of Bioremediation

The advantage of environmental biomonitoring, utilising bioindicators, is an early indication of site contamination from sources such as heavy metals, industrial or agricultural effluent or mine tailings, and therefore, early preventative measures can be implemented. Bioindicators are organisms such as bacteria, plants, plankton, and nematodes that can be utilised to

detect fluctuations in environmental conditions (Parmar *et al.*, 2016). They can be physically counted and easily monitored in the soil by sampling. They are relatively inexpensive to work with, and their use in an environmental context is economically feasible, compared to other specialised monitoring systems. They are found in abundance in all soil types, from clean to contaminated (Bongers and Ferris, 1999). Nematodes, in particular, make excellent bioindicators as they are capable of living in extreme environments (Murfin *et al.*, 2012) and do not relocate from stressful conditions rapidly (Bongers and Ferris, 1999). They are easily influenced by the soil's condition, physical and chemical properties and the soil food-web. They are located in the middle of the food-web (Figure 1.3) and subsequently feed on many organisms in the soil and are a food source for many others (Bongers and Ferris, 1999). Therefore, analysing the nematodes present in a community can give insight into the health of the soil. Nematode composition in the soil can be assessed by morphological assemblage characterisation or molecular community analysis, however, it is suggested by Oliveira *et al.* (2011) that a combination of both methods is more informative.

1.3.3.1 Nematode Assemblage Morphological Assessment

Morphological nematode assemblage analysis is typically conducted by extracting nematodes from the soil, studying their morphological features under a microscope and identifying them taxonomically (Treonis *et al.*, 2018). The most distinguishable features for nematode identification include the buccal cavity, the cuticle and the reproductive organs. The buccal cavity, or the mouth region, is the most important feature in nematode identification as it varies greatly in shape and form, reflecting the feeding type of the nematode, i.e. bacterial feeding, fungal feeding, plant feeding, predator or omnivore (Figure 1.2). It can be absent, minute or have a large open space. Many buccal cavities have movable or immovable projections called stylets and teeth, respectively. There may be rows of small denticles lining the buccal cavity. The tail shape can also be highly characteristic; the tail region varies in shape from rounded to conical, conico-cylindrical or elongated (Bongers, 1994). The cuticle can look entirely smooth or be striated (transversely annulated). There may be dots, punctuation or pores present which can be arranged irregularly or in rows. These features may be confined to the lateral parts of the cuticle or occur in specific regions on the nematode or appear in all regions of the body. The cuticle can also contain sensory organs which occur as projections (sensilla) in the cuticle surface, such as long hair like projections (setae) and nipple-like (papilla) projections (Page and Johnstone, 2007). The reproductive system in nematodes is an important feature in identification; the female may have one or two ovaries (monodelphic/ didelphic). Ovary number and structure are important features and can be used to distinguish major taxonomic groups. The cuticularised copulatory structures are the most important part of male identification as the shape and size of the spicules and guiding piece (gubernaculum) vary considerably.

1.3.3.2 Molecular Characterisation of Nematode Assemblages

Morphological assessments of nematode community structure and diversity are time consuming, require considerable taxonomical knowledge (Treonis *et al.*, 2018), and in order to obtain results fast, it is often just limited to family or genus level. In order to overcome this, molecular approaches are utilised to make such analysis faster and more accessible to researchers. To perform a nematode assemblage molecular analysis, a number of criteria must be met: (1) it is important that the chosen method is capable of processing a large number of samples, (2) that DNA is extracted efficiently, either from soil directly or from extracted nematodes (Griffiths *et al.*, 2006) and (3) that the results are representative of the nematode community present.

Current molecular diversity analysis methods that are utilised to assess an entire nematode community structure include high-throughput sequencing (HTS; Geisen *et al.*, 2018), such as DNA-based metabarcoding, directed terminal-restriction fragment length polymorphism analysis (dT-RFLP; Donn *et al.*, 2012) and denaturing gradient gel electrophoresis (DGGE; Nguyen *et al.*, 2016). For metabarcoding, Treonis *et al.* (2018) explain that species-rich nematode communities are typically dominated by a few species, often with many rare species present. Identification of these rare species can often be difficult, as there are very few representative individual nematodes present in a sample. To overcome this Treonis *et al.* (2018) suggests the use of DNA-based metabarcoding, to increase taxonomic resolution so that rare taxa are captured, preventing missed or misidentified nematodes, and therefore, giving a more complete assessment of the nematode diversity in the samples. The semi-quantitative PCR-based fingerprint technique dT-RFLP, typically used for bacterial community profiling, was explored by Donn *et al.* (2012) for nematode assemblage analysis. This technique is advantageous over other fingerprint profiling methods, due to the inclusion of a size standard with every run that can be used to accurately size fragments, and thus data from different electrophoretic runs can be compared. With known nematode community sequences, the directed version of T-RFLP was utilised to cut DNA in regions that discriminate between taxa of interest (Donn et al., 2012). This method is a rapid way of monitoring changes between soil sites, or to track soil remediation processes.

Denaturing gradient gel electrophoresis (DGGE), the molecular technique of interest in the research reported in this thesis is a fingerprinting method that separates PCR products. Polymerase chain reaction-based DGGE was developed by Foucher *et al.* (2004), Foucher and Wilson (2002), and Waite *et al.* (2003) to estimate nematode biodiversity. DNA sequences from different nematode taxa denature at different denaturant concentrations, which result in a pattern of bands. Each band is representative of an operational taxonomic unit (OTU). In this type of analysis, OTUs are clusters of similar sequences of the 18S rDNA gene, where each cluster is representative of a nematode family. According to Kushida (2013), the advantage of PCR-DGGE analysis is that the bands present in the gel can be excised, sequenced

and compared to known sequences in a DNA database for identification. Unfortunately, a drawback to this technique is that for a community analysis some sensitivity is lost due to numerous species present (Foucher *et al.*, 2004; Kushida, 2013). However, Kushida (2013) found, by using group-specific primer sets in the PCR-DGGE analysis, increased sensitivity in the detection of plant parasitic and fungivorous nematodes in a diverse nematode community.

The effectiveness of molecular tools such as metabarcoding, dT-RFLP and DGGE to identify challenging taxonomic groups more accurately and with greater sensitivity, has helped reduce the necessity of experienced nematologists in taxonomy. Oliveira *et al.* (2011) suggests that a combination of both morphological and molecular techniques would be a more complementary approach and give a more complete picture of nematode diversity in soil assemblages, thus giving a more accurate estimate of soil health in a bioindicator capacity.

1.3.3.3 Nematode Diversity and Food-Web Structure

1.3.3.3.1 Nematode feeding types

There are eight different nematode feeding types, assigned by Yeates *et al.* (1993). Nematodes belonging to each of these groups have different ecological roles within the soil food web (Table 1.1). Omnivorous nematodes (Figure 1.2) are known as generalists and can feed on many soil organisms. Typically, they are large nematodes and are therefore particularly sensitive to soil disturbances, such as tillage, increased fertiliser applications or soil contamination. In a soil community, the presence of omnivorous nematodes is indicative of a diverse and stable food web, whereas the absence of these nematodes is indicative of a disturbed or depleted food web. Fungal-feeding nematodes (Figure 1.2) are responsible for decomposition in the soil, particularly in those soils with a high carbon to nitrogen ratio. They predominate in undisturbed soils and have a short life-cycle of 1-2 weeks. Animal predators (Figure 1.2), are large nematodes that feed on other nematodes. They have long life-cycles and are quite sensitive to contaminants. They have large open mouths, with teeth or spears to pierce their prey or feed on nematode eggs. Due to their size, sensitivity and long life-cycle, omnivores and animal predators, once lost from a food-web can take months to years to return. The feeding types of importance in this study include free-living bacterial feeding and plant parasitic nematodes.

Free-living bacterial feeding nematodes

Free-living bacterial-feeding nematodes (Figure 1.2) are the most abundant nematode group in agricultural soils, due to their small size, fast life-cycle and production of large numbers of eggs. They reside in the rhizosphere, near plant roots that are colonised by bacteria. They are often called enrichment opportunists as their populations tend to increase with

the application of an organic amendment. When a bacterial food source is present in the soil, such as decomposing organic matter, populations can increase rapidly in high densities. Their consumption of bacteria is important for the release of nitrogen in plant available forms (Jiang *et al.*, 2017). They can fix nitrogen by converting it into ammonium. Nematodes feeding on bacteria in the soil stimulate bacterial growth thus controlling the bacteria levels in the soil.

Plant parasitic nematodes

Plant parasitic nematodes (Figure 1.2) can infect all parts of host plants including roots, stems, leaves, flowers or seeds, depending on nematode species and life-cycle. Root-knot nematodes (RKN) belong to the genus *Meloidogyne* and produce galls on plant roots, often on crop roots, which causes severe damage to the productivity of the plants (Abad *et al.*, 2004). Cyst nematodes such as *Heterodera spp.* (Davis and Tylka, 2000) and *Globodera spp.* (Rowe, 2017), produce cysts on the root surface, which harden and fall into the soil and can remain viable in the soil for many years. Members of the genus *Pratylenchus* (Davis and MacGuidwin, 2000), are known as lesion nematodes and cause necrotic lesions throughout the cortex of infected roots. The stubby root nematodes, *Trichodorus spp.*, cause stubby, stunted and malformed roots in crops, affecting the transportation of nutrients and water in the plants (Crow, 2005). Stem nematodes from the genus *Ditylenchus spp.* (Subbotin *et al.*, 2005), can distort stems and cause necrotic patches on host plant leaves.

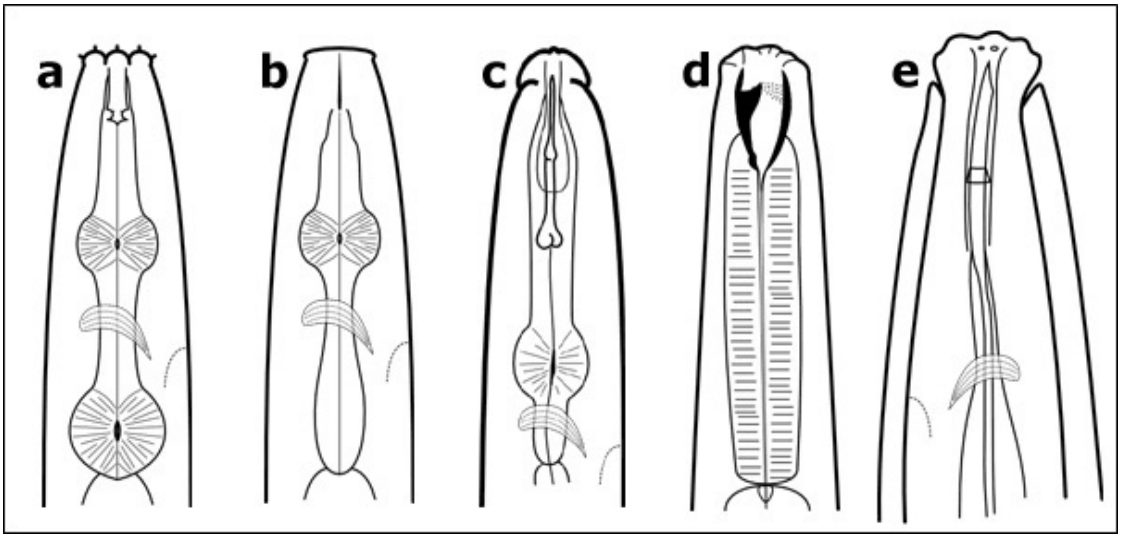

FIGURE 1.2: Schematic representation of nematode feeding types. Nematodes can be classified in different feeding groups based on the structure of their mouthparts. (A) Bacterial feeder, (B) Fungal feeder, (C) Plant feeder, (D) Predator, (E) Omnivore (Ugarte and Zaborski, 2014).

There are three main subgroups of root-infecting/inhabiting nematodes: the free-living ectoparasites, the migratory species, and the sedentary endoparasites. Ectoparasitic nematodes

such as those in the Longidoridae and Trichodoridae families feed on plant tissues from outside the plant (Decraemer and Geraert, 2013). Migratory nematodes can move freely through the soil and plant tissues and endoparasitic nematodes feed inside the plant tissues. Migratory endoparasitic nematodes from the families Pratylenchidae, Anguinidae, and Aphelenchoididae (Moens and Perry, 2009), spend some of their life-cycle moving between the soil and plants, and the remaining of their life within or on the roots. In some species, the adult female becomes swollen and remains in or on the plant roots permanently. They are described as sedentary and include the genera *Heterodera*, *Globodera* and *Meloidogyne* (Abad *et al.*, 2004; Fosu-Nyarko and Jones, 2015; Rowe, 2017).

TABLE 1.1: Nematode feeding types of terrestrial nematodes and the nematode coloniser persister (c-p) scale (Bongers and Bongers, 1998; Yeates *et al.*, 1993).

Feeding Type		**Coloniser-Persister Scale**	
1	Plant feeding	1	Enrichment opportunists
1a.	sedentary parasites		High fecundity
1b.	migratory endoparasites		Small eggs
1c.	semi-endoparasites		Short life-cycle
1d.	ectoparasites		Dauer stage
1e.	epidermal cell feeders		root-hair feeders
1f.	algal, lichen or moss feeders		High gonad: body ratio
1g.	feeders on aboveground plant tissue	2	Basal fauna
2	Fungal feeders		Small nematodes
3	Bacterial feeders		Anhydrobiosis
4	Substrate ingestion		Lower metabolic activity
5	Animal predation		Feeding adaptations
5a.	ingestors	3	Rudimentary food web structure
5b.	piercers		Sensitivity to chemical stressors
6	Unicellular eukaryote feeders feeding on algae diatoms, fungal spores, yeast cells		More food web links (predators and omnivores)
7	Dispersal infective stages of animal parasites	4	Greater food web structure
8	Omnivorous		Greater sensitivity to disturbance
			Larger body size
			Fewer eggs
			Longer life-cycle
		5	Highest food web structure
			Undisturbed conditions
			Large nematodes
			Long-lived
			Narrow ecological amplitude
			Lowest gonad: body ratio

1.3.3.3.2 Assignment to coloniser-persister scale

Nematode populations that fluctuate rapidly in response to favourable conditions are referred to as colonisers, whereas populations that are stable and lacking dominant species, unlike colonisers are referred to as persisters. The coloniser-persister (c-p) scale can be assigned to identified nematodes, to classify them according to their life strategy (Bongers and Bongers, 1998). The scale explained in Table 1.1, ranges from one to five: c-p scale 1 nematodes

behave like an r-strategist (organisms that have large population numbers, that can live in disturbed environments and can produce many offspring). They represent nematodes with short life-cycle, producing many small eggs that are relatively tolerant of pollution and stress. The c-p scale 5 nematodes tend to behave like a K-strategists (organisms that have smaller population numbers, that colonise a stable environment and produces fewer offspring). They represent nematodes that have a long life-cycle, produce a low number of large eggs and are very sensitive to disturbances and pollutants; c-p scale 2 to c-p scale 4 tend to vary between c-p scale 1 and c-p scale 5. Lower c-p values correspond to taxa that are relatively tolerant and larger c-p values are more sensitive to ecological disturbance.

1.3.3.3.3 Maturity index

The maturity index (MI) is described in Bongers (1990) as a semi-quantitative value, that can be utilised to indicate soil condition, determined by the nematode assemblages present. It is based on how nematode communities cope with changes or disturbances in their environment, and thus the success of their survival can be assessed and interpreted into soil condition. The MI (Bongers, 1990) is calculated as the weighted mean of the c-p values (Chapter 4, Table 4.4). Variations of the formula are detailed in Chapter 4, Section 4.2.2.8 and take into consideration the presence of plant-feeding nematodes and enrichment opportunistic c-p 1 nematodes (Neher and Darby, 2006). This useful index has been utilised in many environmental study situations, including a community assessment on reforestation of a Karst soil (Hu *et al.*, 2016) and for assessing the ecological quality status in the Black Sea (Ürkmez *et al.*, 2014).

1.3.3.3.4 Diversity indices

Nematodes belong to one of the most diverse phyla on earth, if not the most, and they are also the most numerous multicellular organisms (Hodda *et al.*, 2009), in terms of individuals. Therefore, utilising nematode diversity as an environmental bioindicator is an informative means of ecologically assessing habitats. The combination of species richness and evenness are termed as diversity (Neher and Darby, 2006), as richness or evenness increases, so does diversity. However, there is no universal index that can be applied to all data types to measure diversity (Morris *et al.*, 2014). There have been many types of indices developed to explore the area of biodiversity, including Shannon Wiener, Pielou's evenness and Jaccards similarity. However, according to Hodda *et al.* (2009), there are different indices more suited for different types of assessments. The Shannon Wiener diversity (H') index assesses the possibility of an individual of an unknown species belonging to the same species in a community assessment. It assumes that all species in the soil sample are represented in that sample and that the soil was sampled at random (Morris *et al.*, 2014). It takes into account both richness and evenness, therefore if there is a large difference in species richness in the assemblage,

it is difficult to compare between communities. The Pielou's evenness index (J') utilises both species richness and Shannon Wiener index to measure abundance similarities between different species. When there are similarities the index is even, however, if there are rare species present it is dissimilar. Jaccard's similarity index is utilised to compare biodiversity levels between communities and is based on species richness (Morris *et al*., 2014). Diversity indices have been utilised to assess aquatic (Bianchelli *et al.*, 2013) and terrestrial (Hu *et al.*, 2016) environments.

1.3.3.3.5 Ecosystem function

Nematodes play a very important role in the soil food web, due to their central position (Figure 1.3). The variation in their feeding types (Figure 1.2 and Table 1.1), enables them to be involved with channelling resources through predation and decomposition by both fungal and bacterial channels (Ferris, 2010), and can increase decomposition rates in the soil. Therefore, they are associated with the distribution of carbon, minerals and subsequently energy in the soil. In addition, through predation, they are involved with the regulation of opportunistic microorganisms, keeping levels in check (Ferris, 2010). Nematodes as bioindicators of ecosystem function therefore can indicate food-web function and structural dynamics. It is possible to conduct a soil food-web analysis, through the organisation of nematode species of similar biological characteristics, into functional guilds. Such an analysis can provide information on the rate of nutrient cycling, such as a high ratio of bacterial to fungal feeding nematodes. A soil dominated by fungal feeding nematodes is indicative of slow nutrient cycling. A soil population that is low in omnivorous nematodes, can indicate soil disturbance, soil contamination or the application of large quantities of fertiliser. Nematode biomass gives an indication of the weight of the nematodes in the different functional guilds. A low predator biomass in comparison to prey biomass, also represented by a low MI, can be indicative of environmental contamination or habitat disturbance. The opposite of this, a high predator biomass in comparison to prey is representative of a stable environmental system (Ferris and Bongers, 2009).

1.3.4 Nematodes as Biosensors of Bioremediation

Transgenic strains of *C. elegans* is well suited for ecotoxicological testing (Anbalagan *et al.*, 2012), taking into consideration (1) the species complete genome sequencing, (2) the ease of producing transgenic strains by micro-injecting DNA constructs and a marker into the nematode gonad (De Pomerai *et al.*, 2002) (3) its small size, (4) its short life cycle and (5) the production of high numbers of progeny (the latter are further described in Section 1.3.7.3). There has been a lot of research carried out on transgenic *C. elegans*, particularly on their suitability for detecting metal contamination, in both aquatic and terrestrial environments.

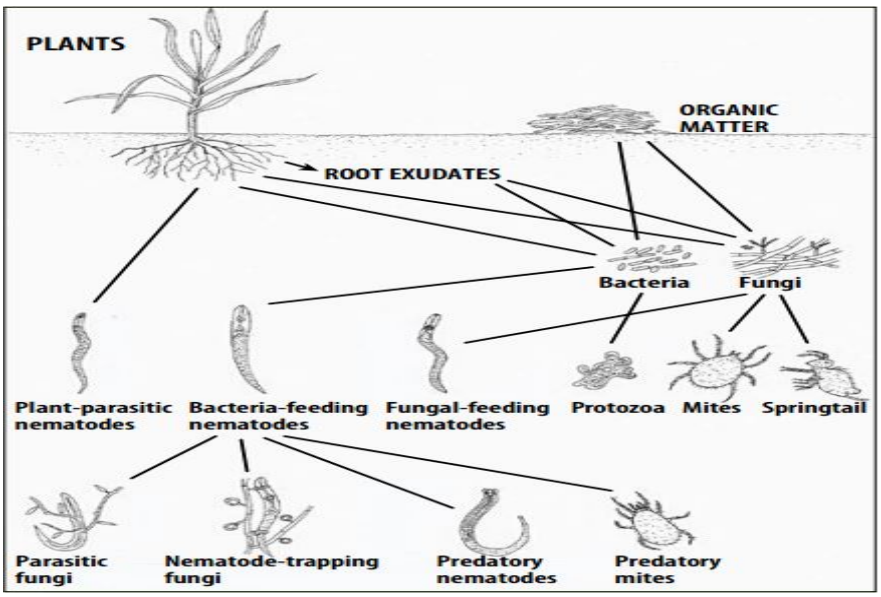

FIGURE 1.3: Soil food web structure. A simplified outline of microorganism interaction in the soil food web (Stirling, 2014)

Specifically, the potential induction of heat-shock protein (HSP), biomarkers of heavy metal stresses, was recently explored by Jiang *et al.* (2016) and Kumar *et al.* (2015).

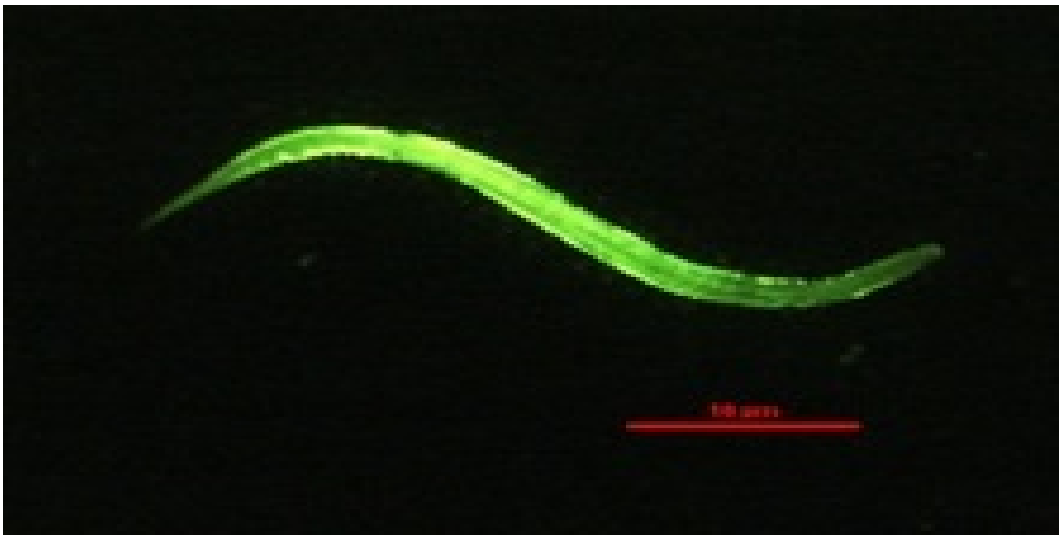

FIGURE 1.4: Transgenic *C. elegans* strain CL2050 *hsp*-16.2::GFP response to nickel.

The *hsp*-16 genes react to a sudden rise in temperature, which activates the 16-kDa proteins (Stringham and Candido, 1994), but any chemical or physical stressors that damages these proteins can also induce a response (De Pomerai *et al.*, 2002). The *hsp* genes are particularly sensitive to heavy metals, inducing a response to Cu, Hg, Ni, Pb and Zn (Anbalagan *et al.*, 2012; Kumar *et al.*, 2015) with a high response to Cd (De Pomerai *et al.*, 2002) to pesticides (Anbalagan *et al.*, 2013), such as paraquat (Link *et al.*, 1999) and to oxidative

stressors (Crombie *et al.*, 2016). Use of transgenic *C. elegans* for ecotoxicological testing, such as in lethality assays, exposure studies (Kumar *et al.*, 2015) and GFP reporter assays (Anbalagan *et al.*, 2012), is a growing area of interest and many studies have demonstrated that *C. elegans* HSP strains are suitable indicators of environmental stress (Anbalagan *et al.*, 2013; De Pomerai *et al.*, 2002; Kumar *et al.*, 2015; Lagido, 2009). The transgenic *C. elegans* HSP strain of interest in this study was developed by Link *et al.* (1999) by combining the *hsp*-16.2 gene and green fluorescent protein (GFP; Shimomura, 1979). The potential of transgenic *C. elegans* CL2050 *hsp*16.2::GFP (Figure 1.4) as biosensor of Ni bioremediation was explored in this research (Chapter 4).

1.3.5 Beneficial Bacteria Phytoparasitic Nematode Biocontrol

Beneficial bacteria, such as *Pseudomonas* spp., are associated with the control of fungal pathogens, insects and nematodes, (Aravind *et al.*, 2010). Siddiqui and Shaukat (2003) suggest that they have the potential to control parasitic nematodes by either direct attack with bacterial metabolites or by provoked systematic resistance. Beneficial bacteria as biocontrol agents are divided into two groups. (1) Bacterial strains that occupy the internal plant tissues and in doing so, reduce nematode invasion by occupying their niche or by antibiosis, or both. (2) Bacterial strains that mainly colonize the root cortex, where they can stimulate plant defence and resistance mechanisms (Siddiqui and Shaukat, 2003). The advantages of using beneficial bacteria over other biocontrol agents are discussed in Sections 1.3.1 and 1.3.2, and include: (i) extensive multiplication in damaged tissues caused by plant-parasitic nematodes, and reduction of root dependence on other environmental factors for their survival; (ii) inside the plant tissue, the beneficial bacteria can escape from microbial competition, unfavourable environmental conditions and can host a response to pathogenic attack; (iii) many PGP bacteria are easy to culture and are easily applied to seed treatments, increasing specificity and reducing the amount of inoculum used; and (iv) they do not produce any phytotoxic symptoms (Siddiqui and Shaukat, 2003).

1.3.5.1 Plant Parasitic Nematodes as Economically Important Crop Pests

Globally, an annual total crop loss caused by phytoparasitic nematodes can range between 3.3% and 20.6%. Economically, the financial impact of PPN damage is estimated to be as high as US$121 billion, including up to US$9.1 billion damage occurring in the USA alone (Degenkolb and Vilcinskas, 2016). Of the 26,000 known species of nematodes, 100 species of phytoparasitic nematodes are considered economically important parasites of crops (Degenklob and Vilcinskas, 2016). In particular, sedentary endoparasites are responsible for

most crop damage (Jansson and Lopez-Llorca, 2007). It was reported in Degenkolb and Vilcinskas (2016), that currently, the most important phytoparasitic nematodes in Europe are the beet cyst nematode *Heterodera schachtii*, the stem and bulb nematode *Ditylenchus dipsaci*, and the golden potato cyst nematode *G. rostochiensis*. However, other invasive cyst nematodes have the potential to outcompete this important crop pest, such as *G. pallida*.

The potato cyst nematode (PCN) *G. pallida* predominantly infects the Solanaceae family, in particular tomato (*Solanum lycopersicum*), melon pear (*S. muricatum*) and eggplant (*S. melongena*). However, it is a major pest of potato crops (*S. tuberosum*) in cool-temperate climates. Geographically they are widespread across Asia, North, Central and South America, New Zealand and Europe, including Ireland and the United Kingdom. It was reported in Jones *et al.* (2017) that they were responsible for an estimated annual loss of £50 million to potato harvests in the United Kingdom, but this is expected to be substantially higher across Europe. They are also estimated to be involved with crop losses of up to 80% in some cases, due to repeated cultivation of potatoes. Economically, *G. pallida* are more serious species compared to its PCN counterpart *G. rostochiensis*, as there are very few cultivars widely grown that have high levels of resistance to this species (Jones *et al.*, 2017).

The RKN *Meloidogyne* spp., are also economically important plant pathogens. Geographically, they are widely distributed, with crop damage and loss reported in South America, Asia, the USA, Africa, Australia and greenhouses in Europe. Specifically *M. hapla*, *M. naasi* and *M. chitwoodi* are predominantly found in temperate regions, whereas *M. fallax*, *M. incognita*, *M. arenaria*, or *M. javanica*, are found in warmer climates and under greenhouse conditions. They have a large host range, with up to 770 host species listed in Goodey *et al.* (1965), including weeds, crop plants and vegetables, specifically tobacco (*Nicotiana tabacum*), watermelon (*Citrullus lanatus* var. *lanatus*), tomato, tea (*Camellia sinensis*) and cotton (*Gossypium* spp.). It is estimated that the damage caused by these phytoparasitic nematodes is in the region of up to €10 billion per year in economic losses to agriculture in Europe (Truong *et al.*, 2015).

1.3.5.2 Plant Parasitic Nematode Management

Management of problematic nematodes is not a simple process. The main objectives in developing management strategies are to increase crop yield and reduce the nematode populations in the soil, therefore limiting damage both economically and environmentally (Coyne, 2009). In the past, chemical nematicides were most commonly utilised in controlling phytoparasitic infections. However, the use of these chemicals is now heavily regulated, due to the impact on human health, livestock and the environment. Nematicides are broad-spectrum toxicants that are highly volatile and water-soluble. They must be able to be evenly distributed throughout the soil without absorbing onto soil particles. To enable this

requirement, high doses of nematicides must be applied to the soil (Degenkolb and Vilcinskas, 2016). There are currently two commonly utilised nematicides, fenamiphos (Nemacur) and ethoprop (Mocap), both of which are classified as organophosphates (Clark and Kenna, 2010). The systemic nematicide, fenamiphos, is classified as restricted-use. It is utilised against most types of PPN, ectoparasitic and endoparasitic, free-living, cyst forming and RKN (Clark and Kenna, 2010). The non-systemic nematicide Ethoprop is nonfumigant and is effective against most soil-dwelling nematodes (Clark and Kenna, 2010). However, the overall efficiency of nematicides is questionable. Most nematicides are not able to penetrate the protein-rich matrix of hardened nematode cysts (Clark and Kenna, 2010), therefore it is important to implement chemical alternative ways of nematode control.

Integrated pest management (IPM) involves a combination of several methods and techniques, to maintain nematodes below economic threshold levels. It is now the most practised method of controlling phytoparasitic nematodes. IPM involves a combination of management techniques, that vary depending on the type of infections in the soil. Crop rotation is a very efficient method of controlling nematode infestations. As some nematodes have a very narrow host range, rotating different crops in the same plot helps prevent an accumulation of parasitic species, allowing for natural mortality to occur to reduce numbers (Chen and Tsay, 2006). Flooding infected land can often aid in reducing problematic nematode numbers. This method can only be implemented if the water level can be controlled and maintained at a high level for several weeks (Guerena, 2006). Nonetheless, one of the most effective means of preventing crop loss to phytoparasitic nematodes is by cultivating resistant plants. However, it is often difficult to ascertain knowledge on the extent and limitations of the resistance required and which phytoparasites are present in the soil in different environmental conditions (Fuller *et al.*, 2008). Resistant crops, including tomatoes, soybeans, cotton and potatoes have already been developed. However, these crops are only resistant to one or two species of nematodes. In the case of the genus *Globodera*, resistance in potato plants to *G. rostochiensis* has been developed in varieties such as Maris Piper and Cara (Trudgill *et al.*, 2003). Although resistant strains have great potential for increasing crop yield, it is also necessary to employ alternative IPM methods to control other nematode species present, that may infect the crop.

The use of beneficial bacteria as a biocontrol agent for pest management has great potential. Some bactericidal, herbicidal, and fungicidal biocontrol commercial products currently available, already contain several *Pseudomonas* strains. Blightban A506 (NuFarm Inc. USA) is utilised to protect fruit-producing plants, such as apple, blueberry, cherry and strawberry, along with and potato against *Erwinia amylovora*. Mycolytin (BioAgri AB, Sweden) is utilised to protect diseases in wheat and barley seeds (Shahid *et al.*, 2017). The potential nematicidal properties of beneficial bacteria have previously been explored by Cronin *et al.* (1997b), Meyer *et al.* (2009), and Singh and Siddiqui (2010), although it is an area that requires further investigation.

1.3.5.3 Beneficial Bacteria Antibiotic Production

The production of secondary metabolites, such as antibiotics, by beneficial bacteria, enables them to compete in the rhizosphere, prior to plant colonisation and also within the plant (Brader *et al.*, 2014) post-colonisation. Beneficial bacteria of the genera *Bacillus* and *Pseudomonas*, are well-characterised species that are known to produce lipopeptides, which are important for antibiosis and for inducing plant defence mechanisms (Brader *et al*., 2014). Pseudomonads, such as *P. fluorescens*, *P. aeruginosa* and *P. putida*, have displayed antifungal and antibacterial activities due to the production of antibiotics, such as phenazines, pyoluteorin and 2,4-DAPG (Shahid *et al.*, 2017).

The phenazine antibiotics are known to play an important role in the biocontrol of lower fungi and most gram-positive and gram-negative bacteria (Shahid *et al*., 2017). Pyoluteorin has bactericidal, herbicidal, and fungicidal activities and is known to control oomycotes, *Pythium spp.* (Vinay *et al.*, 2016) and phytoparasitic nematodes such as *M. incognita* (Singh and Siddiqui, 2010). The antibiotic 2,4-DAPG, displays biocontrol activity against many organisms including bacteria such as *Erwinia carotovora* (Cronin *et al.*, 1997a), fungal disease take all in wheat (Weller, 2007), nematodes *M. incognita, Xiphinema americanum, Heterodera glycines* and *G. rostochiensis* (Cronin *et al.*, 1997b; Meyer *et al.*, 2009) and can induce systemic resistance (Siddiqui and Shaukat, 2003).

1.3.5.4 Induced Systemic Resistance in Plants

The colonisation of beneficial bacteria, best-known strains belonging to the genus *Pseudomonas* (Choudhary *et al.*, 2007), on plant roots can induce a plant immune response or an induced systemic resistance (ISR) response. They do not cause any harm to the plants (Ryan *et al.*, 2008), but increase their resistance to plant pathogens and offer a broad range of protection. The response can also be triggered, not only by live bacteria but also by the presence of bacterial molecules such as siderophores, salicylic acid and flagella (Choudhary *et al.*, 2007), along with the antibiotic 2,4-DAPG (Iavicoli *et al.*, 2003). The induction of a systemic response utilises pathways regulated by jasmonate and ethylene (Choudhary *et al.*, 2007). *Arabidopsis* spp. (Iavicoli *et al.*, 2003), bean, carnation, cucumber, radish, tobacco, and tomato plants have all displayed ISR (Loon *et al.*, 1998) against many pathogenic bacterial, fungal and viral strains (Loon and Glick, 2004), including late blight caused by *Phytophthora infestans* (Yan *et al.*, 2002).

1.3.6 Nematode Characterisation - Novel Methods

Fourier transform infrared microspectroscopy, is an analytical technique that works on the principle of passing electromagnetic radiation in the infrared spectral region through a sample (Ami *et al.*, 2004), causing the chemical bonds to vibrate. These vibrations are recorded and a unique molecular fingerprint is created of the sample. The molecular fingerprint produced provides information on proteins, carbohydrates, lipids and nucleic acids (Ami *et al.*, 2013), all in one reading. This sensitive technique is rapid and non-invasive (Ami *et al.*, 2013), requires a small sample size (even a single nematode) and natural or genetically inserted fluorescence does not interfere with the results (Sheng *et al.*, 2016). It is suggested in Ami *et al.* (2004) that the combination of FT-IR in conjunction with multivariate analysis can be an effective tool for the identification and characterisation of microorganisms. It has been utilised to assess preservation methods for museum specimens (Ami *et al.*, 2004), and has been successfully explored in the biomedical sector (Ami *et al.*, 2013), from the cellular level to more complex tissues (Baker *et al.*, 2014), and in biological systems, including whole organisms, such as *C. elegans, Heterohabditis indica* and *Steinernema glaseri* (San-Blas *et al.*, 2011; Sheng *et al.*, 2016). This instrument has great potential for nematode characterisation, which was further explored in this study in Chapter 5.

1.3.7 Beneficial Bacteria and Nematode Species of Importance in This Study

1.3.7.1 *Pseudomonas fluorescens*

Bacteria belonging to the genus *Pseudomonas*, are cream coloured gram-negative rods. They are motile with polar flagella and some species produce a green fluorescent protein (GFP). They are a diverse group of bacteria and are found in many environments, with over 100 species identified (Garrido-Sanz *et al.*, 2016). There are more than 50 species in the *P. fluorescens* group (Garrido-Sanz *et al.*, 2016) that have been described, which is further divided into subgroups, where variations are identified by multilocus sequence analysis (MLSA) and phylogenomic analysis. This group includes *P. brassicacearum*, *P. protegens*, *P. chlororaphis* and *P. fluorescens* (Table 1.2). They are known as PGPR as they are capable of plant disease suppression caused by plant pathogens, as they can colonise plant tissues. They produce a wide array of antibiotics, and they can induce systemic resistance in the plant. Such antibiotics include nitrogen-containing heterocycles, such as phenazines, pyrrol-type antibiotics, pyo-compounds and indole derivatives (Shanahan *et al.*, 1992). They have also been found

to produce antibiotic compounds that do not contain nitrogen, such as, 2,4-DAPG. These characteristics promote their suitability for biocontrol and biofertilization applications.

Pseudomonas fluorescens strain F113, utilised in this study, is a PGPR strain that was isolated from the rhizosphere of sugar-beet in Ireland (Shanahan *et al*., 1992). They are capable of inhibiting the growth of phytopathogenic bacteria (*Pectobacterium caratovorum*; Cronin *et al.*, 1997a), oomycetes (*Pythium ultimum*; Fenton *et al.*, 1992), fungi (*Fusarium oxysporum*; Barahona *et al.*, 2011) and phytoparasitic nematodes (*Globodera* spp.; Cronin *et al.*, 1997b) due to the production of the secondary metabolite 2,4-DAPG. It is associated with increased activity against plant pathogens and induces plant resistance, resulting in increased crop yields (Meyer *et al.*, 2009). This distinguishes it as a biocontrol microorganism in the agrobiotech sector (Redondo-Nieto *et al.*, 2013). Moreover, it is an excellent rhizosphere coloniser due to its ability to colonise different plant species, including wheat (De La Fuente *et al.*, 2006) and willow (De Cárcer *et al.*, 2007). Therefore, it is typically utilised as a model species for investigating rhizosphere colonisation.

TABLE 1.2: Classification of bacterial species, *P. fluorescens* and *P. agglomerans* utilised in this study.

Phylum	Proteobacteria	Proteobacteria
Class	Gammaproteobacteria	Gammaproteobacteria
Order	Pseudomonadales	Enterobacteriales
Family	Pseudomonadaceae	Enterobacteriaceae
Genus	*Psedomonas*	*Pantoea*
Species	*fluorescens*	*agglomerans*

1.3.7.2 *Pantoea agglomerans*

Bacteria from the genus *Pantoea* are yellow-pigmented, rod-shaped and Gram-negative, and belong to the Enterobacteriaceae family (Walterson and Stavrinides, 2015). *Pantoea agglomerans* (Table 1.2) can colonise a diverse range of environments and has been isolated from soil, water, plants and food. It is also an opportunistic pathogenic species in immunocompromised humans and animals (Büyükcama *et al.*, 2018). This interesting group of bacteria has been described by Dutkiewicz *et al.* (2016) as being both evil and good. *Pantoea agglomerans* is associated with a variety of plant diseases including, cottonseed and boll rot (*Gossypium hirsutum*) grown in the field in the US. It is responsible for 10- 15% loss of cotton yield in the south-eastern US (Dutkiewicz *et al*., 2016). These bacteria have caused serious damage to a variety of both pest and cultivatable grasses including couch grass (*Elytrigia repens*) and onion couch (*Arrhenatherumelatius*). It has been found to reduce the growth of bamboo (*Guadua angustifolia*) shoots cultured *in vitro* and it is associated with inducing gall formation, resulting in tumours in wisteria (*W. sinensis*), Douglas-fir (*Pseudotsuga menziesii*) and

cranberry (*Vaccinium* spp.; Dutkiewicz *et al*., 2016). However, it is not always associated with pathogenic characteristics.

Pantoea agglomerans has been reported to produce secondary metabolites that have biocontrol properties. These metabolites have been developed commercially to produce products such as BlightBan C9-1 and Bloomtime Biological. They are utilised to control fire blight on apple and pear trees (Johnson *et al.*, 2000). It also has bioremediation potential to degrade herbicides, without producing harmful by-products (Pileggi *et al.*, 2012). The traits that *P. agglomerans* display, its versatility and genetic traceability, make it an excellent species for investigating niche-specific adaptation and opportunism and also for the development of commercially relevant medical, agricultural and environmental products (Walterson and Stavrinides, 2015).

1.3.7.3 *Caenorhabditis elegans*

Caenorhabditis elegans (Table 1.3) is a bacterial feeding, self-reproducing hermaphrodite nematode from the family Rhabditidae. It was the first multicellular organism to have its genome completely sequenced (Parkinson *et al.*, 2004). The adults on average are 1 mm in length and contain approximately 600 cells, excluding their reproductive system. There are many advantages to utilising *C. elegans* in research, including ease of culturing in a laboratory environment, food source availability, easy maintenance, and rapid reproduction rate that produces a prolific amount of progeny. They have a short life-cycle of up to 3.5 days when incubated at 20°C (Brenner, 1974), but this is temperature dependent. They have a quick life-cycle, with approximately 300 progenies per self-fertilising hermaphrodite, resulting in several million nematodes per day. *Caenorhabditis elegans* has contributed significantly to medicinal fields, in particular, cancer, ageing and parasitic diseases (Kyriakakis *et al.*, 2015; Tissenbaum, 2015; Weaver *et al.*, 2017).

The initial stage in the life cycle of *C. elegans* is the embryonic stage (Figure 1.5), followed by four larval stages (L1-L4) leading to adulthood. At the end of each larval stage is a molt, where the nematode produces a new cuticle and sheds the old one. The nematodes hatch at the L1 stage, 9 hours post egg laying at 22°C incubation. The L1 stage nematode molts into an L2 stage after 12 hours. It takes 8 hours for *C. elegans* to molt from L2 stage to L3 stage and a further 8 hours to molt from L3 stage to L4 stage. There is another molt from the L4 stage to young adult after 10 hours, followed by a final molt after 8 hours to a mature adult.

The dauer stage develops from a pre-dauer L2 (L2d) stage after 13 hours incubation. The dauer stage is a survival mechanism, that occurs in unfavourable environmental conditions, such as a lack of food (Wolkow and Hall, 2015). It enables *C. elegans* to survive for up to four months, effectively extending the nematodes larval stage. At this stage the nematode's

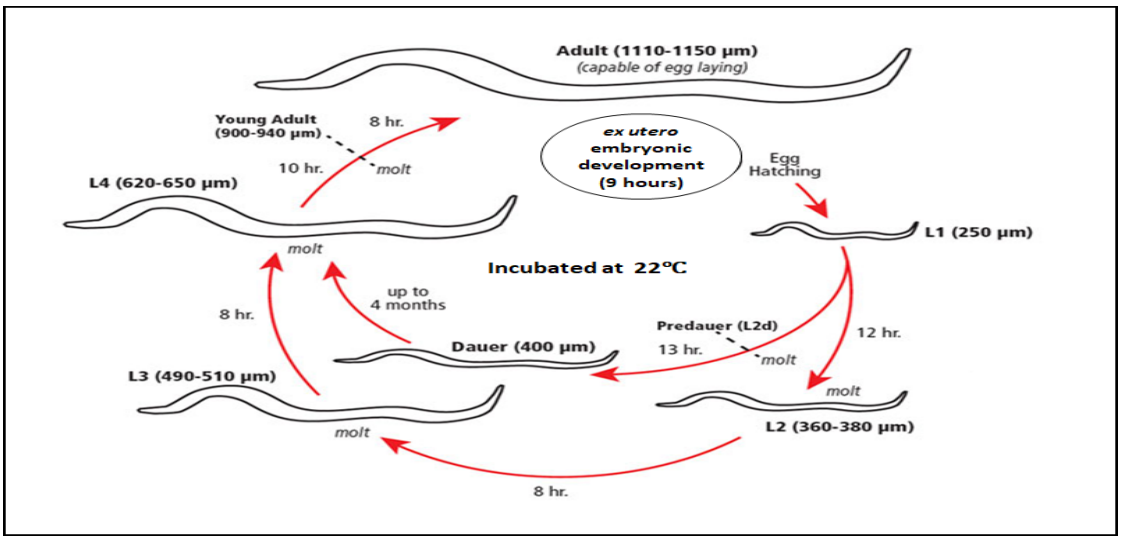

FIGURE 1.5: *Caenorhabditis elegans* life-cycle at 22°C incubation (Wolkow and Hall, 2015).

metabolism alters to allow for fat storage and the development of the gonad is halted. When conditions improve, the nematode continues to develop to the L4 stage.

1.3.7.4 *Pristionchus pacificus*

Pristionchus pacificus (Table 1.3) is a bacterial feeding, self-fertilising hermaphrodite with a four day life-cycle at 20°C (Sommer, 2006) that belongs to the Diplogastridiae family. It has been utilised in the areas of evolutionary developmental biology and ecology. Vulva formation was the first developmental process to be studied in *P. pacificus* (Sommer, 2006). The genetic study of *P. pacificus* has lead to the sequencing of its genome (Dieterich *et al.*, 2008) and more recently, investigating phenotypic plasticity (Rodelsperger *et al.*, 2017). The advantages of utilising *P. pacificus* in a laboratory situation are similar to *C. elegans* as they are easily cultured and have a rapid reproduction rate. Nonetheless, *P. pacificus* development differs from that of *C. elegans* at an early life- stage (Figure 1.6). It has an embryonic molt from J1 stage to J2 stage, before they hatch from the egg. Therefore, the J1 stage is not free-living and is non- feeding. It is suggested that this delay can allow for the development of the complex stoma morphology (Sommer, 2006).

1.3.7.5 *Meloidogyne javanica*

Meloidogyne javanica (Table 1.3) is a sedentary endoparasite and is known as a RKN. The symptoms of RKN infection above ground include plant wilt, stunting and visual signs of nutrient deficiency. The formation of galls on the roots of host plants are the main symptom

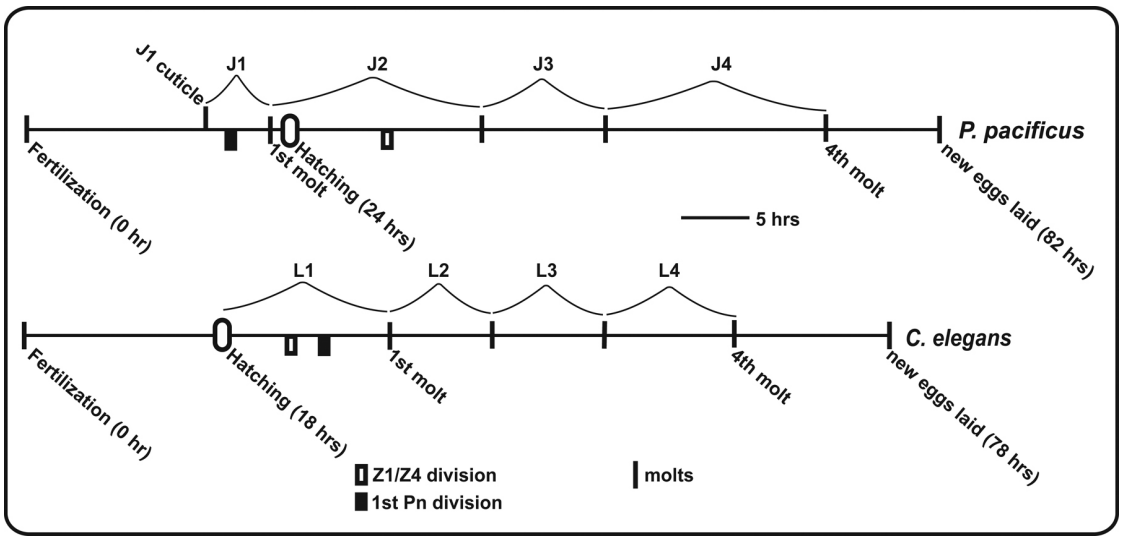

FIGURE 1.6: Comparison of *Pristionchus pacificus* and *Caenorhabditis elegans* life-cycles. Their full life cycle takes approximately four days at 20°C (Hong and Sommer, 2006).

of *M. javanica* infection, below ground. These cause reduced uptake of nutrients and water to the plants due to root damage, resulting in weak plants with poor yields (Abad *et al.*, 2004). The degree of root galling can depend on the nematode population density, the species of *Meloidogyne* and the species of host plant.

TABLE 1.3: Classification of nematode species, *C. elegans*, *P. pacificus*, *M. javanica* and *G. pallida* utilised in this study.

Phylum	Nematoda	Nematoda	Nematoda	Nematoda
Class	Chromadorea	Chromadorea	Secernentea	Secernentea
Order	Rhabditida	Rhabditida	Tylenchida	Tylenchida
Family	Rhabditdae	Diplogastridae	Heteroderidae	Heteroderidae
Genus	*Caenorhabditis*	*Pristionchus*	*Meloidogyne*	*Globodera*
Species	*elegans*	*pacificus*	*javanica*	*pallida*

Nematode development from the J1 to J2 stage occurs within the egg. The J2 infective juvenile stage is motile and migrates through the soil in search of host roots. Plant infection occurs when they enter into the host tissue near the root tip via a stylet and produce cell wall degrading enzymes (Wieczorek *et al.*, 2014). Here they establish a complex host-parasite relationship with the plant (Eisenback and Triantaphyllou, 2009). Their survival is dependent on the establishment of a successful feeding site within the root. They induce a cell differentiation process in the roots resulting in the formation of enlarged cells, known as giant cells, on which they feed.

The J2 stage nematode undergoes a further two molts; these are short and this is a non-feeding stage. The development of *M. javanica* from J3 to the J4 stage is short. The nematode swells and becomes sack like, or saccate, in appearance. They undergo a further two

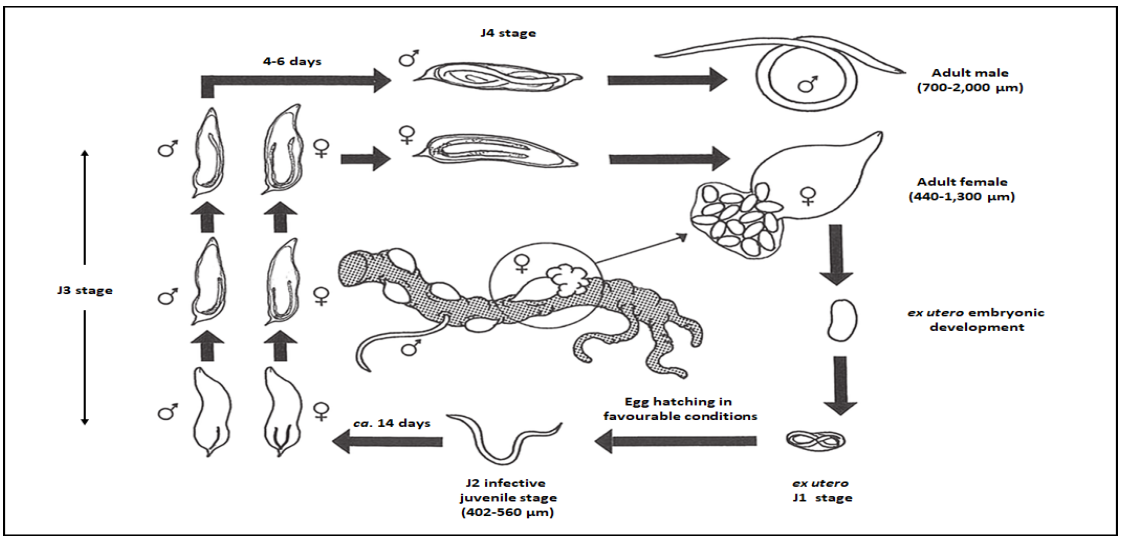

FIGURE 1.7: Life-cycle of *Meloidogyne javanica* in host roots (modified version of Moens *et al.*, 2009).

molts before developing into the J4 stage. The progression from J4 stage to adult takes four to six days when they develop from saccate, to identifiable male and female nematodes. Initially, the young adult females are not egg-laying. As their reproductive system matures into functional gonads, they become mature egg-laying females. The females remain sedentary and are pear to globose. They lay their eggs into a gelatinous matrix, on the root surface (Dávila-Negrón and Dickson, 2013). The saccate male juvenile develops into a vermiform adult male from the J4 stage. The non-feeding nematodes migrate out of the roots (Eisenback and Triantaphyllou, 2009) and search for females to mate. If they are unsuccessful, they remain in the soil and finally die. The rate of nematode stage development is dependent on soil temperature.

1.3.7.6 *Globodera pallida*

Sedentary endoparasite *G. pallida* (Table 1.3) are known as a potato cyst nematode (PCN). Symptoms of PCN infection above ground include stunted plant growth due to reduced circulation of nutrients and poor crop yield. The lower leaves on the plant tend to whither and often die. The upper leaves become discoloured and often the edges display brown spots. In the field, it can often be observed as patches of infected plants. However, all these symptoms can have many other causes (Rowe, 2017), therefore a thorough below ground examination must be performed. Evidence of cysts in the soil or females and cysts on the host roots are all positive means of identifying the cause of the symptoms.

In adequate environmental conditions, correct temperature and on receiving hatching signals (in the form of root exudates) from plants, the J2 infective juvenile stage nematodes hatch

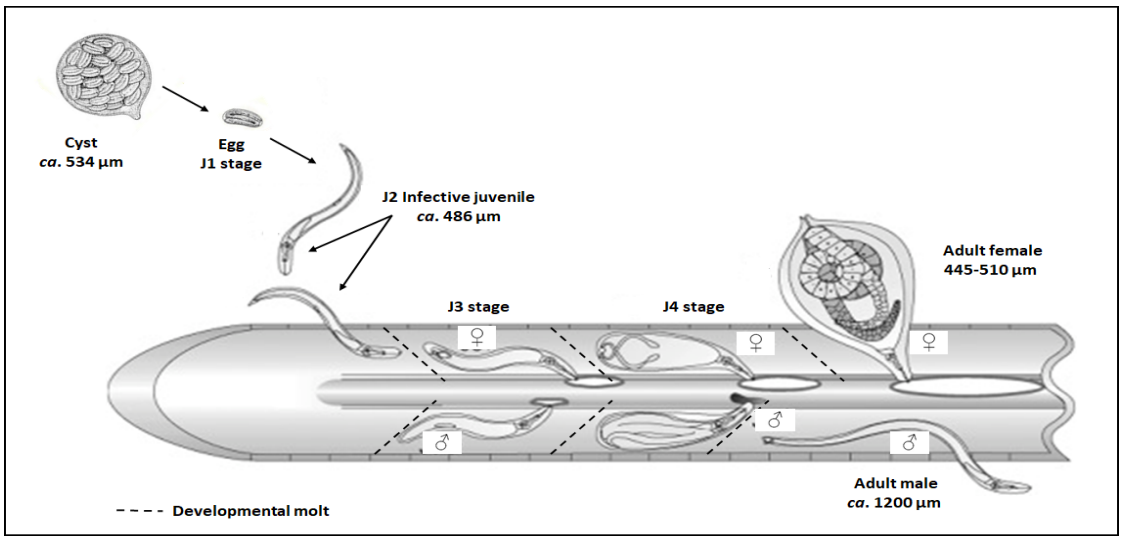

FIGURE 1.8: Life-cycle of *Globodera pallida* in host roots (modified version of Bohlmann, 2015).

and migrate towards host plant roots. There, they penetrate the roots and begin to feed. The plant cells differentiate to form specialised cells (syncytia) which transfer nutrients to the nematodes (Rowe, 2017). The juveniles undergo three more molts to become adults (Figure 1.8). Adult females swell and become globose, breaking through the roots, exposing the posterior portion of their body. Males remain active and continue to feed on the host plant roots until they reach adulthood. On maturity, they cease feeding and leave the root in search of females, surviving for approximately ten days in the soil. *Globodera pallida* adults reproduce sexually. After mating the female produces up to 500 eggs and subsequently dies. The cuticle of the dead female hardens, forms a cyst and can fall off the root into the surrounding soil if disturbed. The eggs can remain dormant in the soil for up to 30 years. In this state, the nematodes are the most resistant to nematicides. The sex of the developing nematodes within the eggs is determined on the availability of food. In adverse conditions and in heavy infestations, more male juveniles develop (Rowe, 2017). It can take between 38-48 days for *G. pallida* to complete its life-cycle, but this is temperature dependent.

1.4 Thesis Structure

Chapter 1

General Introduction

The first chapter introduces the background to this study, and the project aims and objectives. The current literature was utilised to compile a review, which predominantly focused on PGP, biocontrol and bioremediation potential of beneficial bacteria. Use of nematode assemblages as bioindicators was explored with regard to morphological assessments and molecular analysis, along with nematodes as biosensors. The suitability of the instrument, FT-IR for nematode characterisation was further investigated.

Chapter 2

Susceptibility of Nematodes to Plant Growth Promoting Bacteria and their Components

The biocontrol capacity of beneficial bacteria *in vitro* was explored in this chapter. The susceptibility of FLBF and phytoparasitic nematodes to beneficial bacterial strains *P. fluorescens* and *P. agglomerans*, along with their metabolites were investigated, to determine nematode mortality at different life stages, including egg hatch. The toxicity of the antibiotic 2,4-DAPG on the nematode species was also determined. The metabolites produced by the beneficial bacteria were subsequently identified with GC-MS analysis.

Chapter 3

The Effect of Plant Growth Promoting Bacteria on Plant Parasitic Nematodes Biology and Behaviour

The biocontrol capacity of beneficial bacteria *in planta* was explored in this chapter. Nematode attraction to beneficial bacterial strains and 2,4-DAPG was investigated via chemotaxis assays. The influence of beneficial bacteria and 2,4-DAPG on *M. javanica* development, including life stages and infection sites, in tomato plants, was investigated. The capacity of the beneficial bacterial strains to ISR in tomato plants infected with *M. javanica* was evaluated. This was followed by determining the PGP potential of beneficial bacteria inoculated tomato plants.

Chapter 4

Evaluation of Nematodes as Bioindicators of Nickel Bioremediation in an Oilseed Rape Crop

The capacity of beneficial bacteria inoculated OSR, to remediate Ni contaminated soil was explored in this chapter. The potential PGP traits of beneficial bacteria were further investigated in OSR. Nematodes as bioindicators of Ni bioremediation were assessed both by morphological assemblage characterisation and by molecular assessment with the use of DGGE. The c-p scale and nematode feeding types were assigned to the identified nematodes and diversity, maturity and ecological indices were applied to assess the bioremediation process. Transgenic *C. elegans* biosensors were utilised as a novel approach to determine the success of Ni bioremediation.

Chapter 5

Estimating the Potential of Fourier Transform Infrared Spectroscopy as a Novel Tool for Nematode Characterisation

A novel way of nematode characterisation was explored with the use of the analytical technique FT-IR microspectroscopy. Pure cultures of the nematodes (FLBFN, EPN and PPN) were assessed by the instrument, along with pure cultures of recovered nematodes from spiked soil. The data were subjected to principal component analysis and hierarchical clustering to validate the results.

Chapter 6

General Discussion and Future Prospects

This chapter presents an overview of the major findings of this research and discusses the suitability of the IT Carlow PGP bacterial isolates for plant colonisation, increased plant growth and biomass, the effectiveness of beneficial bacteria mediated OSR Ni phytoremediation, the suitability of nematode assemblages as indicators and *C. elegans* as biosensors of Ni bioremediation and the potential of PGP bacteria to manage PPN. The use of FT-IR microspectroscopy as a novel method for nematode characterisation was further discussed. This chapter also discusses future directions for some key findings namely, quantitative analysis of the metabolites produced by the bacteria, utilising nematodes as bioindicators of bioremediation in large-scale studies and the development of a database for FT-IR microspectroscopy comparisons.

Chapter 2

Susceptibility of Nematodes to Plant Growth Promoting Bacteria and their Components

2.1 Introduction

Nematode bacterial interactions are complex associations that can range from beneficial and mutualistic, to harmful and pathogenic (Murfin *et al.*, 2012). Beneficial bacteria, such as bacterial endophytes, particularly their plant colonisation and survival traits, along with their associated plant growth promotion (PGP) and biocontrol, are all areas of interest in current research. However, the interactions between PGP bacteria and nematodes have not received considerable research attention. Plant growth promoting bacteria, such as endophytic bacteria are non-pathogenic microbes, that inhabit the internal structures of host plants. They colonise the same ecological niche as plant pathogens, thus decreasing bacterial, fungal and nematode plant infections and inducing plant defence (Ryan *et al.*, 2008). They increase the plants' ability to cope with abiotic stresses by decreasing exposure to environmental stress factors. These bacteria promote plant growth by increasing the translocation of bacterial metabolites throughout the host plant (Munif *et al.*, 2013).

Bacterial secondary metabolites are produced to increase and ensure the survival of the species. They are synthesised in large quantities between the log and stationary phases of growth, when bacterial growth slows due to decreased availability of nutrients, such as carbon, nitrogen and phosphate (Anantha Padmanabhan *et al.*, 2016). The production of such metabolites increases the availability of nutrients by the production of siderophores, increases protection from environmental stresses by producing pigments, and decreases competition with other organisms by producing antibiotics (Anantha Padmanabhan *et al.*, 2016).

Gas chromatography-mass spectrometry (GC-MS) is an effective technique to identify beneficial metabolites produced by PGP bacteria in complex mixtures of volatile compounds. The instrument separates each component into ions, according to its molecular mass and the results are displayed in the form of a spectrogram with unique peaks. The unknown peaks that are represented as a combination of ions, can be searched on the National Institute Standard and Technology (NIST) database, compared and identified with the name, molecular weight and structure of the component (Anantha Padmanabhan *et al.*, 2016).

The PGP bacterial strains utilised in this study were isolated from the internal tissues of *Miscanthus x giganteus* by previous researchers in enviroCORE, Institute of Technology Carlow (Culhane, 2016; Keogh, 2009; Menton, 2010; Otieno, 2014). The bacterial strains chosen for this research were based on their metabolite production that is associated with PGP and biocontrol. The IT Carlow stocks include members of the genera *Pseudomonas*, *Pantoea* and *Enterobacter* (Keogh, 2009; Otieno, 2014). These bacterial strains are associated with biocontrol of plant pathogenic fungal species *Fusarium oxysporum* and of the plant pathogenic bacterial species *Bacillus subtilis*. Some IT Carlow stock strains produce the antibiotics 2,4-Diacetylphloroglucinol (2,4-DAPG) and pyoluteorin. The PGP traits associated with these strains include the production of the plant growth promoter indole-3 acetic acid (IAA), siderop-hore production, phosphate solubilisation, nitrogen-fixing, production of volatile organic compounds (VOC) and the production of 1-aminocyclopropane-1-carboxylate (ACC) deaminase (Keogh, 2009; Lally, 2016; Otieno *et al.*, 2015).

The bacterium *Pseudomonas fluorescens* F113, utilised in this study as a control strain, is a well-researched and documented plant growth promoting rhizobacterium that has proven to be an efficient biocontrol agent against a range of plant pathogenic bacteria, fungi and nematodes (Redondo-Nieto *et al.*, 2013) including *Globodera rostochiensis* (Cronin *et al.*, 1997b). The biocontrol properties of this rhizobacterium can be attributed to the production of the antibiotic 2,4-DAPG. This metabolite is also produced by some *P. fluorescens* strains utilised in this current study. This antibiotic is directly linked to the biological control of plant pathogens including phytopathogenic bacteria such as *Pectobacterium carotovorum*, oomycetes such as *Pythium spp.* and fungi including *Rhizoctonia solani* (Couillerot *et al.*, 2011). Biological control of the plant parasitic nematodes *Heterodera glycines*, *Meloidogyne incognita* and *Pratylenchus scribneri* has also been reported by Meyer *et al.* (2009).

Nematodes are the most numerous microscopic multicellular animals on earth. They have successfully adapted to every ecosystem and are found in fresh and sea water, on land, in polar regions and in deserts (Murfin *et al.*, 2012). They are found in the middle of the food web (Majdi and Traunspurger, 2015), they feed on bacteria, fungi, plants, protozoan, other nematodes and are a food source for many other taxa. Nematodes vary in their feeding habits, life cycle and habitat according to their life strategy. Free-living nematodes play an important role in nutrient cycling and release of nutrients for plant growth (Wang and McSorley, 2018).

Entomopathogenic nematodes (EPN) reproduce in insect hosts, feeding on their symbiotic bacteria, that inhabits their gut, and it is well reported that EPN can be used to control insect pests (Hurley, 2018; Lacey and Georgis, 2012; Půža, 2015; Zyl and Malan, 2014). Plant parasitic nematodes (PPN) live in the soil, feed on, invade and infect plant roots. They reduce the plant's uptake of water and nutrients, transmit viruses and bacterial infections to plants as they feed.

Plant parasitic nematode control relies heavily on chemical pesticides such as Aldicarb. These chemicals are very toxic and hazardous to humans and the environment and include CMRs that are carcinogenic, mutagenic or toxic to reproduction, POPs which are persistent organic pollutants and PBTs that are persistent bio-accumulative and toxic substances. These nematicides were banned under the European Union (EU) Thematic Strategy for Pesticides, Directive 91/414/EEC, amended in 2007 (Directive, 2007). The aim of this legislation, laid down by this directive, was to minimise the hazards and risks to health and environment, to reduce the levels of harmful active substances and to encourage the use of low-input or pesticide-free crop farming. The outcome of this directive was the requirement to develop newer safer methods of PPN control. There is a constant demand for the establishment of a sustainable, beneficial and safer method of biocontrol, that promotes plant health and development but will inhibit, slow or prevent PPN infection.

Interactions between PGP bacteria and the nematode species *Caenorhabditis elegans*, *Pristionchus pacificus*, *Meloidogyne javanica* and *Globodera pallida* were the main focus of this study. It was hypothesised the PGP bacterial strains and their metabolites would have increase nematode mortality, and that the bacterial strains were producing compounds associated with biocontrol and PGP. Various exposure conditions were established to subject the nematodes at different life stages to PGP bacteria, PGP bacterial metabolites and the antibiotic 2,4-DAPG. The metabolites produced by the bacterial strains were extracted and identified. Encompassing these two groups of organisms, their synergy and antagonism resulted in the main research questions arising: What effect would the PGP bacteria at different concentrations have on nematode survival? Would PGP bacterial metabolites have an effect on nematode survival and egg hatch? What effect would the antibiotic 2,4-DAPG have on nematode survival? What are the compounds that the PGP bacteria produce to cause such a response?

The aims of the research presented in this chapter are as follows:

- To determine the effect of PGP bacteria on the nematode species *C. elegans*, *P. pacificus* and *M. javanica*.
- To investigate the effect of PGP bacterial metabolites on the nematode species *C. elegans*, *P. pacificus*, *M. javanica* and *G. pallida*.

- To explore the effect of PGP bacterial metabolites on *M. javanica* and *G. pallida* egg hatch and to determine the mortality of the hatched juveniles.
- To assess the PGP bacterial strains for the production of antibiotics associated with PGP or compounds that have biocontrol properties, in particular nematicidal effects.

2.2 Materials and Methods

Good laboratory practice and aseptic technique were used when working with bacteria to prevent contamination. *Pseudomonas fluorescens* F113 and PGP bacterial strains were cultured at 30°C and maintained under sterile conditions. Bacterial stocks were prepared and stored at −70°C. Basic testing such as Gram staining, oxidase and catalase testing was carried out on a regular basis along with morphological characterisation to ensure the identity of the strain throughout the project.

All nematode species were cultured at 21-23°C for an appropriate duration to reach the desired life stage or population, depending on the species. *Caenorhabditis elegans* and *P. pacificus* were maintained under sterile conditions, whereas *M. javanica* was maintained in a plant growth room under quarantine and containment. *Globodera pallida* were received as cysts, and were stored in a cool dry place before use (Table 2.1). All PPN waste was disposed of following the appropriate procedures laid down by the department of agriculture, food and marine (DAFM). All nematodes were utilised for assays at J2 life stage unless otherwise stated. Experiments performed in this study were carried out with appropriate replications and controls.

TABLE 2.1: Nematode species utilised during the course of this project (in Chapters 2-5), including the place of origin and the supplier.

Species	Place of Origin	Supplier
Caenorhabditis elegans N2	University of Minnesota, USA	Caenorhabditis Genetics Center
Caenorhabditis elegans CL2050 *hsp*-16.2::GFP	University of Nottingham, UK	Prof David de Pomerai
Globodera pallida	The James Hutton Institute, Dundee, Scotland,UK	Dr John Jones
Heterohabaditis bacteriophora e-nema	Schwentinental, Germany	e-nema
Meloidogyne javanica	National Phyto Pathology Institute, Crete, Greece	Dr Emmanuel Tzortzakakis
Pristionchus pacificus RS 2333	Max-Planck Institute for Developmental Biology, Germany	Dr Ralf Sommer
Steinernema carpocapsae e-nema	Schwentinental, Germany	e-nema
Steinernema feltiae e-nema	Schwentinental, Germany	e-nema
Steinernema feltiae SB 12(1)	Institute of Technology Carlow, Ireland	Dr Stephen Boyle

Bacterial samples that were assessed by GC-MS for metabolite production, were prepared in a fume hood with HPLC grade organic chemicals, in a safe manner following SOPs. Instrument (Rotary evaporator, GC-MS) instruction manuals and EOP's were strictly adhered to.

Statistical analyses were performed on the data with the statistical package SPSS version 23 (IBM SPSS statistics for windows, 2017) unless otherwise stated. Outliers were assessed by a boxplot. All the data was statistically assessed by non-parametric analysis, as the homogeneity of variances and assumption of normality were violated. This test was utilised as it does not make the same assumptions about data distribution (normality) as normally

distributed data. Post hoc analysis was carried out with Dunn (1964) procedure with a Bonferroni correction for multiple comparisons, unless otherwise stated. Statistical significance was set at α = 0.05 level. Values marked with asterisks (*) indicates significant differences in the post hoc analysis between treatments and the control, as follows * ($p \leqslant 0.05$), ** ($p \leqslant 0.01$), *** ($p \leqslant 0.001$) and **** ($p \leqslant 0.0001$). The presence of asterisks in figures and tables indicates a significant difference between treatments and control unless otherwise stated. Data are presented as mean ± standard error of the mean (SEM). GC-MS chromatograms of the bacterial metabolites and broth controls were statistically assessed by OpenChrom® open source software (Community Edition version 1.1.0 Deils).

2.2.1 Plant Growth Promoting Bacterial Strains

Bacterial strains utilised in this study (Chapters 2-4) were isolated from the internal tissues (stems and leaves) of *M. giganteus* plants by previous researchers in enviroCORE, IT Carlow. The bacterial strains have a coding prefix in their ID to indicate the tissue it was isolated from, leaf (L) and stem (S). The original bacterial isolates were sequenced using partial PCR 16S rDNA amplification followed by the closest match with the NCBI BLAST database (Menton, 2010; Otieno, 2014). Table 2.2 explains the percentage BLAST identification and the best matched bacterial strain. The bacterial strains will be referred to from here in according to their strain number. Three *gfp* tagged bacterial strains were utilised in Chapter 4 (Table 2.3). The fluorescent *gfp* gene expresses resistance to the antibiotic kanamycin. Therefore, it increases its trace-ability in soil and plants.

TABLE 2.2: Bacterial strains utilised during the course of this project (in Chapters 2-4), including the host plant they were isolated from and their taxonomical and BLAST identification.

Strain	Host plant	Taxa ID	BLAST ID	Reference
F113	*Beta vulgarus*	*Pseudomonas fluorescens*	-	Fenton *et al.* (1992)
L111	*Miscanthus* leaf	*Pseudomonas fluorescens*	95%	Otieno (2014)
L124	*Miscanthus* leaf	*Pseudomonas fluorescens*	98%	Menton (2010)
L132	*Miscanthus* leaf	*Pseudomonas fluorescens*	93%	Otieno (2014)
L228	*Miscanthus* leaf	*Pseudomonas fluorescens*	99%	Menton (2010)
L321	*Miscanthus* leaf	*Pseudomonas fluorescens*	99%	Otieno (2014)
S110	*Miscanthus* stem	*Pseudomonas fluorescens*	99%	Menton (2010)
S222	*Miscanthus* stem	*Pantoea agglomerans*	99%	Menton (2010)
S118	*Miscanthus* stem	*Pseudomonas fluorescens*	100%	Menton (2010)

Several biochemical tests were performed on *P. fluorescens* F113 and PGP bacterial strains L111, L228, L321 and L132 by Keogh (2009), Otieno (2014), and Otieno *et al.* (2013) to determine plant growth promotion (PGP) traits (Table 2.4). The bacterial strains chosen for this study were based on their biological control properties and PGP traits (Table 2.4). The

biocontrol properties of the bacterial strains were investigated on plant pathogenic fungal species *Fusarium oxysporum*, *Pythium ultimum* and plant pathogenic bacteria *Bacillus subtilis* by past researchers of the enviroCORE group. The bacterial strains interactions with EPN *Steinernema feltiae*, *S. carpocapsae* and *Heterohabditis bacteriophora* have also been previously investigated by Hurley (2018).

2.2.1.1 Culture and Maintenance of Bacterial Strains

Bacterial stocks were prepared for long-term storage by inoculating 10 μl bacterial stock into McCartney bottles containing 10 ml of NB. The bottles were incubated at 30°C for 24 hours in a shaker incubator at 100 rpm. 750μl of bacteria cultures were added to 250 μl 40% glycerol solution. The samples were labelled and stored at -70°C.

TABLE 2.3: *gfp* tagged bacterial strains utilised in Chapter 4.

Strain	Transposon	Genes	Reference
F113 *gfp*	mini-Tn5	*gfp*:km^R	Otieno (2014)
L111 *gfp*	mini-Tn5	*gfp*:km^R	Otieno *et al.* (2013)
L321 *gfp*	mini-Tn5	*gfp*:km^R	Otieno *et al.* (2013)

Bacteria were cultured by inoculating 10 μl of stock bacterial strains aseptically into McCartney bottles containing 10ml sterile nutrient broth (NB). The broths were incubated at 30°C for 24 hours in a shaker incubator at 100 rpm. 10 μl of the culture was streaked onto nutrient agar (NA) plates, using the quadrant streak method and incubated at 30°C for 24 hours. The plates were examined for contaminants and a single colony was picked from the NA plate and re-inoculated into McCartney bottles containing 10ml NB and incubated at 30°C for 24 hours. The bacteria were streaked again onto NA and the colony morphology was visually assessed.

2.2.1.2 Gram Staining

Bacterial smears of each bacterial strain were prepared on glass slides. The slides were then flooded with crystal violet for 30 seconds, followed by a wash with dH_2O. The slides were covered with a mordant of Gram's iodine for 10 seconds, followed by a wash with dH_2O. The smear was subsequently de-colourised with 95% ethanol for 15 seconds, followed by a wash with dH_2O. Finally, the counter-stain safranin was added for 30 seconds, followed by a wash with dH_2O. The slides were blotted dry with tissue paper and left to dry before examining under a microscope with 100 X oil immersion lens. Gram-positive bacteria retain the crystal violet stain in their peptidoglycan layer in the bacterial cell wall and can be visualised as purple/blue cells. Gram-negative bacteria can be visualised as pink/red cells after counterstaining with safranin.

TABLE 2.4: Beneficial bacterial strains utilised during this research (Chapters 2-4), their biological control properties, plant growth promotion traits and antibiotic production.

Strain	Biocontrol properties								PGP traits[3]						References
	Plant pathogen[1]			EPN[2]			Antibiotic gene[4]	Antibiotic	IAA	Siderophore	P sol	N fixing	VOC	ACC	
	FO	*PU*	*BS*	SF	SC	HB									
F113	ND	+	ND	-	-	-	PhlD	DAPG	-	+	+	ND	ND	ND	Cronin *et al.* (1997b) and Hurley (2018)
L111	-	-	ND	-	-	-	-	-	+	+	+	+	-	-	Hurley (2018), Otieno (2014), and Otieno *et al.* (2013)
L124	+	+	+	-	-	-	PhlD, PltB	DAPG, Pyoluteorin	ND	ND	ND	ND	ND	ND	Hurley (2018) and Menton (2010)
L132	-	+	ND	-	-	-	-	-	+	+	+	-	-	-	Hurley (2018) and Otieno (2014)
L228	+	+	+	-	-	-	-	-	-	+	+	-	+	-	Hurley (2018), Menton (2010), and Otieno *et al.* (2013)
L321	-	-	ND	-	-	-	-	-	+	-	+	-	-	+	Hurley (2018) and Otieno *et al.* (2013)
S110	+	+	+	-	-	-	PhlD	DAPG	ND	ND	ND	ND	ND	ND	Hurley (2018) and Menton (2010)
S118	+	-	+	-	-	-	PhlD	DAPG	ND	ND	ND	ND	ND	ND	Hurley (2018) and Menton (2010)
S222	-	+	-	-	-	-	-	-	ND	ND	ND	ND	ND	ND	Hurley (2018) and Menton (2010)

[1] Plant pathogens: FO = *Fusarium oxysporum*, PU = *Pythium ultimum* and BS = *Bacillus subtilis*.
[2] EPN (entomopathogenic nematodes): SF = *Steinernema feltiae*, SC = *S. carpocapsae* and HB = *Heterohabditis bacteriophora*.
[3] PGP (plant growth promoting) traits are referred to as the production of indole-3 acetic acid (IAA), siderophores, phosphate (P) solubilisation, nitrogen (N) fixation, volatile organic compounds (VOC) and 1-aminocyclopropane-1-carboxylate (ACC) deaminase.
[4] Antibiotic gene refers to the antibiotic biosynthetic genes detected by Menton (2010) and the antibiotic they produce.
[5] - = negative effect, + = positive effect and ND = no effect determined.

2.2.1.3 Oxidase and Catalase Biochemical Tests

Oxidase tests were performed on bacterial strains to identify the presence of the enzyme cytochrome c oxidase produced by the bacteria electron transport chain. Bacterial strains were cultured and incubated overnight on NA plates at 30°C. A bacterial colony was transported onto a filter paper disk which contained 5 drops of the reagent 1% tetramethyl-p-phenylenediamine dihydrochloride, with a sterile pick. A positive result was recorded on the development of a dark blue/purple colour within 10 seconds. A negative result was recorded with no colour change.

Catalase test was utilised to determine the production of the enzyme catalase which is responsible for neutralizing toxic forms of oxygen metabolites. Bacterial strains were cultured and incubated overnight on NA plates at 30°C. A bacterial colony was placed onto a glass slide. One drop of fresh 3% H_2O_2 was placed onto the colony. A positive result was determined by effervescence on the colony. A negative result was noted with no reaction.

2.2.1.4 Standard Curves

Bacterial standard curves were utilised to quantify the bacterial concentration in colony forming units (CFU/ml). An optical density (OD) reading of a 24-hour culture of bacteria grown in nutrient broth (NB) was recorded using a Shimadzu UV-1800 UV/Visible scanning spectrophotometer at an OD of 600 nm. The bacteria were diluted from an $OD_{(600)}$ 0.8 to 0.1 using sterile ¼ strength Ringers. A serial dilution of 10^{-1} to 10^{-8} was carried out on each OD bacterial batch, in sterile 1.5 ml tubes containing 900 μl sterile ¼ strength Ringers and 100 μl bacteria culture (Miles and Misra, 1938). Onto NA plates, 30 μl of each dilution was pipetted, in three-fold replications and the plates were incubated at 30°C for 24 hours. The colonies were counted, the CFU/ml was calculated and the standard curve was plotted on a graph using Microsoft Excel (2016).

$$\text{CFU/ml} = \frac{\text{No. colonies} \times \text{dilution factor}}{\text{Volume of culture plate}}$$

2.2.2 Nematode Species Culture and Maintenance

2.2.2.1 *Caenorhabditis elegans* and *Pristionchus pacificus*

Caenorhabditis elegans and *P. pacificus* (Figure 2.1, Images B and C) were utilised in this study as control species. *Caenorhabditis elegans* N2 was obtained from the Genetic Centre University of Minnesota, USA and *P. pacificus* RS 2333 was supplied by Dr Ralf Sommer in the Max-Planck Institute for Developmental Biology, Germany (Table 2.1). Lab-reared

nematodes were cultured on nematode growth medium (NGM) seeded with an *Escherichia coli* OP50 bacterial lawn, sourced from the Genetic Centre University of Minnesota, USA.

2.2.2.1.1 Culture and maintenance

Nematode growth medium was prepared by adding 1.5 g $NaCl_2$ [Sigma], 8.5 g Technical Agar No. 3 [Oxoid] and 1.25 g bacteriological peptone [Lab M] into 500 ml Duran bottle. Following this, 487.5 ml dH_2O was added to the Duran bottle and the mix was autoclaved. After autoclaving, 0.5 ml 1M $CaCl_2$ [Sigma], 0.5 ml cholesterol (5 mg/ ml; [Sigma]) in 95% ethanol [Sigma Aldrich], 0.5 ml 1M $MgSO_4$ [Fisher Scientific] and 12.5 ml 1 M K_2PO_4 buffer were added to the autoclave bottle and mixed (Brenner, 1974). The K_2PO_4 buffer was prepared by adding 136 g KH_2PO_4 dissolved in 1 L H_2O to 182.40 g $K_2HPO_4 \cdot H_2O$ dissolved in 1 L H_2O to increase the pH from pH 4.0 to pH 6.0; the buffer was filter sterilised (Stiernagle, 2006).

The bacterial strain *E. coli* OP50 was cultured by inoculating 10 μl stock culture into a McCartney bottle containing 10ml sterile NB [Lab M]. The broths were incubated at 30°C for 24 hours in a shaker incubator at 100 rpm. Onto a fresh NGM plate, 100 μl overnight bacterial broth culture was pipetted and spread aseptically using the spread plate method. The plates were incubated at 30°C overnight.

An agar chunk of 2 cm^2 was cut from a stock NGM culture plate containing nematodes and eggs. Using a sterile spatula, an agar chunk was placed onto a new seeded NGM plate and sealed with parafilm. The plates were incubated at 20°C for up to eight weeks for stock plates. To increase nematode yield for experiments, up to four agar chunks were added to each fresh NGM plates and incubated at 20°C for up to five days or until the plate was densely populated with the desired life stage.

2.2.2.1.2 Age synchronisation

Age synchronisation was performed on *C. elegans* and *P. pacificus* to eliminate any variation in results due to age differences (Sulston, 1988). This technique was also used to remove fungal contamination from the nematode culture plates (Stiernagle, 2006). The nematodes were cultured on seeded NGM plates for three to five days to ensure an abundance of eggs and gravid females on the plate. The M9 buffer, 2ml in total, was pipetted repeatedly onto the plate and gently swirled to dislodge the nematodes. The M9 buffer was made by adding 6.0 g Na_2HPO_4 [Vickers laboratories], 3.0 gKH_2PO_4 [Merk], 5.0 g $NaCl_2$ and 1.0 ml 1M $MgSO_4$, to a 1 L Duran bottle. The mix was made up to 1 L with dH_2O and filter sterilised using a 0.22 μm filter. The nematodes were collected into a 15 ml falcon tube and left for ten minutes to settle. The settled nematodes were aspirated into 1.5 ml tubes and centrifuge at

2500 rpm for two minutes. The remaining M9 buffer in the 15 ml tubes was left to re-settle and the procedure was repeated until all the nematodes were collected.

A 20% alkaline hypochlorite solution (to make 15 ml; 8.25 ml ddH_2O, 3.75 ml 1M NaOH, [Sigma Aldrich] and 3.0 ml household bleach; made fresh each time (Pires-daSilva, 2013)) was prepared, and 1 ml was added to each 1.5 ml tube. The tubes were mixed gently by inverting every two minutes for ten minutes and centrifuged at 2500 rpm for two minutes. The supernatant was aspirated without disturbing the nematode pellet and 1 ml of M9 buffer was added to each tube and mixed well. The tubes were centrifuged at 2500 rpm for two minutes and the washing procedure was repeated a further three times. To the tubes, 50 μl M9 buffer was added to re-suspend the pellet. The eggs were aseptically pipetted onto NGM plates seeded with *E. coli* OP50 lawn and incubated at 20°C for two days (Sulston, 1988). At this stage, the nematodes had hatched and were age synchronised at J2 life stage.

2.2.2.2 *Meloidogyne javanica*

Meloidogyne javanica (Figure 2.1, Image D) was provided by Dr Emmanuel Tzortzakakis from the National Phyto Pathology Institute, Crete, Greece (Table 2.1). The nematodes were cultured in the roots of tomato plants (*Solanum lycopersicum* var. 'Moneymaker' or *Solanum lycopersicum* var. 'Gardeners delight').

2.2.2.2.1 Culture and maintenance

The nematodes were cultured by removing the infected plant from the plant pot and washing the roots in water to remove the soil. The roots were removed from the plant and placed into a clean Petri dish with water and the egg sacks were observed under the stereoscope and counted. New six to eight-week-old tomato plants grown in sterile general purpose potting compost were infected with the nematodes. Infected roots from stock plants containing five to eight egg sacks were placed into three holes near the base of the roots of new plants at a depth of 5-6 cm. The pots were placed onto plant pot trays and the plants were watered into the trays to avoid washing the nematodes out of the pot. The plants were grown in a plant growth room at 22°C with 16 hours of light and 8 hours of darkness, for three to four months. Plant infection was determined by observing the extent of necrosis of the plant leaves, deterioration of the general health of the plant and the presence of galling on the roots. All nematodes, soil, water used and plant material were treated by autoclaving as per instruction by the DFAM and disposed of subsequently in general waste.

2.2.2.2.2 Extracting *Meloidogyne javanica* from tomato roots

Meloidogyne javanica were extracted from tomato plants using a modified Baermann funnel method (Bezooijen, 2006), which is an effective method of nematode extraction of active

nematodes from plant material. The roots were washed in H_2O and cut into 6-8cm pieces. The chopped roots were placed into a 1mm sieve, lined with a square of loose weave muslin cloth. The sieve was inserted into a dish of H_2O for seven days, ensuring the water was touching the roots. The nematodes emerged out of the roots, moved to the water and settled at the bottom of the dish. They were collected from the water by passing the nematode suspension through a 40 μm sieve to retain them. They were washed off the sieve with H_2O and stored in a falcon tube at 4°C for up to five days. The modified Baermann funnel was refilled with H_2O and the extraction was continued for a further two weeks to ensure the maximum harvest of nematodes.

2.2.2.2.3 Age synchronisation

Infected roots were removed from the tomato plants (as described in Section 2.2.2.2.1), dipped in sterile ddH_2O to remove soil particles and placed into a screw-topped container. The roots were vigorously agitated in 1% sodium hypochlorite solution for three minutes to release the eggs. The suspension was passed through a range of sieves from 150-40 μm to trap debris and soil particles in the larger sieves, and the eggs on the smaller sieves. The eggs on the 40μm were washed with sterile ddH_2O to remove any sodium hypochlorite. A deli dish was filled with the egg suspension and incubated for three to five days at 28°C (Siddiqui and Shaukat, 2003). The hatched nematodes were age synchronised at J2 life stage and were used within five days.

2.2.2.3 *Globodera pallida*

Globodera pallida cysts (Figure 2.1, Image A) were supplied by Dr John Jones from The James Hutton Institute, Dundee, Scotland UK (Table 2.1). The cysts were stored at 21°C in an airtight container until required.

2.2.2.3.1 Potato root diffusate

Potato tubers (*Solanum tuberosum* var. 'Desiree') were stored at 20°C in a dark dry place for three weeks. The potato tubers were subsequently suspended on the surface of sterile H_2O in a beaker to germinate, ensuring the roots were hanging into the water (Bezooijen, 2006). This was performed to obtain root exudates which were required for *G. pallida* eggs to hatch. Once the tubers had germinated and a substantial root was formed, the H_2O or potato root diffusate (PRD) was filter sterilised and stored in 50 ml aliquots at -20°C for further use.

2.2.2.3.2 Maintenance and hatching

The cysts were surface sterilised by placing 30 dry cysts in the syringe and submerging it in ethanol for 15 seconds. They were then transferred to a 1.3% sodium hypochlorite solution until the cysts appeared faded and started to break open, for up to ten minutes (Figure 2.1, Image A). The cysts were rinsed three times in sterile H_2O, placed into a 1.5ml tube and gently agitated three to four times with a sterile micro pestle to help the eggs released from the cysts. The cysts were pipetted onto a watch glass, which was placed into a Petri dish. The watch glass was filled with 5 ml sterile H_2O, the lid was sealed with Parafilm and the dish was incubated in the dark for three days at 18°C. The cysts were transferred to a new watch glass, filled with 5 ml of sterile PRD and incubated again at 18°C for 3-14 days, regularly refilling the watch glass with PRD (ibid.) and monitoring for hatched nematodes. The hatched nematodes, at the J2 life stage, were collected in a deli dish and used within five days.

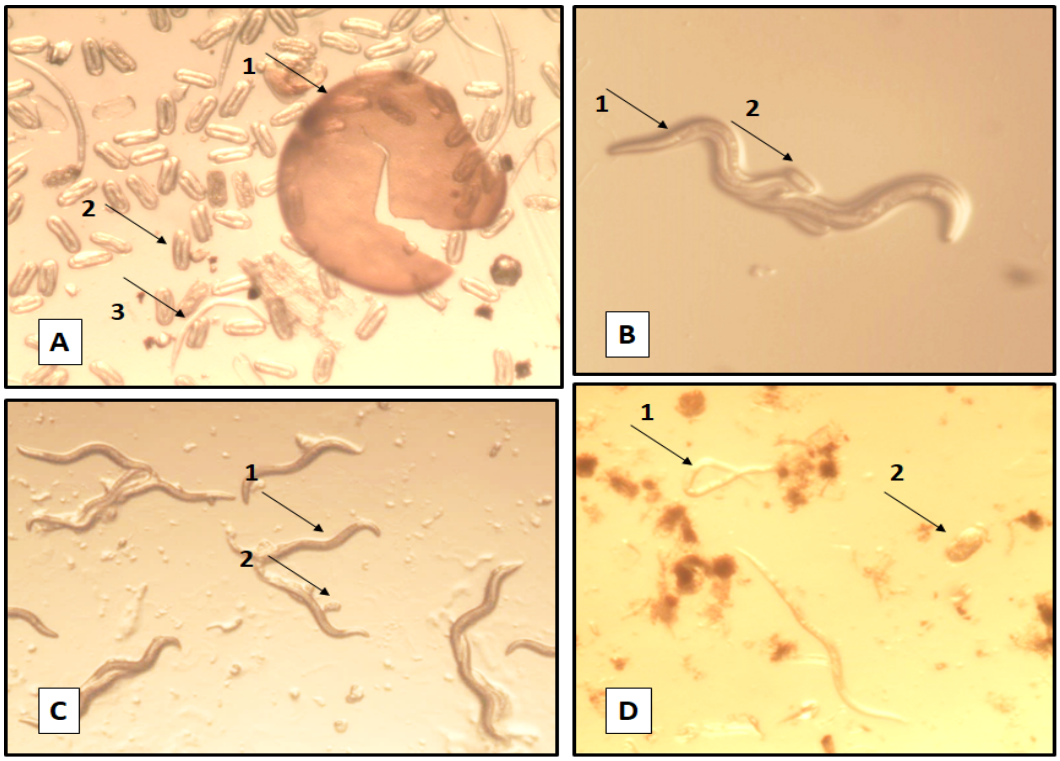

FIGURE 2.1: Nematode species utilised in this study: (A) *Globodera pallida* with (1) open cyst, (2) eggs and (3) J2 nematodes. (B) *Pristionchus pacificus*, with (1) adult nematodes and (2) eggs. (C) *Caenorhabditis elegans* with (1) J4 nematodes and (2) eggs, and (D) *Meloidogyne javanica* with (1) J2 nematodes and (2) eggs.

2.2.3 Susceptibility Testing of Nematodes to PGP Bacteria and their Metabolites

Susceptibility testing was performed to determine the effect of the PGP bacterial strains F113, L228, S118, S222, L124 and L321 and their metabolites on different life stages of the nematodes *C. elegans*, *P. pacificus M. javanica* and *G. pallida* (see Table 2.5 for bacterial concentration, CFU/ ml). Life stages, nematode numbers and exposure times selected for experiments, depended on the life cycle (Table 2.6) and nematode availability in those life stages for each species (Meyer *et al.*, 2009).

2.2.3.1 Susceptibility of Nematodes to PGP Bacteria

Susceptibility of the nematodes *C. elegans*, *P. pacificus* and *M. javanica* to PGP bacteria was established in sterile U-bottom 96 well micro-titre plates. Age synchronised nematodes (Table 2.6), 100 nematodes in 100 μl sterile ¼ strength Ringers were added to each well. An OD reading was taken on a spectrophotometer [Shimadzu] from a 24 hour bacterial culture grown in NB at 30°C (see Table 2.5 for bacterial concentration, CFU/ ml). The liquid culture was diluted with ¼ strength Ringers from an $OD_{(600)}$ 0.8 to $OD_{(600)}$ 0.1. To each well, 100 μl of bacterial culture was added to the nematodes, with six replications of each dilution. Age synchronised nematodes, 100 nematodes in 100 μl sterile ¼ strength Ringers, with six replications, was utilised as a negative control. The nematodes were exposed for 24 and 48 hours at 21-23°C in the dark, after which nematode mortality was recorded. Mortality was determined by typical 'C' shape of nematodes and no movement on prodding with a needle. Percentage mortality was calculated and the results were graphed and statistically assessed.

TABLE 2.5: Bacterial concentrations (CFU/ml) utilised in susceptibility and egg hatch tests.

Strain	**Susceptibility Tests**[1]			**Egg Hatch**[2]
	High	**Medium**	**Low**	
F113	5.29×10^9	4.11×10^8	3.00×10^7	7.78×10^9
L228	9.04×10^8	7.92×10^6	8.93×10^4	2.33×10^9
S222	3.12×10^9	1.72×10^8	1.05×10^7	3.89×10^9
S118	4.56×10^9	4.06×10^8	2.64×10^6	9.56×10^9
L124	5.51×10^9	4.11×10^8	5.25×10^7	8.89×10^9
S110	2.43×10^8	2.54×10^7	6.63×10^5	4.33×10^8
L321	3.74×10^8	1.04×10^8	1.89×10^7	4.89×10^8
L111	8.15×10^7	3.17×10^7	1.03×10^7	1.00×10^8
L132	3.11×10^8	5.56×10^7	9.15×10^6	5.33×10^8

[1] High = $OD_{(600)}$ 0.8 - 0.6, Medium = $OD_{(600)}$ 0.5 - 0.4 and Low = $OD_{(600)}$ 0.3 - 0.1 combined to form the bacterial/ metabolite concentrations for susceptibility tests.
[2] Metabolites of an $OD_{(600)}$ 0.8 reading was utilised in egg hatch tests.

2.2.3.2 Susceptibility of the Nematodes to PGP Bacterial Metabolites

An OD reading was taken on a spectrophotometer [Shimadzu] from 24 hour bacterial cultures of F113, L228, S118, S222, L124 and L321, grown in NB at 30°C (see Appendix A, Table 2.5 for bacterial concentration, CFU/ ml). The liquid culture was diluted with ¼ strength Ringers from an $OD_{(600)}$ 0.8 to $OD_{(600)}$ 0.1. To a 20 ml centrifuge tube, 5 ml of each OD dilution was added and centrifuged twice at 2800 rpm for 20 minutes. The supernatant of each tube was passed through a 0.22 μm sterile filter to remove any remaining bacterial cells. The supernatant was tested for bacterial growth by plating 100 μl of each dilution onto an NA plate. The Petri plate was incubated at 30°C overnight and colony growth was assessed.

Caenorhabditis elegans and *P. pacificus* were cultured on NGM agar plates (Section 2.2.2.1.1) and the nematodes were age synchronised (Section 2.2.2.1.2). The eggs were placed onto NGM agar plates seeded with *E. coli* OP50 and incubated for 14 - 16 hours, after which J1 and J2 were recovered off the plates, by washing the plates with sterile ¼ strength Ringers. Heavily populated NGM plates, with all ages, were washed with sterile ¼ strength Ringers, the washings were passed through nested sieves with a mesh diameter of 125 μm - 60 μm. The nematode life-stages of J3 and J4 were recovered on 60 μm sieves and adults were recovered on 125 μm sieves. Any nematodes present in the samples that were not of this life stage were not counted.

The test was established in sterile U-bottom 96 well micro-titre plates. Nematodes (see Table 2.6 for the number of nematodes utilised) in 100 μl sterile ¼ strength Ringers were added to each well. To each well, 100 μl of bacterial metabolites from each strain were added, with six replications of each dilution. Nematodes in 100 μl sterile ¼ strength Ringers, with six replications, were utilised as negative controls. The nematodes were exposed for 24 hours (*C. elegans* and *P. pacificus* were exposed for 24 and 48 hours) at 25°C in the dark. At this point, nematode mortality was recorded and assessed as described in Section 2.2.3.1.

2.2.4 Sensitivity of Nematodes to 2,4-DAPG

A 1M stock solution of 2,4-DAPG was prepared in 50% methanol (1 mg/ ml). From this 1, 10, 25, 50, 75, 100, 200 and 500 ppm standards were prepared and utilised immediately. A 0 ppm standard of dH_2O was utilised as a control (with 6 replications). The assay was established in a sterile U- bottom 96 well micro-titre plates with age synchronised nematodes (J2 life stage) in 100 μl sterile ¼ strength Ringers (Table 2.6) and 100 μl of 2,4-DAPG. The assay was established for 24 hours at 25°C in the dark, as for Section 2.2.3.1. There

were six replications of each 2,4-DAPG treatment. The assay was established at lower 2,4-DAPG concentrations for *G. pallida*, as the number of nematodes available for this work task, were limited. It was also observed by Cronin *et al.* (1997b) that lower concentrations of the antibiotic had a greater effect on *G. rostochiensis*. Methanol control assays were established parallel to the 2,4-DAPG susceptibility tests under the same test conditions. 99.8% methanol (Sigma-aldrich) was diluted with dH_2O to the equivalent concentrations found in the 2,4-DAPG dilutions: 0.0045%, 0.045% and 0.45%. These methanol concentrations were also tested by Meyer *et al.* (2009) in similar toxicity assays.

2.2.5 Effects of PGP Metabolites on Egg Hatch and Juvenile Mortality

An OD reading was taken on a spectrophotometer [Shimadzu] of a 24-hour bacterial culture grown in NB and diluted with ¼ strength Ringers to $OD_{(600)}$ 0.8 (see Appendix A, Table 2.5 for bacterial concentration, CFU/ ml). The bacterial culture was centrifuged twice at 2800 rpm for 20 minutes and the supernatant was passed through a 0.22 μm sterile filter. The supernatant was tested for bacterial growth by plating 100 μl on an NA plate. The stock solution for the antibiotic 2,4-DAPG was prepared as in Section 2.2.4. From this, 10 and 100 ppm standards were prepared and used immediately.

The assay was established in sterile 24 well tissue culture plates, with eight replications of (1) the bacterial metabolites S110, L124, S222, L321, L228, F113 and S118 and (2) 10 ppm and 100 ppm of synthetic 2,4-DAPG. Nematode suspension, 50 μl in total (*G. pallida* in PRD or *M. javanica* in dH_2O) and surface sterilised eggs (Table 2.6) were added to each well containing 450 μl of bacterial supernatant or 450 μl 2,4-DAPG standard. Controls for the bacterial supernatant were 50 μl of nematode suspension containing surface sterilised eggs and 450 μl NB. Controls for 2,4-DAPG standard were 50 μl of nematode suspension containing surface sterilised eggs and 450 μl dH_2O. *Meloidogyne javanica* and *G. pallida* eggs were incubated at 28°C (Siddiqui and Shaukat, 2003) and 18°C (Bezooijen, 2006) respectively. After five days exposure period for *M. javanica* and seven days for *G. pallida*, egg hatch and juvenile mortality were recorded under a stereoscope [Optika].

2.2.6 Identification of PGP Bacterial Metabolites - Analytical Approach

2.2.6.1 2,4-DAPG Standard

A 1M stock solution of pure synthetic 2,4-DAPG, stored at -20°C in a sealed container, was dissolved in 50% methanol (1 mg/ ml). From this 100 ppm standard was prepared and read

TABLE 2.6: Overview of experimental establishment. Life stages, nematode numbers and exposure times depended on life cycle and availability of life stage for each species (Meyer *et al.*, 2009).

Strain[a]	**Life stage**[b]	**Nematode species**							
		CE[c]		**PP**		**MJ**		**GP**	
		24h[e]	**48h**	**24h**	**48h**	**24h**	**48h**	**24h**	**48h**
Susceptibility to bacteria									
F113	J2	100	100	100	100	100	100	-	-
L228	J2	100	100	100	100	105	105	-	-
S118	J2	100	100	100	100	100	100	-	-
S222	J2	100	100	25	25	100	100	-	-
L124	J2	100	100	100	100	84	100	-	-
L321	J2	100	100	100	100	105	105	-	-
Susceptibility to metabolites									
F113	Adult	83	83	58	58	-	-	-	-
	J3/J4	100	100	30	30	-	-	-	-
	J1/J2	247	247	65	65	75	-	14	-
L228	Adult	132	132	-	-	-	-	-	-
	J3/J4	144	144	74	74	-	-	-	-
	J1/J2	71	71	73	73	75	47	14	-
S118	Adult	83	83	58	58	-	-	-	-
	J3/J4	144	144	100	100	-	-	-	-
	J1/J2	247	247	100	100	75	75	14	-
S222	Adult	132	132	25	25	-	-	-	-
	J3/J4	116	116	100	19	-	-	-	-
	J1/J2	247	247	100	100	75	47	14	-
L124	Adult	83	83	22	22	-	-	-	-
	J3/J4	144	144	74	74	-	-	-	-
	J1/J2	247	247	73	73	75	47	14	-
L321	Adult	-	132	58	58	-	-	-	-
	J3/J4	87	87	13	13	-	-	-	-
	J1/J2	71	71	65	65	75	-	14	-
Sensitivity to 2,4-DAPG[d]									
	J2	100	100	-	-	75	-	14	-
Nematode species egg hatch									
		-	**-**	**-**	**-**	**5d**[d]	**-**	**7d**	**-**
F113	J2	-	-	-	-	95	-	80	-
L228	J2	-	-	-	-	95	-	80	-
S118	J2	-	-	-	-	95	-	80	-
S222	J2	-	-	-	-	95	-	80	-
L124	J2	-	-	-	-	95	-	80	-
L321	J2	-	-	-	-	95	-	80	-
F113 + L321	J2	-	-	-	-	95	-	80	-
F113 + L124	J2	-	-	-	-	95	-	80	-
L321 + L124	J2	-	-	-	-	95	-	80	-
DAPG 10ppm	J2	-	-	-	-	95	-	80	-
DAPG 100ppm	J2	-	-	-	-	95	-	80	-

[a] Strain = Beneficial bacterial strain or metabolites.
[b] Life stage = Nematode life stage
[c] CE = *C. elegans*, PP = *P. pacificus*, MJ = *M. javanica* and GP = *G. pallida*.
[d] DAPG = 2,4- diacetylphloroglucanol.
[e] Susceptibility tests were conducted over 24 and 48 hours. Egg hatch test was assessed after 5 or 7 days.
- = No test performed on this species

on a spectrophotometer [Shimadzu] between the range 220 - 400 nm at an absorbance of 0 - 0.5 (AU). This was carried out to determine the suitability of the compound as a standard, but also to ensure the compound had not degraded or deteriorated in storage.

2.2.6.2 Metabolite Sample Preparation

Pseudomonas fluorescens strains F113, L321, L228, L124, S118 and *P. agglomerans* S222 were cultured in 20 ml LB broth and incubated at 30°C in a shaker incubator for 24, 48 hours and five days. Sterile LB broth samples, incubated parallel to the bacterial cultures, were utilised as the negative control. There were three replications of each bacterial treatment and negative control at each incubation time. Broth (LB) spiked with 10 and 100 ppm 2,4-DAPG were utilised as positive controls. After the incubation period, an $OD_{(600)}$ reading was taken of the bacterial samples. The broths were centrifuged at 3800 rpm for 15 minutes to pellet the bacteria and filtered with Whatman No. 4 filter paper. The samples were acidified to pH < 2.0 with 3M HCl and stored at -20°C (Brucker *et al.*, 2008) until required for chemical analysis.

A liquid solvent extraction was carried out using ethyl acetate (EtOAc) to extract the organic compounds. Supernatants from the three replicates of broth cultures were pooled, and 60 ml were poured into a 250 ml separatory funnel. The aqueous layer was extracted four times with 30 ml and 20 ml EtOAc respectively, and twice with 10 ml EtOAc to remove any remaining broth. The solution was left to separate in-between each extraction for six to ten minutes until a clear separation of liquids was evident. The organic phase was collected in a 250 ml beaker, 3 g Na_2SO_4 were added to the samples to remove any water, and the samples were filtered with Whatman No. 4 filter paper. The EtOAc was evaporated using a rotary evaporator (Rotavapor R-300 with a vacuum pump V-300 and heating bath B-300base, Buchi, Switzerland), set at 176 mbar, 14 rpm at 50°C. 15 ml of the final metabolite sample was made up to 5 ml in a volumetric flask with HPLC grade methanol (Brucker *et al.*, 2008). The samples were prepared for GC-MS analysis by syringe filtering through 0.45 μm PTFE filters. The extract, 800 μl in total was added to a 1 ml glass vial with a split septum. The samples were run immediately on the GC-MS instrument.

2.2.6.3 Gas Chromatography Mass Spectrometer Specifications

Gas chromatography-mass spectrometer analysis was carried out on a Varian 450 GC/ 220 MS ion trap system, which was coupled with a CTC Analytics CombiPAL autosampler, using a modified method by Anantha Padmanabhan *et al.* (2016). A 1µl organic extract sample was injected into the instrument using the autosampler. Helium gas (99%) was utilised as a carrier gas at a constant flow rate of 1 ml/ minute. The injector temperature was maintained at 250°C, placed in splitless mode for 45 seconds, followed by a split ratio of 10: 1. The oven

temperature was held at 110°C for two minutes followed by a temperature ramp to 200°C at 10°C/ minute, with a final temperature increase of 5°C/ minute up to 280°C, which was held for ten minutes. The ion trap temperature was held at 200°C. The GC-resolved components were subjected to 70eV ionisation prior to entering the mass detector. Full scan profiles were generated using the full scan mode 40-650 *m/z* range. The overall GC-MS running time was 36 minutes.

2.2.6.4 Chromatogram Analysis and Compound Identification

Chromatograms were processed by AMDIS (Automated Mass Spectral Deconvolution and Identification) version 2.69 software. A simple analysis was utilised on AMDIS deconvolution settings, for the identification of chromatogram components using standard settings. A minimum match factor (MF) of 60 was set for component identification, with a 32 component width and an adjacent peak subtraction of 2. The medium option was selected for resolution, sensitivity and shape requirements in the deconvolution settings.

The mass spectra of the identified components were compared to the NIST 08 (National Institute of Standards and Technology) version 2.0 software. The software contains 3 electron ionisation (EI) libraries with a combination of 220,460 mass spectra of 192,108 different chemical compounds, which were utilised for resolved component identification (Stein, 2008). The component match factor is referred to as an excellent match if it was 900 or greater, a good match if it ranged between 900-800, a fair match if it ranged between 700-800, and less than 600 was a poor match (Scott, 1990). An average of the forward and reverse match factors was utilised.

The percentage peak area of identified compounds was determined with the use of OpenChrom® (Community Edition version 1.1.0 Deils). The peak of interest on the chromatogram was initially detected by the software with the Manual Peak Detector function, and the Peak Integrator function was utilised to determine the area of the peak. The total integration value was determined by the Sumarea Chromatogram Integrator function, to determine the area of the whole chromatogram.

Percentage peak area was determined by:

$$\% \text{ Peak Area} = 100 \times \frac{\text{Peak Area}}{\text{Sumarea of Chromatogram}}$$

2.2.7 Statistical Analysis

2.2.7.1 Non-Parametric Assessment of Susceptibility Assays

The data from $OD_{(600)}$ 0.8 - 0.6, $OD_{(600)}$ 0.5 - 0.4 and $OD_{(600)}$ 0.3 - 0.1 were combined to form the high, medium and low concentrations of bacteria/ metabolites (Table 2.5). The data was statistically assessed using the non-parametric Kruskal-Wallis H test with Bonferroni pairwise correction. (A) Susceptibility of nematodes to the various bacterial concentrations was determined by comparing percent nematode mortality to the control treatment at each test time. (B) Susceptibility of nematode life stages to various bacterial metabolite concentrations was assessed by comparing percentage mortality of nematode life stages to the control treatment at each test time. (C) The sensitivity of the nematodes to 2,4-DAPG was assessed by comparing percent mortality at the various 2,4-DAPG concentrations to the control treatment after 24 hours. The parallel methanol controls were also statistically assessed by comparing the percent nematode mortality at each methanol concentration to the control treatment after 24 hours. (D) The effects of bacterial metabolites on egg hatch were determined by comparing the percentage of eggs that hatched in bacterial metabolites to the percentage of eggs that hatched in the control treatment after five (*M. javanica*) and seven days (*G. pallida*). Juvenile mortality (%) was assessed by comparing hatched nematodes in bacterial metabolites to the control treatment.

2.2.7.2 Principal Component Analysis of PGP Bacterial Chromatograms

A principal component analysis was performed on AMDIS deconvoluted chromatograms using OpenChrom® (Wenig and Odermatt, 2010) open source software (Community Edition version 1.1.0 Deils). Chromatogram peaks with a retention time of 5 to 16 minutes (approximately the first 1050 scans of each chromatogram, with a retention time window of 200 milliseconds) were utilised for analysis. It is within this time frame that all compounds of interest were retained on the column. This was to reduce the number of descriptors in the files to be analysed, as some contained over 434 peak areas, and to maximise the variance between samples. A bi-plot was generated to display the observations and variables of the multivariate data. It represented the two most significant components of variance produced by the software.

2.3 Results

2.3.1 Plant Growth Promoting Bacterial Strains: Biochemical Tests, Standard Curves and Colony Morphology

Biochemical tests carried out on the strains showed the bacteria were all gram negative, oxidase positive except for S222 and all catalase positive. To display standard curves, the CFU/ml was calculated at each OD dilution and the results were plotted for *P. fluorescens* bacterial strains F113, L228, S118, L124, S110, L111 and L321, and *P. agglomerans* S222 (Appendix A, Section A.1). Bacterial colony morphology was determined, all strains had a mucoidal consistency except S222. The strains L228, L124, L321, L111 and S110 all displayed cream colonies, with F113 exhibiting cream colonies initially which then developed light brown pigments after 5-7 days. The colony surface of L228, S222, L124 and S110 was dull and for F113, S118, L321 and L111 the surface was shiny. Colony elevation was convex in all strains except in L228 which was irregular and spreading. The odour produced by the strains was high for F113, L228 and L124, medium for S118, L321, L111 and S110 and slight for S222. The cells of all bacterial strains were rod-shaped.

2.3.2 Susceptibility Testing of Nematodes to PGP Bacteria and their Metabolites

2.3.2.1 Susceptibility of *Caenorhabditis elegans* to PGP Bacteria

Susceptibility of *C. elegans* (Figure 2.2) to all bacterial strains were statistically significant (Appendix A, Table A.1) compared to the controls, at high and medium bacterial concentrations over 24 and 48 hours exposure. There was a statistical difference between the value assigned to the percentage nematode mortality at low concentration for all bacterial treatments compared to the control, except in those treated with L321 (after 48h) and S222 (after 24 and 48h). A 100% *C. elegans* mortality was recorded in all bacterial treatments at high and medium concentrations after both exposure times. At the low bacterial concentration, there was 100% mortality in all bacterial treatments except for L321 and S222. There was 86% mortality after 24 a hours after exposure to L321, and there was 69% and 62% mortality after 24 and 48 hours exposure to S222 respectively.

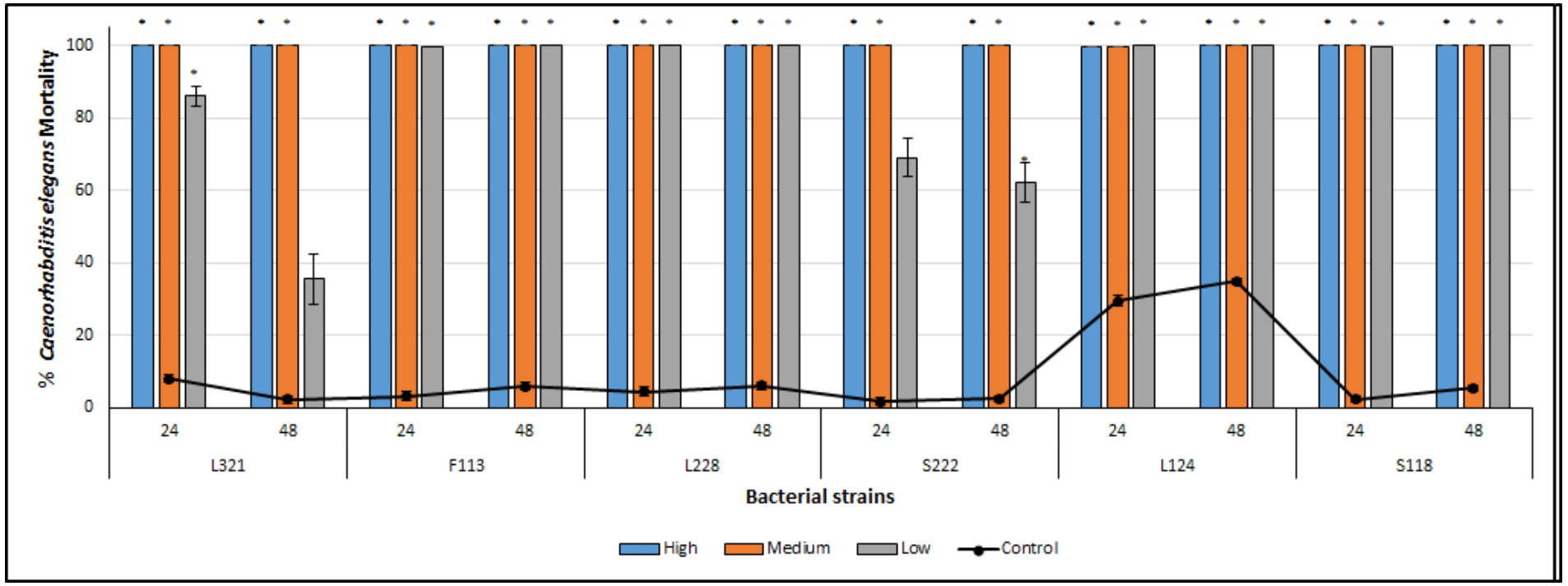

FIGURE 2.2: Mean percentage mortality of *C. elegans* after exposure to PGP bacterial strains at high, medium and low bacterial concentrations (Table 2.5) for 24 and 48 hours. The error bars represent $\pm$ SEM. The presence of asterisks (*) indicates significant differences between PGP bacterial concentrations and the control. The statistical significant differences are represented in Appendix A, Table A.1. Statistical significance $\alpha = 0.05$ level.

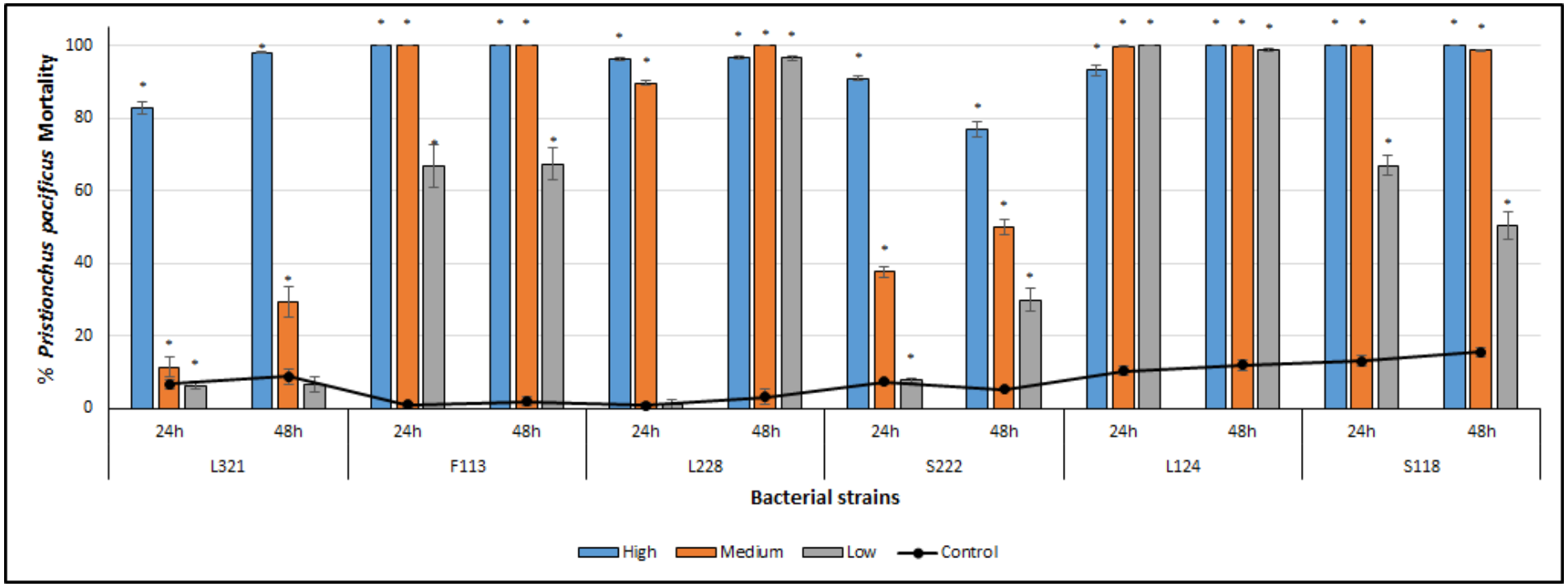

FIGURE 2.3: Mean percentage mortality of *P. pacificus* after exposure to PGP bacterial strains at high, medium and low bacterial concentrations (Table 2.5) for 24 and 48 hours. The error bars represent $\pm$ SEM. The presence of asterisks (*) indicates significant differences between PGP bacterial concentrations and the control. The significant differences are represented in Appendix A, Table A.1. Statistical significance $\alpha = 0.05$ level.

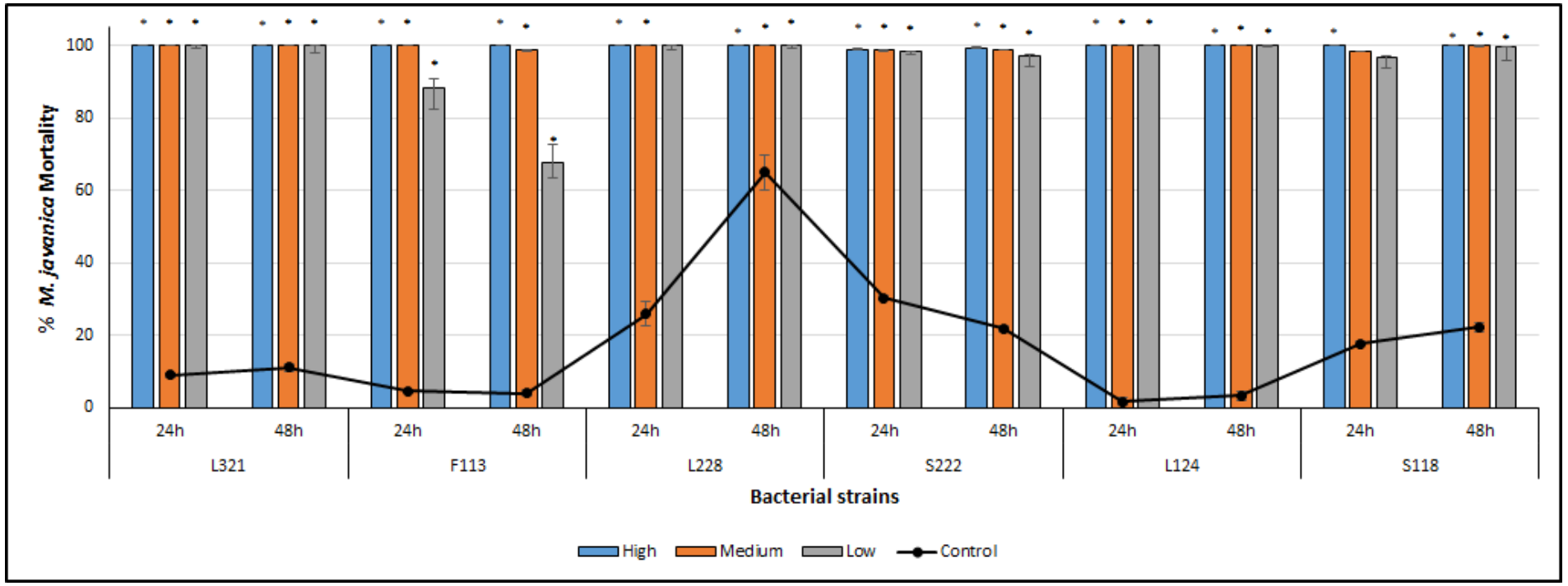

FIGURE 2.4: Mean percentage mortality of *M. javanica* after exposure to PGP bacterial strains at high, medium and low bacterial concentrations (Table 2.5) for 24 and 48 hours. The error bars represent $\pm$ SEM. The presence of asterisks (*) indicates significant differences between PGP bacterial concentrations and the control. The significant differences are represented in Appendix A, Table A.1. Statistical significance $\alpha = 0.05$ level.

2.3.2.2 Susceptibility of *Pristionchus pacificus* to PGP Bacteria

Pristionchus pacificus percentage mortality results at high and medium and low bacterial concentrations over 24 and 48 hours exposure (Figure 2.3) were predominantly statistically significant (Appendix A, Table A.1) when compared to the controls. There was 100% *P. pacificus* mortality on exposure to the bacterial treatments F113, L228, L124 and S118 at various concentrations and exposure times. L321 induced 83% mortality at high, concentration after 24 hours. F113 caused 67% mortality at low concentration after 24 and 48 hours exposure. L228 caused 96% and 90% mortality at high and medium concentrations after 24h and 97% at low concentration after 48h respectively. Bacterial strain S222 induced 23%, and 19% mortality at high concentration after 24 and 48 hours respectively. L124 caused 93% mortality at high concentration after 24h and S118 induced 67% and 50% mortality at low concentration after 24 and 48 hours respectively.

2.3.2.3 Susceptibility of *Meloidogyne javanica* to PGP Bacteria

Mortality of *M. javanica* (Figure 2.4) on exposure to all bacterial treatments were statistically significantly different to that recorded in the control treatment (Appendix A, Table A.1). Bacterial strains L321, L228 and L124 at high, medium and low concentrations caused 100% mortality after both exposure times. Nematodes exposed to S222 induced 100% mortality after 24 hours of exposure. Bacterial strain F113 caused 88% mortality at low concentration after 24 hours, 99% and 68% mortality at medium and low concentrations after 48 hours respectively. The strain S222 caused 99% mortality at high and medium concentration and 97% mortality at low concentration after 24 and 48 hours respectively. Bacterial strain S118 induced 98% and 96% mortality after 24h at medium and low concentrations respectively.

2.3.2.4 Susceptibility of *Caenorhabditis elegans* and *Pristionchus pacificus* to F113 Bacterial Metabolites

Susceptibility of all life stages of *C. elegans* to F113 metabolites (Figure 2.5a) at high, medium and low (low concentration tested with J3/J4 only) concentrations caused 100% mortality after 24 and 48 hours exposure, and were significantly different (Appendix A, Table A.2) to the control treatment. The PGP bacterial metabolites caused 59% mortality at the low concentration after 24 hours of exposure to the adult life stage. After 48 hours of exposure, the metabolites caused 82% and 81% mortality at high and medium concentrations respectively, at the same life stage. The bacterial metabolites induced 49% and 63% mortality to the J1/J2 life stage at low concentration after 24 and 48 hours respectively.

Mortality of all life stages of *P. pacificus* to F113 metabolites (Figure 2.7a) were statistically different to the control treatment at all metabolite concentrations (Appendix A, Table A.2),

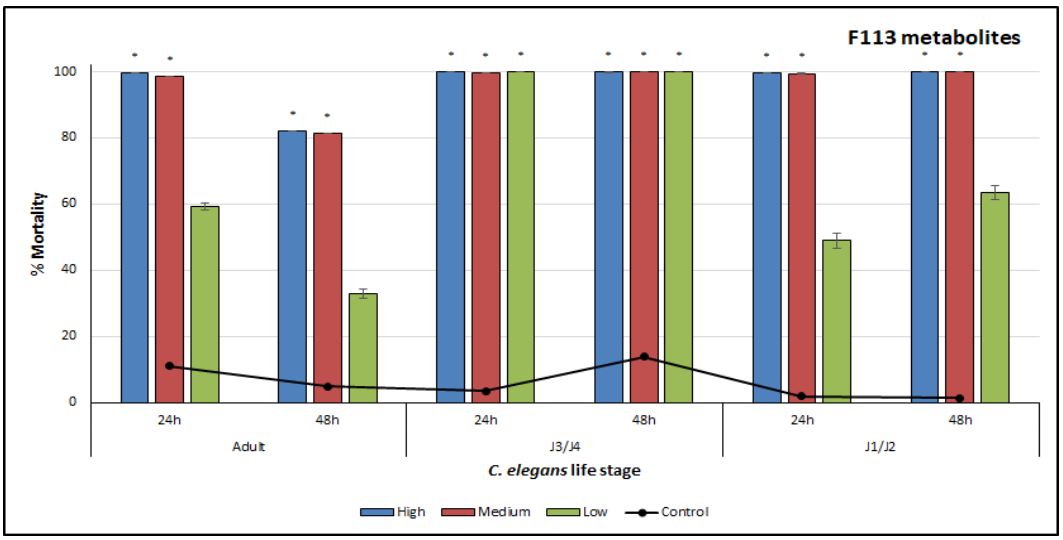

(A)

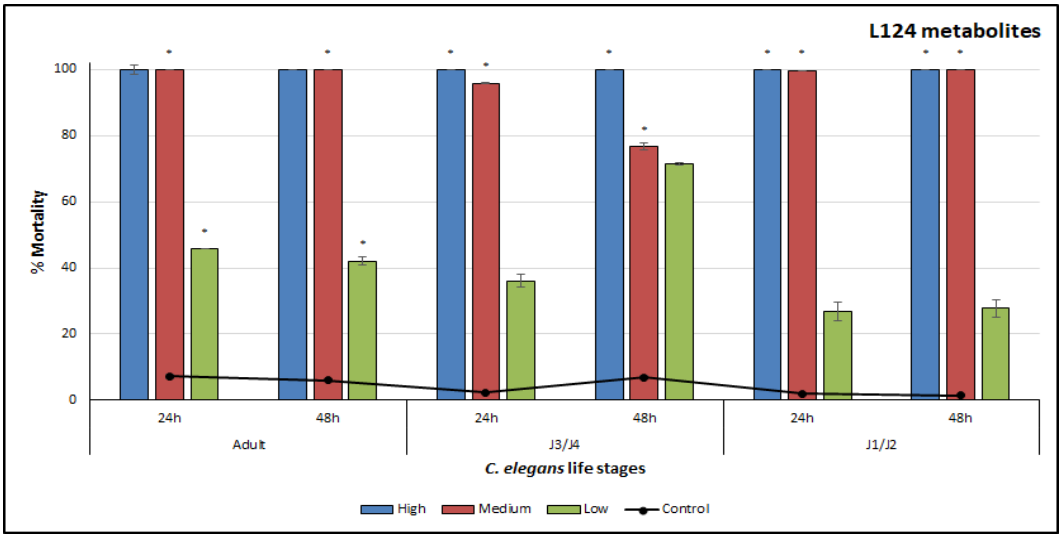

(B)

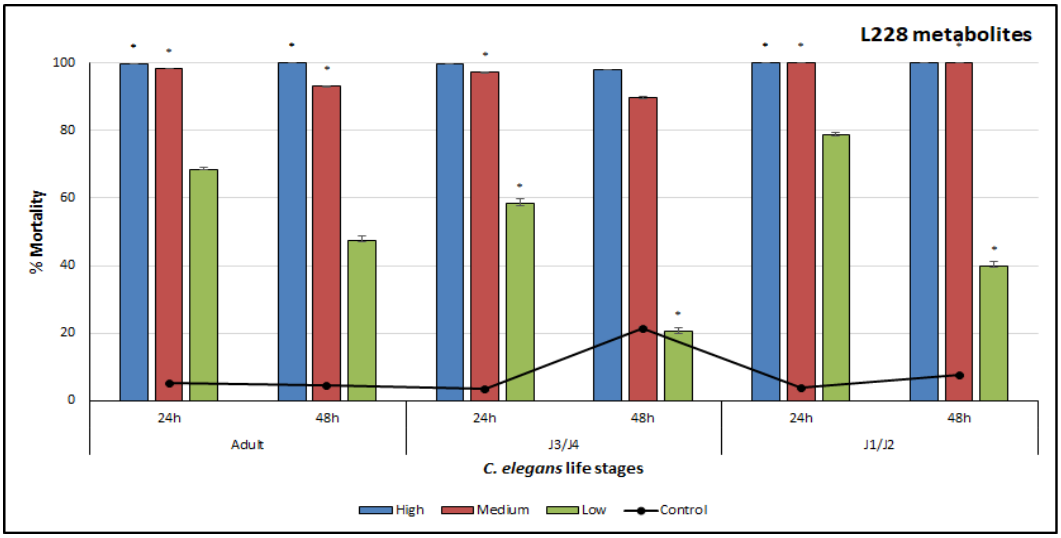

(C)

FIGURE 2.5: Mean percentage mortality of *C. elegans* after exposure to F113, L124 and L228 metabolites at high, medium and low concentrations (Table 2.5) after 24 and 48 hours. The error bars represent ± SEM. The presence of asterisks (*) indicates significant differences between metabolite concentrations and the control. Statistical significance $\alpha = 0.05$ level (Appendix A, Table A.2).

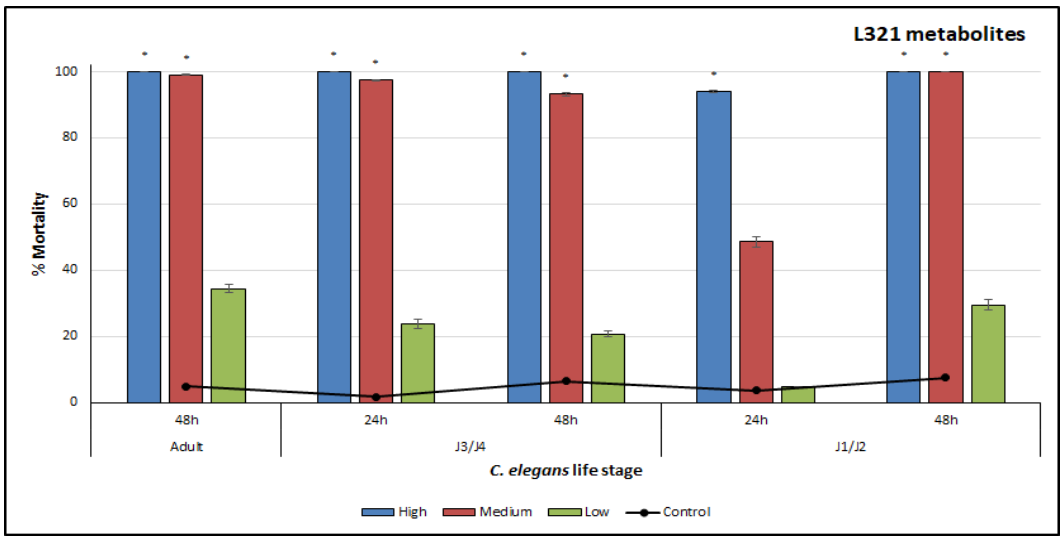

(A)

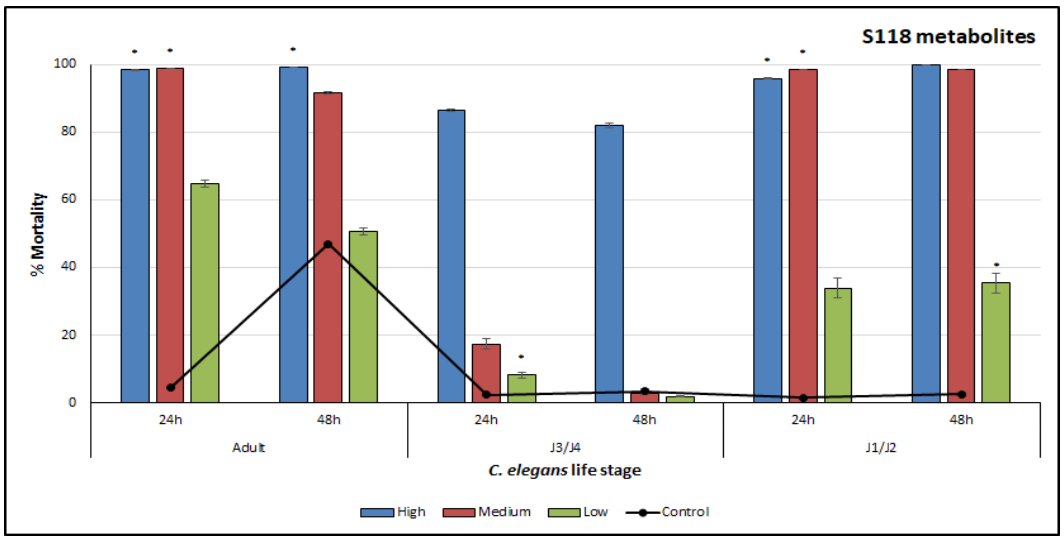

(B)

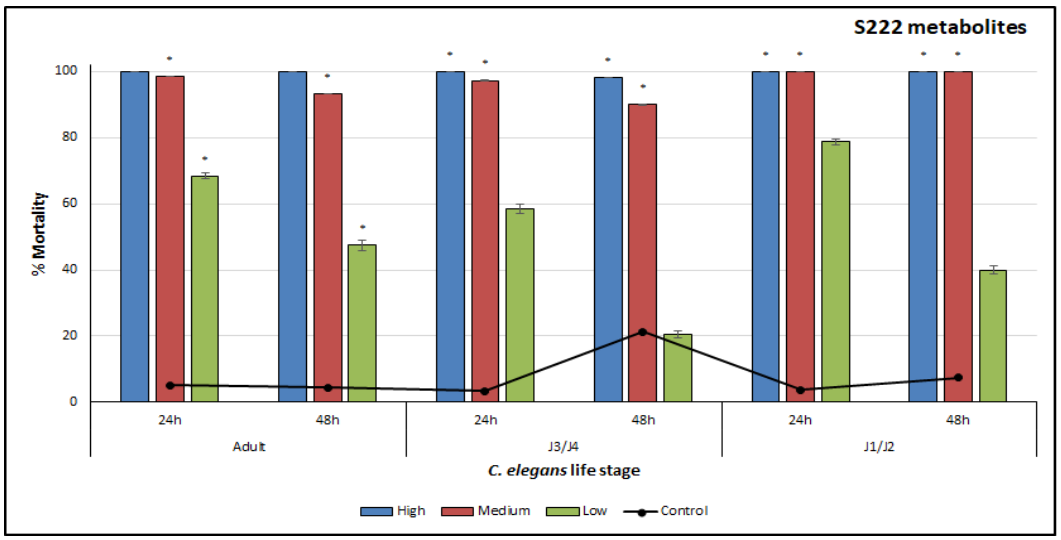

(C)

FIGURE 2.6: Mean percentage mortality of *C. elegans* after exposure to L321, S118 and S222 metabolites at high, medium and low concentrations (Table 2.5) after 24 and 48 hours. The error bars represent $\pm$ SEM. The presence of asterisks (*) indicates significant differences between metabolite concentrations and the control. Statistical significance $\alpha = 0.05$ level (Appendix A, Table A.2).

except for adults exposed to the low concentration after 24 hours, and J1/ J2 exposed to the high concentration after 48 hours. All nematodes exposed to the high metabolite concentration caused 100% mortality, except for the J3/J4 life stage which caused 99% mortality after 48 hours. At the medium metabolite concentration, all the nematode life stages displayed 100% mortality, except for J3/J4, which induced 99% mortality after 24 hours. Low concentration of metabolites also caused 100% mortality after 24 and 48 hours exposure respectively, except for 96% adult mortality after 48 hours and 93% J1/J2 mortality after 48 hours.

2.3.2.5 Susceptibility of *Caenorhabditis elegans* and *Pristionchus pacificus* to L124 Bacterial Metabolites

Mortality of *C. elegans* subjected to L124 bacterial metabolites (Table 2.5b) were significantly different for all metabolite concentrations at most life stages (Appendix A, Table A.2). A 100% nematode mortality occurred at all life stages when exposed to high and medium concentrations of metabolites, except for J3/J4 (J3/J4 were exposed to medium concentration only) after 24 and 48 hours exposure. Adults at low concentrations caused 46% and 42% mortality after 24 and 48 hours respectively. J3/J4 life stage induced 96% mortality after 24 hours, and 77% mortality after 48h at a medium concentration of metabolites.

Pristionchus pacificus mortality on L124 metabolite exposure (Figure 2.7b) were predominantly significantly different to the control at most life stages (Appendix A, Table A.2) after both exposure times. There was 99% adult mortality after 24 hours and 100% after 48 hours exposure to all metabolite concentrations. The J3/J4 life stage exposed to high metabolite concentration caused 100% and 76% mortality and J1/J2 induced 100% and 98% after 24 and 48 hours respectively. The J3/J4 life stage exposed to medium metabolite concentration caused 82% and 58% mortality, and J1/J2 caused 86% and 87% after 24 and 48 hours respectively.

2.3.2.6 Susceptibility of *Caenorhabditis elegans* and *Pristionchus pacificus* to L228 Bacterial Metabolites

Caenorhabditis elegans mortality caused by the bacterial metabolites of L228 (Figure 2.5c) were significantly different to the controls at all life stages (Appendix A, Table A.2). Exposure to the strain caused 98% and 93% adult mortality at medium concentration and 68% and 47% adult mortality at low concentration after 24 and 48 hours exposure respectively. It caused 97% J3/J4 mortality at medium concentration, 58% J3/J4 mortality at low concentration after 24h and 98% and 90% J3/J4 mortality at high and, medium concentrations after 48 hours respectively. It was also responsible for 79% J1/J2 mortality low concentration after 24 hours.

Pristionchus pacificus mortality on exposure to L228 metabolites (Figure 2.7c) were significantly different compared to the control at most life stages (Appendix A, Table A.2). Exposure to the strain caused 74% and 90% J3/J4 mortality at high, 74% and 68% J3/J4 mortality at medium and 43% J3/J4 mortality at low metabolite concentration after 24 and 48 hours respectively. J1/J2 mortality was 100% and 96% at high, metabolite concentration after 24 and 48 hours respectively.

2.3.2.7 Susceptibility of *Caenorhabditis elegans* and *Pristionchus pacificus* to L321 Bacterial Metabolites

Mortality of *C. elegans* exposed to L321 metabolites (Figure 2.6a) was statistically significant for all life stages (Appendix A, Table A.2) at high and medium concentrations over 24 and 48 hours exposure compared to the controls, except for J1/J2 on exposure to medium concentration at 24 hours. A 100% mortality was observed at all life stages on exposure to high concentration of metabolites occurred, except for the J1/J2 life stage, which caused 94% mortality after 24 hours. Exposure of medium metabolite concentration to the adult nematodes caused 99% mortality after 48 hours, J3/J4 caused 97% and 93% mortality, and J1/J2 caused 49% and 100% mortality after 24 and 48 hours respectively.

Pristionchus pacificus mortality to L321 metabolites (Figure 2.8a) were statistically different to the control treatment at most life stages (Appendix A, Table A.2) after both exposure times. A 100% adult mortality in all concentrations after 24 hours occurred. However, after 48 hours it reduced to 77%, 48% and 30% mortality at high medium and low concentrations respectively. Mortality in J3/J4 life stage nematodes after 24 hours was 100%, 99% and 93% and after 48 hours and was 82%, 63% and 69% at high medium and low concentrations respectively. Mortality of J1/J2 life stage after 24 hours was 100%, at high concentrations.

2.3.2.8 Susceptibility of *Caenorhabditis elegans* and *Pristionchus pacificus* to S118 Bacterial Metabolites

Caenorhabditis elegans mortality on exposure to S118 metabolites (Figure 2.6b) were statistically significantly different for most life stages (Appendix A, Table A.2) when compared to the control treatment. Adult mortality on exposure to high concentrations of metabolites caused 98% and 99% mortality, J3/J4 caused 86% and 81% mortality, and J1/J2 caused 95% and 100% mortality after 24 and 48 hours respectively. Adults exposed to medium concentrations of metabolites induced 99% and 92% mortality and J1/J2 caused 98% and 98% mortality after 24 and 48 hours respectively. Adults exposed to low concentrations of metabolites caused 65% and 51% mortality after 24 and 48 hours respectively.

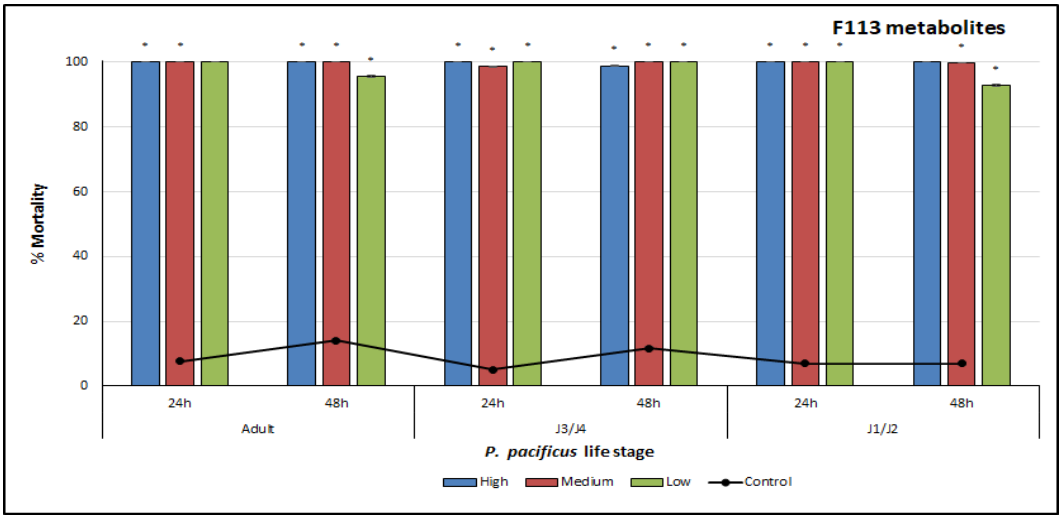

(A)

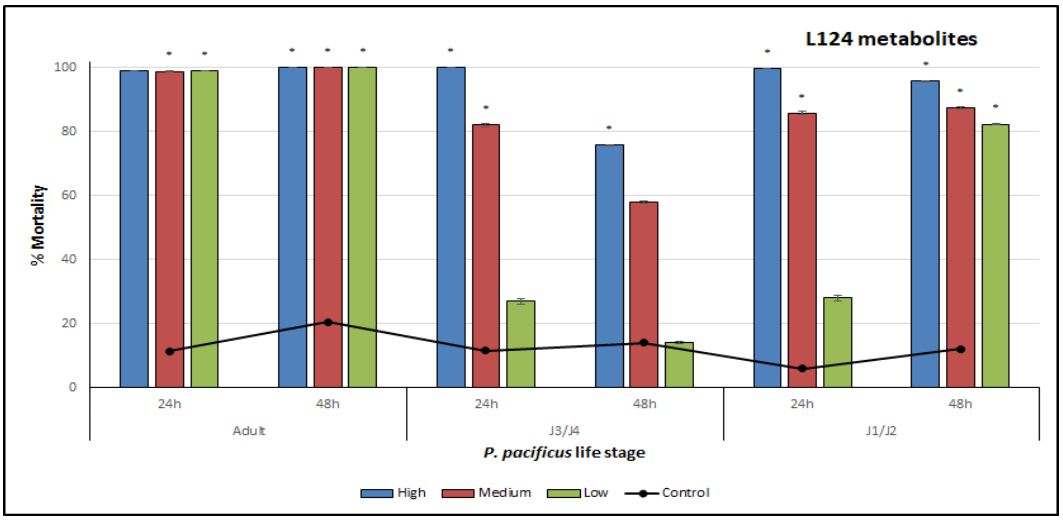

(B)

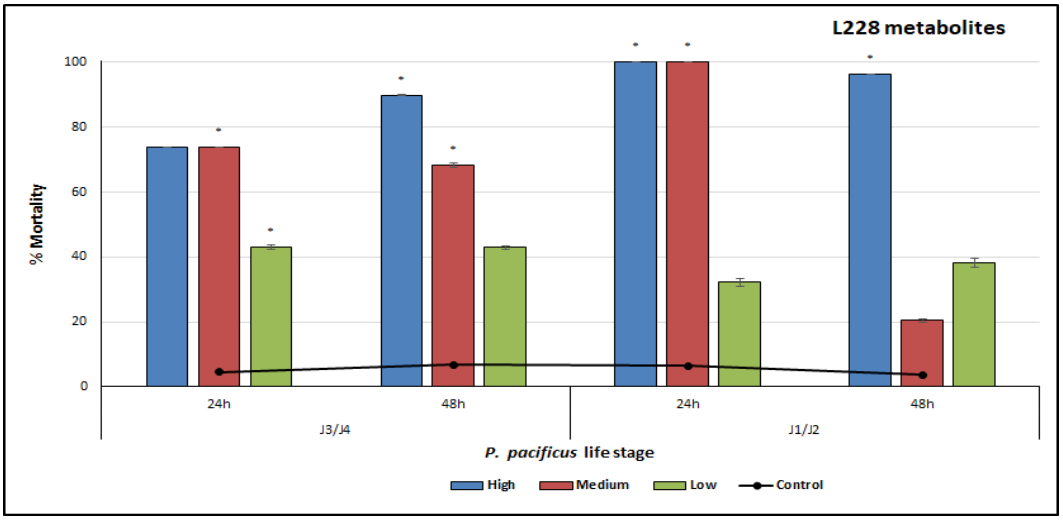

(C)

FIGURE 2.7: Mean percentage mortality of *P. pacificus* after exposure to bacterial metabolites at high, medium and low concentrations after 24 and 48 hours. The error bars represent ± SEM. The presence of asterisks (*) indicate significant differences between metabolite concentrations and the control. Statistical significance $\alpha = 0.05$ level.

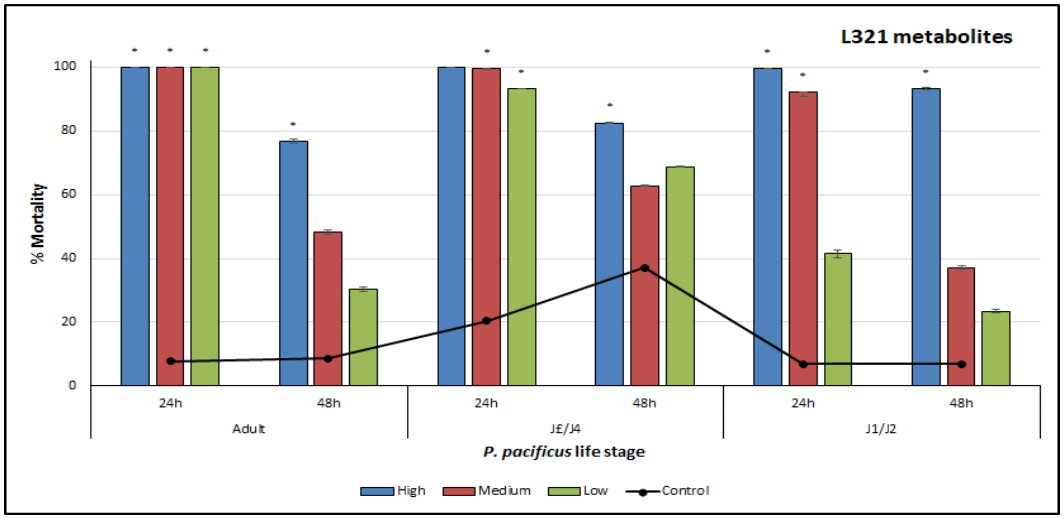

(A)

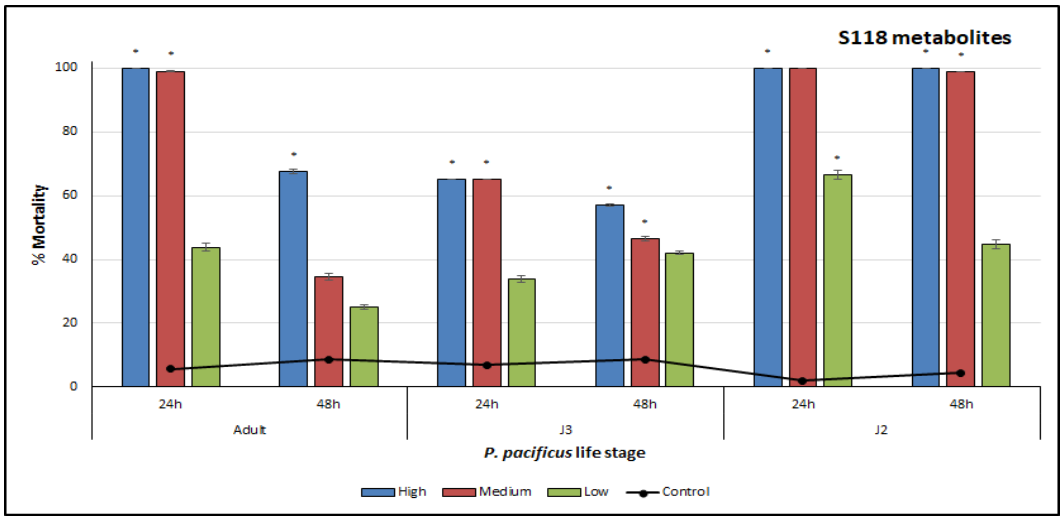

(B)

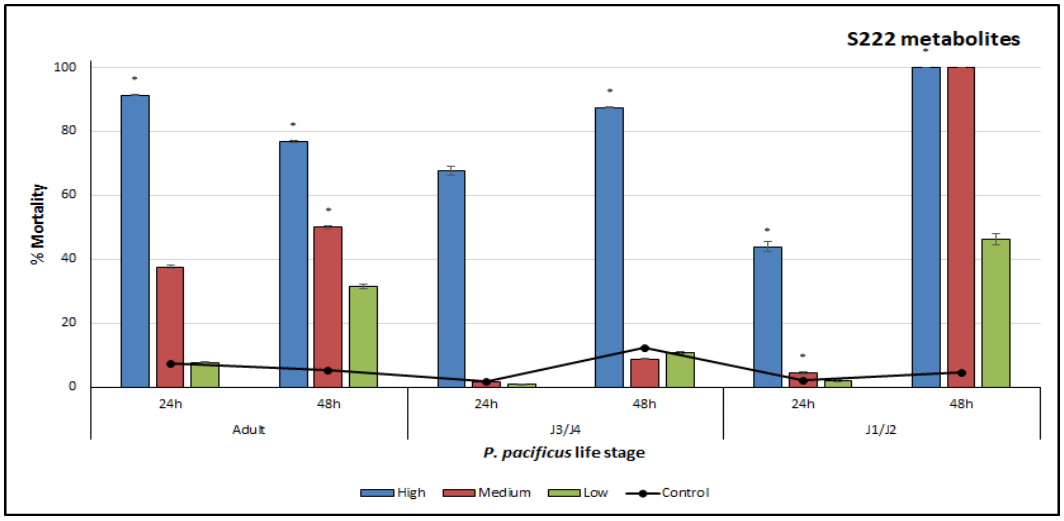

(C)

FIGURE 2.8: Mean percentage mortality of *P. pacificus* after exposure to bacterial metabolites at high, medium and low concentrations after 24 and 48 hours. The error bars represent ± SEM. The presence of asterisks (*) indicates significant differences between metabolite concentrations and the control. Statistical significance $\alpha = 0.05$ level.

Pristionchus pacificus mortality caused by bacterial metabolites of S118 (Figure 2.8b) performed significantly differently from the controls in most life stages (Appendix A, Table A.2). Mortality of the adult life stage after 24 hours exposure was 100% and 99%, and after 48 hours was 68% and 34% at high and medium concentrations respectively. Mortality effect on J3/J4 life stage after 24 hours was 65% and 65%, and after 48 hours was 57% and 46% at high and medium concentrations respectively. The effect of the metabolites on the J1/J2 life stage after 24 hours was 100%, 100% and 67% and after 48 hours was 100%, 98% and 45% at high, medium and low concentrations respectively.

2.3.2.9 Susceptibility of *Caenorhabditis elegans* and *Pristionchus pacificus* to S222 Bacterial Metabolites

Mortality of *C. elegans* to S222 metabolites (Figure 2.6c) were significantly different in most life stages (Appendix A, Table A.2) at both exposure times. A 100% mortality occurred at high metabolite concentration for all life stages, except for J3/J4 life stage with 98% mortality after 48 hours. Exposure to the metabolites at medium concentration caused 98% and 93% adult mortality, 97% and 90% J3/J4 mortality and 100% J1/J2 mortality over 24 and 48 hours exposure. Adult nematode exposure at low metabolite concentration caused 68% and 47% mortality. Low metabolite concentration was also responsible for 58% and 21% J3/J4 mortality and 79% and 40% J1/J2 mortality over 24 and 48 hours exposure respectively.

Pristionchus pacificus mortality on exposure to S222 metabolites (Figure 2.8c) was significantly different compared to the control at high concentration for all life stages (Appendix A, Table A.2), except for the J3/J4 stage after 24 hours and J1/J2 after 48 hours. Subjecting the nematodes to this strain caused 91% adult mortality after 24 hours and after 48 hours it caused 77% at the high concentration. Subjecting the J3/J4 life stage nematodes to the metabolites for 24 hours caused 68% mortality and after 48 hours caused 87% mortality at the high metabolite concentration. The effect of this bacterial stain to the J1/J2 life stage caused 44% mortality after 24 hours at high concentration and 100% mortality at high concentration after 48 hours.

2.3.2.10 Susceptibility of *Meloidogyne javanica* to PGP Bacterial Metabolites

Mortality of *M. javanica* (Figure 2.9a) due to expose to the metabolites of F113, L124, L228, L321, S118 and S222 were significantly different (Appendix A, Table A.2) to that in the controls for most of the concentrations. *Meloidogyne javanica* mortality on exposure to F113 metabolites after 24 hours caused 100%, 100% and 98% mortality, to S118 after 24 hours induced 97%, 95% and 95% mortality and after 48 hours caused 94%, 92% and 87% mortality at high medium and low concentrations respectively. Nematode mortality to S222 metabolites after 24 hours caused 90%, 86% and 92% mortality and after 48 hours

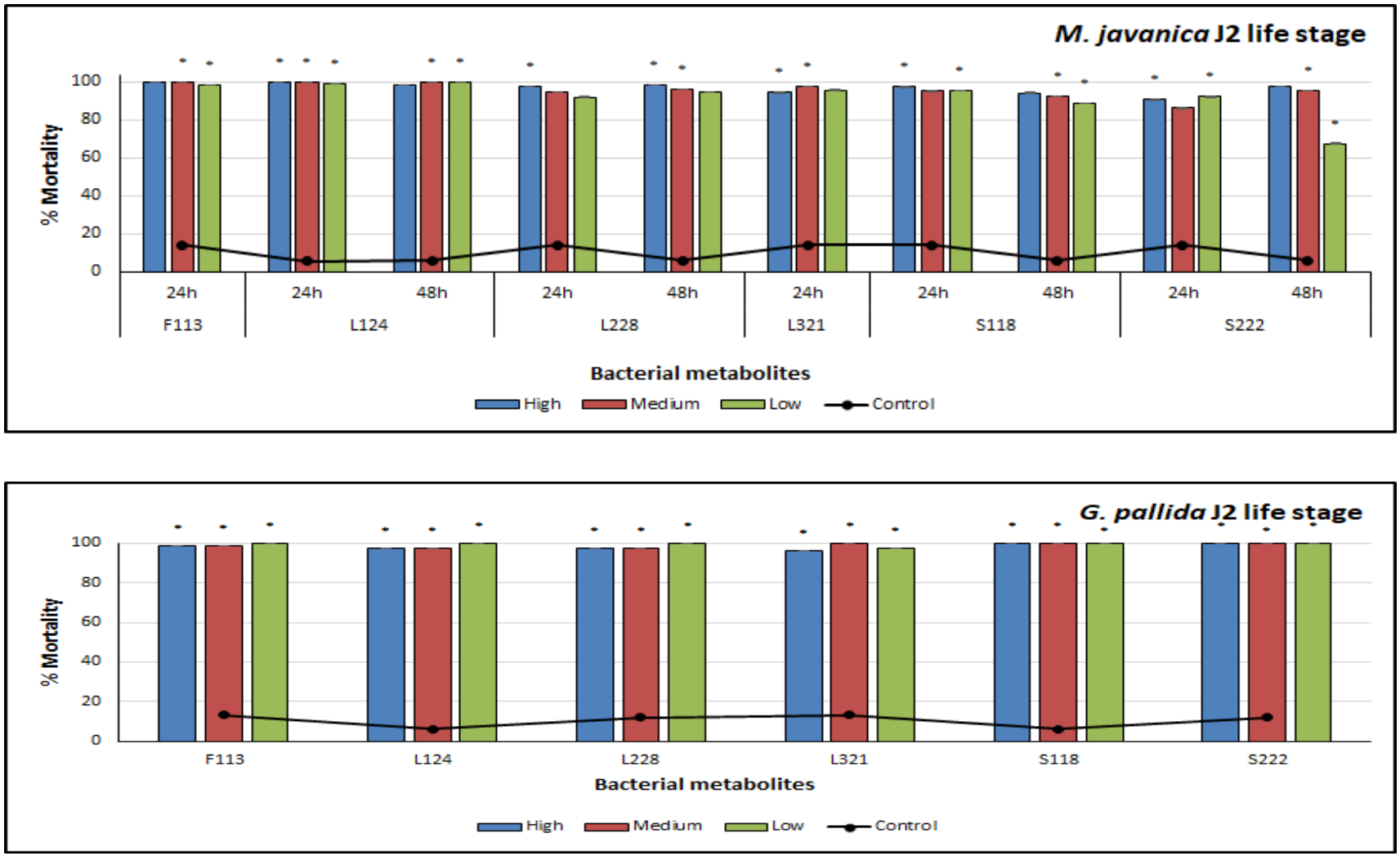

FIGURE 2.9: Mean percentage mortality of *M. javanica* and *G. pallida* after exposure to PGP bacterial metabolites (Table 2.5) for 24 and 48 hours (*M. javanica* only). The error bars represent ± SEM. The presence of asterisks (*) indicates significant differences between PGP bacterial metabolite concentrations and the control. The significant differences are represented in Appendix A, Table A.2. Statistical significance $\alpha = 0.05$ level.

caused 97%, 95% and 67% mortality at high medium and low concentrations respectively. The effect of L321 metabolites on *M. javanica* after 24 hours caused 94%, 98% and 96% mortality at high medium and low concentrations respectively. Mortality on exposure to L124 metabolites after 24 hours caused 100%, 100% and 99% mortality and after 48 hours caused 98%, 100% and 100% mortality at high medium and low concentrations respectively. Bacterial strain L222 metabolites after 24 hours expose caused 98%, 94% and 92% mortality and after 48 hours was 98%, 96% and 94% mortality at high medium and low concentrations respectively.

2.3.2.11 Susceptibility of *Globodera pallida* to PGP Bacterial Metabolites

Mortality of *G. pallida* due to the metabolites of F113, L124, L228, L321, S118 and S222 were significantly different (Appendix A, Table A.2) to that in the controls for all the concentrations. Mortality of *G. pallida* (Figure 2.9b) on exposure to F113 metabolites caused 99%, 99% and 100% mortality, S118 caused 100%, 100% and 100% mortality and S222 caused 100%, 100% and 100% mortality at high, medium and low metabolite concentrations after 24 hours respectively. Nematode mortality on exposure to L124 metabolites caused 98%, 98% and 100% mortality, L228 caused 98%, 98% and 100% mortality and L321 caused 96%, 100% and 98% mortality at high, medium and low concentrations after 24 hours respectively.

2.3.3 Sensitivity of Nematodes to 2,4-DAPG

Caenorhabditis elegans mortality (Figure 2.10a) was significantly different at 500 ppm, 200 ppm and 100 ppm when compared to the effects of the 0 ppm control (Appendix A, Table A.3). Exposure to 500 ppm 2,4-DAPG caused 100% mortality, closely followed by 97% mortality on exposure to 200 ppm. The effect of 100 ppm 2,4-DAPG caused 19% *C. elegans* mortality and the effect of 75 ppm only caused 6% mortality. The parallel methanol controls caused 2%, 1% and 1% *C. elegans* mortality on exposure to 0.45%, 0.045% and 0.0045% methanol respectively.

Meloidogyne javanica mortality subjected to 2,4-DAPG (Figure 2.10b) was statistically significant to the 0 ppm control at 500 ppm and 200 ppm concentrations (Appendix A, Table A.3). Exposure to 500 ppm and 200 ppm 2,4-DAPG caused 100% mortality. The 100 ppm 2,4-DAPG concentration was responsible for 89% *M. javanica* mortality. Subjecting the nematodes to lower concentrations of 2,4-DAPG caused 87% mortality on exposure to 75ppm, 45% mortality on exposure to 50 ppm and 14% mortality on exposure to 10 ppm 2,4-DAPG.

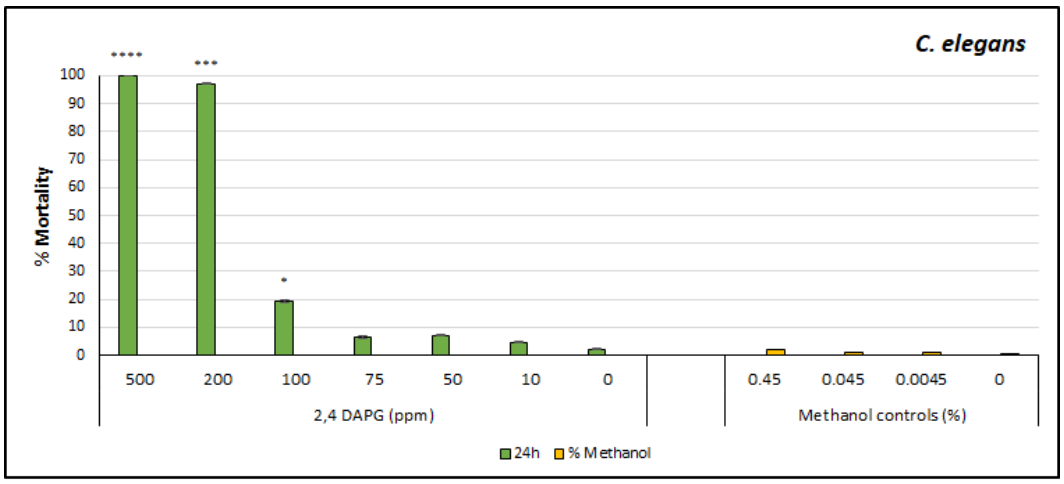

(A)

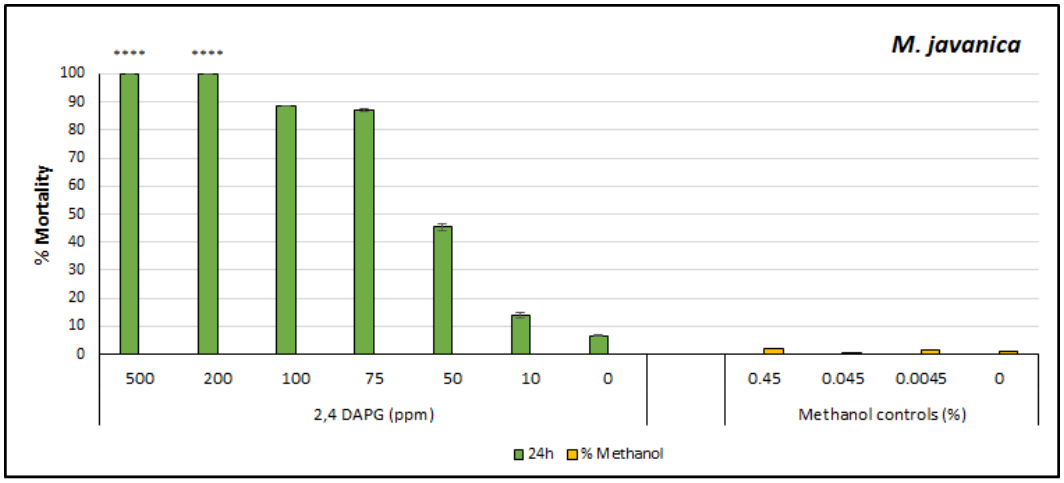

(B)

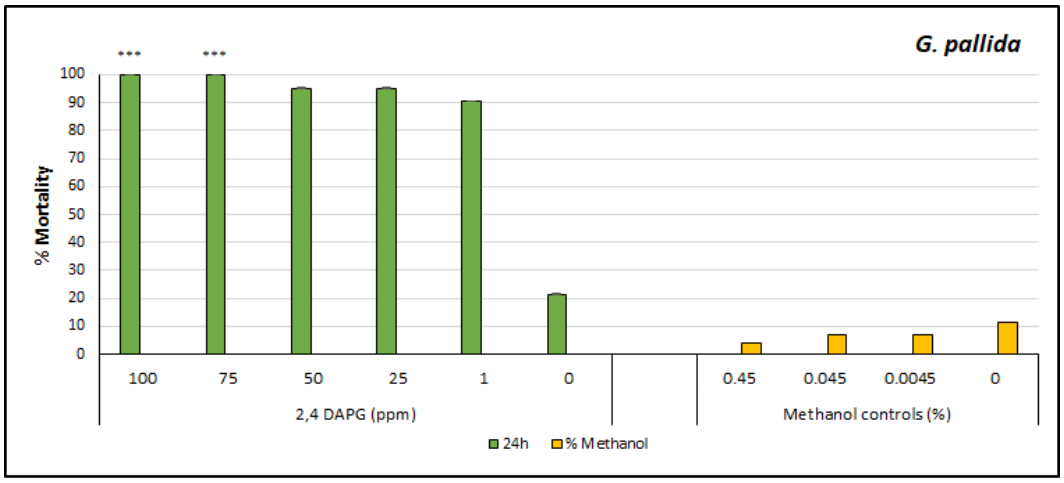

(C)

FIGURE 2.10: Percentage mortality of J2 stage *C. elegans*, *M. javanica* and *G. pallida* after 24 hour exposure to various concentrations of 2,4-DAPG. The error bars represent ± SEM. The presence of asterisks (*) indicates significant differences between 2,4-DAPG treatments and 0 ppm control (green bars). Parallel methanol controls (yellow bars) are presented with equivalent concentrations found in 2,4-DAPG treatments. The p values are represented in Table A.3. Statistical significance $\alpha = 0.05$ level: * $p \leqslant 0.05$, *** $p \leqslant 0.001$ and **** $p \leqslant 0.0001$.

The parallel methanol controls caused 2%, 1% and 1% *M. javanica* mortality on exposure to 0.45%, 0.045% and 0.0045% methanol respectively.

Globodera pallida mortality exposed to 2,4-DAPG (Figure 2.10c) was statistically different to the 0ppm control at 100 ppm and 75 ppm concentrations (Appendix A, Table A.3). *Globodera pallida* mortality on exposure to 100 ppm and 75 ppm 2,4-DAPG caused 100% mortality. Nematode exposure to 50 ppm and 25 ppm were responsible for 95% mortality. Subjecting *G. pallida* to 1 ppm 2,4-DAPG caused 90% mortality. The parallel methanol controls caused 4%, 7% and 7% *G. pallida* mortality to 0.45%, 0.045% and 0.0045% methanol respectively.

2.3.4 Effects of PGP bacterial metabolites on Egg Hatch and Juvenile Mortality

2.3.4.1 Effects of PGP bacterial metabolites on *Meloidogyne javanica* Egg Hatch and Juvenile Mortality

Meloidogyne javanica egg hatch was significantly different to that observed in the control treatments on exposure to all bacterial metabolite treatments, except for bacterial metabolites L111 and L132 (Appendix A, Table A.3). Nematode eggs subjected to L111 metabolites caused 6% egg hatch and *M. javanica* eggs exposed to 100 ppm 2,4-DAPG caused 8% egg hatch (Figure 2.11). The effect of the metabolites of L132, and the metabolite combination F113 + L321 caused 11% egg hatch. Eggs exposed to the metabolite combination of F113 + L124, and to 10 ppm 2,4-DAPG caused 15% egg hatch. Eggs subjected to the bacterial metabolite combination L321 + L124 caused 17% egg hatch. Exposure to the control treatment caused 73% *M. javanica* eggs to hatch.

Meloidogyne javanica juveniles exposed to the various bacterial metabolite treatments caused 100% mortality (Figure 2.11). Except for those exposed to 10 ppm 2,4-DAPG, which was responsible for 95% juvenile mortality. Juveniles subjected to the bacterial metabolites of L124 caused 91% mortality compared to those exposed to the control treatment only caused 4%.

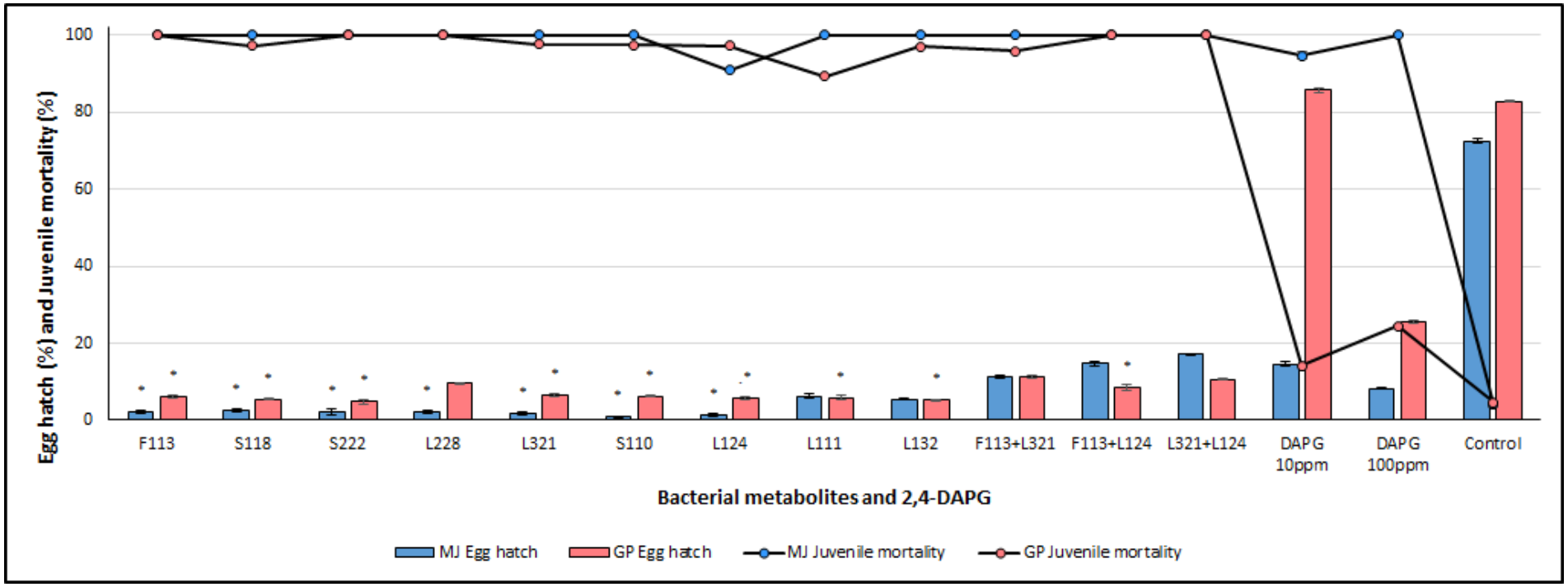

FIGURE 2.11: Percentage of *M. javanica* and *G. pallida* egg hatch and juvenile mortality over various bacterial metabolite treatments and two 2,4-DAPG concentrations. The error bars represent ± SEM. The presence of asterisks (*) indicates significant differences between bacterial metabolites treatments or 2,4-DAPG concentrations and the control. The p values are represented in Table A.3. Statistical significance $\alpha = 0.05$ level.

2.3.4.2 Effects of PGP bacterial metabolites on *Globodera pallida* Egg Hatch and Juvenile Mortality

Globodera pallida egg hatch was significantly different to that observed in the control treatment on exposure to all combinations of bacterial metabolites (Appendix A, Table A.3), except for strain L228. *Globodera pallida* eggs (Figure 2.11) exposed to the bacterial metabolites of S118, S222, and L111 caused 5% egg hatch respectively. Eggs subjected to the metabolites of F113, S110 and L124 caused 6% egg hatch, and exposure to L321 bacterial metabolites caused 7% egg hatch. The effect of the bacterial metabolite combination F113 + L124 and the metabolites of L228 caused 9% and 10% eggs to hatch respectively. *Globodera pallida* eggs exposed to L132 metabolites and to the bacterial metabolite combinations F113 + L321 and L321 + L124 induced 11% eggs to hatch. On exposure to 100 ppm 2,4-DAPG, 25% eggs and at 10 ppm 87% eggs hatched, compared to 83% eggs hatched in the control treatment.

Juvenile mortality of *G. pallida* (Figure 2.11) was significantly different to that observed in the control on exposure to the bacterial metabolites combination L321 + L124 after 7 days. Juveniles subjected to metabolites of S222, L228 and to the metabolite combinations F113 + L124 and L321 + L124 caused 100% juvenile mortality. Exposure to L321 and S110 metabolites caused 98% juvenile mortality, and those subjected to the metabolites of S118, L124 and L111 caused 97% juvenile mortality. The effect of L132 metabolites and bacterial metabolites combination F113 + L321 caused 96% mortality. However, juveniles exposed to 100 ppm and 10 ppm 2,4-DAPG only caused 25% and 5% juvenile mortality respectively, compared to the effect of the control treatment, which caused 5% juvenile mortality.

2.3.5 Identification of PGP Bacterial Metabolites - Analytical Approach

2.3.5.1 2,4-DAPG Standard

The pure synthetic 2,4-DAPG compound was found to have the same peak patterning as Brucker *et al.* (2008), a tall peak (Figure 2.12, point 2) at 270 nm and a smaller shoulder peak (Figure 2.12, point 1) at 330 nm, with a λ_{max} = 268 nm.

To determine the retention time of 2,4-DAPG, initially, a 500 ppm stock solution was prepared in 50% methanol and run on GC-MS using the parameters described in Section 2.2.4. A prominent peak visible in Chromatogram 1 (Figure 2.13), indicated by a black arrow labelled 1A, was generated. The ions 177, 195 and 210 *m/z* associated with the compound 2,4-DAPG, also known as 1,1'-(2,4,6-Trihydroxy-1,3-phenylene) diethanone, as identified

on the NIST library (Figure 2.14a, Images A-C), had a match factor (MF) of 745 and a retention time (RT) of 14.90 minutes.

Following this, sterile LB broth was spiked with 100 ppm and 10 ppm 2,4-DAPG. The samples were prepared as in Section 2.2.4. A large peak was generated in Chromatogram 2 (Figure 2.13), indicated by a black arrow labelled 2A, for 100 ppm spiked broth (MF = 755, RT = 14.85 minutes, Figure 2.14b). A peak was also visible in Chromatogram 3, labelled 3A, that was generated for 10 ppm spiked broth, with an MF of 857 (RT = 14.84 minutes, Figure 2.14c), as identified by NIST. These chromatograms were compared to the broth control to ensure there was no similar peak occurring at that RT.

Pseudomonas fluorescens F113 is a well-known 2,4-DAPG producer (Fenton *et al.*, 1992) and was utilised in this study as a positive control. The strain was assessed to investigate antibiotic production and detection by GC-MS. Figure 2.15 displays the full GC-MS chromatogram (first 20 minutes) of F113 metabolites after 24, 48 hours and 5 days incubation. Also, included are the chromatograms of 10 ppm 2,4-DAPG spiked broth and negative 2,4-DAPG producer, strain L321 after 24 hours incubation. The black arrows on the chromatograms represent 2,4-DAPG retention times for each sample, 14.88 minutes after 24 hours (MF = 878; Chromatogram 1), 14.83 minutes after 48 hours (MF = 857; Chromatogram 2) and 14.85 minutes in the 10 ppm spiked broth control sample (MF = 857; Chromatogram 4) with the ions 177, 195 and 210 *m/z* of interest. There was no 2,4-DAPG peak present in the broth samples after 5 days incubation (Chromatogram 3). The peaks of interest were assessed by the NIST library and identified as 2,4-DAPG (Table 2.8 and Appendix A, Figure A.4).

The percentage peak area of 2,4-DAPG produced by F113 was 0.96% after 24 hours and 0.05% after 48 hours. The PGP bacterial strains L124, L228, S118 and L321 (Figure 2.15), were also assessed for the presence of 177, 195 and 210 *m/z* ions, however, these ions were not present in any bacterial metabolite samples after 24, 48 hours or 5 days incubation.

2.3.5.2 Chromatogram Analysis and Compound Identification

A compound search was conducted on the deconvoluted chromatograms generated by AMDIS for the production of PGP bacterial metabolites. The bacterial strain L124 (Figure 2.16), had 115 matches after 24 hours incubation, 429 matches after 48 hours and 356 matches after 5 days incubation, as identified by AMDIS. Bacterial strain L228 (Figure 2.17) had 96 matches identified after the three incubation times respectively. Plant growth promoting bacterial strain L321 (Figure 2.18) had 137, 60 and 132 matches identified after the three respective incubation times. Strain S118 (Figure 2.19) had 415, 416 and 386 matches identified after the three incubation times. Bacterial strain S222 (Figure 2.20) had 438 matches identified

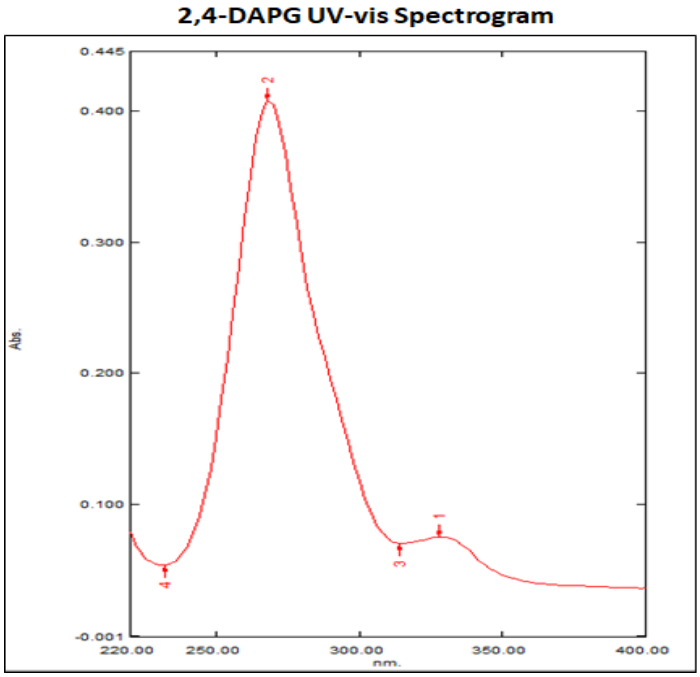

FIGURE 2.12: UV-vis spectrogram of synthetic 2,4-DAPG compound. The compound was represented by a tall peak (point 2) at 270 nm and a smaller shoulder peak (point 1) at 330 nm as confirmed by Brucker *et al.* (2008).

after 24 hours, 429 after 48 hours and 233 matches after 5 days. The broth controls were also assessed (Figure 2.21) by AMDIS with 413 matches after 24 hours, 304 after 48 hours and 108 matches after 5 days.

TABLE 2.7: Bacterial concentrations (CFU/ml) after 24 hours, 48 hours and 5 days growth, for GC-MS analysis.

	Bacterial Growth Period		
Strain	**24 hours**	**48 hours**	**5 days**
F113	3.00 x 10^8 $^{\alpha}$	1.00 x 10^{10}	> 1.00 x 10^{10}
L228	9.00 x 10^7	1.00 x 10^9	8.00 x 10^8
S118	> 1.00 x 10^{10}	> 1.00 x 10^{10}	> 1.00 x 10^{10}
L124	1.00 x 10^{10}	> 1.00 x 10^{10}	> 1.00 x 10^{10}
L321	8.00 x 10^7	2.00 x 10^8	> 5.00 x 10^{10}

$^{\alpha}$ Bacterial concentrations (CFU/ml) were determined from bacterial standard curves (see Appendix A.1).

The peaks on the chromatograms were identified by NIST (Table 2.8). Major peaks and metabolites of interest occurred between 5 and 20 minutes for all bacterial chromatograms. The PGP bacterial metabolite 4-methylbenzenesulphonamide was produced by *P. fluorescens* F113 after 48 hours incubation, with MF of 888 and a percentage peak area of 0.06% (RT = 10.60 minutes; Appendix A, Figure A.4). Plant growth promoting bacterial strain L124

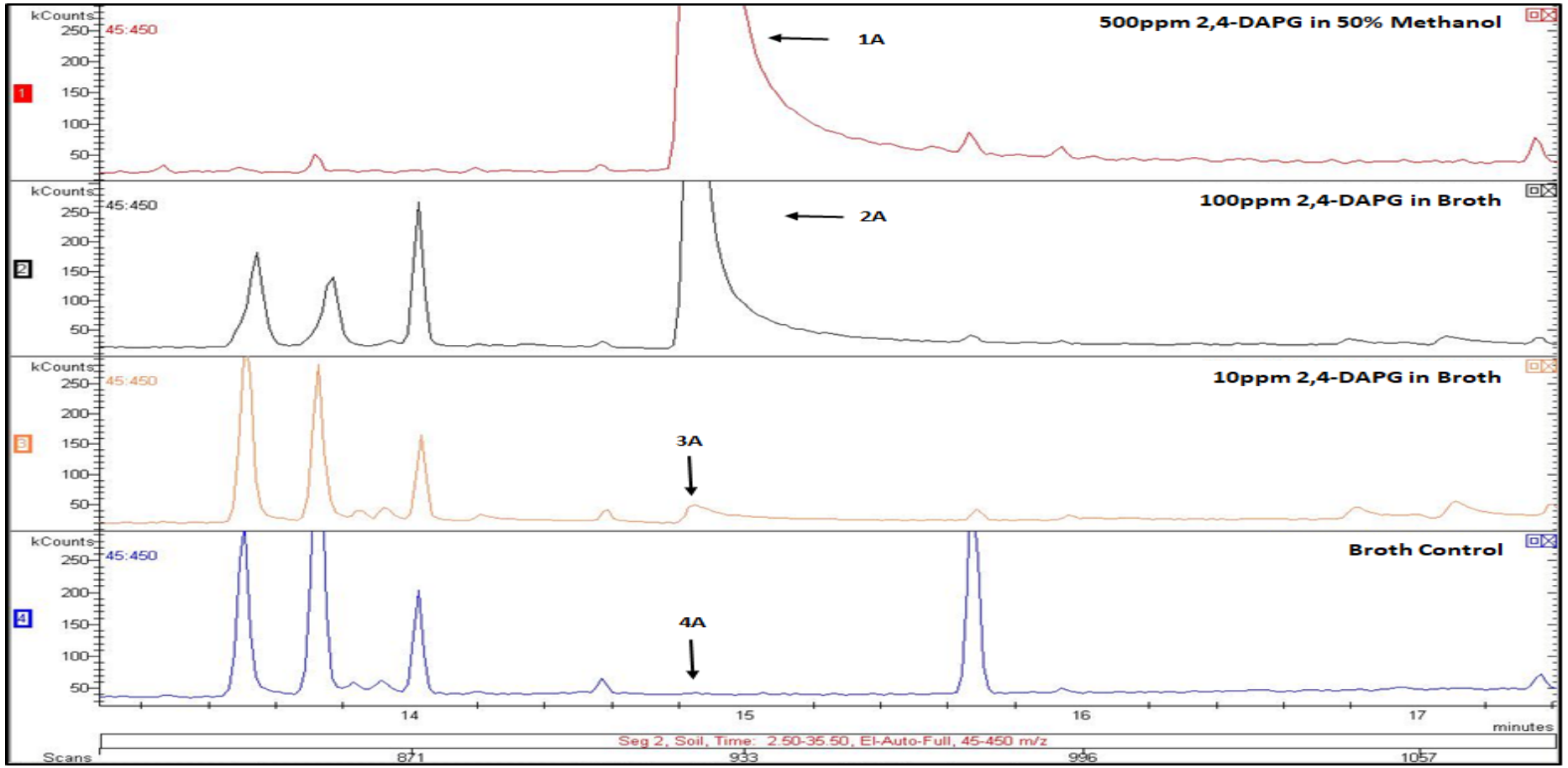

FIGURE 2.13: GC-MS chromatogram of 500 ppm 2,4-DAPG standard dissolved in 50% methanol (1mg/ ml); 100 ppm and 10 ppm 2,4-DAPG spiked broth controls. The peak identified as 2,4-DAPG is indicated in each chromatogram with a black arrow. 1A (MF = 745, RT = 14.89, Figure 2.14a), 2A (MF = 755, RT = 14.85, Figure 2.14b) and 3A (MF = 857, RT = 14.84, 2.14c) = 2,4-DAPG. 4A = Broth control after 24h incubation (No 2,4-DAPG peak present).

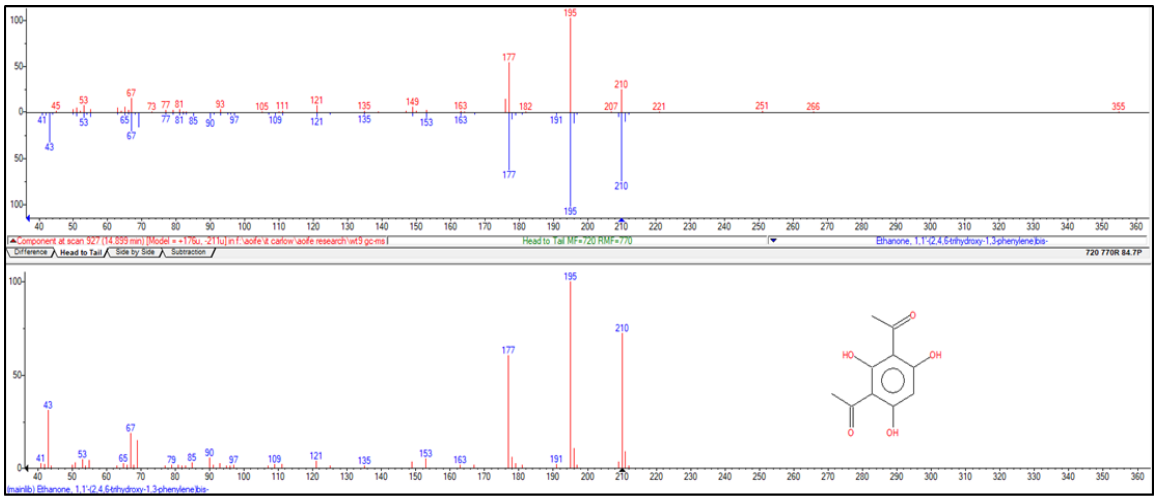

(A)

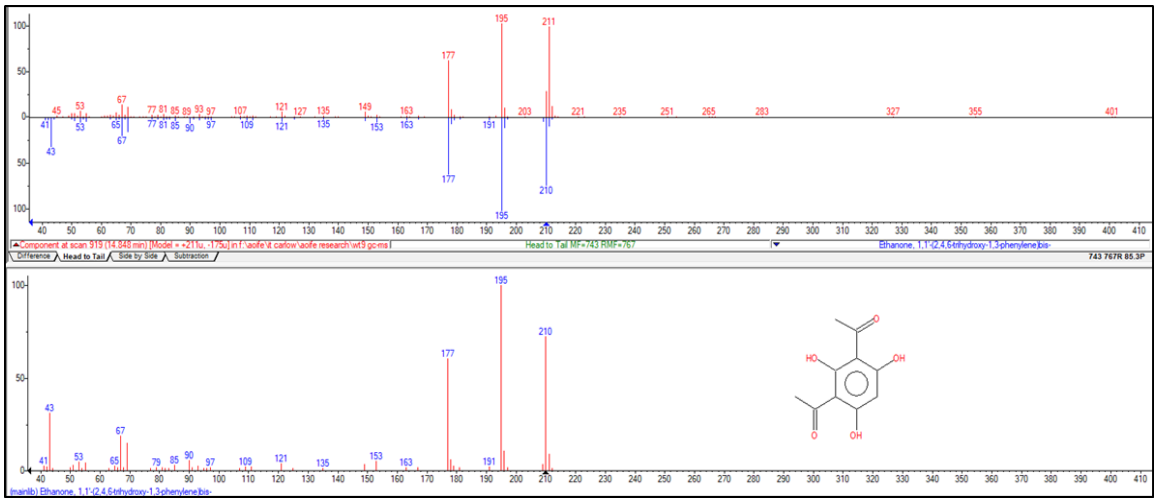

(B)

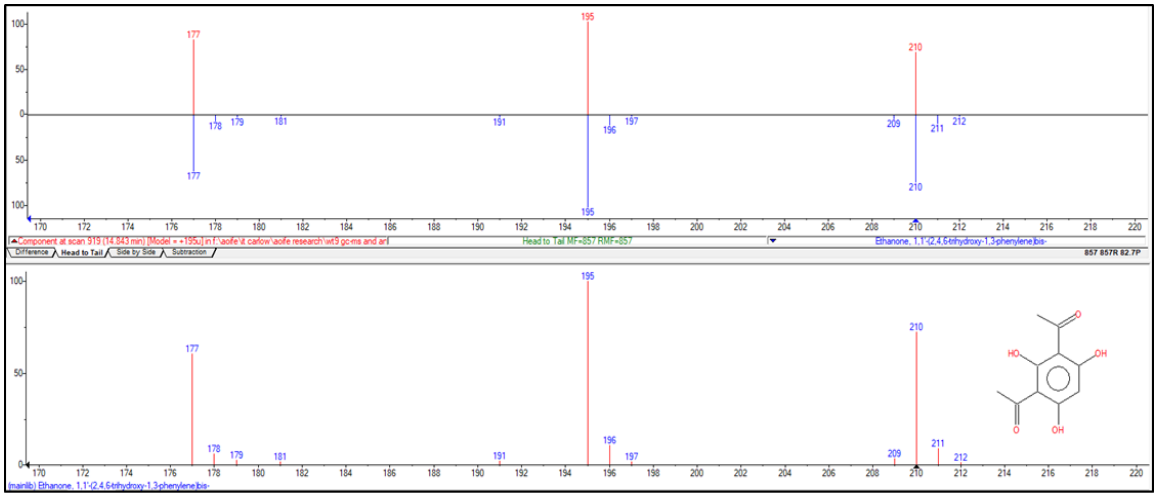

(C)

FIGURE 2.14: NIST identification of 2,4-DAPG in (A) 500 ppm standard dissolved in 50% methanol, (B) 100 ppm and (C) 10 ppm spiked broths. The upper mass spectrum in each figure displays a Head to Tail comparison of the Target (Blue) and the component Hit (Red). The lower mass spectrum in each figure displays the Target compound, with the ions 177, 195 and 210 *m/z* and the compound structure.

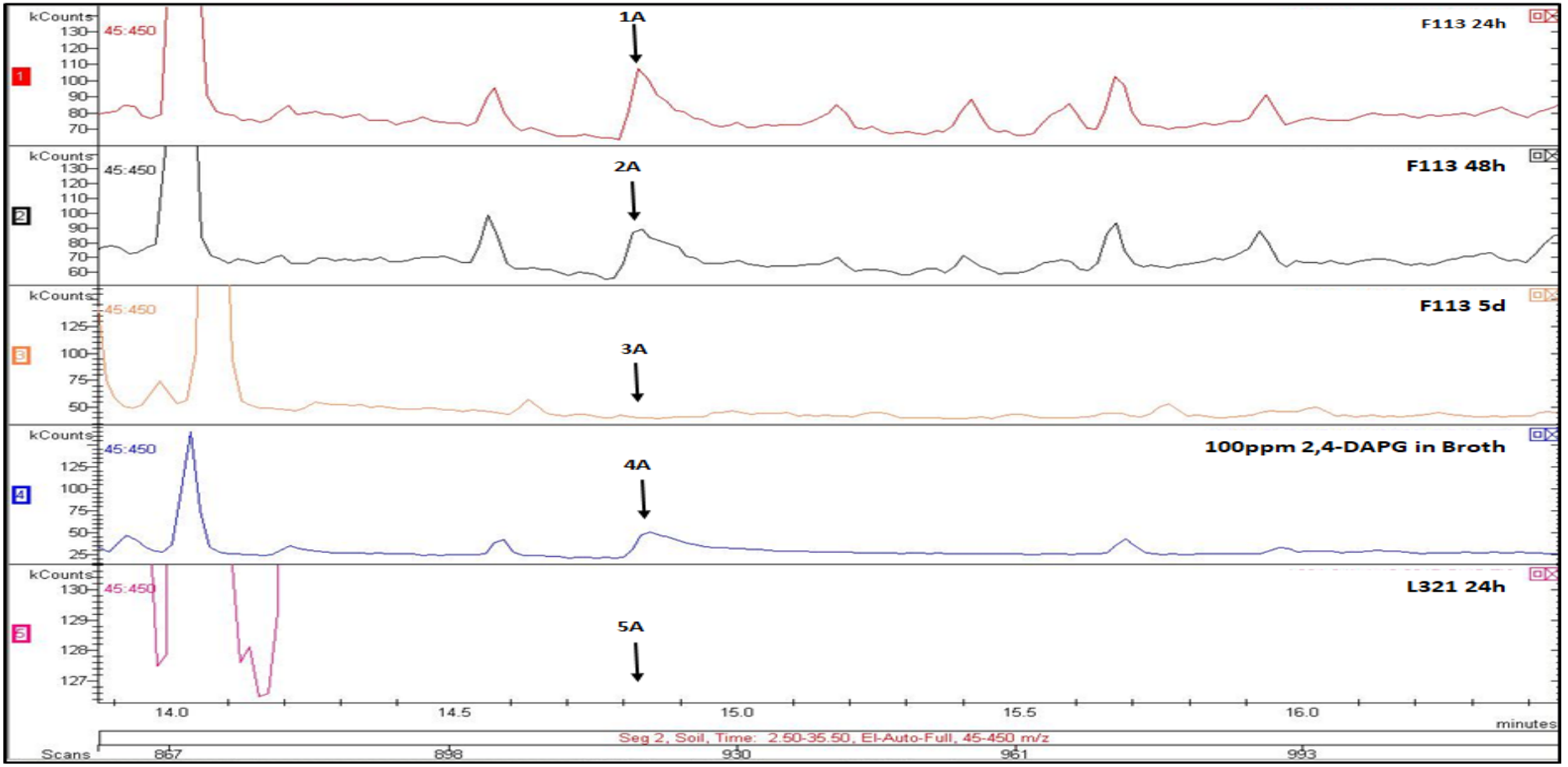

FIGURE 2.15: *Pseudomonas fluorescens* F113 2,4-DAPG production analysed by GC-MS after 24, 48 hours and 5 days growth. The peaks are indicated by a black arrow and are labelled according to the chromatogram number. Chromatogram 1: 1A and Chromatogram 2: 2A = 2,4-DAPG (1,1'-(2,4,6-Trihydroxy-1,3-phenylene) diethanone) peak with target ions 177, 195 and 210 *m/z* (Appendix A, Figure A.4) and retention time 14.83 minutes. Chromatogram 3: 3A = No 2,4-DAPG peak present. Chromatogram 4: 4A = 2,4-DAPG peak (Positive control). Chromatogram 5, 5A = No 2,4-DAPG present (Negative control).

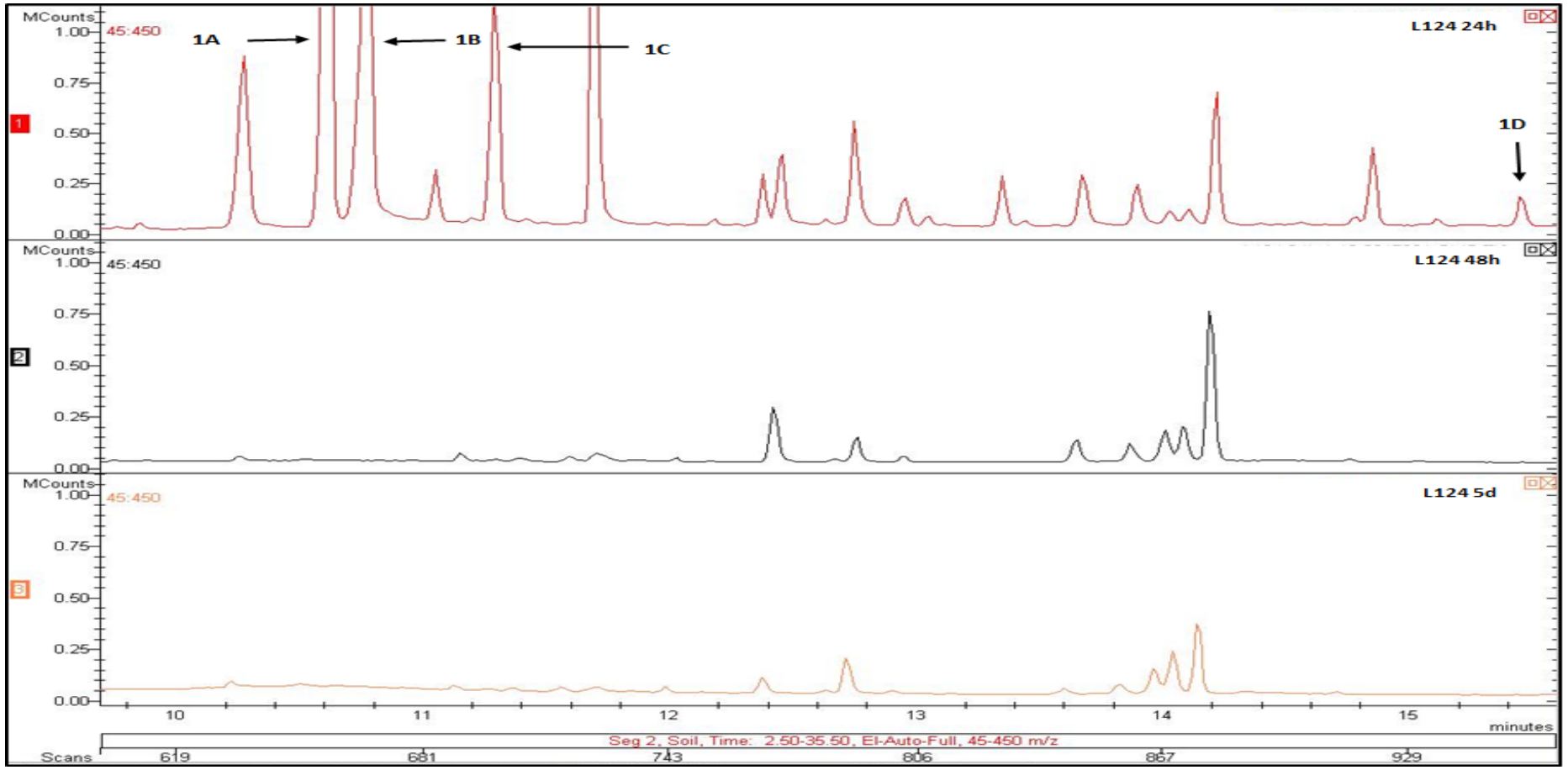

FIGURE 2.16: Plant growth promoting bacterial strain L124 metabolite production analysed by GC-MS after 24, 48 hours and 5 days growth. The metabolites are indicated with black arrows on chromatogram 1. Chromatogram 1: 1A = N-ethyl-2-methylbenzenesulfonamide (RT 10.62 minutes, see Appendix A, Figure A.4), 1B = N-butyl-4-methylbenzenesulfonamide (RT 11.05 minutes, see Appendix A, Figure A.6c), 1C = N-ethyl-4-methylbenzenesulfonamide (RT 11.29 minutes, see Appendix A, Figure A.6a) and 1D = N(-1,1-dimethyl)-4-methylbenzenesulfonamide (RT 15.11 minutes, see Appendix A, Figure A.6b). There were no target metabolites present in L124 after 48 hours or 5 days incubation.

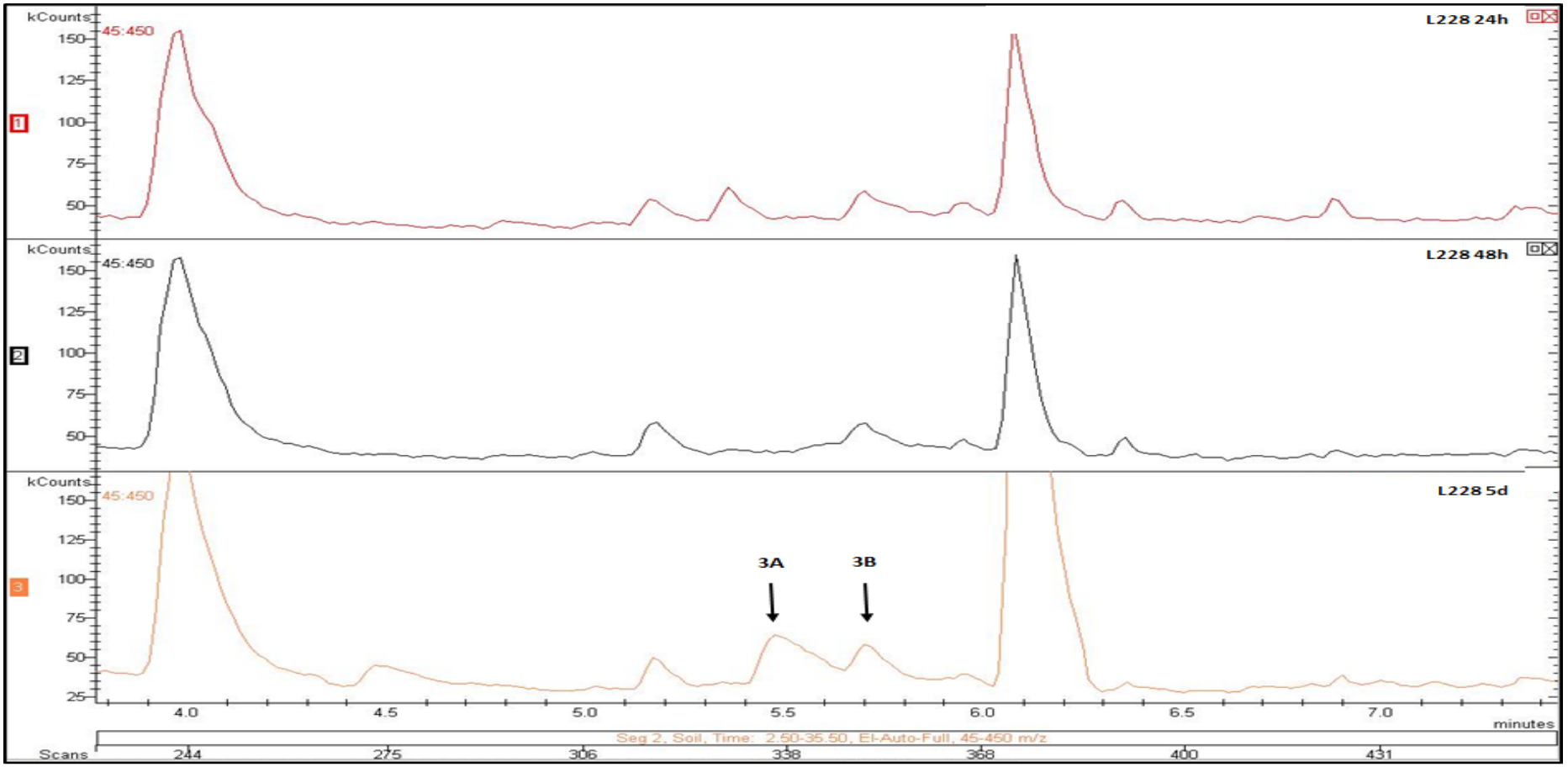

FIGURE 2.17: Plant growth promoting bacterial strain L228 metabolites analysed by GC-MS after 24, 48 hours and 5 days growth. The metabolites are indicated with black arrows on chromatogram 3. Chromatogram 3: 3A = Benzeneacetic acid (RT 5.47 minutes, see Appendix A, Figure A.7a), 3B = 1-(-3-hydroxyphenyl)ethanone (RT 5.70 minutes, see Appendix A A.8b). There were no target metabolites present in L228 after 24 or 48 hours incubation.

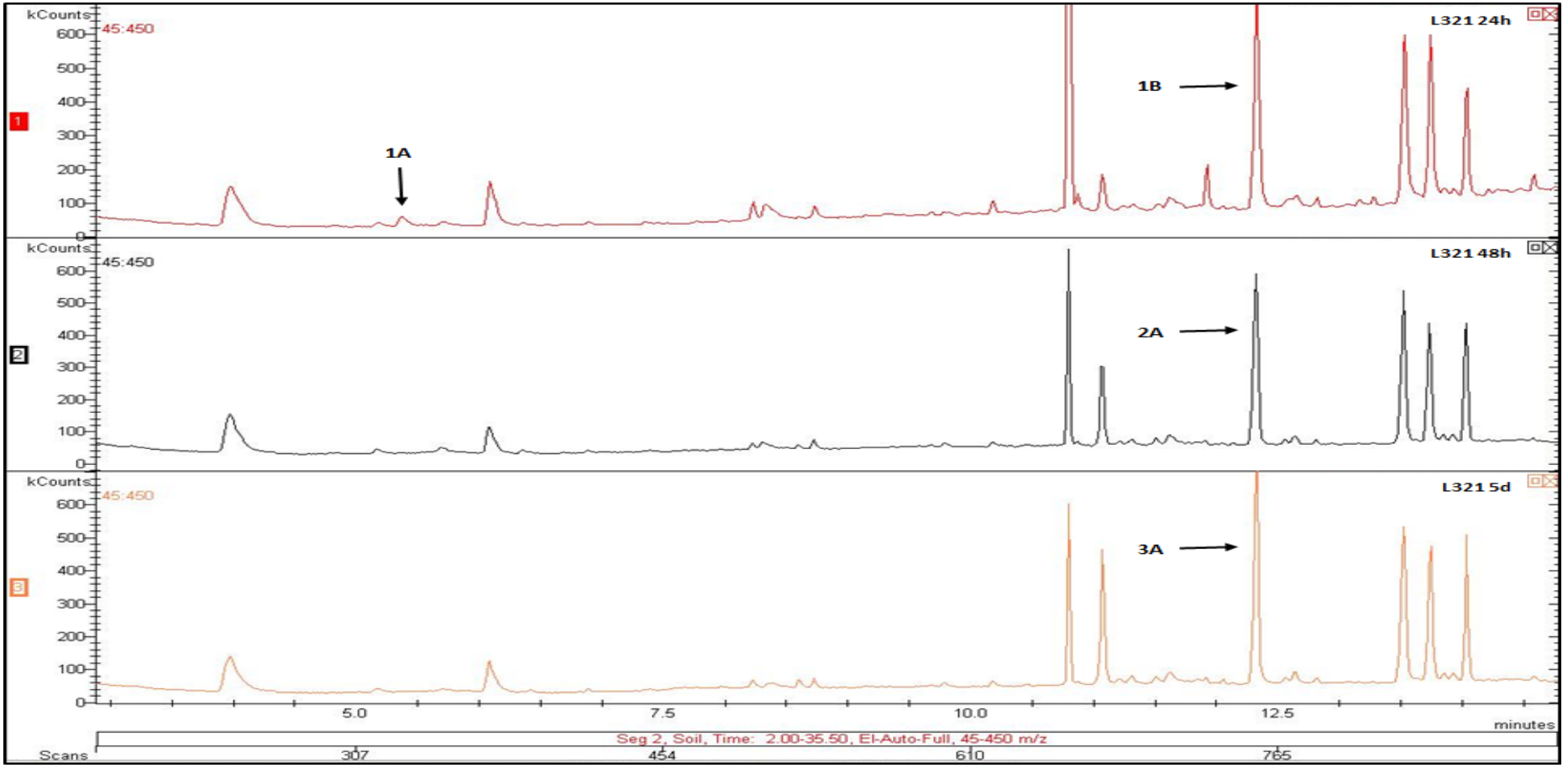

FIGURE 2.18: Plant growth promoting bacterial strain L321 metabolites analysed by GC-MS after 24, 48 hours and 5 days growth. The metabolites are indicated with black arrows on the chromatograms. Chromatogram 1: 1A = Benzothiazole (RT 5.37 minutes, see Appendix A, Figure A.7b) and 1B = 1H Indole-3-carboxaldehyde (RT 12.31 minutes, see Appendix A.7b). Chromatogram 2: 2A = 1H Indole-3-carboxaldehyde (RT 12.30 minutes). Chromatogram 3: 3A = 1H Indole-3-carboxaldehyde (RT 12.31 minutes) There were no target metabolites present in L321 after 5 days incubation.

produced N-ethyl-2-methylbenzenesul- phonamide with MF of 731 and a percentage peak area of 4.64% (RT = 10.62 minutes; Appendix A, Figure A.4), and it produced N-butyl-4-methylbenzenesulphonam-ide with MF of 889 and a percentage peak area of 3.98% (RT = 11.05 minutes; Appendix A, Figure A.6c). Bacterial strain L124 also produced N-ethyl-4-methylbenzenesulphonamide with MF of 780 and a percentage peak area of 1.74% (RT = 11.29 minutes; Appendix A, Figure A.6a) and N-(1,1-dimethyl)-4-methylbenzenesulphonamide with MF of 790, and a percentage peak area of 0.04% (RT = 15.11 minutes; Appendix A, Figure A.6b) after 24 hours. Strain S222 produced 4-methylbenzenesulphonamide with RT of 10.71 minutes, MF of 825 and a percentage peak area of 0.11% after 24 hours, and produced N-butyl-4-methylbenzenesulphonamide with RT of 11.24 minutes, MF of 787 and a percentage peak area of 1.66% after 5 days.

The bacterial metabolite Benzeneacetic acid (Appendix A, Figure A.7a) was produced by strain L228 after 5 days incubation. The compound had a MF of 929 (RT = 5.47 minutes) and a peak area of 0.13% after 5 days. Plant growth promoting bacterial strain L228 also produced 1-(-3-hydroxyphenyl) ethanone (Appendix A, Figure A.8b) after 5 days incubation. The compound had a MF of 899 (RT = 5.70 minutes) and a peak area of 0.05% after 5 days incubation. Plant growth promoting bacterial strain L321 produced the metabolite Benzothiazole (Appendix A, Figure A.7b) with MF of 778 (RT = 5.37 minutes) and a peak area of 0.05%. The strain L321 also produced 1H Indole-3-carboxaldehyde after 24 hours (RT = 12.31 minutes, MF = 872 and % peak area = 0.63%; Appendix A, Figure A.7c), 48 hours (RT = 12.30 minutes, MF = 877 and % peak area = 0.64%) and after 5 days (RT = 12.31 minutes, MF = 898 and % peak area = 1.0%). Bacterial strain S118 produced 2-aminobenzoic acid (Appendix A, Figure A.8a) after 5 days incubation. The compound was identified on NIST with a MF of 929, RT of 7.55 minutes and a peak area of 0.35%.

The identified metabolites produced by the bacteria were compared to the chromatograms of the broth controls at the appropriate incubation times (24, 48 hours or 5 days). None of the metabolites produced by the bacteria were found in the controls. However, the metabolite identified by Pandey *et al.* (2010) as hexahydro-3(2methylpropyl)-pyrrolo[1,2-a]pyrazine-1,4-dione (Appendix A, Figure A.8c) was found in all bacterial strains and broth controls.

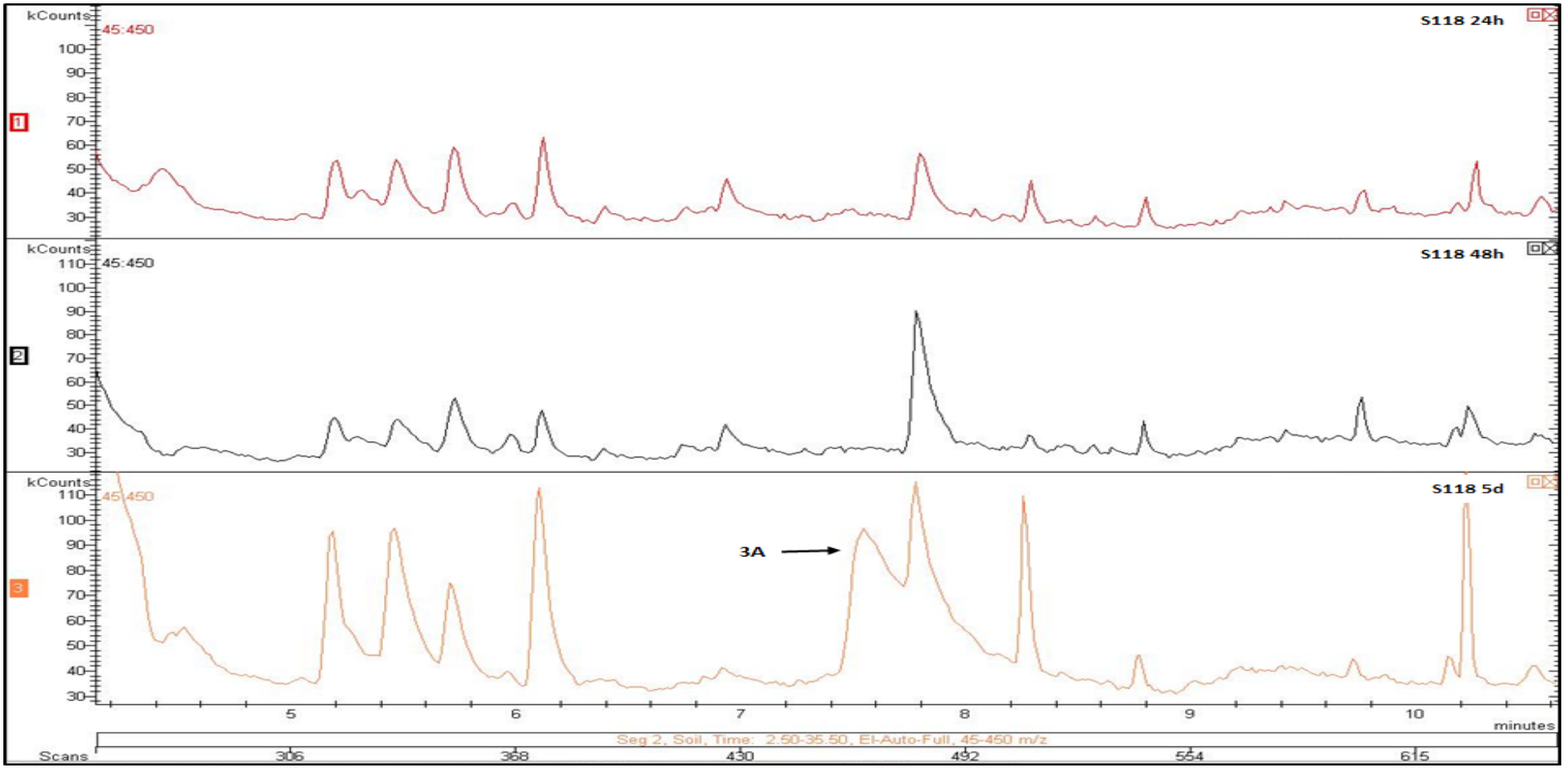

FIGURE 2.19: Plant growth promoting bacterial strain S118 metabolites analysed by GC-MS after 24, 48 hours and 5 days growth. The metabolites are indicated by black arrows on the chromatograms. Chromatogram 3: 3A = 2-aminobenzoic acid, (RT 7.55 minutes, see Appendix A, Figure A.8a). There were no target metabolites present in S118 after 24 and 48 hours incubation.

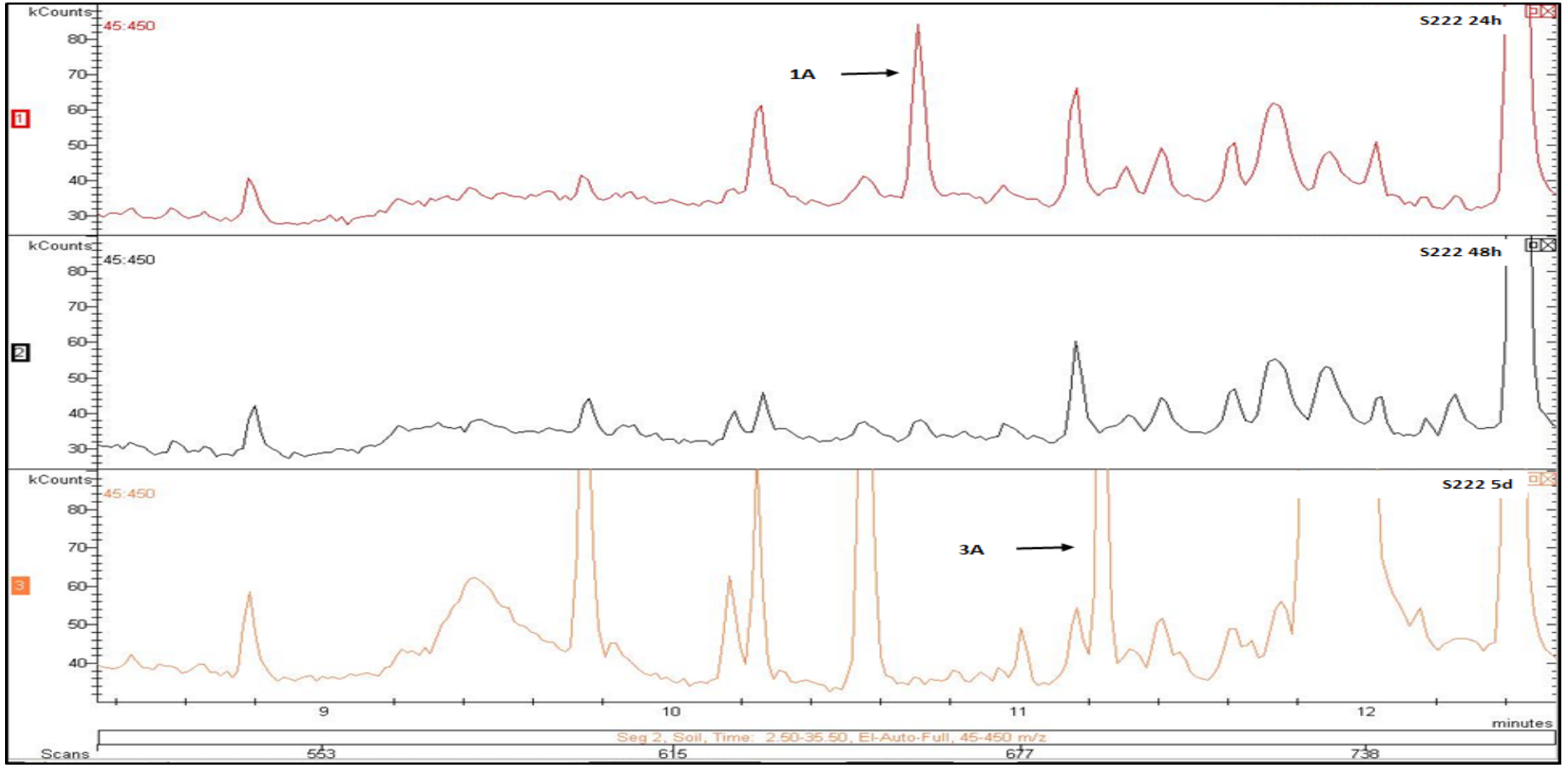

FIGURE 2.20: Plant growth promoting bacterial strain S222 metabolites analysed by GC-MS after 24, 48 hours and 5 days growth. The metabolites are indicated by black arrows on the chromatograms. Chromatogram 1: 1A = 4-methylbenzenesulphonamide (RT 10.71 minutes, see Appendix A, Figure A.4). Chromatogram 3: 3A = N-butyl-4-methylbenzenesulphonamide (RT 11.24 minutes, see Appendix A, Figure A.6c). There were no target metabolites present in S118 after 48 hours incubation.

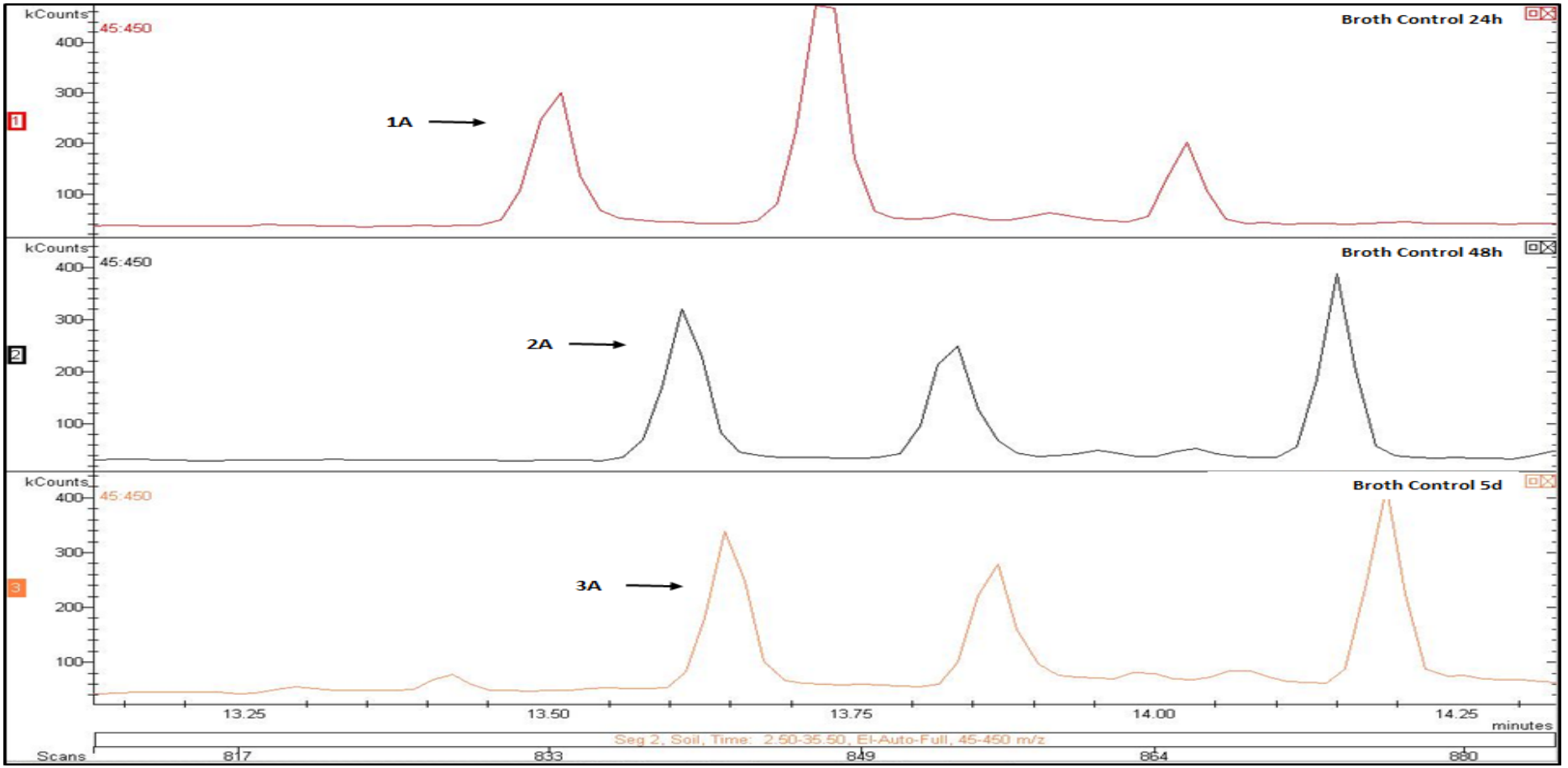

FIGURE 2.21: Broth controls analysed by GC-MS after 24, 48 hours and 5 days incubation. The metabolites are indicated by black arrows on the chromatograms. Chromatogram 1: 1A, Chromatogram 2: 2A and Chromatogram 3: 3A = hexahydro-3(2methylpropyl)-pyrrolo[1,2-a]pyrazine-1,4-dione (RT 13.50, 13.61 and 13.65 minutes respectively; see Appendix A, Figure A.8c).

TABLE 2.8: Plant growth promoting bacterial metabolites produced after 24, 48 hours and 5 days growth. Metabolites present in an ethyl acetate extraction (Brucker *et al.*, 2008) were detected by GC-MS analysis, and the compounds were identified and matched (match factor) by NIST reference library. The percentage peak area was determined by OpenChrom® open source software (Community Edition version 1.1.0 Deils).

Strain[1]	**Incubation**[2]	**RT**[3]	**Compound**	**Molecular formula**	**MF**[4]	**Peak area**
F113	24 h	14.83	1,1'-(2,4,6-Trihydroxy-1,3-phenylene)diethanone	$C_{10}H_{10}O_5$	813	0.96%
	48 h	10.60	4-methylbezenesulfonamide	$C_7H_9NO_2S$	888	0.06%
		14.82	1,1'-(2,4,6-Trihydroxy-1,3-phenylene)diethanone	$C_{10}H_{10}O_5$	850	0.05%
L124	24 h	10.62 - 10.78	N-ethyl-2-methylbenzenesulfonamide	$C_9H_{13}NO_2S$	731 - 855	3.98 - 4.64%
		11.05	N-butyl-4-methylbenzenesulfonamide	$C_{11}H_{17}NO_2S$	889	0.29%
		11.29	N-ethyl-4-methylbenzenesulfonamide	$C_9H_{13}NO_2S$	780	1.74%
		15.11	N-(1,1-dimethyl)-4-methylbenzenesulfonamide	$C_{11}H_{17}NO_2S$	790	0.04%
L228	5 d	05.47	Phenylacetic acid	$C_8H_8O_2$	929	0.13%
		05.70	1-(-3-hydroxyphenyl)ethanone	$C_8H_8O_2$	899	0.05%
L321	24 h	05.37	Benzothiazole	C_7H_5NS	778	0.05%
		12.31	1H Indole-3-carboxaldehyde	C_9H_7NO	872	0.63%
	48 h	12.30	1H Indole-3-carboxaldehyde	C_9H_7NO	877	0.64%
	5 d	12.31	1H Indole-3-carboxaldehyde	C_9H_7NO	898	1.0%
S118	5 d	07.55	2-aminobenzoic acid,	$C_7H_7NO_2$	929	0.35%
S222	24 h	10.71	4-methylbenzenesulfonamide	$C_7H_9NO_2S$	825	0.11%
	5 d	11.24	N-butyl-4-methylbenzenesulfonamide	$C_{11}H_{17}NO_2S$	787	0.12%

[1] Strain = Bacterial strains utilised in this study.
[2] Incubation = Incubation time of bacterial strains prior to GC-MS analysis: 24, 48 hours and 5 days.
[3] RT = Retention time - time (minutes) that the compound was held on the GC column.
[4] MF = Match factor - average of the forward and reverse match factors.

2.3.5.3 Principal Component Analysis of PGP Bacterial Metabolites

Principal component analysis (PCA) was performed on the deconvoluted peaks, of the volatile metabolites produced by the bacterial strains F113, L124, L228, L321, S118 and S222 that were acquired by AMDIS. The peaks were integrated with OpenChrom® and statistically assessed to identify any differences in volatile metabolite production, between 5-16 minutes run time. The results suggest that there is a lot of similarity between the PGP bacterial metabolites that were analysed, and are displayed as a cluster (Red) in the centre of the PC2-PC3 bi-plot (Figure 2.22). This cluster contained the components of the broth controls, L124 and L228 after 24, 48 hours and 5 days incubation, F113 and S222 after 24 hours and 5 days, L321 after 48 hours and 5 days and S118 after 24 and 48 hours. This observation suggests that there is not a significant difference between the controls and bacterial strains and the metabolites they produce.

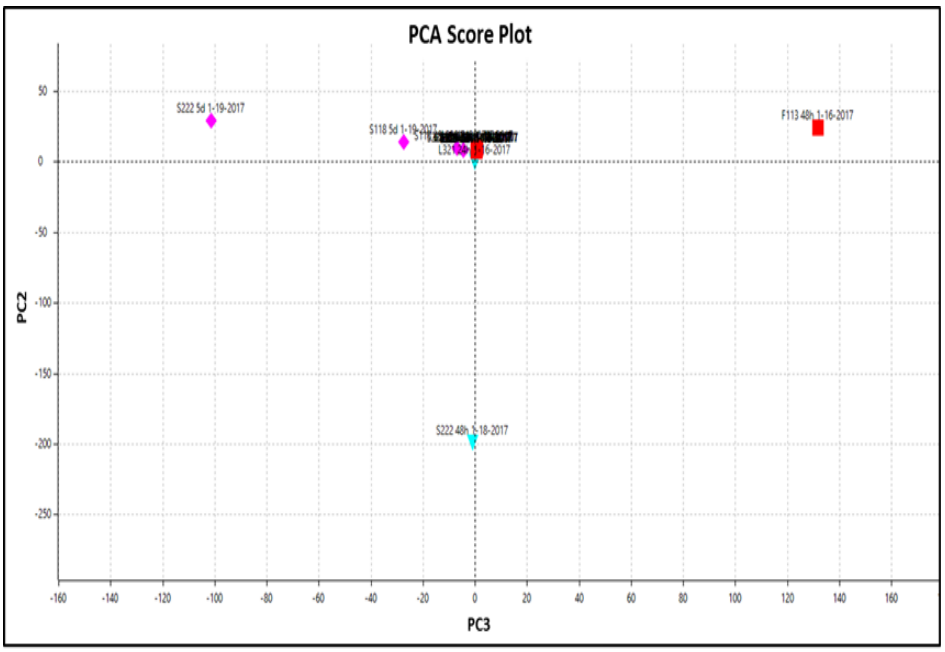

FIGURE 2.22: Principal component analysis bi-plot of GC-MS AMDIS deconvoluted chromatogram files (approximately the first 1050 scans) of PGP bacterial metabolites.

However, of the three clusters produced by OpenChrom®, (Red, Turquoise and Pink), four components loaded positively on PC2, PGP bacterial strains L321 (after 24 hours), S222 and S118 (after 5 days) and, F113 (after 48 hours) incubation. One component loaded negatively on PC3, S222 (after 48 hours) incubation.

2.4 Discussion

Nematode PGP bacterial interactions were explored in this study to assess their effect on nematode survival. The bacterial strains utilised in this study have been extensively investigated by previous IT Carlow researchers. Various biochemical tests were previously performed on the bacterial strains to determine their PGP properties, including IAA, ACC deaminase and VOC production (Otieno *et al.*, 2015). They were also studied in interaction with EPN (Hurley, 2018), plant pathogenic bacteria and for fungus biocontrol (Otieno, 2014; Menton, 2010). The bacterial strains F113, L124, L228, L321, S118 and S222 were chosen for this study due to the extent of information available on them, with a focus on their biocontrol and PGP potential.

The nematodes *C. elegans* and *P. pacificus* were utilised in this study as a control species. *Pristionchus pacificus* stock cultures died during this research due to a fungal infection. Every effort was made to isolate the eggs and re-culture the species by utilising the protocol of Stiernagle (2006) however, it was unsuccessful. Therefore, this nematode was used for susceptibility tests with the beneficial bacteria and bacterial metabolites only. The effect of the bacterial strains and their metabolites on PPN was the focus of this study, with an emphasis on *M. javanica* and *G. pallida*, due to their availability. A limited quantity of *G. pallida* was received from The James Hutton Institute, therefore they were not used in susceptibility tests with bacterial strains. It was originally planned that the PPN *Heterodera cruciferae* and *Pratylenchus penetrans* would also be utilised in this research, however, due to culturing difficulties they were removed from the study.

Susceptibility testing typically involves subjecting an organism to a compound to determine its effect on the organisms mortality. These tests are commonly performed in the medical sector, to determine the effect of an antibiotic on pathogenic bacteria. However, there are many variations to such testing in cases such as: assessing the susceptibility of *E. coli* and *Salmonella typhimurium* to various antibiotics infused on tape in portable culture devices (Deiss *et al.*, 2014), utilising a lectin biosensor on *E. coli* for an antibiotic susceptibility assay (Ma *et al.*, 2015) or the susceptibility of mice to the parasitic nematode *Trichuris muris* infection (Leung *et al.*, 2018). Plant growth promoting bacteria, such as rhizobacteria and endophytic bacteria, are well documented as having biocontrol effects on PPN (Tian *et al.*, 2007), particularly *Pseudomonas* species (Nam *et al.*, 2018; Norabadi *et al.*, 2014; Thiyagarajan and Kuppusamy, 2014; Trifonova *et al.*, 2014). Initially, susceptibility assays in the present study were established to determine the direct effect that PGP bacterial strains had on the survival of *C. elegans*, *P. pacificus* and *M. javanica*. The mortality rate of all three nematode species was significantly high, particularly for *M. javanica*, with up to 100% mortality, even when subjected to low concentrations.

Although high mortality rates were recorded for all nematode species investigated, it was important to determine if nematode mortality was caused by interactions between the bacterial cells directly, or by the secondary metabolites they were producing. Susceptibility of the nematodes utilised in the present study to the bacterial secondary metabolites at various life-stages was thus investigated. Mortality varied significantly for *C. elegans* and *P. pacificus*, between 2% and 100%, depending on the life stage and concentration of the metabolites. However, subjecting *M. javanica* J2 stage to all bacterial metabolites significantly caused up to 100% mortality on exposure to all bacterial concentrations, except for strains S118 and S222. Significantly lower egg hatch was also observed on exposure to all bacterial strains. Equally, *G. pallida* J2 stage mortality was significantly high on exposure to all bacterial metabolite concentrations after 24 hours. Like the effect of the metabolites on *M. javanica* egg hatch, they resulted in significantly low *G. pallida* egg hatch, with a comparatively low percentage of egg hatch on exposure to the metabolite consortium. A similar study was carried out by Cronin *et al.* (1997b). They conducted an egg hatch assay on *G. rotochiensis*, but they exposed the eggs to picrolonic acid (induces egg hatch). In the present study *G. pallida* eggs were exposed to PRD instead of picrolonic acid. Byrne *et al.* (2001) found that *G. pallida* hatched more effectively in response to the natural potato chemicals, alpha-solanine and alpha-chaconine, in comparison to artificial hatching factors.

The results indicated high PPN mortality was caused by the metabolites that the bacterial strains produced. The next step was to investigate what compounds the PGP bacteria were expressing. The control strain *P. fluorescens* F113 has received considerable research attention (Barahona *et al.*, 2011; Redondo-Nieto *et al.*, 2013; Rivilla *et al.*, 2013), particularly on its capacity to produce the compound 2,4-DAPG (Cronin *et al.*, 1997b). The compound has been attributed to the biocontrol of many organisms including plants, fungi, viruses, bacteria and nematodes (Barahona *et al.*, 2011; Cronin *et al.*, 1997a; Fenton *et al.*, 1992; Meyer *et al.*, 2009). Considering it was known that *P. fluorescens* strains L124, S110 and S118 utilised in the present study, all have the PhlD gene associated with 2,4-DAPG production (Menton, 2010), the interactions between the nematodes and the compound were investigated. The synthetic compound viability was assessed on an UV-vis. Brucker *et al.* (2008) established a λ_{max} of 270 nm. In the present study, the λ_{max} was found to be 268 nm. The compound peaks, however, were identical to those found in their paper, and it was concluded that the compound was not degraded in the storage process. The 2,4-DAPG exposure assays suggested that, the nematodes *M. javanica* and *G. pallida* were more sensitive to various concentrations of 2,4-DAPG, compared to *C. elegans*. Interestingly, *G. pallida*, in particular, were more susceptible to the antibiotic than *M. javanica*. It was observed in the present study, *G. pallida* exposure to the compound considerably increased egg hatch, particularly at the lower 2,4-DAPG concentration. It was further noted that on hatching in the antibiotic, in the egg hatch assays, J2 stage *G. pallida* survival increased. Cronin *et al.* (1997b) also observed

increased egg hatch and decreased J2 mortality in the cyst nematode *G. rostochiensis*. However, in the present study, J2 stage *G. pallida* survival on exposure to different concentrations of 2,4-DAPG in the sensitivity assays, caused high mortality even in low concentrations of the compound. Lower concentrations of the antibiotic in the sensitivity assays were utilised in the present study for *G. pallida*, compared to *C. elegans* and *M. javanica*, because Cronin *et al.* (ibid.) observed a lethal effect of the compound on *G. rostochiensis* caused by low concentrations of 2,4-DAPG. Meyer *et al.* (2009) conducted a comparable experiment to this present study. They subjected several nematode species, including RKN and cyst nematodes at different life-stages, to various concentrations of 2,4-DAPG. Their observations suggested that, *M. incognita* did not respond to the 2,4-DAPG treatments, however, it did inhibit egg hatch. This differed considerably from the results in the present study. The antibiotic had a lethal effect on *M. javanica* at various concentrations. However, like Meyer *et al.* (2009) *M. javanica* egg hatch was also inhibited on exposure to various concentrations of 2,4-DAPG.

Bacterial metabolite production had a profound negative effect on nematode survival and egg hatch in the current study. Based on previous enviroCORE researchers findings, in terms of biocontrol and PGP, on the bacterial strains under investigation and the results obtained in the current study, five bacterial strains were chosen for further investigation. Several attempts by enviroCORE researchers to identify the production of the compound 2,4-DAPG derived from IT Carlow stocks were unsuccessful. In the current study, however, for the first time, the antibiotic was discovered to be produced by F113 from the IT Carlow stocks, as assessed by GC-MS analysis. The compound was retained on the instruments column at the same retention time for each run, indicating consistent results. Investigations carried out in enviroCORE by previous researchers on *P. fluorescens* strains L124, L321 and S118, and *P. agglomerans* strain S222 suggested some bacterial strains were associated with the production of the antibiotics 2,4-DAPG and pyoluteorin. Although the capacity of the strains with regards to PGP and biocontrol were known, the compounds the bacterial strains were producing were previously undiscovered, until the present study. The bacterial strains investigated were found to produce many compounds associated with biocontrol and PGP. The bacterial metabolite replications in the present study were pooled together, due to time restrictions using the GC-MS instrument. Anantha Padmanabhan *et al.* (2016) and Pandey *et al.* (2010) carried out similar research to the present study. They assessed the compounds that the bacterial species *Vibrio parahaemolyticus* and *Pseudomonas* were producing. Their findings were utilised in the present study as a reference guide. The compound phenyl acetic acid was only produced by the bacterial strain L228 in the present research, however, Sajid *et al.* (2011) identified *Streptomyces malachitofuscus* as another producer. Phenyl acetic acid is commonly applied in agriculture and utilised in the pharmaceutical industry. It is associated with increased plant growth and development, as it acts as a natural auxin in shoots. It is also associated with antifungal and antimicrobial (Pandey *et al.*, 2010) activity and has been identified as a potential biocontrol agent. The compound Benzenethiazole was produced by *P. fluorescens* L321 in

the present study. The compound is associated with a number of biological processes including antimicrobial and antiviral activity (Ali and Siddiqui, 2013), with antibacterial activity against *Pseudomonas* and *Bacillus* species. 1H Indole-3-carboxaldehyde was also produced by L321 in this current research, and has been identified by Rajalaxmi *et al.* (2016) as an anti-biofilm agent against *Vibrio cholerae* O1. It is also associated with helping bacteria to adapt to stressors. Bommarius *et al.* (2013) established similar sensitivity assays to those utilised in the present study to determine the susceptibility of *C. elegans* to various strains of *E. coli*. They discovered that 1H Indole-3-carboxal- dehyde produced by the bacterial strains had a lethal effect on *C. elegans*. This was comparable to the results obtained in the current study, as high mortality of all life stages of *C. elegans* was observed on exposure to strain L321. The compound Benzenesulphonamide was produced by *P. fluorescens* F113 and L124, and *P. agglomerans* S222 in the present study. The compound has anti-fungal properties and can provide biological control of root pathogens (Kim *et al.*, 2000). It has previously been reported to be produced by *Pseudomonas* spp. (Elleuch *et al.*, 2010). The bacterial strain S118 was identified to produce 2-aminobenzoic acid, this compound is also known as anthranilic acid, and it is associated with improving the effects of plant growth regulators, but they also have a role in the biocontrol activity of soil-borne fungal pathogens (Ownley *et al.*, 2003). There was one commonly occurring compound, hexahydro-3 (2-methylpropyl)-pyrrolo[1,2-a]pyrazine-1,4-dione, throughout all bacterial metabolite treatments and control treatments, appearing at all three-time points. This metabolite has been identified to be involved with antimicrobial, nematicidal and antioxidant activity (Malash *et al.*, 2016; Pandey *et al.*, 2010) and *Bacillus pumilus* is a known producer of this metabolite. However, in the present study, this compound was also identified in the control samples. It can, therefore, be concluded, that it was not produced by the PGP bacteria, but was present in the components of the broth, the bacterial strains were grown in.

One of the aims of this work task was to identify the compounds the bacterial strains were producing in relation to PGP and biocontrol. Although the compounds were identified, the next step would be to quantify the concentration of compounds produced by each strain, with the use of chemical standards. Due to time restrictions, however, this was not achieved. Instead, the percentage peak area was calculated to determine the percent of bacterial metabolite produced in relation to the whole chromatogram. Interestingly, the Benzenesulphonamides had the highest percentage peak areas, up to 5%. Some metabolites had higher percentage peak areas after 24 hours incubation that gradually decreased between 24 and 48 hours of bacterial growth, such as 2,4-DAPG, with no compound being detected after five days. On the other hand, some metabolites were not present after 24 or 48 hours incubation but were produced after a longer incubation time, including phenylacetic acid, 1(-3-hydroxyphenyl)ethanone and 2-aminobenzoic acid. These compounds were present after five days of bacterial growth. The percentage peak area of the compound 1H Indole-3-carboxaldehyde produced by L321 increased consistently over five days of bacterial incubation. This metabolite is persistent and

accumulates over time, which is important as it is associated with biocontrol and bacterial protection. The roles of bacterial secondary metabolite production, are to give the bacteria an advantage in terms of survival and success in an incredibly competitive environment, such as soil. These compounds are associated with increasing the nutrient availability to plants in the soil, niche exclusion of pathogenic bacteria and antimicrobial activity. The manufacturing of secondary metabolites occurs in the late bacterial growth phase after the bacteria have synthesised the primary metabolites necessary for their survival. The stage in the bacteria life-cycle that they produce secondary metabolites is at a genetic level (Ruiz *et al.*, 2010). However, this can be greatly influenced by the environment. Therefore, secondary metabolite production, the number of compounds synthesised and the stage in the life-cycle they are produced are species specific.

In conclusion, the results of the various methods described in this chapter suggest that the PGP bacterial strains and the components they produce have a profound effect on phytoparasitic nematodes. In terms of biotechnology and PPN biocontrol, the PGP bacterial strains and 2,4-DAPG poses to be influential in the development of a control plan against *Globodera* and *Meloidogyne* species. Considering these nematodes can only survive in the soil for 10 to 14 days in the absence of a host; the application of PGP bacterial strains and 2,4-DAPG treatments, with the addition of root diffusates in advance to crop planting, would be advantageous (Cronin *et al.*, 1997b). The outcome of such an approach would be two-fold, (1) egg hatching in the absence of a host plant and (2) the interactions between the antibiotic and the PPN could effect nematode activity.

Key results obtained from the various work tasks in Chapter 2 are the following:

- All PGP bacteria had a lethal effect on *M. javanica* at different concentrations over 24 and 48 hours.
- *Meloidogyne javanica* and *G. pallida* J2 stage exposure to all PGP bacterial metabolites were responsible for up to 100% mortality after 24 and 48 hours.
- The effect of 1 ppm 2,4-DAPG on *G. pallida* J2 stage caused 90% mortality after 24 hours.
- Bacterial metabolites reduced *M. javanica* and *G. pallida* egg hatch, and increased J2 stage mortality compared to the controls.
- The antibiotic 2,4-DAPG reduced *M. javanica* but increased *G. pallida* egg hatch.
- There were 12 different compounds produced by the PGP bacteria identified, that were associated with PGP and biocontrol.

The objective of this study was to identify two to three key strains, that increased PPN mortality and decreased PPN egg-hatch. Surprisingly, however, the bacterial strains caused higher nematode mortality, and therefore, it was not possible to reduce the number of bacterial strains to be further investigated, to that extent. The aims of Chapter 2, to determine the effect of the PGP bacteria and their metabolites on nematode survival and egg hatch, were achieved. The final aim, to identify the compounds produced by the bacterial strains associated with PGP and biocontrol, was also met. The confines of *in-vitro* assays are not representative of the interactions found in a soil microcosm. The next step for this research was to set up plant-based experiments to determine the bacterial nematode interactions in a more complex and natural environment-simulating system. Due to the compounds produced and the effect of the bacterial strains on PPN, *P. fluorescens* F113, L124, L228 and L321 were chosen for further investigation.

Chapter 3

The Effect of Plant Growth Promoting Bacteria on Plant Parasitic Nematode Biology and Behaviour

3.1 Introduction

Plant growth promoting (PGP) bacteria such as endophytic bacteria can colonise living plant tissues and maintain a mutualistic relationship with the host plant. There are many benefits involved with such relationships including increased plant growth and biocontrol against host plant pathogens (Lally *et al.*, 2017; Otieno *et al.*, 2015; Siddiqui and Ehteshamul-Haque, 2001). The colonisation of these bacteria can lead to preconditioning plant defences (Choudhary *et al.*, 2007) by inducing host systemic resistance. The production of secondary metabolites, mainly antibiotics, by PGP bacteria have shown to be an efficient mechanism of PPN control (Cronin *et al.*, 1997b; Meyer *et al.*, 2009; Siddiqui and Shaukat, 2003).

Currently, there are many practices and strategies employed to manage nematode infections in crops including crop rotation (Chen and Tsay, 2006), growing resistant varieties (Fuller *et al.*, 2008), soil steaming (Kokalis-Burelle *et al.*, 2016), supplementing soil with organic matter (Widmer *et al.*, 2002), biocontrol (Cronin *et al.*, 1997b) and the addition of nematicides. Where possible, often these techniques are combined, however, the application of nematicides still dominates. Although these chemicals can be effective, they do not always kill the nematodes in the soil. The use of such chemicals is now heavily regulated due to the hazardous effects on the environment, human health and lack of efficacy. Problematic nematodes in the soil can become resistant to these chemicals, while nematicide compounds often degrade in the soil. Therefore, demand for improved, alternative strategies is increasing. Exploiting the potential biocontrol properties of PGP bacterial colonisation in plants

is a recent development considered for further investigation (Almaghrabi *et al.*, 2013; Jiang *et al.*, 2018; Xiang *et al.*, 2017).

Belowground multitrophic interactions and their influence on plant health and the plant rhizospheric community are not well-known compared to the relevant aboveground processes. The interactions involved may be similar to those aboveground, however, the dispersal of organisms and chemical compounds is lower than that aboveground (Rasmann and Turlings, 2008). Tritrophic interactions in this study refer to the complex interactions among host plants, the mutualistic endophytic bacteria, and problematic plant parasitic nematode (PPN). Plant defence systems can be triggered systemically and expressed in response to biotic stress, such as PPN infection. Plants responding to such stresses and the timing of this response result in the plant either coping or succumbing to the infection. An induced systemic response (ISR) is an enhanced state of defence that can be elicited by the presence of beneficial bacteria, increasing plant protection against subsequent biotic challenges. This enhanced state of resistance is effective against a broad range of pathogens and parasites (Choudhary *et al.*, 2007). Plant colonisation of beneficial bacteria is also effective against the development of giant cells in plant roots, preventing nematode J2 infective juveniles to establish an adequate feeding site. Plant root colonisation by beneficial bacteria also makes roots less attractive (Martinuz *et al.*, 2012) to infective stage nematodes. If these plant defence mechanisms are triggered by a stimulus before being infected, the degree of infection can be reduced (Choudhary *et al.*, 2007).

Chemotaxis is the main sensory mode used by nematodes to orient themselves to their host or food source (Jagodič *et al.*, 2017), such as the entomopathogenic nematode (EPN) *Steinernema feltiae* to its host *Galleria mellonella*, free-living bacterial feeding nematode *Caenorhabditis elegans* to its food source *Escherichia coli*, or the PPN *Meloidogyne javanica* to its tomato plant (*Solanum lycopersicum*) host roots. The nematodes move towards the direction of higher concentrations of plant chemical signals, in the case of PPN. The attraction of PPN to plant roots is due to the production of soluble and gaseous attractants, produced by the roots or by bacteria colonising on the plant roots (Reynolds *et al.*, 2011). There are different classifications of such attractants; (1) long-distance attractants, such as volatile chemicals, that travel quickly by diffusion through the air tends to attract nematodes to the general root area, (2) short-distance attractants, such as water-soluble chemicals that diffuse slowly in the soil tend to attract nematodes to the roots themselves and (3) local attractants, such as compounds produced by bacteria, fungi, plants and other nematodes (Jagodič *et al.*, 2017) that enable PPN to orientate themselves to their preferred invasion site. Phytoparasitic nematode attraction to volatile compounds is an under-researched area (Reynolds *et al.*, 2011), in comparison to the extent of information on EPN in this context. In the present study work focused on the chemotaxis of *C. elegans*, *M. javanica* and *Globodera pallida* to local attractants.

The PGP bacterial strains investigated in this study were known to produce compounds that have biocontrol properties (previously investigated in Chapter 2). Production of these compounds plays an important part in understanding the interactions between PGP bacteria and PPN. The infective stages of the cyst and root-knot nematodes such as *G. pallida* and *M. javanica*, have limited stored energy and must seek their host efficiently and effectively (ibid.). As their lipid reserves deplete, their ability to infect a host plant decreases. The PGP bacterial strains utilised in the attraction assays determined if the treatments were attractive to the nematodes. If roots colonised by beneficial bacteria were not attractive to the PPN or were repulsive to them, the nematodes would not infect the plants and therefore risk running out of energy before infection could take place. Investigating PPN attraction behaviour to PGP bacteria could add to the understanding of belowground multitrophic interactions, and their influences on plant performance and community composition. Understanding these associations could also contribute to the establishment of safer and sustainable bio-nematicide products.

There was two aspects of interest in this chapter: (1) Behaviour of *C. elegans*, *M. javanica*, and *G. pallida* in terms of attraction to PGP bacterial strains and to 2,4-DAPG and (2) the tritrophic interactions between beneficial bacterial strains, *M. javanica* and tomato plants, regarding plant growth promotion and nematode biocontrol. It was hypothesised that the compounds the bacterial strains were producing would reduce nematode infection, hinder nematode development within tomato roots and they would elicit an induced systemic response in tomato plants. Observing the behaviours among these three organisms, their complex interactions and relationships, resulted in the following main research questions arising: If the nematodes were attracted to the bacteria in an environmental situation near a host plant, could their interactions curtail their capacity to infect the host? Could bacterial colonisation on the plant roots impede nematode infection within the plant, and therefore reduce the development of nematodes within the plant, or delay the rate of development? Could the bacteria have an effect on the host plants, with regards to eliciting a systemic response within the plant, to boost their resistance to nematode infection? On the other hand, if the bacteria act as a repellent to the nematode, could this discourage or prevent nematode penetration in host plant roots?

The aims of the research were detailed in this chapter as follows:

- To determine the attraction (or repulsion) of the nematodes *C. elegans*, *M. javanica* and *G. pallida* to *Pseudomonas* species and to the antibiotic 2,4-DAPG.
- To investigate the PGP properties of *P. fluorescens* bacterial strains in PPN infected plants.
- To assess the influence of PGP bacteria and 2,4-DAPG on PPN development in plants.

- To explore the capacity of PGP bacteria and 2,4-DAPG treated plants to elicit induced systemic resistance to PPN infection.

3.2 Materials and Methods

Experiments were carried out with appropriate replications and controls. All culturing was carried out using good laboratory practice to prevent cross contamination of stocks, and under strict quarantine and containment regarding PPN.

Statistical analyses were performed on the data with the package SPSS version 23 (IBM SPSS statistics for windows, 2017), unless otherwise stated. Outliers were assessed by box-plot. All data was statistically assessed by non-parametric analysis, as the homogeneity of variances (Levene's test) and assumption of normality (Shapiro-Wilk test) were violated. The non-parametric analysis determined significant differences among all treatments. Post hoc analysis was carried out with Dunn (1964) procedure with a Bonferroni correction to compare significant differences between the bacterial treatments and the control treatment, unless otherwise stated. The statistical significance was set at $\alpha = 0.05$ level for all tests. The data were presented as ± standard error of the mean (SEM).

3.2.1 Nematode Attraction to PGP Bacteria and 2,4-DAPG

3.2.1.1 Nematode and Bacterial Maintenance and Treatment Preparation

Nematode attraction to PGP bacterial strains F113, L124, L222 and, L321 and to 200 ppm 2,4-DAPG was determined. The bacterial strains, along with *E. coli* OP50 (food source for *C. elegans*) were cultured in 10 ml nutrient broth (NB) and incubated at 30°C for 24 hours (Chapter 2, Section 2.2.1.1). The bacterial concentration utilised was calculated from the standard curves (Chapter 2, Section 2.2.1.4 and Appendix A A.1). Table 3.1, describes the bacterial concentrations utilised in experiments for Chapter 3. The antibiotic 2,4-DAPG was freshly prepared in 50% methanol (Chapter 2, Section 2.2.4). The stock solution was diluted to 200 ppm.

The nematodes were cultured and maintained as described in Chapter 2 (*C. elegans* in Section 2.2.2.1, *M. javanica* in Section 2.2.2.2 and *G. pallida* in Section 2.2.2.3). Potato root diffusate (PRD), a natural stimulant for *G. pallida* (Bezooijen, 2006), was prepared as in Chapter 2 (Section 2.2.2.3.1). Tomato root diffusate (TRD) a natural stimulant for *M. javanica* was prepared, according to Yang *et al.* (2016). Tomato plants, 4-6 weeks old, were carefully uprooted from their pots and the roots were washed free of soil. The plants were placed into a 500 ml beaker containing 300 ml sterile dH_2O overnight at 21°C to enable the root exudates to disperse within the water. The water in the beaker was filter sterilised and stored in 50ml aliquots at -20°C for further use.

TABLE 3.1: Bacterial and antibiotic concentrations utilised in Chapter 3 for attraction assays, nematode development and induced systemic resistance (ISR) in tomato plant experiments.

Strain	Concentration (CFU/ml)		
	Attraction	**Development**	**ISR**
F113	7.78 x 10^9	6.44 x 10^8	6.44 x 10^8
L124	8.89 x 10^9	3.11 x 10^6	3.11 x 10^6
L228	2.33 x 10^9	3.56 x 10^8	3.56 x 10^8
L321	4.89 x 10^8	4.89 x 10^8	4.89 x 10^8
	Concentration (ppm)		
2,4-DAPG	200	200	200

3.2.1.2 Chemotaxis Assay Establishment

The experiment was designed similarly to Jagodič *et al.* (2017). The assay was established on Petri dishes (55 x 16 mm) containing 3 ml sterile 0.8% nutrient agar (NA). The Petri dish was divided into three sections called zones, as shown in Figure 3.1. Zone A = Treatment (bacterial or antibiotic), Zone B = Nematode application (*C. elegans*, *M. javanica* or *G. pallida*) and Zone C = Attractant (*E. coli* OP50, TRD or PRD). There were seven replications of each treatment. The control treatment 1 was established by replacing the bacterial treatment with NB and control treatment 2 involved replacing the antibiotic treatment with 50% methanol) see Table 3.2.

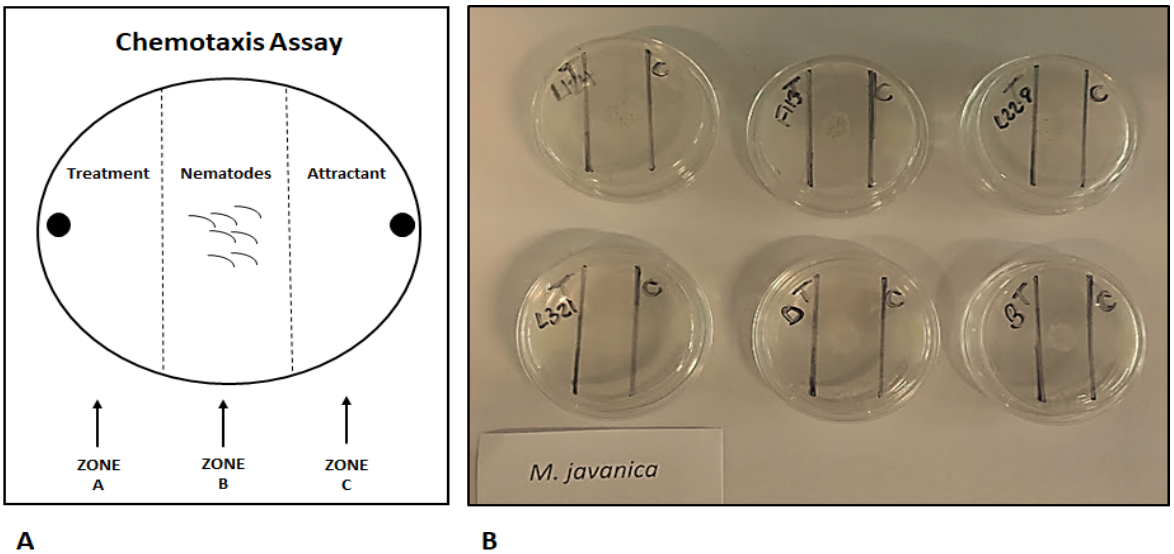

FIGURE 3.1: Chemotaxis index (CI) plate establishment. Figure A: The plates were divided into three zones. A = Treated area (PGP bacteria or 2,4-DAPG), B = Nematode application (*C. elegans*, *M. javanica* or *G. pallida*) and C = Attractant (*E. coli* OP50 or TRD or PRD) see Table 3.2. Figure B: Example of *M. javanica* chemotaxis assay establishment with PGP bacterial, the antibiotic and the control treatment.

The treatment area, Zone A on the test plates contained 10 μl bacteria, either strains F113, L124, L228 or L321 (see Table 3.1 for bacterial concentration) or 10 μl 200 ppm 2,4-DAPG (Figure 3.1A). *Caenorhabditis elegans* (50 nematodes per replication), *M. javanica* (40 nematodes per replication) and *G. pallida* (40 nematodes per replication) were applied to Zone B (Figure 3.1B) in 10 μl water suspension. Different numbers of nematodes were utilised due to availability. In the attractant section, Zone C, 10 μl of *E. coli* OP50, TRD or PRD were added to the Petri dish (Figure 3.1C). *Escherichia coli* OP50, TRD and PRD were utilised as they acted as natural stimulants/ food source to *C. elegans*, *M. javanica* and *G. pallida*, respectively. To Zone A on the control treatment 1 plate, 10 μl NB was added, and 10 μl 50% methanol was added to Zone A on the control treatment 2 plates. These control plates were established to determine if the nematodes were attracted to the broth the bacterial strains were cultured in, or the methanol the 2,4-DAPG was dissolved in. Zones B and C in the control treatment plates were established as for the bacterial and antibiotic treatment plates (Table 3.2).

TABLE 3.2: Chemotaxis assay establishment. The treatments, nematodes and attractants utilised for each assay. There were seven replications of each treatment.

	Zone A	**Zone B**	**Zone C**
Bacterial treatment [1]1	F113	*C. elegans*	*E. coli* OP50
		M. javanica	TRD[2]
		G. pallida	PRD[3]
Bacterial treatment 2	L124	*C. elegans*	*E. coli* OP50
		M. javanica	TRD
		G. pallida	PRD
Bacterial treatment 3	L228	*C. elegans*	*E. coli* OP50
		M. javanica	TRD
		G. pallida	PRD
Bacterial treatment 4	L321	*C. elegans*	*E. coli* OP50
		M. javanica	TRD
		G. pallida	PRD
Antibiotic treatment	200 ppm 2,4-DAPG	*C. elegans*	*E. coli* OP50
		M. javanica	TRD
		G. pallida	PRD
Control treatment 1	NB[4]	*C. elegans*	*E. coli* OP50
		M. javanica	TRD
		G. pallida	PRD
Control treatment 2	50% methanol	*C. elegans*	*E. coli* OP50
		M. javanica	TRD
		G. pallida	PRD

1 Bacterial treatment = *P. fluorescens* strains

2 TRD = Tomato root diffusate

3 PRD = Potato root diffusate

4 NB = Nutrient broth

The assay plates were stored at 20°C for 4 and 24 hours. After this time, the nematodes were immobilised on the plates by exposing them to -20°C for three minutes to stop the assay. The nematode percentage directional response was assessed by counting the number or nematodes that moved from Zone B to either Zone A or Zone C, and the Chemotaxis Index (% CI) was determined according to Jagodič *et al.* (2017) utilising the following equation:

$$\text{CI} = \frac{\text{Number of nematodes in the treatment - Number of nematodes in Control}}{\text{Total Number of nematodes in the assay}}$$

The equation is described as, the number of nematodes in the treatment (refers to the number of nematodes in Zone A on the Petri plate) minus the number of nematodes in the control (refers to the number of nematodes in Zone C on the Petri plate). The total number of nematodes in the assay is the number of nematodes initially added to Zone B at the start of the experiment. The CI criteria are described in Table 3.3. Although 1.0 equals perfect attraction and -1.0 equals perfect repulsion, the criteria were modified by Jagodič *et al*., 2017 to describe CI results with weaker attraction or repulsion observed.

TABLE 3.3: Chemotaxis Index (Jagodič *et al.*, 2017) for determining nematode attraction to bacterial and antibiotic treatments.

Chemotaxis Index	Description
1.0	Perfect attraction
$\geq$ 0.2	Attractant
0.2 to 0.1	Weak attractant
0.1 to -0.1	No effect
-0.1 to -0.2	Weak repellent
$\leq$ -0.2	Repellent
-0.1	Perfect repulsion

3.2.2 Influence of PGP Bacteria and 2,4-DAPG on *Meloidogyne javanica* Development in Plants

3.2.2.1 Establishment of a Plant Trial to Assess *Meloidogyne javanica* Development in Tomato Plants Inoculated with PGP Bacteria or Spiked with 2,4-DAPG

Topsoil was autoclaved and passed through a 2 mm sieve to remove stones or large debris. Plastic pots, 8 cm in diameter, were filled with 350 g of sterile soil each. Bacterial strains, F113, L321, L124 and L228, were cultured in 10 ml NB and incubated at 30°C for 24 hours (Chapter 2, Section 2.2.1.1). The bacterial OD was read on a spectrophotometer at $OD_{(600)}$ 0.8 and the bacterial concentration utilised was calculated from the standard curves (Chapter 2, Section 2.2.1.4 and Appendix A, Section A.1). Table 3.1 describes the bacterial

concentrations utilised in this experiment. 25 ml of bacterial cultures, were added to the soil in each pot. The antibiotic 2,4-DAPG, was freshly prepared in 50% methanol (Chapter 2, Section 2.2.4). 4 ml 200 ppm 2,4-DAPG was added to the soil of in each pot. The treated soils were mixed well to ensure even distribution of bacteria or antibiotic.

TABLE 3.4: Experimental design to assess *M. javanica* development in tomato plants inoculated with PGP bacteria or spiked with 2,4-DAPG. There were 18 replications of each treatment, with six pots assessed after 20, 50 and 70 days post inoculation, respectively.

	Strain	**Nematode**	**Plant**
Bacterial treatment [1]1	F113	*M. javanica*	Tomato
Bacterial treatment 2	L124	*M. javanica*	Tomato
Bacterial treatment 3	L228	*M. javanica*	Tomato
Bacterial treatment 4	L321	*M. javanica*	Tomato
Antibiotic treatment	2,4-DAPG	*M. javanica*	Tomato
Control treatment 1	- [2]	*M. javanica*	Tomato
Control treatment 2	-	-	Tomato

1 Bacterial treatment = *Pseudomonas fluorescens* strains

2 - = Not present in the pot

After the application of each treatment, one 2 week old tomato plant (*Solanum lycopersicum* var. 'Money maker') was planted in each pot. The plants were left to establish for 1 week before 1000 *M. javanica* J2 infective juveniles were added to the roots of each plant. The nematodes were added to three 2 cm deep holes, 1 cm from the plant base. The pots were kept on trays in a plant growth room set to 22°C with 16 hours of light and 8 hours of darkness. The control treatments were established at the same time, Control 1 = nematodes and no bacteria, Control 2 = no nematodes and no bacteria (see Table 3.4 for experimental design). There were 18 replications of each treatment, with six pots assessed after 20, 50 and 70 days post-inoculation, respectively (Martinuz *et al.*, 2012). Bacterial treatments were added to the relevant pots a further two times throughout the plant trial, after 20 and 50 days, in the form of a bacterial drench. After this time the plants were harvested (Appendix B, Figure B.2), the roots, stem and leaf were measured and weighed, and the number of leaves per plant was counted. The plant roots were stained (Section 3.2.2.2) and assessed for nematode infection with a microscope [Optika] at each harvest. Once the severity of nematode infection was determined (Section 3.2.2.3), the roots, stem and leaf were oven dried at 60°C and the plant biomass was calculated.

3.2.2.2 Staining Plant Roots

Tomato roots were carefully rinsed to remove soil particles, and a stock solution of acid fushin was prepared (25 ml glacial acetic acid, 75 ml dH_2O and 0.35 g acid fushin dissolved)

according to Byrd *et al.* (1983). Tomato roots (1 g) were added to 50 ml dilute sodium hypochlorite (5.25% NaOCl) solution in a 250 ml beaker, for four minutes, swirling occasionally. The contents of the beaker were poured over a 1 mm mesh sieve and the tissue was rinsed under a tap for 45 seconds. The roots were placed into a 250 ml beaker with 150 ml water for 15 minutes. After which, the roots were added to a 250 ml beaker containing, 50 ml water and 1 ml acid fushin stock solution. The beakers were boiled on a hot plate for 30 seconds in a fume hood, after which, the stained roots were removed with a forceps and was placed onto a 1 mm mesh sieve. The roots were washed under tap water, blotted dry (Figure 3.2, Image A) and stored in labelled 50 ml tubes containing 30 ml acidified glycerol (3ml 5M HCl in 100 ml glycerol). Larger roots from 50 and 70 days old plants were cut into sections up to 5 cm long, prior to staining.

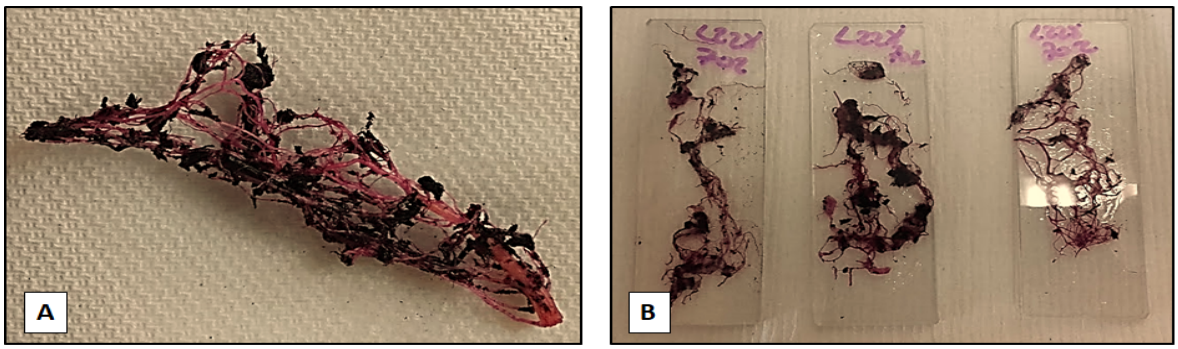

FIGURE 3.2: Tomato roots 70 days post nematode infection, stained with acid fushin (A) and mounted between two glass slides (B) prior to identifying nematode development in the roots.

3.2.2.3 Determining Nematode Infection

The stained roots were removed from the acidified glycerol, blotted in tissue paper to remove any excess and mounted onto slides. The roots were gently pressed between two glass slides (Figure 3.2, Image B) to increase the visibility of nematodes within plant tissues. The length of plant tissue in the glass slide was observed under a high powered microscope (Optika) at 10x magnification. The presence of nematodes was recorded, their developmental stage (Table 3.5) was noted and their numbers were counted. Feeding sites and the number of egg masses were also counted and digital images were captured.

TABLE 3.5: Description of *M. javanica* life stages for identification in tomato plant roots (Dávila-Negrón and Dickson, 2013; Eisenback and Triantaphyllou, 2009).

Life Stage	Description
J2 Infective juvenile	Vermiform shape
J3/ J4 stage	Saccate, swollen sack like
Young Adult Female	Swollen, pear-shape body, non-egg laying stage
Mature Adult Female	Swollen, pear to globose shape body, egg laying stage
Feeding site	Cluster of enlarged plant cells or giant cells
Egg mass	Groups of eggs in gelatinous matrix

3.2.3 Resistance of Treated Tomato Plants to *M. javanica* Infection: Split Root System

3.2.3.1 Induced Systemic Resistance: Part I

Bacterial strains, F113, L321, L124 and L228, were cultured as described in Section 3.2.2.1. The bacterial OD was read on a spectrophotometer at $OD_{(600)}$ 0.8 and the bacterial concentration utilised was calculated from the standard curves (Chapter 2, Section 2.2.1.4 and Appendix A.1). Table 3.1 describes the bacterial concentrations utilised in this experiment. The antibiotic 2,4-DAPG was freshly prepared in 50% methanol (Chapter 2, Section 2.2.4) prior to use.

Topsoil was autoclaved and passed through a 2 mm sieve to remove stones or large debris. Tomato seeds (*Solanum lycopersicum* var. 'Money maker') were surface sterilised in 95% ethanol for 3 minutes and planted in pots, 8 cm in diameter, filled with 350 g of sterile soil. After 3 weeks, the tomato seedlings were uprooted, washed with tap water and the roots were split into two halves with a sterilised dissecting scalpel. Each half of the root system was immediately transplanted into two separate pots 8 cm in diameter (Figure 3.3). The pots contained 350 g soil per pot and the two pots were attached together on the outside with a masking tape. A plastic plant label was placed between the two pots and provided support to the plant.

TABLE 3.6: Induced systemic resistance of treated tomato plants to *M. javanica* infection, the experimental design. There were six replications of each treatment for each experiment.

	ISR I		**ISR II**	
	Left	**Right**	**Left**	**Right**
Bacterial treatment [1]1	F113	MJ	MJ	F113 + MJ
Bacterial treatment 2	L124	MJ	MJ	L124 + MJ

Continued on next page

Table 3.6 – *Continued from previous page*

	ISR I		ISR II	
	Left	**Right**	**Left**	**Right**
Bacterial treatment 3	L228	MJ	MJ	L228 + MJ
Bacterial treatment 4	L321	MJ	MJ	L321 + MJ
Antibiotic treatment	DAPG	MJ	MJ	DAPG + MJ
Control treatment	- [2]	MJ	MJ	MJ

1 Bacterial treatment = *P. fluorescens* strains

2 - = Nothing added to the pot

The treatment was added to the root system on the left (Figure 3.3, Image 1), either 25 ml bacterial culture or 4 ml 200 ppm 2,4-DAPG. The plants were left to establish for one week to ensure bacterial colonisation had taken place. After this time 1000 *M. javanica* J2 infective juveniles were added to the root system on the right (Table 3.6). The control treatment had nematodes added to the root system on the right with no bacterial strains or antibiotic added to the soil (Figure 3.3, Image 2). There were six replications of each treatment (bacterial, antibiotic or control). After 30 days post nematode infection, the plants were carefully removed from the pots. A piece of nylon thread was tied around the root system from the left pot, to distinguish it from the root system from the right pot. Tomato roots were rinsed with tap water to remove soil and blotted on tissue paper. Their height was measured and the number of leaves was counted. The fresh weight was recorded and the roots were stained by boiling them in 0.1% lactic acid fuchsin (Section 3.2.2.2). The number of adults, feeding sites and egg masses were identified in the roots and recorded. After this, the roots, stem and leaves from both sides of the plant were oven dried at 60°C and the plant biomass was calculated.

3.2.3.2 Induced Systemic Resistance: Part II

The second experiment was prepared and established as described in Section 3.2.3.1. However, to the root system on the right (Figure 3.4, Image 3), the treatment was added, either 25ml bacterial culture or 4 ml 2,4-DAPG. The plants were left to establish for one week and to ensure bacterial colonisation had taken place. After this time, 1000 *M. javanica* J2 infective juveniles were added to the root system on the right and left. In the control treatment (Figure 3.4, Image 4) nematodes were added to the left and right root systems, with no other treatments added to the pots (Table 3.6). There were six replications of each bacterial or antibiotic treatment and control treatment. After 30 days post nematode infection, the plants were removed from the pots. Plant height and number of leaves per plant were recorded. The

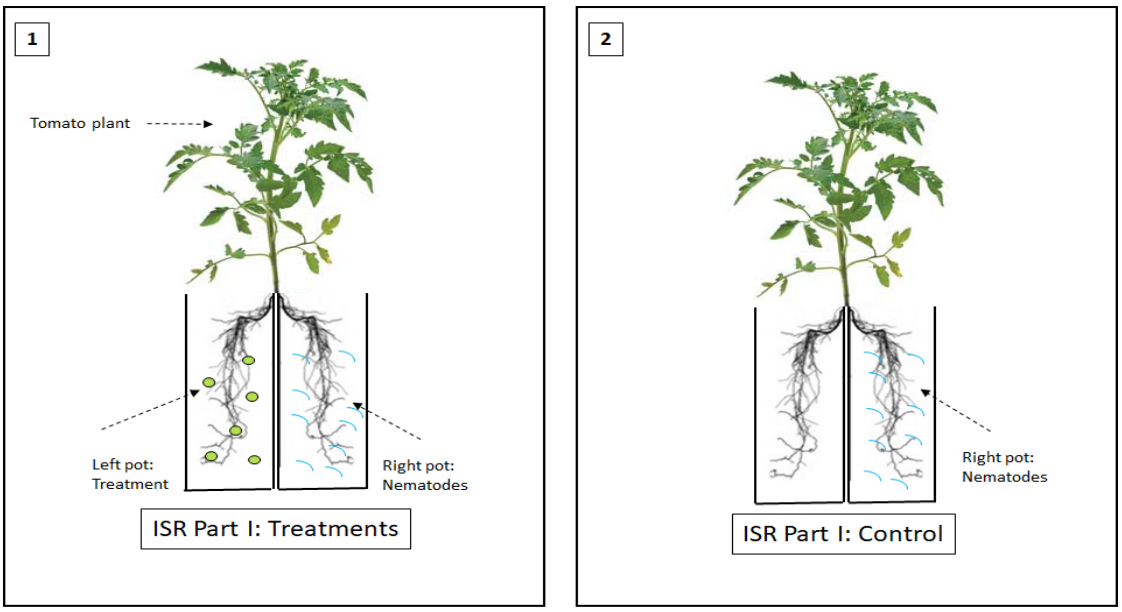

FIGURE 3.3: Schematic representation of the ISR Part I experiment establishment (Siddiqui and Shaukat, 2003). Treated (Image 1): Bacterial strains or the antibiotic were added to the pots on the left and *M. javanica* J2 were added to the pots on the right. Control (Image 2): No bacteria or antibiotic were added to the pots on the left but nematodes were added to the pot on the right.

fresh and dry weight of the plants were determined. The roots were stained and the number of nematode adults, feeding sites and egg masses was counted.

3.2.4 Statistical analysis

The data for each experiment failed the assumption of a normal distribution (Shapiro Wilk, $p > 0.05$). A Kruskal Wallis H test was employed with the post hoc test, Bonferroni pairwise correction. This statistical test was performed on the following experiments, (A) Nematode attraction to treatments and the chemotaxis Index, (B) plant biomass in nematode development and ISR experiments, (C) nematode development in tomato plants, all life stages and (D) induced systemic resistance to *M. javanica* infection, Part I and Part II.

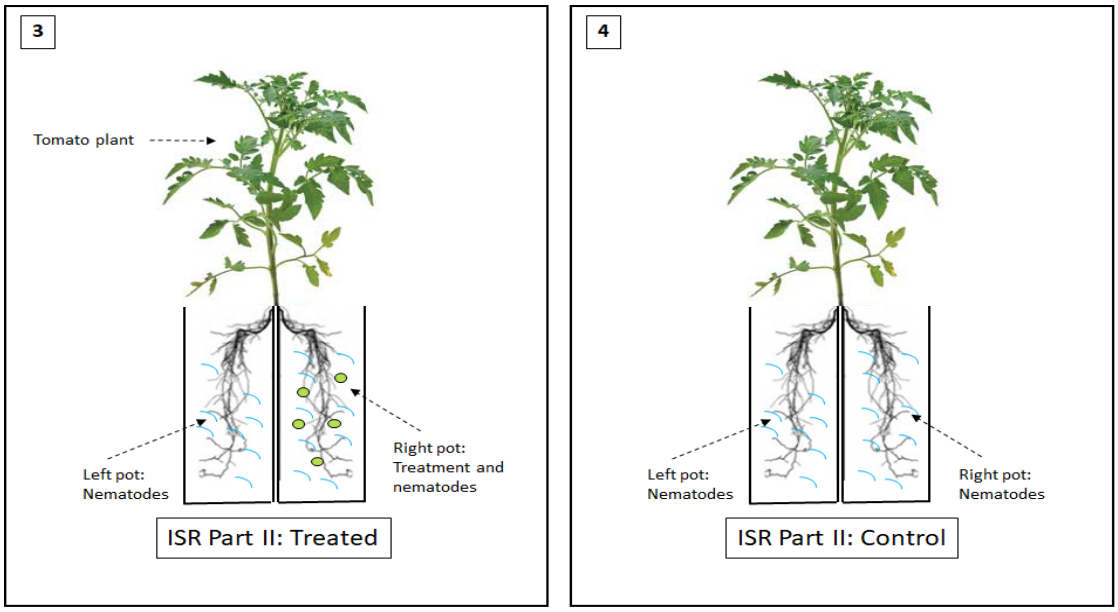

FIGURE 3.4: Schematic representation of the ISR Part II experiment establishment (Siddiqui and Shaukat, 2003). Treated (Image 3): Bacterial strains or the antibiotic were added to the pots on the right, and *M. javanica* J2 were added to the pots on the right and left. Control (Image 4): No bacteria or antibiotic were added to the pots but nematodes were added to the pot on the right and left.

3.3 Results

3.3.1 Nematode Attraction to PGP Bacteria and 2,4-DAPG

3.3.1.1 Chemotaxis Assay Assessment

Bacterial treatment L124 acted as a weak repellent (see Table 3.3 for the criteria determining attraction and Table 3.7 for results) to *C. elegans* (CI = -0.19%) and a weak attractant to *G. pallida* (CI = 0.15%) after 4 hours respectively. *Globodera pallida* attraction to L124 was significantly different to the control (p = 0.012; see Table B.1). *Caenorhabditis elegans* was weakly attracted to strain L321 after 4 hours (CI = 0.11%) and 24 (CI = 0.14%) hours. *Caenorhabditis elegans* was not attracted to the antibiotic 2,4-DAPG, a repellent response was determined according to Jagodič *et al*., (2017; Table 3.3) after 4 (CI = - 0.41%) and 24 (CI = - 0.37%) hours exposure. *Meloidogyne javanica* were weakly repelled to the antibiotic after 4 hours. The control treatment acted as a repellent to *C. elegans* after 4 (CI = - 0.23%) and 24 (CI = - 0.25%) hours, however it had no effect on the other nematode taxa.

TABLE 3.7: Nematode attraction to PGP bacterial and antibiotic treatments, as assessed by the chemotaxis Index (Jagodič *et al*. 2017).

Treatments	**Chemotaxis Index**					
	Caenorhabditis elegans		***Meloidogyne javanica***		***Globodera pallida***	
	4 hours	**24 hours**	**4 hours**	**24 hours**	**4 hours**	**24 hours**
L124	WR	NE	NE	NE	WA *[1]	NE
F113	NE	NE	NE	NE	NE	NE
L228	NE	NE	NE	NE	NE	NE
L321	WA	WA	NE	NE	NE	NE
2,4-DAPG	R	R	NE	NE	NE	NE
Control	R	R	NE	NE	NE	NE

1 * = significant difference between the values assigned to L124 and the control (p = 0.012)

WR = Weak repellent, NE = No effect, WA = Weak attractant, WR = Weak repellent, R = Repellent

3.3.2 Influence of PGP Bacteria and 2,4-DAPG on *Meloidogyne javanica* Development in Tomato Plants

3.3.2.1 Effect of PGP Bacteria and 2,4-DAPG on *M. javanica* Infected Tomato Plant Biomass

Mean tomato plant height (Figure 3.5) was greatest for those treated with the antibiotic 2,4-DAPG (Appendix B, Figure B.2), F113 ($p = 0.006$ compared to C1, see Appendix B, Table B.2; Appendix B, Figure B.2) and L124 (Appendix B, Figure B.2) after 20 (30.33 cm), 50 (49.40 cm) and 70 (77.40 cm) days respectively on exposure to *M. javanica*. The mean number of leaves per plant (Figure 3.5) were highest in plant treated with 2,4-DAPG, F113 and L228 after 20 (37.17 leaves), 50 (61.20 leaves) and 70 (94.80 leaves) days respectively when subjected to *M. javanica*. The effect of the treatments 2,4-DAPG, F113 and L124 caused increased tomato stem and leaf fresh weight (Figure 3.6a) after 20 (5.00 g), 50 (17.67 g) and 70 (94.80 g) days respectively in the presence of *M. javanica*. An increase in tomato plant roots fresh weight (Figure 3.6a) was observed in those treated with 2,4-DAPG after 20 (0.28 g) days and F113 and after 50 (0.47 g) and 70 (1.02 g) days respectively on *M. javanica* exposure. The dry weight of tomato plant stem and leaf (Figure 3.6b) was increased in those treated with 2,4-DAPG after 20 days (0.27 g) and F113 after 50 (0.96 g) and 70 (1.36 g) days respectively when subjected to *M. javanica*. The dry weight of tomato roots (Figure 3.6b) were increased in plants treated with F113, L321 and L228 after 20 (0.18 g), 50 (0.40 g) and 70 (0.33 g) days respectively when subjected to *M. javanica* infection.

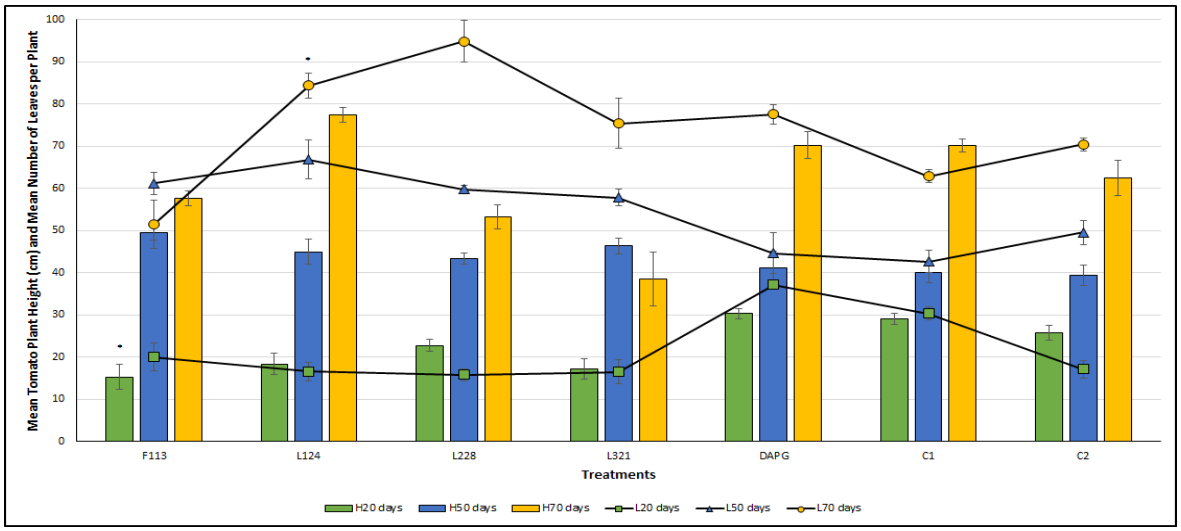

FIGURE 3.5: Mean plant height and leaf number after 20, 50 and 70 days *M. javanica* infection. H = plant height and L = number of leaves. Error bars = ± SEM (see Table B.2 for statistical assessment).

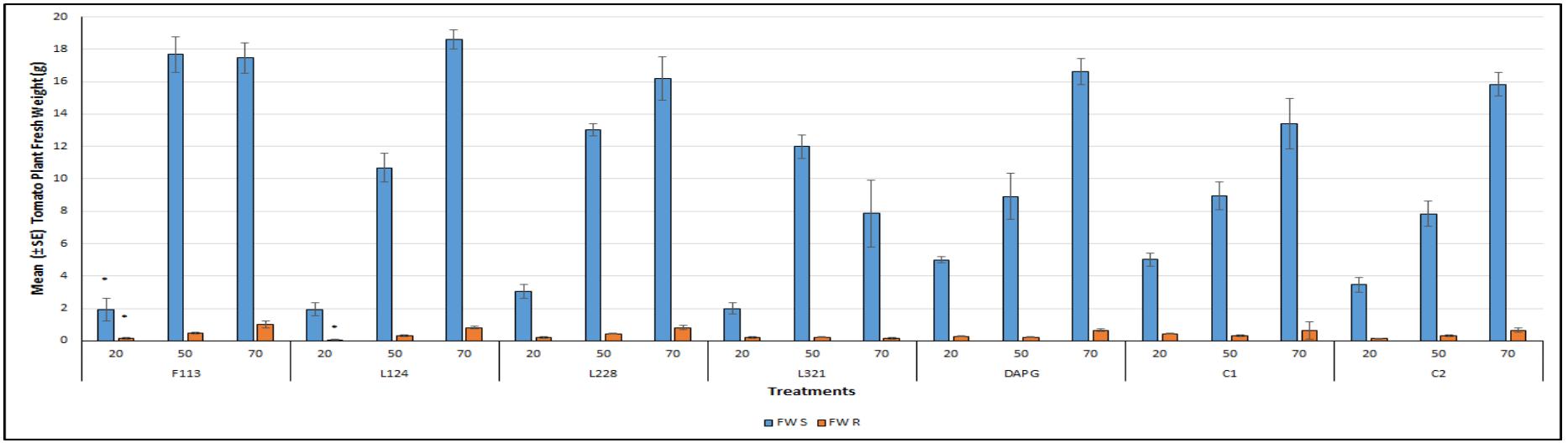

(A)

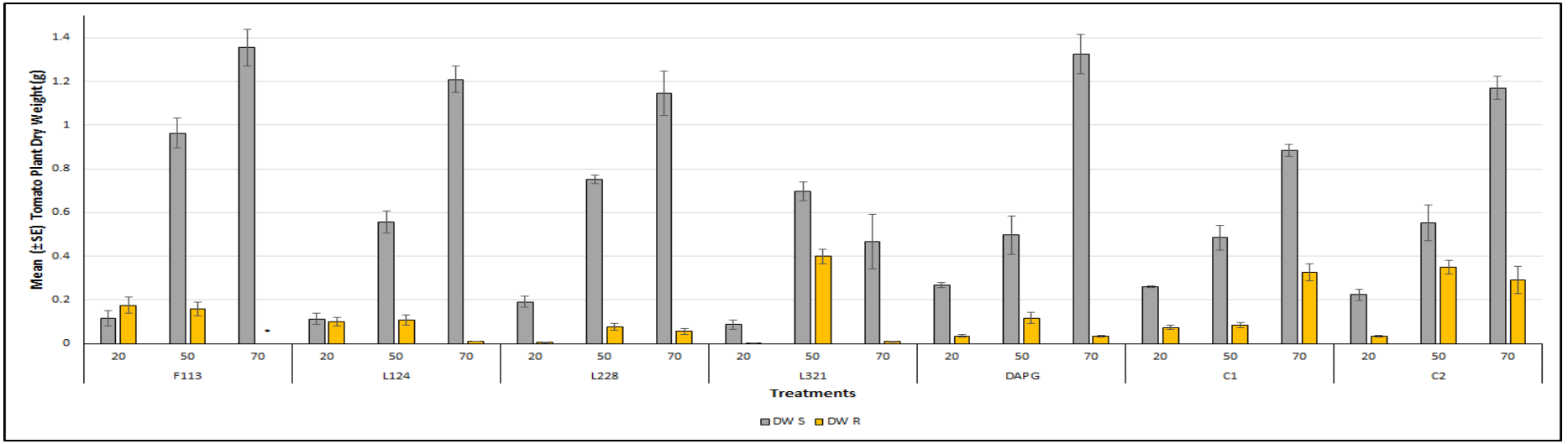

(B)

FIGURE 3.6: Biomass of tomato plants inoculated with PGP bacteria or spiked with 2,4-DAPG after 20, 50 and 70 days *M. javanica* infection. Figure (A) FW = fresh weight, S = stem and leaf and R = roots. Figure (B) DW = dry weight. Error bars = ± SEM, see Appendix B, Table B.2 for statistical assessment.

3.3.2.2 *Meloidogyne javanica* Development in Tomato Plants Treated with PGP Bacterial strains and 2,4-DAPG

3.3.2.2.1 Development after 20 days

Meloidogyne javanica infection in tomato plants after 20 days was low. There were no J2 infective juvenile (Figure 3.9a) present in the roots at this time point (Table 3.8), except in plants treated with F113 (mean = 0.20 nematodes; see Figure 3.7 for visual representation of the life stages). J3/ J4 stage (Figure 3.9b) was highest in plants treated with strain L228 (mean = 2.17 nematodes), compared to those assigned to the control treatment C1 (mean = 0.50 nematodes). There were no J3/ J4 stage nematodes found in plants treated with L124 or 2,4-DAPG. There was a significant difference between those treated with L124 ($p = 0.012$) and the control treatment C1 (Appendix B, Table B.3) in the post hoc test.

TABLE 3.8: Presence of *M. javanica* developmental stages in tomato plants (see Figures 3.7 and 3.8 for visual description on the nematode life stages). Plants were inoculated with bacterial treatments F113, L124, L228, L321 or spiked with antibiotic treatment 2,4-DAPG. Control treatment C1 = Nematodes and no bacteria.

Treatments	**Time after infection**		
	20 days	**50 days**	**70 days**
F113	J2 infective juvenile	Egg mass	Feeding site
	Young adult female	Mature adult female	
L124	Young adult female	Egg mass	J2 infective juvenile
	Mature adult female	J3/ J4 stage	
		Feeding site	
L228	J3/ J4 stage	Egg mass	J2 infective juvenile
	Mature adult female		J3/ J4 stage
	Feeding site		
L321	J3/ J4 stage	Egg mass	Feeding site
	Mature adult female	Young adult female	
2,4-DAPG	Young adult female	Egg mass	J2 infective juvenile
	Mature adult female	J3/ J4 stage	
	Feeding site		
C1	J3/ J4 stage	Egg mass	
	Young adult female	J2 infective juvenile	
	Mature adult female	Feeding site	

Young adult females (Figure 3.9c) were found in plants treated with L124 (mean = 0.40 nematodes) and 2,4-DAPG (mean = 0.33 nematodes), however the largest number was found in the control treatment C1 (mean = 5.68 nematodes). There were significant differences among treatments (Appendix B, Table B.3) at the young adult females life stage ($\chi^2 = 25.47$,

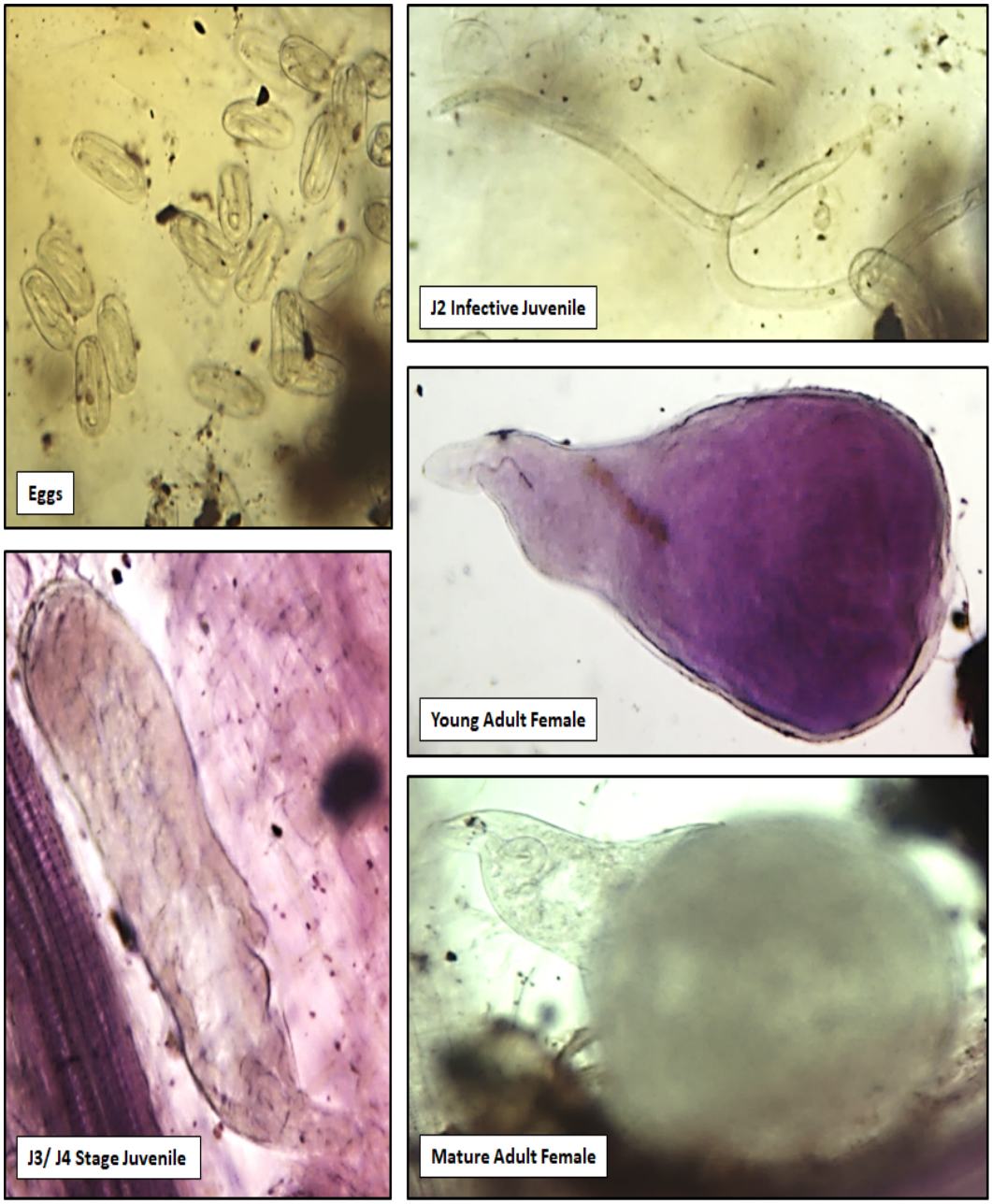

FIGURE 3.7: Development of *M. javanica* in tomato plants inoculated with bacterial and antibiotic treatments. Nematode developmental life stages (Table 3.5) were identified and captured with Optika Vision Pro software: Eggs = from an egg mass in a C1 plant after 50 days. J2 infective juvenile = just hatched from an egg mass in a C1 plant after 50 days. J3/ J4 stage nematode = inside an infection site of a C1 plant after 50 days. Adult males were not observed. Young adult female = located near an infection site of a C1 plant after 20 days. Mature adult female = located beside tomato roots inoculated with L124 after 50 days.

p = 0.000), with significance between the control C1 and the treatments L321 (p = 0.008), F113 (p = 0.003), L228 (p = 0.002) and 2,4-DAPG (p = 0.010) in the post hoc test. Mature adult females (Figure 3.10a) were found in all plants inoculated/ spiked with bacteria and the 2,4-DAPG treatment. The highest number of mature adult females occurred in roots treated with L228 (mean = 6.50 nematodes). The control treatment C1 was higher than all other treatments (mean = 4.00 nematodes), except for those treated with L228. There was a significant difference (Appendix B, Table B.3) between those treated with F113 (p = 0.043) and the control treatment C1 in the post hoc test.

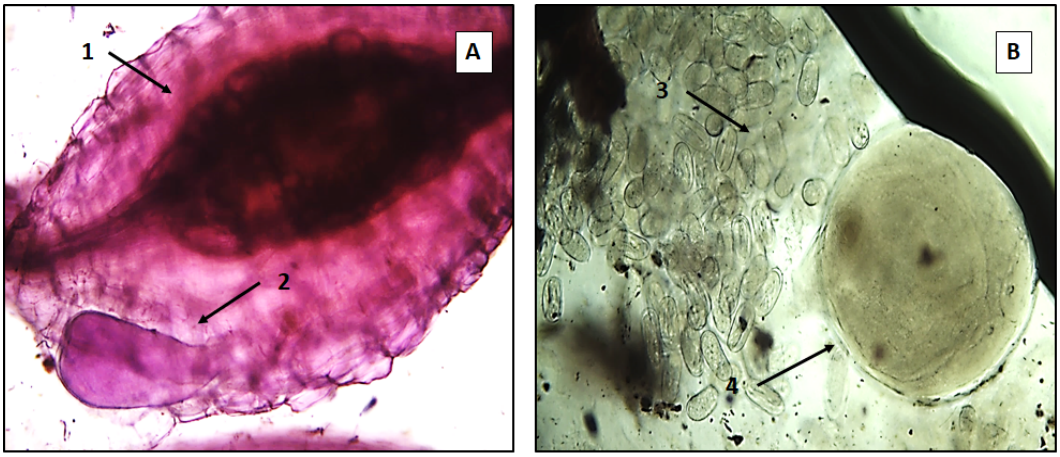

FIGURE 3.8: Development of *M. javanica* feeding site and egg masses in tomato plants inoculated with bacterial and antibiotic treatments. Figure A: (1) Feeding site on a tomato root with enlarged, giant cells and (2) a young adult female at the feeding site. Figure B: (3) An egg mass with (4) a mature adult female.

Feeding sites (Figure 3.10b) were only present in plants treated with L228 (mean = 3.33 sites) and 2,4-DAPG (mean = 0.17 sites) at this time point. There was a significant difference (Appendix B, Table B.3) between the control treatment and bacterial strain L228 (p = 0.004) in the post hoc test. There were no egg masses present in any plants at any of the treatments at this time point.

3.3.2.2.2 Development after 50 days

Development of *M. javanica* in tomato roots after 50 days post-infection, had advanced compared to 20 days post-infection (Table 3.8). There were no J2 infective juveniles (Figure 3.9a) observed in plant roots for any treatments at this time, except for control treatment C1 (mean = 0.40 nematodes; see Figure 3.7 for a visual representation of the life stages). J3/ J4 stage nematodes (Figure 3.9b) were found in the roots of plants of all treatments, with the highest found in plants treated with L124 (mean = 5.60 nematodes). However, the values assigned to the control treatment C1 were the highest (mean = 7.20 nematodes).

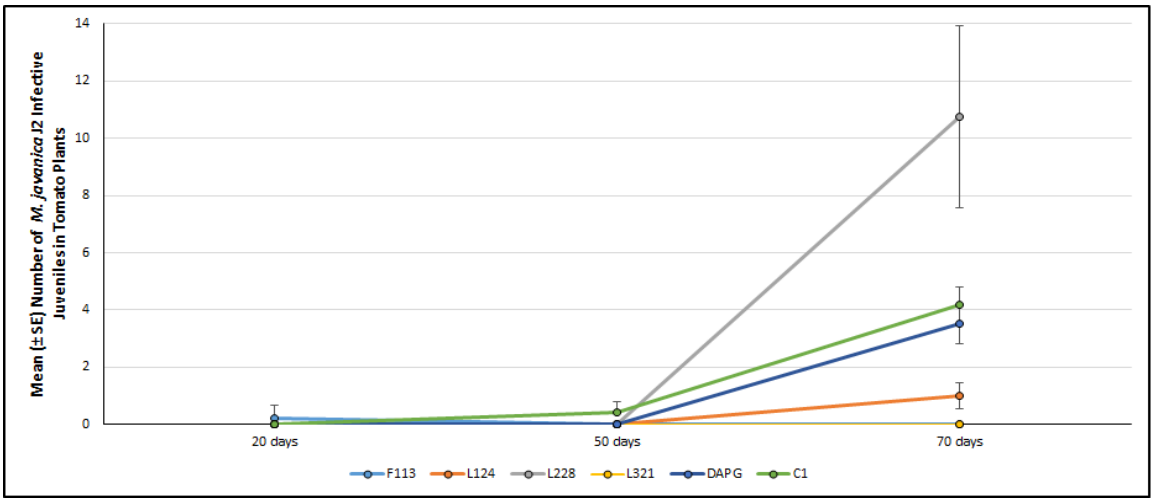

(A)

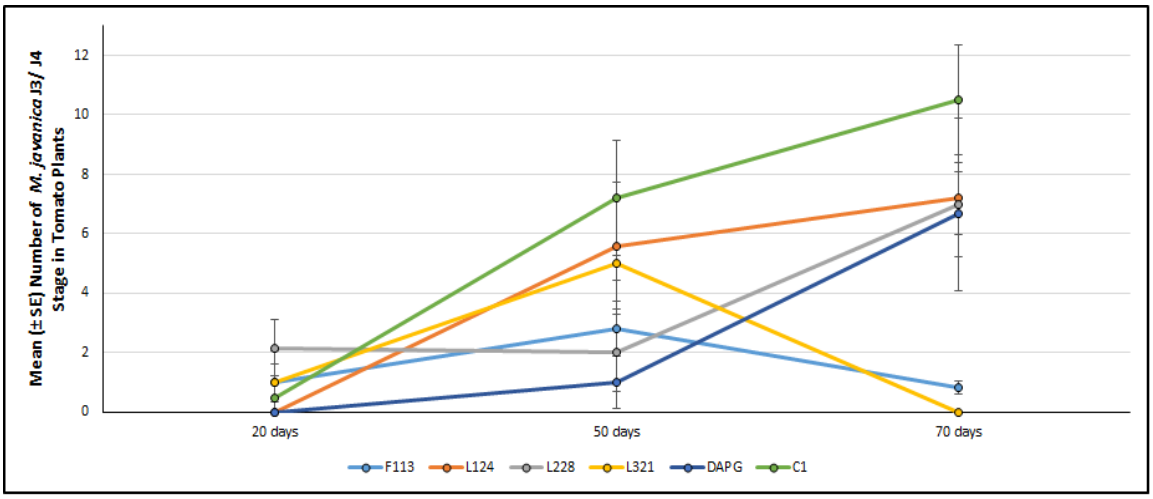

(B)

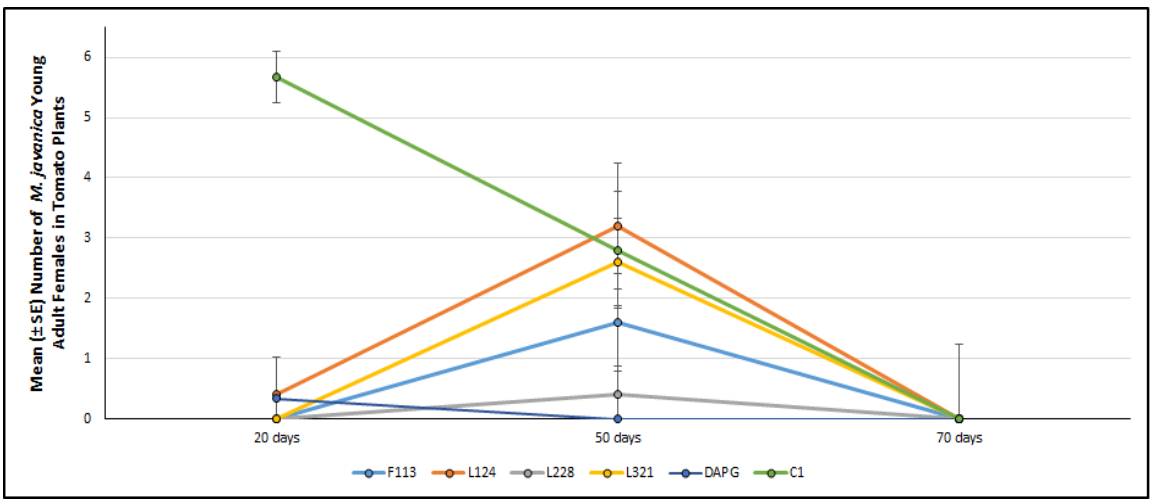

(C)

FIGURE 3.9: Development of *M. javanica* in tomato plants treated with bacteria and 2,4-DAPG, 20, 50 and 70 days post nematode infection. The number of (Figure A) J2 infective juvenile, (Figure B) J3/ J4 stage and (Figure C) young adult female observed at each time are displayed. Error bars represent ± SEM (see Appendix B, Table B.3 for the statistical analysis results).

Young adult females (Figure 3.9c) were found in plants of all treatments, except in plants treated with 2,4-DAPG. Young adult females in plants treated with bacterial strain L124 (mean = 3.20 nematodes) were the highest at this time point. There were significant differences among treatments at the young adult female stage (χ^2 = 13.10, p = 0.042). There were also significant differences between the control treatment C1 and the treatments F113 (p = 0.003), L228 (p = 0.002) and 2,4-DAPG (p = 0.010) in the post hoc test (Appendix B, Table B.3). Mature adult females (Figure 3.10a) were found in plant roots of all treatments and those treated with the bacterial strain L124, had the highest number of mature adults in their roots (mean = 12.40 nematodes). However, the mean number of mature adults present in the control treatment C1, was higher than all other treatments (mean = 10.00 nematodes), except for those treated with L124 and 2,4-DAPG.

Feeding sites (Figure 3.10b) were only observed in roots treated with L124 (mean = 5.20 sites) and L228 (mean = 0.20 sites). There were no feeding sites found in roots of any other treatment or in the control treatment C1. There was a significant difference in the post hoc test for the values assigned to L124 (p = 0.000) when compared to the control treatment C1 (Appendix B, Table B.3). Egg masses (Figure 3.10c)were found in the roots of plants from all treatments. The highest number of egg masses were found in those treated with bacterial strain L228 (mean = 15.40 egg masses). The values assigned to the control treatment were higher (mean = 15.20 egg masses) than all other treatments, except for those treated with L228.

3.3.2.2.3 Development after 70 days

Nematode J2 (Figure 3.9a) infective juveniles (see Figure 3.7 for visual representation of the life stages) were observed in tomato plant roots, treated with L124 (mean = 1.00 nematodes), L228 (mean = 10.75 nematodes) and 2,4-DAPG (mean = 3.50 nematodes). The control treatment C1 (mean = 4.17 nematodes) was high, compared to the other bacterial treatments. Plants treated with L321 and F113 had no J2 stage nematodes present in the roots. There was a significant difference (Appendix B, Table B.3) between control treatment C1 and F113 (p = 0.036), in the post hoc test. J3/ J4 stage (Figure 3.9b) were found in the roots of all treatments except those treated with L321. The highest J3/J4 stage was found in the roots treated with L124 (mean = 7.20 nematodes), followed by L228 (mean = 7.00 nematodes) and 2,4-DAPG (mean = 6.67 nematodes). However, the control treatment C1 for J3/J4 was the highest (mean = 10.50 nematodes).

No young adult females (Figure 3.9c) were observed in any tomato plant roots, from any treatment after 70 days infection. Mature adult females (Figure 3.10a) were present in the roots from all treatments. The highest number were found in plants treated with L124 (mean = 36.40 nematodes). The control treatment C1 was higher than all other treatments (mean = 27.00 nematodes), except for roots treated with L124.

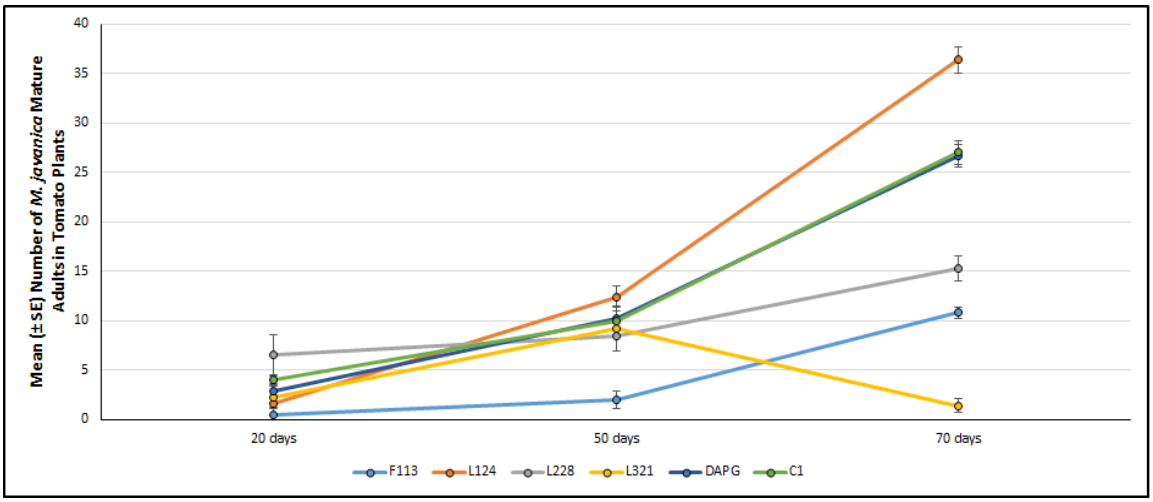

(A)

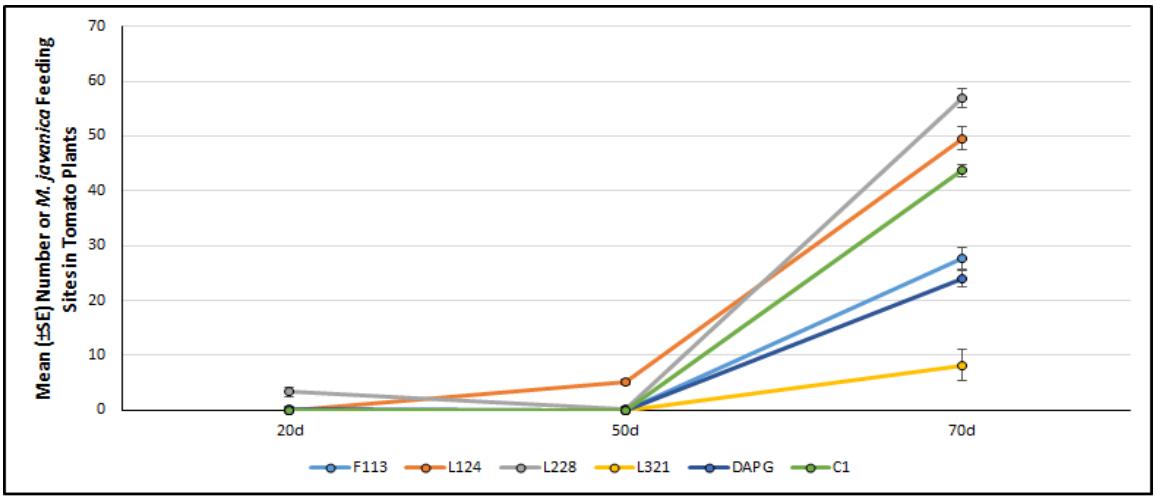

(B)

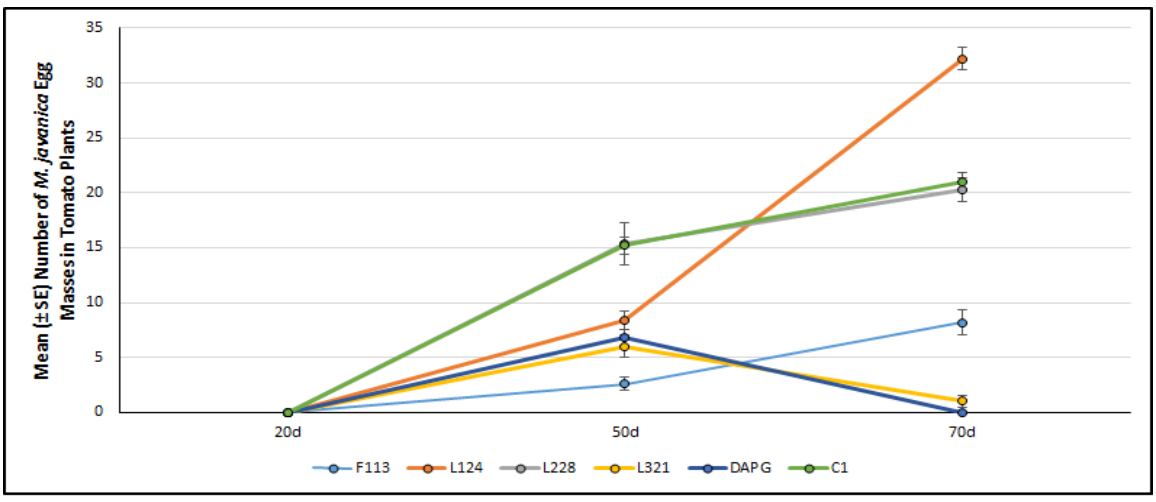

(C)

FIGURE 3.10: Development of *M. javanica* in tomato plants treated with bacteria and 2,4-DAPG, 20, 50 and 70 days post nematode infection. The number of (Figure A) mature adult females, (Figure B) feeding sites and (Figure B) egg masses observed at each time are displayed. Error bars represent ± SEM (see Appendix B, Table B.3 for the statistical analysis results)

Feeding sites (Figure 3.10b) occurred in all treatments, with the highest observed in roots treated with L228 (mean = 57.00 sites). The values assigned to the control treatment, C1 were also high (mean = 43.67 sites), but not as high as those assigned to L228 and L124. Egg masses (Figure 3.10c) were present in the roots of all treatments except for those treated with 2,4-DAPG. The highest number occurred in the roots treated with L124 (mean = 32.20 egg masses). Control treatment C1, was higher than all other treatments (mean = 21.00 egg masses), except for those treated with L124. There was a significant difference between the control treatment C1 and 2,4-DAPG (p = 0.015; see Appendix B, Table B.3).

3.3.3 Resistance of Treated Tomato Plants to *M. javanica* Infection: Split Root System

3.3.3.1 Induced Systemic Resistance: Part I

3.3.3.1.1 Part I: Tomato plant biomass

The mean plant height and the number of leaves 30 days post nematode infection from the first experiment (Figures 3.11a) and 3.12), were recorded. The tallest plants were treated with PGP bacterial strain L124 (mean = 37.10 cm), followed by F113 (mean = 32.50 cm). The control-treated plants (mean = 24.50 cm) were taller than the plants treated with the antibiotic 2,4-DAPG (mean = 21.40 cm). Similarly to the height data, the mean number of leaves (Figure 3.12) were the highest in plants treated with L124 (mean = 43.40 leaves) followed by those in plants treated with F113 (mean = 41.40 leaves). The mean number of leaves for the control treatment (mean = 36.00 leaves) were also higher than plants treated with 2,4-DAPG (mean = 34.80 leaves).

The fresh weights recorded of the stem and leaf (Figure 3.13a) were highest in plants treated with F113 (mean = 6.42 g) followed by plants treated with L228 (mean = 5.26 g). The mean fresh weight of plant roots (Figure 3.13a) was highest in those treated with L124 (mean = 0.30 g) followed by F113 (mean = 0.23 g) and L228 (mean = 0.22 g). The dry weight of plant stem and leaf (Figure 3.13b) was highest in plants treated with bacterial strain L124 (mean = 0.47 g), followed by F113 and L228 (mean = 0.32 g respectively). The mean dry weight of tomato plant roots (Figure 3.13b) was highest in plants treated with L228 (mean = 0.32 g). However, the control plants were heavier than all other treatments (mean = 0.22 g). There were significant differences between the control plant stem and leaf and those treated with 2,4-DAPG (p = 0.000) and L124 (p = 0.046) (Appendix B, Table B.5), in the post hoc test.

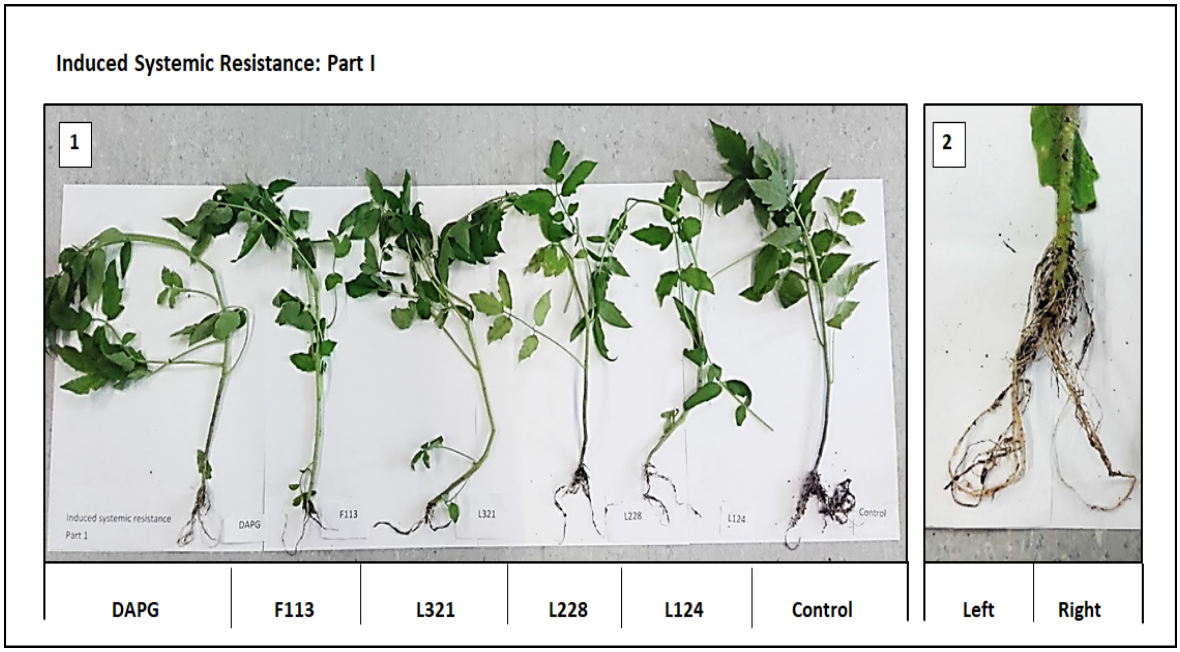

(A)

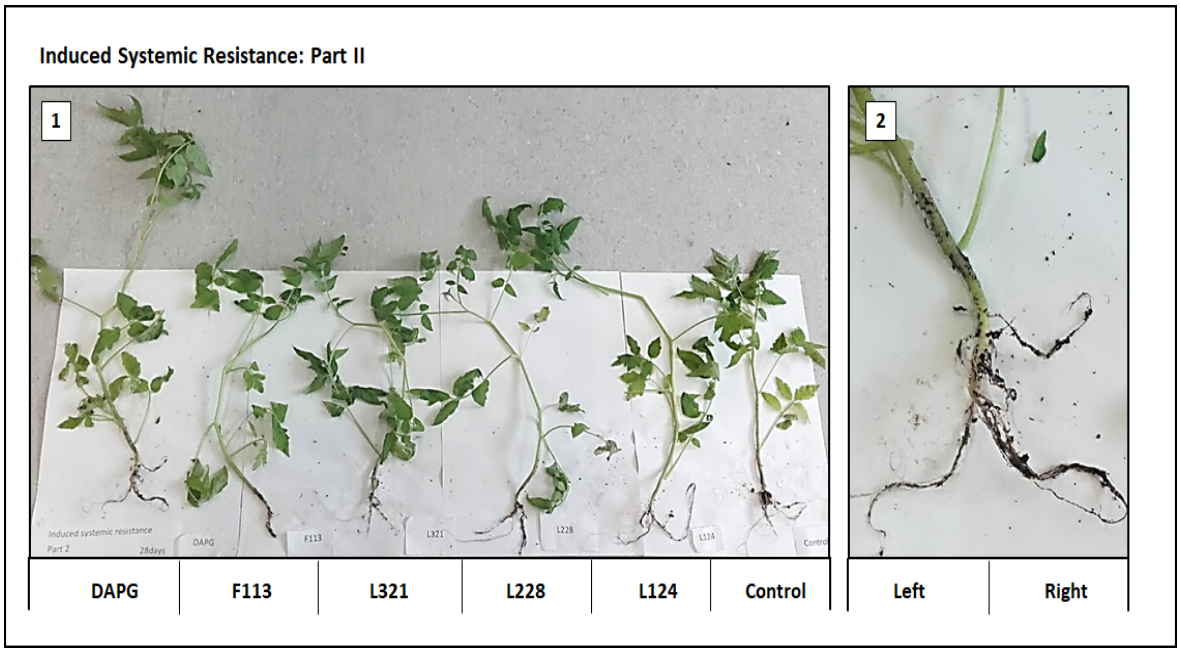

(B)

FIGURE 3.11: Split root tomato plants treated with PGP bacterial strains and 2,4-DAPG. The plants were infected with *M. javanica*, and plant biomass was assessed after 30 days (see Figures 3.3 and 3.4 for details) Figures (1): Representation of tomato plants per treatment, displaying a split root. Figures (2) Established split root system in plants from ISR Part I and Part II.

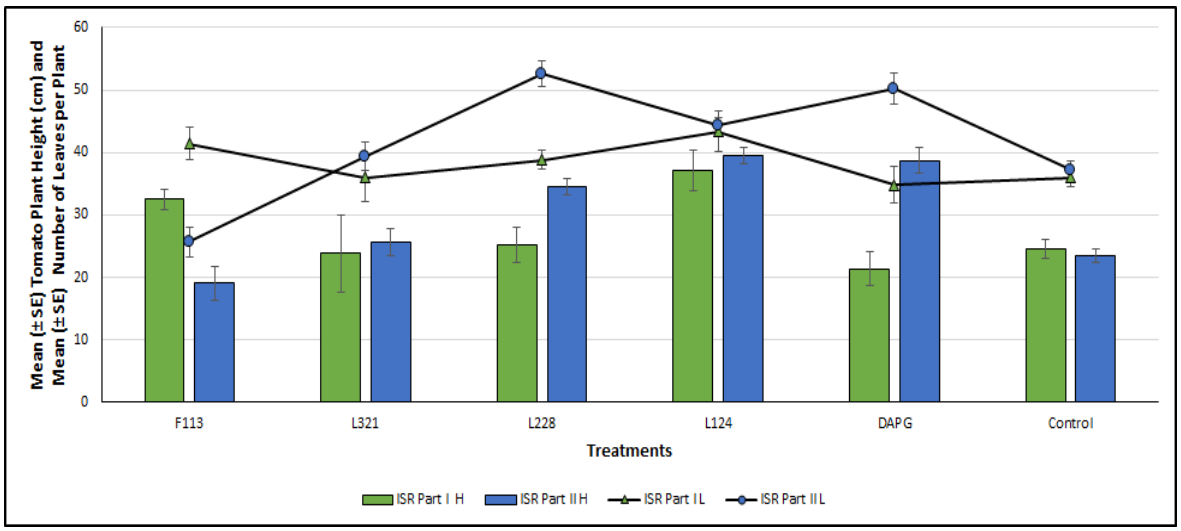

FIGURE 3.12: Mean tomato plant height and number of leaves after 30 days *M. javanica* infection. H = plant height and L = number of leaves assessed in the ISR Part I and Part II experiments. Error bars = ± SEM.

3.3.3.1.2 Part I: Treated tomato plants resistance to *M. javanica* infection

In the ISR trial Part I (Figure 3.3A), the root system in the pot on the left contained no nematodes, infection sites or egg masses in any of the replications for all treatments and control (Figure 3.3 B). The number of adults (Figure 3.14a) in the root system on the right was highest in plants treated with L124 (mean = 7.00 adults), followed by plants treated with L228 (mean = 2.20 adults). In the control treatment, the number of adults was higher (mean = 5.50 adults) than all other treatments, except for those treated with strain L124.

The number of feeding sites (Figure 3.14b) was higher in the root system treated with 2,4-DAPG (mean = 0.67 feeding sites) and L228 (mean = 0.20 feeding sites) when compared to the control roots (mean = 0.17 feeding sites). However, plants treated with F113, L321 and L124 had no feeding sites on their roots. There were no egg masses (Figure 3.14c) present on the roots of any of the plant for any treatment, except for the roots of the control treatment (0.83 egg masses).

3.3.3.2 Induced Systemic Resistance: Part II

3.3.3.2.1 Part II: Tomato plant biomass

The mean plant height and the number of leaves 30 days post nematode infection from the second experiment (Figures (Figure 3.11b) and 3.12), were recorded. The tallest plants, as in ISR: Part I, were those treated with PGP bacterial strain L124 (mean = 45.00 cm). This was followed by plants treated with 2,4-DAPG (mean = 38.75 cm) and L228 (mean = 34.60 cm). The control plants were the smallest plants (mean = 23.42 cm) when compared to the

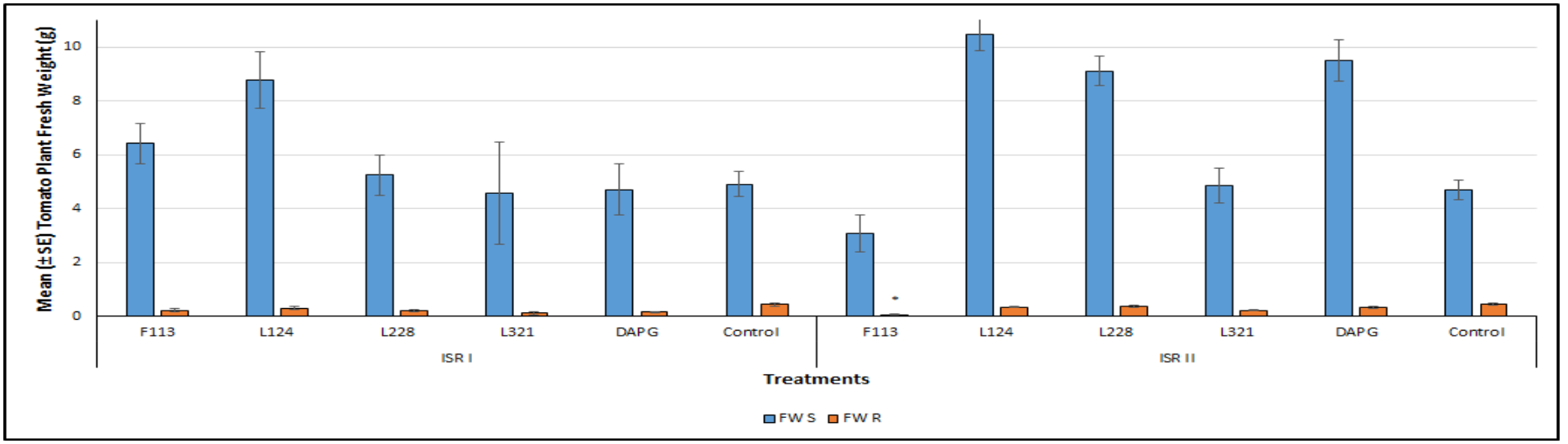

(A)

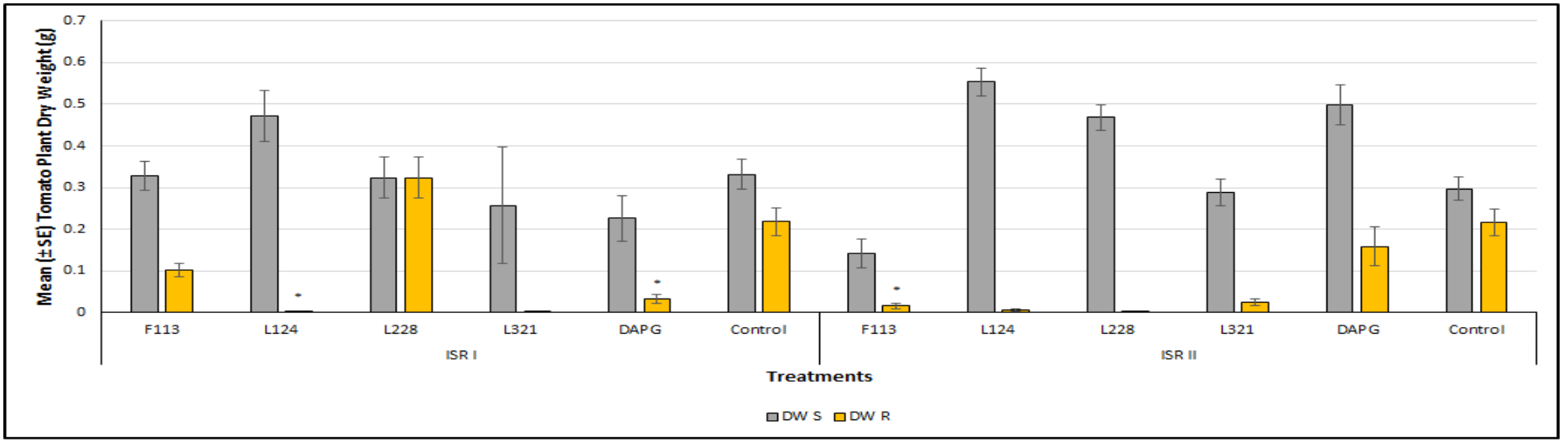

(B)

FIGURE 3.13: Biomass of tomato plants inoculated with PGP bacteria or spiked with 2,4-DAPG after 30 days *M. javanica* infection. Figure (A) fresh weight (FW) of stem and leaf (S), and roots (R) and Figure (B) dry weight (DW) of stem and leaf, and roots were recorded for induced systemic resistance (ISR) experiments, Part I and Part II. Error bars ± SEM, see Appendix B, Table B.5 for statistical assessment.

plant height of all other treatments. The mean number of leaves per plant (Figure 3.12) were highest for those treated with PGP bacterial strain L228 (mean = 52.60 leaves/ plant), this was followed by plants treated with the antibiotic 2,4-DAPG (mean = 50.17 leaves/ plant). The control plants had a low number of leaves (mean = 37.17 leaves/ plant), however plants treated with F113 (mean = 25.67 leaves/ plant) were the lowest.

The fresh weight of stem and leaf (Figure 3.13a) was the heaviest in those plants treated with L124 (mean = 10.50 g) followed by 2,4-DAPG (mean = 9.51 g). The control plants were lower (mean = 4.71 g) than all other treatments except for plants treated with F113 (mean = 3.07 g). The mean fresh weight of tomato roots (Figure 3.13a) was highest for those treated with L228 (mean = p = 0.36 g), followed by L321 and 2,4-DAPG (mean = 0.34 g respectively). However, the control plant roots were higher (mean = 0.44 g) than those in all other treatments. There was a significant difference between the control plants fresh weight of root and bacterial treatment F113 (p = 0.027) (Appendix B, Table B.5), in the post hoc test.

The dry weight of the stem and leaf (Figure 3.13b) was heaviest in plants treated with L124 (mean = 0.55g), followed by 2,4-DAPG (mean = 0.50g). The control plants (mean = 0.30 g) were lower than all other treatments, except for those treated with F113 (mean = 0.14 g). The mean dry weight of plant roots (Figure 3.13b) was heaviest in plants treated with 2,4-DAPG (mean = 0.16 g). However, all other treatments were low (mean = 0.00 - 0.02 g) when compared to the control plants (mean = 0.22 g). There was a significant difference between the control plant dry weight of roots and those treated with F113 (p = 0.048; Appendix B, Table B.5), in the post hoc test.

3.3.3.2.2 Part II: Treated tomato plants resistance to *M. javanica* infection

In the ISR trial Part II (Figure 3.4 A), the number of adults in the root system in the pot on the left were highest in roots treated with L228 (mean = 5.00 adults), followed by 2,4-DAPG (mean = 4.67 adults). The number of adults was lower in the other treatments when compared to the control treatment (Figure 3.4 B; mean = 4.17 adults), with no adult nematodes present in plants treated with F113. In the pots on the right, the highest number of adults were present in the root system that was treated with 2,4-DAPG (mean = 2.00 adults), this was followed by L124 (mean = 1.67 adults) and L228 (mean = 1.60 adults). However, the number of adults in the control plants (mean = 5.17 adults) were the highest.

The mean number of feeding sites in the left root system was highest in plants treated with L124 (mean = 0.67 sites), followed by plants treated with L321 and L228 (mean = 0.40 sites respectively). There were no feeding sites present in roots treated with F113 or 2,4-DAPG. The control (mean = 0.50 sites) was higher than all treatments except for those treated with L124. The number of feeding sites present in the right root system was highest in those treated with 2,4-DAPG (mean = 0.50 sites) followed by L124 (mean = 0.17 sites).

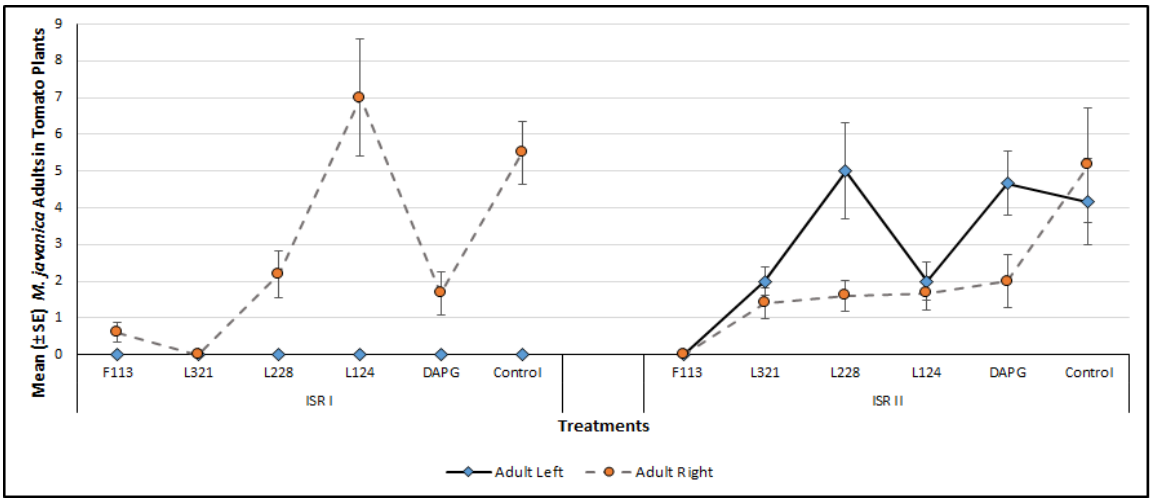

(A)

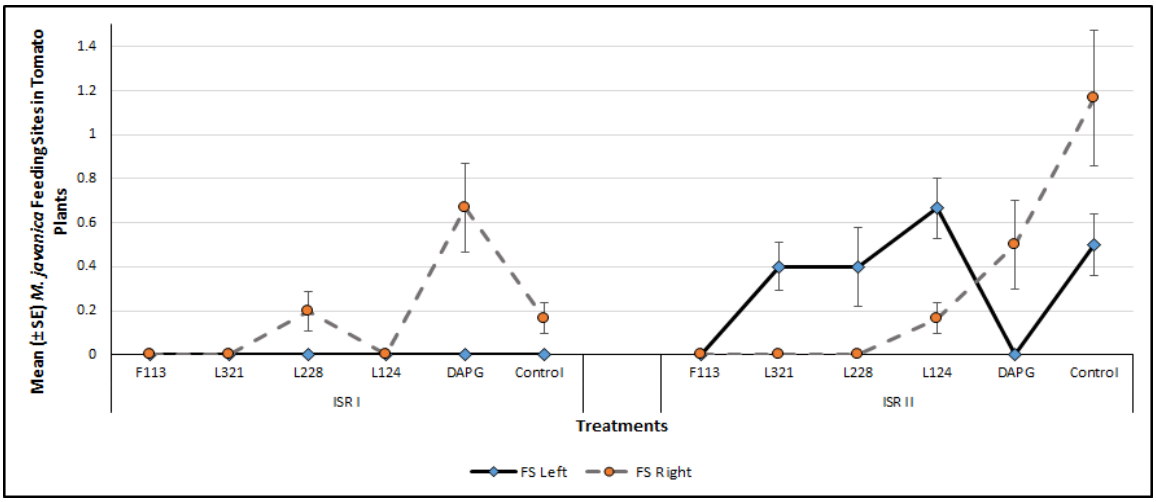

(B)

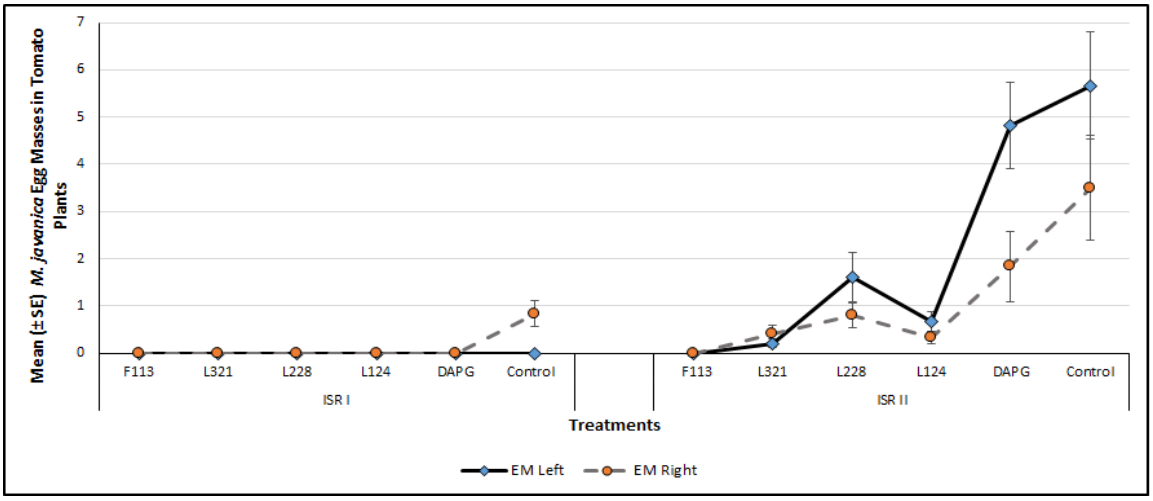

(C)

FIGURE 3.14: *Meloidogyne javanica* infection in tomato plants with a split root system, treated with PGP bacteria and 2,4-DAPG after 30 days. The mean number of adult nematodes (Figure A), feeding sites (FS; Figure B) and egg masses (Figure C; EM) observed in roots from pots on the left and the right, are displayed. Error bars represent ± SEM. Statistical analysis results, see Appendix B, Table B.4.

The control treatment had the highest number (mean = 1.17 sites) compared to all other treatments. There were no feeding sites present in roots treated with F113, L321 or L228.

Egg masses present in the left root system were highest of plants treated with 2,4-DAPG (mean = 1.83 egg masses), followed by L228 (mean = 1.60 egg masses). There were no egg masses present in plants treated with F113. The control plants had the highest number of egg masses (mean = 5.67 egg masses) when compared to all other treatments. Egg masses in the right root system were highest in plants treated with 2,4-DAPG (mean = 1.83 egg masses), followed by L228 (mean = 0.80 egg masses). There were also no egg masses present in roots inoculated with F113. The control plants had the highest number of egg masses (mean = 3.5 egg masses) when compared to all other treatments.

3.4 Discussion

The complex tritrophic interactions between *M. javanica*, bacterial treatments and tomato plants were explored here, in various experiments including (1) attraction of nematodes to bacterial and antibiotic treatments, (2) influence of bacterial and antibiotic treatments on *M. javanica* development in tomato plants and (3) resistance of tomato plants to *M. javanica* infection. This chapter is a continuation of the work carried out in Chapter 2. By focusing on just three beneficial bacterial strains, that proved in Chapter 2 to be the most effective in terms of PGP and biocontrol, and the antibiotic, these interactions were further investigated in this study with a focus on nematode behaviour and biology.

The PGP strains were chosen, to be utilised in the experiments for this chapter were *P. fluorescens* L124, L228 and L321. *Pseudomonas fluorescens* F113 was used in this chapter as a positive control, as it is a well-known producer of 2,4-DAPG (Cronin *et al.*, 1997b; Fenton *et al.*, 1992). The synthetic 2,4-DAPG antibiotic was utilised as a comparison for the DAPG producing strains. The four PGP bacterial strains utilised in this study were previously analysed by gas chromatography-mass spectrometry (GC-MS) in Chapter 2, to identify the compounds the strains were producing, that are associated with PGP and biocontrol. The GC-MS analysis results in Chapter 2 indicated that strain L124 was producing compounds associated with biocontrol (Kim *et al.*, 2000), and that strain L228 produced compounds associated with antimicrobial and antiviral activity (Pandey *et al.*, 2010). The analysis also suggested that the strain L312 produced compounds that were associated with adapting to stresses (Rajalaxmi *et al.*, 2016).

The research area of nematode attraction and chemotaxis is predominantly focused on the nematode response, particularly EPN, to synthetic VOCs (Jagodič *et al.*, 2017), directly to roots (Reynolds *et al.*, 2011) or exploring different media that replicate soil (Hida *et al.*, 2015; Spence *et al.*, 2008). There is no literature published, however, exploring the attraction of the nematodes studied in this chapter, to PGP bacteria in a chemotaxis bioassay. This experiment was established to investigate the nematodes response to their natural chemoattractant, or to the presence of bacterial strains, or the antibiotic (Jagodič *et al.*, 2017), in terms of attraction or repulsion. The chemotaxis attraction assay established by Jagodič *et al.* (2017) investigated the chemosensation of EPN IJ to different VOCs released from *Brassica nigra* roots damaged by cabbage root fly larvae. Like the results obtained in the present study, they found relatively weak attractions between nematodes and VOCs compared to other related publications. In the present study, the PGP strain L321 acted as a weak attractant for *C. elegans* consistently over the two time points. The nematode *G. pallida* was weakly attracted and *C. elegans* was weakly repelled to the bacterial strain L124. This bacterial strain was producing a compound that had an antagonistic effect on the PPN and a positive effect on the bacterial feeding nematode. Although Jagodič *et al.* (2017) were investigating the

attraction of different nematode species and different attractants from those in this study, it is interesting that in the present study, a weak response was also observed.

Plant growth promotion traits of the bacterial strains chosen for this study were explored in the developmental and the ISR experiments by assessing plant biomass. The highest tomato plant biomass overall (including plant height, number of leaves, fresh and dry weight of stem and leaf, and roots) in the development and ISR experiments combined, occurred in plants treated with bacterial strains F113 and L124. The lowest biomass occurred in tomato plants treated with bacterial strain L321, which was also observed by Culhane (2016) in *Lolium perenne*, however, this was not observed by Lally *et al.* (2017) in *Brassica napus* or Otieno *et al.* (2015) in *Pisum sativum* L, who found the bacterial strain to increase biomass.

The plant-based experiments, nematode development and ISR, were established to determine the development and numbers of *M. javanica* in tomato plants and *G. pallida* in potato plants, however, no nematode infection was observed in potato roots in any treatment, at any time point post root staining. The reason for the lack of infection could be temperature. This experiment was conducted in the greenhouse (average temperature of 18 - 25°C) which spanned the summer months. *Globodera pallida* eggs hatch at 10°C or less, and they have adapted to complete their life- cycle between between 10 - 18°C (Rowe, 2017). Due to a lack of space in the plant growth room to establish this experiment, it had to be carried out in the greenhouse at that time. The *G. pallida* cysts utilised in this chapter, from which eggs were extracted, were received from the James Hutton Institute. It is possible that the eggs had degraded, although, it is known that *G. pallida* eggs can remain viable for many years in the soil, before gradually deteriorating (Rowe, 2008). Only the results of *M. javanica* development in tomato roots, therefore are discussed in this chapter. Development and resistance experimental establishment, along with potato plant biomass data are presented in Appendix B.

Developmental stages of *M. javanica* were assigned according to Eisenback and Triantaphyllou (2009), who describe very little variation physically between *M. javanica* developmental stages J3 and J4. The vermiform shape of the J2 infective juveniles begin to get swollen and they are a non-egg laying stage (Dávila-Negrón and Dickson, 2013). The differences visually between male and female J3 and J4 stages, when identifying them within roots, were difficult to determine. Due to this, any nematodes that had the appearance of a swollen version of a J2 infective juvenile (Figure 3.7) but not the characteristic globose appearance of an adult female, were classified at the J3/ J4 stage. This experiment was conducted over a period of 70 days, much longer than the previous *M. javanica* development experiments carried out (Nyczepir *et al.*, 1999; after 24 days and Martinuz *et al.*, 2012; after 35 days) in tomato plants.

Overall plants treated with the bacterial strains F113 and L321, particularly after 70 days had

the lowest number of nematodes present in their roots. Plants treated with the antibiotic 2,4-DAPG also had low numbers of nematode present in the roots of all developmental stages, except for the adult stage. In a study carried out by Martinuz *et al*. (2012), inoculating tomato plants with the endophytic bacterium *Rhizobium etli*, strain G12, interfered with the correct development of the plant root giant cells which are necessary for the establishment of successful feeding sites. They found that this obstructed, or delayed J2 infection, restricting nutrient availability to the nematodes. Likewise, although different bacterial strains were utilised, in the present study it was observed that there were few J2 stage nematodes present in the roots up to 50 days compared to the control treatment C1, however, this increased considerably after 70 days. The bacterial strains utilised in the present study, however, could have had a similar effect on the development of giant cells in tomato roots. Martinuz *et al*. (2012) also observed that *R. etli*, strain G12, slowed the development of *M. incognita* J2 infective juveniles to the J3 stage after 15 days. Similarly, in the present study, the observed number of J3/J4 stage *M. javanica* was lowest in the roots after 20 days compared to the control treatment C1 and peaked at 70 days, however in those plants treated with L321 and F113 the presence of J3/J4 stage had decreased after 50 days. It is possible that in the present study the bacterial strains and the compounds they produce are responsible for the low numbers of nematodes present in the roots and for the slow development of *M. javanica* J2 to the J3/J4 stage. However, plants treated with 2,4-DAPG had the lowest numbers of J3/ J4 stage, consistently throughout all three-time points, as well as young adult females. The biocontrol properties of the antibiotic could be involved with this developmental delay. Martinuz *et al*. (2012) further observed a reduction of adult nematodes compared to the controls after 21 days in plants treated with *R. etli*, strain G12. Similarly, the results in this study, also show a low number of adult nematodes (except for those plants treated with L228) after 20 days. Reimann *et al.* (2008) had studied the effects of the same endophyte and nematode species as Martinuz *et al.* (2012) in tomato plants, but they determined that their treated plants produced fewer egg masses when compared to control plants after 56 days. A similar result was also evident in the present study, however, reduced egg masses were further observed in the 70-day plants compared to the control treatment C1. It is clear from the results in the present study, the treatments had a negative effect on nematode fecundity, particularly those plants treated with strains L321 and F113.

The concept of priming a plant to precondition its defences prior to infection (Choudhary *et al.*, 2007) was investigated in the ISR experiments. The experiment was divided into two parts to determine if the production of secondary metabolites, by the bacterial strains tested, acted as an inducer of systemic resistance to *M. javanica* infection, in tomato plants. It was planned to have a second control in these experiments, involving a split root tomato plant with no treatments or nematodes added, however, due to the delicate nature of splitting the

tomato seedling roots, there were some plant fatalities. The experimental design was therefore determined by the number of viable plants available. After the application of the bacteria or antibiotic, the plants were left for one week for bacterial colonisation and secondary metabolite production. In this experiment, the presence of adult females, feeding sites and egg masses were counted, as indicators of an ISR response. According to Choudhary *et al.* (2007) there have been several rhizobacterial strains found to be efficient at eliciting an ISR response in different plant species. Some of these strains are more specific, however, indicating a plant species-specific recognition between the colonising bacteria and receptors on the root surface. To confirm bacterial plant colonisation and viability of the bacterial strains in the tomato roots, a plate count method could have been conducted, but it was not eventually done, as nematode development and tomato plant resistance were the main focus in this study. Nevertheless, it is known that *Pseudomonas* species are effective colonisers of tomato plant roots (Gamalero *et al.*, 2004).

In the ISR Part I experiment (Figure 3.3) there were no nematodes found in the pots on the left, indicating that no nematodes were washed out of the pots on the right during plant watering, or re-infected the roots on the left. Although the bacterial strains and the nematodes were added to two separate pots, those plants treated with bacterial strains L321 and F113 were indicative of a reduction in plant infection, compared to the control treatment. Likewise, the results in the ISR Part II experiment (Figure 3.4) are also suggestive that a systemic resistance response was induced in the treated tomato plants, particularly in those plants treated with F113 and L321. Overall, in the ISR Part II experiment, the pots on the right, which contained both the bacterial or antibiotic treatment and nematodes, indicated reduced root infection compared to the control treatment. The number of nematodes present in the pots on the left, that contained only nematodes was considerably higher than the number of nematodes in those on the right, however, the results are variable. The ISR Part I and II results indicate a systemic response did occur in the tomato plants, particularly in those plants treated with F113 and L321. Similarly, Siddiqui and Shaukat (2003) determined that *P. fluorescens* strain CHA0 reduced *M. javanica* infection in tomato plants by eliciting a systemic resistance response in the plants, in the case of ISR Part I, as the bacteria and nematodes were spatially separated. The ISR Part II results suggest that the interactions between the bacteria and the nematodes directly slowed the development of the nematodes in tomato roots, therefore reducing the number of feeding sites and nematode fecundity. These traits were also observed in the development experiment in the present study, after 20 and 50 days.

The biocontrol properties of 2,4-DAPG were observed in Siddiqui and Shaukat (2003), who noted that the production of the antibiotic by *P. florescences*, strain CHA0, was important in the suppression of *M. javanica* infection, and was also attributed to ISR against *M. javanica* in tomato roots. Choudhary *et al.* (2007) likewise, identified that a 2,4-DAPG producing *Pseudomonas* species was inducing determinants associated with eliciting an ISR response.

Similarly, this was observed in the present study, in both ISR Part I and II, in tomato plants treated with the 2,4-DAPG producer F113, however, the results were variable in those plants treated with both L124 and the synthetic form of the antibiotic. Considering a high (200 ppm) concentration of synthetic 2,4-DAPG was added to the soil near the plant roots, the results on nematode development and ISR do not consistently reflect its biocontrol potential. This suggests that the application of 2,4-DAPG in this form did not reduce nematode infection as much as the natural antibiotic producers did. Some ISR response in tomato plants did occur however, an infection was not consistently higher than the controls, but it was not as efficient as the other bacterial strains. This may have occurred due to the application of 2,4-DAPG, in a form not easily absorbed by the tomato plant roots. This result was consistent with the results of the development experiment, previously discussed in this chapter. Notably, however, in the present study, in both the development and ISR experiments, plants treated with bacterial strain L321, which is not a 2,4-DAPG producer, consistently had lower nematode numbers present in the roots compared to the control. Therefore, the compounds L321 was producing, increased plant resistance to nematode infection.

The results gathered in this chapter suggest that the benefits of PGP bacterial colonisation of tomato roots are two-fold: (1) Plant biomass (expressed as plant height, number of leaves, plant fresh and dry weight) consistently increased over the four time points (20, 50 and 70 days in the development and 30 days in the ISR experiments), particularly in plants treated with L124 and F113. (2) The biocontrol capacity of the bacterial strains and synthetic 2,4-DAPG varied between the sampling times however, plants treated with the bacterial strains F113 and L321 were the most consistent regarding the degree of infection, nematode development within the plants and the number of nematodes present in the roots in the development and ISR experiments. It was also found in the present study, that plants treated with F113 and L321 elicited a systemic response that was responsible for lowering nematode infection and development within the roots. The outcome of these results suggests, that there should be an emphasis on inoculating tomato plants as early as possible for the induction of plant defence. In an agricultural context, pre-treating seeds prior to sowing or inoculating seedlings early, before planting in a field situation, may be an effective approach to the control of PPNs. There is a concern, however, on the viability of the bacterial strains, in terms of their capacity to colonise host plants and the extent they would remain within the plant, in order to induce a systemic response. Application rates of biocontrol bacteria and nematode population density, in the soil and plants, play an important role in the degree of suppression of PPNs (Siddiqui and Shaukat, 2003). However, it is known that the production of antibiotics by beneficial bacterial strains, can improve the ecological fitness of the bacteria (Chandra and Kumar, 2017), which can further influence long-term biocontrol efficacy.

In conclusion, the results of the various methods described in this chapter suggest that the bacterial strains and the components they produce (1) have an effect on the capacity of *M. javanica* to infect their host and (2) delay nematode development within the roots. Through

exploring the biology and behaviour of these nematodes, their tritrophic interactions in attraction assays, their development in tomato plants and tomato plant resistance experiments, two strains were identified that had promising potential regarding PGP and biocontrol. These results indicate that overall, the bacterial strain L321 was the most successful strain at the biocontrol of *M. javanica* and bacterial strain L124 was the most successful strain for increasing tomato plant biomass. The positive control strain *P. fluorescens* F113 also proved to be effective at increasing tomato plant biomass and *M. javanica* biocontrol. Although the experiments carried out in this chapter give a greater insight into the role of *P. fluorescens* F113, the IT Carlow bacterial strains and the antibiotic 2,4-DAPG in the suppression of *M. javanica* infection in tomato plants, there is scope for further investigations to be carried out in the context of environmental conditions, such as temperature and soil type, bacterial application and dose rates, the duration of beneficial colonisation with host plants, 2,4-DAPG formulation, and host/plant species, that result in the optimum production of bacterial antibiotics to induce plant resistance and increase PGP.

Key results obtained from the work tasks in Chapter 3 are the following:

- Bacterial strain L124 acted as a weak attractant to *G. pallida*
- Highest PGP effects, in terms of biomass, were observed in tomato plants treated with strain L124
- The most consistent biocontrol effects of *M. javanica* was observed in plants treated with bacterial strain L321
- Plants treated with bacterial strains L124 and L321 displayed delayed *M. javanica* J2 infective juvenile infection
- Reduced numbers of adult females, feeding sites and egg masses were recorded in plants treated with bacterial strain L321
- An ISR response was observed in plants treated with bacterial strain L321

The objective of this study was to assess tomato plants treated with bacteria and infected with *M. javanica*, and to further explore the bacterial strains biocontrol and PGP capacity. The aims of this chapter, to determine nematode attraction to the bacterial strains and the antibiotic 2,4-DAPG were achieved. The capacity of the PGP bacterial strains to increase plant growth was investigated. The bacterial strains ability to affect *M. javanica* development in tomato roots was assessed. The final aim, which was the concept of eliciting an ISR in treated tomato plants was also explored. The boundaries of these bacterial strains were

further investigated to assess their limitations in a complex natural environment-simulating system, resulting in positive interactions in terms of combating RKN plant infections.

Chapter 4

Nickel Bioremediation Capacity of *Pseudomonas fluorescens* in an Oilseed Rape Crop, Assessed by Nematode Bioindicators

4.1 Introduction

Currently, there are up to 2.5 million contaminated sites across Europe (EEA, 2018), of these, 14% are so heavily contaminated they will require some form of remediation, either mechanical, chemical or biological. Environmental contamination such as heavy metals can cause major health problems in humans and animals due to their cytotoxicity, mutagenicity and carcinogenicity (Ma *et al.*, 2011b). Naturally, the heavy metal Ni occurs in the environment at levels, between 0.5 and 100 ppm (McGrath and Fleming, 2007). Nickel compounds readily absorb to soil particles that are released to the environment and become immobile. The main sources of Ni contamination in the soil are from metal plating industries, combustion of fossil fuels, and through the application of sewage and sludge to land. The use of hyperaccumulating plants, grown on contaminated land, decreases the bioavailability of metals in contaminated soil (Vassilev *et al.*, 2004), in a process known as phytoremediation. Bioenergy crops, such as oilseed rape (OSR; *Brassica napus*) are becoming a popular alternative to meet the demands of fuel and alternative energy sources, they are also known hyperaccumulators and are resilient to toxic heavy metals (Mourato *et al.*, 2015). Although these type of plants are typically utilised for their phytoremediation capacity, there is also potential to utilise *B. napus* oil for energy consumption post phytoremediation (Park *et al.*, 2012) therefore, increasing the profitability of growing OSR as a bioenergy crop.

Beneficial bacteria, such as plant growth promoting (PGP) *Pseudomonas* strains have great potential for transforming sustainable agriculture and increasing the production potential of biofuels (Montalbán *et al.*, 2016). They can enhance plant growth either directly by increasing the availability of nutrients to plants by nitrogen fixation, mineral solubilisation or increased iron uptake, or indirectly by preventing pathogens colonising through niche exclusion. The application of naturally occurring or introduced microorganisms to decontaminate soil is known as bioremediation. Plant growth promoting bacteria are an ideal amendment to contaminated soils, particularly in a phytoremediation capacity, due to their inexpensive production costs, they are environmentally sustainable and they have the ability to increase host plant biomass. Utilising nematodes as bioindicators of bioremediation is a rapid and non-invasive method.

Nematodes are representative of their habitat, they respond quickly to any disturbance or change in the soil composition, and are, therefore, well suited as bioindicators of environmental monitoring (Bongers and Ferris, 1999). Utilising nematodes as indicators of a process such as bioremediation has many benefits including, they can give a real-time insight into the present soil condition, they are easily sampled without disturbing the growing crop, they are found in abundance in the soil and are relatively inexpensive to work with. Nematode morphological identification is a very specialised and time-consuming process (Treonis and Wall, 2005) and requires considerable taxonomical knowledge. It involves focusing mainly on the buccal and tail regions of the nematode, but also taking into account the cuticle, gender and reproductive organs of the individual. However, often molecular techniques are employed to speed up the identification process. Many molecular tools and techniques have been developed for nematode identification and classification, with a polymerase chain reaction (PCR), transforming the study of nematology. PCR based molecular assessments provide accurate and sensitive descriptive information (Oliveira *et al.*, 2011). The molecular fingerprinting technique, denaturing gradient gel electrophoresis (DGGE), separates PCR products according to their molecular weight, resulting in a series of bands that are representative of different nematode genera, which can be utilised to evaluate nematode diversity (Foucher *et al.*, 2004). However, progressive as molecular techniques are, they are no replacement for classical morphological and taxonomic analysis, and a combination of both techniques should be utilised to consolidate findings and give more informative results. (Oliveira *et al.*, 2011).

Transgenic *Caenorhabditis elegans* as an environmental biosensor has multiple applications across a wide variety of settings including toxicology, genetics, pharmacology and cell biology (Leung *et al.*, 2008). They are easily cultured and maintained in the lab, and they respond rapidly to external stressors. Much research has been invested in the suitability of transgenic *C. elegans* as a biosensor for detecting metal contamination, in both aquatic and terrestrial environments. In particular the induction of heat-shock protein (HSP) such as *hsp*-16.2 output genes in response to Cu, Hg, Ni and Zi (Anbalagan *et al.*, 2012; Kumar *et al.*, 2015). The use of these transgenic strains is a growing area of interest and many studies

have demonstrated that *C. elegans* HSP strains are suitable indicators of environmental stress (Anbalagan *et al.*, 2013; De Pomerai *et al.*, 2002; Kumar *et al.*, 2015; Lagido, 2009).

The bioremediation and PGP capacity of different strains of *P. fluorescens* inoculated OSR plants, grown in Ni contaminated soil, were investigated in this chapter. The efficiency of this process was monitored by utilising nematode assemblages as bioindicators, and it was assessed by (1) determining PGP bacterial strains viability in the rhizosphere and the colonisation in OSR, (2) measuring OSR biomass, (3) identifying nematode assemblages by (a) morphological assessment and (b) molecular analysis utilising the molecular fingerprinting method DGGE, and by assigning diversity, maturity and functional indices to the results, and (4) exploring transgenic *C. elegans* as biosensors of Ni bioremediation. It was hypothesised that OSR inoculated with *P. fluorescens* would be effective at bioremediating Ni contamination from the soil, and that nematode assemblages as bioindicators would be an informative method of monitoring the process. There are a number of interactions taking place in this work, between the PGP bacteria and OSR, between the colonised OSR and the heavy metal Ni, between the nematode assemblages and the rhizosphere of the OSR plants and between transgenic *C. elegans* and the Ni soil pore water, to take into consideration. A detailed and encompassed study such as this gives a great insight into these types of interactions resulting in the following research questions arising: Are OSR capable of Ni bioremediation, and is a three to six-month trial a sufficient length of time for OSR Ni bioremediation to occur? How long will the PGP bacterial strains colonise and remain viable within and in the rhizosphere of the OSR plants? Is a morphological assemblage assessment sensitive enough to detect Ni bioremediation? Does the molecular assessment reflect the morphological findings? Can transgenic *C. elegans* be utilised as a measure of bioremediation?

The aims of the research detailed in this chapter are as follows:

- To determine the colonisation and viability of *P. fluorescens* strains F113, L111, L132 L321 in the rhizosphere and within inoculated OSR
- To investigate the OSR PGP capacity of the bacterial strains when grown in Ni contaminated soil
- To measure the ability of OSR inoculated with PGP bacteria to sequester Ni in the roots, stem and leaves
- To analyse the suitability of nematode communities as bioindicators of OSR Ni bioremediation by utilising a morphological assessment
- To evaluate the suitability of the molecular fingerprinting technique PCRDGGE, to assess nematode assemblages as bioindicators of OSR Ni bioremediation.
- To explore the suitability of transgenic *C. elegans* as a biosensor of Ni bioremediation.

4.2 Materials and Methods

Bacterial strains and transgenic *C. elegans* were cultured and maintained, using good lab practice. Experiments were established with appropriate replications and controls. Soil A, the control soil was utilised immediately, it was not spiked with Ni and OSR was not grown in it. Soil B, the experimental soil, was spiked with Ni and OSR inoculated with bacterial strains were grown in it. Pots assigned to control treatment C1 contained 125 ppm Ni and no bacteria. The treated pots designated to Soil B were statistically compared to the control treatment C1. Pots assigned to control treatment C2 were similar to Soil A, as it contained no bacterial treatments or Ni, however, this soil had OSR growing in it for 3 months. Pots designated to Soil A were statistically compared to control treatment C2.

Statistical analyses were performed on the data with the statistical package SPSS, version 23 (IBM SPSS statistics for windows, 2017) unless otherwise stated (see Table 4.3 for statistical tests and software utilised for each experiment). Outliers were assessed by a boxplot. Where the data met the homogeneity of variances (Levene's test; $p < 0.05$) and the assumption of normality (Shapiro-Wilk test; $p > 0.05$), it was assessed by a one-way analysis of variance (ANOVA) with a Tukey post hoc test. If the data did not meet the assumption of homogeneity of variances, a Welch ANOVA was utilised with Games-Howell post hoc test. Where the homogeneity of variances and assumption of normality were violated, a non-parametric Kruskal Wallis with a Bonferroni post hoc test alternative was applied. A non-parametric Mann-Whitney U test was employed to compare the results obtained from Soil A to those in Soil B control treatment C2 throughout this chapter (Table 4.3).

Statistical significance was set at $\alpha = 0.05$ level. Values marked with asterisks (*) indicate significant differences, as follows * ($p \leqslant 0.05$), ** ($p \leqslant 0.01$), *** ($p \leqslant 0.001$) and **** ($p \leqslant 0.0001$), that were detected following post hoc analysis. The presence of asterisks in figures and tables indicates either, a significant difference between the results assigned to Soil A and those in Soil B control treatment C2, or statistical significance among the results determined from Soil B bacterial treatments and those associated with control treatment C1 unless otherwise stated. Results were presented as mean ± standard error of the mean (SEM).

4.2.1 Oilseed Rape Microcosm Establishment

Soil utilised in this experiment was sampled and collected from the rhizosphere of an OSR crop, in Teagasc Oakpark Co. Carlow. It was stored at 4°C and processed within two days to minimise any change in nematode numbers. The soil was split evenly into two parts (Table 4.1) and labelled Soil A (untreated soil) and Soil B (treated soil). Soil A represented the total control samples, without the addition of amendments. This soil was homogenised, divided into four parts as replications and utilised immediately. Soil B represented the experimental

soil to which 125 ppm Ni ($NiCl_2$) and bacteria strains were added. The rhizosphere bacteria *Pseudomonas fluorescens* F113 is well-known for its biocontrol properties and PGP capabilities, previously outlined in Chapter 2 (see Table 2.4). It was utilised in this experiment as a positive control. *Pseudomonas fluorescens* strains L321, L111 and L132 were also utilised for their biocontrol properties and PGP traits. The secondary metabolites produced by these strains are associated with these traits and they were identified in this research in Chapter 2 (see Table 2.8). Within the untreated and treated soil samples, the soil was further divided according to each work task (See Tables 4.1 and 4.2). Prior to dividing the soil, a soil profile was determined. Two plant trials were established to evaluate the bioremediation capacity of spring OSR (*Brassica napus* var. Tamarin) grown in Ni contaminated soil in the presence of these bacterial strains. The Ni concentration that was utilised in this present work, was determined via a plant trial, carried out by Dr Nicholas Otenio (Otieno, 2014). This concentration was assessed to cause stress to OSR plants but did not have any lethal effect.

4.2.1.1 Overview of Plant Trial 1

A plant trial was established with soil assigned to Soil B. Plant pots, 2 L in capacity were lined with plastic (to prevent leaching of Ni) and filled with 500 g of soil. The pots were labelled according to the bacterial treatment they were to contain, either L321, L132, L111 or F113. The control treatments were labelled C1 (which contained Ni and no bacterial treatments) and C2 (which contained no Ni and no bacterial treatments). There were four replications of each bacterial and control treatment. Nickel (125 ppm) was added to each pot, except for the pots labelled C2. The pots were left in the greenhouse for four weeks to enable the Ni to stabilise, ensuring the soil remained moist to maintain the viability of the nematode populations. The pots were subsequently planted with three OSR seeds. The seeds were coated with the bacteria (see Table 4.1 for information on the bacterial strains utilised in this plant trial) in the form of an alginate bead (see Section 4.2.1.4). The two weakest plants were removed from the pots four weeks post planting. The remaining plants were grown for a further three months (Figure 4.1, image C), after which they were harvested, weighed, oven dried at 60°C and the biomass was calculated. The soil was further utilised for morphological and molecular nematode assemblage assessment.

4.2.1.2 Overview of Plant Trial 2

The second plant trial was established with the same conditions as for Plant Trial 1 (described in Section 4.2.1.1), except that the plants were grown for 6 months (Figure 4.1 image D) before harvesting. *P. fluorescens gfp* tagged strains (see Table 4.1 for information on the *gfp* tagged bacterial strains) were utilised to determine bacterial colonisation and viability in rhizosphere (soil), root and phyllosphere (plant stem and leaf) of OSR after 6 months.

The remaining roots, phyllosphere and soil were oven dried at 60°C for 48 hours and plant biomass was determined. Nickel concentrations in the rhizosphere and within OSR were measured by atomic absorption spectroscopy (AAS). In addition, soil pore water extractions (SPW) were performed on the soil samples from this plant trial, to determine the suitability of transgenic *C. elegans* as biosensors of Ni bioremediation.

TABLE 4.1: Summary of Chapter 4 experimental design for Plant Trial 1 and Plant Trial 2. The soil was further divided and utilised in the different work tasks.

	Plant Trial 1		**Plant Trial 2**
	Soil A	**Soil B**	**Soil B**
Bacterial treatment [1]1	-	F113wt[2]+ Ni[3]	F113*gfp*:km^{R}[4]+ Ni
Bacterial treatment 2	-	L111wt + Ni	L111*gfp*:km^{R} + Ni
Bacterial treatment 3	-	L132wt + Ni	L132wt + Ni
Bacterial treatment 4	-	L321wt + Ni	L321*gfp*:km^{R} + Ni
Control treatment C1	-	Ni + No bacteria	Ni + No bacteria
Control treatment C2	-	No Ni + No bacteria	No Ni + No bacteria
Work tasks		OSR biomass	OSR biomass
	Morphological analysis	Morphological analysis	Bacterial colonisation
	Molecular assessment	Molecular assessment	OSR Ni AAS analysis
			Transgenic *C. elegans* biosensor
Time assessed	Immediately	After 3 months	After 6 months
Statistical comparisons	Soil A - Soil B C2	Soil B treatments - C1	Soil B treatments - C1
			Soil B treatments - C2

[1] Bacterial treatment = *P. fluorescens* strains

[2] Wt = Wild type strains with no genetic alterations.

[3] Ni = 125ppm $NiCl_2$

[4] *gfp*:km^{R} = Bacterial strains tagged with green fluorescent protein construct that are kanamycine resistant.
- = No Ni or bacteria added

4.2.1.3 Soil Profile Analysis

Soil profile analysis was carried out to determine the soil composition (Figure 4.1 image A). The soil was oven dried for 48 hours at 60°C. It was passed through a 2 mm mesh sieve to remove any large stones and debris and crushed with a pestle and mortar. The soil was further passed through a 1 mm mesh sieve and mixed well. To a 500 ml graduated cylinder, 100 g of dry ground soil (see Table 4.2), 300 ml tap water and 2 g non-foaming laboratory grade dish-washing power was added. It was sealed with parafilm and agitated for ten minutes. The graduated cylinder was left to stand undisturbed for three days. After which, the defined layers of soil were measured (Whiting *et al.*, 2014). The total soil volume was determined and the percent of sand, silt and clay were calculated. The soil type was identified using a soil texture triangle (Appendix C, Figure C.1). This was repeated a further two times.

TABLE 4.2: The quantity of soil utilised per treatment replication, that was assigned to each work task in Chapter 4.

Work task	Section	Plant Trial 1		Plant Trial 2	Additional soil
		Soil A	Soil B	Soil B	
Morphological analysis	4.2.2.1	400 g	100 g		
Molecular assessment	4.2.3.1	10 g	10 g		
Bacteria viability	4.2.1.5			5 g	
Ni bioremediation	4.2.1.6.3			5 g	
Transgenic Biosensors	4.2.4.2			250 g	
Soil profile	4.2.1.3				100g
MHC[1]of soil	4.2.4.1				10 g

[1] MHC = Moisture holding capacity of soil

4.2.1.4 Alginate Beads

In Plant Trial 1, the bacterial strains L111, L321, L132 and F113, were cultured in NB, at 30°C overnight. For Plant Trial 2, the *gfp* tagged bacterial strains (Table 4.1) were cultured in *Pseudomonas* selective broth (SGA broth; 20 g sucrose, 22 g glutamic acid, 1 g K_2HPO_4 and 5 ml 10% w/v $MgSO_4$ per litre) supplemented with kanamycin (50 µg/ l) at 30°C overnight. Oilseed rape seeds were surface sterilised in 95% ethanol for three minutes and coated in the bacteria in the form of an alginate bead. Stock solutions for the alginate beads comprised of 5% sodium alginate, 2% $CaCl_2$ and 5 g powdered semi-skimmed milk in 50 ml dH_2O. The solutions were autoclaved at 121°C at 15 psi for 15 minutes; the skimmed milk solution was autoclaved for ten minutes, to prevent coagulation of milk proteins. The working solution consisted of 5 ml semi-skimmed milk, 15 ml sodium alginate and 5 ml bacterial inocula (10^7 CFU/ ml). These components were placed on a sterile Petri dish and mixed well with a sterile inoculating loop. The mix was poured into a 20 ml sterile syringe barrel and the OSR seeds were added. They were dropped out of the syringe into a beaker containing 250 ml sterile $CaCl_2$ and a magnetic stirrer to prevent the beads from clumping. Control seed coatings consisted of SGA broth without any inoculum. The beads were rinsed three times with sterile deionised water and stored in a sealed plastic bag for 2-3 days at 4°C before use.

4.2.1.5 Plant Growth Promoting Bacterial Colonisation in OSR

Once the OSR plants in Plant Trial 2 were harvested, 1.5 g of phyllosphere, along with 1.5g of roots were weighed, ensuring the roots were free of soil and debris. 1.5 g rhizosphere (Table 4.2) from the pots were also weighed to determine any bacterial colonisation in the soil. The phyllosphere and the roots were surface sterilised with 10% sodium hypochlorite followed by an aseptic 95% ethanol dip. Once the ethanol had evaporated the plant tissues were crushed with a sterile pestle and mortar. From the crushed plant tissue, 0.1 g of root

and phyllosphere, and 0.1 g from the rhizosphere were placed into a 1.5ml tube containing 900 µl sterile Ringers.

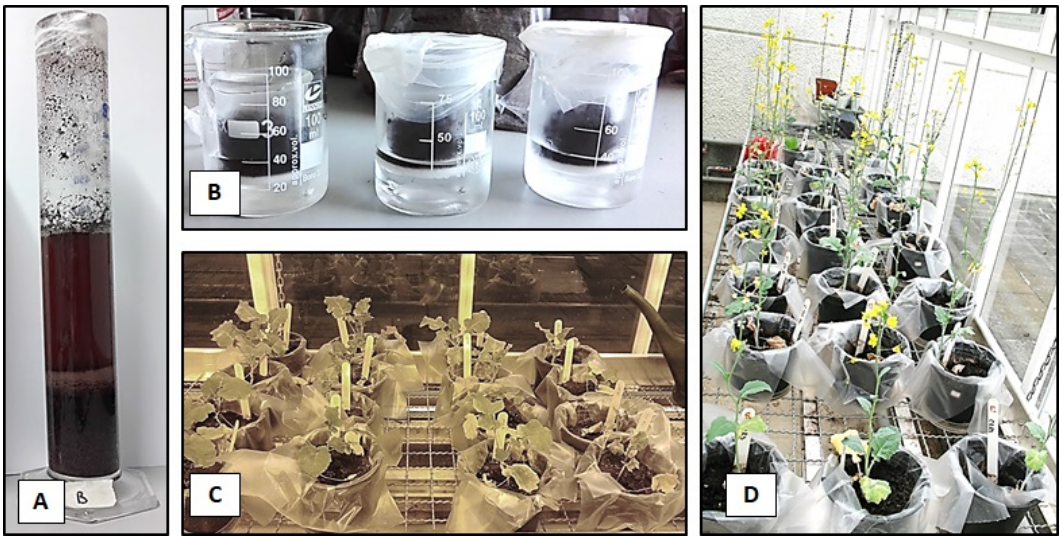

FIGURE 4.1: Oilseed rape microcosm establishment. Examples of the (A) soil profile, (B) MHC of the soil, and (C) OSR plants after 3 months and (D) after 6 months growth in Ni contaminated soil, treated with *P. fluorescens* strains. Control treatments: C1 = Ni and no bacteria and C2 = No Ni and no bacteria.

Serial dilutions (10^{-1} to 10^{-6}) were performed on the soil and plant matter. Bacterial colonisation was only determined for *gfp* tagged strains F113, L321 and L111. Colonisation was also investigated for the control treatment, which was utilised as a negative control. The dilutions were plated out in triplicate on *Pseudomonas* selective agar, (SGA agar; sucrose glutamic acid agar; 20 g sucrose, 22 g glutamic acid, 2 g K_2HPO_4 and 1 g Technical agar No. 1 per litre. After autoclaving, 5 ml 10% w/v $MgSO_4$ was added to the molten agar before the plates were poured.) The selective media contained the antibiotic kanamycin sulphate (0.05 mg ml^{-1}) to select for the kanamycin resistant bacteria (see Table 4.1). The media also contained cycloheximide (32.5 mg ml^{-1}) to prevent fungal growth on the plates. Petri plates were incubated at 30°C for 24-36 hours until bacterial growth was clearly visible. The visible colonies were counted, verified under UV light for fluorescence and the CFU g^{-1} was determined.

4.2.1.6 Sample Preparation for Atomic Absorption Spectroscopy

4.2.1.6.1 Soil pore water acidification

Acid digestion was carried out on soil pore water (SPW) samples (see Section 4.2.4.2 for details), following the EPA Method 3005A (USEPA, 1992). The SPW samples were centrifuged for 20 minutes at 3800 rpm. To a 50 ml volumetric flask, 5 ml SPW sample and

1.25 ml nitric acid (HNO_3) was added. The solution was made up to 50 ml with dH_2O. The solution was filtered using Whatman No. 4 filter paper into a 50 ml falcon tube and stored at 4°C for 2-3 days for further use.

4.2.1.6.2 Microwave digestion of oilseed rape

Oven dried plants were pulverised with a pestle and mortar and digested via a microwave digester (Milestone Start D Microwave digestion system). The procedure was implemented according to the manufacturers' instructions and user manual. The method for digestion of dried plant matter (Application note DG-AG-02) was employed. To the microwave digester ceramic containers, 0.5 g dry plant matter and 7 ml HNO_3 and 1ml 30% hydrogen peroxide (H_2O_2) was added, ensuring to wash all the plant matter from the container sides into the solution. The containers were sealed and loaded into the microwave, ensuring the device was balanced. The plant matter was digested for 25 minutes at 1000 Watts at 200°C followed by a cool down step of 90 minutes at 1000 Watts at 40°C. On completion of the cycles, the ceramic containers were removed from the device and the contents rinsed into a 100 ml volumetric flask. The solutions were filtered with Whatman No. 4 filter paper and were stored at 4°C for 2-3 days.

4.2.1.6.3 Acid digestion of soil

A strong acid digestion was performed on the dried soil (Table 4.2), following the EPA Method 3050B (USEPA, 1996). To a 250 ml glass beaker, 1 g dried sieved soil samples, 10 ml 1:1 HNO_3: H_2O was added and mixed well. The sample was covered with a clock glass, heated to 95°C for 10-15 minutes without boiling, followed by cooling. Once cool, 5 ml concentrated HNO_3 was added to the soil samples, and the beakers were covered, heated without boiling to evaporate the solution to 5ml. Once cool, 2 ml H_2O along with 3 ml 30% H_2O_2 were added to the beakers. The beakers were covered with a clock glass and heated until effervescence had subsided. The beakers were further heated to evaporate the solutions to 5 ml. When cool the solution was filtered with Whatman No. 4 filter paper, made up to 100 ml with dH_2O and syringe filtered with a 0.45 μm filter. The solution was stored at 4°C for 2-3 days.

4.2.1.7 Analysis of Soil and Plant Tissues for the Presence of Nickel

The nickel concentration present in the acidified SPW digested soil and plant tissues in Plant Trial 2 (Section 4.2.1.2) were determined by AAS. Nickel standards were prepared from a concentrated 1000 ppm Ni standard solution [Sigma-Aldrich]. The standards utilised for digested soil samples were 0.5 ppm, 1.0 ppm, 2.0 ppm and 10.0 ppm. For acidified SPW and

digested plant matter, the standards were 0.5 ppm, 1.0 ppm and 2.0 ppm. Nickel concentration present in the experimental samples determined the standard concentrations. Whereby a range was chosen on the lowest and highest Ni concentrations, with a third concentration, that was between the two, were chosen to create the standard curve.

The acidified and digested solutions were analysed by AAS using an AAnalyst 100 Spectrometer [Perkin Elmer] with an air-acetylene flame and a Ni lamp, according to the manufacturers' instructions. To ensure instrument accuracy, continuous calibration of a Ni standard was run through the system after every ten samples measured. The samples were read three times on the instrument to ensure reproducible results. The results were collated and the Ni concentration was determined, taking the dilution factor into consideration.

4.2.1.8 Statistical Analysis

Statistical analysis was conducted, as described in Section 4.2 with respect to OSR biomass, including viability of the bacterial strain in the rhizosphere, in OSR roots and the phyllosphere, along with assessing the success of bioremediation of OSR via AAS (see Table 4.3).

TABLE 4.3: Statistical tests utilised in Chapter 4. The statistical analysis performed on each work task and the software packages employed for each test.

Plant Trial	Experiment	Section	Soil A	Soil B		Statistical Software
			Statistical test	Statistical test	Post hoc test	
Oilseed Rape Microcosm Establishment						
2	Bacterial viability after 6 months	4.3.1.2		Kruskal Wallis	Bonferroni	SPSS[2]
2	OSR bioremediation of Ni	4.3.1.3		Kruskal Wallis	Bonferroni	SPSS
1 and 2	OSR Biomass after 3 and 6 months growth	4.3.1.4		Kruskal Wallis	Bonferroni	SPSS
Nematode Assemblage Characterisation: Morphological Analysis						
1	Mean % c-p scale	4.3.2.2.1	Mann-Whitney U	Kruskal Wallis	Bonferroni	SPSS
1	Mean % trophic groups	4.3.2.2.2	Mann-Whitney U	Kruskal Wallis	Bonferroni	SPSS
1	Mean nematode abundance per soil type and treatment	4.3.2.3.1	Mann-Whitney U	Kruskal Wallis	Bonferroni	SPSS
1	Mean nematode biomass and C per soil type and treatment	4.3.2.4.2	Mann-Whitney U	Kruskal Wallis	Bonferroni	SPSS
1	Mean % biomass per trophic groups	4.3.2.4.3	Mann-Whitney U	Kruskal Wallis	Bonferroni	SPSS
1	Pielous evenness index (J')	4.3.2.5.1	Mann-Whitney U	one-way ANOVA	Tukey	SPSS
1	Shannon Wiener diversity index (H')	4.3.2.5.3	Mann-Whitney U	Welch ANOVA	Games-Howell	SPSS
1	Jaccard similarity coefficient	4.2.2.7.2	Mann-Whitney U	Kruskal Wallis	Bonferroni	SPSS
1	Maturity index (MI)	4.3.2.6.1	Mann-Whitney U	one-way ANOVA	Tukey	SPSS
1	Sum of maturity index ($\sum$MI)	4.3.2.6.3	Mann-Whitney U	Kruskal Wallis	Bonferroni	SPSS
1	Plant parasitic index (PPI)	4.3.2.6.2	Mann-Whitney U	Welch ANOVA	Games-Howell	SPSS
1	Enrichment index	4.3.2.7.2	Mann-Whitney U	Kruskal Wallis	Bonferroni	SPSS
1	Structure index	4.3.2.7.3	Mann-Whitney U	Kruskal Wallis	Bonferroni	SPSS
1	Basal index	4.3.2.7.4	Mann-Whitney U	one-way ANOVA	Tukey	SPSS

Continued on next page

Table 4.3 – *Continued from previous page*

Plant Trial	Experiment	Section	Soil A	Soil B		Statistical Software
			Statistical test	Statistical test	Post hoc test	
Nematode Assemblage Characterisation: Molecular Assessment						
1	Jaccard similarity coefficient	4.3.3.1.2	Mann-Whitney U	Kruskal Wallis	Bonferroni	SPSS
1	Pielous evenness index (J')	4.3.3.1.1	Mann-Whitney U	Kruskal Wallis	Bonferroni	SPSS
1	Shannon Wiener diversity index (H')	4.3.3.1.3	Mann-Whitney U	Kruskal Wallis	Bonferroni	SPSS
1	Cluster analysis	4.3.3.2.1	UPGMA	UPGMA		CLIQS[3]
1	Multidimensional scaling (MDS)	4.3.3.2.2				XLSTAT[4]
Biosensors of Ni Bioremediation						
2	GFP reporter assay	4.3.4.1		ANOVA	Tukey	SPSS
2	Image J analysis	4.3.4.2		Kruskal Wallis	Bonferroni	SPSS

[1] Soil A statistical test = No post hoc test as it was only compared to Soil B control treatment C2.

[2] SPSS version 23 (IBM SPSS statistics for Windows, 2017)

[3] CLIQS 1D Pro version 1.1 (TotalLab)

[4] XLSTAT (XLSTAT, 2017)

4.2.2 Nematode Assemblage Characterisation using Morphological Techniques

4.2.2.1 Nematode Extraction from Soil

In Plant Trial 1 (Table 4.1) the nematodes were extracted from the untreated soil, Soil A (400cm^3 soil per replication, with four replications, see Table 4.2) immediately. In Soil B, the nematodes were extracted from pots containing Ni and bacterial treatments L321, L111, L132 and F113 (100cm^3 soil per replication, with four replications per treatment) after three months. There was less soil available for each replication for Soil B, compared to Soil A, as the soil was divided and utilised in further work tasks. The experiments in this section required an assessment of the nematode community in an environmental soil sample. The soil utilised in this experiment was not dried and weighed (as this would lead to nematode mortality), instead, soil volume was measured.

Nematode extraction techniques included a combination of decanting, sieving and sugar floatation. The soil sample was placed into a 5 L jug containing 2 L of tap water, it was manually stirred and mixed well to remove any lumps. The mixture was poured through a 2 mm sieve into a clean 5 L jug to remove the large debris and plant matter. It was left to settle for 10 seconds and then decanted into a clean 5 L jug; the dense debris and sediment were discarded. Decanting continued until there was little sediment remaining in the jug. Some soil mixture was poured onto a 40 μm sieve; the sieve was attached to a 5 L jug and placed onto an orbital shaker table [Stuart Scientific] set to a low rotation. This procedure was continued until all the contents of the jug were passed through the 40 μm sieve and the

water ran clear. The nematodes on the 40 μm sieve were condensed and rinsed into a beaker with 200 ml of the silica colloidal solution Ludox [Sigma Aldrich] and left to settle for up to 1 hour. Prior to this, Ludox was diluted to 1.18 specific gravity (s.g.); this is the optimum s.g. to ensure the nematodes are suspended in the liquid and the heavier soil particles sink to the bottom of the beaker (Bezooijen, 2006). The Ludox suspension was passed through a 40 μm sieve, leaving the sediment in the bottom of the beaker. This procedure was repeated a further two times, using a clean beaker each time. Following this, the nematodes were rinsed off the sieve, with tap water into a 50 ml falcon tube. The tubes containing the extracted nematodes were stored at 4°C for up to 24 hours before fixing.

4.2.2.2 Nematode Fixing and Mounting

The extracted nematodes were preserved in DESS (dimethyl sulphoxide, disodium EDTA, and saturated with NaCl; Yoder *et al.*, 2006). A stock solution of 0.25 M EDTA disodium salt was prepared by adding 23.27 g of salt and 50 ml of deionised water to a 250 ml beaker. It was heated to 30°C and stirred continuously to mix the solution. 100 ml 1M NaOH was prepared and added to the EDTA solution until a pH 7.5 was achieved. When the EDTA salt was dissolved, the volume was brought up to 200 ml with deionised water. 50 ml 20% DMSO was added to the solution and mixed well. NaCl was added to the beaker over heat until the solution was saturated and the salt no longer dissolved. The solution was poured into a 250 ml Duran bottle leaving the remaining salt crystals in the beaker.

Extracted nematodes were preserved by concentrating the nematode/ water suspension on a 40 μm sieve. The preservative DESS was poured onto the nematodes on the sieve, the contents were stored in 50 ml falcon tubes, in the dark at room temperature for 24 hours. Following this, the nematodes in DESS were again poured onto a 40 μm sieve and washed with deionised water to remove any salt crystals. The preserved nematodes were added to shallow cavity blocks which were placed in an airtight container containing 5 ml 96% ethanol. They were incubated at 40°C for 12 hours, after which the cavity blocks were removed and placed onto trays. The opening on the cavity blocks was covered by two-thirds to enable slow evaporation. They were filled every 3 hours for 12 hours with Solution II (95 parts of 96% ethanol and 5 parts glycerol). The nematodes were stored in the cavity blocks until they were mounted onto slides.

The nematodes were mounted onto glass slides for identification. Paraffin ring mounts (Bezooijen, 2006) were prepared by heating a copper tube on a Bunsen burner, dipping it into a dish containing solid paraffin wax and stamping the tube onto a glass slide. Once the paraffin ring had cooled and solidified, a small drop of 100% glycerol was added to the centre of the ring. The nematodes were observed in the cavity block under a stereoscope [Optika]. They were picked from the cavity block using a picking needle and placed into the glycerine drop

on the glass slide. Five preserved nematodes were mounted on each slide, a coverslip was placed onto the paraffin ring and the slide was heated on a hot plate for 3 - 5 seconds to melt the wax and seal the specimens. Once the wax was cooled the specimens were ready for observation under the microscope.

4.2.2.3 Morphological Identification of Nematodes

The preserved nematodes were identified using a high-powered microscope [Optika], under 100x oil immersion lens to genus and some to species level using the keys of Zullini (2007); Chen *et al.* (2004); Siddiqi (2001); Bongers (1994); Hunt (1993) and Holovachov (1982). To observe the different characteristic features of a nematode, minute changes in focusing distance allowed for observation within different planes of focus. The two main specific regions to observe when identifying nematodes were, the buccal cavity and the tail shape. However other important characteristics include cuticle pattern and, location and formation of reproductive organs (Barriére and Félix, 2006).

The nematodes were identified to genus and to some species level. They were recorded according to the pot and treatment they were extracted from (Section 4.2.2.1). The slides were labelled according to the sampling time, soil treatment, replication and slide number, along with the number of nematode per slide. Up to 200 nematodes were identified per replication in Soil A. Up to 200 nematodes were identified per treatment (50 nematodes per replication identified) in Soil B. More nematodes were identified in Soil A, as this was a larger volume of soil compared to Soil B (previously described in Section 4.2.2.1). The nematode length and diameter was measured using the calliper and polyline functions (Figure 4.2) on Optika Vision Pro software and were recorded along with a reference number. Digital copies of the head, tail and whole nematodes were taken using Optika Vision Pro software for reference.

4.2.2.4 Assignment to the Coloniser- Persister Scale, Trophic Groups and Feeding Types

The coloniser-persister scale was assigned to identified nematodes to classify them according to their life strategy (Bongers and Bongers, 1998). The scale, (explained in Table 1.1) ranges from 1-5 whereby 1 represents the colonisers and 5 is associated with persisters. The identified nematodes were assigned to trophic groups according to their feeding type (Bongers and Bongers, 1998), to determine the relationship between nematode population and soil environment. Feeding habits of nematodes differ greatly among species; therefore some genera of nematodes may have more than one feeding type. Feeding types (described in Table 1.1) ranged from 1-8 and included plant feeders, fungal feeders, bacterial feeders and omnivores.

4.2.2.5 Nematode Abundance

Nematode abundance was expressed as the number of individuals in Soil A (400 cm^3 soil per replication, with four replications) and Soil B, bacterial and control treatments (100 cm^3 soil per replication, with four replications per treatment). The variation in soil volume, between Soil A and Soil B, occurred as the soil assigned to Soil B was divided up for further work tasks. This was previously described at the beginning of Section 4.2 (see Table 4.2).

Rank abundance curves (Whittaker plot; Whittaker, 1965) were employed to display relative species abundance. The x-axis represents the abundance rank, whereby the most abundant species is assigned to rank one, the second most abundant is assigned to rank two, this is continued until all the abundance data are assigned to a rank. The y-axis represents the proportional abundance or the relative abundance, which is a measure of species abundance (the number of individuals) relative to the abundance of other species; this is measured on a log scale. Rank abundance curves give a visual representation of species richness and evenness. Species richness is represented by the number of different species on the graph (the number of species ranked). Species evenness is reflected in the slope of the line. A steep slope is indicative of low evenness (the high-ranking species have much higher abundances than the low-ranking species). A shallow gradient indicates high evenness (as the abundances of different species are similar).

4.2.2.6 Nematode Biomass and Carbon Content

Nematode biomass was calculated to indicate food web structure. While the nematodes were identified, the body length and diameter were recorded using Optika Vision Pro software (Figure 4.2). The polyline function was employed to measure nematode length and calliper function was utilised to determine the widest part of the nematode. The microscope was calibrated with a calibration slide and the software was adjusted accordingly. Nematode biovolume was calculated using the formula of Andrassy (Pusceddu *et al.*, 2014).

Andrassy's equation (Table 4.4) describes nematode body mass, where W is the mass (fresh weight μg) per individual, L is nematode length (μm) and D is the body diameter (μm) taken at the widest part of the nematode. It is based on a cylindrical shape representing the elongated morphology of nematodes. The average density for each genus of nematode was calculated by multiplying the fresh weight by 1.13g cm^{-3}. Nematode biomass (dry weight) was recorded as 25% of the average density (Soetaert *et al.*, 2009). The carbon content of the genera was considered to be 40% of the dry weight (Bianchelli *et al.*, 2013).

FIGURE 4.2: Example of body measurements of a nematode, using Optika Vision Pro software, employing the caliper and polyline functions, respectively. Digital images show an adult *Achromadora spp.* in (A) diameter and in (B) length.

4.2.2.7 Diversity Indices

4.2.2.7.1 Nematode evenness

Pielou's evenness index (J'; Neher and Darby, 2009) measures diversity and species richness. It refers to how close in numbers different species are in each sample. The equation (Table 4.4) describes the evenness index J', where H' is the Shannon Wiener diversity index and S is the total number of species. It ranges from 0 (no evenness or dissimilar abundance) to 1 (complete evenness). The closer the values are to 0, the less variation there are between species in the samples and can be indicative of a dominant species. The closer the values are to 1, the more diverse the species are in the sample. This can be indicative of complete evenness between species.

4.2.2.7.2 Jaccard similarity coefficient

Jaccard similarity coefficient (S_j; Neher and Darby, 2006) compares the percent similarity and diversity of sample sets. Soil A was compared to Soil B control treatment C2. Each of the bacterial treatments, F113, L132, L111 and L321 were compared to control treatment C1. The index represents the percent taxa present that are both shared and distinct to Soil A and Soil B. It is a form of binary data (presence and absence) expression. The index can be described as the fraction of species that are shared between the sampling times (Table 4.4), where a represents the number of taxa unique to group A, b represents the number of taxa unique to group B, and c represents the number of taxa common to group A + B. It is a measure of similarity between the two sets of data, with a range from 0% (low similarity) to 100% (high similarity).

TABLE 4.4: Ecological indices describing diversity, dominance, evenness, similarity and functional indices calculated for nematode community analysis.

Name	Equation	Reference
Biovolume		
Andrassys Equation	$W = \frac{(L*D^2)}{(1.6*10^6)}$	Pusceddu *et al.* (2014)
Diversity Indices		
Pielou's Evenness Index	$J' = \frac{H'}{ln(S)}$	Neher and Darby (2009)
Shannon Wiener Diversity[1]	$H' = -\sum_{i=1}^{s} \rho_i \ln \rho_i$	Neher and Darby (2006)
Jaccard Similarity	$S_j = 100 * \frac{c}{a+b+c}$	Neher and Darby (2006)
Functional Indices		
Maturity Index	$MI = \sum_{i=1f} \frac{v_i n_i}{n_i}$	Neher and Darby (2006)
Basal Index[2]	$BI = 100 * \frac{b}{(e+s+b)}$	Berkelmans *et al.* (2003)
Enrichment Index	$EI = 100 * \frac{e}{(e+b)}$	Neher *et al.* (2004)
Structure Index	$SI = 100 * \frac{s}{(s+b)}$	Neher *et al.* (2004)

[1] ρ_i = Proportion of individuals found in species i, n_i = Number of individuals in species $_i$, N = Total number of individuals in the community and S = Total number of species

[2] b = (Ba_2 + Fu_2) * W2,
e = (Ba_1* W1) + (Fu_2 * W2),
s = ((Ba_n * Wn) + (Ca_n * Wn) + (Fu_n * Wn) + (Om_n * Wn)) where n = 3-5 (referring to c-p).
W1 = 3.2, W2 = 0.8, W3 = 1.8, W4 = 3.2 and W5 = 5.0

[3] Ba = Bacterivore, Fu = Fungivore, Om = Omnivore, Ca = Carnivore. (Ferris *et al.*, 2001).

4.2.2.7.3 Shannon Wiener diversity index

Shannon Wiener diversity index (H'; Neher and Darby, 2006) is a measure of the number of individuals observed for each species in the same sample (Table 4.4). As H' increases, the species richness and evenness of the nematodes also increase. The index is described as, the total number of species in the community (richness), where pi is the proportion of individuals found in species i. Proportion is estimated as (pi= n*i*/N), where ni is the number of individuals in species *i* and N is the total number of individuals in the community. The values range between 1.5 and 3.5, rarely exceeding a value greater than 4.

4.2.2.8 Maturity Index Family

4.2.2.8.1 Maturity index

Maturity Index (MI; Bongers, 1999) is a measure of environmental disturbance. It is based on the proportion of colonisers (r-strategists) and persisters (K-strategists) in a sample, including all five levels of the c-p scale, however, it omits plant-feeding nematodes. For MI, the index

of interest is described as Vi which is the c-p value assigned to each taxon i, ni which is the number of nematodes in each of the f taxa, and f representing the abundance of nematodes that meet the criteria (Table 4.4). The MI is based on the sum of the weighted proportion of nematodes in the sample. Low MI represents a disturbed or enriched environment in comparison to high MI which indicates a stable environment (Bongers, 1989).

4.2.2.8.2 Plant parasitic index

The plant-parasitic index (PPI) is calculated only for plant-feeding nematodes. It can be utilised as an indicator of system enrichment, under the assumption that the abundance of plant-feeding nematodes are dependent on the availability and health of their host plants. In enriched conditions, an increase in higher plants results in increased PPI and decreased MI (Bongers *et al.*, 1991). The PPI is also expected to be higher than MI in disturbed soil conditions, the inverse of the response of the MI to disturbance (Bongers, 1990).

4.2.2.8.3 Sum of Maturity index 2-5

Sum of Maturity Index 2-5 ($\sum$ MI 2-5) is calculated only for nematodes in the c-p range of 2-5, including PPN. The nematodes assigned c-p scale 1 are enrichment opportunists and respond positively to a disturbed environment, therefore they are omitted. This index differs from MI 2-5 as it recognises the input of plant-feeding nematodes with regard to environmental stress.

4.2.2.9 Indicators of Ecosystem Function

4.2.2.9.1 Functional guilds

A functional guild is an assemblage of species with similar biological characteristics and is utilised as a tool for their organisation in a food web analysis (Bongers and Bongers, 1998). There are three components in a food web (1) basal, (2) enriched, and (3) structured, with associated indicator guilds: bacterivores (Ba_x), fungivores (Fu_x), carnivores (Ca_x), plant feeders (Pl_x) and omnivores (Om_x), where x = c-p scale 1-5. The numbers W1 = 3.2, W2 = 0.8, W3 = 1.8, W4 = 3.2 and W5 = 5.0, refer to a weighting system for nematode guilds described in Ferris *et al.* (2001). The absence of a guild indicates disturbance and the presence of a guild indicates lack of disturbance or soil recovery. Functional guild indicators were classified as showing basal (b), enrichment (e) and structural (s) components. The weighting

system (W1-5) was assigned to the values, according to Ferris *et al.*, (2001) along the structure and enrichment trajectories (Figure 4.3), for the determination of the enrichment index (EI), structure index (SI) and basal index (BI) of the food web:

b = $((Ba_2 + Fu_2) * W2)$

e = $((Ba_1 * W1) + (Fu_2 * W2))$

s = $((Ba_n * Wn) + (Ca_n * Wn) + (Fu_n * Wn) + (Om_n * Wn))$

where n = 3-5 (referring to c-p), W1 = 3.2, W2 = 0.8, W3 = 1.8, W4 = 3.2 and W5 = 5.0.

4.2.2.9.2 Enrichment index

Enriched food webs are representative of disturbance and availability of resources such as organic matter. They can occur due to a rise in organism mortality, an increase in microbial activity and favourable environmental conditions. The enrichment index (EI; Neher *et al.*, 2004) is represented by Ba_1 and Fu_2. The index is described (Table 4.4) as the percentage of e divided by the sum of e and b (described in Section 4.2.2.9.1).

4.2.2.9.3 Structure index

Structured food webs follow the flow of carbon through a system. The availability of carbon affects the structure, dynamics and activities of the food web. Food webs that are low in resources, such as organic matter, tend to be short and dominated by opportunistic nematodes. Those with sustained resources tend to be longer, with greater nematode abundance and biomass. The structure index (SI; Neher *et al*., 2004) indicates food web structure and stability. It is represented by c-p scale 3-5 in the nematode guilds. In Table 4.4, SI is described as the percentage of s divided by the sum of s and b (as described in Section 4.2.2.9.1).

The orientation of bacterivore, fungivore, omnivore and carnivore functional guilds in a food web are represented in faunal profiles (Figure 4.3). They describe the condition of the food web and are orientated along the structure (x-axis) and enrichment (y-axis) trajectories. Both trajectories have cp-2 guilds which are indicators of basal conditions. The quadrats (A-D) are described in Table 4.5.

4.2.2.9.4 Basal index

Basal food web structure is based on fundamental resources such as, living plant tissue, root exudates or dead organic matter which occupy the lowest trophic level. These food webs

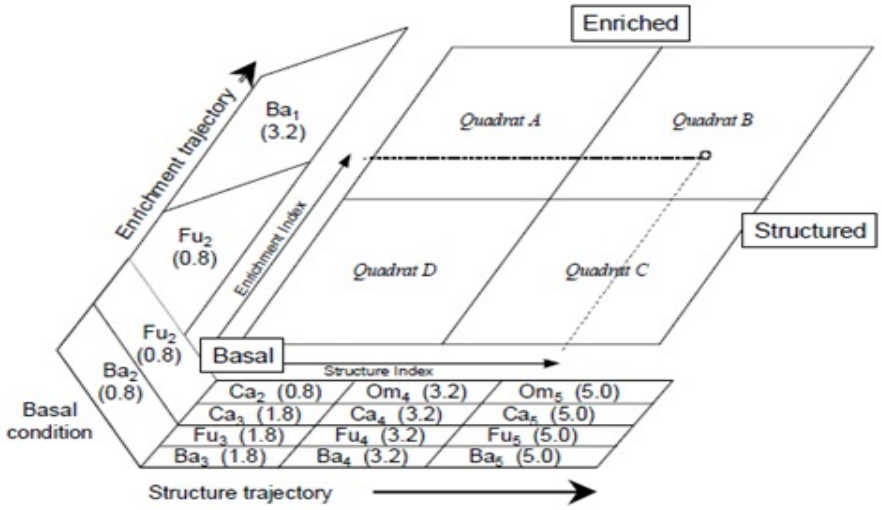

FIGURE 4.3: Nematode faunal profile (Ferris and Bongers, 2009). The x-axis describes the structure trajectory and the y-axis describes the enrichment trajectory. The quadrats (A-D) represent the condition of the soil food web and its environment (Table 4.5).

TABLE 4.5: Description of the soil food web condition and its environment based on weighted nematode faunal analysis (Ferris *et al.*, 2001). Quadrats refer to faunal ordination in the faunal profile (Figure 4.3).

Description	Quadrat A	Quadrat B	Quadrat C	Quadrat D
Disturbance	High	Low to moderate	Undisturbed	Stressed
Enrichment	N-enriched	N-enriched	Moderate	Depleted
Decomposition channels	Bacterial	Balanced	Fungal	Fungal
C:N ratio	Low	Low	Moderate to high	High
Food web condition	Disturbed	Maturing	Structured	Degraded

can decline due to a lack of resources or by adverse environmental conditions. The basal index (BI) is indicative of stress, unfavourable environmental conditions, or contamination. Nematodes in the c-p 2 class predominate the basal food web, which consists of bacterial scavengers (Ba_2) and fungal feeders (Fu_2). They are considered basal (b) to both enrichment and structure trajectories. Table 4.4, describes BI, as the percentage of b divided by the sum of e, b and s (described in Section 4.2.2.9.1; Berkelmans *et al.*, 2003).

4.2.2.10 Statistical Analysis

The results assigned to the c-p scale, trophic groups and feeding types and abundance, followed by nematode biomass and carbon content, and diversity, maturity and functional indices were statistically assessed (Table 4.3 for details). The statistical comparisons for each task are described in Table 4.1.

4.2.3 Nematode Assemblage Characterisation utilising Molecular Techniques

4.2.3.1 DNA Extraction from Soil using a Commercial Soil Kit

The DNA extraction was carried out on soil from Plant Trial 1 (Section 4.2.1.1) according to manufacturers instructions for the PowerSoil® DNA Isolation Kit (Mo Bio, Laboratories Inc.). From each OSR pot, 10g soil was collected and stored at $4°$C overnight (Table 4.2) in a sealed bag. To a power bead tube, 0.25 g soil was added. The soil was homogenised and enzymatically treated using proteinase K and SDS. The DNA was filtered and purified using column purification and a silica membrane. It was stored at $-20°$C for further analysis. Four DNA extractions were performed on each soil replication, from Soil A (four soil replications) and Soil B (six treatments with four soil replications of each). The DNA was quantified and concentrations were recorded.

4.2.3.2 Polymerase Chain Reaction Amplification

A PCR was utilised to amplify the target regions in the nematode genes. Four different primer sets (Table 4.6) were initially assessed to determine the most efficient at amplifying the 18S ribosomal gene and to identify their suitability for DGGE. A GC clamp was added to the 5' end of each forward primer sequence to prevent complete denaturation of DNA during DGGE. PCR amplifications were carried out in 25 μl volumes, containing 2 μl extracted DNA (60-80 ng/μl), 11 μl 2X GoTaq® Green Master Mix (2 X Taq DNA polymerase, 400 μM dNTPs and 3 mM $MgCl_2$ [Promega]) and 0.5 μl of 0.2 μM of each primer [Eurofins Genomics]. The final volume was obtained with PCR grade water. The reaction was processed in a G-Storm GS1 thermocycler. The reaction conditions according to Bhadury *et al.* (2006), Foucher and Wilson (2002), Takemoto *et al.* (2010), and Waite *et al.* (2003) are outlined in Table 4.6. A negative control contained no DNA template and was used for each PCR thermocycler run. The PCR products were electrophoresed at 80V for 60 minutes on 0.8% agarose gel in 1x TAE buffer (0.04 M Tris acetate, 0.001 M EDTA, pH 8.5) and stained with 0.5 μg/ ml GelRed™ [VWR]. A 100 bp DNA ladder [Thermo scientific] was used for reference. The gel was visualised and the images were captured on a red ™ Personal Gel Imaging System.

4.2.3.3 Denaturing Gradient Gel Electrophoresis Establishment

The molecular fingerprinting technique DGGE was utilised to visualise the PCR products and determine nematode biodiversity. Electrophoresis was executed on a BIO Rad DCode™

universal mutation detection system. The apparatus was assembled according to manufacturers instructions (Bio-Rad, 1996). The tank was filled with 6.5 L of 1x TAE (2% 50x TAE and 8% dH_2O) buffer and heated to 65°C. Two clean glass plates (10 cm and 16 cm in height) were clamped into the core unit. A 6% polyacrylamide gel (to select for 300-1000 bp sized DNA fragments) with a gradient of 20-50% denaturing solution was used to achieve optimum banding clarity. The 20% (15 ml 40% acrylamide/ bis [BioRad], 2 ml 50x TAE buffer [BioRad], 8 ml deionised formamide [BioRad] and 8.4 g urea [BioRad]) and 50% (15 ml 40% acrylamide/ bis, 2 ml 50x TAE buffer, 20 ml deionised formamide and 21 g urea) stock denaturing solutions were prepared in 250 ml brown Duran bottles. Both solutions were made up to 100 ml with dH_2O and stored at 4°C. The gel was prepared by adding 20 ml 20% and 50% denaturing solution into two 30 ml tubes. To each tube, 180 μl 10% APS [BioRad] and 18 μl TEMED [BioRad] were added. To the 50% denaturing solution, 30 μl DCode dye solution was added. The denaturing solutions were poured into a gradient maker, the gel was cast and left to solidify for up to 4 hours at room temperature. The wells were washed with 1x TAE buffer and the gel

TABLE 4.6: Primer sets and PCR reaction conditions used for the amplification of 18S rDNA. The GC clamp was utilised with all primer sets, except for the SSU9R GC clamp which was utilised with SSU9R primer. F= forward primer and R= reverse primer.

Primer Set	Oligonucleotide Sequence	Amplicon Size	Reaction Conditions	Reference
nem 1 (F) nem 2 (R)	5'-GCA AGT CTG GTG CCA GCA GC-3' 5'-CCG TGT TGA GTC AAA TTA AG-3'	630 bp	2 min at 94°C, followed by four cycles of 40 s at 48°C, 2 min at 72°C and 30 s at 94°C and then 10 cycles of 25 s at 49°C, 90 s at 72°C, 15 s at 94°C, followed by 15 cycles of 20 s at 50°C, 120 s at 72°C and 15 s at 94°C with one more cycle of 20 s at 50°C, 4 min at 72°C and 1 min at 10°C.	Foucher and Wilson (2002)
NEMF1 (F) NEM896r (R)	5'-CGC AAA TTA CCC ACT CTC-3' 5'-TCC AAG AAT TTC ACC TCT MAC G-3'	469 bp	30 cycles of 1 min at 94°C, 1 min at 53°C and 2 min at 72°C.	Waite *et al.* (2003)
G18S4F (F) MN18F (F) 22R (R)	5'-TTG TCT CAA AGA TTA AGC C-3' 5'-CGC GAA TRG CTC ATT ACA ACA GC-3' 5'-GCC TGC TGC CTT CCT TGG A-3'	400 bp 345 bp	4 min at 95°C, 36 cycles of 1 min at 94°C, 1 min at 56°C, 90 s at 72°C, and one cycle of 2 min at 56°C and 30 min at 72°C	Bhadury *et al.* (2006)
SSU9R (F) SSU18A (R)	5'-GAG CTG GAA TTA CCG CGG CTG-3' 5'-AAA GAT TAA GCC ATG CAT G-3'	610 bp	3 min at 98°C, followed by 26 cycles of 10 s at 98°C, 15 s at 52°C, 40 s at 72°C and 10 min at 72°C.	Takemoto *et al.* (2010)
		GC Clamp		
	5'-CGC CCG CCG CGC GCG GCG GGC GGG GCG GGG GCA CGG GGG GCC-3'			Bhadury *et al.* (2006)
		SSU9R GC Clamp		
	5'-CGC CCG CCG CGC CCC GCG CCC 5 GGC CCG CCG CCC CCG CCC-3'			Takemoto *et al.* (2010)

was loaded onto the amber holder. It was placed into the tank containing 1x TAE buffer preheated to 60°C. The wells were loaded with 10 μl PCR product and 5 μl 2x loading dye. The gel was run on constant for 18 hours at 80 V.

It was stained in 400 ml 1x TAE buffer and 20 μl gel red, for 30 minutes, followed by a de-stain in H_20 for 15 minutes. The gel was visualised on red™ Personal Gel Imaging System and digital images were recorded. Due to low diversity visualised on the DGGE gels, Soil B PCR product replications were pooled together according to the bacterial or control treatment. Three replications of pooled PCR products were loaded onto DGGE gels for electrophoresis. To obtain a broad overview of the nematode diversity in the untreated soil, 18 replications of Soil A PCR products were electrophoresed on DGGE.

4.2.3.4 Denaturing Gradient Gel Electrophoresis Profile Analysis

The DGGE gels were digitally documented and analysed using CLIQS 1D Pro v 1.1 (TotalLab). The agglomerative hierarchical cluster method, unweighted pair group method with arithmetic mean (UPGMA) analysis was employed to assess the gels. Lanes were assigned and bands representing the operational taxonomic units (OTUs) were detected. Gel background subtraction was performed utilising the rolling ball background selection, set to 100. The band positions were normalised and any gel distortion was repaired, with the Rf calibration. Gel lanes were matched and band classes were created using the parameter Rf vector set at 0.02. The data obtained was assessed with two methods (1) binary data (presence = 1 and absence = 0 of bands) analysis, or (2) relative band intensity profile analysis (Chhabra, 2012).

4.2.3.5 Diversity Indices on DGGE Profiles

Nematode evenness was assessed with Pielous evenness index (J') to determine the closeness, in relative intensity, of each OTU (Section 4.2.2.7.1) in the samples. Shannon Wiener diversity index (H') was utilised to characterise the relative intensity of the nematode OTUs diversity (Section 4.2.2.7.3). Jaccard's similarity coefficient (S_j) was calculated to compare the similarity and diversity of OTUs present (Section 4.2.2.7.2) in the different soil types. The equations for these diversity indices (Neher and Darby, 2009) are found in Table 4.4.

4.2.3.6 Statistical Analysis

The results assigned to the diversity indices for the molecular analysis were statistically assessed (see Table 4.3). The statistical comparisons for each task are described in Table 4.1. A hierarchical cluster analysis, UPGMA (Table 4.3), was conducted on the OTUs determined from the values assigned to Soil A and Soil B. This type of clustering utilises an algorithm,

that determines the distance between two groups. It defines the distance as the average distance between each of their members. The data was assessed by the software package CLIQS 1D Pro (TotalLab). The results were used to present this information in the form of a dendrogram (Gafan *et al.*, 2005). Dice similarity coefficient was utilised to express the overall similarities of OTUs between samples. This coefficient is a measure similar to Jaccard's similarity coefficient except, the matching bands are weighted twice. A dendrogram hierarchically nests OTUs into increasingly more inclusive groups. The degree of similarity was represented by branch length. Multidimensional scaling (MDS performed on XLSTAT 2017), was used to observe the dissimilarities or the distances between Soil A and Soil B.

4.2.4 Transgenic *C. elegans* as a Biosensor of Nickel Bioremediation in an Oilseed Rape Crop

4.2.4.1 Determining Moisture Holding Capacity of Soil

A filter crucible containing 10 g oven dried, untreated soil (no bacteria or Ni; Table 4.2), was placed into a beaker with 30 ml sterile ddH_2O (Figure 4.1 Image B). The beaker was covered with parafilm and stored at 4°C overnight to allow the soil to become saturated, and for the water level to stabilise. The volume of water absorbed by the soil was measured, noted and subtracted from 30 ml. This volume of water was indicative of 100% moisture holding capacity (MHC) of the soil. Anbalagan *et al.* (2012) and Power and Pomerai (1999) used 50% MHC of soil, to carry out soil pore water extractions, to the test soil. The same MHC level was used in this research. To find 50% MHC of the soil, the water volume taken up by the soil was halved. The MHC was repeated six times.

4.2.4.2 Soil Pore Water Extractions

In Plant Trial 2, the soil was removed from pots that contained OSR inoculated with *P. fluorescens* treatments F113, L321, L111 and L132 (see Section 4.2.1.2). The samples were oven dried at 70°C for 48 hours. The soil, 250 g (Table 4.2) in total, was passed through a 2 mm sieve to remove large debris. The samples were stored in sealed bags, in a cool dry place for further analysis. To each beaker, 60 ml sterile ddH_2O was added to 120 g sieved dry soil. The soil was mixed vigorously using a glass rod to ensure all the soil was exposed to the water. The beaker was sealed with 2 layers of parafilm and stored overnight at 4°C. The wet soil was split between two 20 ml syringe barrels plugged with plastic mesh and glass wool, as described in Anbalagan *et al.* (2012). The syringe barrels were placed into 50 ml plastic tubes and sealed in place with masking tape. The tubes were centrifuged at

3,800 rpm for 20 minutes at room temperature. The filtrate or soil pore water (SPW) was poured into clean 30 ml tubes and labelled. More soil was added to the syringe barrels, and the samples were centrifuged again. This was repeated until all the soil was processed. In total, 15-20 ml of soil pore water was recovered from each soil sample after 2–4 centrifuge cycles. Soil pore water extracts were re-centrifuged at 3,800 rpm for 20 minutes to remove any remaining sediment. This was repeated for each bacterial and control treatment. There were four replications per treatment (see Table 4.7 for details).

TABLE 4.7: Replications utilised for SPW and GFP reporter assays

Work task	**Replications**
Plant trial	Pots per treatment = 4
SPW extractions	Replications per pot = 1
GFP reporter assay	Pseudo replications per SPW sample = 6

Bacterial treatments = F113, L111, L132 and L321
Control treatments; C1 = Ni and no bacteria and C2 = No Ni and no bacteria

4.2.4.3 Culture and Maintenance of Transgenic *C. elegans*

Transgenic *C. elegans* CL2050 *hsp*-16.2::GFP (Chapter 2, Table 2.1) were cultured on NGM agar plates (Chapter 2, Section 2.2.2.1), seeded with an *E. coli* OP50 lawn. The nematodes were incubated at 20°C for 3-5 days until the plates were heavily populated. Nematodes of all ages (Anbalagan *et al*., 2012) were washed off the NGM plates with ice-cold K medium (53 mM NaCl and 32 mM KCl; Williams and Dusenbery, 1990). The nematodes were left to settle on ice for 5-10 minutes and re-suspended in fresh K medium to remove bacteria, this was repeated a further 2-3 times. Once the nematodes had settled, they were removed to a 30ml falcon tube and re-suspended in 10 ml K medium. The nematode concentration was estimated via counting in 20μl aliquots under a low-power stereoscope.

4.2.4.4 GFP reporter assay

A bioassay was established to expose transgenic *C. elegans* to SPW extractions (Anbalagan *et al.*, 2012). To each well, of a 24-well flat-bottomed tissue culture plate, 1000 nematodes in 50 μl K medium and 250 μl SPW were added. The nematodes were exposed to the SPW for 24 hours. There were six pseudo - replications taken from each SPW sample (see Table 4.7 for replications) which were representative of each OSR plant pot. Two negative controls were prepared by (1) replacing the SPW with sterile ddH_2O, these contained nematodes and (2) ddH_2O only in each well.

After 24 hours, the contents of each 24 well-plate were removed and placed into black U-bottomed 96-well micro titre-plate (Cruinn Diagnostics) and read on a micro-titre plate

reader (see Figure 4.4for an example of the 96-well plate Bioassay Plate 1). The results were statistically compared to Control 1 on plate 1. Bacterial treatment L321 and control treatment C1 were read on Bioassay Plate 2 and were also statistically compared to Control 1 on plate 2. The 96 well-plates were kept on ice for 15 minutes for the nematodes to settle to the bottom of the wells. The fluorescent response of the transgenic nematodes after 24 hours exposure was measured using Tecan GENios Fluorescent plate reader with excitation (485 nm) and emission (525 nm) filters. Plates were read three consecutive times in the plate reader. The data was collated with the software Magellan, normalised and the nematodes were assessed for mortality.

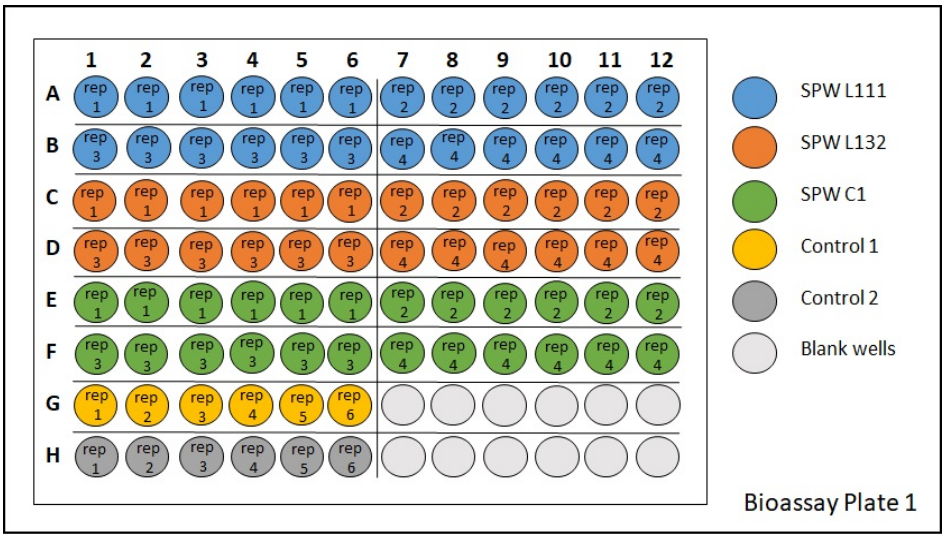

FIGURE 4.4: Example of the establishment of a 24 hour GFP reporter assay to expose transgenic *C. elegans* CL2050 to SPW extractions (Table 4.8). Treatment replication = the treated plant replications (1-4), 96-well plate replication = the coloured wells (1-6). A second plate was also established parallel to the present plate, with the same lay-out for the remaining bacterial and control treatments.

TABLE 4.8: Description of GFP reporter assay 96 well plate contents (Figure 4.4).

Treatment	Colour	Contents of the well
L111	Blue	1000 nematodes and 250 μl SPW[1]from pots treated with L111
L132	Orange	1000 nematodes and 250 μl SPW from pots treated with L132
C1[2]	Green	1000 nematodes and 250 μl SPW from pots assigned to C1
Control 1	Yellow	1000 nematodes and and 250 μl sterile ddH_2O
Control 2	Grey	250 μl sterile ddH_2O
Blank	White	-

[1] SPW = Soil pore water
[2] C1 = Control treatment 1 = Pots treated with Ni but no bacteria
- = Nothing added to the wells

4.2.4.5 Data Analysis with Image J

Following 24 hours of exposure to SPW, the nematodes were removed from the black 96 well plates (continuation from the previous experiment in Section 4.2.4.4) and mounted onto glass slides. The slides were passed through a Bunsen burner to fix the nematodes. Digital images were immediately taken of the fluorescing nematodes with a Nikon eclipse 80i epi-fluorescence microscope with NIS-Elements software. Ten images of fluorescing nematodes were captured per treatment. Ten background images were captured and utilised to calculate mean background fluorescence. The images were assessed using the open-sourced image processing and analysis program, Image J version 1.6.0. (Burgess *et al.*, 2010). Individual nematodes were observed on the images, for GFP expression. The area of GFP production in the nematode was outlined using the 'freehand selection' function, to define the region of interest (ROI). Measurements for analysis were set utilising the area, integrated density and mean greyscale functions (Cramer, 2012). The ROI of 10 fluorescing adult nematodes from each treatment, randomly selected, were determined. The data was assessed and the corrected total GFP fluorescence (McCloy *et al.*, 2014) was calculated in Microsoft Excel, using the formula:

Total GFP Fluorescence = Integrated Density - (Nematode Area x Mean Fluorescent Background)

4.2.4.6 Statistical Analysis

The results assigned to the GFP reporter assays and those determined for the Image J analysis were statistically assessed (see Table 4.3). The statistical comparisons for each task are described in Table 4.1.

4.3 Results

4.3.1 Oilseed Rape Microcosm Establishment

4.3.1.1 Soil Profile Analysis

A soil profile analysis, on soil utilised in this experiment, collected from Teagasc Oakpark, Co. Carlow was determined. It contained 40% sand, 40% silt and 20% clay. The soil type was identified as loam using a soil texture triangle (Appendix C, Figure C.1).

4.3.1.2 Plant Growth Promoting Bacteria Colonisation in Oilseed Rape

In the rhizosphere, the highest colony counts were recorded in pots treated with F113 with 2.43 log CFU g^{-1}, (Figure 4.5) followed by those treated with L321 with 1.34 log CFU g^{-1}. There was a statistical difference (see Appendix C, Table C.1) between the soil that contained OSR treated with bacterial treatment F113 (p = 0.01) and the control treatment.

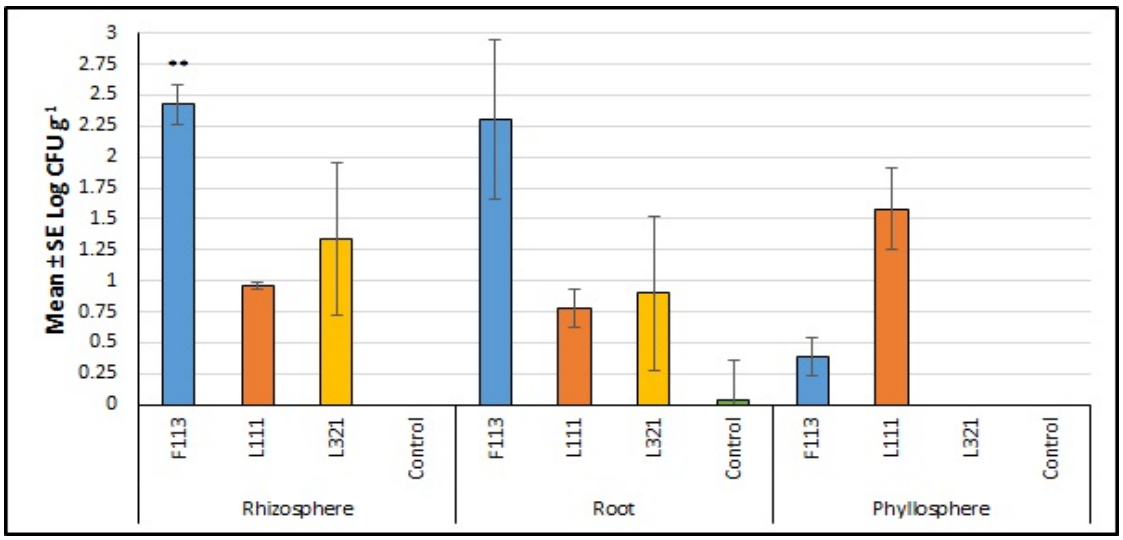

FIGURE 4.5: Viability of PGP bacteria (Log CFU g^{-1}) in the rhizosphere, roots and phyllosphere of oilseed rape after 6 months plant growth. Control = No bacteria. The error bars represent ± SEM. ** $p \leqslant 0.01$.

Similarly to the rhizosphere results, the presence of bacteria in OSR roots (Figure 4.5) were highest in plants inoculated with strain F113 with 2.30 log CFU g^{-1}, followed by those treated with L321 with 0.90 log CFU g^{-1}. Bacterial colonisation in the phyllosphere (Figure 4.5) were highest in plants inoculated with strain L111 with 1.58 log CFU g^{-1} followed by those treated with F113 with 0.39 log CFU g^{-1}.

4.3.1.3 Analysis of Soil and Plant Tissue for the Presence of Nickel

The Ni concentration in SPW samples after six months plant growth was highest in pots treated with L132 (0.94 ppm), followed by F113 (0.88 ppm). Soil pore water from the control treatment C1 contained 2.83 ppm and C2 contained 0.001 ppm (Figure 4.6). In the rhizosphere (Figure 4.7) the highest Ni concentration occurred in pots treated with the bacterial strain L132 (21.34 ppm), followed by L111 (21.19 ppm). The SPW concentration analysed from the rhizosphere in control treatment C1 contained 25.48 ppm, and those from C2 contained 10.44 ppm and those from C3 contained 37.67 ppm.

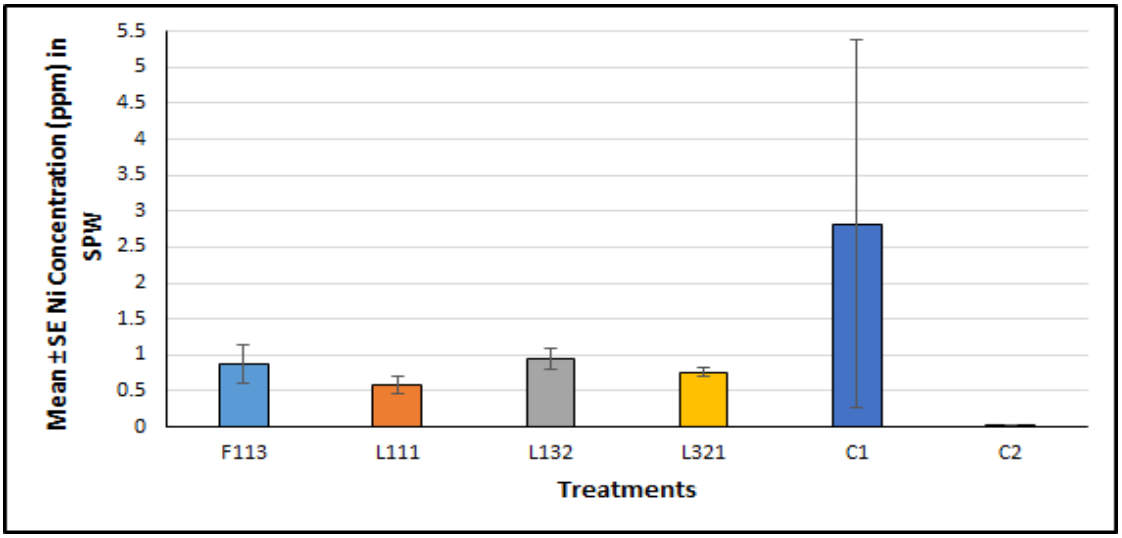

FIGURE 4.6: Nickel concentration in the SPW samples from each bacterial and control treatment. C1 = Ni and no bacteria and C2 = No Ni and no bacteria. The error bars represent ± SEM.

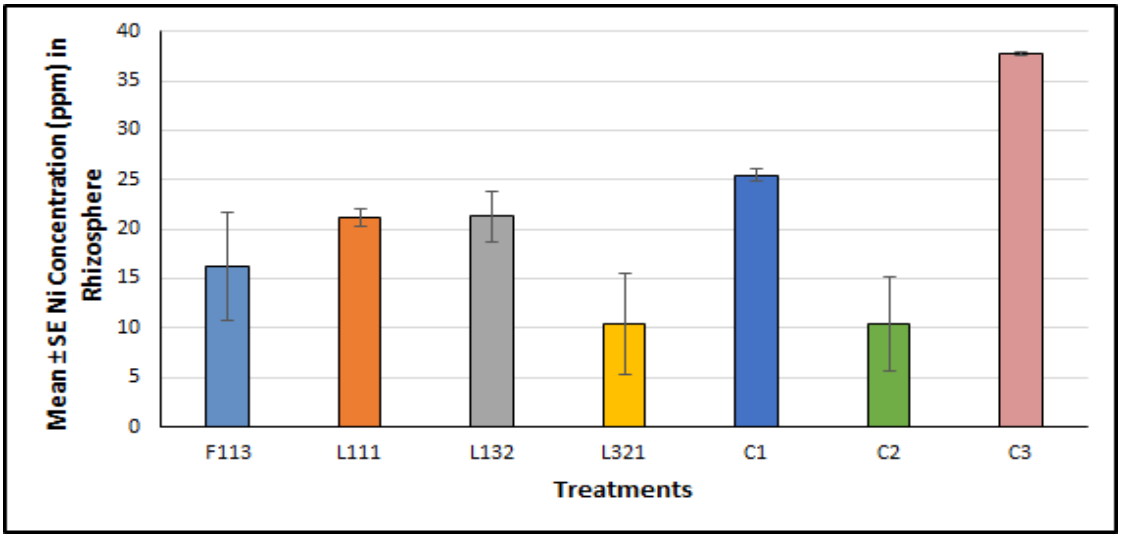

FIGURE 4.7: Nickel concentration in the rhizosphere samples from each bacterial and control treatment. C1 = Ni and no bacteria, C2 = No Ni and no bacteria and C3 = Ni spiked soil and no plant. The error bars represent ± SEM.

The Ni concentration in OSR (Figure 4.8) after 6 months, was highest in plants inoculated with F113 (2.10 ppm), followed by L111 (1.36 ppm). Plants assessed from the control treatment C1 contained 2.60 ppm and from C2 contained 0.11 ppm. There was a significant difference (Appendix C, Table C.1) between the control treatments C1 and C2 (p = 0.040).

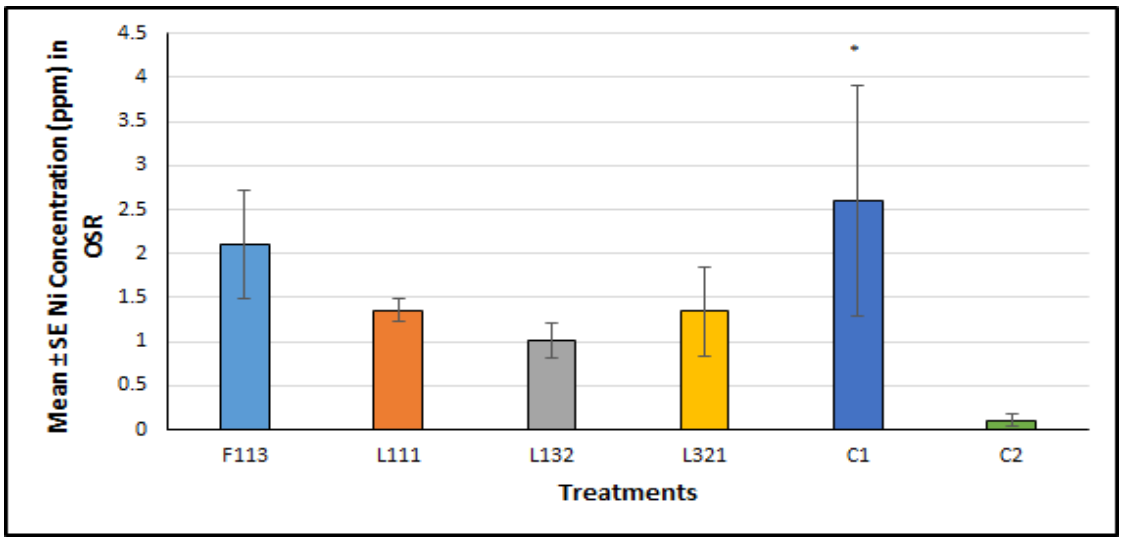

FIGURE 4.8: Nickel concentration in the OSR samples from each bacterial and control treatment. C1 = Ni and no bacteria and C2 = No Ni and no bacteria. The error bars represent ± SEM. Statistical significance α= 0.05 level; * p $\leqslant$ 0.05.

4.3.1.4 Plant Biomass

Biomass assessed from OSR roots and shoots (FW) after three months growth (Figure 4.9) were highest in plants treated with L111 (2.76 g and 7.45 g respectively). Subsequently, the total FW was highest in plants treated with L111 after 3 months growth. Root and shoot FW after six months growth was highest in those treated with bacterial strain L321 (1.60 g and 5.33 g respectively). Therefore the total FW after six months was highest in plants inoculated with L321.

Oilseed rape root biomass (DW) after three months growth (Figure 4.10 and Appendix C, Table C.2) was highest in plants treated with L321 (0.64 g). Biomass (DW) was highest in OSR shoots treated with L111 (1.38 g). The total DW after three months of growth, therefore, was highest in plants treated with the bacterial treatment L111 (2.02 g). The root and shoot biomass (DW) after six months growth was highest in plants treated with L321 (0.37 g and 1.24 g respectively). However, the total DW after six months growth was highest in the plants inoculated with L111 (1.43 g). There was a significant difference between plants treated with bacterial treatment L321 and control treatment C2, for plant FW (Root, p = 0.010; Shoot, p = 0.006; Total p = 0.003) and DW (Root, p = 0.024; Shoot, p = 0.047; Total, p = 0.027) after six months growth (Appendix C, Table C.2). There was also a significant difference in

the data assigned to the OSR shoots (DW), between the bacterial treatment L111 and control treatment C2 ($p = 0.034$) after six months.

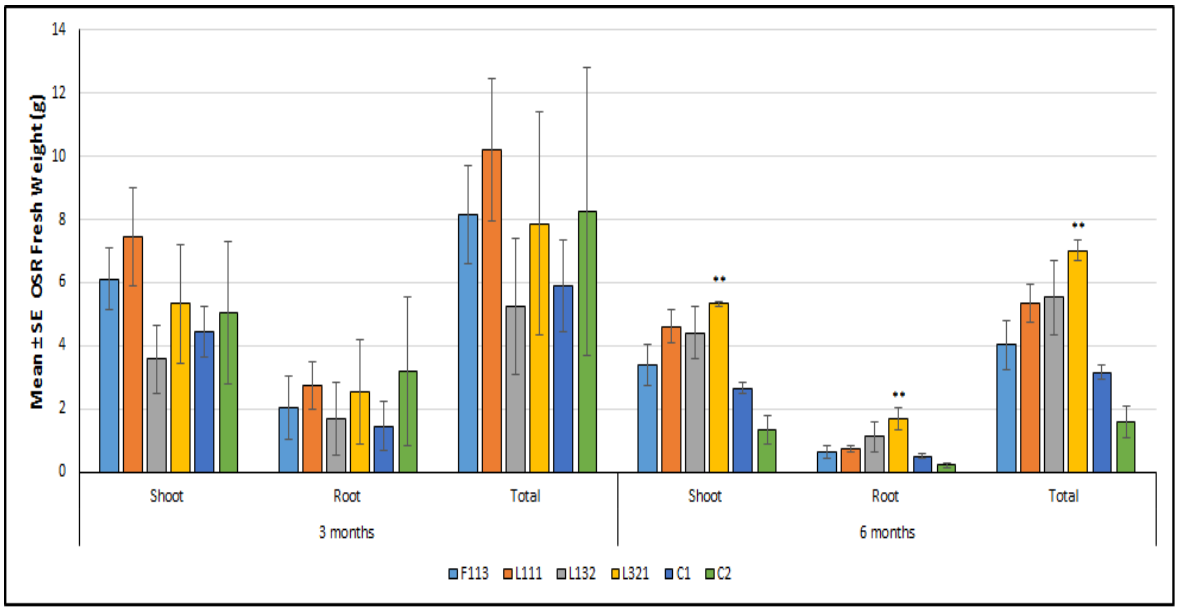

FIGURE 4.9: Oilseed rape fresh weight biomass inoculated with *P. fluorescens* strains after three and six months Ni exposure. The bars represent ± SEM. The presence of asterisks indicate significant differences between the bacterial treatments and control treatment C2. Statistical significance $\alpha = 0.05$ level; * $p \leqslant 0.05$, ** $p \leqslant 0.01$.

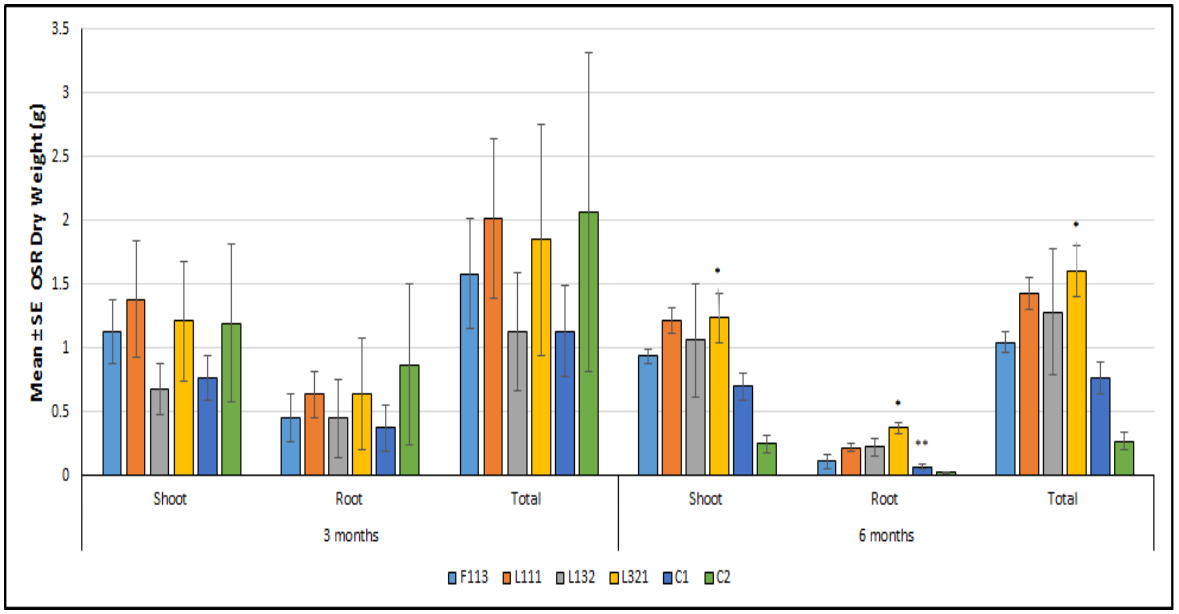

FIGURE 4.10: Oilseed rape dry weight biomass inoculated with *P. fluorescens* strains after three and six months Ni exposure. The bars represent ± SEM. The presence of asterisks indicate significant differences between the bacterial treatments and control treatment C2. Statistical significance $\alpha = 0.05$ level; * $p \leqslant 0.05$, ** $p \leqslant 0.01$.

4.3.2 Nematode Assemblage Characterisation Utilising Morphological Techniques

4.3.2.1 Morphological Identification of Nematodes

Up to 200 nematodes were identified per replication in Soil A (Table 4.9) and up to 50 nematodes were identified, per treatment replication (replications = 4) in Soil B. Therefore 200 nematodes per treatment were identified in total. However, if the required number of nematodes were not present in the samples, all the nematodes present were identified.

TABLE 4.9: Number of nematodes identified in Soil A and Soil B.

Soil	Treatment	Replication	Identified
A		1	212
		2	181
		3	183
		4	199
B	F113	Combined	194
	L132	Combined	198
	L111	Combined	185
	L321	Combined	170
	C1	Combined	192
	C2	Combined	195

4.3.2.1.1 Predatory nematodes

Predatory nematodes or carnivores have a large buccal cavity, which is adapted to the food the nematode eats. They feed on other soil nematodes, including both plant-parasitic and free-living nematodes and on other animals of various sizes. The buccal cavity of predatory nematodes such as *Anatonchus* spp. and *Mylonchulus* spp., contains thick ridges that run vertically (Figure 4.11, Images A, B and E) towards the oesophageal region. Often predatory nematodes have teeth in the buccal cavity ranging from a single mural tooth, as seen in *Mylonchulus sigmaturus* and *Clarkus papillatus* (Figure 4.11, Images C, E and F), up to three teeth in *Anatonchus tridentatus* (Figure 4.11, Images A and B).

4.3.2.1.2 Bacterial feeding nematodes

Bacterial feeding nematodes or bacterivores have a narrow stoma, which is a hollow tube adapted to ingest bacteria, as seen in *Rhabditis* spp. and *Eucephalobus* spp. (Figure 4.12, Images A, B and D). Many kinds of free-living nematodes feed only on bacteria and are generally abundant in the soil, such as *Eucephalobus* spp. (Figure 4.12 image B) which have projections or probolae on the top of the head or *Achromadora* spp. (Figure 4.12 image C)

which are distinguishable with a spiral amphid, situated just behind the level of the base of the stoma. They also contain small apical papilla on each of the six lips.

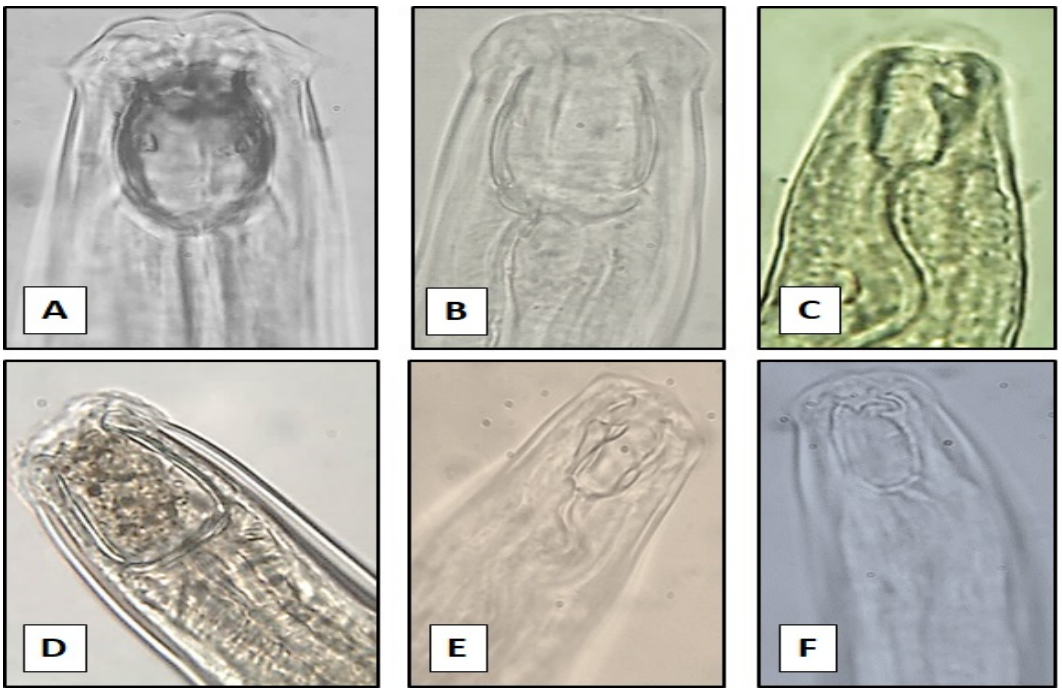

FIGURE 4.11: Carnivore nematodes displaying large buccal cavities and some teeth. A = *Anatonchus tridentatus* B = *Anatonchus* spp. C = *Clarkus* spp. D = *Miconchus* spp. E = *Mylonchulus sigmaturus* F = *Clarkus papillatus*.

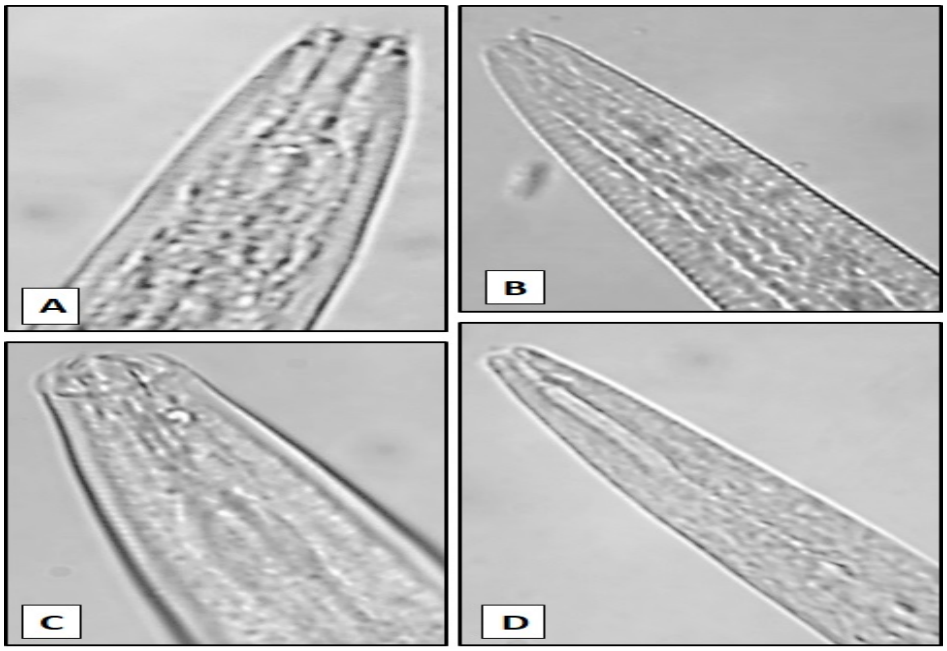

FIGURE 4.12: Bacterial feeding nematodes displaying a narrow stoma for the ingestion of bacteria. A = *Rhabditis* spp. B = *Eucephalobus* spp. C = *Achromadora* spp. D = *Rhabditis* spp.

4.3.2.1.3 Omnivorous and plant feeding nematodes

Omnivorous nematodes are generalists and feed on more than one type of food including fungal spores, bacteria, algae and other animals; or they may have a different diet at each life stage. Nematode omnivores have a stylet, a spear like projection that can either be solid or hollow. Plant-feeding nematodes have a stylet that is adapted to penetrate plant cells. The spear is retractable as for omnivorous nematodes *Aporcelaimellus* spp., *Mesodorylaimus* spp. and *Prodorylaimus* spp. This is also evident in plant-feeding nematodes *Pungentus* spp. and *Pratylenchus* spp. (Figure 4.14, Images A, F, G and H, and Figure 4.13, Images A and B) and is used for feeding. Some nematodes such as omnivorous *Aporcelaimellus* spp. contain an onchiostyle (Figure 4.14, Images D and E). Basal knobs were present in the omnivorous nematode *Mesodorylaimus* spp. and plant feeding nematode *Bitylenchus* spp. (Figure 4.14, image F and Figure 4.13 image G); they are attached to a barb and shaft. The median bulb, in omnivorous nematode *Prodorylaimus* spp. (Figure 4.14, Image H) is another identifiable feature and can contain a valve. Some nematodes have a guiding ring either at the base or the tip of the stylet, that helps to guide the spear through the region, as seen for plant feeding nematode *Pratylenchus* spp. (Figure 4.13, Image B).

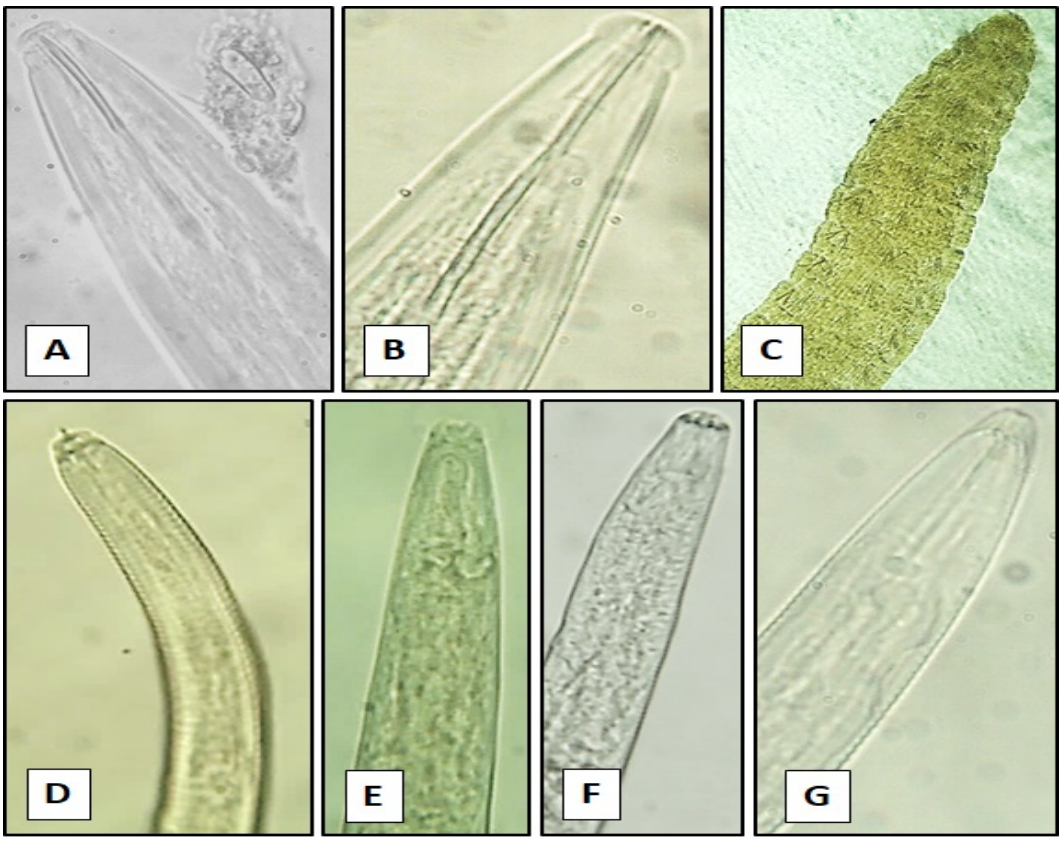

FIGURE 4.13: Plant feeding nematodes displaying stylets or spear-like projections in their oesophageal region, which are adapted for their food source. A = *Pungentus* spp. B = *Pratylenchus* spp. C = *Criconema* spp. D = *Helicotylenchus* spp. E = *Tylenchus* spp. F = *Dolichorhynchus* spp. G = *Bitylenchus* spp.

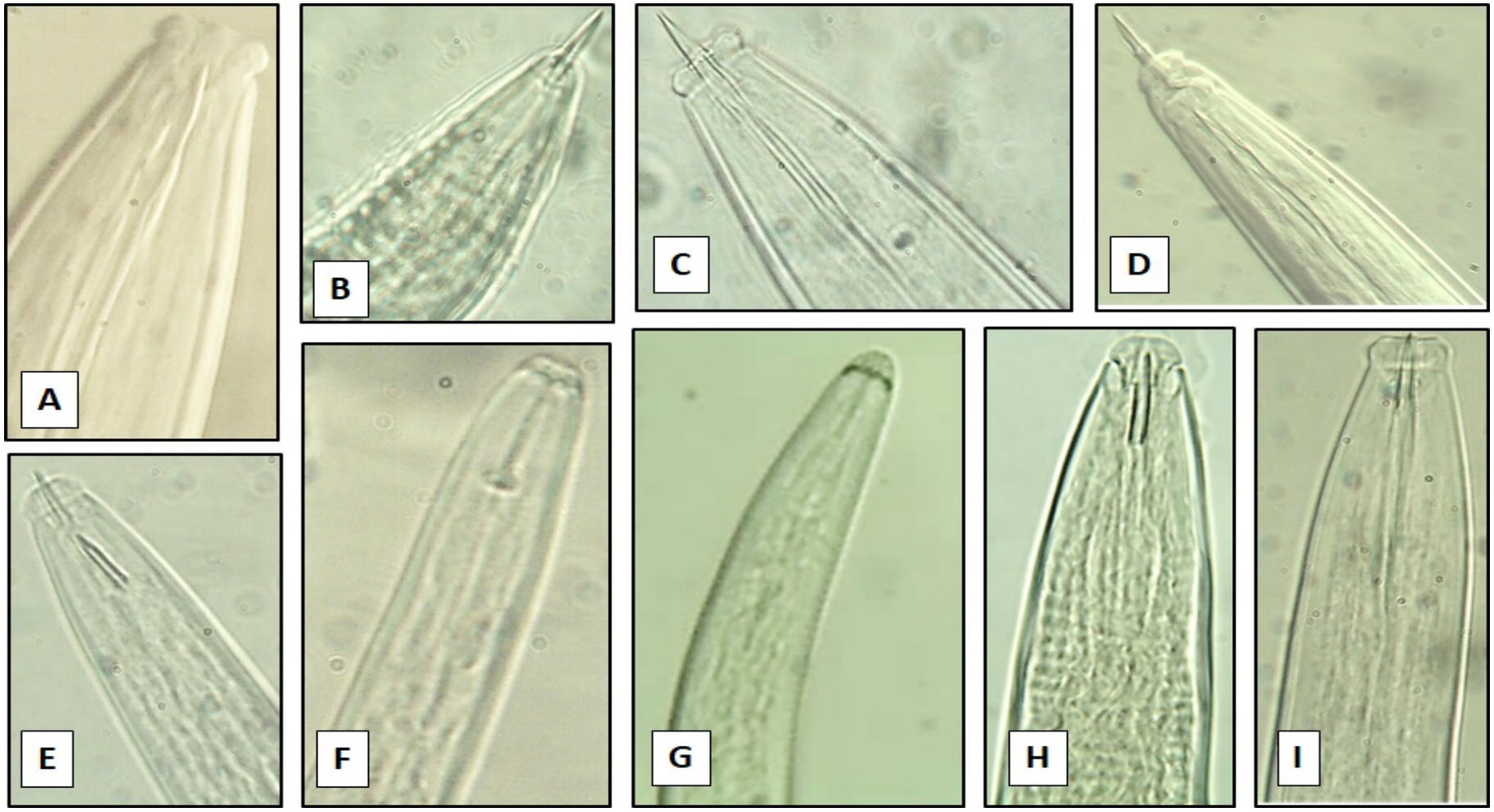

FIGURE 4.14: Omnivorous nematodes displaying stylets or spear-like projections in their oesophageal region. A = *Aporcelaimellus spp.* B = *Mesodorylaimus* C = *Aporcelaimellus tritichi* D = *Aporcelaimellus obtusicladatus* E = *Aporcelaimellus* spp. F = *Mesodorylaimus* spp. G = *Mesodorylaimus* spp. H = *Prodorylaimus* spp. and I = *Aporcelaimellus* spp.

4.3.2.1.4 Cephalic region

The cephalic region contains the mouth, lips, pore like amphid and papillae. Some cephalic regions are lobed, such as the predatory nematodes *A. tridentatus*, *Miconchus* spp. and *Mylonchulus* spp. (Figure 4.11, Images A, B, D and F), bacterial feeding nematodes *Rhabditis spp.* and *Achromadora* spp. (Figure 4.12, Images A, C and D), omnivorous nematodes *Aporcelaimellus* spp. (Figure 4.14, Images A, C D E and I), and plant feeding nematodes *Tylenchus* spp. and *Dolichorhynchus* spp. (Figure 4.13, Images E and F). Other nematodes have a smooth cephalic region such as omnivorous nematodes *Mesodorylaimus* spp. and *Aporcelaimellus* spp. (Figure 4.14, Images B, D, E, F, G and H) and plant feeding nematodes *Pratylenchus* spp., *Helicotylenchus* spp. and *Bitylenchus* spp. (Figure 4.13, Images B, D and G).

4.3.2.1.5 Tail region

The shape and form of the tail region in nematodes is an important feature in their identification and varies among species. The tail terminus of the predatory nematode *M. sigmaturus* (Figure 4.3.2.1.5, Image C) is blunt and rounded with a short projection, unlike the tail region of *Ditylenchus* spp. (Figure 4.3.2.1.5, Image E) which is narrow and pointed. *Clarkus papillatus*, *A. tridentatus* and *C. parvus* (Figure 4.3.2.1.5, Images A, B and D) all have similarly shaped tails where the tail terminus is long, curved and conoid, however *A. tridentatus* tail is more rounded at the tip compared to *C. papillatus* and *C. parvus*, which belong to the same family, Monochidae. Some bacterial feeding nematode tails are long and filiform such as in *Heterocephalobus spp.* (Appendix C, Figure C.2, Image D). The tail terminus can be pointed or convex-conoid, as for *Rhabditis* spp. (Appendix C, Figure C.2, Image B) or rounded and blunt as for *Eucephalobus* spp. and *Acrobeloides* spp. (Appendix C, Figure C.2, Images C and E, respectively). Some nematodes have a small pointed projection or a spinneret at the end of the tail such as *Achromadora* spp. (Appendix C, Figure C.2, Image A). The tail region of the omnivorous nematode *Prodorylaimus* spp. is long and filiform (Appendix C, Figure C.3, Images A and C) and slightly tapering in Image C. The omnivorous nematode *Eudorylaimus* spp. (Appendix C, Figure C.3, Images D and E) has a round tail terminus with a subdigitate pointed projection at the end. The nematode *A. obtusicaudatus* (Appendix C, Figure C.3, Image B) and the plant feeding nematode *Pungentus* spp. (Appendix C, Figure C.4, Image A) tails and are bluntly conoid and round cylindroid respectively. The plant feeding nematode *Malenchus* spp. (Appendix C, Figure C.4, Image D) has a pointed tail terminus which is convex ovoid in form, while the plant feeding nematodes *Pratylenchus* spp. and *Helicotylenchus* spp. (Appendix C, Figure C.4, Images C and B) both have a blunt boxy tail terminus.

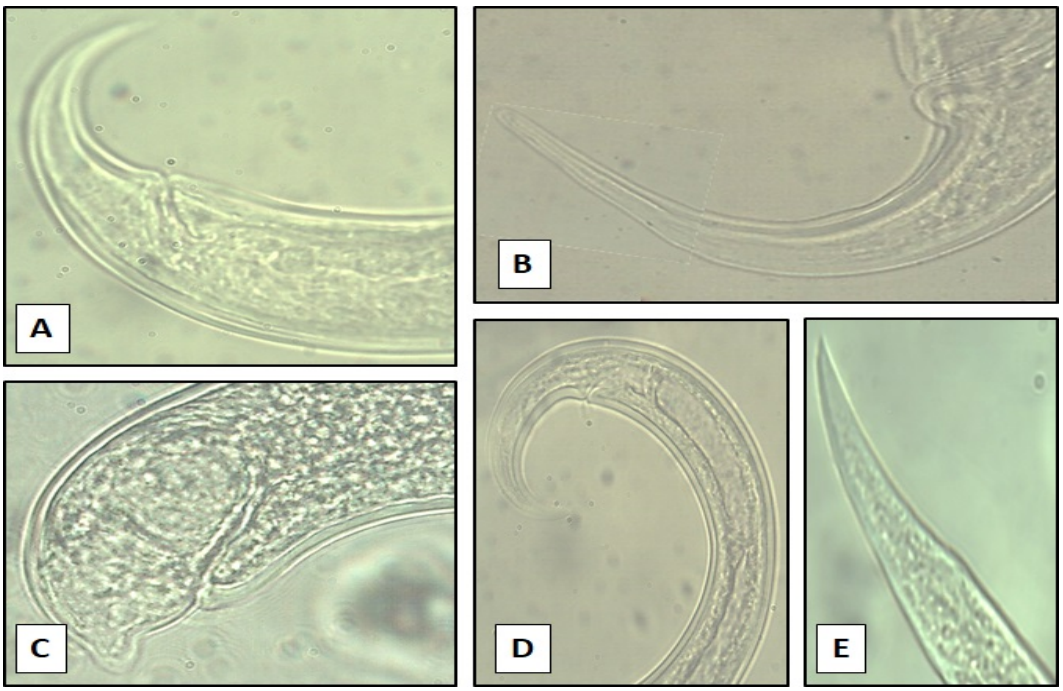

4.3.2.1.6 Nematode cuticle

The nematode cuticle can be used to confirm nematode identification. The bacterial feeding nematodes *Rhabditis* spp. (Figure 4.12, images A and D), *Acrobeloides* spp. and *Eucephalobus* spp. (Figure C.2, Images E and D), all have striation on their bodies that are transversly annulated. The omnivorous nematode *Mesodorylaimus* spp. (Figure 4.14, Image B) and plant feeding nematode *Helicotylenchus* spp. (Figure 4.13, image D) are also transversly annulated. Some nematodes cuticle can be entirely smooth such as, that of the omnivorous nematodes *Aporelaimellus* spp. and the Dorylaimids (Figure 4.14, Images A, C, D, E, F, G, H and I). Some nematode species have striation on specific regions on their body such as in the carnivorous nematode *A. tridentatus* (Appendix C, Figure 4.3.2.1.5, Image B) and the plant feeding nematodes *Malenchus* spp. (Appendix C, Figure C.4, Image B), which have course striation on their tail region. The plant feeding nematode *Criconema* spp. has course striation, with scale like projections (Figure 4.13, Image C).

4.3.2.1.7 Nematode reproductive structures

Nematode reproduction features are important characteristics for nematode identification, including the presence or absence of a male nematode within a species. The distance of the female vulva, or male spicule, to the tail is representative of some species. The retractable male spicule is evident in *Anatonchus* spp. (Figure 4.15, Images A and G). The spicule is supported by a gubernaculum, for *Rhabditis* spp. and *M. sigmaturus* (Figure 4.15, Images A and F). The female nematodes *Aporcelaimellus* spp. and *Xiphinema* spp. (Figure 4.15, Images C, D and E) clearly show the vulva and two ovaries.

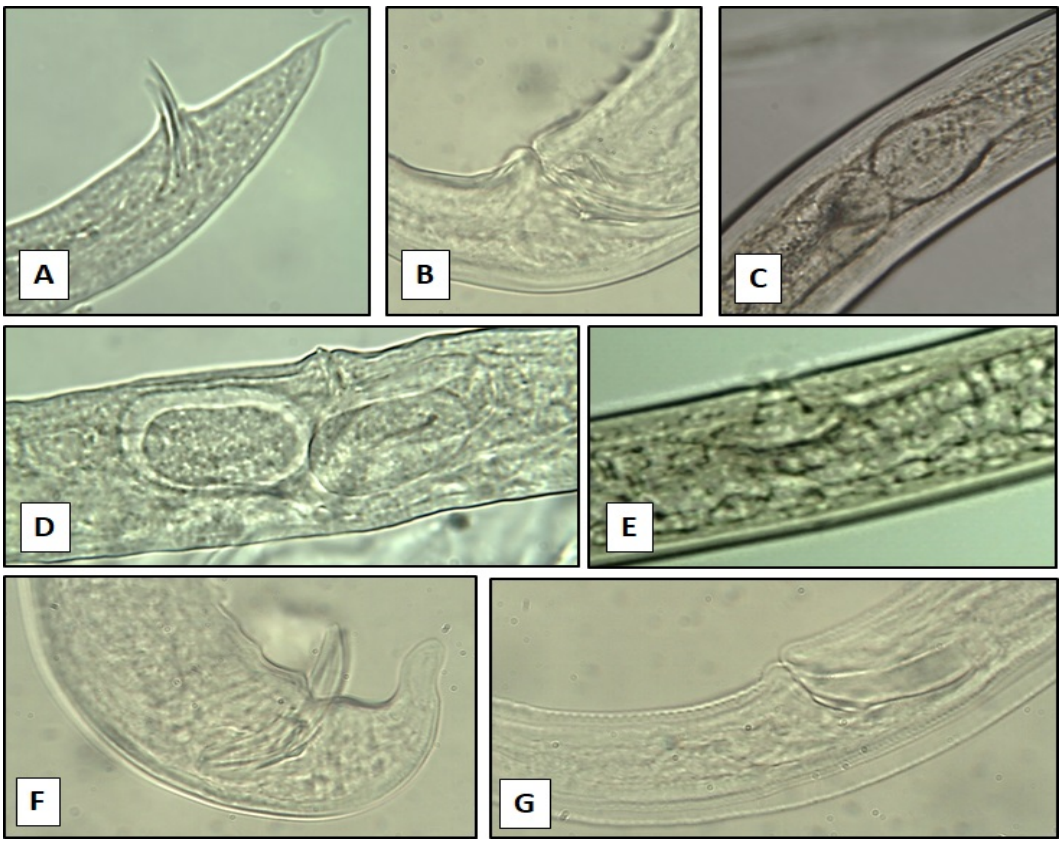

FIGURE 4.15: Nematode reproductive structures displaying ovaries and copulatory structures. A = *Rhabditis* spp. B = *Anatonchus tridentatus* C = *Aporcelaimellus* spp. D = *Aporcelaimellus* spp. E = *Xiphinema* spp. F = *Mylonchulus sigmaturus* G= *Anatonchus* spp.

4.3.2.1.8 Nematode form and shape

Images of whole nematodes were captured to determine nematode biomass, by measuring nematode width and length, but also to aid in the identification process. The differences in the nematode body form varied considerably between genera, such as *Prodorylaimus* spp. (Figure 4.16, Image B) compared to *Anatonchus tridentatus* (Figure 4.16, Image G). The shape of the preserved nematodes, is also an indication of their genus, as some take up a 'J' shape, such as *Pungentus* spp. (Figure 4.16, Image C) and *Mylonchulus* spp.(Figure 4.16, Image F), while others are straighter in form, such as *Pratylenchus* spp. (Figure 4.16, Image A) and *Aporcelaimellus* spp (Figure 4.16, Image E).

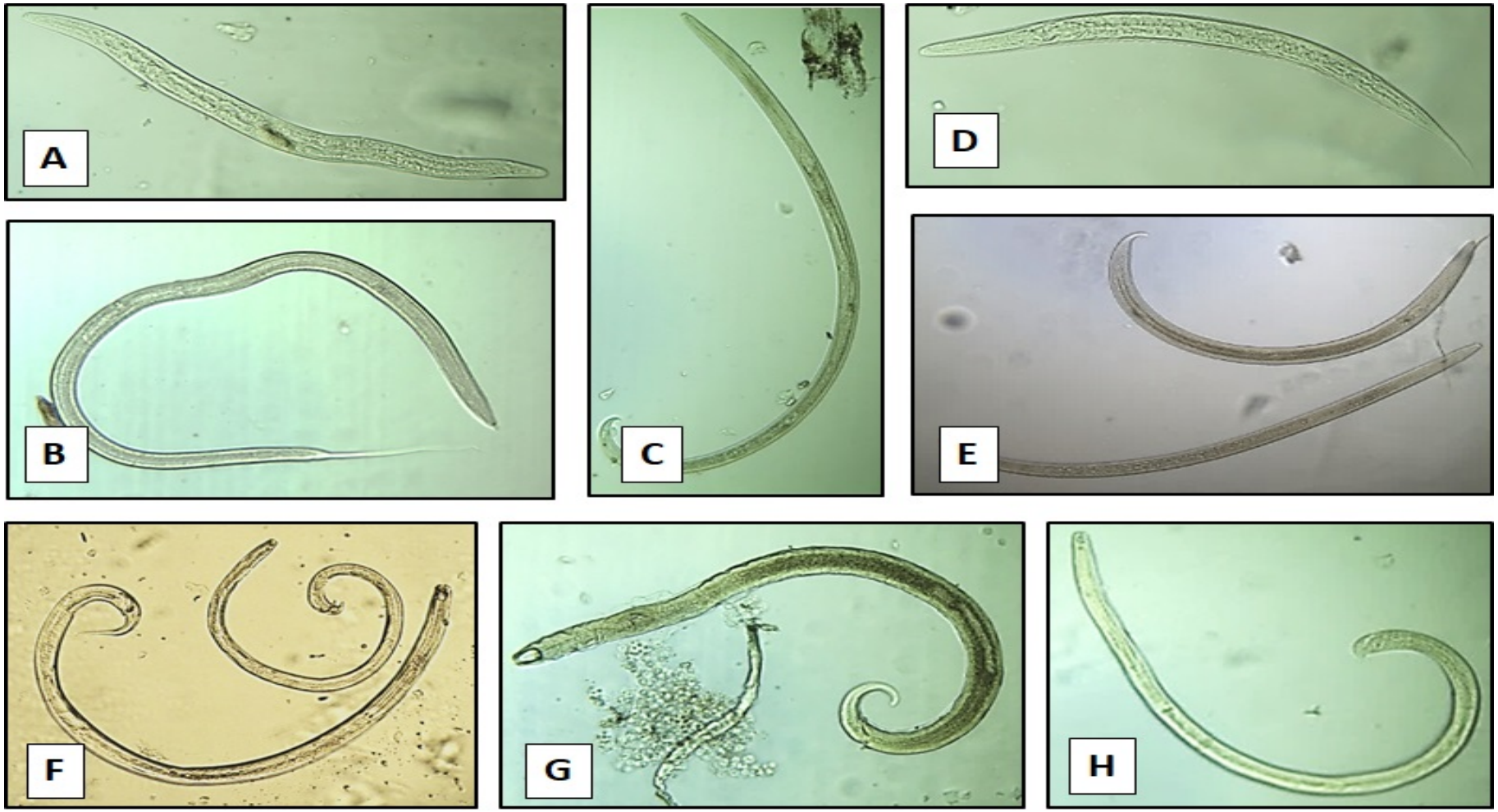

FIGURE 4.16: Examples of whole nematode images, captured to measure nematode length and width to determine nematode biomass and for nematode identification. A = *Pratylenchus* spp. B = *Prodorylaimus* spp. C = *Pungentus* spp. D = *Heterocephalobus* spp. E =*Aporcelaimellus* spp. (both) F = *Mylonchulus* spp. (top) *Anatonchus tridentatus* (bottom) G = *Anatonchus tridentatus* H = *Mylonchulus* spp.

TABLE 4.10: Identified nematodes from Soil A and Soil B according to family, genus and some species level. The coloniser-persister scale (c-p) and nematode feeding type were assigned. The identified nematodes, their corresponding c-p scale and feeding type were arranged according to their trophic grouping (Bongers and Bongers, 1998; Zullini, 2007). Their indicator guilds were assigned according to Ferris *et al.* (2001). Ca= Carnivore; Ba= Bacterivore; Fu= Fungivore; Om= Omnivores; and Pl= Plant feeders. The number following each indicator guild refers to the c-p scale.

Family	Genera and species		C-P	Feeding type	Guild
	Soil A	**Soil B**			
		Predator			
Alaimidae	*Amphidelus*	-	4	3	Ca_4
Anatonchidae	-	*Anatonchus*	5	5a	Ca_5
Anatonchidae	*Anatonchus tridentatus*	*Anatonchus tridentatus*	5	5a	Ca_5
Mononchidae	*Clarkus papillatus*	*Clarkus papillatus*	3	5a	Ca_3
Mononchidae	*Coomansus*	*Coomansus*	4	5a	Ca_4
Mononchidae	*Coomansus parvus*	*Coomansus parvus*	4	5a	Ca_4
Leptolaimidae	*Deontolaimus*	-	4	3	Ca_4
Diplogasteridae	*Diplogasteritus*	-	4	3	Ca_4
Diplogasteroididae	*Diplogasteroides*	*Diplogasteroides*	5	3	Ca_5
Anguinidae	*Ditylenchus*	*Ditylenchus*	4	2,1b	Ca_4
Anatonchidae	*Miconchus*	-	4	5a	Ca_4
Anatonchidae	*Miconchus studeri*	-	4	5a	Ca_4
Mononchidae	*Mononchus*	*Mononchus*	4	5a	Ca_4
Mononchidae	*Mylonchulus*	*Mylonchulus*	4	5a	Ca_4
Mononchidae	-	*Mylonchulus rotundicaudatus*	4	5a	Ca_4
Mononchidae	*Mylonchulus sigmaturus*	*Mylonchulus sigmaturus*	4	5a	Ca_4
Nygolaimidae	*Nygolaimus macrobrachyuris*	-	5	5	Ca_5
Mononchidae	*Prionchulus punctatus*	-	4	5a	Ca_4
		Bacterial feeders			
Achromadoridae	*Achromadora pseudomicoletzkyi*	-	4	6	Ba_4
Cephalobidae	*Acrobeloides*	-	3	3	Ba_3
Alaimidae	*Alaimus*	-	4	3	Ba_4
Plectidae	*Anaplectus*	*Anaplectus*	5	3	Ba_5
Cephalobidae	*Cephalobus*	*Cephalobus*	4	3	Ba_4
Cephalobidae	*Eucephalobus*	*Eucephalobus*	2	3	Ba_2
Cephalobidae	*Heterocephalobus*	-	3	3	Ba_3
Plectidae	*Plectus*	*Plectus*	2	3	Ba_2
Neodiplogasteridae	*Pristionchus*	-	1	3, 5a	Ba_1
Neodiplogasteridae	*Pristionchus lheritieri*	-	1	3, 5a	Ba_1
Desmodoridae	*Prodesmodora*	*Prodesmodora*	3	3	Ba_3
Rhabditidae	*Protorhabditis*	-	1	3	Ba_1
Rhabditidae	*Rhabditis*	*Rhabditis*	1	3	Ba_1
Rhabditidae	*Rhabditis terricola*	-	1	3	Ba_1
Rhabdolaimidae	*Rhabdolaimus*	-	3	3	Ba_3
		Hyphal feeders			
Aphelenchidae	*Aphelenchus*	-	2	2, 1e	Fu_2
Leptonchidae	*Tylencholaimus*	-	4	2	Fu_4
		Omnivores			
Aporcelaimidae	*Aporcelaimellus*	*Aporcelaimellus*	4	5, 8	Om_4
Aporcelaimidae	*Aporcelaimellus tritici*	-	4	5,8	Om_4
Aporcelaimidae	*Aporcelaimellus obtusicaudatus*	-	4	5,8	Om_4
Aporcelaimidae	*Aporcelaimellus simplex*	-	1	5,8	Om_1

Continued on next page

Table 4.10 – *Continued from previous page*

Family	Genera and species		C-P	Feeding type	Guild
	Soil A	Soil B			
Dorylaimidae	*Dorylaimus*	*Dorylaimus*	5	8	Om_5
Qudsianematidae	*Epidorylaimus*	-	4	8	Om_4
Qudsianematidae	*Eudorylaimus*	*Eudorylaimus*	3	5,8	Om_3
Qudsianematidae	*Eudorylaimus centrocercus*	-	3	5,8	Om_3
Thornematidae	*Mesodorylaimus*	*Mesodorylaimus*	5	8	Om_5
Thornematidae	*Mesodorylaimus derni*	-	5	8	Om_5
Qudsianematidae	*Microdorylaimus*	-	4	8	Om_4
Thornematidae	*Prodorylaimus*	*Prodorylaimus*	5	8	Om_5
Thornematidae	*Prodorylaimus rotundiceps*	-	5	8	Om_5
		Plant feeders			
Dolichodoridae	*Amplimerlinius*	*Amplimerlinius*	3	1d	Pl_3
Aphelenchoididae	*Aphelenchoides*	*Aphelenchoides*	2	2, 1b, 1e, 1f	Pl_2
Tylenchidae	*Bitylenchus*	-	2	1d	Pl_2
Tylodoridae	*Cephalenchus*	-	4	1d	Pl_4
Criconematidae		*Criconema*	3	1d	Pl_3
Dolichodoridae	*Dolichorhynchus*	-	3	1d	Pl_3
Hoplolaimidae	*Helicotylenchus*	*Helicotylenchus*	3	1c	Pl_3
Hoplolaimidae	*Helicotylenchus digonicus*	-	3	1c	Pl_3
Hemicycliophoridae	*Hemicycliophora*	-	3	1d	Pl_3
Ironidae	*Ironus*	-	2	5a, 6	Pl_2
Tylenchidae	*Malenchus*	*Malenchus*	2	1e	Pl_2
Meloidogynidae	*Meloidogyne*	-	3	1a	Pl_3
Paratylenchidae	*Paratylenchus*	-	2	1d	Pl_2
Paratylenchidae	*Pratylenchoides*	-	2	1b	Pl_2
Pratylenchidae	*Pratylenchus*	-	3	1b	Pl_3
Nordiidae	*Pungentus*	-	4	1d, 5, 8	Pl_4
Nordiidae	*Pungentus silvestris*	-	4	1d, 5, 8	Pl_4
Hoplolaimidae	*Rotylenchus*	*Rotylenchus*	3	1c	Pl_3
Trichodoridae	*Trichodorus*	-	4	1d	Pl_4
Dolichodoridae	*Tylenchorhynchus*	-	3	1d	Pl_3
Dolichodoridae	*Tylenchorhynchus striatus*	-	3	1d	Pl_3
Tylenchidae	*Tylenchus*	*Tylenchus*	2	1f,2	Pl_2
Longidoridae	*Xiphinema*	*Xiphinema*	5	1d	Pl_5
Longidoridae	*Xiphinema diversicaudatum*	-	5	1d	Pl_5

4.3.2.2 Assignment to the Coloniser-Persister Scale, Trophic Groups and Feeding Types

4.3.2.2.1 Mean percentage c-p scale

The coloniser persister (c-p) scale (described in Chapter 1, Table 1.1) was assigned to the identified nematodes (Table 4.10) using the tables of Bongers *et al.* (1991) and Bongers and Bongers (1998). The identified nematodes in Soil A, were predominantly c-p 1 (30%), followed by c-p 4 (29%). There was good nematode diversity throughout the soil, as the identified nematodes included all five groups on the c-p scale (Figure 4.17). There was a

significant difference between the values assigned to Soil A and to Soil B control treatment C2 (Appendix C, Table C.3) for c-p 1 ($p = 0.003$), c-p 3 ($p = 0.006$), c-p 4 ($p = 0.002$) and c-p 5 ($p = 0.004$).

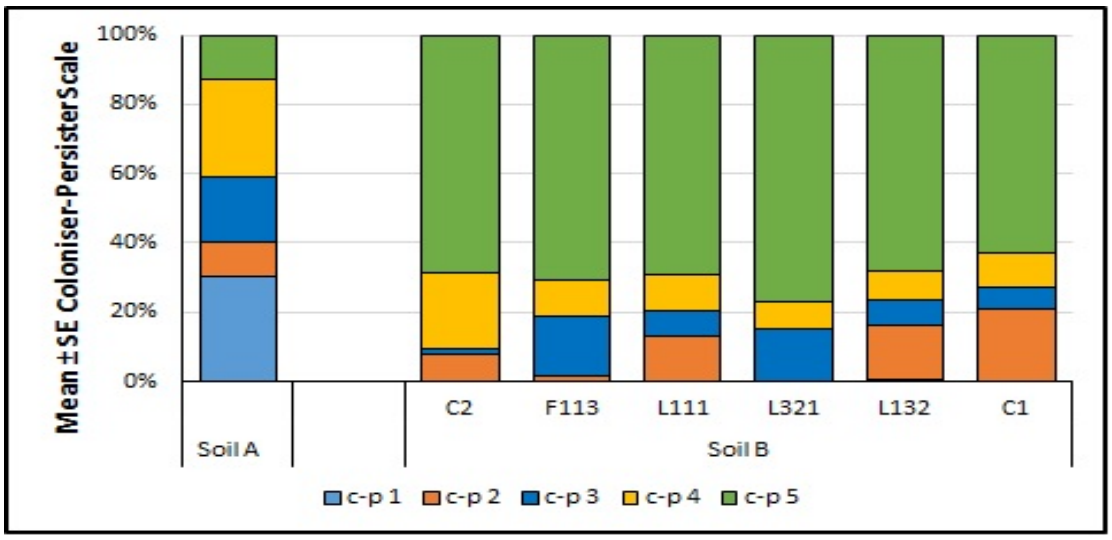

FIGURE 4.17: Mean percentage c-p composition of nematode assemblages in Soil A and Soil B per *P. fluorescens* treatments and control treatments. C1 = Ni and no bacteria. C2 = No Ni and no bacteria.

In Soil B, the identified nematodes were predominantly c-p 5 (Figure 4.17). The values assigned to strain F113 were the highest (71%), followed by L132 (68%) and L111 (69%). Control treatment C1 percent c-p 5 value determined was 63% and C2 was 69%. In pots treated with F113, L111, L321, C1 and C2 there were no nematodes classified as c-p 1. There was a significant difference between the values assigned to the control treatment C1 and to F113 ($p = 0.007$) and to L321 ($p = 0.031$) for c-p 3 (Appendix C, Table C.3).

4.3.2.2.2 Mean percentage trophic groups

The trophic groups (Table 4.10) were referred to as (Bongers and Bongers, 1998); predator (P), bacterial feeder (BF), fungal feeder (FF), omnivores (OM), and plant feeder (PF). The BF were the predominant group in Soil A (Figure 4.18) with 43% , which was statistically different to Soil B control treatment C2 ($p = 0.003$; Appendix C, Table C.3). The P group was also high with 22%. The trophic group OM dominated all six treatments in Soil B (Figure 4.18). Percent OM group assigned to strain F113 was 65%, L132 was 68%, L111 was 69% and L321 was 79%. The P value assigned to control treatment C1 was 63% and C2 was 72%. The trophic group FF was absent from all treatments, except L111. There was a significant difference between the values assigned to the strains L321 and F113 when compared to the control treatment C1 ($p = 0.002$ and $p = 0.007$ respectively) in the BF group. There was also

a significant difference to the values assigned to the trophic group PF between F113 and C1 (p = 0.013) in the post hoc test (Appendix C, Table C.3).

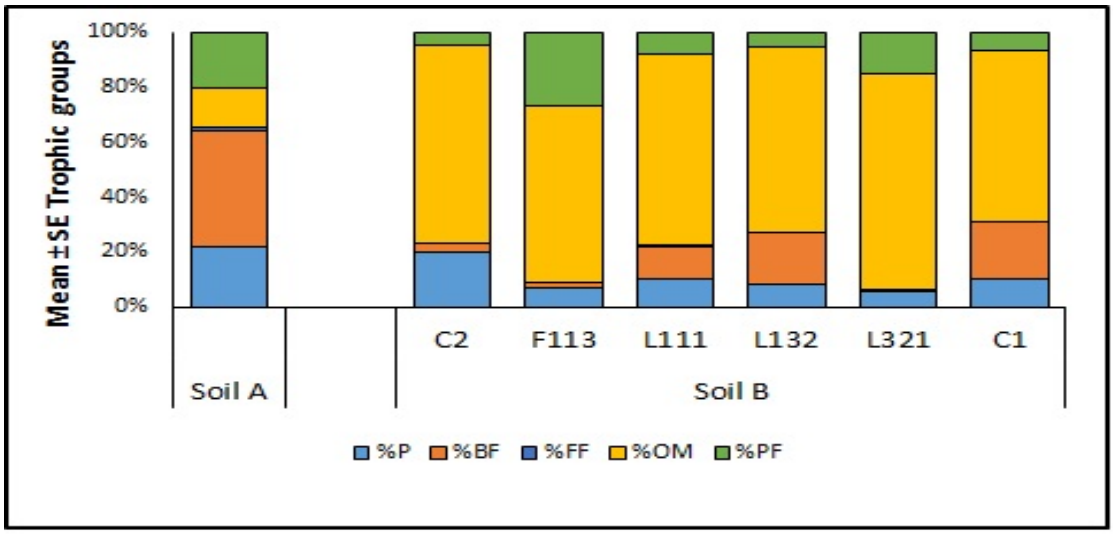

FIGURE 4.18: Mean percentage trophic group assigned to Soil A and Soil B per PGP bacterial treatment. C1 = Ni and no bacteria. C2 = No Ni and no bacteria. Trophic groups P = predator, BF = bacterial feeders, FF = fungal feeders, OM = omnivores and PF = plant feeders (see Appendix C, Table C.3 for statistical analysis).

4.3.2.2.3 Nematode feeding types

In Soil A, the feeding types (Table 4.10) present in the trophic group predators, ranged from 1b, 2, 3, 5 and 5a, with the majority type being 5a. Bacterial feeders ranged from 3, 5a and 6, but were predominately type 3. Hyphal feeders ranged from 1e and 2, with type 2 dominating. Omnivores ranged between, 5, 5a and 8, but it was predominantly type 8. Plant feeders ranged between 1a, 1b, 1d, 1e, 1f, 2, 5, 5a and 8 with type 1d dominating the trophic group. In Soil B, the feeding types present in the predator trophic group, ranged from 1b, 2, 3 and 5a, with the majority being type 5a. Feeding type 3 was the only feeding type present in the bacterial feeders trophic group. There were no hyphal feeders present in Soil B. Omnivores ranged between 5, 5a and 8 with type 8 dominating. Plant feeders ranged from 1b, 1c, 1d, 1e, 1f, and 2 with type 1d dominating the trophic group.

4.3.2.3 Nematode Abundance

4.3.2.3.1 Mean abundance of nematode species identified

Mean nematode genera abundance per soil is displayed in Table 4.11. The data points in bold highlight the most abundant genera of nematodes in Soil A and Soil B. Soil A was dominated by *Rhabditis* with the greatest mean abundance of 55.83 nematodes followed by *Aporcelaimellus* with 22.50 nematodes (Figure 4.3.2.3.1). There were also high abundances

of *Prodorylaimus* with 12.67 nematodes and *Clarkus* with 12.16 nematodes. Soil B was dominated by *Aporcelaimellus* with 123.83 nematodes (Figure 4.3.2.3.1). There were high abundances of *Eucephalobus* with 25.50 nematodes followed by *Ditylenchus* with 21.50 nematodes, *Mononchus* with 20.00 and *Helicotylenchus* with 19.42 nematodes.

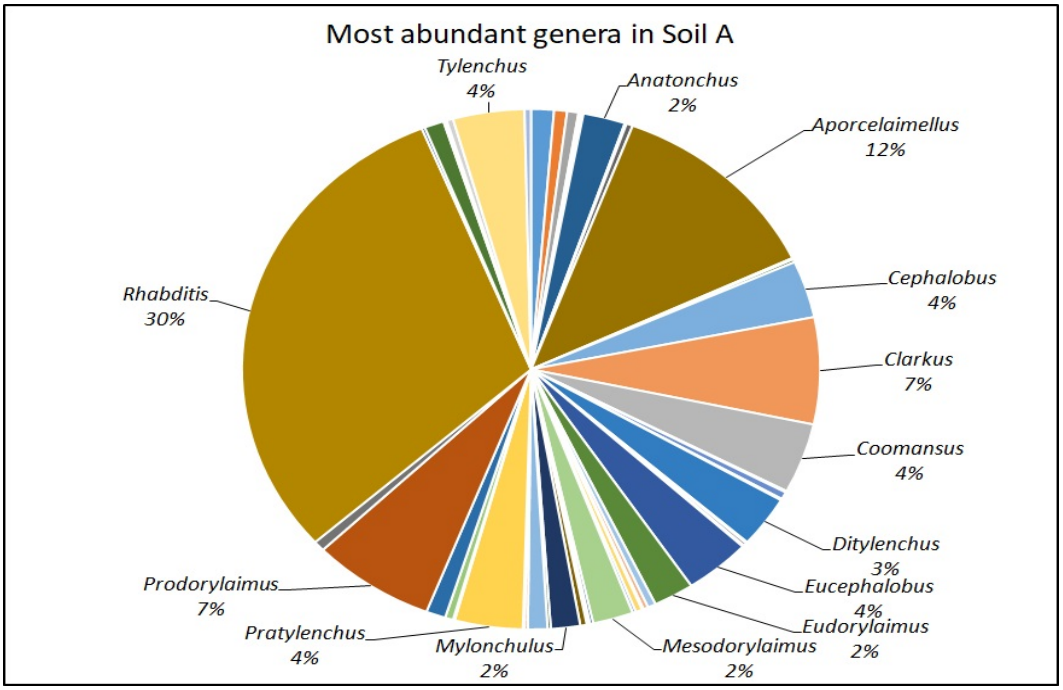

(A)

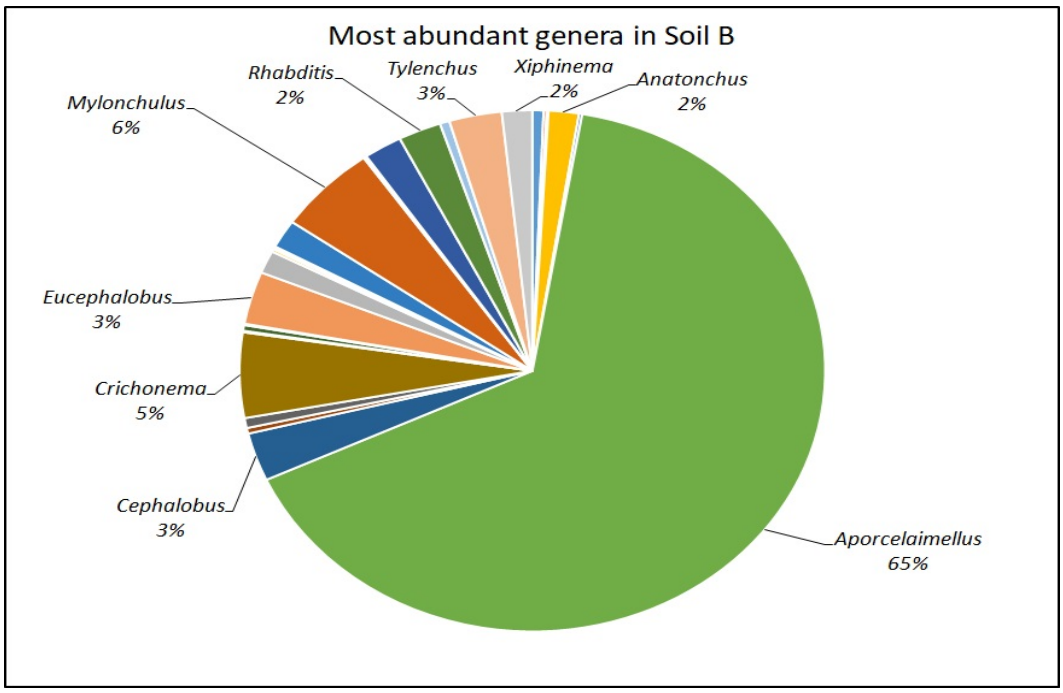

(B)

FIGURE 4.19: Nematode abundance in the rhizosphere samples assigned to (A) Soil A and (B) Soil B. The most abundant nematodes are indicated with their percentage occurrence.

4.3.2.3.2 Mean nematode abundance per soil type and treatment

Mean abundance of identified nematodes in Soil A (181.33 nematodes/ 400 g), was lower than Soil B, control treatment C2 (195.00 nematodes/ 400 g). In Soil B (Table 4.12), nematode abundance was highest in pots treated with bacterial strain L132 (198.00 nematodes/ 400 g), followed by F113 (195.00 nematodes/ 400 g) and L111(186.00 nematodes/ 400 g). The control treatment C1 had an abundance of 192.00 nematodes/ 400 g.

4.3.2.3.3 Rank abundance curves

The rank abundance curve determined for Soil A abundance (Figure 4.3.2.3.3), indicated a greater number of different species, with 69 species ranked, compared to Soil B with 31 species ranked. The curve developed for Soil B (Figure 4.3.2.3.3) indicated bacterial treatment L111 had the greatest number of different species identified, with 14 species ranked. This was followed by strain L132 with 13 species ranked. The ranked abundances for the bacterial treatments were lower when compared to the control treatments (C1 had 15 species and C2 had 16 species ranked).

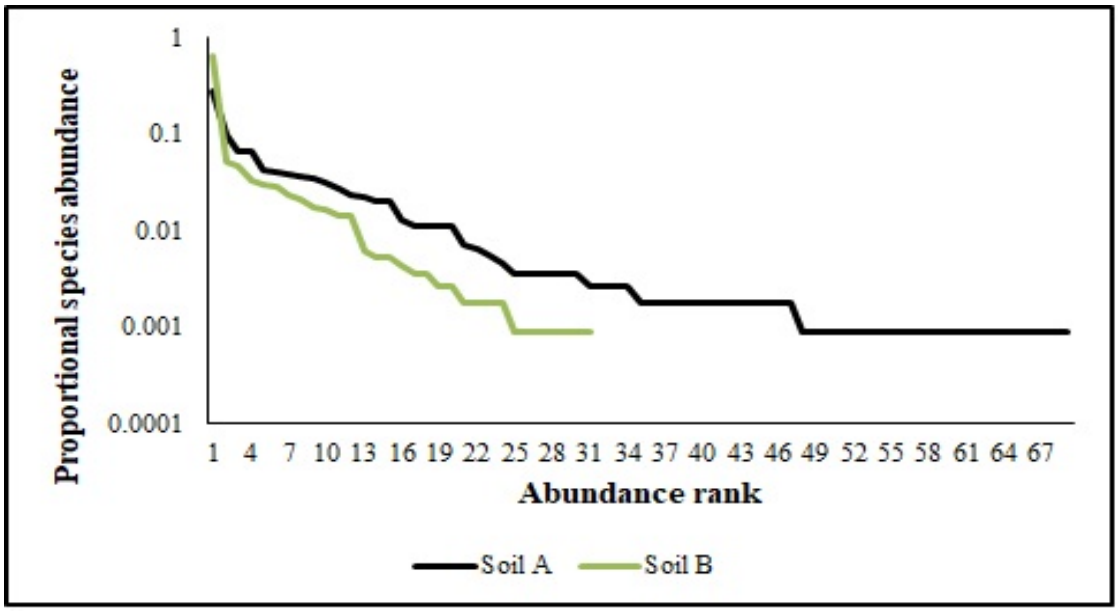

FIGURE 4.20: Rank abundance curve assigned to Soil A and Soil B. C1 = Ni and no bacteria. C2 = No Ni and no bacteria. x-axis = abundance rank and y-axis = proportional species abundance, a measure of species abundance.

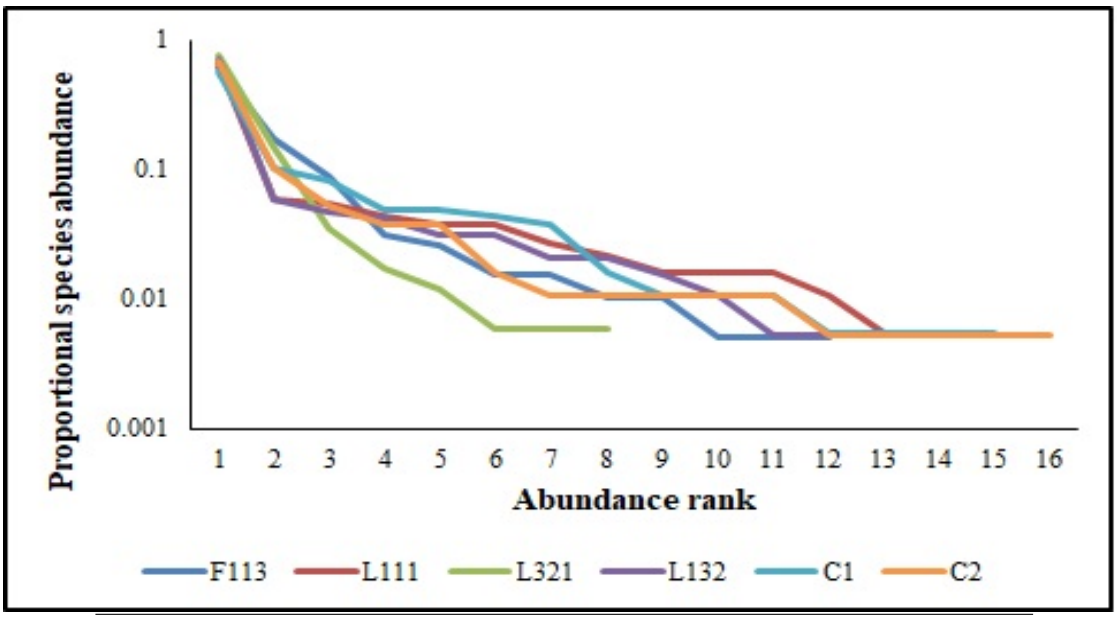

FIGURE 4.21: Rank abundance curve assigned to Soil B bacterial and control treatments. C1 = Ni and no bacteria. C2 = No Ni and no bacteria. x-axis = abundance rank and y-axis = proportional species abundance, a measure of species abundance.

4.3.2.4 Nematode Biomass and Carbon Content

4.3.2.4.1 Nematode biomass and carbon content per genus

Helicotylenchus spp. had the greatest mean biomass in Soil A (77.76 μg/ 2.4 kg) with a carbon content of 7.77% (Table 4.11), followed by *Ironus* spp. (22.82 μg/ 2.4 kg) with a carbon content of 9.13%. *Prodesmodora* spp. also had a high biomass (20.25 μg/ 2.4 kg) with a carbon content of 2.06% along with *Aporcelaimellus* spp. (19.12 μg/ 2.4 kg) with a carbon content of 7.65%. *Anatonchus* spp. biomass dominated Soil B (268.45 μg/ 2.4 kg) with a a carbon content of 107.38%, followed by *Criconema* spp. (176.75 μg/ 2.4 kg) with a carbon content of 70.70%. *Aporcelaimellus* spp. was also dominant (4.89 μg/ 2.4 kg) with a carbon content of 5.96% along with *Cephalobus* spp. (11.36 μg/ 2.4 kg) with a carbon content of 4.54%.

4.3.2.4.2 Nematode biomass and carbon content per soil type and treatment

The mean biomass of Soil B control treatment C2 (16.73 μg/ 400 g) was much lower than Soil A (75.26 μg/ 400 g). Nematode biomass in Soil B bacterial treatment L321 was the highest (545.44 μg/ 400 g), followed by F113 (89.91 μg/ 400 g), L132 (31.44 μg/ 400 g) and L111 (8.17 μg/ 400 g). The control treatment C1 was low with 31.44 μg/ 400 g (Table 4.12). Mean percentage nematode carbon content (Table 4.12) of Soil B control treatment C2 (6.69%) was also much lower than Soil A (30.10%). Soil B carbon content was the highest for bacterial treatment L321 (218.17%) followed by F113 (35.96%). The control treatment C1 was low with 12.57%.

TABLE 4.11: Mean abundance, biomass and percentage carbon content assigned to the nematode genera identified in Soil A and Soil B (± SEM). Figures highlighted in bold represent the most abundant genus, highest biomass or carbon content. - = Not present in the soil sample.

	Mean nematode abundance ($mean\ number\ of\ nematodes\ in\ 2.4kg\ soil\ /soil\ type$)		**Mean nematode biomass** ($\mu g\ nematode/2.4kg\ soil$)		**C content** ($\%/soil\ type$)	
Genera	**Soil A**	**Soil B**	**Soil A**	**Soil B**	**Soil A**	**Soil B**
Achromadora	**7.00** ± 1.89	2.33 ± 0.44	0.14 ± 0.31	1.09 ± 0.34	0.06	0.44
Acrobeloides	1.33 ± 0.83	-	0.49 ± 0.34	-	0.19	-
Alaimus	1.17 ± 0.61	-	0.36 ± 0.30	-	0.15	-
Amphidelus	1.00 ± 0.00	-	0.57 ± 0.58	-	0.23	-
Amplimerlinius	1.00 ± 0.00	2.00 ± 0.00	0.57 ± 0.28	0.15 ± 0.31	0.23	0.06
Anaplectus	1.00 ± 0.00	1.00 ± 0.00	0.73 ± 0.72	0.67 ± 0.59	0.29	0.27
Anatonchus	4.33 ± 0.44	3.17 ± 0.34	**18.88** ± 2.53	**268.45** ± 8.83	**7.55**	**107.38**
Aphelenchoides	1.00 ± 0.00	2.00 ± 0.00	0.09 ± 0.23	0.11 ± 0.24	0.04	0.04
Aphelenchus	1.00 ± 0.58	-	1.27 ± 0.68	-	0.51	-
Aporcelaimellus	**22.5** ± 0.67	**123.83** ± 0.28	**19.12** ± 1.79	**14.89** ± 0.54	**7.65**	**5.96**
Bitylenchus	0.50 ± 0.70	-	0.17 ± 0.31	-	0.07	-
Cephalenchus	1.00 ± 1.00	-	0.20 ± 0.34	-	0.08	-
Cephalobus	6.50 ± 0.62	6.80 ± 1.21	5.48 ± 0.93	**11.36** ± 1.81	2.19	**4.54**
Clarkus	**12.16** ± 0.66	1.33 ± 0.29	**13.76** ± 1.46	0.25 ± 0.79	5.50	0.10
Coomansus	**8.00** ± 0.79	3.50 ± 0.80	4.12 ± 0.96	1.55 ± 0.68	1.65	0.62
Criconema	-	**15.00** ± 2.13	-	**176.75** ± 6.07	-	**70.70**
Deontolaimus	1.00 ± 0.00	-	0.41 ± 1.65	-	0.16	-
Diplogasteritus	4.24 ± 0.95	-	4.24 ± 0.50	-	1.70	-
Diplogasteroides	1.00 ± 0.00	1.00 ± 0.00	0.80 ± 1.01	0.02 ± 0.11	0.32	0.01
Ditylenchus	**7.00** ± 0.95	**21.50** ± 0.00	5.37 ± 0.85	0.16 ± 0.32	2.15	-
Dolichorhynchus	1.00 ± 0.00	-	1.23 ± 2.07	-	0.49	-
Epidorylaimus	1.00 ± 0.00	-	**7.27** ± 0.31	-	**2.91**	-
Eucephalobus	6.83 ± 0.61	**25.50** ± 1.17	**7.10** ± 3.92	0.65 ± 0.21	**2.55**	0.26
Eudorylaimus	5.00 ± 0.73	5.3 ± 0.52	**7.10** ± 1.07	6.17 ± 1.00	*2.84*	2.47
Helicotylenchus	1.25 ± 0.22	**19.42** ± 0.00	**77.76** ± 3.26	-	**7.77**	-
Heterocephalobus	1.00 ± 0.00	-	0.33 ± 0.31	-	0.13	-
Ironus	1.00 ± 0.00	-	**22.82** ± 4.02	-	**9.13**	-
Malenchus	1.33 ± 0.29	1.00 ± 0.00	0.80 ± 0.34	0.02 ± 0.10	0.32	0.01
Meloidogyne	1.00 ± 0.00	-	0.19 ± 0.33	-	0.08	-
Mesodorylaimus	4.17 ± 0.67	1.00 ± 0.00	1.16 ± 0.33	4.32 ± 0.36	0.46	0.10
Miconchus	2.00 ± 0.00	-	0.20 ± 0.34	-	0.08	
Microdorylaimus	1.00 ± 0.00	-	0.47 ± 0.53	-	0.19	-
Mononchus	4.00 ± 0.00	**20.00** ± 0.00	0.56 ± 0.57	-	0.2	-
Mylonchulus	3.00 ± 0.49	**10.50** ± 0.62	4.69 ± 1.04	4.32 ± 0.60	1.88	1.73
Nygolaimus	2.00 ± 0.00	-	0.16 ± 0.31	-	0.07	-
Paratylenchus	2.40 ± 0.26	-	**7.59** ± 2.00	-	**3.04**	-
Plectus	1.00 ± 0.00	1.00 ± 0.00	0.79 ± 0.49	0.47 ± 0.50	0.32	0.12

Continued on next page

Table 4.11 – *Continued from previous page*

	Mean nematode abundance ($mean\ number\ of\ nematodes\ in\ 2.4kg\ soil\ /soil\ type$)		**Mean nematode biomass** ($\mu g\ nematode/2.4kg\ soil$)		**C content** ($\%/soil\ type$)	
Genera	**Soil A**	**Soil B**	**Soil A**	**Soil B**	**Soil A**	**Soil B**
Pratylenchoides	1.00 ± 0.00	-	0.92 ± 0.81	-	0.37	-
Pratylenchus	**7.00** ± 1.06	-	4.56 ± 0.79	-	1.82	-
Prionchulus	1.00 ± 0.00	-	0.93 ± 0.74	-	0.37	-
Pristionchus	2.50 ± 0.32	-	5.06 ± 1.70	-	2.02	-
Prodesmodora	3.00 ± 1.15	5.14 ± 0.00	**20.25** ± 1.50	-	**2.06**	-
Prodorylaimus	**12.67** ± 0.58	3.53 ± 0.60	**14.14** ± 1.51	0.43 ± 0.22	**1.41**	0.17
Pungentus	2.33 ± 0.44	-	0.06 ± 0.24	-	0.02	-
Rhabditis	**55.83** ± 0.87	4.50 ± 0.81	4.80 ± 0.95	1.58 ± 0.49	1.92	0.63
Rhabdolaimuss	1.00 ± 0.00	-	0.32 ± 0.34	-	0.13	-
Rotylenchus	2.00 ± 0.26	3.00 ± 0.58	**12.88** ± 1.66	0.24 ± 0.22	*5.15*	0.09
Trichodorus	1.00 ± 0.00	-	0.01 ± 0.08	-	0.01	-
Tylencholaimus	1.00 ± 0.00	-	0.09 ± 0.23	-	0.04	-
Tylenchorhynchus	4.00 ± 0.00	-	0.14 ± 0.287	-	0.06	-
Tylenchus	**7.33** ± 1.11	6.60 ± 0.61	5.88 ± 1.02	1.71 ± 0.36	2.35	0.68
Xiphinema	1.33 ± 0.29	**9.50** ± 2.76	3.30 ± 0.62	**7.35** ± 1.67	1.32	**2.94**

4.3.2.4.3 Mean percentage biomass per trophic groups

The mean percentage nematode biomass (Figure 4.22 and Appendix C, Table C.3 for statistical results) determined from Soil A were highest for those assigned to the trophic group P, followed by PF and BF. The biomass values assigned to Soil B bacterial treatment F113 were largest for trophic group PF (72.10%) followed by BF (17.33%), strain L321 were greatest for trophic group BF (81.10%) and PF (17.12%), L111 were highest for trophic group PF (40.45%) and P (36.46%), and the values assigned to L132 were greatest for P (32.27%) followed by BF (30.85%). Control treatment C1 percent biomass values were largest for trophic group BF (88.13%) followed by P (10.17%), control treatment C2 values were highest for trophic group BF (51.91%) followed by P (24.24%).

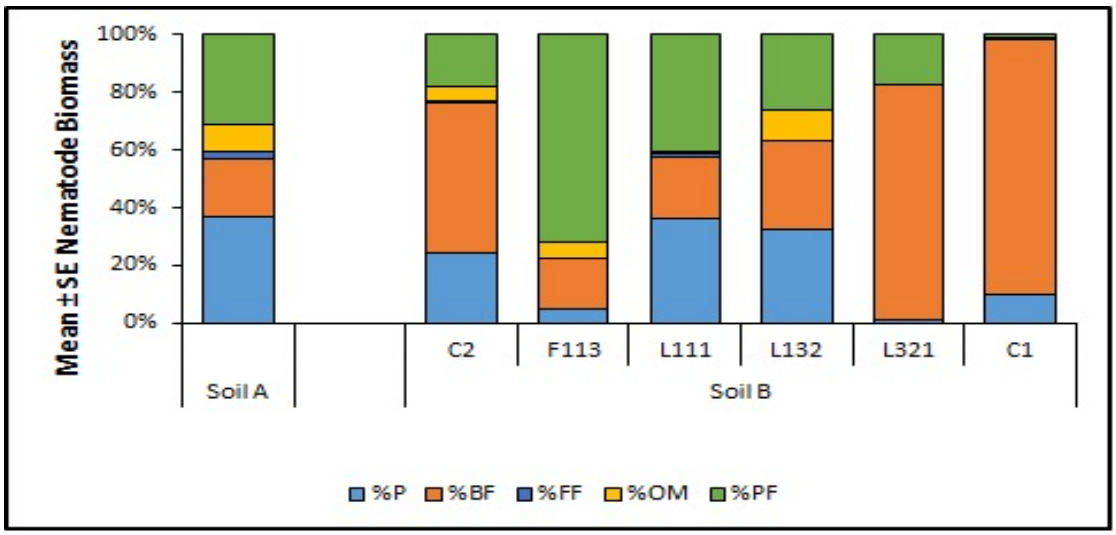

FIGURE 4.22: Mean percentage nematode biomass per trophic group per PGP bacterial strain and control treatment assigned to Soil A and Soil B. C1 = Ni and no bacteria. C2 = No Ni and no bacteria. Trophic groupings consist of P= predator, BF= bacterial feeders, FF= fungal feeders, OM= omnivorous and PF= plant feeders (see Table C.3, for statistial analysis).

4.3.2.5 Diversity Indices

4.3.2.5.1 Nematode evenness

The J' value assigned to Soil A (Figure 4.23, morphological analysis) was higher (J' = 0.45) compared to Soil B control treatment C2 (J' = 0.26). In Soil B, the mean evenness assigned to bacterial treatment L111 was highest (J' = 0.29), followed by L132 (J' = 0.26) and F113 (J' = 0.25). However, all J' values were lower for bacterial treatments compared to control treatment C1 (J' = 0.30). There was a significant difference between the values assigned to Soil A and to Soil B control treatment C2 (p = 0.002) and between Soil B bacterial treatment L321 and Soil B control treatment C1 (p = 0.01; Appendix C, Table C.4).

TABLE 4.12: Mean abundance, biomass and carbon content of identified nematodes in Soil A and Soil B per *P. fluorescens* bacterial and control treatments. The results are represented by ± SEM. C1 = Ni and no bacteria. C2 = No Ni and no bacteria.

Treatments	**Abundance** ($number\ of\ nematodes\ in\ 400g\ soil\ /soil\ type\ or\ treatment$)	**Biomass** ($\mu g\ nematode/400g\ soil$)	**Carbon Content** ($\%/soil\ type\ or\ treatment$)
Soil A	181.33 ± 0.85	75.26 ± 0.70	30.10 ± 0.70
Soil B F113	195.00 ± 2.63	89.91 ± 2.19	35.96 ± 2.19
Soil B L321	170.00 ± 3.67	545.44 ± 6.58	218.17 ± 6.58
Soil B L111	186.00 ± 2.27	8.17 ± 0.32	3.27 ± 0.32
Soil B L132	198.00 ± 2.40	8.56 ± 0.42	3.42 ± 0.42
Soil B C1	192.00 ± 2.15	31.44 ± 1.23	12.57 ± 1.23
Soil B C2	195.00 ± 2.35	16.73 ± 0.51	6.69 ± 0.51

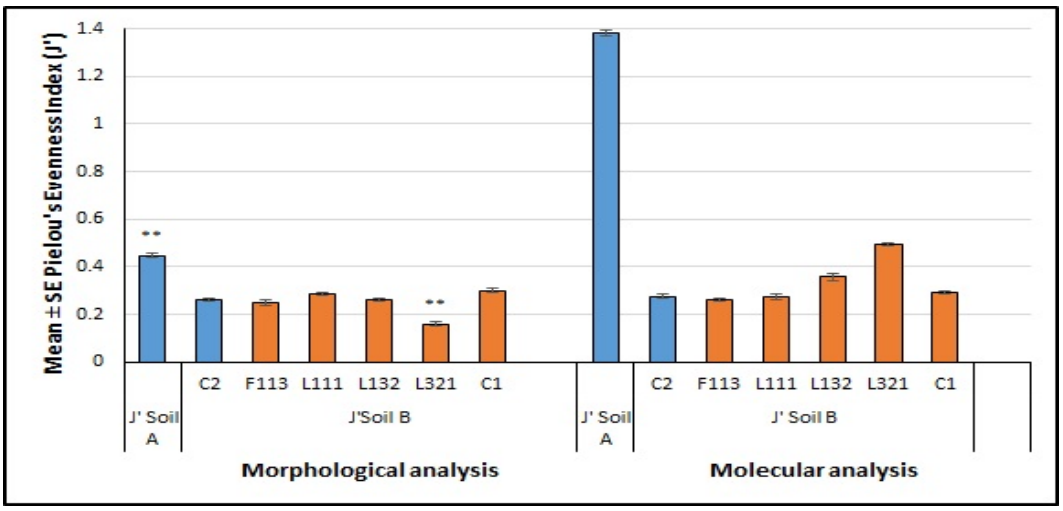

FIGURE 4.23: Pielou's evenness index (J') was assigned to Soil A and Soil B nematode assemblage values determined from the morphological and molecular analysis. Asterisks indicates a significant difference between the values assigned to Soil A and Soil B C2 (blue bars) or among Soil B bacterial treatments and C1 (orange bars). Statistical significance α = 0.05 level; ** $\leqslant$ 0.01.

4.3.2.5.2 Jaccard similarity coefficient

The similarity between the value determined for Soil A and Soil B control treatment C2 was 26% (Figure 4.24, morphological analysis). The similarity between the values assigned to Soil B control treatment C1 and bacterial treatment L111 was 50%, L132 was 42%, F113 was 35% and L321 was 25% (Figure 4.24, morphological analysis). There was a significant difference between Soil A and Soil B control treatment C2 (p = 0.000; Appendix C, Table C.4).

4.3.2.5.3 Shannon Wiener diversity index

The mean Shannon Wiener diversity index (H') value assigned to Soil A was higher (H' = 4.05) than control treatment C2 (H' = 1.37). In Soil B (Figure 4.28, morphological analysis) the mean H' highest value was assigned to bacterial treatment L321 (H' = 1.49) followed by L111 (H' = 1.39) and F113 (H' = 1.31). The value for control treatment C1 was high with H' = 1.58. There was a significant difference between the values assigned to Soil A and Soil B control treatment C2 (p = 0.002). There was also a significant difference between the values assigned to strain L321 and control treatment C1 (p = 0.004; Appendix C, Table C.4).

4.3.2.6 Maturity Index Family

4.3.2.6.1 Maturity index

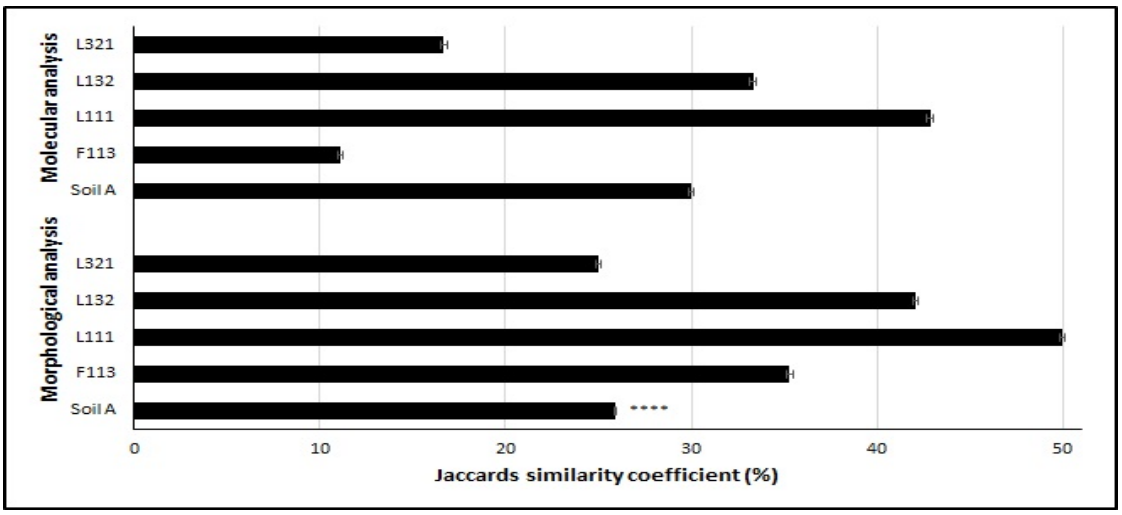

FIGURE 4.24: Jaccard similarity coefficient (S_j) was assigned to Soil A and Soil B nematode assemblage values determined from morphological and molecular analysis. It assessed the percentage similarity between (1) Soil A and Soil B control treatment C2 and (2) Soil B bacterial treatments and control treatment C1. Error bars represent $\pm$ SEM. Statistical significance α = 0.05 level; **** $p \leqslant 0.0001$.

Mean maturity index (MI) value assigned to Soil A (MI = 2.45) was lower compared to Soil B control treatment C2 (MI = 3.95). In Soil B (Figure 4.25), the mean MI value was greatest for those assigned to bacterial treatment F113 (MI = 4.83), followed by L321 (MI = 3.93) and L111 (MI = 3.83). The MI value assigned to control treatment C1 was 3.90. There was a significant difference between Soil A and Soil B control treatment C2 (p = 0.002; Appendix C, Table C.4).

4.3.2.6.2 Plant parasitic index

Mean plant parasitic index (PPI) value assigned to Soil B control treatment C2 (PPI = 3.65) was higher than that assigned to Soil A (2.81). In Soil B (Figure 4.25), the mean PPI value was greatest for bacterial treatment L111 (PPI = 3.74), followed by F113 (PPI = 3.72) and L132 (PPI = 3.45). However, the PPI value assigned to control treatment C1 was the highest of all treatments (3.89). There was a statistical difference between the PPI values determined for Soil A and Soil B control treatment C2 (p = 0.002). There was also a statistical difference between control treatment C1 and F113 (p = 0.019), L321 (p = 0.002) and L111 (p = 0.002) in the post hoc test (Appendix C, Table C.4).

4.3.2.6.3 Sum of maturity index 2-5

The mean sum of maturity index 2-5 ($\sum$ MI 2-5) values assigned to Soil A ($\sum$ MI 2-5 = 3.63) were lower than Soil B control treatment C2 ($\sum$ MI 2-5 = 3.89). The values assigned to bacterial treatment F113 were highest ($\sum$ MI 2-5 = 4.50) in Soil B followed by L321 ($\sum$

MI 2-5 = 4.06) and L111 ($\sum$ MI 2-5 = 3.68). The control treatment C1 $\sum$ MI 2-5 value was low with 3.76. There was a statistical difference between Soil A and Soil B control treatment C2 (p = 0.002). There was also a statistical difference between the bacterial strains F113, L321 and L111 (p = 0.000, p = 0.000 and p = 0.001 respectively) when compared to the control treatment C1 (Appendix C, Table C.4).

4.3.2.7 Indicators of Ecosystem Function

4.3.2.7.1 Functional guilds

Functional guilds were assigned to the identified nematodes identified (Table 4.10). They are determined by combining nematode feeding habits and the c-p scale. Functional guilds were described as Ca= carnivore, Ba= bacterivore, Fu= fungivore, Om = omnivore and Pl= herbivore.

4.3.2.7.2 Enrichment index

The mean enrichment index (EI) values assigned to Soil A were much lower (EI = 14.00) compared to Soil B control treatment C2 (EI = 100). Soil B (Figure 4.26), EI values were greatest for bacterial treatment F113 (EI = 33.33) followed by L111 (EI = 22.22) and L132 (EI = 13.79). The results were further represented in the nematode faunal profile (Figure 4.27).

4.3.2.7.3 Structure index and nematode faunal profile

The structure index (SI) value assigned to Soil A was 97.67 compared to Soil B control treatment C2 which was 100.00. In Soil B (Figure 4.26), the SI values assigned to the values determined from the morphological analysis were highest for bacterial treatment L321 (SI = 100.00) followed by F113 (SI = 99.75) and L111 (SI = 98.34). The SI value determined for the control treatment C1 was 94.65. There was a significant difference between Soil A and Soil B control treatment C2 (p = 0.001; Table C.4). There was a significant difference between the values assigned to the bacterial treatment L111 and to C1 (p = 0.007). In the nematode faunal profile (Figure 4.27), the values assigned to soil A and Soil B bacterial treatments F113, L132, L111 and L321 along with control treatment C1 appear in Quadrat C. The values assigned to Soil B, control treatment C2 occurs in Quadrat B.

4.3.2.7.4 Basal index

The BI value assigned to Soil A (BI = 2.31) was higher than Soil B control treatment C2 (BI = 0.00). The differences between them were also significantly different (p = 0.004). In Soil B (Figure 4.26) the BI values assigned to bacterial treatment L132 were the highest (BI =

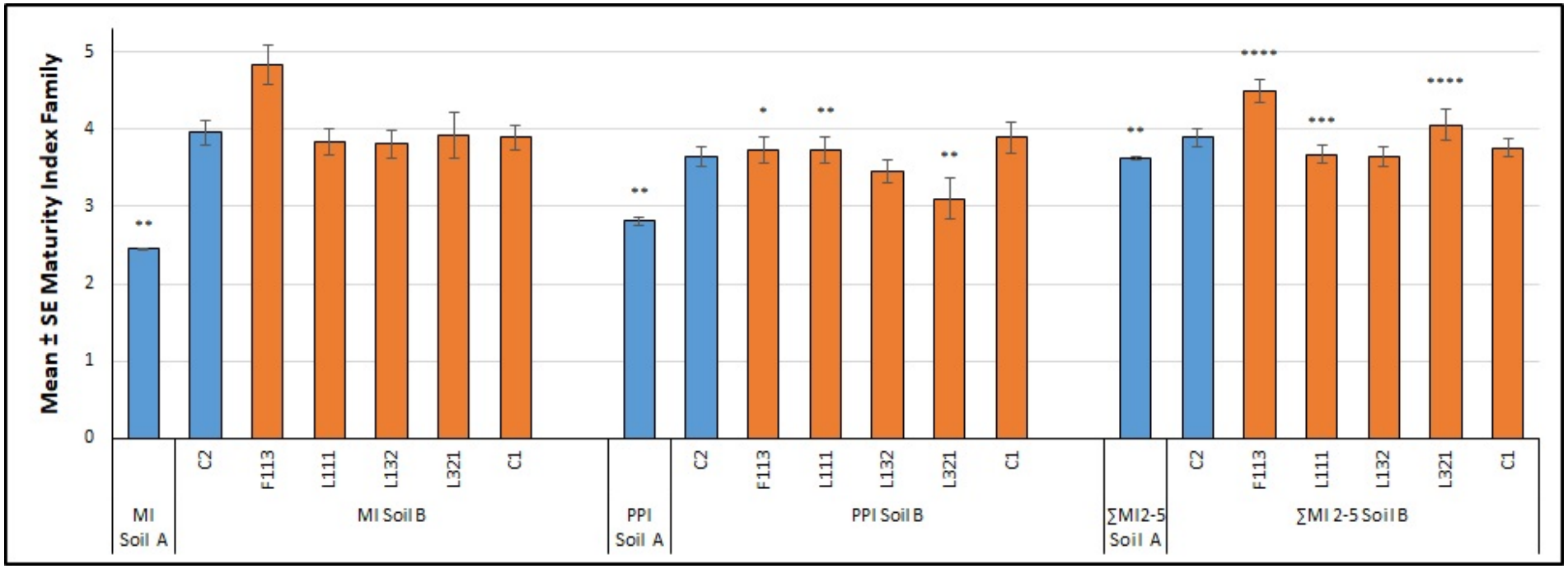

FIGURE 4.25: Maturity index family (Neher and Darby, 2006) values assigned to Soil A and Soil B *P. fluorescens* treatments. C1 = Ni and no bacteria. C2 = No Ni and no bacteria. MI = maturity index, PPI = plant parasite index and $\sum$MI 2-5 = maturity index omitting c-p 1 and including plant feaders. The error bars represent $\pm$ SEM. Asterisks indicate significant differences between the values assigned to Soil A and Soil B control treatment C2 (blue bars) or Soil B bacterial treatments and control treatment C1 (orange bars). Statistical significance α= 0.05 level; * $p \leqslant 0.05$, ** $p \leqslant 0.01$.

2.77), followed by those determined for L111 (BI = 1.65) and F113 (BI = 0.25), however, the BI value assigned to bacterial treatment L321 was 0. The BI values determined for control treatment C1 were the greatest (BI = 5.35). The difference between strain L111 (p = 0.024) and control treatment C1 was significantly different (Appendix C, Table C.4).

4.3.3 Nematode Assemblage Characterisation Utilising Molecular Techniques

Total soil DNA was extracted from OSR pots and the 18S rDNA was amplified by PCR using the primer set MN18F and 22R (Bhadury *et al.*, 2006). All rDNA samples were amplified with this primer set, as the best amplification and cleanest PCR product was evident when visualised via gel electrophoresis.

4.3.3.1 Diversity Indices Assigned to DGGE Profiles

4.3.3.1.1 Pielous evenness index

The Pielous evenness index (J') was determined for the values assigned to in Soil A , which was higher (J' = 1.38) than Soil B control treatment C2 (J' = 0.28). Soil B evenness values (Figure 4.23, molecular analysis) determined for the bacterial treatments were greatest for those assigned to L321 (J' = 0.49), followed by F113 (J' = 0.26) and L132 (J' = 0.36). The value assigned to the control treatment C1 was J' = 0.29.

4.3.3.1.2 Jaccard similarity coefficient

Jaccard similarity coefficient (S_j) value determined for Soil A and Soil B control treatment C2 was 30.00% (Figure 4.24, molecular analysis). The similarity value assigned to Soil B bacterial treatment L111 was 42.86, L132 was 33.33%, L321 16.67% and F113 was 11.11%, compared to control treatment C1.

4.3.3.1.3 Shannon Wiener diversity index

Shannon Wiener diversity index (H') value assigned to Soil A (H' = 0.32) was similar to Soil B control treatment C2 (H' = 0.35). The values assigned to Soil B (Figure 4.28, molecular analysis) were highest for L132 (H' = 0.36), followed by L321 (H' = 0.34) and F113 (H' = 0.34). The H' value determined for control treatment C1 was 0.35.

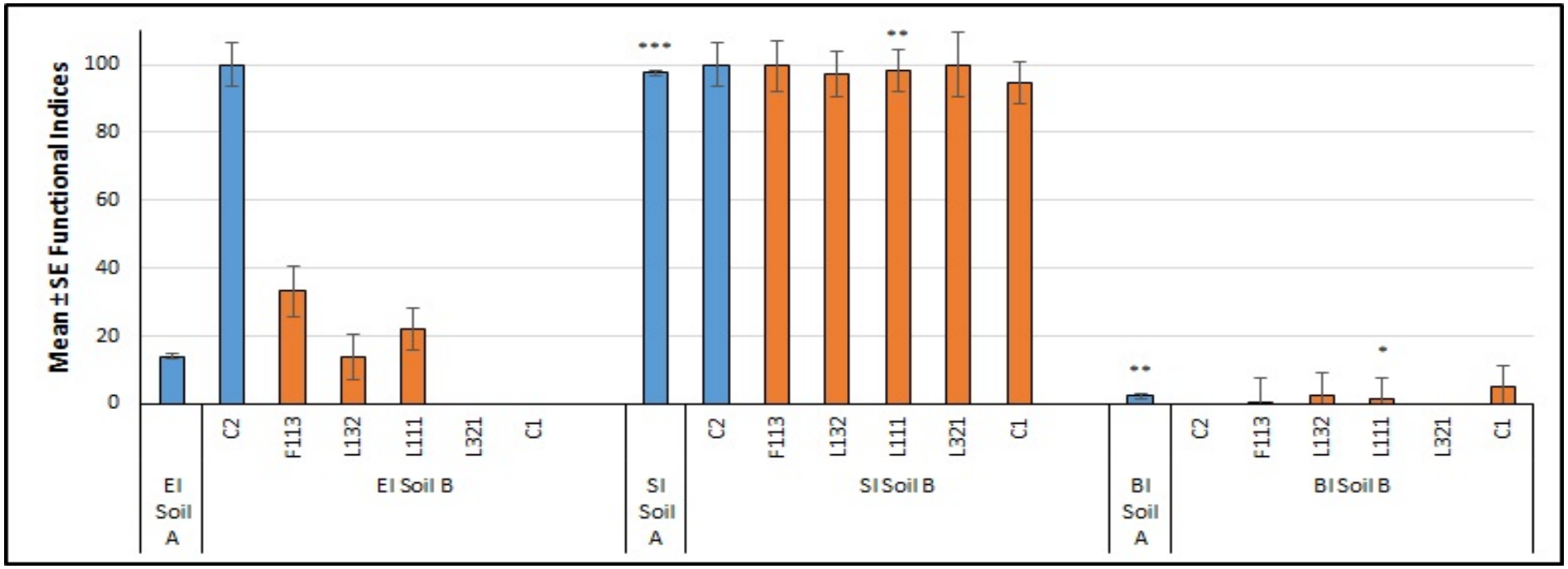

FIGURE 4.26: The functional indices; Enrichment Index (EI), Structure Index (SI), and Basal Index (BI), were assigned to the values determined for Soil A and Soil B. They were utilised to determine food-web structure and function. C1 = Ni and no bacteria. C2 = No Ni and no bacteria. The error bars represent $\pm$ SEM. The presence of asterisks indicate either a significant difference between Soil A and and Soil B control treatment C2 (blue bars) or among Soil B bacterial treatments and control treatment C1 (orange bars) in the respective index. Statistical significance α= 0.05 level; * $p \leqslant 0.05$, ** $p \leqslant 0.01$ and *** $p \leqslant 0.001$.

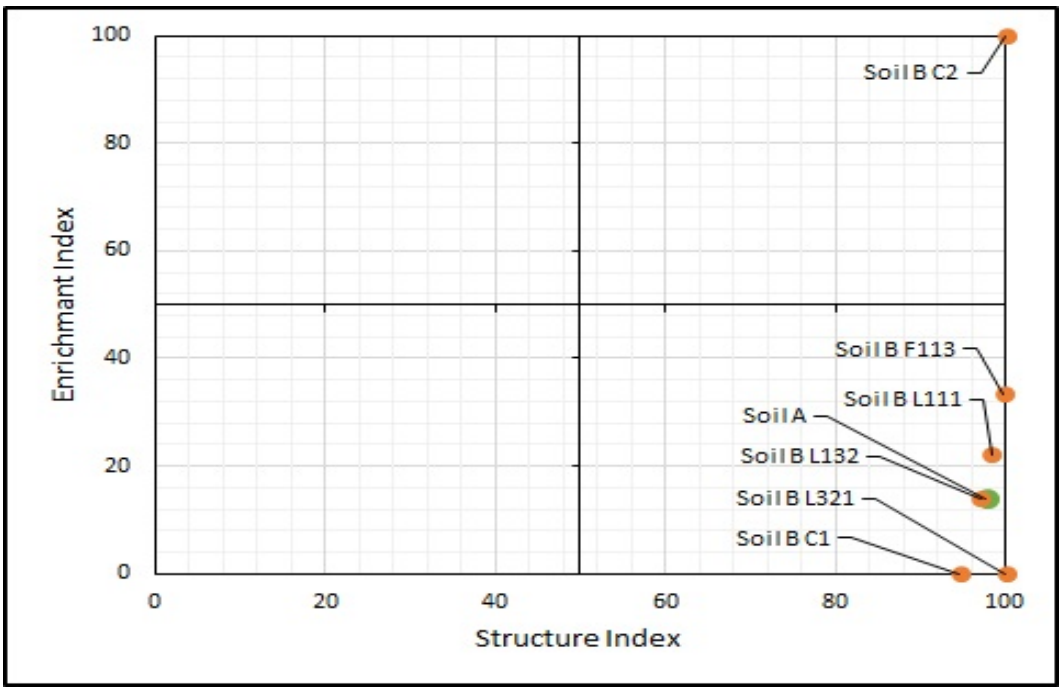

FIGURE 4.27: Nematode faunal profile was applied to the values determined for Soil A and Soil B, as an overall representation of the soil food web and environmental condition (Ferris and Bongers, 2009). It describes the orientation of functional guilds along the structure (x-axis) and enrichment (y-axis) trajectories (Figure 4.3 and Table 4.5). Soil A = green circle. Soil B bacterial and control treatments = orange circles. C1 = Ni and no bacteria. C2 = No Ni and no bacteria.

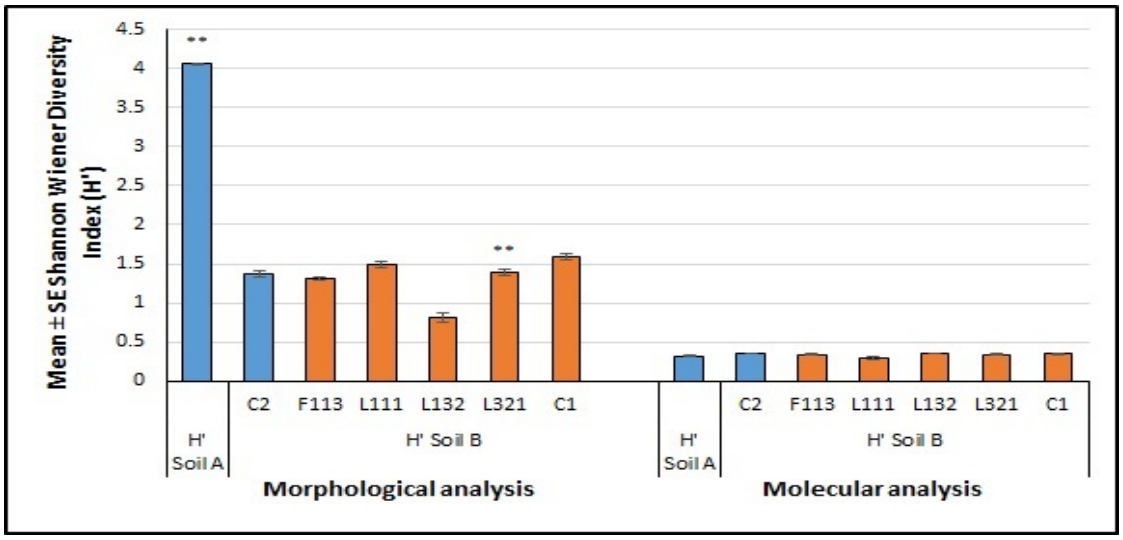

FIGURE 4.28: Mean Shannon Wiener diversity index was assigned to Soil A and Soil B nematode assemblage values. The error bars = ± SEM. C1 = Ni and no bacteria. C2 = No Ni and no bacteria. Asterisks indicate a significant difference between the values assigned to Soil A and Soil B C2 (blue bars) or among Soil B treatments and C1 (orange bars; ** $p \leqslant 0.01$).

4.3.3.2 Agglomerative Hierarchical Clustering

4.3.3.2.1 Cluster Analysis

There were three distinct clusters identified on the dendrogram (Figure 4.30), indicated by red (cluster 1 at a distance of 0.8), green (cluster 2 at a distance of 0.6) and blue (cluster 3 at a distance of 0.75) circles. The cluster groups that were similar included Soil A replications 13-14 (a distance of 0.4), 9-11 (a distance of 0.25), 6-8 (a distance of 0.6), 1 and 3-4 (a distance of 0.15). Similar clustering was evident in Soil B, bacterial treatments F113 replications 1 and 3 (a distance of 0.15), L321 replications 1 and 2, and L111 replication 3 (a distance of 0.45). There was also similar clustering for L132 replications 1-3 and L111 replication 1 (a distance of 0.2). The control treatments in Soil B clustered similarly for C1 replications 1 and 2 (a distance of 0.15), and C2 replications 2 and 3 (a distance of 0.25). However, there was a mixed treatment cluster for bacterial treatment L111 replication 2 and control treatments, C1 replication 3 and C2 replication 1 (a distance of 0.3).

4.3.3.2.2 Multi Dimensional Scaling

Soil A (Figure 4.29) displayed dissimilarities among replications 01, 06, 11, 13, 16 and 17 in the Dim 1- (negative) and Dim 2+ (positive) quadrant of the graph. There were dissimilarities in values assigned to Soil A between replications 03, 07, 09 and 12 in the Dim 1+ and Dim 2+ quadrants. Soil A replications 02, 04, 14 and 15 were located in the Dim 1- and Dim 2- quadrants, and 08 and 10 were represented in the Dim 1+ and Dim 2- quadrants of the graph, which were also dissimilar.

In Soil B there were dissimilarities between bacterial treatment L111 replication 1 and 3 in the Dim 1+ and Dim 2- quadrants of the graph. The data points for bacterial treatment L321, although closely positioned on the graph, they appeared in different quadrants, replication 1 was located in Dim 1+ and Dim 2- compared to replication 3 which was positioned in quadrant Dim 1- and Dim 2+. Bacterial strain L132 data point replications 2 and 3 were both situated in the same quadrant, Dim 1+ and Dim 2+. The control treatment C1 dissimilarity points were also located in different quadrants. Replication 1 was located in Dim 1- and Dim 2-, replication 2 was positioned in Dim 1+ and Dim 2- and replication 3 was situated in Dim 1- and Dim 2+.

4.3.4 Transgenic *C. elegans* as a Biosensor of Nickel Bioremediation in an Oilseed Rape Crop

4.3.4.1 GFP Reporter Assay

The highest GFP fluorescence expression value (Figure 4.3.4.1) was assigned to bacterial treatments L321 (RFU = 0.96), followed by L111 (RFU = 0.92) and L132 (RFU = 0.88). The control treatment C1 value was high (RFU = 0.93). There was a significant difference

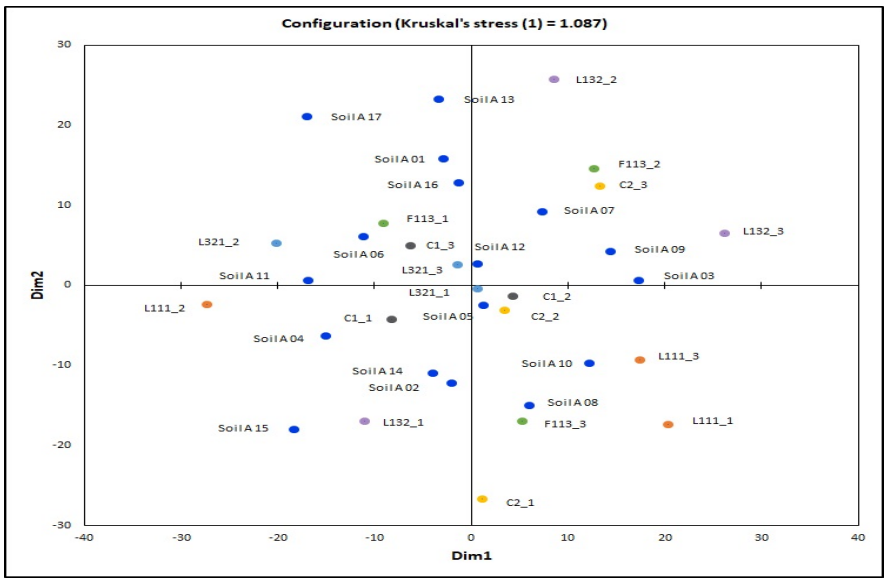

FIGURE 4.29: Multidimensional scaling on observed dissimilarities between OTUs in Soil A (blue points) and Soil B bacterial strains F113 (green points), L321 (light blue), L111 (orange points), L132 (purple points); and control treatments C1 (grey points) and C2 yellow points), across the two dimensions (Dim 1 = x-axis and Dim 2 = y-axis).

between the values assigned to control 1 plate 1 and to bacterial strain F113 (p = 0.000), and between control 1 plate 2 and strain L132 (p = 0.003).

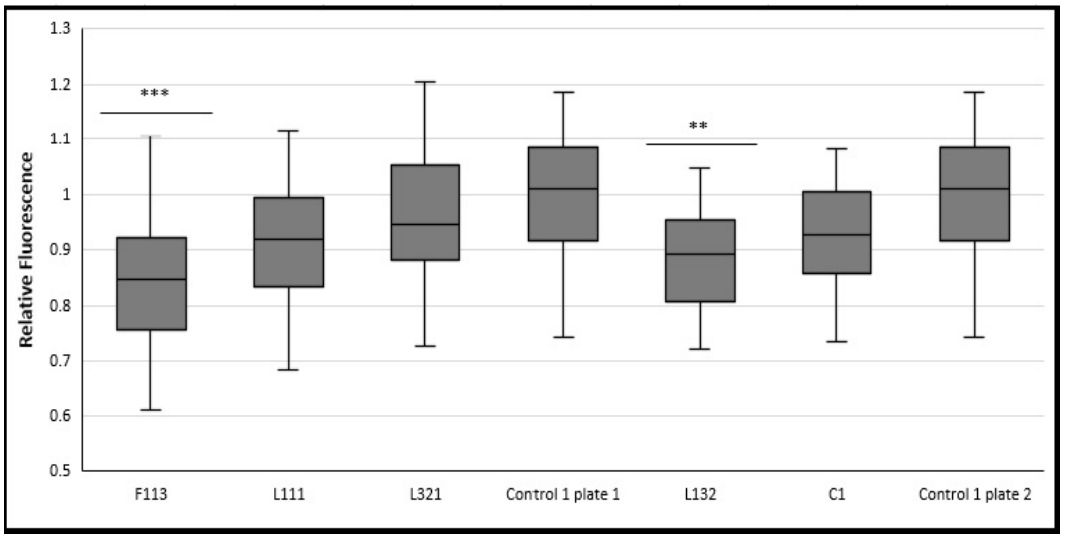

FIGURE 4.31: Transgenic *C. elegans* CL2050 *hsp* 16-2 biosensor response to SPW, as assessed by the GFP reporter assay. The treatments F113, L111 and L321 were statistically compared to Control 1 plate 1 and treatments L132 and C1 were compared to Control 1 plate 2. The error bars represent ± SEM. Statistical significance α= 0.05 level; ** $p \leqslant 0.01$ and *** $p \leqslant 0.001$.

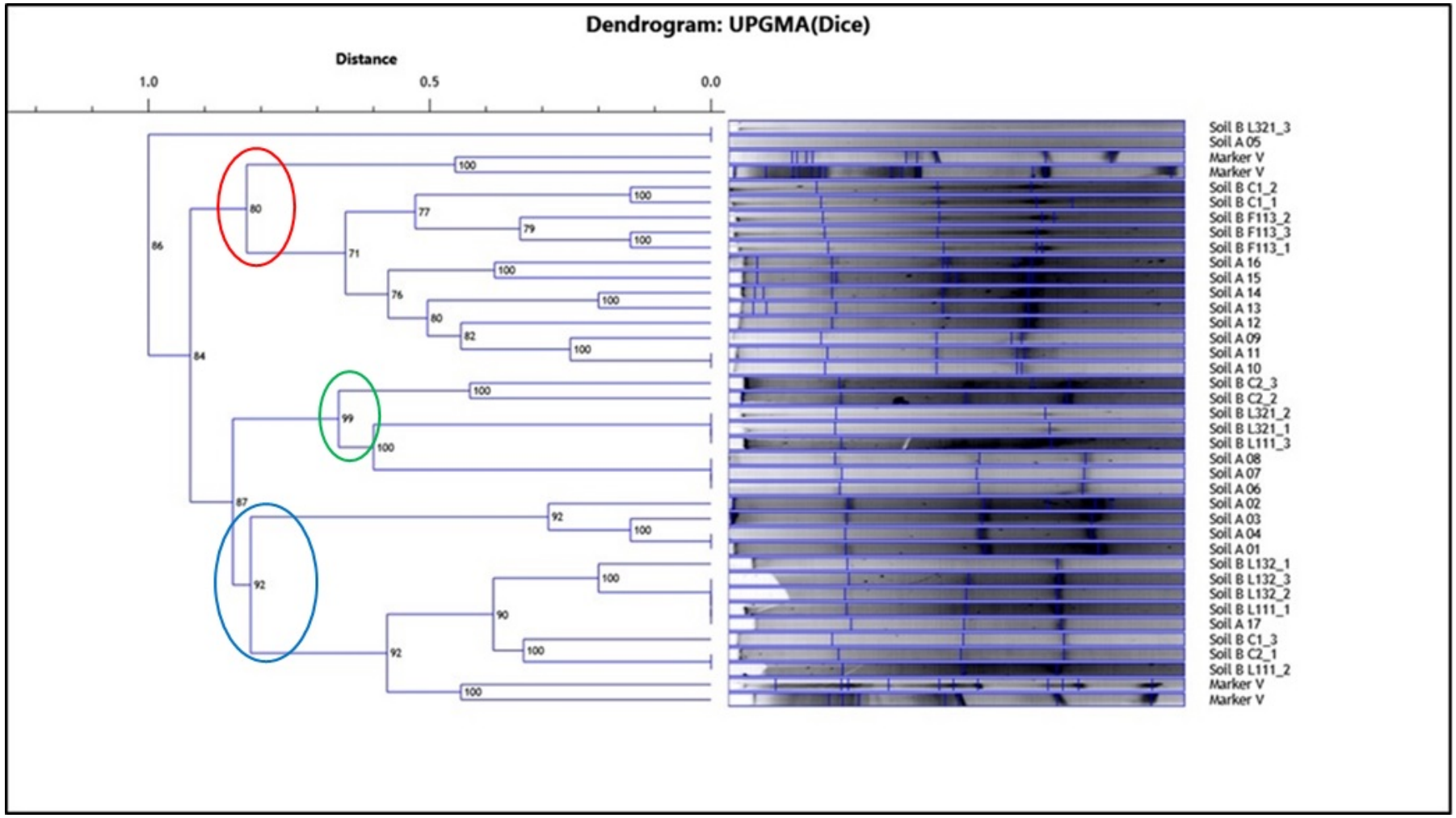

FIGURE 4.30: Dendrogram based on UPGMA with Dice similarity coefficient representing OTUs present in Soil A and Soil B, assigned to *P. fluorescens* treatments. C1 = Ni and no bacteria. C2 = No Ni and no bacteria. Cluster 1 = red circle, Cluster 2 = green circle and Cluster 3 = blue circle. The DGGE gel lanes are labelled according to Soil A (replications 1-17) and Soil B treatments (3 replications per treatment).

4.3.4.2 Data Analysis with Image J

The fluorescing transgenic *C. elegans* images assessed with the software Image J, revealed the bacterial strain F113 had the highest fluorescent response with 3.3 x 10^5 RFU followed by L321 with 2.7 x 10^5 RFU (Figure 4.3.4.2). The bacterial strains L111 and L132 both had the same RFU value with 2.2 x 10^5 respectively. The control treatment C1 had 2.1 x 10^5 RFU. The Control, which contained nematodes and ddH_2O, had a value of 8.4 x 10^4 RFU. There was a significant difference between the values assigned to the control and bacterial treatments L111 and L132 (p = 0.016 respectively), F113 (p = 0.003), L321 (p = 0.002) and C1 (p = 0.043).

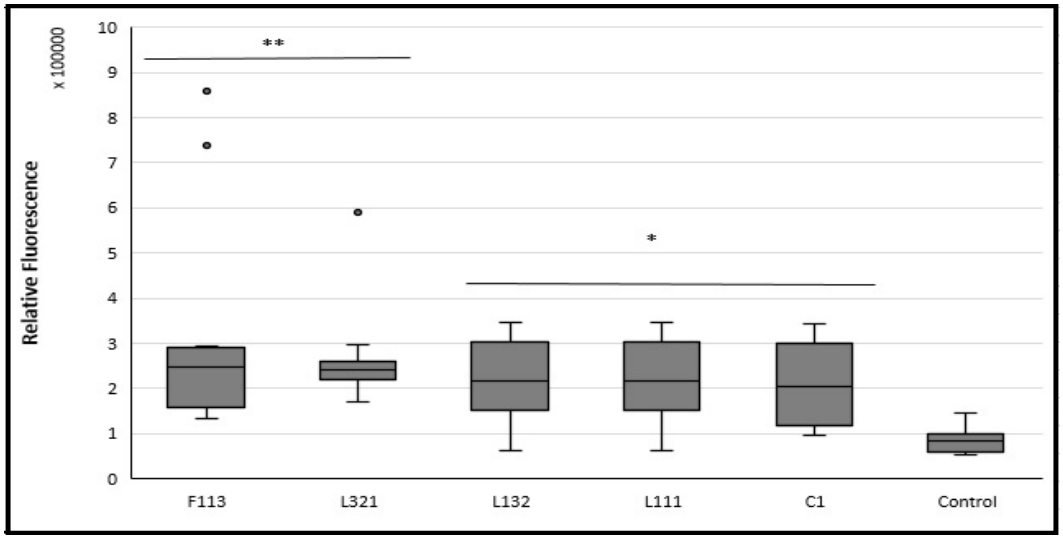

FIGURE 4.32: Transgenic *C. elegans* CL2050 *hsp* 16-2 biosensor response to SPW, assessed with the software Image J (Burgess *et al.*, 2010). The error bars represent ± SEM. Statistical significance α= 0.05 level; * $p \leqslant 0.05$ and ** $p \leqslant 0.01$.

4.4 Discussion

Beneficial bacteria as bioremediators of heavy metal contaminants are environmentally favourable and are a sustainable means of soil decontamination. There are many benefits of such bacterial plant interactions including, PGP, bioremediation and increased plant resistance to infection. The *P. fluorescens* bacterial strains utilised in this study have been extensively explored by previous researchers in enviroCORE. The strains L111, L132 and L321 were chosen for this current chapter of work due to their PGP traits which include, their capacity for IAA and siderophore production, phosphate solubilization and nitrogen fixing, as determined by Culhane (2016), Lally *et al.* (2017), and Otieno *et al.* (2015). This was also supported by work carried out in Chapter 2, whereby the compounds produced by the bacterial strains were identified. The results in Chapter 2 suggested that the strains were producing secondary metabolites associated with antimicrobial and antiviral activity, therefore increasing the plants' vigour and potential for bioremediation. The bacterial strain F113, is a well-known plant growth promoter (Cronin *et al.*, 1997a; Meyer *et al.*, 2009; Shanahan *et al.*, 1992) and was utilised as a positive control in the present study.

The first aim in the current study was to determine if *P. fluorescens* strains were capable of colonising OSR and to determine the viability of these colonising strains. In order to track the bacterial strains in the rhizosphere and plant tissues, *gfp* labelled bacterial isolates were utilised. These strains were labelled with a kanamycin resistant gene to ensure they could be traced. The bacterial strain L132 however, was not utilised to determine colony viability in OSR, as it was not *gfp* tagged and therefore, could not be traced in the rhizosphere or OSR. Previous researchers in enviroCORE found the bacterial strains chosen for this study, were successful at OSR colonisation, however, in the current research the bacteria also had to interact with the heavy metal Ni in the soil samples. The strain L321 colonisation of OSR was determined to be the most successful, regarding bacterial viability. The bacteria were present in the rhizosphere and roots after six months. These results are consistent with Lally *et al.* (2017), who tracked L321 colonisation in the rhizosphere and roots of OSR for five months. However, it is suggested in this present study, that strain L321 has the potential to remain viable for considerably longer in the rhizosphere and OSR roots, due to high bacterial numbers present. Lally *et al*. (2017) observed a decline in colonisation in the phyllosphere after this time, which was also evident in the current study.

High bacterial colonisation in the rhizosphere could be accredited to the seed inoculation technique (in the form of an alginate bead), prior to planting. The rationale for introducing the bacterial strains in this manner was to increase bacterial viability and colonisation of OSR, by ensuring the bacteria were in direct contact with the emerging seedling. Considering the field collected soil was utilised in this experiment, it was important to ensure the introduced bacteria would thrive over the natural predators and pathogens present in the soil,

and indeed cope with the presence of Ni in the soil. Seed inoculation, predominantly with *Pseudomonas* species has been attributed to increased colonisation (O'Callaghan, 2016) and yield, in a wide variety of crops including, sugarbeet (*Beta vulgaris*), onion (*Allium cepa*), wheat (*Triticum aestivum*) and barley (*Hordeum vulgare*).

Pseudomonas spp. have received considerable research attention regarding their PGP capabilities in a wide range of plants, including OSR (David *et al.*, 2018). Belimov *et al.* (2002) recorded increased root and shoot growth in *B. napus* var. oleifera L. when inoculated with *P. putida*, particularity with the addition of P amendment. Ma *et al.* (2016) also reported increased *B. oxyrrhina* growth when inoculated with *P. libanensis* TR1 and *P. reactans* Ph3R3. These inoculated plants demonstrated the capacity to phytoremediate Cu and Zn, even in drought conditions. Plant biomass in the present study was determined at different harvest times, after three and six months of growth. The plants inoculated with strain L321 and grown in Ni spiked soil after six months had significantly higher fresh and dry weight biomass, in both the shoots and roots compared to the control treatment C1 and compared to the bacterial strain F113. This increase could be as a result of the colonising bacterial strain L321, producing the hormone IAA, which is associated with plant growth regulation, unlike strain F113 which is not a producer. Likewise, Lally *et al.* (2017) reported increased OSR fresh weight biomass when inoculated with *P. fluorescens* strain L321 after five months growth. The biomass results after six months growth are more informative than three months of growth, as they give an insight into these interactions over a longer time period. Notably, however, in the present study, six months after inoculation, OSR growth and fresh weight biomass had decreased compared to the plants grown for only three months. This reduction is indicative of a loss in nutrients from the soil and reduced plant vigour with the onset of senescence. The concentration of Ni that was added to the soil did not affect the growth of these plants, however, it is evident from the results that the plants inoculated with the PGP bacterial strains, all had increased biomass.

The capacity of inoculated OSR to bioremediate Ni contaminated soil was investigated in the present study with an aim to determine which if any bacterial strain was beneficial at bioremediation. It has been reported that there are over 317 Ni-hyperaccumulating plant taxa identified, including the genera Brassicaceae (Baker *et al.*, 2000). Although there is very little literature published regarding OSR (*B. napus*) Ni accumulation, it has been reported that *Brassica juncea*, which is closely related to *B. napus* has great potential for use in the phytoextraction process (Muthukumar *et al.*, 2007). In this present study, however, Ni spiked rhizosphere samples treated with bacterial strain L321 had the lowest levels of Ni present in the samples, levels that are comparable to the Ni concentration determined in control treatment C2. This result is interesting as, the control treatment C2, had no Ni and no bacteria added to it. The result suggests that the presence of the bacterial strain L321 was influential in cleaning the soil of Ni to the levels observed in C2. Therefore, OSR is capable of Ni accumulation at low levels, particularly when inoculated with the bacterial strain F113. However,

considering the concentration of Ni in the OSR control treatment C1 was higher than the OSR treated with the bacterial strains, it is unclear how beneficial the bacterial strains are at aiding the Ni phytoremediation process.

It can be proposed, therefore, that the interactions between the bacterial strains and the soil directly have a greater effect on Ni decontamination in the soil, rather than their capacity to help OSR bioremediate the soil. Naz *et al.* (2016) investigated the biosorption potential, the removal of metals and compounds from a solution by microorganisms such as bacteria (Mustapha and Halimoon, 2015), of *Pseudomonas* spp. to reduce the concentration of heavy metals in industrial effluent from a sugar factory. They discovered that *Pseudomonas* spp. reduced Ni levels by 32%. López *et al.* (2000) investigated the influence of pH on the biosorption of heavy metals by *Pseudomonas fluorescens* 4F39. They observed that the bacterial strain had the highest affinity for the accumulation of Ni, compared to the other heavy metals investigated, including Hg, Cd and Pb. It is also possible, that by the bacterial strains colonising the roots of OSR, prevented Ni sequestering. Rajkumar *et al.* (2013) reported reduced Ni uptake by *B. juncea* after inoculation of Ni-resistant serpentine isolate *Bacillus megaterium* SR28C. However, there is very little published on the potential of *P. fluorescens* to reduce heavy metal uptake by plants.

The result also suggests that there was a low concentration of Ni present naturally in the soil, prior to the commencement of the experiment. North County Carlow, where the environmental soil was sampled, according to The National Soil Database is above the Ni threshold level by 23% (McGrath and Fleming, 2007). This may account for the raised Ni levels naturally occurring in the soil.

Nematode assemblages and their associated indices have been assessed for their capacity to identify changes in environmental characteristics in many different types of ecosystems (Neher *et al.*, 2005). Traditional and novel methods were employed in this chapter to investigate nematode assemblages present in the environmental soil as bioindicators of Ni bioremediation in OSR. Due to their small size and morphological similarity, nematodes are considered to be of the most difficult organisms to identify at species level (Oliveira *et al.*, 2011). The soil nematode assemblage structure and taxa identified, indicated rich diversity in Soil A with a total abundance of 69 taxa, more than double than those identified in Soil B, with a total abundance of 30 taxa. It has been determined, however, that heavy metal soil contamination is associated with reduced nematode numbers (Korthals *et al.*, 1996). The results that represent nematode diversity in the present study were supported by the H' index in the morphological analysis, which indicates that Soil A was significantly the most diverse and dominant group of all soils assessed. The most frequently occurring nematodes in Soil A were *Rhabditis* spp. (30%) and *Aporcelaimellus* spp. (10%), in comparison to the nematodes *Aporcelaimellus* spp. (65%) and *Mylonchulus* (6%) occurring in Soil B. This was

reflected in the most commonly occurring trophic groups, whereby Soil A was predominantly BF (43%) and Soil B was dominated by OM (63-79%) across treatments. However nematode biomass was greatest in Soil A for the nematode *Helicotylenchus* spp., and in Soil B with *Anatonchus* spp. Soil A, therefore, differed considerably in comparison to Soil B, however, Soil A in the present study was only utilised as a total control giving a snapshot of the nematode assemblage prior to the addition of any treatment. Thus, Soil A would be expected to be representative of a balanced undisturbed environment. Interestingly, however, the nematodes identified that were represented by c-p scale 4, were more abundant in the soil (29%), but the nematodes assigned to c-p scale 1 were more dominant (30%). This result was also reflected in the values assigned to the diversity and maturity indices, which were all significantly lower compared to Soil B control treatment C2, indicating an increase in the environmental disturbance. The application of fertiliser or amendments to the OSR crop in the field, prior to soil sampling, could result in a fluctuation of c-p scale 1 nematodes, however, this was not reflected in the values assigned to EI, indicating a less enriched system. Despite the fact that Soil A values assigned to SI, which consists of higher c-p scale values (c-p 3-5), and therefore stable food webs (Ferris *et al.*, 2001), were high, they were still significantly lower than control treatment C2. However, the BI values assigned to Soil A were significantly higher than control treatment C2, indicating unfavourable environmental conditions (Berkelmans *et al.*, 2003).

Although the results recorded from Soil A give a comprehensive insight into the soil condition before the addition of amendments, the interactions among the nematode assemblages, the introduced PGP bacterial strains, the Ni treatment and OSR plants in Soil B are the main focus in the present study. Soil B was utilised as the experimental soil, to which Ni and PGP bacteria were added. Considering the addition of these amendments, it was expected that the trophic groups and c-p scale values assigned to Soil B, would be representative of a stressed ecosystem. However, the nematodes present in the soil indicated an undisturbed environment, dominated by c-p scale 5, with the highest c-p scale 5 value observed in those treated with L312. There are many factors that can account for the differences between Soil A and Soil B. Soil A was sampled from the environment and assessed immediately, unlike Soil B which was placed into pots and spiked with Ni. The confined, unnatural space of the plant pot, along with the presence of OSR plants growing in them, in such close proximity to the nematode assemblages was a forced, artificial environment. Also, Soil B samples were exposed to greenhouse conditions of approximately 21-24°C, much warmer than the daily Spring temperature of Carlow (8-15°C) for that time of year. The trophic groups and c-p scale values assigned to control treatment C2, that contained no Ni and no bacteria, were also similar to the values assigned to the bacterial treatments and control treatment C1.

The nematode taxa and trophic groups, in Soil B, determined their capacity to adapt to the Ni contaminated soil conditions, demonstrating tolerance to the presence of Ni. Other than the predominant *Aporcelaimellus* spp. that occurred in Soil B, the PF group nematode

Criconema spp. (up to 17%), the BF group nematode *Cephalobus* spp. (10%), and the P group nematode *Mylonchulus* spp. (up to 9%) were dominant in some treatments, in particular the latter nematode which frequently occurred throughout four of the six treatments. Many nematodes only occurred in one treatment, including the genera *Amperlimerlinius* spp., *Anaplectus* spp., *Ditylenchus* spp. and *Mesodorylaimus* spp. On the other hand, several taxa occurred throughout all six treatments including *Anatonchus* spp., *Aporcelaimellus* spp., *Mylonchulus* spp. and *Rhabditis* spp. Although low nematode diversity (H') was recorded from the molecular results, it was evident in the morphological analysis that the values assigned to Soil A were the highest, indicating high levels of nematode diversity. The most even (J') nematode assemblage were those assessed from pots treated with the bacterial strain L321, as determined by the molecular analysis, representing high variation among nematode species for that treatment. These results indicate that some taxa, typically the higher trophic OM and P groups, that were high in abundance across treatments, were capable of overcoming changes in their environment and persisting. Therefore, indicating more established communities.

The dominant taxa, in Soil B, ranged between c-p 3 to cp-4 which were representative of an actively recovering, to a stable environment. This was supported by the MI for all treatments, particularly the values assigned to strain F113. The PPI was not as high as the control treatment, and it was particularly low for the values assigned to treatment L321, which was significantly different. The PPI is indicative of system enrichment with the understanding that, as the presence of plants increases in an area, so do the presence of PPN. Interestingly, however, the increased level of PPI in Soil B compared to Soil A is substantial, demonstrating that the PPN level in a confined artificial environment increased. The values assigned to $\sum$MI 2-5, which takes into account all c-p values except c-p 1 and PF, are highest in those treated with L321, other than those assigned to F113. This gives a good overall representation of community structure and therefore suggests, that the values assigned to L321 are indicative of a more stable system compared to the other treatments. The results for all the bacterial strains are also supported by EI, indicating no enrichment (Ferris *et al.*, 2001), SI, indicating stability and sustained resources, and BI, indicating a favourable environment for nematodes identified from soil treated with that strain (Berkelmans *et al.*, 2003). With all treatments and soils occurring in the same quadrant for the nematode faunal profile, which is representative of an undisturbed and structured position in the soil food web, suggesting very little variation at an ecological level between them.

The molecular fingerprinting technique PCRDGGE was utilised to estimate nematode biodiversity. This technique originally developed by Foucher and Wilson (2002) and was further developed by Foucher *et al.* (2004) and Waite *et al.* (2003). Kushida (2013) suggests that the development and improvement of group-specific primers would increase the suitability of DGGE. Nguyen *et al.* (2016) reports in their study that DGGE has great potential for nematode identification even up to species level. However, in the present study, the results

suggest reduced diversity in both soils A and B, and they did not reflect the morphological assessment. The dendrogram results for the MDS also confirmed low nematode OTU diversity in dissimilarity between reps and treatments. There were no specific cluster groups evident from the graph. Suggesting that there were very little variation between OTUs identified in DGGE analysis. There are several reasons for this occurrence. The DNA extraction kit utilised in the present study extracted DNA that was representative of 0.5% of the total soil sample, in comparison to 20% utilised for nematode identification,in the morphological assessment. Degradation of DNA samples due to repeated freeze-thaw could have assisted in reduced diversity. Another reason could be associated with the instrument DGGE and the sensitivity of it, due to large volumes of species DNA as suggested by Foucher *et al.* (2004). Currently, there are many other HTS techniques that are more sensitive, more specific and more representative of a whole nematode assemblage such as dT-RFLP as previously outlined in Chapter 1.

Transgenic *C. elegans* was utilised as a biosensor to further assess OSR Ni bioremediation after six months plant growth, however, the results varied. Transgenic *C. elegans* is a well-established biosensor of metal contamination using the well-characterised heat-shock *hsp*-16.2 gene as a metal induced biomarker (Anbalagan *et al.*, 2012; Jiang *et al.*, 2016; Kumar *et al.*, 2015). Kumar *et al.* (2015) and Lagido (2009) also suggests that they are suitable indicators of environmental stress. Yet, this was not reflected in the present study. It was expected that the level of fluorescence response elicited by the transgenic nematodes would be representative of the concentration of Ni present in the soil, and therefore, indicative of OSR Ni bioremediation. In the bioassay experiments, GFP expression for all treatments was lower than the control plates (blank wells). This was a recurring problem. Other transgenic *C. elegans* strains were also trialled, including PC161 (*hsp*-16.1::GFP:*lacZ*), 87-35A2prIII-GFP (*cyp*35A2::GFP) and BC20334 (*cyp*-29A2::GFP), obtained from Dr. De Pommerai, nonetheless similar results were observed. It is unclear why the results in the present study differed considerably to Anbalagan *et al.* (2012). Many obvious issues were addressed including, reading the bioassay plate on different plate readers and increasing the number of nematodes per well. Considering, it was suggested by Dr De Pommerai, that *hsp* 16.2 should elicit the strongest RFU response to Ni, Kumar *et al.* (2015) reported that direct exposure of transgenic nematodes to environmental waters resulted in a reduced, or uninformative response compared to the nematodes expression when exposed to the metals directly. The transgenic nematodes in this study were not exposed to the soil directly, in order to reduce nematode loss due to the extraction and cleaning process, as advised by Dr De Pommerai. The software package Image J was utilised as an alternative method to assess the nematodes fluorescent response to Ni, which proved to be more successful. Burgess *et al.* (2010) and McCloy *et al.* (2014) successfully utilised this programme to determine total corrected cellular fluorescence of immunofluorescent stained HeLa cells. Cramer (2012) utilised this software to assess the ROI of transgenic nematodes *gfp* fluorescent response to various heavy

metals. More recently, Escorcia *et al.* (2018) utilised the software to quantify the abundance and distribution of lipids in *C. elegans* stained with Nile Red and Oil Red O. The results of the Image J assessment in the present study looked more promising than the bioassay results, as the treatment values occurred higher than the control value. The digital images of the fluorescing *C. elegans* as assessed by the software Image J, indicated that the RFU values assigned to strains F113 and L111 were higher than the control treatment C1. The RFU values assigned to both, strains F113 and L132 in the bioassay and Image J assessment, were significant when compared to either the control plate in the bioassay analysis or the control image for the Image J assessment. However, the results for the bioassay and Image J software are not comparable considering there was so much variation in significance with the controls. There were outliers present on the graph displaying the results for the Image J analysis, these could have occurred due to dust in the plate well, autofluorescence, or by the nematodes moving in the wells. These contradictory results are indicative that transgenic *C. elegans hsp* 16.2 is not a reliable or effective method for assessing Ni bioremediation in OSR. This is particularly true in an agricultural setting, with the addition of amendments to the soil, where transgenic nematodes would fluoresce regardless of remediation. This conclusion is also confirmed by Cramer (2012), who found that the strain *hsp* 16.2 failed to show any expression modulation following exposure in a toxicity assay. He continued to declare that the *hsp* 16.2 gene was not suitable for use as a bioindicator.

The results compiled in the present chapter suggest that the interaction between PGP bacterial strains colonising OSR, increased plant biomass, this was confirmed by; (1) bacterial OSR colonisation and viability after 6 months, and (2) oilseed rape biomass (expressed as shoot and root fresh and dry weight) was higher for all treatments compared to the control treatment C1, after both time points. However, OSR inoculated with PGP bacterial strains, did not increase the plants capacity to bioremediate Ni from soil, this was indicated by; (1) the AAS analysis, which revealed variations in bioremediated Ni concentrations between treatments in the rhizosphere and in OSR, however all results were lower than the control treatment C1, and (2) the similarity between treatments assigned to Soil B in the nematode morphological assessment as determined by the c-p scale and trophic groups, diversity, maturity and ecological indices. It was also determined in the present study that the molecular technique was not a suitable method of community analysis, as it did not confirm the morphological findings. It can be concluded that transgenic *C. elegans* as biosensors were not sufficient at accurately indicating any difference between treatments or controls, and were, therefore, an unsuccessful tool for this type of analysis. The outcome of the results discussed in this chapter indicate that OSR are not suitable plants for Ni phytoremediation, however, there is great potential for biosorption of Ni by strain L321. The concept of applying this bacterial strain to contaminated soil and growing OSR on the land still has great potential, with a positive outcome, as the soil will become remediated of the heavy metal and the bacterial strain will promote OSR growth, which in turn can be utilised as a source of bioenergy

(Park *et al.*, 2012).

Key results obtained from the work tasks in Chapter 4 are the following:

- The bacterial strain L321 is a successful rhizosphere and root coloniser of OSR for at least six months
- *Pseudomonas fluorescens* L321 has biosorption potential of Ni
- Highest PGP effects, in terms of biomass, were observed in OSR plants treated with strain L321
- Soil A was dominated by the bacterial feeding *Rhabditis* and Soil B by the omnivorous *Aporcelaimellus*
- Largest nematode diversity was observed in Soil A
- All nematodes identified from Soil A and Soil B occupy the same position in the soil food-web

In conclusion, the results of the various methods described in this chapter suggest that the interactions between OSR and the PGP bacterial strains increase the plants' growth, however, the presence of the bacterial strains in the rhizosphere and within the plants did not increase bioremediation. Through exploring the interactions between OSR, PGP bacterial strains, Ni contamination and nematode assemblages, in morphological and molecular assessments one bacterial strain, L321, was identified as promoting OSR growth and has the capacity for Ni biosorption. Therefore there is further scope to investigate the biosorption potential of other PGP bacterial strains from the IT Carlow stocks, along with utilising nematode assemblages as bioindicators of other microbiological remediation processes. The objective of this study was to assess the capacity of OSR colonised by PGP bacterial strains to bioremediate Ni contaminated soil and to determine the efficacy of nematode assemblages as bioindicators of the process. The aims of this chapter to investigate the viability of the *P. fluorescens* strains and their capacity to colonise OSR were achieved. The bacterial strain's potential for PGP in Ni contaminated soil was demonstrated. An investigation into the ability of PGP bacterial strains to promote Ni bioremediation and sequester Ni within the plants was completed, however, the results were not promising. Utilising nematode assemblages, with both morphological and molecular techniques, as bioindicators of this bioremediation process were performed, however, with varying results due to the failure of OSR to bioremediate the Ni. Likewise, the suitability of transgenic *C. elegans* as biosensors of the bioremediation process was evaluated, but it was not found to be a suitable tool for this type of analysis. Both the capacity of the *P. fluorescens* bacterial strains to promote PGP and Ni bioremediation, and the nematodes, both as assemblages and as single species (transgenic *C. elegans*) were explored. A variety of techniques were were also employed to derive decisive results on the

positive interactions between increasing the capacity of the bioenergy crop OSR to be grown on contaminated soil for use as biofuel, and the ability of the bacterial strains for heavy metal biosorption in contaminated land.

Chapter 5

Estimating the Potential of Fourier Transform Infrared Spectroscopy as a Novel Tool for Nematode Characterisation

5.1 Introduction

Fourier transform infrared microspectroscopy (FT-IR) has been utilised in the identification, classification and characterisation of many organisms, including some species of pathogenic bacteria (Zarnowiec *et al.*, 2015), food spoilage filamentous fungi (Shapaval *et al.*, 2012) and preliminary for entomopathogenic nematodes (EPN) (San-Blas *et al.*, 2011). This technique is advantageous as it can rapidly produce the spectra of microorganisms without the need for complex extraction methods or equipment, DNA amplification, or specific staining protocols (Tague, 2008). This technique can also produce results much quicker than traditional identification methods.

The instrument, FT-IR, measures the absorption of electromagnetic radiation in the infrared spectral region (San-Blas *et al.*, 2012), which causes the vibration of different compounds. The vibrational spectrum of a molecule is unique and characteristic of that molecule. Coates (2000) suggests that this infrared spectrum can be used for identification, by comparing the spectrum of an unknown to a reference spectrum, or database. He also suggests that it is possible to identify, to a basic level, the spectrum in the absence of a reference database. This is performed by identifying specific structural features of the molecule.

In this study, it was hypothesised that FT-IR microspectroscopy is capable of determining unique fingerprint regions between nematode genera. The absorption spectra of free-living

bacterial-feeding nematodes (FLBFN; *Caenorhabditis elegans* and *Pristionchus pacificus*), entomopathogenic nematodes (EPN; *Steinerne-ma feltiae* e-nema, *S. feltiae* SB 12(1), *S. carpocapsae* and *Heterohabditis bacteriophora*) and plant parasitic nematodes (PPN; *Meloidogyne javanica* and *Globodera pallida*) of pure cultures and those incorporated in soil, were assessed. In theory, the FT-IR absorption bands representing functional groups could be specific to each genus of nematode, if not species, and therefore a unique spectral fingerprint could be recorded for each nematode taxon (San-Blas *et al.*, 2011).

This study was conducted around the research question: Has FT-IR the potential to be utilised as a novel tool for nematode identification, with the aim to characterise an environmental nematode community (Barthés *et al.*, 2011), and thus overcoming the difficulties of morphological identification, such as their small size and morphological similarity (Oliveira *et al.*, 2011), for the use of nematodes as environmental bioindicators? This study investigated the proposed question.

The aims of the research presented in this chapter are as follows:

- To assess the suitability and reproducibility of FT-IR, as a tool for identifying FLBFN, EPN and PPN, to explore current literature on similar organisms and to compare it to the results of this study.
- To compare pure cultured nematode absorption spectra with those of the nematodes mixed in soil to identify and distinguish fingerprint bands, or regions, on the absorption spectra and 2^{nd} order derivative spectra.
- To perform multivariate statistical analysis on spectra data, to identify a nematode that may be a suitable bioindicator for this type of analysis.

5.2 Materials and Methods

Experiments performed in this study were carried out with appropriate replications. All nematode species were cultured at 21-23°C, under aseptic conditions to prevent cross-contamination of the species and strains. The nematodes *C. elegans* and *P. pacificus* were maintained under sterile conditions. Statistical analyses were performed on the data using Microsoft Excel with the statistical add-in package XLSTAT (XLSTAT, 2017) unless otherwise stated.

5.2.1 Nematode Cultures

The FLBFN (Chapter 2, Table 2.1) *C. elegans* (N2) and *P. pacificus* (RS2333) were cultured on NGM plates seeded with *E. coli* OP50 and incubated at 20°C for 3-5 days, until well established and adult females were present. The NGM plates populated with gravid females were treated with a 20% sodium hypochlorite solution to release their eggs, which were age synchronised (previously described in Chapter 2, Section 2.2.2.1.1). The age synchronised nematodes were washed off the Petri dishes with sterile $^1/_4$ strength Ringers solution and left to settle in a 50ml tubes. The nematodes were aspirated into a clean 50ml tubes and washed 3 times with sterile $^1/_4$ strength Ringers solution to remove any bacteria present.

The EPN *S. feltiae* SB 12(1) (Boyle, 2007), *S. feltiae* e-nema, *S. carpocapsae* e-nema and *H. bacteriophora* e-nema (Chapter 2, Table 2.1) were cultured in the last instar larvae of *Galleria mellonella* (Live Foods Direct, Sheffield, UK; Shapiro-Ilan *et al.*, 2012). Petri dishes (92 X 16mm) were inverted and the lids were lined with two sheets of Whatman filter paper (No. 4). 1ml of approximately 5,000 infective juveniles (IJ) H_2O stock suspension was added to the filter paper. Five *G. mellonella* were placed onto the filter paper, the Petri dish was sealed and incubated at 21°C for 3-10 days until mortality occurred. *Galleria mellonella* mortality was confirmed via colour change and by probing with a blunt instrument. *Galleria mellonella* infected with *S. feltiae* SB 12(1) and *S. feltiae* e-nema turned black, infected with *S. carpocapsae* turned brown and infected with *H. bacteriophora* turned red. Once mortality was confirmed, the infected *G. mellonella* were placed on modified White traps (White, 1927). A small Petri dish (55 x 16mm) was inverted and the lid placed onto the Petri dish base, a platform was created by placing filter paper (Whatmann No. 4) over the Petri dish. The platform was placed into a 12 oz transparent deli dish (JFK disposables) and dH_2O was added until the edges of the filter paper touched the water. The infected *G. mellonella* were placed onto the platform and incubated at room temperature for up to 14 days. After emergence, nematodes were harvested by decanting the water into an empty deli dish. The transparent dish containing the infected insects was replenished with ddH_2O and incubated for a further 1-3 days. This was continued until the desired amount of nematodes was harvested.

The PPN *M. javanica* were cultured in four-week-old tomato plants (*Solanum lycopersicum*) var. 'Gardeners Delight', for 3-4 months (previously explained in Chapter 2, Section 2.2.2.2.1). The plant roots were chopped into 3 cm pieces and the nematodes were extracted on a modified Baermann funnel (Chapter 2, Section 2.2.2.2.2). *Globodera pallida* cysts were surface sterilised in ethanol for 15 seconds and then transferred to a 1.3% sodium hypochlorite solution until the cysts appeared faded and started to break open. The cysts were rinsed in sterile dH_2O and placed into a transparent deli dish filled with 5 ml sterile dH_2O and sealed. The cysts were incubated in the dark for three days at 18°C after which the cysts were transferred to a new deli dish and filled with 5 ml sterile potato root diffusate (PRD; Chapter 2, Section 2.2.2.3.2). The cysts were incubated again at 18°C for 3-14 days regularly refreshing the deli dish with PRD (Bezooijen, 2006) until hatched.

5.2.2 Nematode Spiked Soil Pots

The nematodes *C. elegans*, *S. feltiae* SB 12(1), *S. feltiae* e-nema, *S. carpocapsae*, *H. bacteriophora* and *M. javanica* were cultured (as described in Section 5.2.1). 20 g of sterile air dried topsoil was placed into 5 cm pots. 1000 nematodes of each species were added to each pot, with seven pot replications per species. The number of replications was determined by the availability of the nematodes. The pots were stored at 18°C in the dark for four weeks. The soil was kept moist with sterile dH_2O to maintain 10% moisture holding capacity (MHC; Chapter 4, Section 4.2.4.1).

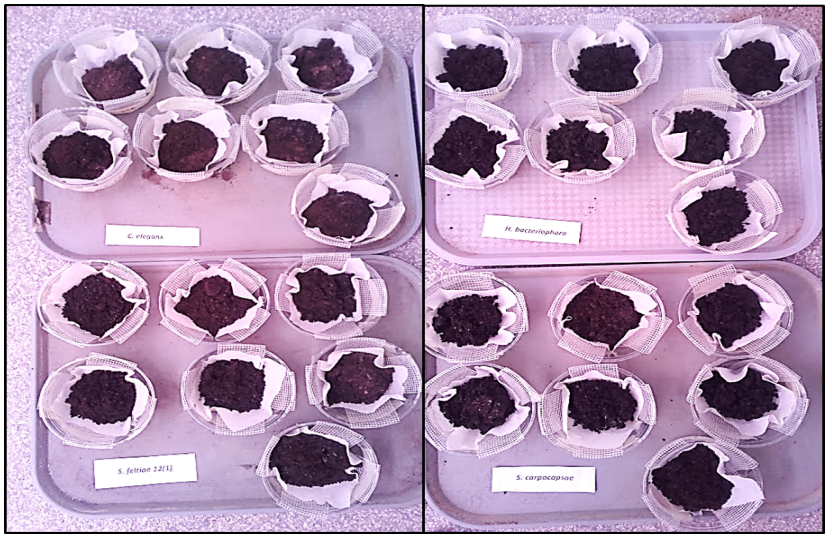

FIGURE 5.1: Extracting the nematodes from nematode spiked soil pots. The pots were spiked with the nematodes *C. elegans*, *S. feltiae* SB 12(1), *S. feltiae* e-nema, *S. carpocapsae*, *H. bacteriophora* and *M. javanica* using modified White traps (White, 1927).

The nematodes were extracted from the soil using modified Baermann funnel. They were constructed by crossing over two pieces of fibreglass adhesive tape into a deli dish, ensuring the tape didn't touch the bottom of the dish. The fibreglass adhesive tape was secured to the deli dish to prevent it from moving. A 4x4 cm piece of tissue paper was placed on top of the fibreglass adhesive tape, where the two pieces of tape crossed over. The nematode containing soil was placed onto the tissue paper and the dish was filled with sterile dH_2O until the bottom of the soil was level with the water (Figure 5.1). The Baermann funnels were incubated at 18°C for two weeks. After this time the dH_2O nematode suspension was passed through a series of sieves ranging from 40-150 μm in diameter, to remove any soil debris. The seven nematode replications were pooled together due to a low number of nematode emergence from the soil.

5.2.3 Nematode Sample Preparation for FT-IR analysis

The nematodes from the pure cultures and those that emerged from the soil were surface sterilised. The nematode suspension for each species was placed into an individual 50 ml tube. The tubes were centrifuged at 3800 rpm for 20 minutes and the supernatant was removed by avoiding disturbing the pellet. 20 ml of 10% sodium hypochlorite solution was added to each tube. The tubes were placed on a shaker table diagonally for ten minutes. They were then centrifuged again at 3800 rpm for 20 minutes. The supernatant was removed without disturbing the pellet and 20 ml sterile dH_2O was added to each tube. This process was repeated a further three times to remove all the sodium hypochlorite from the nematodes. After the final wash, the nematode pellet was mounted onto a glass microscope slide and labelled. There were seven species of pure culture with ten replications and six species of nematodes emerged from the soil with three replications. The slides were left to air dry in the dark for a week.

5.2.4 Analysing Nematode Samples on FT-IR

Spectra from 3500-650 cm^{-1} were acquired from a PerkinElmer Spectrum 65 Fourier transform infrared spectrometer [PerkinElmer]. The spectrometer setting conditions were as follows: 4 cm^{-1} spectral resolution, 150 scans with a squared triangular apodisation. 149 data points were used for slope calculation. A blank run was performed on the instrument initially to ensure the instrument was calibrated. The prepared samples on the glass microscope slides were carefully scraped off and placed on the crystal head and the pressure clamp was applied according to manufacturers instructions. The spectra were analysed using PerkinElmer Spectrum software.

5.2.5 Analysis of Spectral Data

5.2.5.1 Absorbance Spectra

The spectra were baseline corrected to eliminate any dissimilarities between them, due to shifts in the baseline. The data was transformed and normalised, in order to set the minimum and maximum between 0- 1 to eliminate the path length variation and to reduce fluctuation between the replications. The data were converted to absorbance from transmittance. The absorbance spectrum data in the range of 3500- 600 cm^{-1} was graphed using Microsoft Excel 2016. The number of discriminative features and fingerprint regions associated with the nematode spectra were highlighted using data points and described.

5.2.5.2 Second Order Derivative Transfored Spectra

Second order derivative transformations of the absorbance spectra were employed to reduce variability in replications, prevent baseline shift and separate out overlapping peaks (San-Blas *et al.*, 2011). The FT-IR spectra of the three nematode categories, (1) FLBFN *C. elegans* and *P. pacificus*, (2) EPN *S. feltiae* SB 12(1), *S. feltiae* e-nema, *S. carpocapsae* and *H. bacteriophora*, (3) PPN *M. javanica* and *G. pallida* were transformed to the second order derivative using PerkinElmer Spectrum software. The data was plotted and the number of discriminative features and peaks, associated with the nematode spectra, were highlighted using data points and described.

5.2.6 Statistical Analysis

5.2.6.1 principal Component Analysis

All multivariate statistics were performed on Microsoft Excel (2016) with statistical add-in package XLSTAT (2017). A principal component analysis (PCA) was performed on the 2^{nd} order derivative transformed spectra for all nematodes utilised in this study. The statistic analysed pure cultured nematodes (*C. elegans*, *S. feltiae* e-nema, *S. carpocapsae*, *H. bacteriophora*, *M. javanica* and *G. pallida*) with ten replications of each species. They were grouped accordingly; (1) all pure cultured nematodes, (2) pure cultured FLBFN, (3) pure cultured EPN, and (4) pure cultured PPN. Following this analysis, PCA was performed on the data extrapolated from the nematodes exposed to the soil (*C. elegans*, commercial *S. feltiae* e-nema, wild *S. feltiae* SB 12(1), *S. carpocapsae*, *H. bacteriophora* and *M. javanica*), with three replications of each species. They were grouped as follows (1) all nematodes

exposed to soil and (2) EPN exposed to soil. The groupings for PCA of pure cultured nematodes and those exposed to soil were explored to observe the orientation and clustering of components (San-Blas *et al*., 2011).

An investigation of the correlation matrix utilised to determine linearity between all variables (Statistics, 2015) showed that all variables had at least one correlation coefficient greater than 0.4. The Kaiser-Meyer-Olkin (KMO) test was utilised to measure the linear relationships between variables and determine the appropriateness of PCA analysis on the data was employed. The test values range between 0 to 1, with values above 0.8 considered good and suitable for analysis on PCA. A Bartlett's test of sphericity, which tests for correlations between variables, and determines if the correlation matrix is an identity matrix (1 on the diagonal and 0 on all the off-diagonal elements) was utilised. Bartlett's test of sphericity was statistically significant ($p < 0$ .0005) for all data analysed, indicating the data could be factorised (Statistics, 2015). A scree plot, which is a plot of the total variance explained by each component against its respective component, was utilised to determine how many components should be retained in the analysis (Cattell, 1966). The PCA threshold value employed was 0.4. A Varimax orthogonal rotation was employed to aid interpretability (Statistics, 2015) of the results.

Bi-plots were utilised to interpret the similarities and differences between the nematodes species (*C. elegans*, *P. pacificus*, *S. feltiae* SB 12(1) and e-nema, *S. carpocapsae*, *H. bacteriophora*, *M. javanica* and *G.pallida*) and nematode category (FLBFN, EPN and PPN) for pure cultured nematodes and for nematodes exposed to soil. The closer the samples were within the bi-plot, the more similar they were with respect to the principal component score evaluated. The replications on the graph are not labelled due to space restrictions. In the results section, the replications are labelled according to the initials of the nematode species they represent, followed by the replication number 1-10.

5.2.6.2 Agglomerative Hierarchical Clustering

An agglomerative hierarchical clustering (AHC) analysis (XLSTAT, 2017) was employed to identify and classify groups into clusters. This approach clusters each observation in its own cluster; as dissimilarity increases the clusters are merged in a bottom-up approach. The analysis was performed on 2^{nd} order derivative data in the region of 900-1300 cm^{-1}. Dissimilarity clustering with Euclidean distance, to measure the distance between pairs of observations, was utilised along with Ward's method, to measure the increase in variance for the cluster being merged as the agglomeration method.

5.3 Results

5.3.1 Analysis of Spectral Data

5.3.1.1 Absorbance Spectra of Pure Cultured Nematodes

Bands in the region of 2800 and 3350 cm^{-1} were assigned to the C-H stretching vibrations of methyl (CH_3) and methylene (CH_2) groups within the range of 2800– 2950 cm^{-1}, seen in the spectra of *S. feltiae* e-nema (Figure 5.3a), *S. carpocapsae* (Figure 5.4a) and *H. bacteriophora* (Figure 5.5a) pure cultures (Table 5.1). Bands between 3284 and 3350 $^{-1}$ were assigned to CH stretching vibrations, with a shoulder between 3088 and 3054 cm^{-1} in *S. feltiae* e-nema (Figure 5.3a), *S. carpocapsae* (Figure 5.4a) , *H. bacteriophora* (Figure 5.5a) and *G. pallida* (Figure 5.7b), due to the CH trans stretching vibration (Table 5.1). The asymmetric CH (–CH_2–) stretching vibration, in bands between 2921 and 2926 cm^{-1} presents a strongly overlapped band in *S. feltiae* e-nema (Figure 5.3a), *S. carpocapsae* (Figure 5.4a) , *H. bacteriophora* (Figure 5.5a) and *G. pallida* (Figure 5.7b) in Table 5.1. The band between 2852 and 2855 cm^{-1} in *S. feltiae* e-nema (Figure 5.3a), *S. carpocapsae* (Figure 5.4a), *H. bacteriophora* (Figure 5.5a) and *G. pallida* (Figure 5.7b) also came from the symmetric CH (–CH_2–) stretching vibration. The –C O phosphidiester group stretching vibration of triglycerides band can be seen between 1739 and 1745 cm^{-1} in *S. feltiae* e-nema (Figure 5.3a), *S. carpocapsae* (Figure 5.4a), *H. bacteriophora* (Figure 5.5a) and *G. pallida* (Figure 5.7b) in Table 5.1.

The bands between 1630 and 1636 cm^{-1} were assigned to the vibrations of C O groups of the -sheet amide I of the secondary structure for *S. feltiae* e-nema (Figure 5.3a), *S. carpocapsae* (Figure 5.4a), *H. bacteriophora* (Figure 5.5a), *M. javanica* (Figure 5.6a) and *G. pallida* (Figure 5.7b) and the amide II band between 1535 and 1536 cm^{-1} for *S. feltiae* e-nema (Figure 5.3a) and *G. pallida* (Figure 5.7b) respectively (Table 5.1). The amide III band at 1234 and 1235cm^{-1} in *H. bacteriophora* (Figure 5.5a) and *S. feltiae* e-nema (Figure 5.3a) respectively represent CN stretching and NH, and it is also involved with the triple helical structure of collagen (Table 5.1).

The vibrational modes of collagen carbohydrate residues appear between 1027 and 1038 cm^{-1} in *P. pacificus* (Figure 5.7a), *S. feltiae* e-nema (Figure 5.3a), *M. javanica* (Figure 5.6a) and *G. pallida* (Figure 5.7b) in Table 5.1. The amide III/CH_2 wagging vibrations of collagen appear between 1235 and 1243 cm^{-1} in *S. feltiae* e-nema (Figure 5.3a), *S. carpocapsae* (Figure 5.4a), *H. bacteriophora* and (Figure 5.5a) *M. javanica* (Figure 5.6a) reported in Table 5.1. Therefore, the peaks between 1077 and 1078 cm^{-1} in *S. carpocapsae* (Figure 5.4a) and *H. bacteriophora*, and 1234 and 1235 cm^{-1} in *H. bacteriophora* (Figure 5.5a) and

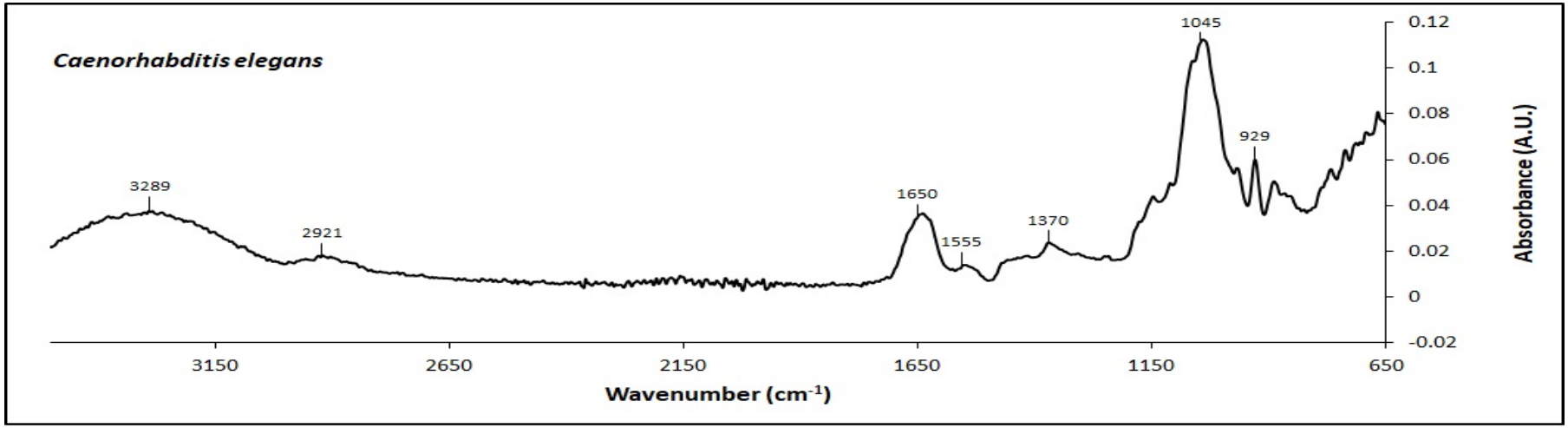

(A)

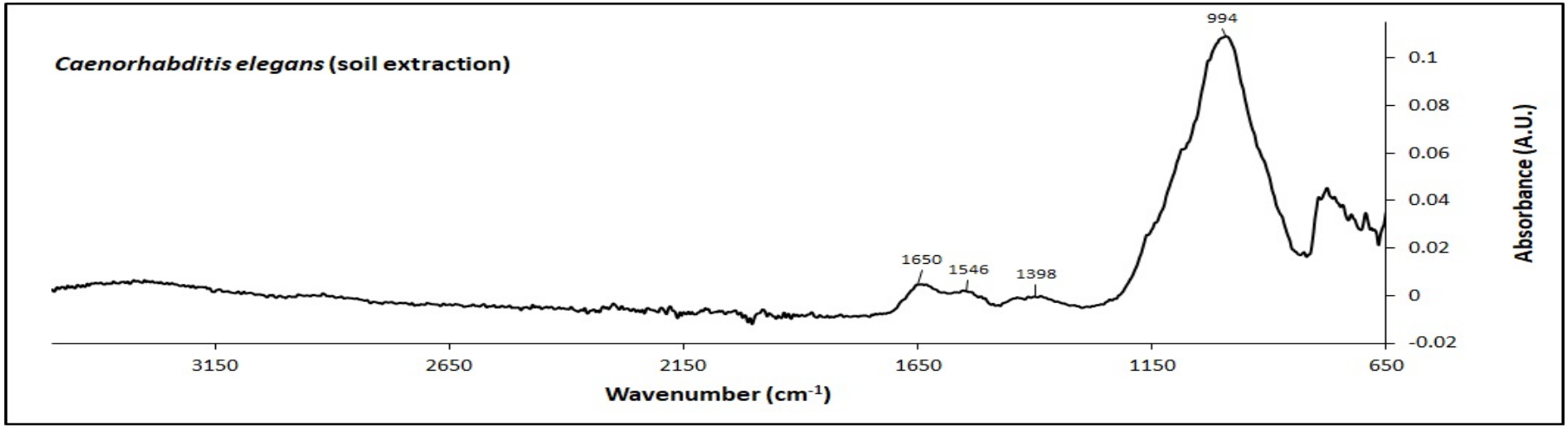

(B)

FIGURE 5.2: FT-IR absorbance spectrum of *C. elegans* directly from pure cultures and extracted from soil. The spectrum results were averaged and baseline corrected. (A) = pure cultured *C. elegans* with prominent peaks at 929, 1045, 1370 and 1650 cm^{-1}. (B) = *C. elegans* extracted from soil with prominent peaks at 994, 1398, 1546 and 1650 cm^{-1}. The x-axis describes the wavenumber in the range 3500 - 600 cm^{-1}. The y-axis describes IR absorbance in AU.

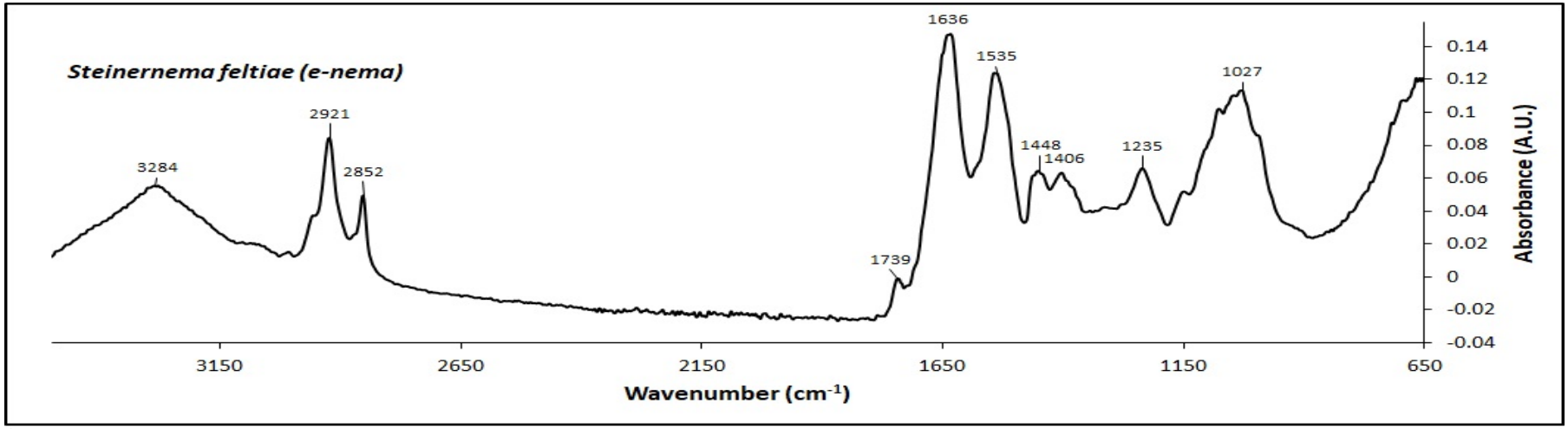

(A)

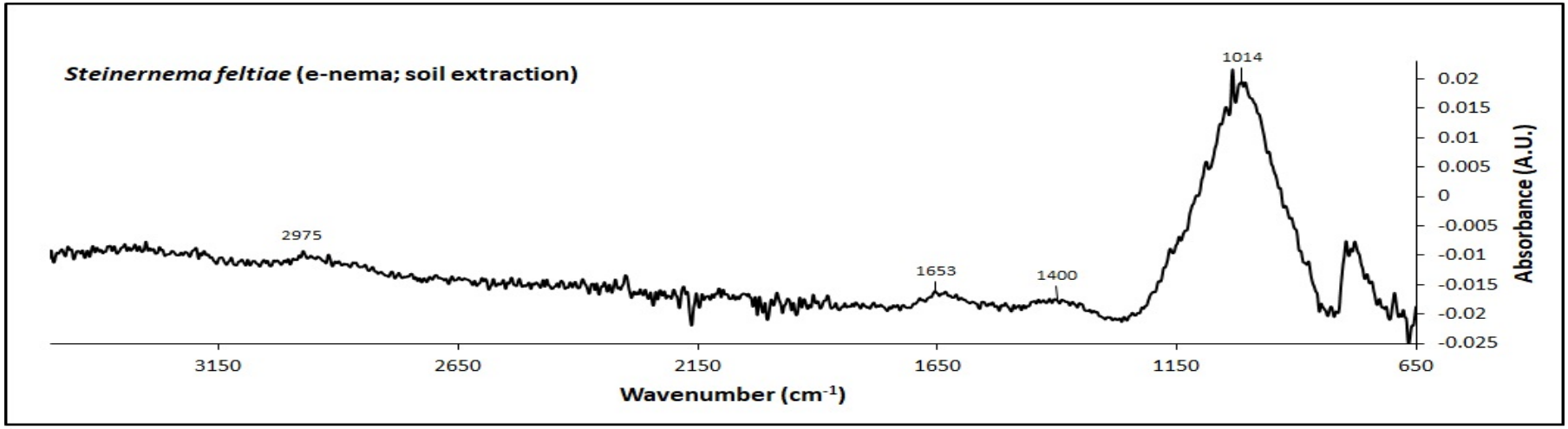

(B)

FIGURE 5.3: FT-IR absorbance spectrum of *S. feltiae* e-nema directly from pure cultures and extracted from soil. The spectrum results were averaged and baseline corrected. (A) = pure cultured *S. feltiae* e-nema with prominent peaks at 1027, 1235, 1535, 1636 and 2921 cm^{-1}. (B) = and *S. feltiae* e-nema extracted from soil with prominent peak at 1014 cm^{-1}. The x-axis describes the wavenumber in the range 3500- 600 cm^{-1}. The y-axis describes IR absorbance in AU.

S. feltiae e-nema (Figure 5.3a) are from both collagen and the symmetric and asymmetric phosphate (PO_2 2+) stretching modes (sPO_2 2+ and $asPO_2$ 2+), respectively (Table 5.1).

The bands between 1148 and 1161 cm^{-1} in *P. pacificus* (Figure 5.7a), *S. carpocapsae* (Figure 5.4a), *H. bacteriophora* (Figure 5.5a) and *G. pallida* (Figure 5.7b) represent the C–O stretching modes of the C–OH groups of proteins and C–O stretching vibration in all cases (Table 5.1). Nitrogenous compounds contributed to the absorption band in the region between 1357 and 1375 cm^{-1} (Table 5.1) in *C. elegans* (Figure 5.2a), *P. pacificus* (Figure 5.7a), *M. javanica* (Figure 5.6a) and *G. pallida* (Figure 5.7b). The band 1045 cm^{-1} in *C. elegans* (Figure 5.2a) was assigned to C–C, C–O, C–O–C stretching vibration of carbohydrates (Table 5.1). The band at 991 cm^{-1} (Table 5.1) in *S. carpocapsae* (Figure 5.4a) was assigned to a stretching vibration band of the -1,1 linkage. It is difficult to assign spectral features below 900cm^{-1} as the resolution of the spectra becomes poorer.

The spectra between the three nematode categories, FLBFN, EPN and PPN, shows some similarities but also marked differences between them. The band at 3277 cm^{-1} is associated with O-H symmetric stretching and was only found in *G.pallida* (Figure 5.7b, Table 5.1). The band at 2925 cm^{-1} is associated with lipids and the asymmetric stretching vibration of the CH_2 acyl chains was only found in *M. javanica* (Figure 5.6a). The band between 2852 and 2855 cm^{-1} was assigned to the symmetric stretching of the CH_2 bonds and was found in all three EPN species spectra, and also in *G. pallida* spectrum (Table 5.1). Similarly, the bands between 1739 and 1745 cm^{-1} were assigned to CO of phosphodiester and were found in the three EPN species along with *G. pallida* (Table 5.1). Both *C. elegans* and *P. pacificus* have prominent peaks at 1650 and 1652 cm^{-1} (Table 5.1) assigned to C=C uracyl, C=O and collagen (San-Blas *et al.*, 2011). These peaks were not found in any of the other nematode species investigated.

Both *C. elegans* and *P. pacificus* were lacking bands in the region of 1420-145 cm^{-1} which are associated with the asymmetric CH_3 bending of the methyl groups of lipids and the CH_2 deformation of lipids and Amide II. These bands were found in the EPN and PPN families (Table 5.1). The bands between 1357 and 1370 cm^{-1} (Table 5.1) associated with nitrogenous compounds, were found in the FLBFN and the PPN but were completely absent in the EPN species. The FLBFN and *G. pallida* were lacking bands between 1234 and 1243 cm^{-1} (Table 5.1) which are involved with the overlapping of Amide II and PO asymmetric stretching of PO_2 (San-Blas *et al.*, 2011). The EPN *S. carpocapsae* and *H. bacteriophora* had bands at 1077 and 1078 cm^{-1}, respectively. which were associated with symmetric phosphate stretching (Table 5.1). These bands were absent in all the other nematode species investigated. The bands in the range of 1200–900 cm^{-1} were found in all categories of nematodes.

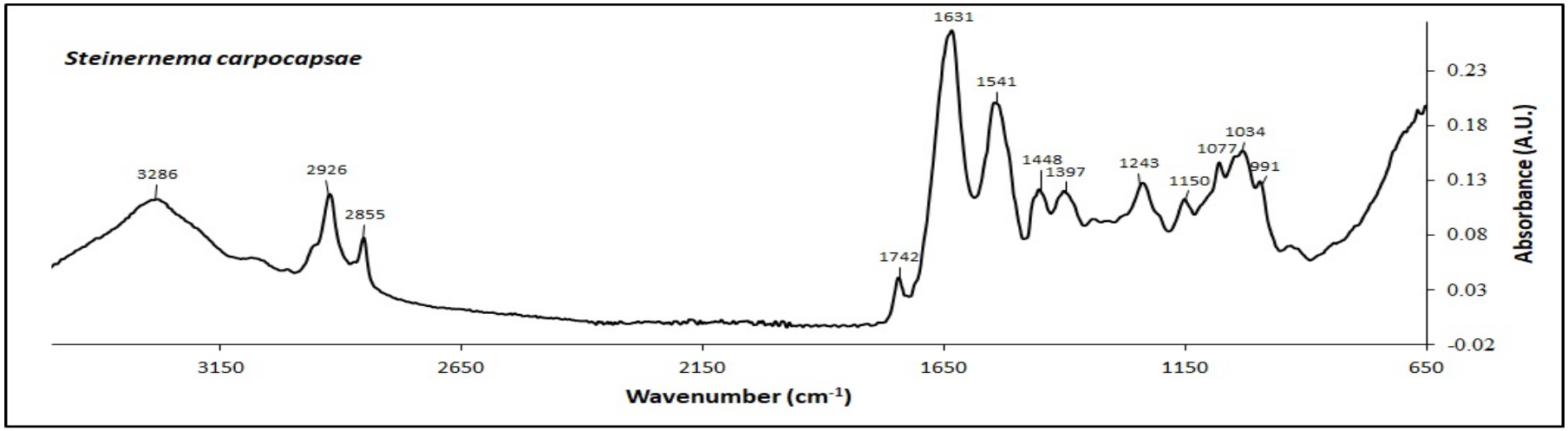

(A)

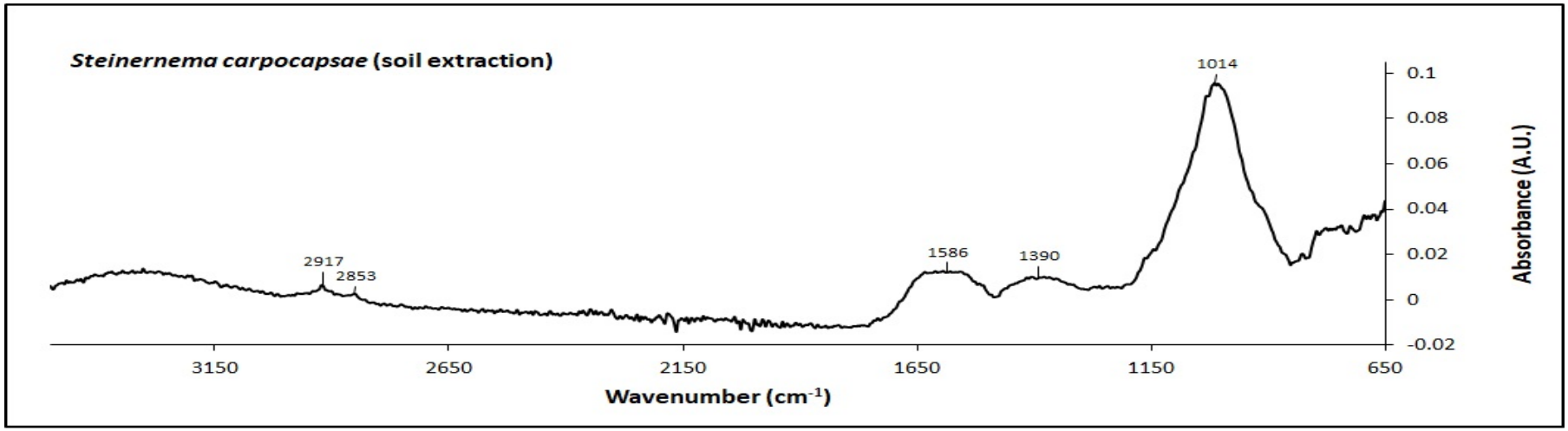

(B)

FIGURE 5.4: FT-IR absorbance spectra of *S. carpocapsae* e-nema directly from pure cultures and extracted from soil. The spectrum results were averaged and baseline corrected. (A) = pure cultured *S. carpocapsae* e-nema with prominent peaks of 1034, 1243, 1541, 1631 and 2926 cm^{-1}. (B) = *S. carpocapsae* e-nema extracted from soil with prominent peaks of 1014, 1390 and 1586 cm^{-1}. The x-axis describes the wavenumber in the range 3500- 600 cm^{-1}. The y-axis describes IR absorbance in AU.

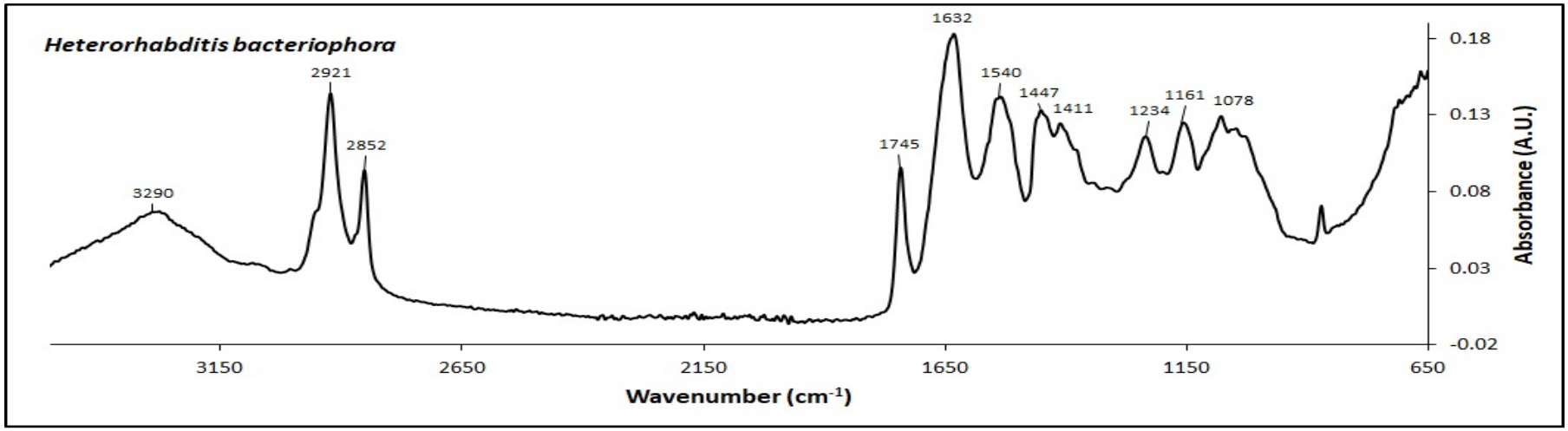

(A)

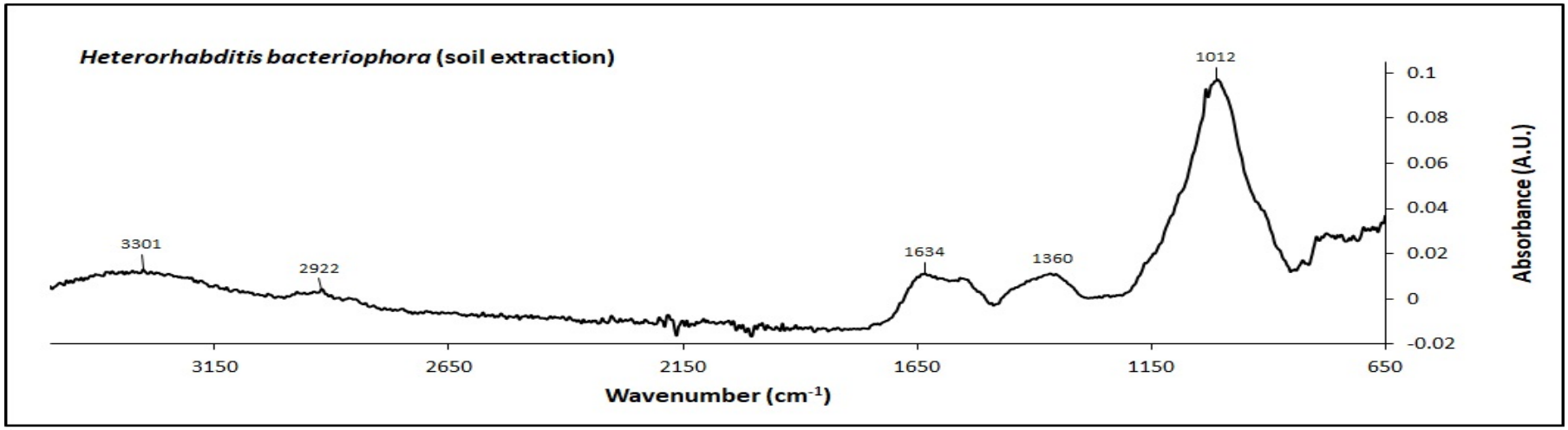

(B)

FIGURE 5.5: FT-IR absorbance spectraum of *H. bacteriophora* e-nema directly from pure cultures and extracted from soil. The spectrum results were averaged and baseline corrected. (A) = *H. bacteriophora* e-nema with prominent peaks of 1161, 1234, 1540, 1632, 1745 and 2921 cm^{-1}. (B) = *H. bacteriophora* e-nema extracted from soil with prominent peaks of 1012, 1360 and 1634 cm^{-1}. The x-axis describes the wavenumber in the range 3500- 600 cm^{-1}. The y-axis describes IR absorbance in A.U.

TABLE 5.1: Assignment of FTIR-ATR absorption bands of free living nematodes *C. elegans* and *P. pacificus*, entomopathogenic nematodes *S. feltiae* e-nema, *S. carpocapsae* e-nema and *H. bacteriophora* e-nema and plant parasitic nematodes *M. javanica* and *G. pallida* from pure cultures.

C. elegans	*P. pacificus*	*S. feltiae*	*S. carpocapsae*	*H. bacteriophora*	*M. javanica*	*G. pallida*	**Assignment**	**Reference**
3289	3323	3284	3286	3290	3350	3289	-C=CH: C-H stretch Amide A N-H stretching Asymmetric stretching N-H	San-Blas *et al.* (2011)
-	-	-	-	-	-	3277	Stretching O-H symmetric	San-Blas *et al.* (2012)
2921	2903	2921	2926	2921	-	2925	Asymmetric stretching vibration of CH_2 acyl chains (lipids)	San-Blas *et al.* (2012, 2011)
-	-	-	-	-	2871	-	Stretching C-H and N-H Symmetric stretching vibration of CH_3 acyl chains (lipids) νs CH_3	San-Blas *et al.* (2012)
-	-	2852	2855	2852	-	2855	C-H stretching (symmetric) CH_2 νs CH_2 of lipids Asymmetric CH_2 stretching mode of the methylene chains in membrane lipids C=O phosphidiester group stretching vibration of triglycerides	San-Blas *et al.* (2012, 2011)
-	-	1739	1742	1745	-	1742	C=O stretching in saturate esters of triglycerides	San-Blas *et al.* (2012)
1650	1652	1636	1631	1632	1636	1630	Ring C-C stretch of phenyl C=C uracyl C=O, Collagen Amide I (β pleated sheet)	San-Blas *et al.* (2012, 2011)
1555	-	1535	1541	1540	-	1536	Stretching C=N, C=C, Amide II	San-Blas *et al.* (2012)
-	-	1448	1448	1447	1420	1455	Asymmetric CH_3 bending of the methyl groups of lipids	San-Blas *et al.* (2012)
							C-H def of CH_2 deformation mainly lipids or Amide II	San-Blas *et al.* (2011)
-	-	1406	-	1411	-	-	C-C stretch (in ring)	Coates (2000)
-	-	-	-	1397	-	-	Symmetric CH_3 bending of the methyl groups of proteins or COO- symmetric stretching of aspartic acid	San-Blas *et al.* (2012)
1370	1366	-	-	-	1357	1375	Nitrogenous compounds Aromatic secondary amine CN stretch	Coates (2000)
-	-	1235	1243	1234	1242	-	Collagen CH_2 wagging Overlapping of the protein Amide III and the nucleic acid phosphate vibration PO asymmetric stretching of PO_{2-}	San-Blas *et al.* (2012, 2011)
-	1148	-	1150	1161	-	1152	νas CO-O-C, C-O, C-C stretching C-O-H, C-O-C deformation of glycogen	San-Blas *et al.* (2012, 2011)
-	-	-	1077	107	-	-	Symmetric phosphate[PO_2-(sym)] stretching	Coates (2000)
1045	-	-	-	-	-	-	C-O, C-C stretching, C-O-H, C-O-C of carbohydrates	San-Blas *et al.* (2011)
-	1038	1027	-	-	1033	1034	Glycogen and collagen C-OH stretching	San-Blas *et al.* (2011)
-	-	-	991 -	-	-	-	Stretching vibration of the α,α-1, 1 linkage of trehalose	San-Blas *et al.* (2011)
929	929	-	-	-	912	-	R-CH=CH_2	San-Blas *et al.* (2011)

5.3.1.2 Absorbance Spectra of Nematodes Exposed to Soil

Bands in the region of 2800 and 3301 cm^{-1} were assigned to the C– H stretching vibrations of methyl (CH_3) and methylene (CH_2) groups within the range of 2800–2950 cm^{-1}, as seen for *S. feltiae* SB 12(1) (Figures 5.8b) and e-nema (Figure 5.3b), *S. carpocapsae* (Figure 5.4b), *H. bacteriophora* (Figures 5.5b) and *M. javanica* (Figures 5.6b) in Table 5.2. The asymmetric CH (–CHV–) stretching vibration, in bands between 2915 and 2923 cm^{-1} presents a strongly overlapped band in *S. feltiae* SB 12(1) (Figures 5.8b), *S. carpocapsae* (Figures 5.4b), *H. bacteriophora* (Figures 5.5b) and *M. javanica* (Figures 5.6b) in Table 5.2. The band at 2853 cm^{-1} in *S. carpocapsae* (Figures 5.4b) represents the symmetric CH ($–CH_2–$) stretching vibration. The bands at 1631 and 1634 cm^{-1} found in *M. javanica* (Figures 5.6b) and *H. bacteriophora* (Figures 5.5b), respectively, were associated with the vibrations of C O groups of the -sheet amide I of secondary structure and the amide II band at 1537 cm^{-1} for *M. javanica* (Table 5.2). The symmetric bending vibration of CH_3 were represented at band 1400 and 1405 in *S. feltiae* e-nema (Figure 5.3b) and SB 12(1) (Figures 5.8b), respectively (Table 5.2). The amide III band at 1245 cm^{-1} in *M. javanica* (Figures 5.6b) represent CN stretching and NH and it is also involved with the triple helical structure of collagen.

The spectra among the three nematode categories, FLBFN, EPN and PPN, shows some similarities but also marked differences. The band at 3301 cm^{-1} associated with N- H stretching only occurred in *H. bacteriophora* (Figures 5.5b). The band at 2975 cm^{-1} is associated with O-H symmetric stretching and was only found in *S. feltiae* (Table 5.2). The band between 2915 and 2923 cm^{-1} found in *S. feltiae* SB 12(1), *S. carpocapsae*, *H. bacteriophora* and *M. javanica* respectively is associated with lipids and the asymmetric stretching vibration of the CH_2 acyl chains (Table 5.2). The band at 2853 cm^{-1} was assigned to the symmetric stretching of the CH_2 bonds and was found only in *S. carpocapsae* (Figures 5.4b). *Caenorhabditis elegans* (Figures 5.2b) was found to have distinct peaks at the band 1650 cm^{-1} assigned to C=C uracyl, C=O and collagen and shouldered by the band 1546 cm^{-1} associated with asymmetric CH_3 bending of the methyl groups of lipids and the CH_2 deformation of lipids and Amide II (Table 5.2).

Similarly, *H. bacteriophora* (Figures 5.5b) was found to have distinct peaks at the band 1634 (Table 5.2) associated with ring C-C stretch of phenyl, C=C uracyl, C=O and collagen along with Amide I (β pleated sheet). This was shouldered by a smaller peak with the band 1549 cm^{-1} (Table 5.2) which is associated with C=N stretching, C=C and Amide II. *M. javanica* (Figures 5.6b) has unique sharp peaks in the region of 1631-1245 cm^{-1} (Table 5.2). *S. feltiae* SB 12(1) (Figures 5.8b) had a broad band at 1609 cm^{-1} (Table 5.2) which was absent in *S. feltiae* e-nema (Figures 5.3b). *S. feltiae* e-nema and *S. carpocapsae* (Figures 5.4b) have distinctive double broad peaks in the region of 1653 and 1586 cm^{-1} followed by peaks in the region of 1405 and 1390 cm^{-1} along with *S. feltiae* SB 12(1) (Table 5.2). The bands between 1360 and 1398 cm^{-1} (Table 5.2), associated with nitrogenous compounds,

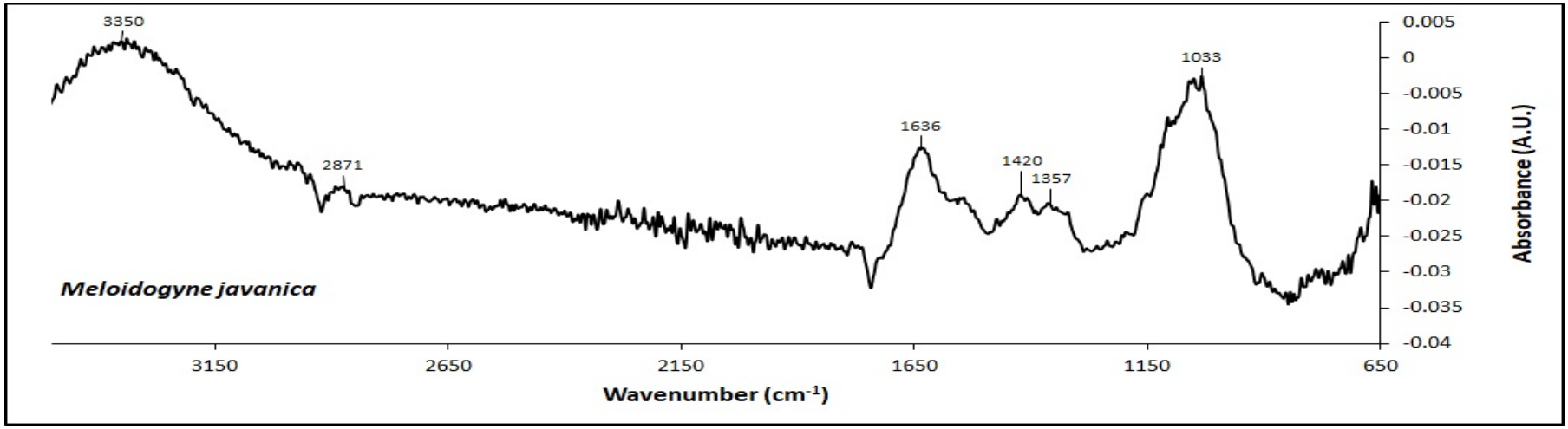

(A)

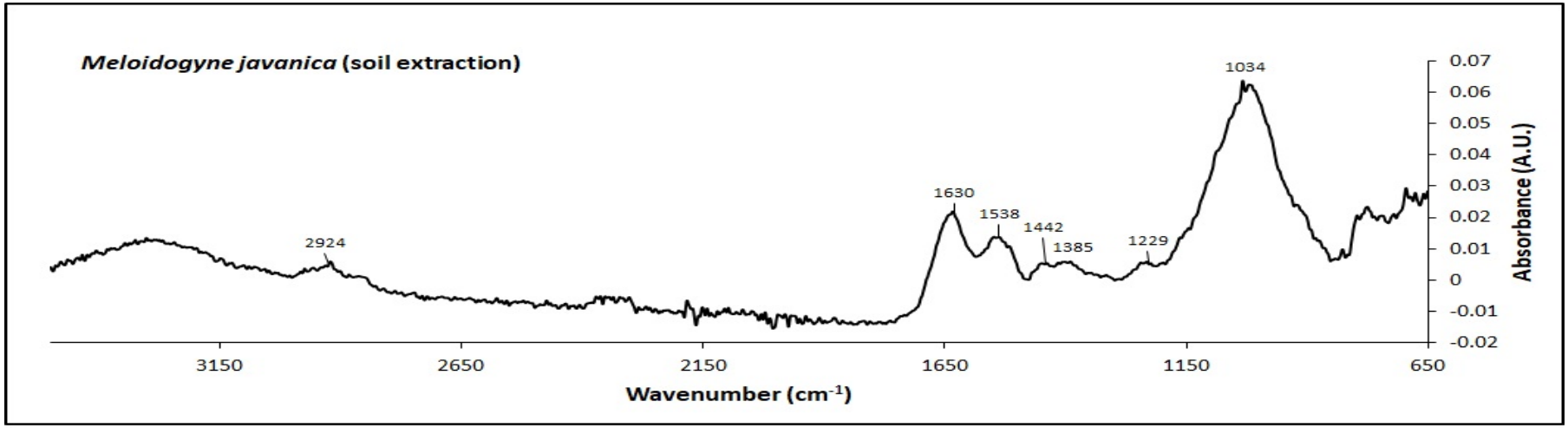

(B)

FIGURE 5.6: FT-IR absorbance spectrum of *M. javanica* directly from pure cultures and extracted from soil. The spectra results were averaged and baseline corrected. (A) = *M. javanica* with prominent peaks at 1033 and 1636 cm^{-1}. (B) = *M. javanica* extracted from soil with prominent peaks at 1034, 1538 and 1630 cm^{-1}. The x-axis describes the wavenumber in the range 3500- 600 cm^{-1}. The y-axis describes IR absorbance in A.U.

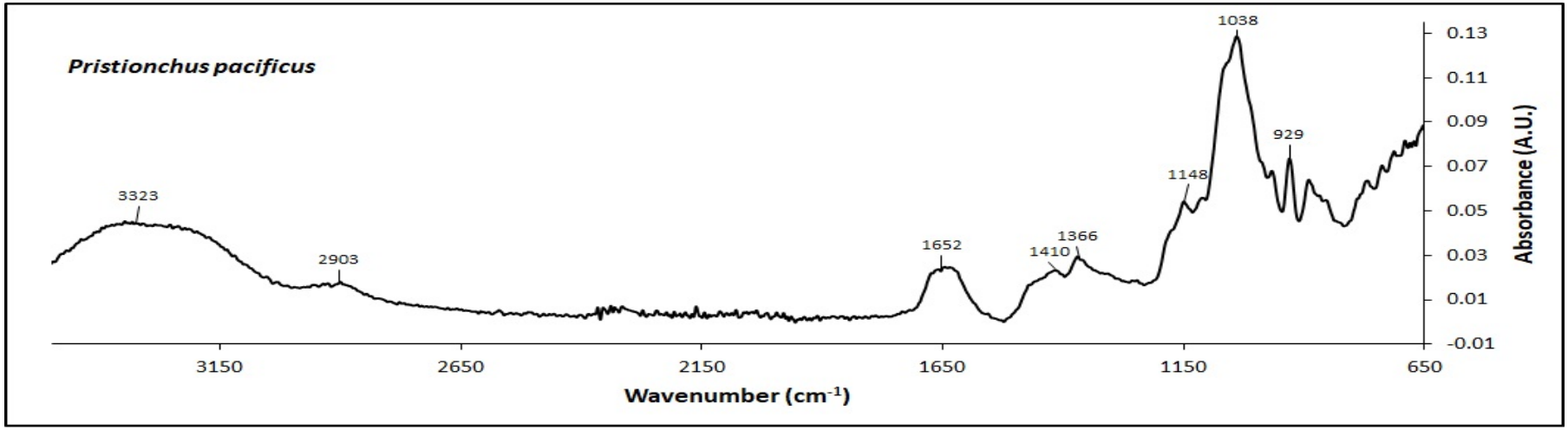

(A)

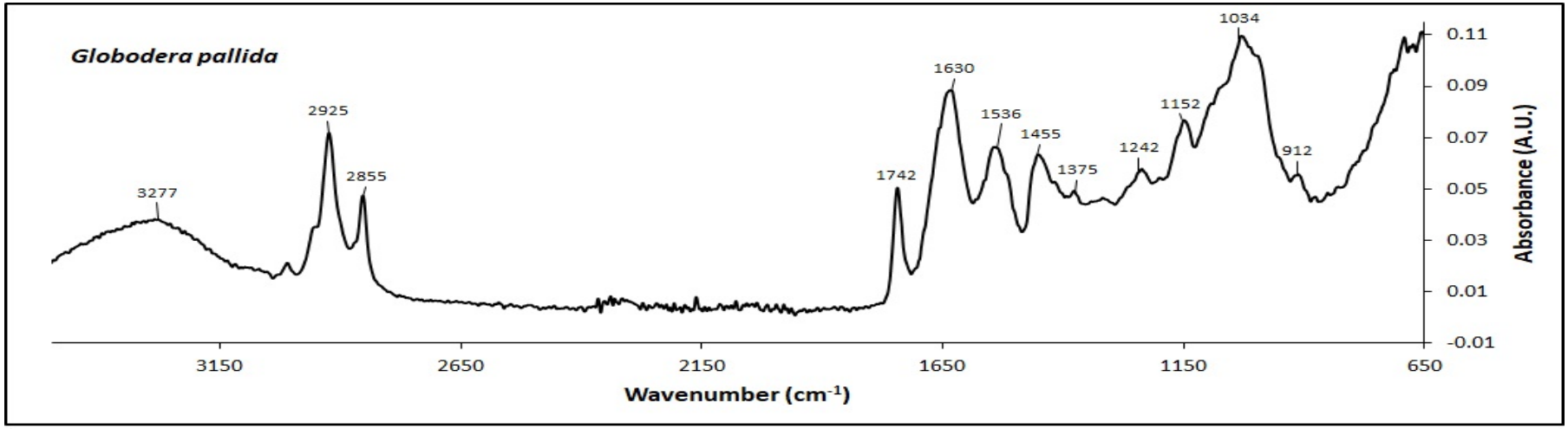

(B)

FIGURE 5.7: FT-IR absorbance spectra of *P. pacificus* and *G. pallida* from pure cultures. The spectrum results were averaged and baseline corrected. (A) = *P. pacificus* with prominent peaks at 1038, 1366 and 1652 cm^{-1}. (B) = *G. pallida* with prominent peaks at 1034, 1455, 1536, 1630, 1742 2855 and 2925 cm^{-1}. The x-axis describes the wavenumber in the range 3500- 600 cm^{-1}. The y-axis describes IR absorbance in A.U.

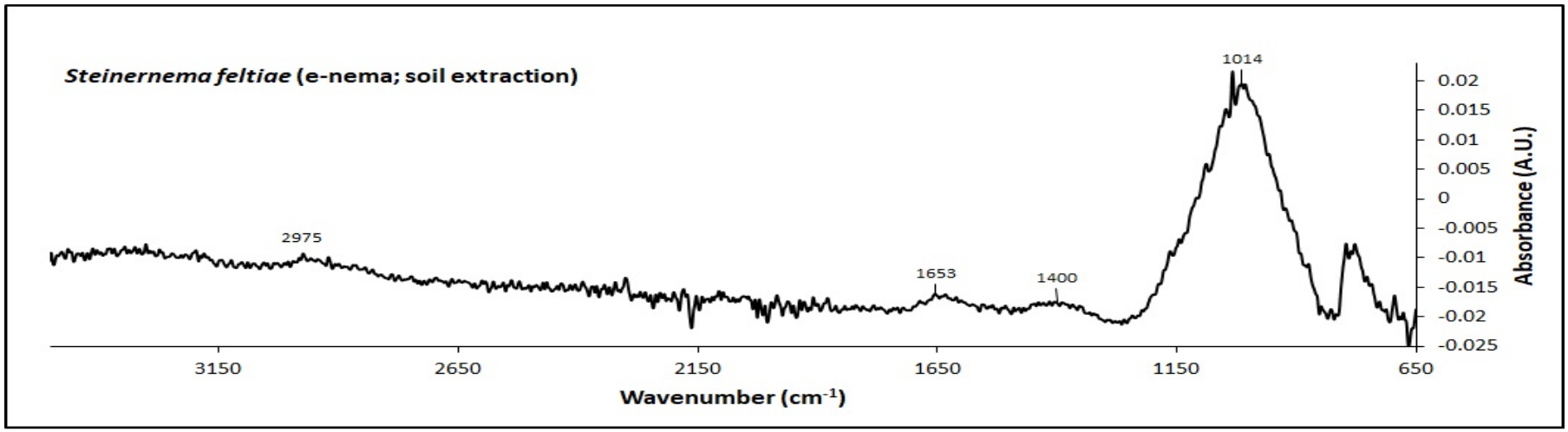

(A)

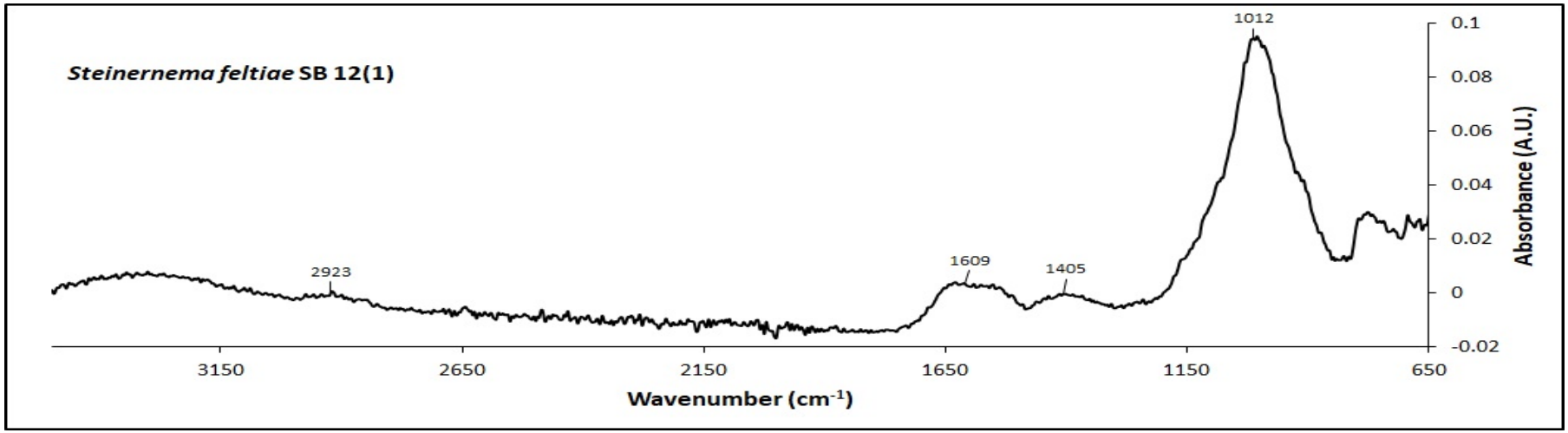

(B)

FIGURE 5.8: Comparison of FT-IR absorbance spectra of commercial *S. feltiae* e-nema and wild species *S. feltiae* SB 12(1) similarities, extracted from soil. The spectra results were averaged and baseline corrected. Similarities between the two spectra occurr with a prominent peak at 1012 and 1014 cm^{-1}, followed by two broader peaks at 1400 (A) and 1405 (B) cm^{-1}, and 1658 (A) and 1609 (B) cm^{-1}. The x-axis describes the wavenumber in the range 3500 - 600 cm^{-1}. The y-axis describes IR absorbance in A.U.

were absent in *S. feltiae* (e-nema and SB 12 (1)). Only *M. javanica* (Figures 5.6b) spectrum had the band at 1245 cm^{-1}, which is involved with the overlapping of Amide II and PO asymmetric stretching of PO_2.

The comparison between nematodes from pure cultures and the nematodes extracted from soil pots varies greatly. The band regions of 1077 and 1078 cm^{-1} were unique to *S. carpocapsae* (Figures 5.4a) and *H. bacteriophora* (Figures 5.5a) in nematodes from pure cultures but was absent in the spectra from nematodes exposed to soil (Table 5.2). The band regions at 1148- 1161 cm^{-1}, 1357- 1375 cm^{-1} and 1420-1455 cm^{-1} (Tables 5.2 and 5.1) that were present in the spectra of the pure cultured nematodes were absent from the spectra of nematodes exposed to the soil. The bands at 1400-1406 cm^{-1} were unique to *S. feltiae*, in both pure culture and extracted from the soil for both the wild (Figure 5.8b) and commercial nematodes (Figures 5.3a and 5.3b). Visually, the spectra for the nematodes from pure cultures show a greater number of distinct, sharp and broad bands in the 2852 -3290 cm^{-1} region. In comparison, the nematodes exposed to soil had very small and largely undefined bands in the same region. The pure cultured nematodes show a large number of unique sharp and prominent bands in the region of 1027- 1745 cm^{-1} that are clearly identifiable with the species. Again in comparison with the nematodes extracted from the soil the uniqueness of the bands is indistinguishable and the bands' prominence and sharpness is suppressed.

TABLE 5.2: Assignment of FTIR-ATR absorption bands of of the free living nematode *C. elegans*, entomopathogenic nematodes *S. feltiae* 12(1), *S. feltiae* e-nema, *S. carpocapsae* and *H. bacteriophora* and plant parasitic nematode *M. javanica* exposed to soil.

C. elegans	***S. feltiae* SB 12(1)**	***S. feltiae* e-nema**	***S. carpocapsae***	***H. bacteriophora***	***M. javanica***	**Assignment**	**Reference**
-	-	-	-	3301	-	N-H stretch	San-Blas *et al.* (2011)
-	-	2975	-	-	-	Stretching O-H symmetric	San-Blas *et al.* (2012)
-	2923	-	2917	2922	2915	C-H stretching (asymmetric) CH_2 Asymmetric stretching vibration of CH2 and acyl chains (lipids)	San-Blas *et al.* (2011)
-	-	-	2853	-	-	C-H stretching (symmetric) CH_2 νs CH_2 of lipids Asymmetric CH_2 stretching mode of the methylene chains in membrane lipids -C=O phosphidiester group stretching vibration of triglycerides	San-Blas *et al.* (2011) San-Blas *et al.* (2012) San-Blas *et al.* (2012)
1650	1653	-	-	-	-	2° amine, NH bend	Coates (2000)
-	-	-	1634	1631	-	Ring C-C stretch of phenyl C=C uracyl C=O, Collagen Amide I (β pleated sheet)	San-Blas *et al.* (2012, 2011)
-	-	1586	-	-	-	2° amine, NH bend	Coates (2000)
-	1609	-	-	-	-	N-H bend 2° amines	Coates (2000)
1546 -		-	-	-	1537	Stretching C=N, C=C, Amide II	San-Blas *et al.* (2012, 2011)
-	-	-	-	-	1449	Asymmetric CH3 bending of the methyl	San-Blas *et al.* (2012)
-	-	-	-	-		groups of lipids C-H def of CH_2 deformation mainly lipids or Amide II	San-Blas *et al.* (2011)
-	1405	1400	-	-	-	Symmetric bending vibration of CH_3	San-Blas *et al.* (2011)
1398-		-	1390	1360	1391	Symmetric CH_3, bending of methyl groupsof proteins or COO^- symmetric stretch of aspartic acid	San-Blas *et al.* (2012)
-	-	-	-	-	1245	Collagen CH_2 wagging Overlapping of the protein Amide III and the nucleic acid phosphate vibration PO asymmetric stretching of PO_2	Coates (2000) and San-Blas *et al.* (2011)
-	-	1032 -	-	-	1034	Glycogen and collagen C-OH stretching	San-Blas *et al.* (2011)
-	1012	-	1008	1006	-	C-C vibrations C-O stretch	Coates (2000)

5.3.1.3 Second Order Derivative Transformed Spectra

The mean spectral difference of the second order derivative of the nematodes investigated in the range of 1300-900 cm^{-1} were identified visually. When the FLBFN were assessed directly from pure cultures, *C. elegans* (Figure 5.9), displayed a strong band signal at 1051 followed by a medium band at 1168 cm^{-1} in comparison to *P. pacificus* (Figure 5.14b), which had a small band at 1132, followed by a small peak at 1098 and a shoulder in the 900 cm^{-1} region. There was a prominent peak common to all three pure cultured EPN, *S. feltiae* e-nema (Figure 5.10b) at 944 cm^{-1} region, *S. carpocapsae* (Figure 5.11b) at 944 cm^{-1} and *H. bacteriophora* (Figure 5.12a) at 954 cm^{-1}. *S. feltiae* e-nema had two shoulders at 1068 and 1141 cm^{-1}, in comparison to small bands at 1143 and 1074 cm^{-1} in *S. carpocapsae* and strong band at 1112 and 1045 in *H. bacteriophora*. The spectra for the PPN were very different, with a steep broad band at 950 cm^{-1} in *G. pallida* (Figure 5.13c) compared to wider peak in *M. javanica* (Figure 5.12c) at the same wavenumber. A medium sized band was evident in *M. javanica* at 1038 cm^{-1} in comparison to two small bands at 1052 and 1139 cm^{-1} in *G. pallida*. There was also a similar steep peak at 1280 in *M. javanica* and 1270 cm^{-1} in *G. pallida*, at the end of the wavenumber rage of interest.

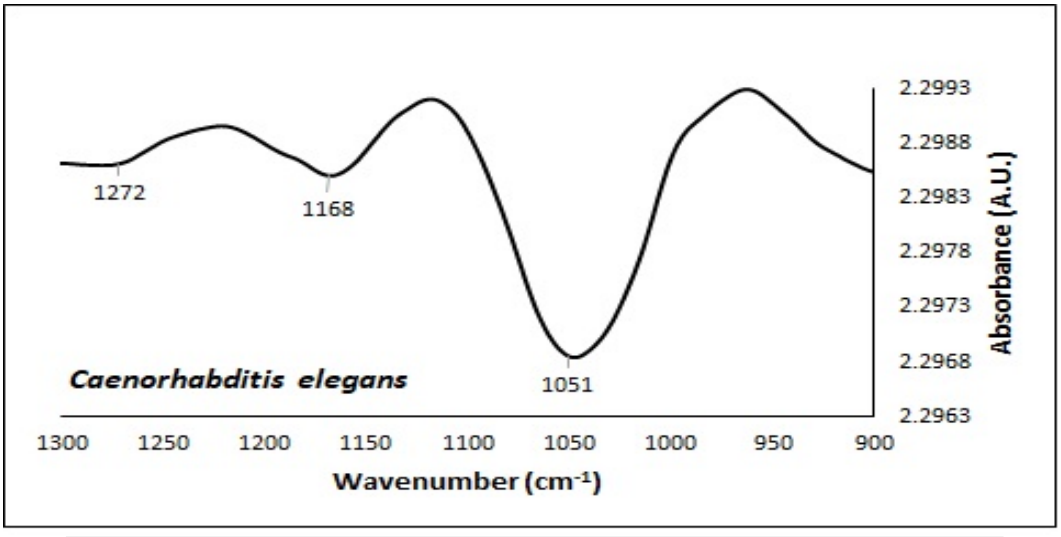

FIGURE 5.9: A 2^{nd} order derivative transformation spectrum display of pure cultured *C. elegans* with prominent peaks at 1051 and 1168 cm^{-1}. The x-axis describes the wavenumber in the range 1300-900 cm^{-1}. The y-axis describes absorbance in AU.

Caenorhabditis elegans (Figure 5.10a) exposed to soil had a strong band at 1019 cm^{-1} followed by a shoulder at 1138 cm^{-1} and another strong band at 1249 cm^{-1}. There were distinct differences and similarities among the EPN exposed to soil. *Steinernema feltiae* SB 12(1) (Figure 5.14b), *S. feltiae* e-nema (Figure 5.14a), *S. carpocapsae* (Figure 5.11c) and *H. bacteriophora* (Figure 5.12b) all had strong bands at 1024, 1023, 1024 and 1026 cm^{-1} respectively with *S. feltiae* e-nema having a stronger signal than the other three species. Both *S. feltiae*

SB 12(1) and e-nema had a broad shoulder starting from 1136 and 1135 cm^{-1} respectively. Similarly both *S. carpocapsae* and *H. bacteriophora* had a broad shoulder starting from 1129 and 1132 cm^{-1} respectively. Unlike the other EPN tested, *S. feltiae* e-nema had a small distinct shoulder at 1207 cm^{-1}. All four EPN tested had a strong band between 1255-1260 cm^{-1}.

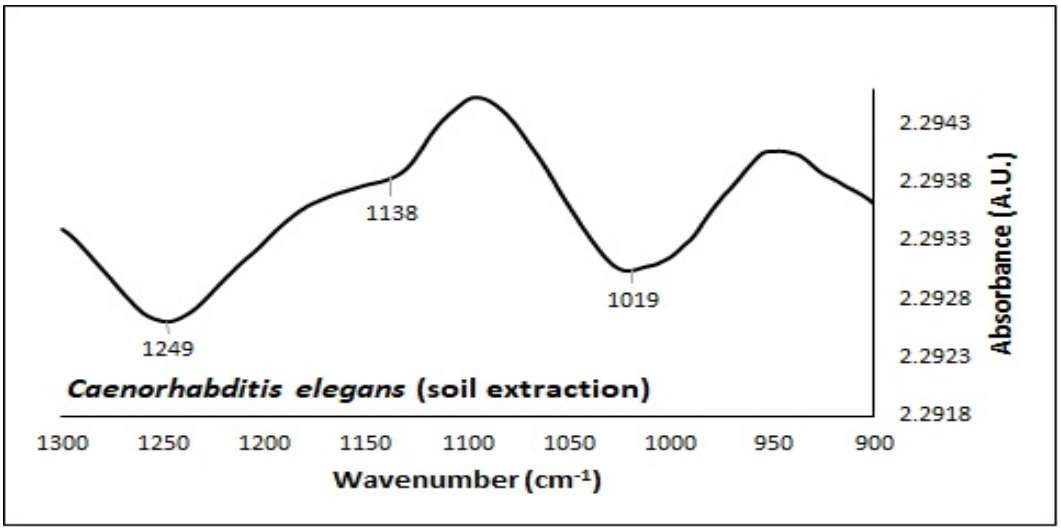

(A)

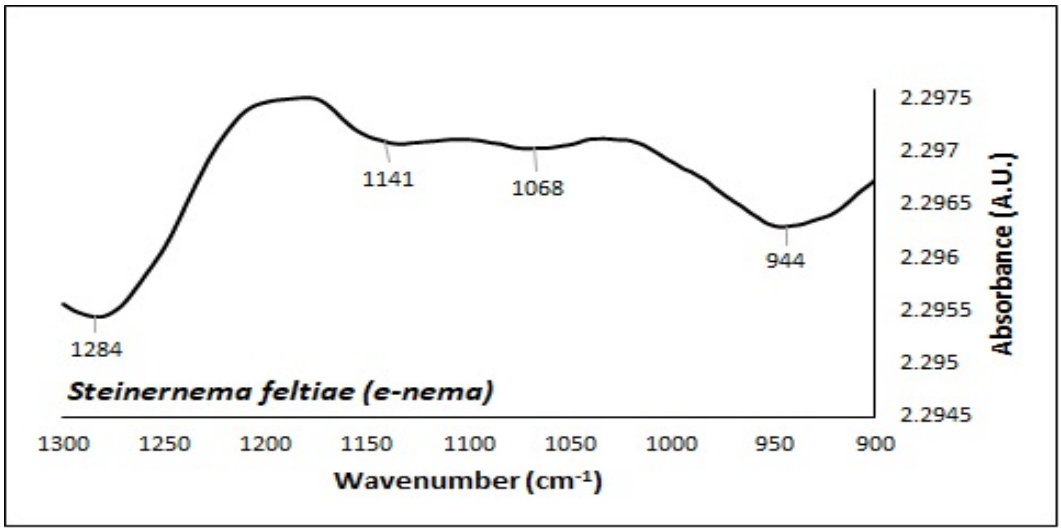

(B)

FIGURE 5.10: The 2^{nd} order derivative transformation spectrum display of (A) *C. elegans* exposed to soil with prominent peaks at 1019 and 1249 cm^{-1} and (B) *S. feltiae* e-nema from pure cultures with prominent peaks at 944 and 1284 cm^{-1}. The x-axis describes the wavenumber in the range 1300- 900 cm^{-1}. The y-axis describes absorbance in AU.

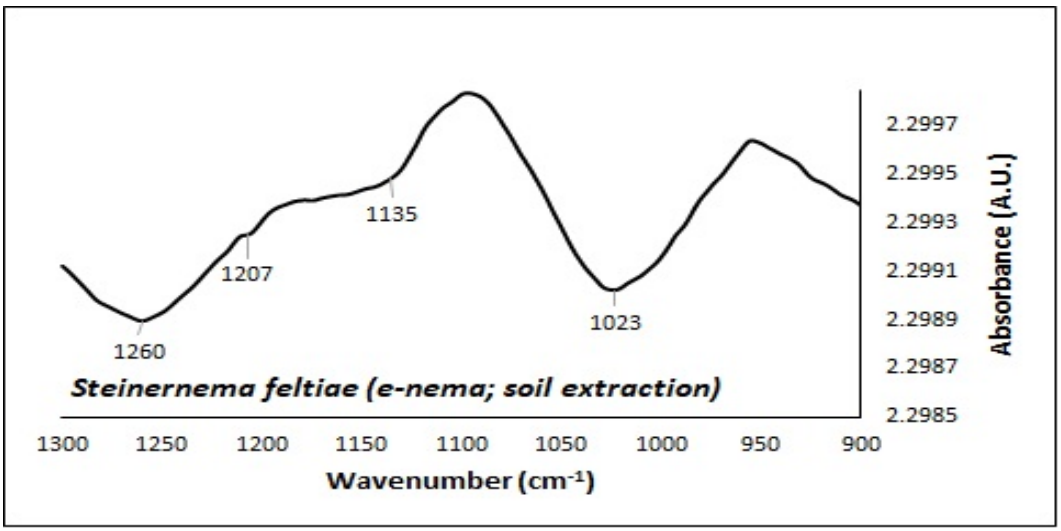

(A)

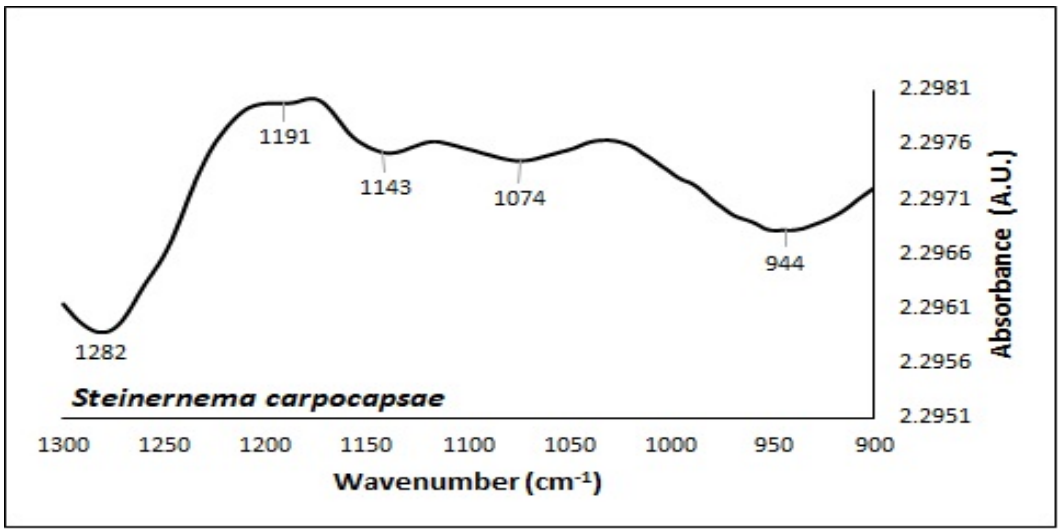

(B)

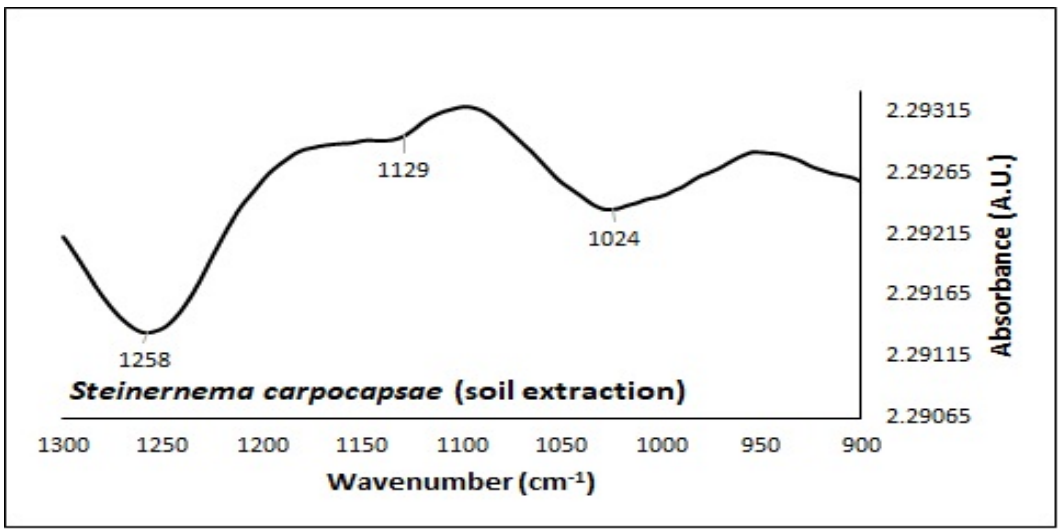

(C)

FIGURE 5.11: The 2^{nd} order derivative transformation spectra display of (A) *S. feltiae* e-nema that was exposed to soil with prominent peaks at 1023 and 1260 cm^{-1}, (B) *S. carpocapsae* e-nema from pure cultures with prominent peaks at 944 and 1143 and 1282 cm^{-1} and (C) *S. carpocapsae* e-nema that was exposed to soil with prominent peaks at 1024 and 1258 cm^{-1}. The x-axis describes the wavenumber in the range 1300- 900 cm^{-1}. The y-axis describes absorbance in AU.

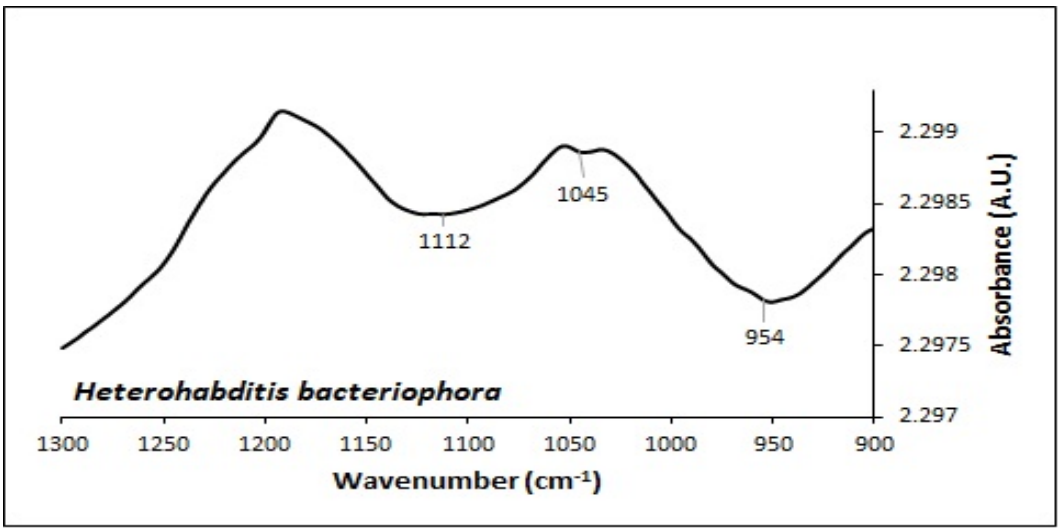

(A)

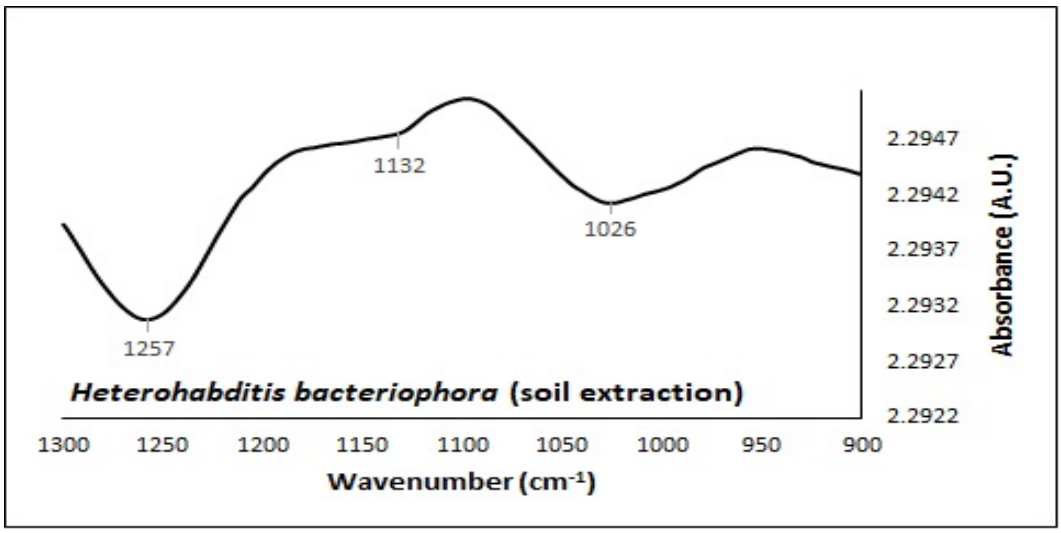

(B)

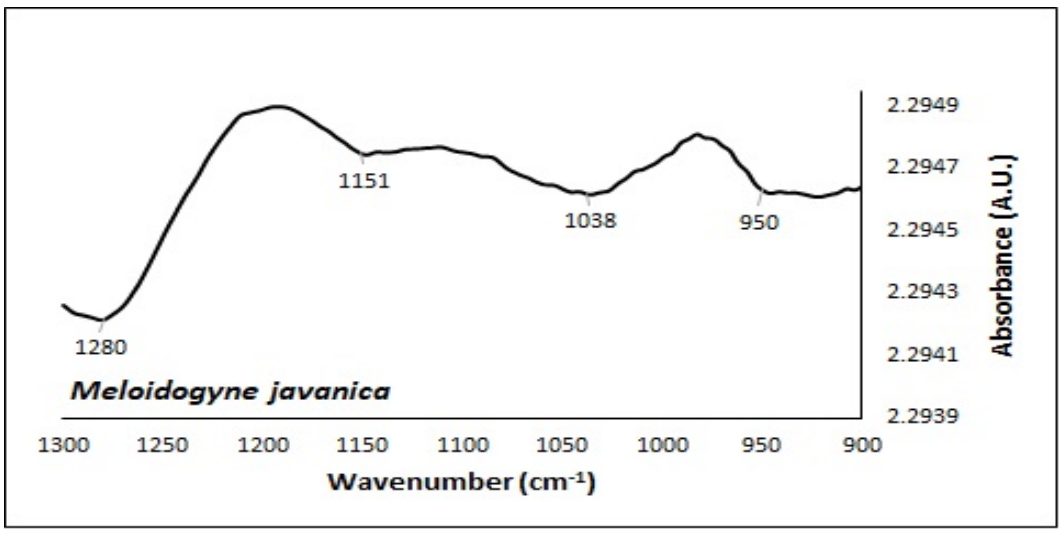

(C)

FIGURE 5.12: A 2^{nd} order derivative transformation spectrum display of (A) *H. bacteriophora* e-nema from pure cultures with a prominent peak at 954 cm^{-1}, (B) *H. bacteriophora* e-nema that was exposed to soil with prominent peaks at 1026 and 1257 cm^{-1} and (C) *M. javanica* from pure cultures with prominent peaks at 1038 and 1280 cm^{-1} . The x-axis describes the wavenumber in the range 1300- 900 cm^{-1}. The y-axis describes absorbance in AU.

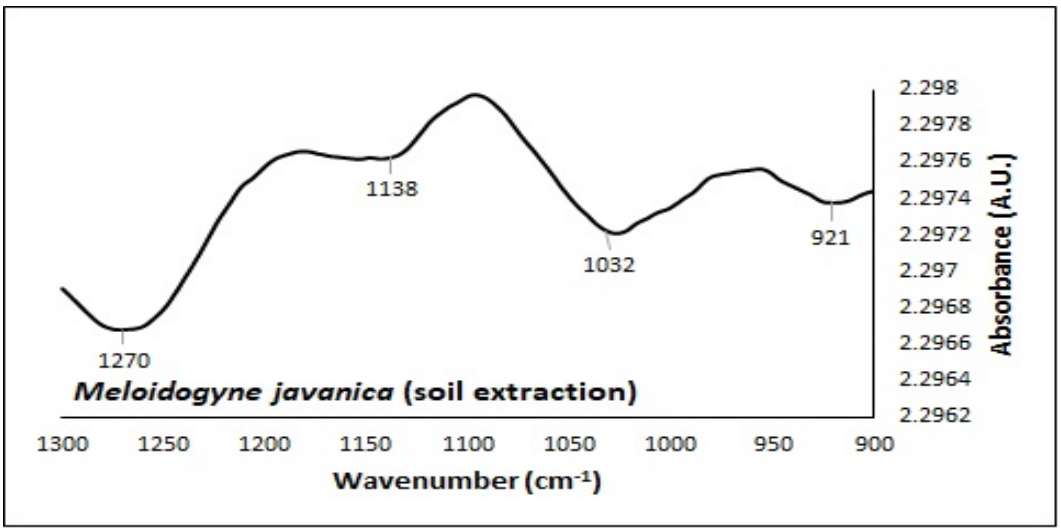

(A)

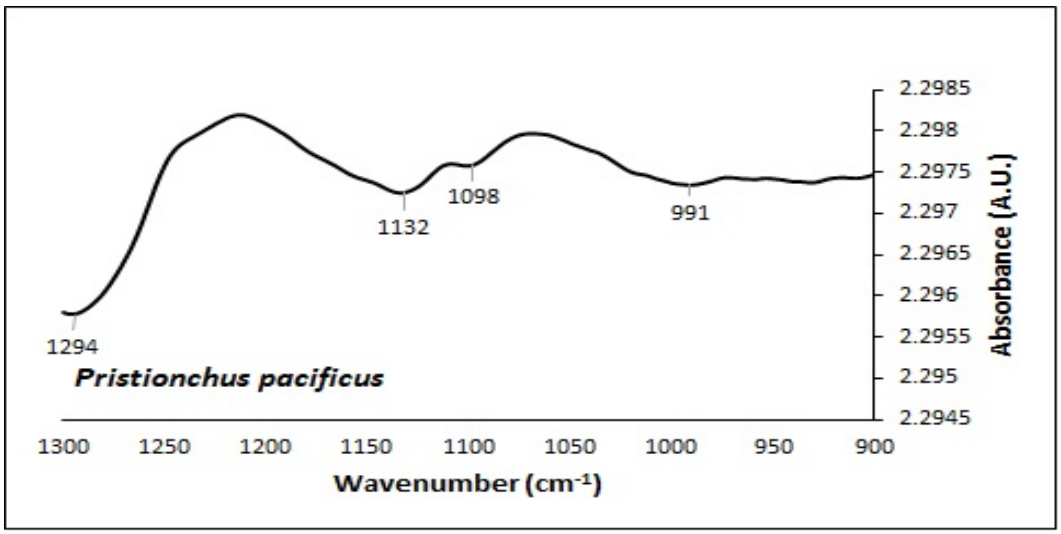

(B)

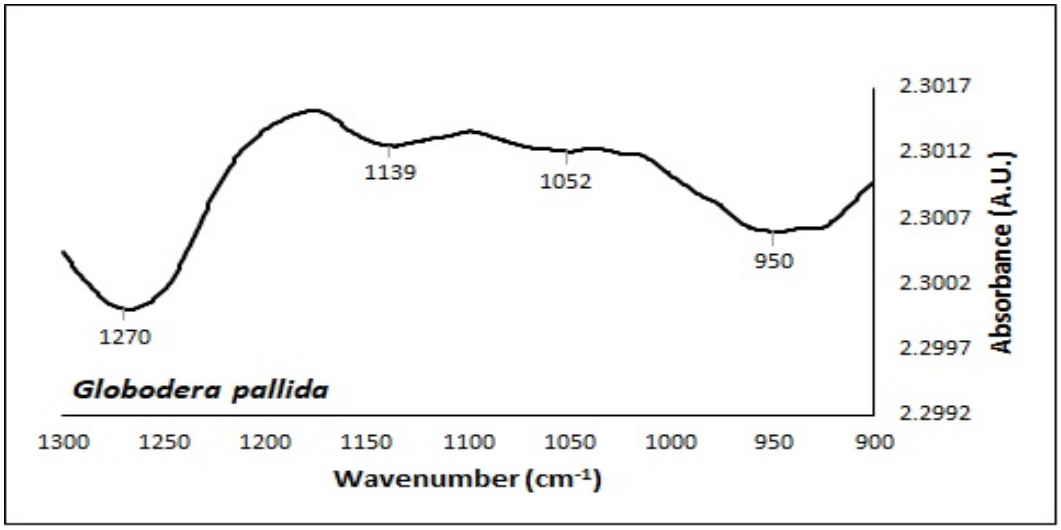

(C)

FIGURE 5.13: A 2^{nd} order derivative transformation spectrum display of (A) *M. javanica* that was exposed to soil with prominent peaks at 921, 1032 and 1270 cm^{-1}, (B) *P. pacificus* from pure cultures with prominent peaks at 1098 and 1132 cm^{-1} and (C) *G. pallida* from pure cultures with prominent peaks at 1139 and 1270 cm^{-1}. The x-axis describes the wavenumber in the range 1300- 900 cm^{-1}. The y-axis describes absorbance in AU.

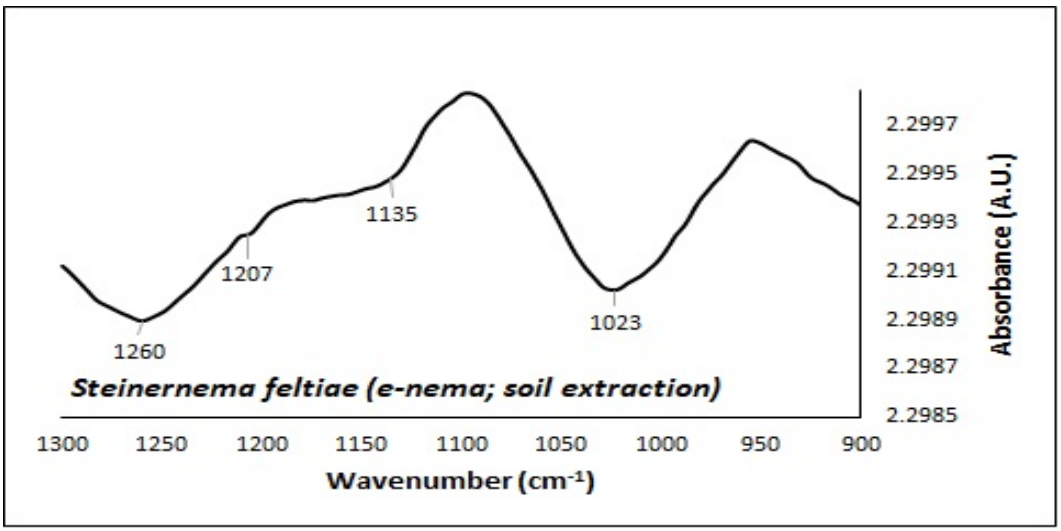

(A)

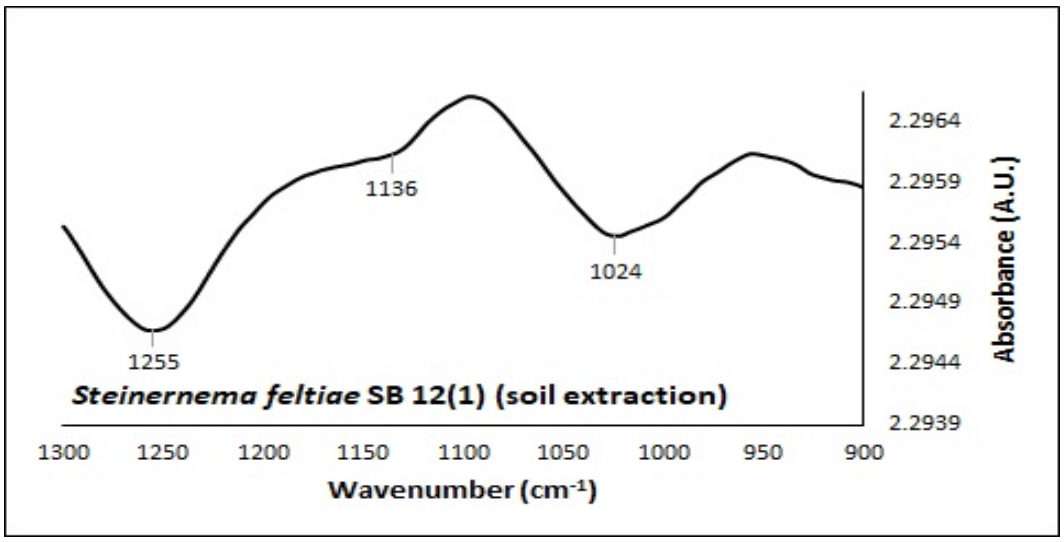

(B)

FIGURE 5.14: Comparison of 2^{nd} order derivative transformation spectra of (A) *S. feltiae* e-nema and (B) *S. feltiae* SB 12(1) with prominent peaks at 1024 and 1255 cm^{-1} exposed to soil. The x-axis describes the wavenumber in the range 1300- 900 cm^{-1}. The y-axis describes absorbance in arbitrary units (A.U.).

The comparison between nematodes from pure cultures and of nematodes exposed to soil shows distinct differences. Pure cultured *C. elegans* (Figure 5.2a) has a strong sharp band at 1051 cm^{-1} which is not evident in *C. elegans* (Figure 5.10a) exposed to soil. Likewise *C. elegans* exposed to soil has two distinct sharp bands at 1019 and 1249 cm^{-1} that are absent *C. elegans* directly assessed from cultures.

Steinernema feltiae e-nema exposed to soil had a strong, large band at 1023 cm^{-1} followed by a medium sized band a 1260 cm^{-1}, which were absent in pure cultured *S. feltiae* e-nema. In comparison, pure cultured *S. feltiae* e-nema had a medium band at 944 cm^{-1} and two shoulders at 1064 and 1141 cm^{-1} that were absent in *S. feltiae* e-nema exposed to soil. *Steinernema carpocapsae* exposed to soil had strong bands at 1024 and 1258 cm^{-1} which were absent in pure cultured *S. carpocapsae*. Likewise pure cultured *S. carpocapsae* had a

weak band at 1024 cm^{-1} and a strong band at 1258 cm^{-1}. Pure cultured *H. bacteriophora* had a strong band at 954 cm^{-1}, followed by a medium band at 1112 cm^{-1} which was lacking in *H. bacteriophora* exposed to soil. *H. bacteriophora* exposed to soil had a medium band at 1026 cm^{-1} followed by a strong band at 1257 cm^{-1} that were absent in the pure cultures.

Pure cultured *M. javanica* (Figure 5.12c) and *M. javanica* (Figure 5.13a) exposed to soil had similar small peaks at 950 cm^{-1} in pure cultured and 921 cm^{-1} in soil exposure, a small peak at 1038 cm^{-1} in pure cultures and a medium peak at 1032 cm^{-1} in soil exposure and strong peaks at 1280 cm^{-1} in pure culture and 1270 cm^{-1} in soil exposure. The comparisons between wild *S. feltiae* SB 12(1) and the commercial type e-nema were similar, with prominent peaks at 1023 and 1024, 1135 and 1136, and 1260 and 1255, for commercial and wild respectively.

5.3.2 Statistical Analysis

5.3.2.1 Principal Component Analysis on Pure Nematode Cultures

principal Component Analysis on all nematodes directly assessed from pure cultures revealed seven components that had eigenvalues greater than one which explained 44.12%, 18.17%, 14.52%, 10.22% 6.94% 3.93% and 1.34% of the total variance, respectively. Visual inspection of the scree plot also indicated that seven components should be retained. However, a forced factor extraction was performed on the data and a five component solution was retained to explain 62.28% of the total variance. The overall KMO measure was 0.925 with individual KMO measures all greater than 0.8. *C. elegans* shared components 1 and 4, with even loading in both components. *S. feltiae* e-nema and *S. carpocapsae* shared components 1 and 5 with dominant loading in component 1. *P. pacificus* and *H. bacteriophora* both had dominant loading in component 1 and did not share with any other component. *M. javanica* and *G. pallida* both had component loading in components 2 and 3, with *M. javanica* dominating component 3 and *G. pallida* dominating component 2. Component loadings of the rotated solution are presented in Appendix D (Table D.1).

A further PCA was carried out on each nematode group, to determine any similarities or differences within nematode lifestyles. For the FLBFN *C. elegans* and *P. pacificus* (Appendix D Figure D.1.2), the overall KMO measure was 0.915 with individual KMO measures all greater than 0.8. PCA revealed 2 components that had eigenvalues greater than one and which explained 72.40% and 24.64% variance per component and explained 97.04% of the total variance. There were strong loadings in component 1 for *C. elegans* and component 2 for *P. pacificus*. Component loadings were presented in, Appendix D (Table D.2).

PCA on the EPN, *S. feltiae* e-nema, *S. carpocapsae* and *H. bacteriophora* (Appendix D, Figure D.1.2), had a KMO measure of 0.918, with individual KMO measures all greater than

0.8. PCA revealed 3 components that had eigenvalues greater than one and which explained 73.14% 18.31% and 4.37% of the total variance, respectively. Visual inspection of the scree plot indicated that 2 components should be retained, to explain 95.82% of the total variance. There were strong loadings in component 1 for *S. feltiae* e-nema, *S. carpocapsae* and *H. bacteriophora*. However, *S. feltiae* e-nema and *S. carpocapsae* also shared component 2. Component loadings of the rotated solution were presented in Appendix D (Table D.2).

For the PPN *M. javanica* and *G. pallida* (Appendix D, Figure D.1.2) the KMO measure was 0.881 with individual KMO measures all greater than 0.8. PCA revealed two components that had eigenvalues greater than one and which explained 52.80% and 44.99% of the total variance, respectively. Visual inspection of the scree plot indicated that two components should be retained to explain 97.79% of the total variance. There were strong loadings in component 1 for *M. javanica* and component 2 for *G. pallida*. Component loadings of the rotated solution were presented in, Appendix D (Table D.2).

5.3.2.2 Principal Component Analysis on Nematodes Exposed to Soil

principal component analysis was run on 2^{nd} order derivative data extrapolated from, nematodes exposed to the soil, in a pot based experiment. There were three replications of each species (Figure 5.16). Inspection of the correlation matrix showed that all variables had at least one correlation coefficient greater than 0.4. PCA revealed 2 components that had eigenvalues greater than one and which explained 78.66% and 9.67% of the total variance, respectively. Visual inspection of the scree plot indicated that 2 components should be retained to explain 88.33% of the total variance. There were strong loadings in component 1 for *C. elegans*, and component 2 for *M. javanica*. The other species investigated shared both components. Component loadings of the rotated solution were presented in Appendix D (Table D.3).

The EPN PCA scores for *S. feltiae* SB 12(1), *S. feltiae* e-nema, *S. carpocapsae* and *H. bacteriophora* (Appendix D, Figure D.1.2), revealed 2 components that had eigenvalues greater than one and which explained 81.45% and 8.63% of the total variance. Visual inspection of the scree plot also indicated that 2 components explained 90.08% of the total variance. The KMO measure was 0.885, with individual KMO measures all greater than 0.7. All EPN shared the two components. Component loadings of the rotated solution were presented in, Appendix D (Table D.3).

5.3.2.3 Principal Component Analysis Bi-Plots

Bi-plots were constructed for all PCA analyse including: (1) all pure cultured nematode species (Figure 5.15), (2) pure cultured FLBFN, (Appendix D, Figure D.1.2), (3) pure cultured EPN (Appendix D, Figure D.1.2), and (4) pure cultured PPN (Appendix D, Figure D.1.2), along with bi-plots for (5) all nematode species exposed to soil (Figure, 5.16) and (6) EPN exposed to soil (Appendix D, Figure D.1.2). The cluster structure of the data allowed to observe seven clear consistent clusters of cases for combined pure cultured nematodes (Figure 5.15), six clusters of cases (Figure 5.16) for combined nematodes exposed to soil, three clusters of cases (Appendix D, Figure D.1.2) for pure cultured EPN and two clusters of cases (Appendix D, Figure D.1.2) for pure cultured PPN and (Appendix D, Figure D.1.2) for EPN exposed to soil.

In Figure 5.15, displaying the pure cultured nematodes, the clusters of cases were individually clustered according to species for *G. pallida*, *M. javanica*,*C. elegans* and *S. feltiae* e-nema except for the replication SFE 9, for all 10 replications. The groups were mainly distributed along the PC1, except for *G. pallida*, which was distributed along the PC2. There was close groupings of *C. elegans*, *P. pacificus*, *H. bacteriophora* except for replication HB 3 and replication HB 5 and *S. carpocapsae* except for replication SC6.

The clusters of cases for the FLBFN in Appendix D (Figure D.1.2), were tightly clustered for *C. elegans* and more loosely clustered for *P. pacificus* mainly along the PC1. There is a clear distinction between the EPN clusters of cases in Appendix D (Figure D.1.2). Specifically, *S. feltiae* e-nema was tightly clustered except for replications SFE2 and SFE9, *H. bacteriophora* was tightly clustered except for replications HB3 and HB5, and *S. carpocapsae* was tightly clustered except for replications SC6 and SC10, along with the PC1. The PPN clusters of cases (Appendix D, Figure D.1.2), for *M. javanica* were tightly clustered along the far end of the positive PC1 and *G. pallida* was clustered along the far end of the positive PC2. There was no sharing between species when analysed according to their life strategy.

In Figure 5.16, nematodes that were exposed to soil, the clusters of cases for all species were more loosely clustered compared to the pure cultured nematodes. *S. carpocapsae* was closely clustered except for replication SC2 along PC1. *M. javanica* was loosely clustered for all 3 replications and MJ3 shared with replication SC1, SC3 and HB2 . *S. feltiae* SB 12(1) and *S. feltiae* e-nema were loosely distributed and the replications did not cluster together along PC1 except for replication SFE2 which was distributed close to PC2. *H. bacteriophora* (replications HB1 and HB3) and *C. elegans* (replications CE2 and CE3) cluster of cases were closely distributed along PC1.

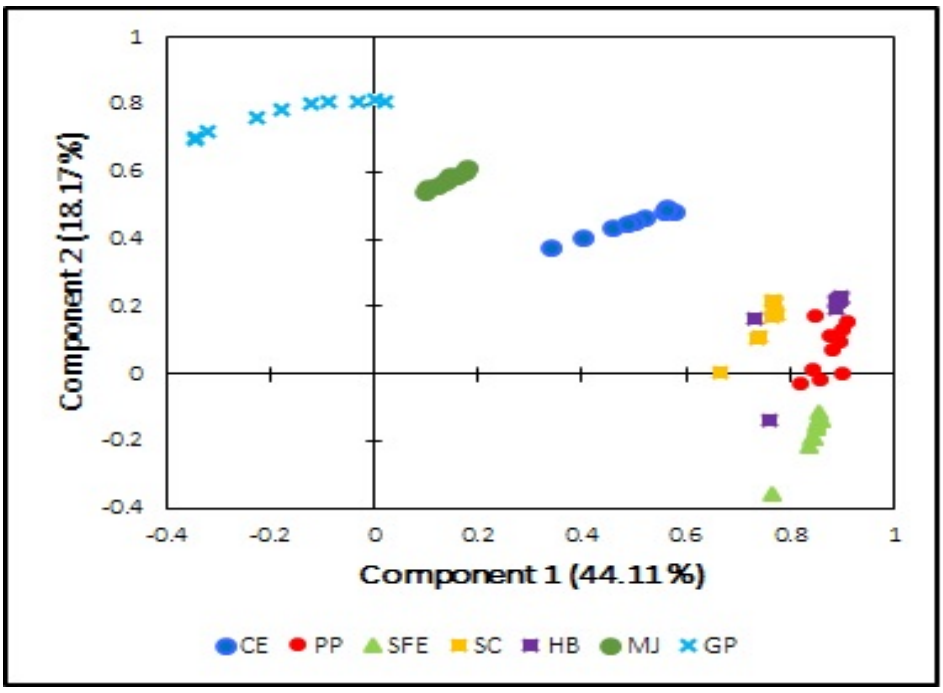

FIGURE 5.15: Principal component analysis of FTIR spectra of nematodes assessed directly from cultures, that were baseline corrected in the 2^{nd} order derivative, with 10 replications of each species. PCA was performed on data in the range of 900-1350cm^{-1}. Component 1 describes 44.11% and component 2 describes 18.17% of the total variance. Component loadings of the rotated solution were presented in, Appendix D (Table D.1). The nematodes are described as CE = *C. elegans*, PP = *P. pacificus*, SFE = *S. feltiae* e-nema, SC = *S. carpocapsae*, HB = *H. bacteriophora*, MJ = *M. javanica* and GP = *G. pallida*.

In Appendix D (Figure D.1.2), the EPN exposed to soil were all loosely clustered. *H. bacteriophora* (replications HB1 and HB3) clusters of cases were closely clustered along PC1. *Steinernema carpocapsae* (replications SC1 and SC3) clusters of cases were closely clustered along PC1 with an overlap of replication HB2. *Steinernema feltiae* SB 12(1) and *S. feltiae* e-nema cluster of cases were loosely distributed along PC1 except for replication SFE2 which was closely distributed along PC2. When comparing Appendix D Figure D.1.2 to Figure D.1.2, there are clearly defined cluster of cases for nematodes from pure cultures and mixed clusters for nematodes exposed to soil.

5.3.2.4 Agglomerative Hierarchical Clustering

Agglomerative hierarchical cluster analysis was employed on the 2^{nd} order derivative data in the region of 900-1300 cm^{-1} to identify groups and classify them into clusters. It was also utilised to confirm that the replications were grouped by species (San-Blas *et al.*, 2011). The AHC of all pure cultured nematodes (Figure 5.17) shows individual clusters of each nematode species, with no overlap or sharing of clusters between 0-500 on the dissimilarity scale. Between 500-1000 dissimilarity *C. elegans* and *P. pacificus* share a cluster, likewise

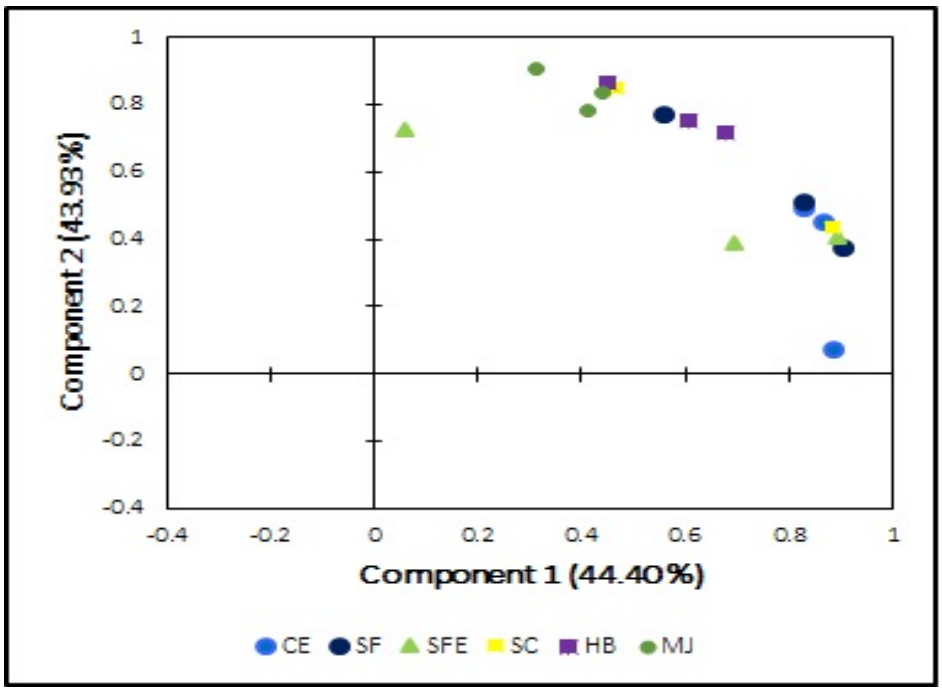

FIGURE 5.16: Principal component analysis on FT-IR spectra of nematodes exposed to soil, that were baseline corrected in the 2^{nd} order derivative, with 3 replications of each species. PCA was performed on data in the range of 900-1350cm^{-1} . Component 1 describes 86.41% and component 2 describes 7.59% of the total variance. Component loadings of the rotated solution were presented in, Appendix D (Table D.3). The nematodes are described as CE = *C. elegans*,SF = *S. feltiae* SB 12(1), SFE = *S. feltiae* e-nema, SC = *S. carpocapsae*, HB = *H. bacteriophora* and MJ = *M. javanica*.

H. bacteriophora and *S. carpocapsae* share a cluster. The nematode *M. javanica* distantly shares a cluster with *H. bacteriophora* and *S. carpocapsae* at 2500 on the dissimilarity scale. However *G. pallida*, as a group, appeared alone, as they shared a cluster with all groups at 4500 dissimilarity.

The AHC for the nematodes exposed to soil (Figure 5.18) is more varied compared to the pure cultured nematodes. There were two prominent clusters present. The nematode *M. javanica* was the only species to have all three replications grouped together between 0-25 dissimilarity. However *M. javanica* was further clustered with *S. feltiae* e-nema replication 2 at 100 dissimilarity. This was clustered again at 200 dissimilarity with the remaining *S. feltiae* e-nema replication 1, *S. feltiae* SB 12(1) replications 2 and 3, *S. carpocapsae* replications 1 and 3 and *H. bacteriophora* replication 2 and 3. The 2^{nd} cluster contained *S. carpocapsae* replication 2, *S. feltiae* SB 12(1) replication 1, *S. feltiae* e-nema replication 3, *C. elegans* replications 2 and 3 along with *H. bacteriophora* replication 1 at 50 dissimilarity. This group was closely clustered with *C. elegans* replication 1 at 225 dissimilarity. *S. feltiae* SB 12(1) was clustered with all nematode species at 1500 dissimilarity. The results observed after AHC confirmed the PCA results for both nematodes from pure cultures and for nematodes exposed to soil.

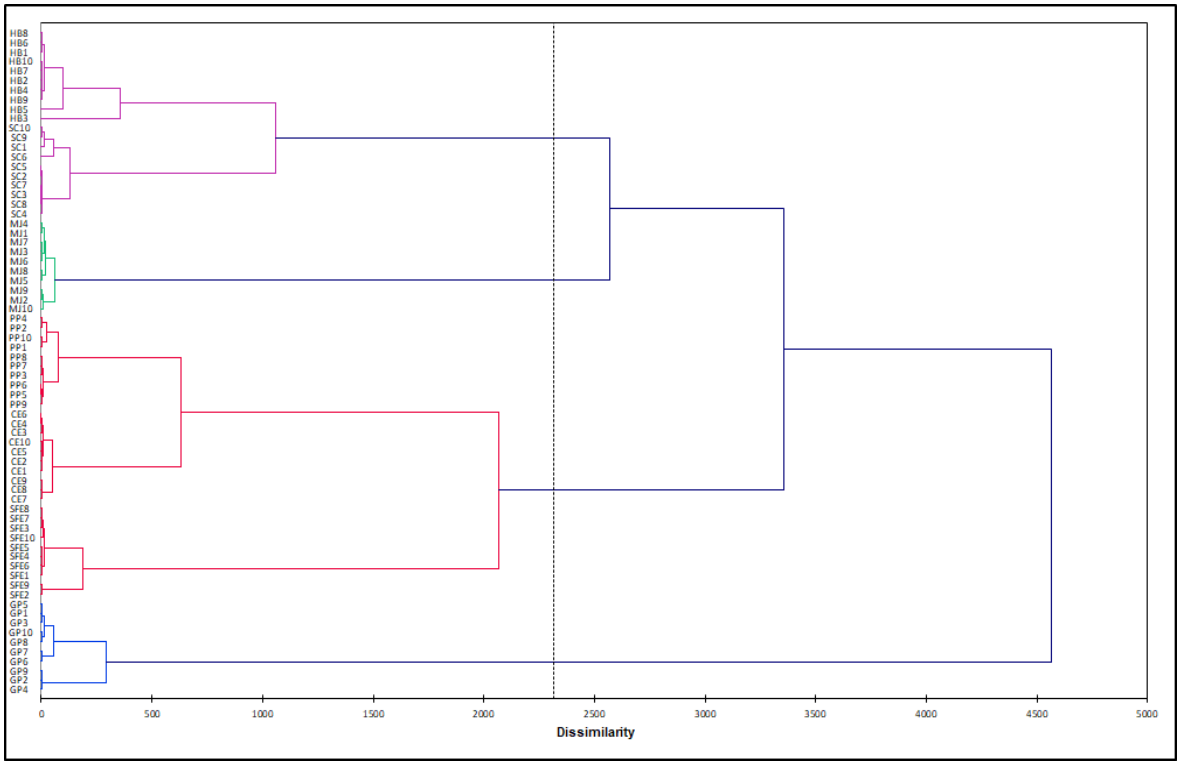

FIGURE 5.17: Hierarchical clustering of 2^{nd} order derivative transformation data of nematodes assessed directly from pure cultures. The nematodes are described on the y-axis as CE = *C. elegans*, SF = *S. feltiae* SB 12(1), SFE = *S. feltiae* e-nema, SC = *S. carpocapsae*, HB = *H. bacteriophora* and MJ = *M. javanica*. The nematodes are numbered according to the replications 1-10. The x-axis describes the dissimilarity distance.

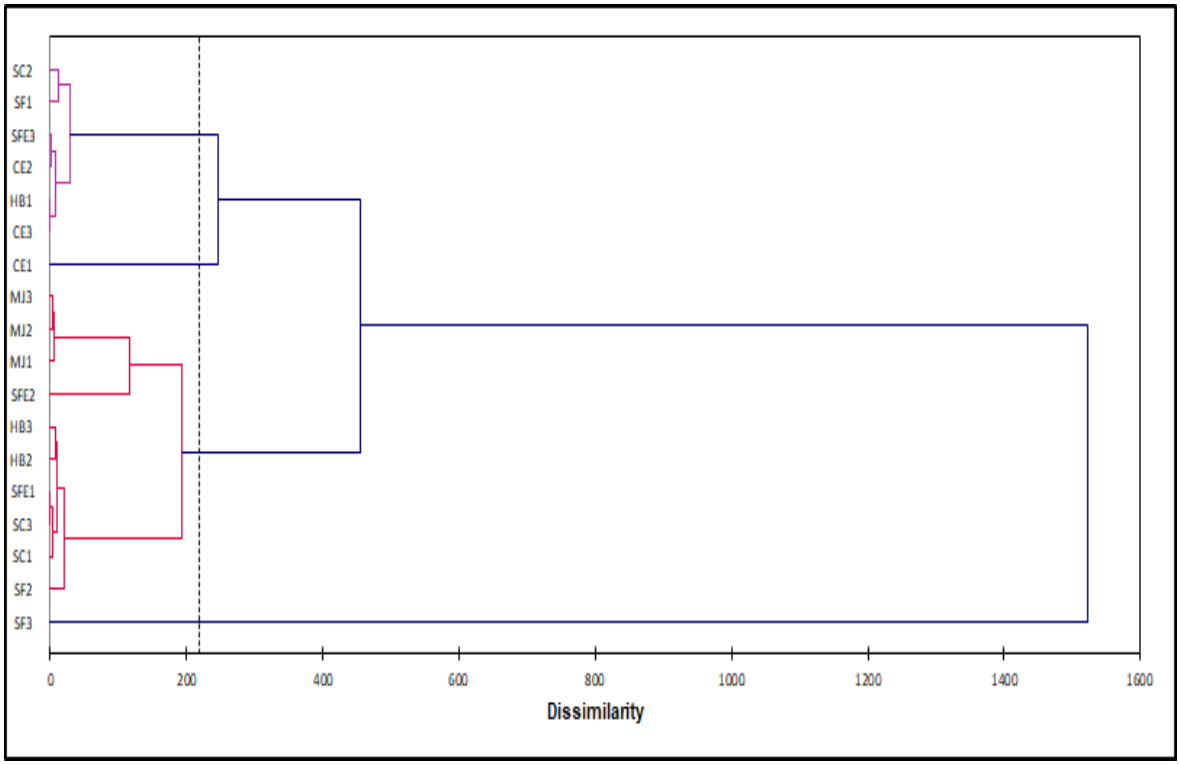

FIGURE 5.18: Hierarchical clustering of 2^{nd} order derivative transformation data of pure cultured nematodes. The nematodes are described on the y-axis as CE = *C. elegans*, SF = *S. feltiae* SB 12(1), SFE = *S. feltiae* e-nema, SC = *S. carpocapsae*, HB = *H. bacteriophora* and MJ = *M. javanica*. The nematodes are numbered according to the replications 1-3. The x-axis describes the dissimilarity distance.

5.4 Discussion

Nematodes are diverse complex multicellular organisms that have very different life strategies ranging from free-living to entomopathogenic, to phytoparasitic. Nematodes, specifically PPN, are responsible for up to 21% loss of crop yield worldwide with an estimated crop loss of $121 billion globally (Degenkolb and Vilcinskas, 2016). Due to this, it is necessary for a rapid and reliable nematode identification system to be a key factor in the decision making for PPN management and the implementation of adequate control measures. In addition, a rapid indication of a nematode community would be beneficial to give a quick diagnosis of soil contamination and environmental stress. Nematodes, however, are still one of the most difficult organisms to be identified, due to their indistinguishable features and microscopic size (Carneiro *et al.*, 2017). Classical nematode identification techniques are time-consuming and require a high level of expertise and training. Currently, new molecular methods and techniques are being investigated and employed, but are still highly reliant on morphological analysis for more accurate results.

The FT-IR absorbance spectra for pure cultured nematodes and for nematodes exposed to soil were initially assessed in the 650- 3500 cm^{-1} region, to give a visual representation of the full spectrum and an indication of any specific differences and similarities between the nematode species. It was found that the spectra displayed intense absorbance bands in the mid-IR region for all nematode species investigated. In the pure cultured nematodes, the band at 991 cm^{-1} in *S. carpocapsae* was assigned to a stretching vibration band of the -1,1 linkage, this band was also found in San-Blas *et al.* (2011) at 992 cm^{-1}. This is characteristic of trehalose, an important disaccharide of glucose. Its function regarding nematodes is for protection against environmental stresses such as heat, cold and desiccation San-Blas *et al.* (2011). The bands between 1400-1406 cm^{-1} were unique to *S. feltiae*, in both pure cultures and extracted from the soil for both the wild and commercial nematodes. The band at 2853 cm^{-1} was assigned to the symmetric stretching of the CH_2 bonds and was found only in *S. carpocapsae*. The nematode *M. javanica* had a unique band found at 2925 cm^{-1}. This band is important as it is associated with recognising the compound as an organic compound, that contains an aliphatic group, and in this case, it is associated with lipids. The band at 2975 cm^{-1} is associated with O-H symmetric stretching and was only found in *S. feltiae*. The band at 3301 cm^{-1} associated with N- H stretching only occurred in *H. bacteriophora*. The band at 3277 cm^{-1} region, was unique to *G. pallida* , Coates (2000) suggests that this band region, which is associated with hydroxyl absorption, is one of the most important bands in the infrared spectrum. However, other vibrations are important to characterise the compound.

The three EPN species also shared some bands with the PPN *G. pallida*, such as the bands between 2852 and 2855 cm^{-1} which are associated with the aliphatic functional group methylene, along with the bands 1739 and 1745 cm^{-1} which is associated with the carbonyl functional groups aldehyde and ester Coates (2000). The FLBFN assessed, had prominent bands at 1650 and 1652 cm^{-1} which belong to the olefinic group. However, they were lacking bands at the 1420-1455 region which may be associated with inorganic carbonate ion, these bands were present in the EPN and PPN groups. The bands between 1357 and 1370 cm^{-1} were found in the FLBFN and the PPN, yet, they were absent in the EPN group. Nitrogenous compounds contributed to the absorption of the band in this region for the FLBFN and PPN and may represent nematode waste products (including ammonia) secreted through the excretory pores and through the cuticle (San-Blas *et al.*, 2011). Interestingly, the EPN *S. carpocapsae* and *H. bacteriophora* had bands present at 1077 and 1078 cm^{-1} which were completely absent in all other nematode species investigated. These bands are associated with numerous functional groups including the aliphatic organohalogen compound group (aliphatic fluoro compounds), the ether and oxy compound groups and the amine and amino group. The bands in the range of 1200–900 cm^{-1} were found in all categories of nematodes and are associated with many bands assigned to lipids and carbohydrates.

San-Blas *et al.* (2011), observed in their study with the EPN species *S. glaseri* and *H.indica* that the most important variations occurred at band 1745 cm^{-1}, which is characteristic of triglycerides, when compared to *C. elegans*. Similarly to this investigation, a distinct band was also visualised at 1739cm^{-1} in *S. carpocapsae*, and 1745cm^{-1} in *H. bacteriophora*, which confirms their observations. However, there was a band present at 1742cm^{-1} for *G. pallida* in this investigation, which suggests that it is not a unique fingerprint region to EPN. It was observed in the present study that the bands in the 1300-800 region were notably distinct across all nematode species investigated, this was also noted in San-Blas *et. al.* (2011), who suggested this as the fingerprint region for all organisms.

The spectral profile of the nematodes that were exposed to soil, indicated that the groups, FLBF, EPN and PPN had some similarities, but also marked differences among them. The spectra output, visually, for these nematodes differed greatly compared to the pure cultured nematodes, particularity in the 1850-3150 cm^{-1} region, with major differences in bands between 900-1650 for all nematodes. This band range was higher than the pure cultured nematodes. *Heterohabditis bacteriophora* had unique bands at 3301 cm^{-1} that is associated with the hydroxy compound group, 1634 cm^{-1} that is associated with the olefinic group and 1549 cm^{-1} that is associated with the amine compound group. *Steinernema feltiae* SB 12(1) and e-nema had a unique band at 2975 cm^{-1}, which is associated with the aliphatic group and *S. carpocapsae* had a unique band at 2853 cm^{-1}, which is associated with the saturated aliphatic methylene group. *Meloidogyne javanica* had distinctive sharp peaks in the 1631-1245 cm^{-1} region associated with the amine compound group, the carbonyl compound group, the nitrogen compound group and the simple hetero-oxy compounds (Coates, 2000).

The EPN *S. feltiae* SB 12(1), *S. feltiae* e-nema, and *S. carpocapsae* had common bands at 1653 and 1586 cm^{-1} which are associated with the olefinic groups and aromatic ring groups, along with 1405 and 1390 cm^{-1} which belong to the saturated aliphatic and carbonyl compound groups. *Steinernema feltiae* SB 12(1), *S. feltiae* e-nema, *S. carpocapsae* and *H. bacteriophora* all had strong bands at 1024, 1023, 1024 and 1026 cm^{-1} respectively with *S. feltiae* e-nema having a stronger signal than the other three species. There was a prominent peak common to all three pure cultured EPN, *S. feltiae* e-nema at 944 cm^{-1} region, *S. carpocapsae* at 944 cm^{-1} and *H. bacteriophora* at 954 cm^{-1}.

The comparison between the spectra of the nematodes directly assessed from pure cultures and the nematodes exposed to soil vary considerably. *Steinernema carpocapsae* and *H. bacteriophora* had common bands in the pure cultured nematodes but were absent from the spectra in the soil nematodes. *Steinernema feltiae* e-nema had similar bands present in both the pure cultured and soil spectra. The spectra for pure cultured *M. javanica* and those exposed to soil differed from all the other nematode spectra. The absorbance spectra were very distorted and not very smooth in comparison to the other absorbance spectra. This may be due to *M. javanica* being the only nematode investigated in this study that was cultured directly in the soil. It is very difficult to remove all soil particles from the nematodes and they may have caused some interference when reading the absorbance on FT-IR. Although unique and identifiable features are visible between the pure cultured nematodes and the nematodes from soil pots, the peaks are more subtle and therefore one would be reluctant to give a confident identification of the nematode species.

In order to increase the discriminating features of the spectra results for the nematodes, the 2^{nd} order derivative was assessed. The benefits of such approach are (1) absorption bands can be identified even if two peaks overlap and (2) it helps the identification of weaker absorption bands, even if obscured by a sharper absorbance peak. The 2^{nd} order derivative exposed a prominent peak common to all pure cultured EPN, this was similar to the EPN exposed to soil, where they all had strong bands in the 1023-1026 cm^{-1} region. Both *S. feltiae*, SB 12(1) and e-nema, had a broad-shouldered peak in the same region. There were also marked differences between the pure cultured nematodes and the soil nematodes 2^{nd} order derivative spectra.

The results in this study, compared to those in San-Blas *et al.* (2011), varied considerably. The spectra in this study were lacking many peaks, particularly in the 2^{nd} order derivative transformed data and this is due to different specifications of the FT-IR instruments used. In their study, their FT-IR instrument had an absorption spectra range of 3700- 550 cm^{-1} compared to 3700- 650 in this study, with accurate results up to 900 cm^{-1}. For the 2^{nd} order derivative transformed data, which looked at the wavenumber range of 1300-900, there was more scope with their instrument, as the accuracy of the instrument utilised in this study begins to diminish after 900 cm^{-1}. The detector on their instrument was also a much higher

specification compared to the instrument used in this study. They had a DLATGS detector coupled to a 6mm three-reflection diamond/ ZnSe crystal ATR plate MIRacle ^{TM} with a high-pressure clamp (2000 psi). In comparison in this study, an ATR Universal detector was utilised with a ZnSe crystal and a clamp with 150 psi. These differences reflect the resolution of the graphs, which is notable in the figures presented in this chapter. It is also difficult to directly compare the results when there is so much variation in the specifications of the instruments. Nonetheless, there are some similarities visible when comparing spectra results in this study to that of San-Blas *et al.* (ibid.). principal component analysis was utilised to identify any patterns or relationships (similarities or differences) in the spectral data. The results suggest that a combination of variables are evident that can distinguish between the nematode categories, FLBFN, EPN and PPN, but also between nematodes directly assessed from cultures and nematodes exposed to soil. The principal component loadings for all nematodes from pure cultures, along with all nematodes exposed to soil describe the effect of the original variables on the principal components and can be used as a basis for data interpretation. However, there are large differences between the nematodes extracted from the soil and pure cultured nematodes, in terms of clustering. The PCA results for the nematodes from pure cultures, explained 62% of the variance for all the pure cultured nematodes, 97% variance in the pure cultured free-living bacterial-feeding nematodes, 96% variance in the pure cultured EPN and 98% variance on the pure cultured PPN. The most important clusters structure of the data were represented on bi-plots, with very different and cohesive clusters of cases which were completely separated from each other on the plots. Specifically *G. pallida*, *M. javanica*, *C. elegans* and *S. feltiae* e- nema had no overlapping or sharing of clusters. These results were further confirmed with hierarchical cluster analysis. Each nematode group was clustered according to the species, again with no overlapping or sharing. The groups that are notable in the pure cultured analysis is the PPN *G. pallida*, as it showed a stand-alone cluster and only shares clusters with the other species at 4500 dissimilarity. In nematodes exposed to soil, PCA analysis explained 88% variance for all nematodes and 90% variance for the EPN. The results represented on bi-plots for the nematode data exposed to soil are very different to those recorded in the pure cultured nematodes, with the cluster of cases not being very closely related or cohesive. There is a lot of overlapping and sharing of components. This result is confirmed by hierarchical cluster analysis, where two defined clusters are present that represent all the nematodes tested. There is a sharing of clusters with different species and replications with no consistency. The PPN *M. javanica* is the only species group that does not share or overlap with another species for all replications in both the bi-plot and the AHC analysis.

Similarly to San-Blas *et al.* (2011), who suggest that the technique FTIR along with the multivariate data analysis has the potential to become a successful method for studying EPN, this too has been suggested by this study for the pure cultured nematodes, particularity the EPN and FLBFN. This technique worked more efficiently for lab-reared nematodes. It is

also suggested in the present study, that there is potential for assigning multiple bands in the EPN spectra to be used for rapid identification and classification, along with industrial production potential. This may be true for lab cultured nematodes, utilised for commercial applications.

This study revealed that nematodes that were exposed to soil, extracted and read on FT-IR did not give clear spectra readings. One of the issues associated with this procedure was the difficulty in getting the nematodes completely free of soil particles. The presence of soil may have interfered with the FT-IR spectra reading. However, if this technique is to be utilised as a means of identifying nematodes from an environmental soil sample, there must be more research invested in developing a more efficient and effective sample preparation step. It is notable that the PPN *M. javanica* and *G. pallida*, both lab cultured and in the case of *M. javanica* exposed to soil, did show some potential that this technique was working, throughout this study from absorbance spectra, to 2^{nd} order derivative transformed data, to PCA and AHC. *Meloidogyne javanica* were the only nematodes to be clustered in a group on their own through all analysis types used in this study. This is interesting for *M. javanica*, as it was the only nematode utilised in this study, that was also cultured in the soil.

Key results obtained from the various work tasks in Chapter 5:

- The bands between 1400-1406 cm^{-1} were unique to *S. feltiae*, in both pure cultures and extracted from the soil for both the wild and commercial nematodes.
- *Steinernema carpocapsae* and *H. bacteriophora* had bands present at 1077 and 1078 cm^{-1} which were completely absent in all other nematode species investigated.
- *Meloidogyne javanica* had a unique band found at 2925 cm^{-1}
- *Meloidogyne javanica* is the only species group that did not share or overlap with any another species in both the bi-plot and the AHC analysis.

The objective of this study was to assess the use of FT-IR as a tool to distinguish nematodes, with a further view towards analysing nematode assemblages as bioindicators and in other environmental and agricultural studies. The aim of Chapter 5, to assess the suitability of FT-IR as a tool for identifying different nematode genera with different survival strategies, was met. Current literature was explored and compared to the findings in the present study. The absorption spectra and the 2^{nd} order derivative transformed data of the nematodes investigated were assessed and some fingerprint regions were identified. Multivariate statistical analysis was also successful in identifying *M. javanica* as a suitable indicator species for this type of analysis. There is potential for success in utilising this technique as a rapid means of

nematode identification, but, the suitability of this technique for this purpose must be further researched.

Chapter 6

General Discussion and Future Prospects

6.1 General Discussion

Growing bioenergy crops for the production of biofuels is associated with one of the UN sustainable agricultural goals (Brodt *et al.*, 2011), relating to energy efficiency and conservation. Food demands are predicted to increase by 98% in some parts of the world by 2050 (Elferink and Schierhorn, 2016) and currently, there is a global shortage of land for food production. In addition, there are up to 2.5 million contaminated sites reported across Europe (EEA, 2018). This has led to an increase in research on the use of bioenergy plants for phytoremediation of these contaminated sites. Beneficial bacteria, like *P. fluorescens*, colonising on or within plants, either native or introduced have demonstrated increased plant growth and enhance plant defence. The combination of phytoremediating bioenergy crops and PGP bacteria have the potential to revolutionise the decontamination of brown field sites and increase the viability of land agricultural processes. Another branch of the UN sustainable agricultural goals focuses on biologically integrated farming systems including IPM. Considering that up to 20% of food crops are lost to phytoparasitic nematodes annually (Dauck, 2018), there are requirements for the advancement of efficient sustainable biocontrol products, that are both beneficial to plants, and have a predominantly negative effect on PPN. Beneficial bacteria, like *P. fluorescens* have considerable potential for the development of a high-impact, bio-based nematicidal product, capable of biocontrol, as a viable means of implementing sustainable agriculture.

This study set out to exploit and further investigate the capacity of beneficial *P. fluorescens* strains, specifically (1) their efficiency at OSR and tomato PGP, (2) their capability for PPN biocontrol and (3) their Ni OSR bioremediation potential. The suitability of nematodes and their assemblages as biosensors and bioindicators of Ni bioremediation were also assessed

in this research. The PGP bacterial metabolites were identified by GC-MS analysis to consolidate the results of the *in vitro* and *in planta* experiments. In addition, a novel method for nematode characterisation was evaluated, by utilising FT-IR microspectroscopy.

This study is the first of its kind to combine various aspects of beneficial bacteria to investigate their potential for PPN biocontrol, to enhance plant growth, and to bioremediate Ni while evaluating this with nematodes as bioindicators of the process.

The main findings of this research are:

1. *Pseudomonas fluorescens* strain L321 was:
    - an effective coloniser of OSR plants, measured by bacterial viability tests.
    - associated with increased OSR plant growth as estimated by plant biomass.
    - capable of Ni biosorption, determined analytically by AAS.
    - most efficient strain at PPN biocontrol as assessed by *in vitro* nematode susceptibility and *in planta* nematode development and ISR experiments.
    - associated with delayed *M. javanica* infection in tomato plants.
    - producing secondary metabolites investigated by GC-MS analysis, associated with antimicrobial, anti fungal and anti viral properties, biocontrol, stress tolerance, and PGP.
2. *Pseudomonas fluorescens* strain L124 was:
    - capable of increasing tomato plant growth, as assessed by plant biomass.
    - producing compounds investigated by GC-MS analysis, related to the biocontrol of root pathogens, including nematicidal, antimicrobial and anti-fungal properties.
3. Nematode assemblages, through a morphological assessment, are informative bioindicators of Ni contaminated soil condition and the soil food-web structure.
4. There is potential for the use of FT-IR as a novel technique for nematode characterisation, in particular PPN.

Previous members of enviroCORE have extensively researched the characteristics of these bacterial strains, from IT Carlow stocks. Many strains were discovered to be associated with IAA and siderophore production, phosphate solubilisation and nitrogen fixation (Menton, 2010; Otieno *et al.*, 2015), all of which, are related to increased plant growth. The PGP properties of the *P. fluorescens* strains were explored in Chapter 3, in tomato and Chapter 4, in OSR plants, to identify their ability to increase plant biomass. Although two different

bacterial application methods were utilised, a drench for tomato and an alginate bead for OSR, two bacterial strains were identified as successful growth promoters. *Pseudomonas fluorescens* L321 proved to be an excellent OSR coloniser, remaining viable six months after inoculation. Not only is this strain efficient at colonising OSR in plant microcosms, but Lally *et al.* (2017) also reported it to be successful at colonising OSR in field trials. This strain also had the capacity to increase OSR root and phyllosphere biomass in the presence of Ni contaminated soil. The rhizosphere or internal colonisation capabilities by the *P. fluorescens* strains in tomato plants were not examined in the present study. However, Gamalero *et al.* (2004) report that *P. fluorescens* is a well-known coloniser of tomato plants. Elevated plant growth was also recorded in tomato plants investigated in Chapter 3, particularly in the phyllosphere, when treated with the PGP bacterial strain L124. This was observed in both the development and the ISR experiments, after 30 and 70 days from *M. javanica* infection. Almaghrabi *et al.* (2013) too, observed increased tomato plant growth when inoculated with this bacterial species.

The biocontrol capacity of the PGP bacterial strains from the IT Carlow stocks was also previously assessed by past members of enviroCORE (Hurley, 2018; Menton, 2010; Otieno *et al.*, 2013). Yet, the PPN biocontrol capacity of these *P. fluorescens* strains have not previously been explored. As biocontrol agents, all the PGP bacterial strains tested were particularly effective at disrupting the early phase (penetration and J2 infective juvenile stage) of *M. javanica* life cycle (Chapter 3). A collective examination of results recorded in the susceptibility assays (Chapter 2), development experiments and in ISR tests (Chapter 3) indicate that the bacterial strain L321 was the most successful isolate for *M. javanica* biocontrol. Furthermore, GC-MS analysis presented in Chapter 2, indicates that a potential mode of action is the production of antimicrobial compounds associated with biocontrol and increased stress tolerance.

Although the aim of Chapter 4 was to assess the capacity of OSR inoculated with PGP bacterial strains to bioremediate Ni, the results suggested that this process did not occur. The presence of Ni was examined in the rhizosphere and in the OSR plants with AAS analysis. Considering that the Ni concentration in the rhizosphere treated with strain L321 was reduced by 41% and that this uptake was not accounted for within the OSR plants, this finding indicates that the Ni was not phytoremediated by the plants. It is possible nonetheless, that the strain L321 was involved with some form of remediation, such as Ni biosorption, which is an important biological process associated with the removal of organic or inorganic compounds by microorganisms (Fomina and Gadd, 2014). The Ni biosorption capacity of *Pseudomonas* spp is well supported by López *et al.* (2000), Naz *et al.* (2016), and Zhang *et al.* (2016), however, further research is needed on this process regarding strain L321. It was not possible, therefore, to utilise nematode assemblages as bioindicators of Ni bioremediation, nematodes did indicate differences between the untreated and the treated soil,

through morphological analysis by assigning the c-p scale and trophic groups, and by determining nematode abundance. Other indices assigned via both morphological and molecular assessments, such as the diversity, maturity and ecological indices, suggest that there are similarities between treatments assigned to the treated soil and that there are differences between the untreated and treated soils, which consolidated the results.

The application of FT-IR microspectroscopy has been suggested by San-Blas *et al.* (2011) as a novel alternative to classical morphological nematode identification techniques (Chapter 4). This is due to its capacity to produce an informative organism spectrum in seconds. San-Blas *et al*. (2011) successfully utilised this technique to determine spectral differences among species of EPN. To build on this work, and advance this technique to the next stage, three categories of nematodes were investigated in the present study: PPN, FLBFN and EPN, with nematodes from both lab cultures and those exposed to soil (Chapter 5). The results suggested that this type of analysis has great potential for nematode characterisation, particularly for the PPN *M. javanica*. This nematode showed the most consistent results throughout all the spectra readings and associated statistical analysis, in the absorbance spectra, the 2^{nd} order derivative transformed data, the PCA and in the AHC analysis. However, to continue building upon these positive results, further research must be invested in developing a more efficient and effective sample preparation step, to sufficiently remove soil from the nematode cuticle.

The work in this thesis contributed to two of the three UN sustainable agriculture goals (Brodt *et al.*, 2011) by, firstly exploring the capacity of PGP bacteria colonising OSR to bioremediate Ni. This adds to the knowledge base in relation to OSR for phytoremediation of brown field sites, which further contributes to the area of energy efficiency and conservation. Secondly, by assessing the potential biocontrol abilities of *P. fluorescens* isolates against phytoparasitic nematodes. This also justifies further research regarding their use for IPM and contributes to the area of biological farming systems. Despite the numerous known benefits associated with beneficial bacteria - plant relationships, including PGP, reduced plant stress, increased plant health and infection prevention, these beneficial bacteria currently are not widely utilised in agriculture. Therefore, growers continue to be heavily reliant on the application of commercial chemical treatments (Le Cocq *et al.*, 2017). Other than their associations with plants, these beneficial bacteria are also favourable to soil health by increasing the availability of nutrients to plants, and by soil decontamination in a phytoremediation capacity (Vassilev *et al.*, 2004). The present work is imperative for a better understanding of PGP bacterial associations, both with plants and with problematic nematodes, to develop robust, reliable and sustainable alternatives to agrochemicals and encourage the use of bio-based solutions.

Not only has this project significantly contributed to the knowledge of sustainable agricultural practices but, it has also identified two key *P. fluorescens* stains (L124 and L321) that

can be used as sustainable, innovative, low-cost and effective alternatives to chemical applications for PGP, PPN biocontrol and Ni biosorption.

6.2 Future Prospects

- GC-MS analysis to identify *Pseudomonas* spp. metabolites is a relatively new approach in enhancing knowledge in this area, that requires further development and improvement. The qualitative analysis carried out in this study gave a good representation of the types of compounds produced by the bacterial strains. However, a quantitative analysis would enhance the results, therefore a series of standard compounds would be required. The software package metaMS has great potential as an untargeted method to analyse GC-MS compounds, to accelerate the analysis and assess entire spectra, without missing important component peaks. The sequenced genomes of *P. fluorescens* L111, L228, and L321 by previous researchers in enviroCORE could be investigated for regions associated with biocontrol or PGP, to consolidate findings in this work.
- There are more than 460 isolated bacterial strains in the IT Carlow collection, and many are yet to be characterised. Therefore, there is a large scope for further assessments, both *in vitro* and *in planta*, to test these strains in the areas of phytoparasitic biocontrol and bioremediation.
- The use of PGP bacterial strains for bioremediation in this work was limited to a greenhouse based experiment, in heavy metal spiked environmental soil. There are several areas for future development of this type of research. Further greenhouse experiments could be conducted with environmentally contaminated soil that would contain the native nematode populations from that site. As different bioenergy crops are effective at phytoremediating various sources of contamination, there is scope for further research on different plant genera in this capacity. Exploration of the *P. fluorescens* strains L321 and L124 colonisation potential, in different bioenergy crop types, to assess their capacity for bioremediation utilising the methods in this work, should also be considered. The next stage of this research would be to establish field trials in a contaminated site, as this would provide a natural representation of the nematode assemblages and would give insight into the PGP bacteria- plant dynamics, in a competitive environment.
- FT-IR microspectroscopy has good potential as a tool for rapid nematode identification for various types of environmental assessment to increase the popularity of utilising nematodes as environmental indicators and to accelerate the manual nematode identification process. The development of a comprehensive database, inclusive of all spectra from many nematode species of all feeding types, from lab cultures and those extracted from various soil types and sediments, and environmental conditions, would be an excellent basis for quick comparison and identification.

Bibliography

Abad, P., Favery, B., Rosso, M.N., and Castagnone-Sereno, P. (2004). Rootknot nematode parasitism and host response: molecular basis of a sophisticated interaction. *Molecular Plant Pathology* 4 (4):217–224.

Ali, R and Siddiqui, N. (2013). Biological Aspects of Emerging Benzothiazoles: A Short Review. *Journal of Chemistry*:1–12.

Almaghrabi, O.A., Massoud, S.I., and Abdelmoneim, T.S. (2013). Influence of inoculation with plant growth promoting rhizobacteria (PGPR) on tomato plant growth and nematode reproduction under greenhouse conditions. *Saudi Journal of Biological Sciences* 20 (1):57–61.

Ami, D., Mereghetti, P., and Doglia, S.M. (2013). Multivariate Analysis for Fourier Transform Infrared Spectra of Complex Biological Systems and Processes. *Multivariate Analysis in Management, Engineering and the Sciences*. Ed. by L. V. de Freitas and A. P. de Freitas. Rijeka: IntechOpen. Chap. 10.

Ami, D., Natalelloa, A., Zullinia, A., and Dogliaa, S.M. (2004). Fourier transform infrared microspectroscopy as a new tool for nematode studies. *FEBS Letters* 576:297–300.

Anantha Padmanabhan, S., Deventhiran, M., Saravanan, P., Anand, D., and Rajarajan, S. (2016). A comparative GC-MS analysis of bacterial secondary metabolites of Pseudomonas species. *The Parma Innovation Journal* 5 (4):84–890.

Anbalagan, C., Lafayette, I., Antoniou-Kourounioti, M., Gutierrez, C., Martin, J.R., Chowdhuri, D.K., and De Pomerai, D.I. (2013). Use of transgenic GFP reporter strains of the nematode *Caenorhabditis elegans* to investigate the patterns of stress responses induced by pesticides and by organic extracts from agricultural soils. *Ecotoxicology* 22 (1):72–85.

Anbalagan, C., Lafayette, I., Antoniou-Kourounioti, M., Haque, M., King, J., Johnsen, B., Baillie, D., Gutierrez, C., Martin, J.A.R., and Pomerai, D. de (2012). Transgenic nematodes as biosensors for metal stress in soil pore water samples. *Ecotoxicology* 21 (2):439–455.

Andersson-Sköld, Y., Hagelqvist, A., Crutu, G., and Blom, S. (2014). Bioenergy grown on contaminated land- a sustainable bioenergy contributor? *Biofuels* 5 (5):487–498.

Angus, J.F., Kirkegaard, J.A., Hunt, J.R., Ryan, M.H., Ohlander, L., and Peoples, M.B. (2015). Break crops and rotations for wheat. *Crop and Pasture Science* 66 (6):523–552.

Aravind, R., Eapen, S.J., Kumar, A., Dinu, A., and Ramana, K.V. (2010). Screening of endophytic bacteria and evaluation of selected isolates for suppression of burrowing nematode (*Radopholus similis* Thorne) using three varieties of black pepper (*Piper nigrum* L.) *Crop Prot* 29:318–324.

Baker, M.J., Mc Grath, S.P., Reeves, R.D., and Smith, J.A. (2000). *Metal hyperaccumulator plants: A review of the ecology and physiology of a biological resource for phytoremediation of metal-polluted soils*. Ed. by N. Terry and G. Banuelos. Lewis Publishers. Chap. 5, pp. 85–107.

Baker, M.J. *et al.* (2014). Using Fourier transform IR spectroscopy to analyze biological materials. *Nature Protocols* 9 (8):1771–1791.

Barahona, E., Navazo, A., Martínez-Granero, F., Zea-Bonilla, T., Pérez-Jiménez, R.M., Martín, M., and Rivilla, R. (2011). *Pseudomonas fluorescens* F113 mutant with enhanced competitive colonization ability and improved biocontrol activity against fungal root pathogens. *Applied Environmental Microbiology* 77 (15):5412–5419.

Barriére, A. and Félix, M.A. (2006). Isolation of *C. elegans* and related nematodes. *WormBook*:1–9.

Barthés, B.G., Brunet, D., Rabary, B., Ba, O., and Villenave, C. (2011). Near infrared reflectance spectroscopy (NIRS) could be used for characterization of soil nematode community. *Soil Biology and Biochemistry* 43 (8):1649–1659.

Belimov, A.A., Safronova, V.I., and Mimura, T. (2002). Response of spring rape (*Brassica napus* var. oleifera L.) to inoculation with plant growth promoting rhizobacteria containing 1-aminocyclopropane-1-carboxylate deaminase depends on nutrient status of the plant. *Canadian Journal of Microbiology* 48 (2):189–199.

Berkelmans, R., Ferris, H., Tenuta, M., and Bruggen, A.H.C. van (2003). Effects of long-term crop management on nematode trophic levels other than plant feeders disappear after 1 year of disruptive soil management. *Applied Soil Ecology* 23:223–235.

Bezooijen, J. (2006). *Methods and techniques for nematology*.

Bhadury, P., Austen, M.C., Bilton, D.T., Lambshead, P.J., Rogers, A.D., and Smerdon, G.R. (2006). Molecular detection of marine nematodes from environmental samples: overcoming eukaryotic interference. *AQUATIC MICROBIAL ECOLOGY* 44:97–103.

Bianchelli, S., Gambi, C., Mea, M., Pusceddu, A., and Danovare, R. (2013). Nematode diversity patterns at different spatial scales in bathyal sediments of the Mediterranean Sea. *Biogeosciences* 10.

Bio-Rad (1996). *The DCode^{TM} Universal Mutation Detection System*. English. Bio-Rad Laboratories. 85 pp.

Bohlmann, H. (2015). Introductory Chapter on the Basic Biology of Cyst Nematodes. *Plant Nematode Interactions - A View on Compatible Interrelationships*. Vol. 73. Advances in Botanical Research. Chap. 2, p. 33–59.

Bommarius, B., Anyanful, A., Izrayelit, Y., Bhatt, S., Cartwright, E., Wang, W., Swimm, A. I., Benian, G., Schroeder, F.C., and Kalman, D. (2013). A family of indoles regulate virulence and shiga toxin production in pathogenic *E. coli*. *PLoS ONE* 8 (1):1–16.

Bongers, T. (1990). The Maturity Index: an ecological measure of environmental disturbance based on nematode species composition. *Oecologia* 83:14–19.

– (1994). *De Nematoden Van Nederland*. Utgeverij Pirola Schoorl.

– (1999). The Maturity Index, the evolution of nematode life history traits, adaptive radiation and cp-scaling. *Plant and Soil* 212:13–22.

Bongers, T., Alkemade, R., and Yeates, G.W. (1991). Interpretation of Disturbance-Induced Maturity Decrease in Marine Nematode Assemblages by Means of the Maturity Index. *Marine Ecology Progress Series* 76 (2):135–142. ISSN: 0171-8630.

Bongers, T. and Bongers, M. (1998). Functional diversity of nematodes. *Applied Soil Ecology* 10:239–251.

Bongers, T. and Ferris, H. (1999). Nematode Community Structure as a Bioindicator in Environmental Monitoring. *Tree* 14:224–228.

Boyle, S.G. (2007). An investigation on the intraspecific genetic variation and genetic structure of Irish and exotic *Steinernema feltiae* (Nematoda: Steinernematidae). Thesis.

Brader, G., Compant, S., Mitter, B., Trognitz, F., and Sessitsch, A. (2014). Metabolic potential of endophytic bacteria. *Current Opinion in Biotechnology* 27 (100):30–37.

Brenner, S. (1974). The genetics of *Caenorhabditis elegans*. *Genetics* 77 (1):71–94.

Brodt, S., Six, J., Feenstra, G., Ingels, C., and Campbell, D. (2011). Sustainable Agriculture. *Nature Education Knowledge* 3 (10):1.

Brucker, R.M., Baylor, C.M., Walters, R.L., Lauer, A., Harris, R.N., and Minbiole, K.P. (2008). The identification of 2,4-diacetylphloroglucinol as an antifungal metabolite produced by cutaneous bacteria of the salamander *Plethodon cinereus*. *J Chem Ecol* 34 (1):39–43.

Burgess, A., Vigneron, S., Brioudes, E., Labbé, J.C., Lorca, T., and Castro, A. (2010). Loss of human Greatwall results in G2 arrest and multiple mitotic defects due to deregulation of the cyclin B-Cdc2/PP2A balance. *Proc Natl Acad Sci USA* 107:12564–12569.

Büyükcama, A., Tuncerb, Ö., Gürb, D., Sancakb, B., Ceyhana, M., Cengiza, A.B., and Karaa, A. (2018). An improved technique for clearing and staining plant tissue for detection of nematodes. *Journal of Nematology* 14:142–143.

Byrd, D.W., Kirkpatrick, J.T., and Barker, K.R. (1983). An improved technique for clearing and staining plant tissue for detection of nematodes. *Journal of Nematology* 14:142–143.

Byrne, J.T., Maher, N.J., and Jones, P.W. (2001). Comparative Responses of *Globodera rostochiensis* and *G. pallida* to Hatching Chemicals. *Journal of Nematology* 33 (4):195–202.

Carneiro, R.M. ., Oliveira Lima, F.S. de, and Correia, V.R. (2017). *Methods and Tools Currently Used for the Identification of Plant Parasitic Nematodes*. Ed. by M. M. Shah. InTech. Chap. 2, pp. 19–35.

Cattell, R.B. (1966). The scree test for the number of factors. *Multivariate Behavioural Research* 1:245–276.

Chandra, N. and Kumar, S. (2017). Antibiotics Producing Soil Microorganisms. *Antibiotics and Antibiotics Resistance Genes in Soils: Monitoring, Toxicity, Risk Assessment and Management*. Ed. by M. Z. Hashmi, V. Strezov, and A. Varma. Springer International Publishing, p. 1–18.

Chen, P. and Tsay, T. (2006). Effect of Crop Rotation on *Meloidogyne* spp. and *Pratylenchus* spp. Populations in Strawberry Fields in Taiwan. *Journal of Nematology* 38 (3):339–344.

Chen, Z., Chen, S., and Dickson, D. (2004). *Nematology: Advances and Perspectives*. Vol. Nematode Morphology, Physiology and Ecology. CABI Publishing.

Cheng, S.F., Huang, C.Y., Chen, K.L., Lin, S.C., and Lin, Y.C. (2015). Exploring the benefits of growing bioenergy crops to activate lead-contaminated agricultural land: a case study on sweet potatoes. *Environmental Monitoring and Assessment* 187 (3):144.

Chhabra, S. (2012). Soil metagenome analysis and bacterial ecology of a low-input tillage agroecosystem. PhD thesis. Institute of Technology Carlow, Ireland.

Choudhary, D.K., Prakash, A., and Johri, B.N. (2007). Induced systemic resistance (ISR) in plants: mechanism of action. *Indian Journal of Microbiology* 47:289–297.

Clark, J.M. and Kenna, M.P. (2010). Lawn and Turf: Management and Environmental Issues of Turfgrass Pesticides. *Hayes' Handbook of Pesticide Toxicology 3rd Edition*. Academic Press. Chap. 47, p. 1047–1076.

Coates, J. (2000). *Interpretation of Infrared Spectra, A Practical Approach*. Vol. Encyclopedia of Analytical Chemistry. Encyclopedia of Analytical Chemistry. Chichester: John Wiley and Sons Ltd.

Couillerot, O., Combes-Meynet, E., Pothier, J.F., Bellvert, B., Challita, E., Poirier, M., Rohr, R., Comte, G., Möenne-Loccoz, Y., and Prigent-Combaret, C. (2011). The role of the antimicrobial compound 2,4-diacetylphloroglucinol in the impact of biocontrol *Pseudomonas fluorescens* F113 on *Azospirillum brasilense* phytostimulators. *Microbiology* 157:1694–1705.

Coyne, D. (2009). Pre-empting plant-parasitic nematode losses on banana in Africa: which species do we target? *Acta Horticulturae* 828:227–236.

Cramer, P.B. (2012). Using transgenic *Caenorhabditis elegans* as a bioindicator; A useful tool for examining potential environmental hazards, or just a bunch of glowing worms? Thesis.

Crombie, T.A., Tang, L., Choe, K. P., and Julian, D. (2016). Inhibition of the oxidative stress response by heat stress in *Caenorhabditis elegans*. *Journal of Experimental Biology* 219:2201–2211.

Cronin, D., Möenne-Locco, Y., Fenton, A., Dunne, C., Dowling, D.N., and O' Gara, F. (1997a). Ecological interaction of a biocontrol *Pseudomonas fluorescens* strain producing 2,4-diacety- lphloroglucinol with the soft rot potato pathogen *Erwinia carotovora* subsp. atroseptica. *FEMS Microbiology Ecology* 23 (2):95–106.

Cronin, D., Möenne-Locco, Y., Fenton, A., Dunne, C., Dowling, D.N., and O'Gara, F. (1997b). Role of 2,4-Diacetylphloroglucinol in the Interactions of the Biocontrol Pseudomonad Strain F113 with the Potato Cyst Nematode *Globodera rostochiensis*. *Applied and Environmental Biology* 63 (4):1357–1361.

Crow, W.T. (2005). Diagnosis of *Trichodorus obtusus* and *Paratrichodorus minor* on turfgrasses in the Southeastern United States. *Plant Health Progress*.

Culhane, J. (2016). Investigation of plant growth promotion endophytic isolates as microbial inoculants for application in the bioremediation of oil contaminated soil. PhD thesis. Institute of Technology, Carlow, Ireland.

Dauck, H. (2018). Nematodes – A Hidden Threat. *Bayer Crop Science*.

David, B.V., Chandrasehar, G., and Selvam, P.N. (2018). *Pseudomonas fluorescens*: A plant-growth-promoting rhizobacterium (PGPR) with potential role in biocontrol of pests of crops. *Crop Improvement Through Microbial Biotechnology*. Ed. by R. Prasad, S. S. Gill, and N. Tuteja. Elsevier. Chap. 10, p. 221–243.

Dávila-Negrón, M. and Dickson, D.W. (2013). Comparative Thermal-Time Requirements for Development of *Meloidogyne arenaria*, *M. incognita*, and *M. javanica*, at Constant Temperatures. *Nematropica* 43 (2):152–163.

Davis, E.L. and MacGuidwin, A.E. (2000). Lesion nematode disease. *The Plant Health Instructor, American Phytopathological Society*.

Davis, E.L. and Tylka, G.L. (2000). Soybean cyst nematode disease. *The Plant Health Instructor, American Phytopathological Society*.

De Cárcer, D.A., Martín, M., Mackova, M., Macek, T., Karlson, U., and Rivilla, R. (2007). The introduction of genetically modified microorganisms designed for rhizoremediation induces changes on native bacteria in the rhizosphere but not in the surrounding soil. *ISME J* 1 (3):215–223.

De La Fuente, L., Landa, B.B., and Weller, D.M. (2006). Host crop affects rhizosphere colonization and competitiveness of 2,4-Diacetylphloroglucinol-producing *Pseudomonas fluorescens* Phytopathology. *Journal of Nematology* 96 (7):751–762.

De Pomerai, D.I., David, H.E., Power, R.S., Mutwakil, M.H., and Daniells, C. (2002). Transgenic Nematodes as Biosensors of Environmental Stress. *Biotechnology for the Environment: Strategy and Fundamentals. Focus on Biotechnology*. Ed. by S.N. Agathos and W. Reineke. Vol. 3A. Dordrecht: Springer, p. 221–236.

Decraemer, W. and Geraert, E. (2013). Ectoparasitic nematodes. *Plant Nematology, 2nd Edition*. Ed. by R. N. Perry and M. Moens. Wallingford, U.K: CABI. Chap. 6, p. 179–218.

Degenkolb, T. and Vilcinskas, A. (2016). Metabolites from nematophagous fungi and nematicidal natural products from fungi as an alternative for biological control. Part I: metabolites from nematophagous ascomycetes. *Appl Microbiol Biotechnol* 100:3799–3812.

Deiss, F., Funes-Huacca, M.E., Bal, J., Tjhung, K.F., and Derda, R. (2014). Antimicrobial susceptibility assays in paper-based portable culture devices. *Lab Chip* 14 (1):167–171.

Dieterich, C. *et al.* (2008). The *Pristionchus pacificus* genome provides a unique perspective on nematode lifestyle and parasitism. *Nature Genetics* 40:1193–1198.

Directive, EU (2007). Thematic strategy for pesticides. *Directive 91/414/EU*.

Dodds, W. K. and Whiles, M. R (2010). Multicellular Animals. *Freshwater Ecology (Second Edition)*. Ed. by W.K. Dodds and M.R. Whiles. Second Edition. Aquatic Ecology. London: Academic Press. Chap. 10, p. 221–257.

Donn, S., Neilson, R., Griffiths, B.S., and Daniell, T.J. (2012). A novel molecular approach for rapid assessment of soil nematode assemblages – variation, validation and potential applications. *Methods in Ecology and Evolution* 3:12–23.

Dunn, O.J. (1964). Multiple comparisons using rank sums. *Technometrics* 6:241–252.

Dutkiewicz, J., Mackiewicz, B., Kinga, L., Golec, M., and Milanowski, J. (2016). *Pantoea agglomerans*: a mysterious bacterium of evil and good. Part III. Deleterious effects: infections of humans, animals and plants. *Annals of Agricultural and Environmental Medicine* 23 (2):197–205.

Ebbs, S.D. and Kochian, L.V. (1997). Toxicity of zinc and copper to *Brassica* species: Implications for phytoremediation. *Journal of Environmental Quality* 26:776–781.

EEA (2018). Soil contamination widespread in Europe. Copenhagen, Denmark: European Environment Agency, p. 1–6.

Eisenback, J.D. and Triantaphyllou, H.H. (2009). Root-knot nematodes: *Meloidogyne* species and races. *Manual of Agricultural Nematology*. Ed. by W. R. Nickle. New York: Marcell Dekker, p. 191–274.

Elferink, M. and Schierhorn, F. (2016). *Global demand for food is rising. Can we meet it?* Tech. rep.

Elleuch, L., Shaaban, M., Smaoui, S., Mellouli, L., Karray-Rebai, I., F.L., Fourati-Ben, Shaaban, K.A., and Laatsch, H. (2010). Bioactive Secondary Metabolites from a New Terrestrial *Streptomyces* sp. TN262. *Applied Biochemistry and Biotechnology* 162 (2):579–593.

EPA (2017). National Soils Database. *Environmental Protection Agency*.

Escorcia, W., Ruter, D.L., Nhan, J., and Curran, S.P. (2018). Quantification of Lipid Abundance and Evaluation of Lipid Distribution in *Caenorhabditis elegans* by Nile Red and Oil Red O Staining. *Journal of Visualized Experiments* 133.

Fay, D., Kramers, G., Zhang, C., McGrath, D., and Grennan, E. (2007). Soil Geochemical Atlas of Ireland. Ed. by G. Kramers. Teagasc and the Environmental Protection Agency, p. 120.

Fenton, A.M., Stephens, P.M., Crowley, J., O'Callaghan, M., and O'Gara, F. (1992). Exploitation of gene(s) involved in 2,4-diacetylphloroglucinol biosynthesis to confer a new biocontrol capability to a Pseudomonas strain. *Applied and Environmental Microbiology* 58:3873–3878.

Ferris, H. (2010). Contribution of Nematodes to the Structure and Function of the Soil Food Web. *Journal of Nematology* 42 (1):63–67.

Ferris, H and Bongers, T. (2006). Nematode indicators of organic enrichment. *Journal of Nematology* 38:3–12.

Ferris, H. and Bongers, T. (2009). Indices Developed Specifically for Analysis of Nematode Assemblages. *Nematodes as Environmental Biondicators*. Ed. by M. Wilson and T. Kakouli-Duarte. Wallingford, U.K: CABI. Chap. 5, p. 124–145.

Ferris, H, Bongers, T, and R.G.M., Goede (2001). A framework for soil food web diagnostics: extension of the nematode faunal analysis concept. *Applied Soil Ecology* 18:13–29.

Fomina, M. and Gadd, G.M. (2014). Biosorption: current perspectives on concept, definition and application. *Bioresource Technology* 160:3–14.

Fosu-Nyarko, J. and Jones, M.G. (2015). *Application of Biotechnology for Nematode Control in Crop Plants*. Vol. 73. Chap. 14, pp. 339–376.

Foucher, A., Bongers, T., Noble, L.R., and Wilson, M. (2004). Assessment of nematode biodiversity using DGGE of 18S rDNA following extraction of nematodes from soil. *Soil Biology and Biochemistry* 36 (12):2027–2032.

Foucher, A. and Wilson, M. (2002). Development of a polymerase chain reaction-based denaturing gradient gel electrophoresis technique to study nematode species biodiversity using the 18s rDNA gene. *Molecular Ecology Notes* 2:45–48.

Fuller, V., Lilley, C.J., and Urwin, P.E. (2008). Nematode resistance. *New Phytologist* 108:27–44.

Gafan, G.P., Lucas, V.S., Roberts, G.J., Petrie, A., Wilson, M., and Spratt, D.A. (2005). Statistical analyses of complex denaturing gradient gel electrophoresis profiles. *Journal of Clinical Microbiology* 43 (8):3971–3978.

Gamalero, E., Lingua, G., Caprí, F. G., Graziella, A. F., and Lemanceau, B. P. (2004). Colonization pattern of primary tomato roots by *Pseudomonas fluorescens* A6RI characterized by dilution plating, flow cytometry, fluorescence, confocal and scanning electron microscopy. *FEMS Microbiology Ecology* 48 (1):79–87.

Garrido-Sanz, D., Meier-Kolthoff, J. P., Göker, M., Martín, M., Rivilla, R., and Redondo-Nieto, M. (2016). Genomic and Genetic Diversity within the *Pseudomonas fluorescens* Complex. *PLoSONE* 11 (2):1–30.

Geisen, S., Snoek, L. B., Hooven, F. C. ten, Duyts, H., Kostenko, O., Bloem, J., Martens, H., Quist, C. W., Helder, J. A., and Putten, W. H. van der (2018). Integrating quantitative morphological and qualitative molecular methods to analyse soil nematode community responses to plant range expansion. *Methods in Ecology and Evolution* 9 (6):1366–1378.

Goodey, J. B., Franklin, M. T., and Hooper, D. J. (1965). *The Nematode Parasites of Plants Catalogued under their Hosts. 3rd. ed.* CAB International, Wallingford, UK, pp. 4–214.

Goudaa, S., Kerryb, R.G., Dasc, G., Paramithiotisd, S., Shine, H.S., and Patra, J. K. (2018). Revitalization of plant growth promoting rhizobacteria for sustainable development in agriculture. *Microbiological Research* 206:131–140.

Griffiths, B.S., Donn, S., Neilson, R., and Daniell, T.J. (2006). Molecular sequencing and morphological analysis of a nematode community. *Applied Soil Biology* 32:325–337.

Guerena, M. (2006). Nematode: Alternative Controls. *NCAT Agriculture Specialist*:1–14.

Guilini, K., Soltwedel, T., Oevelen, D. van, and Vanreusel, A. (2011). Deep-sea nematodes actively colonise sediments, irrespective of the presence of a pulse of organic matter: results from an in-situ experiment. *PloS one* 6:1–12.

Hernández-Allica, J., Becerril, J. M., and Garbisu, C. (2008). Assessment of the phytoextraction potential of high biomass crop plants. *Environmental Pollution* 152:32–40.

Hida, H., Nishiyama, H., Sawa, S., Higashiyama, T., and Arata, H. (2015). Chemotaxis assay of plant-parasitic nematodes on a gel-filled microchannel device. *Sensors and Actuators B: Chemical* 221:1483–1491.

Hodda, M., Peters, L., and Traunspurger, W. (2009). Nematode diversity in terrestrial, freshwater aquatic and marine systems. *Nematodes as Environmental Biondicators*. Ed. by M. Wilson and T. Kakouli-Duarte. Wallingford, U.K: CABI. Chap. 2, p. 124–145.

Holovachov, O. (1982). *Morphology and Systematics of the Order Plectida*. Malakhov (Nematoda).

Hong, R.L. and Sommer, R.J. (2006). *Pristionchus pacificus*: a well-rounded nematode. *Bioessays* 28:651–659.

Hu, N., Li, H., Tang, Z., Li, Z., Tian, J., Lou, Y., Li, J, Li, G, and Hu, X. (2016). Community diversity, structure and carbon footprint of nematode food web following reforestation on degraded Karst soil. *Scientific Reports* 6:1038.

Huang, Xianqing, Zhang, X., and Xu, Y. (2008). Positive Regulation of Pyoluteorin Biosynthesis in *Pseudomonas* sp. M18 by Quorum-Sensing Regulator VqsR. *Journal of Microbiological Biotechnology* 18 (5):828–836.

Hunt, D. (1993). *Aphelenchida, Longidoridae and Trichodoridae. Their Systematics and Bionomics.* International Institute of Parasitology. An Institute of CAB International.

Hurley, M.J. (2018). An investigation on the interactions between entomopathogenic nematodes and plant growth promoting bacteria. PhD thesis. Institute of Technology Carlow, Ireland.

Iavicoli, A., Boutet, E., Buchela, A., and Métraux, J.P. (2003). Induced systemic resistance in *Arabidopsis thaliana* in response to root inoculation with *P. fluorescens* CHA0. *Molecular Plant-Microbe Interactions* 16:851–858.

Jagodič, A, Ipavec, N., Trdan, S, and Laznik, Z. (2017). Attraction behaviours: are synthetic volatiles, typically emitted by insect-damaged *Brassica nigra* roots, navigation signals for

entomopathogenic nematodes (*Steinernema* and *Heterorhabditis*)? *International Organization for Biological Control*.

Jansson, H.B. and Lopez-Llorca, L.V. (2007). Control of nematodes by fungi. *Fungal Biotechnology in Agricultural, Food, and Environmental Applications*. Ed. by D.P. Arora. New York: Marcel Dekker. Chap. 30, p. 205–215.

Jiang, C.H., Xie, P., Li, K., Xie, Y.S., Chen, L.J., Wang, J.S., Xua, Q., and Guo, J.H. (2018). Evaluation of root-knot nematode disease control and plant growth promotion potential of biofertilizer Ning shield on *Trichosanthes kirilowii* in the field. *Brazilian Journal of Microbiology* 49:232–239.

Jiang, Y., Chen, J., Wu, Y., Wang, Q., and Li, H. (2016). Sublethal Toxicity Endpoints of Heavy Metals to the Nematode *Caenorhabditis elegans*. *PLoS ONE* 11 (1):1–12.

Jiang, Y., Liu, M., Zhang, J., Chen, Y., Chen, X., Chen, L., Li, H., Zhang, X.X., and Sun, B. (2017). Nematode grazing promotes bacterial community dynamics in soil at the aggregate level. *The ISME Journal* 11:2705–2717.

Johnson, K.B., Stockwell, V.O., Sawyer, T.L., and Sugar, D. (2000). Assessment of environmental factors influencing growth and spread of *Pantoea agglomerans* on and among blossoms of pear and apple. *Phytopathology* 90:1285–124.

Jones, L.M., Koehler, A.K., Trnka, M., Balek, J., Challinor, A.J., Atkinson, H.J., and Urwin, P.E. (2017). Climate change is predicted to alter the current pest status of *Globodera pallida* and *G. rostochiensis* in the United Kingdom. *Global Change Biology* 23 (11):4497–4507.

Keogh, E. (2009). The isolation and characterisation of bacterial endophytes and their potential applications for improving phytoremediation. PhD thesis. Institute of Technology, Carlow, Ireland.

Kim, k.K., Kang, J.G., Moon, S.S., and Kang, K.Y. (2000). Isolation and Identification of Antifungal 7V-Butylbenzenesulphonamide Produced by *Pseudomonas* sp. AB2. *Journal of Antibiotics* 53 (2):131–136.

Kokalis-Burelle, N., Rosskopf, E.N., Butler, D.M., Fennimore, S.A., and Holzinger, J. (2016). Evaluation of Steam and Soil Solarization for *Meloidogyne arenaria* Control in Florida Floriculture Crops. *Journal of Nematology* 48 (3):183–192.

Korthals, G.W., Ende, A. van de, Megen, H. van, Lexmond, T.M., Kammenga, J., and Bongers, T. (1996). Short-term effects of cadmium, copper, nickel and zinc on soil nematodes from different feeding and life-history strategy groups. *Applied Soil Ecology* 4 (2):107–117.

Kumar, R., Pradhan, A., Khan, F.A., Lindström, P., Ragnvaldsson, D., Ivarsson, P., Olsson, P.E., and Jass, J. (2015). Comparative Analysis of Stress Induced Gene Expression in *Caenorhabditis elegans* following Exposure to Environmental and Lab Reconstituted Complex Metal Mixture. *PLoS ONE* 10 (7):1–21.

Kushida, A. (2013). Design and Evaluation of PCR Primers for Denaturing Gradient Gel Electrophoresis Analysis of Plant Parasitic and Fungivorous Nematode Communities. *Microbes and Environments* 28 (2):269–274.

Kyriakakis, E., Markaki, M., and Tavernarakis, N. (2015). *Caenorhabditis elegans* as a model for cancer research. *Molecular and Cellular Oncology* 2 (2):1–11.

Lacey, L.A. and Georgis, R. (2012). Entomopathogenic Nematodes for Control of Insect Pests Above and Below Ground with Comments on Commercial Production. *Journal of Nematology* 44 (2):218–225.

Lagido, C. (2009). Transgenic *Caenorhabditis elegans* as Biosensors. *Nematodes as Environmental Indicators*. Ed. by M.J. Wilson and T. Kakouli-Duarte. Oxfordshire: CABI. Chap. 10, p. 225–252.

Lally, R.D. (2016). Investigating the application, plant growth promotion and genetic potential of three endophytic *Pseudomonas fluorescens* isolates for use in sustainable agriculture. PhD thesis. Institute of Technology, Carlow, Ireland.

Lally, R.D., Galbally, P., Moreira, A.S., Spink, J., Ryan, D., Germaine, K., and Dowling, D.N. (2017). Application of Endophytic *Pseudomonas fluorescens* and a Bacterial Consortium to *Brassica napus* Can Increase Plant Height and Biomass under Greenhouse and Field Conditions. *Frontiers of Plant Science* 8 (2193):1–10.

Le Cocq, K., Gurr, S.J., Hirsch, P.R., and Mauchline, T.H. (2017). Exploitation of endophytes for sustainable agricultural intensification. *Molecular Plant Pathology* 18 (3):469–473.

Leung, J.M., Budischak, S.A., Chung The, H., Hansen, C., Bowcutt, R., Neill, R., Shellman, M., Loke, P., and Graham, A.L. (2018). Rapid environmental effects on gut nematode susceptibility in rewilded mice. *PLOS Biology* 16 (3):1–28.

Leung, M.C., Williams, P.L., Benedetto, A., Au, C., Helmcke, K.J., Aschner, M., and Meyer, J.N. (2008). *Caenorhabditis elegans*: An emerging model in biomedical and environmental toxicology. *Toxicological Sciences* 106:5–28.

Leveau, J.H. and Lindow, S.E. (2005). Utilization of the Plant Hormone Indole-3-Acetic Acid for Growth by *Pseudomonas putida* Strain 1290. *Applied Environmental Microbiology* 71 (5):2365–2371.

Link, C.D., Cypser, J.R., Johnson, C.J., and Johnson, T.E. (1999). Direct observation of stress response in *Caenorhabditis elegans* using a reporter transgene. *Cell Stress and Chaperones* 4 (4):235–242.

Lone, M.I., He, Z., Stoffella, P.J., and Yang, X. (2008). Phytoremediation of heavy metal polluted soils and water: Progresses and perspectives. *Journal of Zhejiang University SCIENCE B* 9 (3):210–220.

Loon, L.C. van, Bakker, P.A., and Pieterse, C.M. (1998). Systemic resistance induced by rhizosphere bacteria. *Annual Review of Phytopathology* 36:453–483.

Loon, L.C. van and Glick, B.R. (2004). Increased plant fitness by rhizobacteria. *Molecular ecotoxicology of plants*. Ed. by Sandermann H. Heidelberg, Berlin: Springer-Verlag. Chap. 7, p. 177–205.

López, A., Lázaro, N., Priego, J. M., and Marqués, A. M. (2000). Effect of pH on the biosorption of nickel and other heavy metals by *Pseudomonas fluorescens* 4F39. *Journal of Industrial Microbiology and Biotechnology* 24:146–151.

Ma, F., Rehman, A., Sims, M., and Zeng, X. (2015). Antimicrobial Susceptibility assays based on the Quantification of Bacterial Lipopolysaccharides via a Label Free Lectin Biosensor. *Analytical Chemistry* 87:4385–4393.

Ma, Y., Prasad, M., Rajkumar, M., and Freitas, H. (2011a). Plant Growth Promoting Rhizobacteria and Endophytes Accelerate Phytoremediation of Metalliferous Soils. *Biotechnology Advances* 29:248–258.

Ma, Y., Rajkumar, M., Luoa, Y. M., and Freitas, H. (2011b). Inoculation of endophytic bacteria on host and non-host plants — Effects on plant growth and Ni uptake. *Journal of Hazardous Materials* 195:230–237.

Ma, Y., Rajkumar, M., Zhang, C. H., and Freitas, H. (2016). Inoculation of *Brassica oxyrrhina* with plant growth promoting bacteria for the improvement of heavy metal phytoremediation under drought conditions. *Journal of Hazardous Materials* 320:36–44.

Majdi, N. and Traunspurger, W. (2015). Free-Living Nematodes in the Freshwater Food Web: A Review. *Journal of Nematology* 47 (1):28–44.

Malash, M.A., El-Naggar, M.M., Abou El Hassayeb, H. E., and Ibrahim, M.S. (2016). Production of antimicrobial pyrrol-derevatives acting against some fish pathogens from marine *Bacillus pumilusmmm*. *Global Veterinaria* 17 (6):495–504.

Martinuz, A., Schouten, A., and Sikora, R. A. (2012). Post-infection development of *Meloidogyne incognita* on tomato treated with the endophytes *Fusarium oxysporum* strain Fo162 and *Rhizobium etli* strain G12. *BioControl* 58 (1):95–104.

McCloy, R. A., Rogers, S., Caldon, C.E., Lorca, T., Castro, A., and Burgess, A (2014). Partial inhibition of Cdk1 in G 2 phase overrides the SAC and decouples mitotic events. *Cell Cycle* 13:1400–1412.

McGrath, D. and Fleming, G.A. (2007). *Trace Elements and Heavy Metals in Irish Soils*. Teagasc, p. 216.

Menton, C. (2010). Microbiology of bio-energy crops: pathogen fate and bioremediation enhancement. PhD thesis. Institute of Technology, Carlow, Ireland.

Meyer, S.L., Everts, K., McSpadden Gardener, B., Masler, E.P., Abdelnabby, H.M.E., and Skantar, A M. (2016). Assessment of DAPG-producing *Pseudomonas fluorescens* for Management of *Meloidogyne incognita* and *Fusarium oxysporum* on Watermelon. *Journal of Nematology* 48 (1):43–53.

Meyer, S.L., Halbrendt, J.M., Carta, L.K., Skantar, A.M., Liu, T., Abdelnabby, H.M.E., and Vinyard, B.T. (2009). Toxicity of 2,4-diacetylphloroglucinol (DAPG) to plant-parasitic and bacterial-feeding nematodes. *Journal of Nematology* 41 (4):274–280.

Miles, A.A. and Misra, S.S. (1938). The estimation of the bactericidal power of the blood. *Journal of Hygiene* 38:732–749.

Moens, M. and Perry, R.N. (2009). Migratory plant endoparasitic nematodes: a group rich in contrasts and divergence. *Annual Review of Phytopathology* 47:313–332.

Moens, M., Perry, R.N., and Starr, J.L. (2009). *Meloidogyne* Species – a Diverse Group of Novel and Important Plant Parasites. *Root-knot Nematodes*. Ed. by R.N. Perry, M. Moens, and J.L. Starr. Oxfordshire: CABI. Chap. 1, p. 1–17.

Montalbán, B., Croes, S., Weyens, N., Lobo, M.C., Pérez-Sanz, A., and Vangronsveld, J. (2016). Characterization of bacterial communities associated with *Brassica napus* L. growing on a Zn-contaminated soil and their effects on root growth. *International Journal of Phytoremediation* 18:985–993.

Montalbán, B., Thijs, S., Lobo, M., Weyens, N., Ameloot, M., Vangronsveld, J., and Pérez-Sanz, A. (2017). Cultivar and Metal-Specific Effects of Endophytic Bacteria in *Helianthus tuberosus* Exposed to Cd and Zn. *International Journal of Molecular Sciences* 18 (2026):985–993.

Morris, E.K. *et al.* (2014). Choosing and using diversity indices: insights for ecological applications from the German Biodiversity Exploratories. *Ecol Evol* 4 (18):3514–24.

Mourato, M.P., Moreira, I.N., Leitão, I., Pinto, F.R., Sales, J.R., and Louro Martins, L. (2015). Effect of Heavy Metals in Plants of the Genus *Brassica*. *International Journal of Molecular Sciences* 16 (8):17975–17998.

Munif, A., Hallmann, J., and Sikora, R.A. (2013). The influence of endophytic bacteria on *Meloidogyne incognita* infection and tomato plant growth. *J. ISSAAS* 19 (2):68–74.

Murfin, K.E., Dillman, A.R., Foster, J.M., Bulgheresi, S., Slatko, B.E., Sternberg, P.W., and Goodrich-Blair, H. (2012). Nematode-Bacterium Symbioses - Cooperation and Conflict Revealed in the 'Omics' Age. *Biol Bull* 223 (1):85–102.

Mustapha, M.U. and Halimoon, N. (2015). Microorganisms and Biosorption of Heavy Metals in the Environment: A Review Paper. *Journal of Microbial and Biochemical Technology* 7:253–256.

Muthukumar, B., Yakubov, B., and Salt, D. E. (2007). Transcriptional activation and localization of expression of *Brassica juncea* putative metal transport protein BjMTP1. *BMC Plant Biology* 7 (32):1–12.

Nam, H.S., Anderson, A.J., and Kim, Y.C. (2018). Biocontrol Efficacy of Formulated Pseudomonas chlororaphis O6 against Plant Diseases and Root-Knot Nematodes. *The Plant Path-ology Journal* 34 (3):241–249.

Naz, T., Khan, M.D., Ahmed, I., Rehman, S., ur Rha, E.S., Malook, I., and Jamil, M. (2016). Biosorption of heavy metals by Pseudomonas species isolated from sugar industry. *Toxicology and Industrial Health* 32 (9):1619–1627.

Neher, D.A., Bongers, T., and Ferris, H. (2004). Computation of Nematode Community Indices. *Society of Nematologists, Estes Park, Colorado*.

Neher, D.A. and Darby, B.J. (2006). *Computation and application of nematode community indices: general guidelines*. Freshwater nematodes: Ecology and Taxonomy. CABI.

– (2009). Community Indices that can be used for Analysis of Nematode Assemblages. *Nematodes as Environmental Indicators*. Ed. by M.J. Wilson and T. Kakouli-Duarte. Oxfordshire: CABI. Chap. 4, p. 107–123.

Neher, D.A., Wu, J., Barbercheck, M.E., and Anas, O. (2005). Ecosystem type affects interpretation of soil nematode community measures. *Applied Soil Ecology* 30:47–64.

Nguyen, P., Nguyen, H., Ha, D.N., and Duong, D.H. (2016). Application of PCR-DGGE method for identification of nematode communities in pepper growing soil. *Journal of Vietnamese Environment* 7 (1):9–14.

Norabadi, M. T., N., Sahebani, and Etebarian, H. R. (2014). Biological control of root-knot nematode (*Meloidogyne javanica*) disease by *Pseudomonas fluorescens* (Chao). *Archives of Phytopathology and Plant Protection* 47 (5):615–621.

Nyczepir, A.P., Beckman, T.G., and Reighard, G.L. (1999). Reproduction and Development of *Meloidogyne incognita* and *M. javanica* on Guardian Peach Rootstock. *Journal of Nematology* 31 (3):334–340.

O'Callaghan, M. (2016). Microbial inoculation of seed for improved crop performance: issues and opportunities. *Applied Microbiology and Biotechnology* 100:5729–5746.

Oliveira, C.M.G., Monteiro, C.M., and Monteiro, A.R. (2011). Morphological and molecular diagnostics for plant-parasitic nematodes: working together to get the identification done. *Tropical Plant Pathology* 36:65–73.

Ortíz-Castro, R., Contreras-Cornejo, H. A., Macías-Rodríguez, L., and López-Bucio, J. (2009). The role of microbial signals in plant growth and development. *Plant signalling and behaviour* 4:701–712.

Otieno, N. (2014). Development of plant growth promoting endophytic isolates as microbial inoculants for practical application in bioenergy species. PhD thesis. Institute of Technology, Carlow, Ireland.

Otieno, N., Culhane, J., Germaine, K.J., Brazil, D., Ryan, D.A., and Dowling, D.N. (2013). Screening of large collections of plant associated bacteria for effective plant growth promotion and colonisation. *Aspects of Applied Biology* 120:23–28.

Otieno, N., Lally, R.D., Kiwanuka, S., Lloyd, A., Ryan, D., Germaine, K.J., and Dowling, D.N. (2015). Plant growth promotion induced by phosphate solubilizing endophytic Pseudomonas isolates. *Frontiers in Microbiology* 6.

Ownley, B.H., Duffy, B.K., and Weller, D.M. (2003). Identification and Manipulation of Soil Properties To Improve the Biological Control Performance of Phenazine-Producing *Pseudomonas fluorescens*. *Applied and Environmental Biology* 69 (6):3333–3343.

Page, A.P. and Johnstone, I.L. (2007). The cuticle, WormBook, ed. The *C. elegans* Research Community, WormBook.

Pandey, A., Naik, M.M., and Dubey, S.K. (2010). Organic metabolites produced by *Vibrio parahaemolyticus* strain An3 isolated from Goan mullet inhibit bacterial fish pathogens. *African Journal of Biotechnology India* 9 (42):7134–7140.

Park, J., Kim, J.Y., and Kim, K.W. (2012). Phytoremediation of soil contaminated with heavy metals using *Brassica napus*. *Geosystem Engineering* 15:9–17.

Parkinson, J. *et al.* (2004). A transcriptomic analysis of the phylum Nematoda. *Nature Genetics* 36:1259–1267.

Parmar, T.K., Rawtani, D., and Agrawal, Y.K. (2016). Bioindicators: the natural indicator of environmental pollution. *Frontiers in Life Science* 9 (2):110–118.

Phelan, S. (2017). *Crops Costs and Returns 2017*. booklet. Crops, Environment and Land-Use Programme, Teagasc, Oak Park.

Pileggi, M., Pileggi, S.A, Olchanheski, L.R., Silva, P.A. da, Munoz Gonzalez, A.M., Koskinen, W.C., Barber, B, and Sadowsky, M.J. (2012). Isolation of mesotrione-degrading bacteria from aquatic environments in Brazil. *Chemosphere* 86:1127–1132.

Pires-daSilva, A. (2013). *Pristionchus pacificus protocols*. The C. elegans Research Community: WormBook, ed, pp. 1–20.

Power, R.S. and Pomerai, D.I. de (1999). Effect of Single and Paired Metal Inputs in Soil on a Stress-Inducible Transgenic Nematode. *Archives of Environmental Contamination and Toxicology* 37:503–511.

Purakayastha, T.J., Viswanath, T., Bhadraray, S., Chhonkar, P.K., Adhikari, P.P., and Suribabu, K. (2008). Phytoextraction of zinc, copper, nickel and lead from a contaminated soil by different species of brassica. *Int. J. Phytoremediat* 10:61–72.

Pusceddu, A., Gambi, C., Corinaldesi, C., Scopa, M., and Danovaro, R. (2014). Relationships between Meiofaunal Biodiversity and Prokaryotic Heterotrophic Production in Different Tropical Habitats and Oceanic Regions. *PLoS ONE* 9 (3):e91056.

Půža, Vladimír (2015). Control of Insect Pests by Entomopathogenic Nematodes. *Principles of Plant-Microbe Interactions: Microbes for Sustainable Agriculture*. Ed. by Ben Lugtenberg. Cham: Springer International Publishing, p. 175–183.

Rajalaxmi, M., Beema Shafreen, R., Iyer, P.M., Sahaya Vino, R., K., Balamurugan., and Pandian, S.K. (2016). silico, in vitro and in vivo investigation of indole-3-carboxaldehyde identified from the seawater bacterium *Marinomonas* sp. as an anti-biofilm agent against *Vibrio cholerae* O1. *Biofouling* 32:1–12.

Rajkumar, M., Ma, Y., and Freitas, H. (2013). Improvement of Ni phytostabilization by inoculation of Ni resistant *Bacillus megaterium* SR28C. *Journal of Environmental Management* 128:973–980.

Rasmann, S. and Turlings, T.C. (2008). First insights into specificity of belowground tritrophic interactions. *Oikos* 117 (3):362–369.

Redondo-Nieto, M. *et al.* (2013). Genome sequence reveals that *Pseudomonas fluorescens* F113 possesses a large and diverse array of systems for rhizosphere function and host interaction. *BMC Genomics* 14:54.

Reimann, S., Hauschild, R., Hildebrandt, U., and Sikora, R.A. (2008). Interrelationship between *Rhizobium etli* G12 and *Glomus intraradices* and multitrophic effects in the biological control of the root-knot nematode *Meloidogyne incognita* on tomato. *Journal of Plant Diseases and Protection* 115 (3):108–113.

Reynolds, A.M., Dutta, T.K., Curtis, R. H., Powers, S.J., Gaur, H.S., and Kerry, B.R. (2011). Chemotaxis can take plant-parasitic nematodes to the source of a chemo-attractant via the shortest possible routes. *Journal of the Royal Society Interface* 8:568–577.

Rivilla, R., Martínez-Granero, F., and Martín, M. (2013). Motility, Biofilm Formation, and Rhizosphere Colonization by *Pseudomonas fluorescens* F113. *Molecular Microbial Ecology of the Rhizosphere, 1 and 2*. Ed. by F. J. de Bruijn. Wiley. Chap. 68.

Rodelsperger, C., Meyer, J.M., Prabh, N., Lanz, C., Bemm, F., and Sommer, R.J. (2017). Single-Molecule Sequencing Reveals the Chromosome-Scale Genomic Architecture of the Nematode Model Organism *Pristionchus pacificus*. *Cell Reports* 21:834–844.

Rowe, J. (2017). *Globodera pallida (white potato cyst nematode)*. IACR-Rothamsted, Rothamsted Experimental Station, Harpenden, Hertfordshire, AL5 2JQ, UK: CABI publishing.

Ruiz, B., Chávez, A., Forero, A., García-Huante, Y., Romero, A., Sánchez, M., Rocha, D., Sánchez, B., Rodríguez-Sanoja, R., Sánchez, S., and Langley, E. (2010). Production of microbial secondary metabolites: Regulation by the carbon source. *Critical Reviews in Microbiology* 32:146–167.

Ryan, R.P., Germaine, K., Franks, A., Ryan, D.J., and Dowling, D.N. (2008). Bacterial endophytes: recent developments and applications. *Federation of European Microbiological Societies (FEMS) Microbiol Lett* 278:1–9.

Sajid, I., Shaaban, K.A., and Hasnain, S. (2011). Identification, isolation and optimization of antifungal metabolites from the *Streptomyces malachitofuscus* ctf9. *Brazilian Journal of Microbiology* 42:592–604.

San-Blas, E., Cubillán, N., Guerra, M., Portillo, E., and Esteves, I. (2012). Characterization of *Xenorhabdus* and *Photorhabdus* bacteria by Fourier transform mid-infrared spectroscopy with attenuated total reflection (FT-IR/ATR). *Spectrochim Acta A Mol Biomol Spectrosc* 93:58–62.

San-Blas, E., Guerra, M., Portillo, E., Esteves, I., Cubillán, N., and Alvarado, Y. (2011). ATR/ FTIR characterization of *Steinernema glaseri* and *Heterohabditis indica*. *Vibrational Spectroscopy* 57 (2):220–228.

Sas-Nowosielska, A., Kucharski, R., Malkowski, E, Pogrzeba, M., Kuperberg, J., and Kryński, K. (2004). Phytoextraction crop disposal-an unsolved problem. *Environmental Pollution* 128 (3):373–379.

Scott, D. (1990). The NIST/EPA/MSDC mass spectral database, personal computer versions 1.0 and 2.0. *Chemometrics and Intelligent Laboratory Systems* 8 (1):3–5.

Shahid, I., Rizwan, M., Baig, D.N., Saleem, R. ., Malik, K.A., and Mehnaz, S. (2017). Secondary Metabolites Production and Plant Growth Promotion by *Pseudomonas chlororaphis* and *P. aurantiaca* Strains Isolated from Cactus, Cotton, and Para Grass. *Journal of Microbiology and Biotechnology* 27 (3):480–491.

Shanahan, P., O'Sulivan, D.J., Simpson, P., Glennon, J.D., and O'Gara, F. (1992). Isolation of 2,4-Diacetylphloroglucinol from a Fluorescent Pseudomonad and Investigation of Physiological Parameters Influencing Its Production. *Applied and Environmental Biology*:353–358.

Shapaval, V., Schmitt, J., Møretrø, T., Sus, H. P., Skaar, I., Åsli, A.W., Lillehaug, G., and Kohler, A. (2012). Characterization of food spoilage fungi by FTIR spectroscopy. *Journal of Applied Microbiology* 114:788–796.

Shapiro-Ilan, D., Han, R., and Dolinksi, C. (2012). Entomopathogenic Nematode Production and Application Technology. 44 (2):206–217.

Sheng, M., Gorzsás, A., and Tuck, S. (2016). Fourier transform infrared microspectroscopy for the analysis of the biochemical composition of *C. elegans* worms. *Worm* 5 (1):1–14.

Shimomura, O. (1979). Structure of the chromophore of *Aequorea* green fluorescent protein. *FEBS Letters* 104:220–222.

Siddiqi, M. (2001). *Tylenchida: Parasites of Plants and Insects*. CABI Publishing.

Siddiqui, I. A. and Ehteshamul-Haque, S. (2001). Suppression of the root rot–root knot disease complex by *Pseudomonas aeruginosa* in tomato: The influence of inoculum density, nematode populations, moisture and other plant-associated bacteria. *Plant and Soil* 237:81–89.

Siddiqui, I.A. and Shaukat, S.S. (2003). Suppression of root-knot disease by *Pseudomonas fluorescens* CHA0 in tomato: importance of bacterial secondary metabolite, 2,4-diacetylpholoroglucinol. *Soil Biology and Biochemistry* 35 (12):1615–1623.

Singh, P. and Siddiqui, Z.A. (2010). Biocontrol of root-knot nematode *Meloidogyne incognita* by the isolates of *Pseudomonas* on tomato. *Archives of Phytopathology and Plant Protection* 43 (14):1423–1434.

Sochová, I., Hofman, J., and Holoubek, I. (2006). Using nematodes in soil ecotoxicology. *Environment international* 32:374–383.

Soetaert, K., Franco, M., Lampadariou, N., and Muthumbi, A. (2009). Factors affecting nematode biomass, length and width from the shelf to the deep sea. *Marine Ecology Programme Series* 392:123–132.

Sommer, R.J. (2006). *Pristionchus pacificus*. *WormBook*:1–8.

Spence, K.O., Lewis, E.E., and Perry, R.N. (2008). Host finding and invasion by entomopathogenic and plant-parasitic nematodes: Evaluating the ability of bioassays to predict field results. *Journal of Nematology* 40 (2):93–98.

Statistics, Laerd (2015). Principal components analysis (PCA) using SPSS Statistics. *Statistical tutorials and software guides*.

Stein, S.E. (2008). NIST/EPA/NIH Mass Spectral Library (NIST08) and NIST Mass Spectral Search Program (Version 2.0f).

Stiernagle, T. (2006). *Maintenance of C. elegans*. The *C. elegans* Research Community: WormBook, edition, pp. 1–11.

Stirling, G.R. (2014). *Biological Control of Plant-parasitic Nematodes: Soil Ecosystem Management in Sustainable Agriculture*. Biological Crop Protection Pty. Ltd, Australia: CABI, p. 536.

Stringham, E. and Candido, E.P. (1994). Transgenic *hsp*16-*lacZ* strains of the soil nematode *Caenorhabditis elegans* as biological monitors of environmental stress. *Environmental Toxicology and Chemistry* 13:1211–1220.

Subbotin, S.A., Madani, M., Krall, E., Sturhan, D., and Moens, M. (2005). Molecular Diagnostics, Taxonomy, and Phylogeny of the Stem Nematode *Ditylenchus dipsaci* Species Complex Based on the Sequences of the Internal Transcribed Spacer-rDNA. *American Phytopathological Society* 95:1308–1315.

Sulston, J. (1988). *Cell lineage. In The nematode C. elegans (ed. W.B. Wood)*. Cold Spring Harbor, New York: Cold Spring Harbor Laboratory Press, pp. 587–606.

Tague, T. (2008). Microbial identification using FT-IR. *Spectroscopy*.

Takemoto, S., Niwa, S., and Okada, H. (2010). Effect of Storage Temperature on Soil Nematode Community Structures as Revealed by PCR-DGGE. *Journal of Nematology* 42 (4):324–331.

Tangahu, B.V., Abdullah, S.R., Basri, H., Idris, M., Anuar, N., and Mukhlisin, M. (2011). A Review on Heavy Metals (As, Pb, and Hg) Uptake by Plants through Phytoremediation. *International Journal of Chemical Engineering* 2011:31.

Thiyagarajan, S.S. and Kuppusamy, H. (2014). Biological control of root knot nematodes in chillies through *Pseudomonas fluorescens*'s antagonistic mechanism. 2:152–158.

Tian, B., Yang, J., and Zhang, K.Q. (2007). Bacteria used in the biological control of plant-parasitic nematodes: populations, mechanisms of action, and future prospects. *FEMS Microbiology Ecology* 61 (2):197–213.

Tissenbaum, H.A. (2015). Using *C. elegans* for aging research. *Invertebrate Reproduction and Development* 59 (S1):59–63.

Treonis, A.M., Unangst, S.K., Kepler, R.M., Buyer, J.S., Cavigelli, M.A., Mirsky, S.B., and Maul, J.E. (2018). Characterization of soil nematode communities in three cropping systems through morphological and DNA metabarcoding approaches. *Scientific Reports* 8 (2004):1–12.

Treonis, A.M. and Wall, D.H. (2005). Soil Nematodes and Desiccation Survival in the Extreme Arid Environment of the Antarctic Dry Valleys. *Integrative and Comparative Biology* 4:258–268.

Trifonova, Z., Tsvetkov, I., Bogatzevska, N., and Batchvarova, R. (2014). Efficiency of Pseudomonas spp. for biocontrol of the potato cyst nematode *Globodera rostochiensis* (Woll.) *Bulgarian Journal of Agricultural Science* 20:666–669.

Trudgill, D.L., Elliott, M.J., Evans, K., and Phillips, S. (2003). The white potato cyst nematode (*Globodera pallida*) a critical analysis of the treat in Britain. *Annals of Applied Biology* 143 (1):73–80.

Truong, N.M., Nguyen, C.N., Abad, P., Quentin, M, and Favery, B. (2015). Function of Root-Knot Nematode Effectors and Their Targets in Plant Parasitism. *Advances in Botanical Research*. Ed. by C. Escobar and C. Fenoll. Vol. 73. New York: Academic Press. Chap. 12, p. 293–324.

Ugarte, C. and Zaborski, E. (2014). Soil Nematodes in Organic Farming Systems. *Extension*.

Ürkmez, D., Sezgin, M., and Bat, L. (2014). Use of nematode maturity index for the determination of ecological quality status: a case study from the Black Sea. *Journal of the Black Sea/ Mediterranean Environment* 20 (2):96–107.

USEPA (1992). EPA Method 3005A. Acid Digestion of Waters for Total Recoverable or Dissolved Metals for Analysis by FLAA or ICP Spectroscopy. *United State Environmental Protection Agency*.

– (1996). EPA Method 3050B. Acid Digestion of Sediments, Sludges and Soils. *United State Environmental Protection Agency*.

Vasile, A.J., Andreea, I.R., Popescu, G.H., Elvira, N., and Marian, Z. (2016). Implications of agricultural bioenergy crop production and prices in changing the land use paradigm- The case of Romania. *Land Use Policy* 50:399–407.

Vassilev, A., Schwitzguebel, J.P., Thewys, T., Lelie, D. van der, and Vangronsveld, J. (2004). The Use of Plants for Remediation of Metal Contaminated Soils. *The Scientific World Journal* 4:9–34.

Vejan, P., Abdullah, R., Khadiran, T., Ismail, S., and Nasrulhaq Boyce, A. (2016). Role of Plant Growth Promoting Rhizobacteria in Agricultural Sustainability. *Molecules* 21 (573):1–17.

Vinay, J. U., Naik, M. K., Rangeshwaran, R., Chennappa, G., Shaikh, S. S., and Sayyed, R. Z. (2016). Detection of antimicrobial traits in fluorescent pseudomonads and molecular characterization of an antibiotic pyoluteorin. *3 Biotech* 227:1–11.

Voijant Tangahu, B., Siti Rozaimah Sheikh, A., Basri, H., Isris, M., Anuar, N., and Mukhlisin, M. (2011). A Review on Heavy Metals (As, Pb, and Hg) Uptake by Plants through Phytoremediation. *International Journal of Chemical Engineering* 2011:1–31.

Waite, I.S. *et al.* (2003). Design and evaluation of nematode 18S rDNA primers for PCR and denaturing gradient gel electrophoresis (DGGE) of soil community DNA. *Soil Biology and Biochemistry* 35 (9):1165–1173.

Walterson, A. M. and Stavrinides, J. (2015). *Pantoea*: insights into a highly versatile and diverse genus within the Enterobacteriaceae. *FEMS Microbiology Reviews* 39:968–984.

Wang, K.H. and McSorley, R. (2018). Effects of Soil Ecosystem Management on Nematode Pests, Nutrient Cycling, and Plant Health. *American Phytopathological Society*.

Weaver, K.J., May, C.J., and Ellis, B.L. (2017). Using a health-rating system to evaluate the usefulness of *Caenorhabditis elegans* as a model for anthelmintic study. *PLOS ONE* 12 (6).

Weller, D.M. (2007). *Pseudomonas* Biocontrol Agents of Soilborne Pathogens: Looking Back Over 30 Years. *Symposium The Nature and Application of Biocontrol Microbes III: Pseudomonas spp.* 97 (2).

Wenig, P. and Odermatt, J. (2010). OpenChrom: a cross-platform open source software for the mass spectrometric analysis of chromatographic data. *BMC Bioinformatics* 11.

Weyens, N., Van der Lelie, D., Taghavi, S., and Vangronsveld, J. (2009). Phytoremediation: Plant- Endophyte Partnerships Take the Challenge. *Current Opinion in Biotechnology* 20 (2):248–254.

White, G.F. (1927). A method for obtaining infective nematode larvae from cultures. *Science* 66:302–303.

Whiting, D., Wilson, C., and Reeder, J. (2014). Estimating Soil Texture: Sand, Silt or Clayey? *Colorado State University Extension*.

Whittaker, R.H. (1965). Dominance and Diversity in Land Plant Communities: Numerical relations of species express the importance of competition in community function and evolution. *Science* 147 (3655):250–260.

Widmer, T.L., Mitkowski, N.A., and G.S., Abawi. (2002). Soil Organic Matter and Management of Plant-Parasitic Nematodes. *Journal of Nematology* 34 (4):289–295.

Wieczorek, K, Elashry, A., Quentin, M., Grundler, F., Favery, B., Seifert, G.J., and Bohlmann, H. (2014). A distinct role of pectate lyases in the formation of feeding structures induced by cyst and root-knot nematodes. *Molecular Plant-Microbe Interactions* 27 (9):901–912.

Williams, P.L. and Dusenbery, D.B. (1990). Aquatic Toxicity Testing using the Nematode *Caenorhabditis elegans*. *Environmental Toxicology and Chemistry* 9 (10):1285–1290.

Wolkow, C.A. and Hall, D.H. (2015). *Introduction to the Dauer Larva, Overview*. WormAtlas.

Xiang, N., Lawrence, K.S., Kloepper, J.W., Donald, P.A., and McInroy, J.A. (2017). Biological control of *Heterodera glycines* by spore-forming plant growth-promoting rhizobacteria (PGPR) on soybean. *PLOS ONE* 12:1–19.

XLSTAT (2017). XLSTAT 2017: Data Analysis and Statistical Solution for Microsoft Excel. *Addinsoft, Paris, France*.

Yan, Z., Reddy, M.S., Ryu, C.M., McInroy, J.A., Wilson, M., and Kloepper, J. W. (2002). Induced Systemic Protection Against Tomato Late Blight Elicited by Plant Growth-Promoting Rhizobacteria. *Phytopathology* 92 (12):1329–1333.

Yang, G., Zhou, B., Zhang, X., Zhang, Z., Wu, Y., Zhang, Y., Lu, S., Zou, Q., Gao, Y., and Teng, L. (2016). Effects of Tomato Root Exudates on *Meloidogyne incognita*. *PLoS One* 11 (4).

Yeates, G. W., Bongers, T., Goede, R.G.M. de, Freckman, D.W, and Georgieva, S.S. (1993). Feeding habits in soil nematode families and genra- an outline for soil ecologists. *Journal of Nematology* 25:315–331.

Yoder, M., Tandingan De Lay, I., King, I.W., Mundo-Ocampo, M., Mann, J., Blaxter, M., Poiras, L., and De Lay, P. (2006). DESS: a versatile solution for preserving morphology and extractable DNA of nematodes. *Nematology* 8 (3):367–376.

Zahoor, F. and Forristal, D. (2000). *CROP QUEST Oilseed rape: Crop report*. Teagasc, Oak Park , Carlow.

Zarnowiec, P., Zarnowiec, L., Czerwonka, G., and Kaca, W. (2015). Fourier Transform Infrared Spectroscopy (FTIR) as a Tool for the Identification and Differentiation of Pathogenic Bacteria. *Current Medicinal Chemistry* 22 (14):1710–1718.

Zhang, J., Yang, K., Wang, H., Lv, B., and Ma, F. (2016). Biosorption of copper and nickel ions using *Pseudomonas* sp. in single and binary metal systems. *Desalination and Water Treatment* 57 (6):2799–2808.

Zullini, A. (2007). *Identification manual for freshwater nematode genra*. Universita di Milano-Bicocca.

Zyl, C. van and Malan, A.P. (2014). The Role of Entomopathogenic Nematodes as Biological Control Agents of Insect Pests, with Emphasis on the History of Their Mass Culturing and in vivo Production. *African Entomology* 22:235–249.

Appendix A

Supplementary Information for Chapter 2

A.1 Bacterial Standard Curves

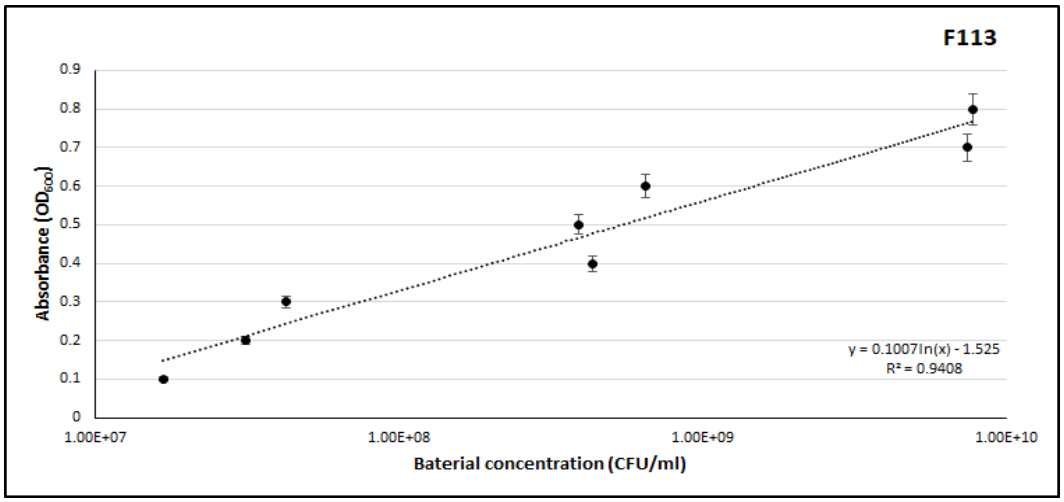

(A)

FIGURE A.1: Standard curves of (A) PGP bacterial strain F113. Bacterial concentration, colony forming units per ml (CFU/ml), were plotted against the absorbance, of bacterial cells at various OD readings ($OD_{(600)}$ 0.1 - 0.8) after 24 hours growth.

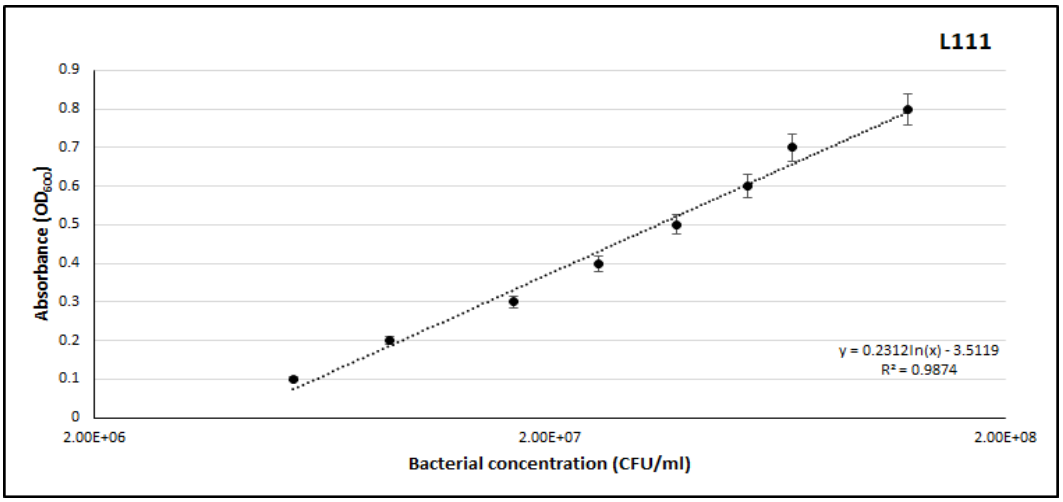

(A)

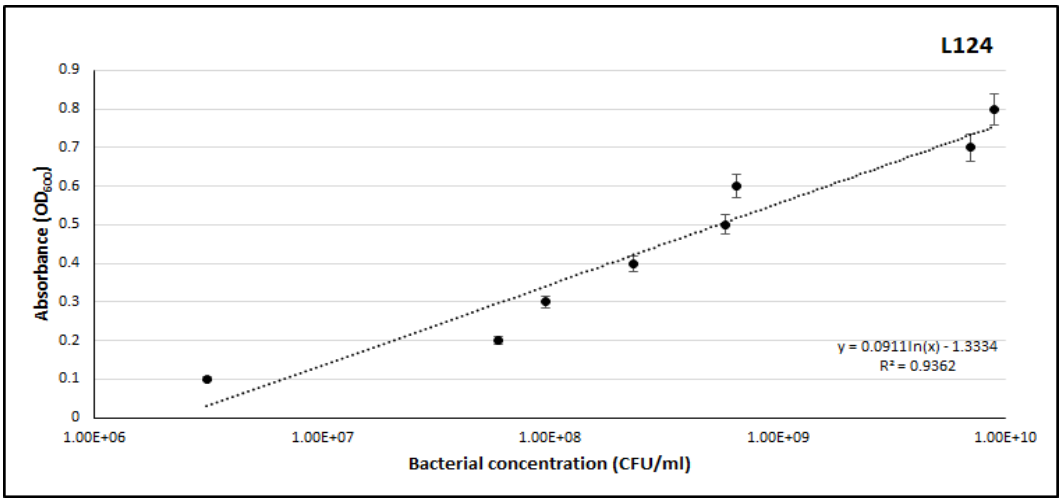

(B)

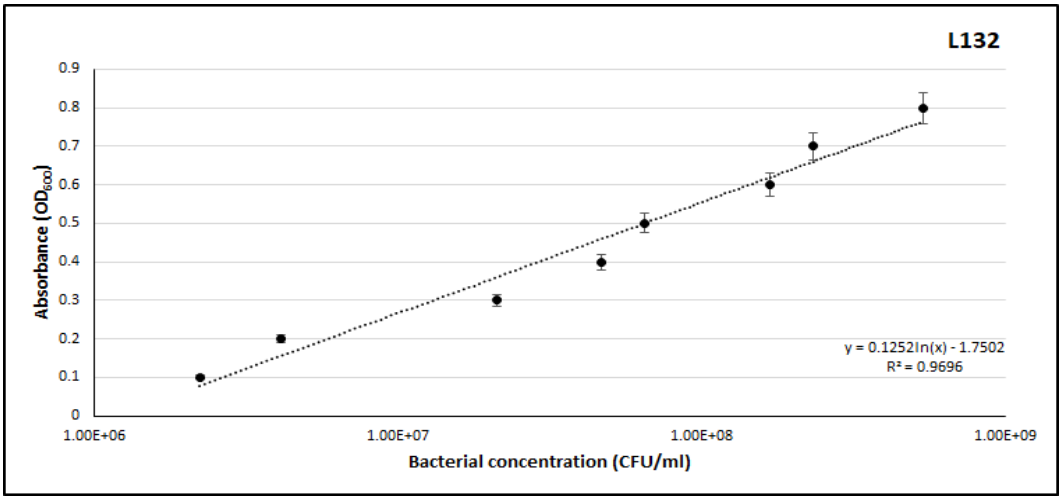

(C)

FIGURE A.2: Standard curves of PGP bacterial strains (A) L111, (B) L124 and (C) L132. Bacterial concentration, colony forming units per ml (CFU/ml), were plotted against the absorbance of bacterial cells at various OD readings ($OD_{(600)}$ 0.1 - 0.8) after 24 hours growth.

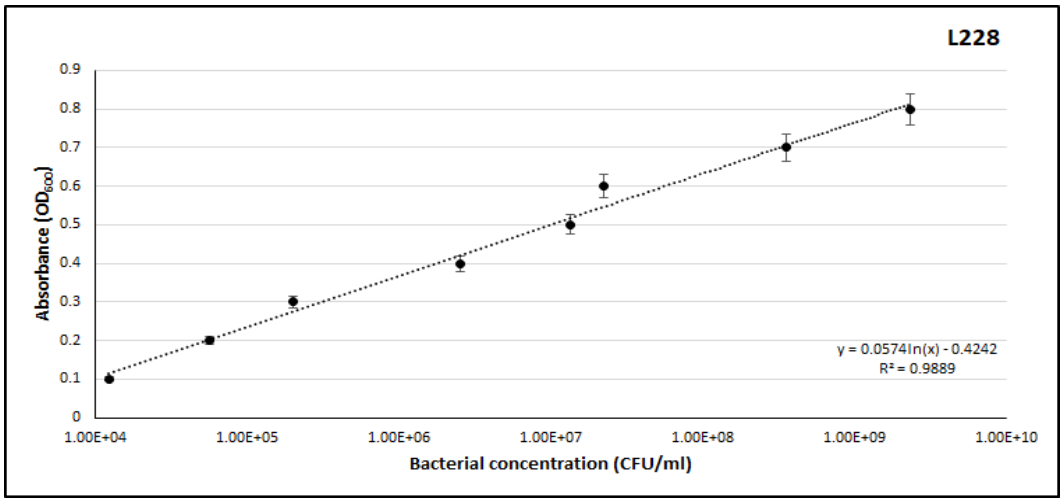

(A)

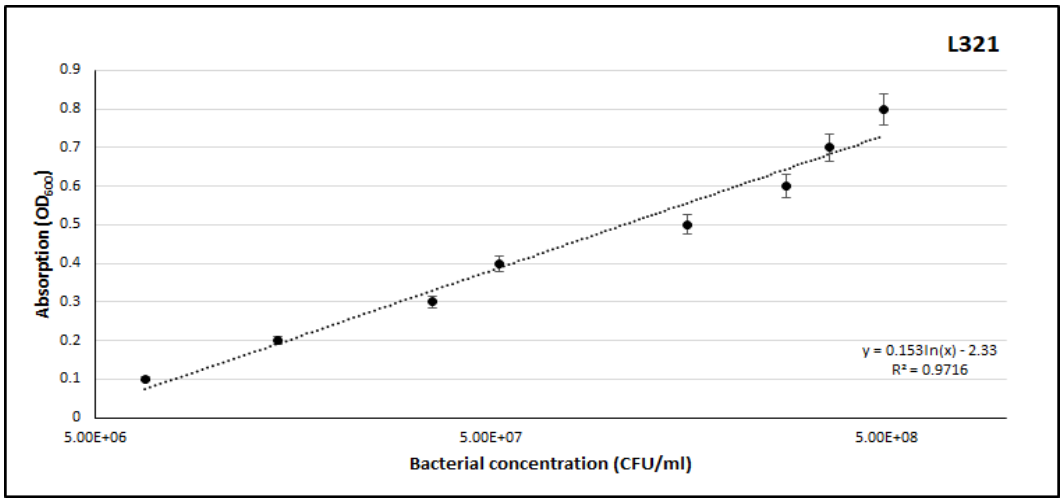

(B)

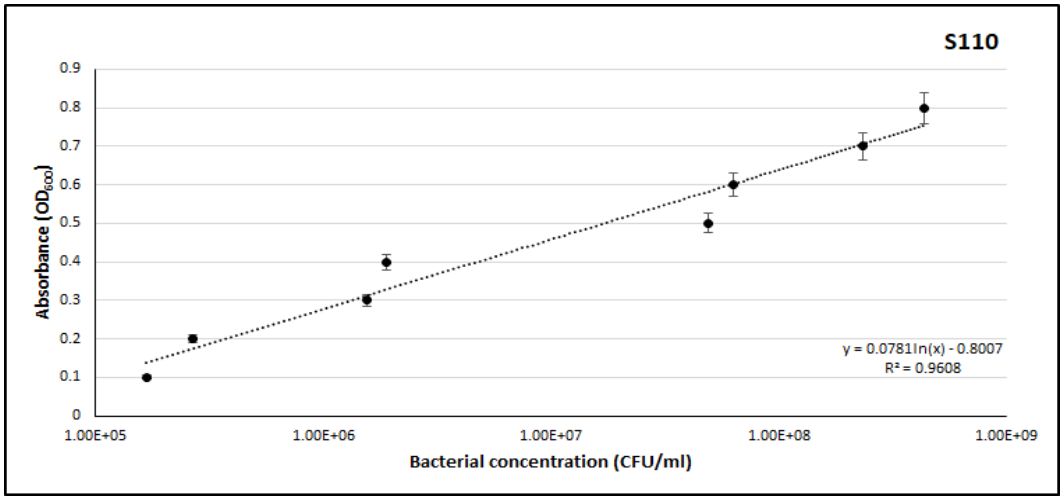

(C)

FIGURE A.3: Standard curves of PGP bacterial strains (A) L228, (B) L321 and (C) S110. Bacterial concentration, colony forming units per ml (CFU/ml), were plotted against the absorbance of bacterial cells at various OD readings ($OD_{(600)}$ 0.1 - 0.8) after 24 hours growth.

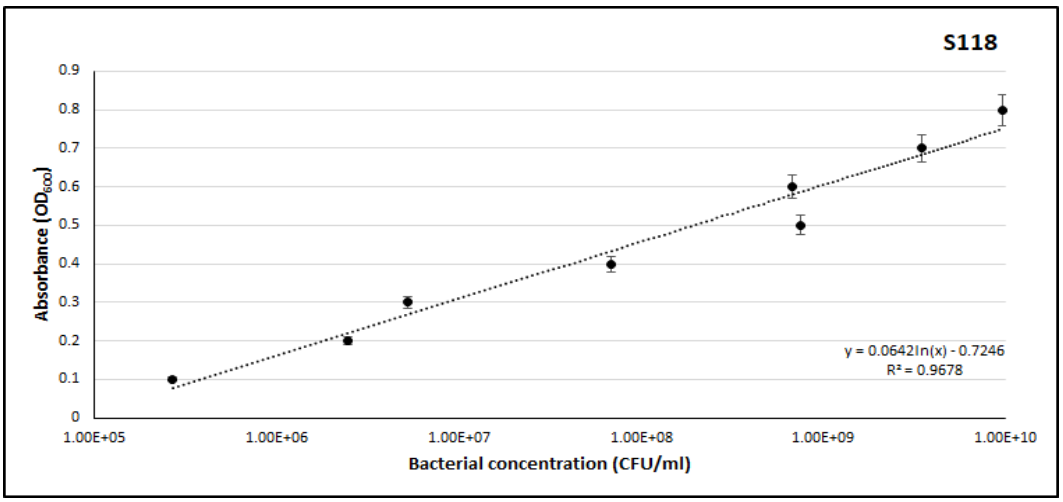

(A)

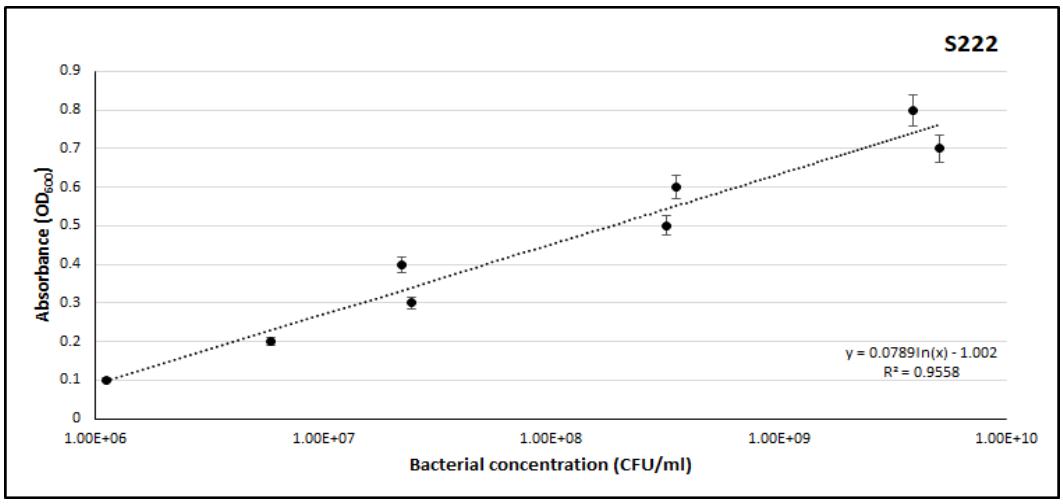

(B)

FIGURE A.4: Standard curves of PGP bacterial strains (A) S118 and (B) S222. Bacterial concentration, colony forming units per ml (CFU/ml), were plotted against the absorbance of bacterial cells at various OD readings ($OD_{(600)}$ 0.1 - 0.8) after 24 hours growth.

A.2 Susceptibility Testing of Nematodes to PGP Bacteria and their Metabolites

TABLE A.1: Statistical assessment of the percentage mortalities of *C. elegans*, *P. pacificus* and *M. javanica* to PGP bacterial strains at high, medium and low concentrations after 24 and 48 hour exposures. Bacterial concentrations for each strain are reported in Table 2.5. Non-parametric Kruskal-Wallis H test was performed on the bacterial treatments and controls with a Bonferroni pairwise correction.

Strain[1]	**Time (h)**[2]	**Kruskal-Wallis**	**Bonferroni**[3]		
			H-C	**M-C**	**L-C**
		Caenorhabditis elegans			
L321	24	χ^2 = 56.51, p = 0.000	p = 0.000	p = 0.000	p = 0.000
	48	χ^2 = 78.86, p = 0.000	p = 0.000	p = 0.000	-
F113	24	χ^2 = 68.26, p = 0.000	p = 0.000	p = 0.000	p = 0.000
	48	χ^2 = 81.67, p = 0.000	p = 0.000	p = 0.000	p = 0.000
L228	24	χ^2 = 88.61, p = 0.000	p = 0.000	p = 0.000	-
	48	χ^2 = 88.60, p = 0.000	p = 0.000	p = 0.000	p = 0.000
S222	24	χ^2 = 52.62, p = 0.000	p = 0.000	p = 0.000	p = 0.000
	48	χ^2 = 65.04, p = 0.000	p = 0.000	p = 0.000	p = 0.000
L124	24	χ^2 = 20.28, p = 0.000	p = 0.001	p = 0.019	p = 0.000
	48	χ^2 = 38.78, p = 0.000	p = 0.000	p = 0.000	p = 0.000
S118	24	χ^2 = 63.35, p = 0.000	p = 0.000	p = 0.000	p = 0.000
	48	χ^2 = 81.67, p = 0.000	p = 0.000	p = 0.000	p = 0.000
S110	24	χ^2 = 21.56, p = 0.000	p = 0.001	p = 0.000	p = 0.001
	48	χ^2 = 24.90, p = 0.000	p = 0.000	p = 0.000	p = 0.000
		Pristionchus pacificus			
L321	24	χ^2 = 37.19, p = 0.000	p = 0.000	-	-
	48	χ^2 = 41.91, p = 0.000	p = 0.001	-	-
F113	24	χ^2 = 27.83, p = 0.000	p = 0.000	p = 0.000	p = 0.015
	48	χ^2 = 29.38, p = 0.000	p = 0.000	p = 0.000	p = 0.005
L228	24	χ^2 = 42.87, p = 0.000	p = 0.000	p = 0.049	-
	48	χ^2 = 26.47, p = 0.000	p = 0.007	p = 0.000	p = 0.000
S222	24	χ^2 = 46.20, p = 0.000	p = 0.000	-	-
	48	χ^2 = 27.46, p = 0.000	p = 0.000	p = 0.018	-
L124	24	χ^2 = 24.50, p = 0.000	p = 0.034	p = 0.000	p = 0.000
	48	χ^2 = 27.80, p = 0.000	p = 0.000	p = 0.000	p = 0.000
S118	24	χ^2 = 45.97, p = 0.000	p = 0.000	p = 0.000	-
	48	χ^2 = 38.06, p = 0.000	p = 0.000	p = 0.001	-
S110	24	χ^2 = 38.50, p = 0.000	p = 0.000	p = 0.001	-
	48	χ^2 = 34.02, p = 0.000	p = 0.000	p = 0.000	-
		Meloidogyne javanica			
L321	24	χ^2 = 52.76, p = 0.000	p = 0.000	p = 0.000	p = 0.000
	48	χ^2 = 52.76, p = 0.000	p = 0.000	p = 0.000	p = 0.000
F113	24	χ^2 = 66.72, p = 0.000	p = 0.000	p = 0.000	p = 0.05
	48	χ^2 = 66.46, p = 0.000	p = 0.000	p = 0.000	p = 0.037
L228	24	χ^2 = 52.76, p = 0.000	p = 0.000	p = 0.000	p = 0.000
	48	χ^2 = 50.90, p = 0.000	p = 0.000	p = 0.000	p = 0.000
S222	24	χ^2 = 17.02, p = 0.001	p = 0.000	p = 0.003	p = 0.003
	48	χ^2 = 23.26, p = 0.000	p = 0.000	p = 0.002	p = 0.028
L124	24	χ^2 = 43.73, p = 0.000	p = 0.000	p = 0.000	p = 0.000

Continued on next page

Table A.1 – *Continued from previous page*

Strain	Time (h)	Kruskal-Wallis	Bonferroni		
			H-C	M-C	L-C
	48	χ^2 = 44.73, p = 0.000	p = 0.000	p = 0.000	p = 0.000
S118	24	χ^2 = 31.59, p = 0.000	p = 0.000	p = 0.000	p = 0.000
	48	χ^2 = 27.85, p = 0.000	p = 0.000	p = 0.000	p = 0.001

[1] Strain = endophytic bacterial strain utilised.

[2] Time = % mortality was assessed after 24 and 48 hours exposure.

[3] H - C represents the Bonferroni significance between the high endophytic bacterial treatments, M - C represents the medium and L - C represents the low endophytic bacterial treatments compared to the control (sterile ¼ strength Ringers) treatment. - represents no statistically significant difference between bacterial treatments and control. Statistical significance at α = 0.05 level.

TABLE A.2: Statistical assessment of the mortalities recorded in *C. elegans*, *P. pacificus* and PPN exposed to PGP bacterial metabolites at high, medium and low concentrations (see Table 2.5 for bacterial concentrations) for 24 and 48 hours exposure. Non-parametric Kruskal Wallis H test was performed on the bacterial treatments and control with a Bonferroni pairwise correction.

Metabolites[1]	Life stage	Hours[2]	Kruskal Wallis	Bonferroni		
				H-C[3]	M-C	L-C
			Caenorhabditis elegans			
F113	Adult	24	χ^2 = 34.62, p = 0.000	p = 0.000	p = 0.000	-
		48	χ^2 = 34.05, p = 0.000	p = 0.000	p = 0.000	-
	J3/J4	24	χ^2 = 31.96, p = 0.000	p = 0.000	p = 0.000	p = 0.000
		48	χ^2 = 46.35, p = 0.000	p = 0.000	p = 0.000	p = 0.000
	J1/J2	24	χ^2 = 25.01, p = 0.000	p = 0.000	p = 0.003	-
		48	χ^2 = 42.78, p = 0.000	p = 0.000	p = 0.000	-
S118	Adult	24	χ^2 = 33.81, p = 0.000	p = 0.000	p = 0.000	-
		48	χ^2 = 36.36, p = 0.000	p = 0.000	-	-
	J3/J4	24	χ^2 = 30.67, p = 0.000	p = 0.032	-	p = 0.000
		48	χ^2 = 42.92, p = 0.000	p = 0.040	-	-
	J1/J2	24	χ^2 = 33.82, p = 0.000	p = 0.001	p = 0.000	-
		48	χ^2 = 33.99, p = 0.000	-	-	p = 0.000
L228	Adult	24	χ^2 = 44.69, p = 0.000	p = 0.000	p = 0.008	-
		48	χ^2 = 45.66, p = 0.000	p = 0.000	p = 0.009	-
	J3/J4	24	χ^2 = 42.72, p = 0.000	-	p = 0.004	p = 0.000
		48	χ^2 = 42.17, p = 0.000	-	-	p = 0.011
	J1/J2	24	χ^2 = 36.23, p = 0.000	p = 0.000	p = 0.000	-
		48	χ^2 = 31.62, p = 0.000	-	p = 0.000	p = 0.000
S222	Adult	24	χ^2 = 38.62, p = 0.000	-	p = 0.002	p = 0.000
		48	χ^2 = 33.64, p = 0.000	-	p = 0.009	p = 0.000
	J3/J4	24	χ^2 = 15.91, p = 0.001	p = 0.049	p = 0.044	-
		48	χ^2 = 41.74, p = 0.000	p = 0.000	p = 0.000	-
	J1/J2	24	χ^2 = 18.55, p = 0.000	p = 0.038	p = 0.000	-
		48	χ^2 = 45.08, p = 0.000	p = 0.000	p = 0.000	-
L124	Adult	24	χ^2 = 29.13, p = 0.000	-	p = 0.002	p = 0.005
		48	χ^2 = 47.42, p = 0.000	-	p = 0.000	p = 0.000
	J3/J4	24	χ^2 = 34.98, p = 0.000	p = 0.049	-	p = 0.001
	J1/J2	24	χ^2 = 41.25, p = 0.000	p = 0.000	p = 0.002	-

Continued on next page

Table A.2 – *Continued from previous page*

Metabolites	Life stage	Hours	Kruskal Wallis	Bonferroni		
				H-C	M-C	L-C
		48	χ^2 = 47.87, p = 0.000	p = 0.000	p = 0.000	-
L321	Adult	48	χ^2 = 47.52, p = 0.000	p = 0.000	p = 0.000	-
	J3/J4	24	χ^2 = 33.89, p = 0.000	p = 0.000	p = 0.000	-
		48	χ^2 = 44.33, p = 0.000	p = 0.000	p = 0.003	-
	J1/J2	24	χ^2 = 30.93, p = 0.000	p = 0.000	-	-
		48	χ^2 = 19.83, p = 0.000	p = 0.003	p = 0.003	-
			Pristionchus pacificus			
F113	Adult	24	χ^2 = 52.78, p = 0.000	p = 0.000	p = 0.000	-
		48	χ^2 = 39.01, p = 0.000	p = 0.000	p = 0.000	p = 0.000
	J3/J4	24	χ^2 = 46.58, p = 0.000	p = 0.000	p = 0.000	p = 0.000
		48	χ^2 = 41.98, p = 0.000	p = 0.000	p = 0.000	p = 0.000
	J1/J2	24	χ^2 = 52.78, p = 0.000	p = 0.000	p = 0.000	p = 0.000
		48	χ^2 = 32.84, p = 0.000	p = 0.000	p = 0.000	p = 0.002
S118	Adult	24	χ^2 = 35.09, p = 0.000	p = 0.000	p = 0.002	-
		48	χ^2 = 25.40, p = 0.000	p = 0.000	-	-
	J3/J4	24	χ^2 = 18.95, p = 0.000	p = 0.000	p = 0.004	-
		48	χ^2 = 22.75, p = 0.000	p = 0.000	p = 0.027	-
	J1/J2	24	χ^2 = 28.70, p = 0.000	p = 0.000	-	p = 0.014
		48	χ^2 =29.99, p = 0.000	p = 0.000	p = 0.003	-
L228	J3/J4	24	χ^2 = 31.43, p = 0.000	-	p = 0.000	p = 0.009
		48	χ^2 = 40.67, p = 0.000	p = 0.000	p = 0.010	-
	J1/J2	24	χ^2 = 78.62, p = 0.000	p = 0.000	p = 0.000	-
		48	χ^2 = 26.62, p = 0.000	p = 0.000	-	-
S222	Adult	24	χ^2 = 46.21, p = 0.000	p = 0.000	-	-
		48	χ^2 = 26.73, p = 0.000	p = 0.000	p = 0.017	-
	J3/J4	24	χ^2 = 34.42, p = 0.000	-	-	-
		48	χ^2 = 31.25, p = 0.000	p = 0.000	-	p = 0.000
	J1/J2	24	χ^2 = 26.68, p = 0.000	p = 0.018	-	-
		48	χ^2 = 28.19, p = 0.000	p = 0.001	p = 0.001	-
L124	Adult	24	χ^2 = 26.86, p = 0.000	-	p = 0.000	p = 0.000
		48	χ^2 = 52.79, p = 0.000	p = 0.000	p = 0.000	p = 0.000
	J3/J4	24	χ^2 = 43.67, p = 0.000	p = 0.000	p = 0.005	-
		48	χ^2 = 42.95, p = 0.000	p = 0.000	-	-
	J1/J2	24	χ^2 = 44.79, p = 0.000	p = 0.000	p = 0.001	-
		48	χ^2 = 20.77, p = 0.000	p = 0.000	p = 0.005	p = 0.022
L321	Adult	24	χ^2 = 52.78, p = 0.000	p = 0.000	p = 0.000	p = 0.000
		48	χ^2 = 28.55, p = 0.000	p = 0.000	-	-
	J3/J4	24	χ^2 = 30.14, p = 0.000	p = 0.000	p = 0.000	p = 0.003
		48	χ^2 = 10.32, p = 0.016	p = 0.026	-	-
	J1/J2	24	χ^2 = 27.35, p = 0.000	p = 0.000	p = 0.006	-
		48	χ^2 = 39.27, p = 0.000	p = 0.000	-	-
			Meloidogyne javanica			
F113	J2	24	χ^2 = 17.99, p = 0.000	-	p = 0.005	p = 0.001
S118	J2	24	χ^2 = 13.71, p = 0.003	p = 0.024	-	p = 0.005
		48	χ^2 = 14.12, p = 0.003	-	p = 0.016	p = 0.004
S222	J2	24	χ^2 =14.18, p = 0.003	p = 0.004	-	p = 0.012
		48	χ^2 = 19.74, p = 0.000	-	p = 0.003	p = 0.001
L124	J2	24	χ^2 = 16.58, p = 0.001	p = 0.003	p = 0.003	p = 0.021
		48	χ^2 = 16.62, p = 0.001	-	p = 0.003	p = 0.003
L228	J2	24	χ^2 = 15.89, p = 0.001	p = 0.001	-	-
		48	χ^2 = 16.48, p = 0.001	p = 0.000	p = 0.038	-

Continued on next page

Table A.2 – *Continued from previous page*

Metabolites	Life stage	Hours	Kruskal Wallis	Bonferroni		
				H-C	M-C	L-C
L321	J2	24	χ^2 = 13.81, p = 0.003	p = 0.031	p = 0.004	-
			Globodera pallida			
F113	J2	24	χ^2 = 18.67, p = 0.000	p = 0.002	p = 0.002	p = 0.005
S118	J2	24	χ^2 = 22.48, p = 0.0001	p = 0.001	p = 0.000	p = 0.001
S222	J2	24	χ^2 = 22.48, p = 0.000	p = 0.001	p = 0.000	p = 0.001
L124	J2	24	χ^2 = 14.94, p = 0.002	p = 0.012	p = 0.015	p = 0.015
L228	J2	24	χ^2 = 15.70, p = 0.001	p = 0.004	p = 0.015	p = 0.015
L321	J2	24	χ^2 = 17.38, p = 0.001	p = 0.031	p = 0.000	p = 0.043

1 Metabolites refers to the endophytic bacterial metabolites utilised in these tests.

2 Assays were assessed after 24 and 48 hours.

3 H - C represents the Bonferroni significance between the high endophytic bacterial treatments, M - C represents the medium and L - C represents the low endophytic bacterial treatments compared to the control (sterile ¼ strength Ringers) treatment. - = No significance. Statistical significance at α = 0.05 level.

A.3 Sensitivity of Nematodes to 2,4-DAPG and the Effect of PGP Bacterial Metabolites on Egg Hatch and Juvenile Mortality

TABLE A.3: Statistical assessment of (1) the sensitivity of the nematodes to 2,4-DAPG, (2) the sensitivity of the nematodes to the parallel methanol controls, (3) the effect of PGP bacterial metabolites on nematode egg hatch and (4) on juvenile mortality of the nematodes *C. elegans* and PPN. Non-parametric Kruskal Wallis H test was performed on all treatments compared to the controls with a Bonferroni pairwise correction post-hoc test.

Nematode	Time	Kruskal Wallis	Bonferroni
		2,4-DAPG	
C. elegans	24h	χ^2 = 37.48, p = 0.000	500 ppm, p = 0.000
			200 ppm, p = 0.002
			100 ppm, p = 0.046
	48h	χ^2 = 36.06, p = 0.000	500 ppm, p = 0.000
			200 ppm, p = 0.000
M. javanica	24h	χ^2 = 38.27, p = 0.000	500 ppm, p = 0.000
			200 ppm, p = 0.000
G. pallida	24h	χ^2 = 23.67, p = 0.000	100 ppm, p = 0.002
			75 ppm, p = 0.002
		Methanol	
C. elegans	24h	χ^2 = 3.90, p = 0.273	-
M. javanica	24h	χ^2 = 2.78, p = 0.427	-
G. pallida	24h	χ^2 = 7.53, p = 0.570	-
		Egg hatch	
M. javanica	5d	χ^2 = 91.41, p = 0.000	S110, p = 0.000
			L124, p = 0.000

Continued on next page

Table A.3 – *Continued from previous page*

Nematode	Time	Kruskal Wallis	Bonferroni
			S222, p = 0.000
			L321, p = 0.000
			L228, p = 0.000
			F113, p = 0.000
			S118, p = 0.002
G. pallida	7d	χ^2 = 61.65, p = 0.000	S222, p = 0.000
			S118, p = 0.000
			L132, p = 0.000
			L124, p = 0.004
			L111, p = 0.005
			F113, p = 0.026
			S110, p = 0.029
			L321, p = 0.048
			F113 + L124, p = 0.014
Juvenile mortality			
M. javanica	5d	χ^2 = 83.07, p = 0.000	-
G. pallida	7d	χ^2 = 33.37, p = 0.003	L321 + L124, p = 0.022

Statistical significance at α = 0.05 level.

- = No significant difference between the treatments and the control in the post hoc test

A.4 Mass Spectral Display of Compounds Identified

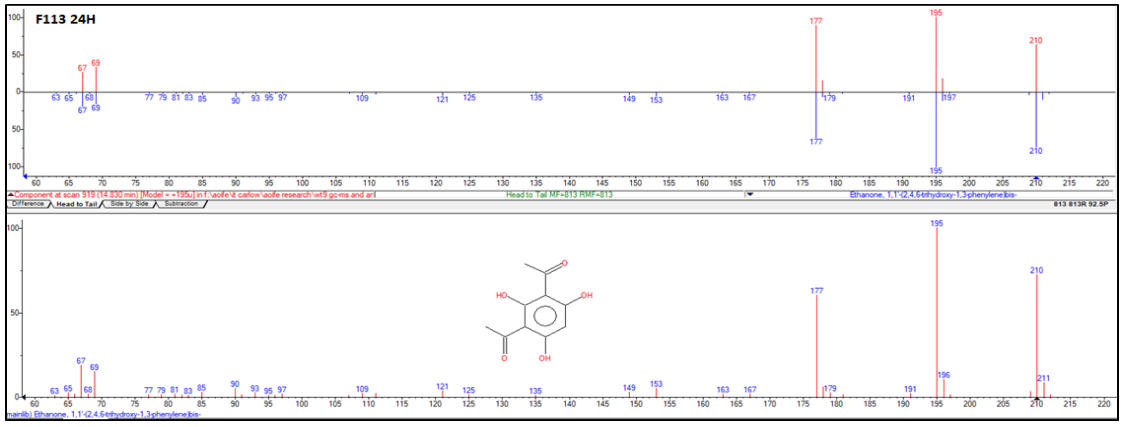

(A)

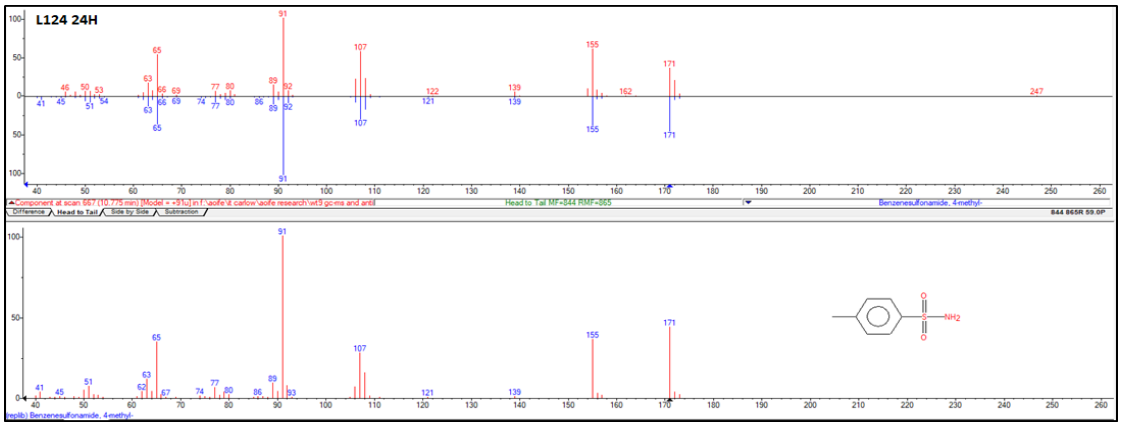

(B)

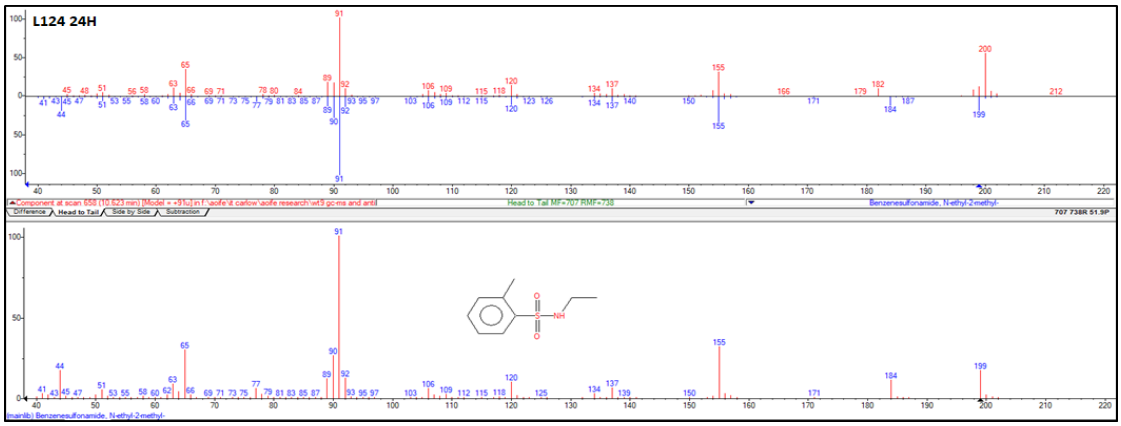

(C)

FIGURE A.5: Mass spectral display of bacterial metabolites identified on the NIST library: (A) Ethanone, 1,1'- (2,4,6-trihydroxy-1,3-phenylene)dis- (Ions: 177, 195, 210 *m/z*. RT = 14.83 and MF = 813), (B) 4-methylbenzenesulfonamide (Ions: 91, 107, 155 *m/z*. RT = 10.71 and MF = 825) and (C) N-ethyl-2-methylbenzenesulfonamide (Ions: 65, 91, 200 *m/z*. RT = 10.62 and MF = 723). The upper mass spectrum in each figure displays a Head to Tail comparison of the Target (Blue) and the component Hit (Red). The lower mass spectrum displays the Target compound, with ions of interest and compound structure.

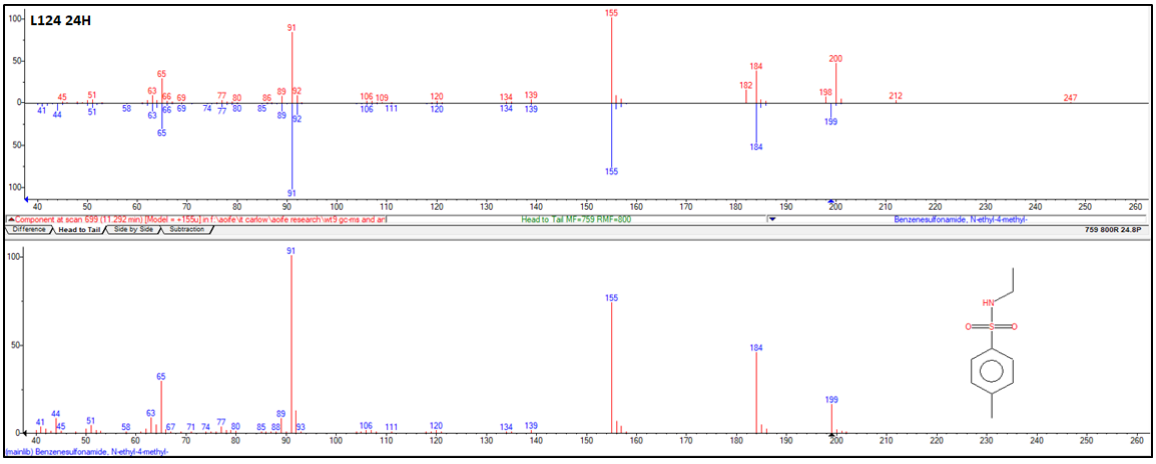

(A)

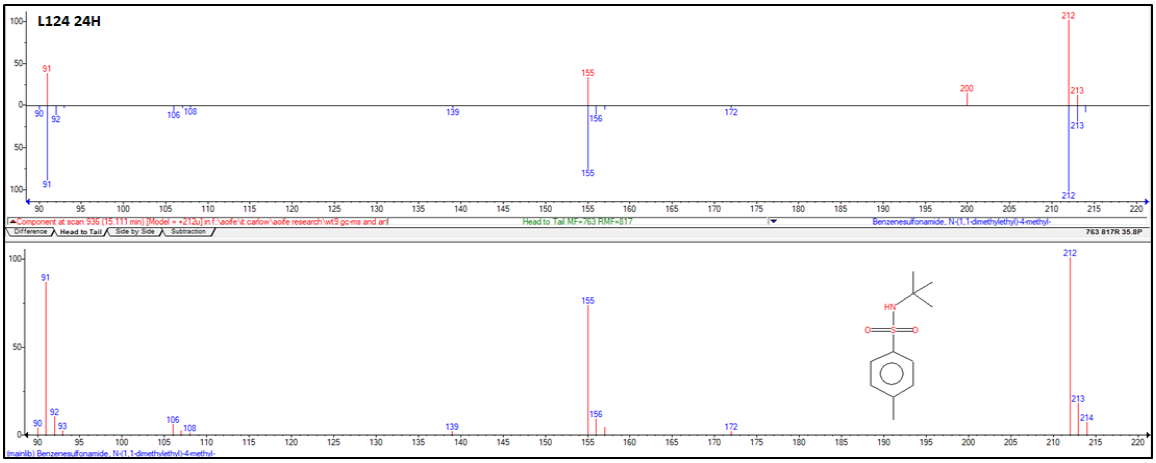

(B)

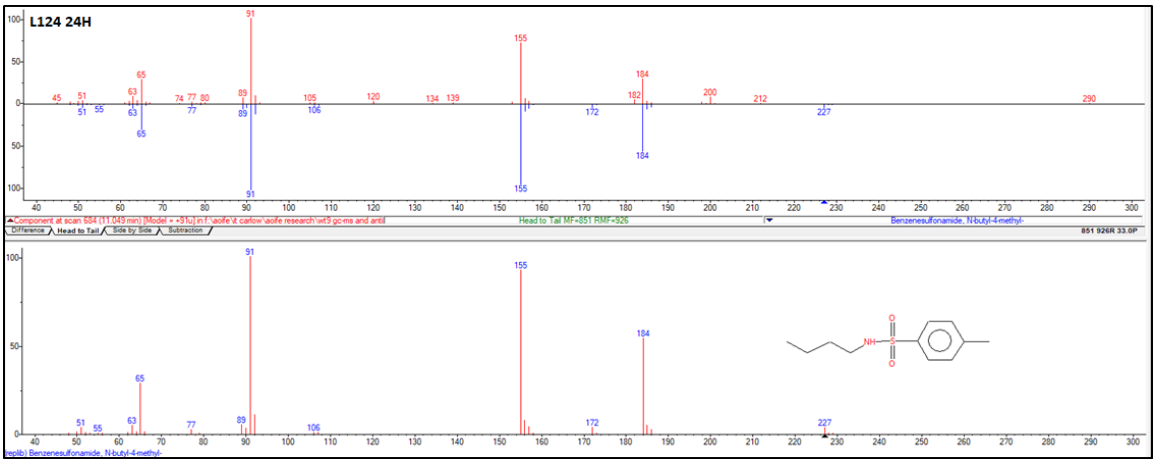

(C)

FIGURE A.6: Mass spectral display of bacterial metabolites identified on NIST library: (A) N-ethyl-4-methylbenzenesulfonamide (Ions: 91, 155, 200 *m/z*. RT = 11.29 and MF = 780), (B) N-(1,1-dimethylethyl)-4-methylbenzenesulfonamide (Ions: 91, 155, 212 *m/z*. RT = 15.11 and MF = 790) and (C) N-butyl-4-methylbenzenesulfonamide (Ions: 91, 155, 184 *m/z*. RT = 11.05 and MF = 889). The upper mass spectrum in each figure displays a Head to Tail comparison of the Target (Blue) and the component Hit (Red). The lower mass spectrum displays the Target compound, with ions of interest and compound structure.

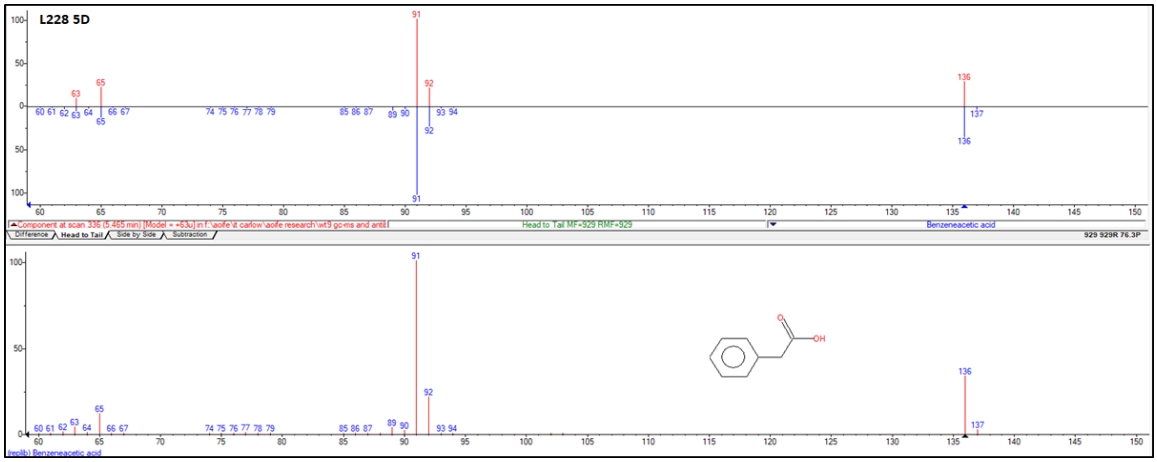

(A)

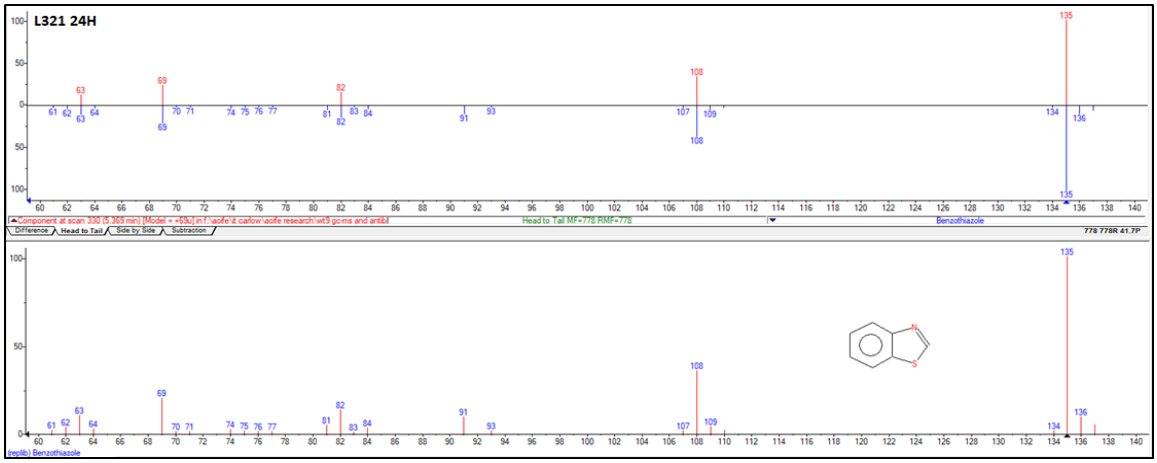

(B)

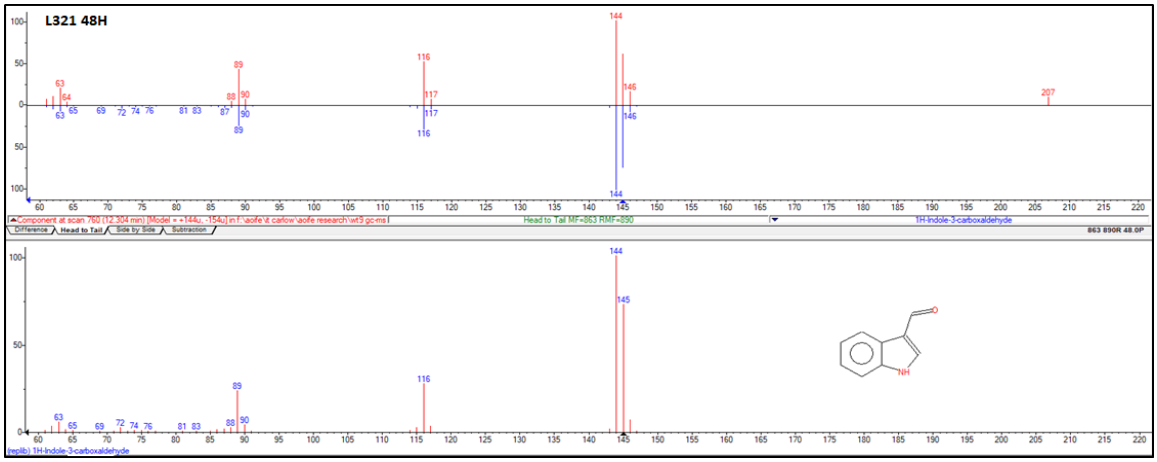

(C)

FIGURE A.7: Mass spectral display of bacterial metabolites identified on NIST library: (A) Benzeneacetic acid (Ions: 91, 92, 136 *m/z*. RT = 05.47 and MF = 929), (B) Benzothiazole (Ions: 69, 108, 135 *m/z*. RT = 5.37 and MF = 778) and (C) 1H Indole-3-carboxaldehyde (Ions: 89, 116, 144 *m/z*. RT = 12.30 and MF = 877). The upper mass spectrum in each figure displays a Head to Tail comparison of the Target (Blue) and the component Hit (Red). The lower mass spectrum in each figure displays the Target compound, with ions of interest and compound structure.

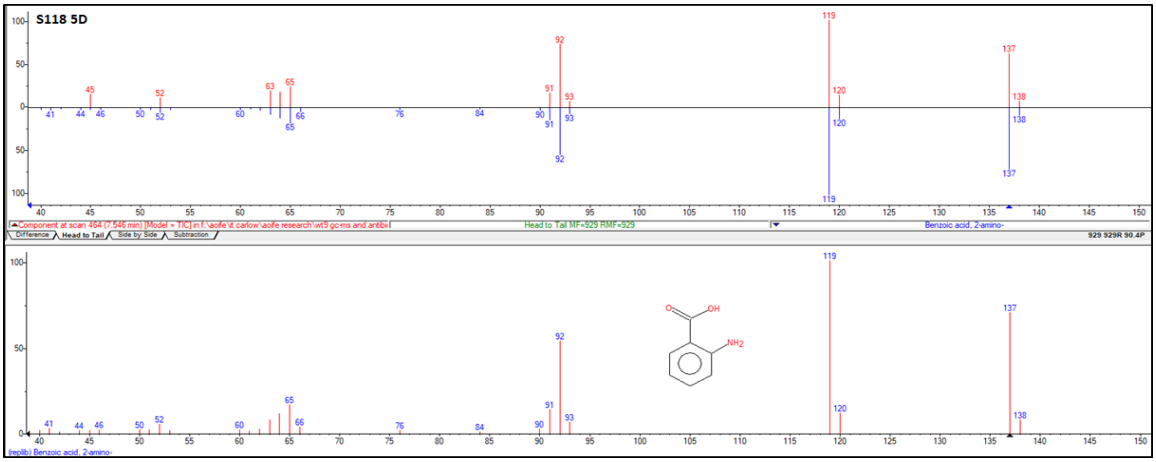

(A)

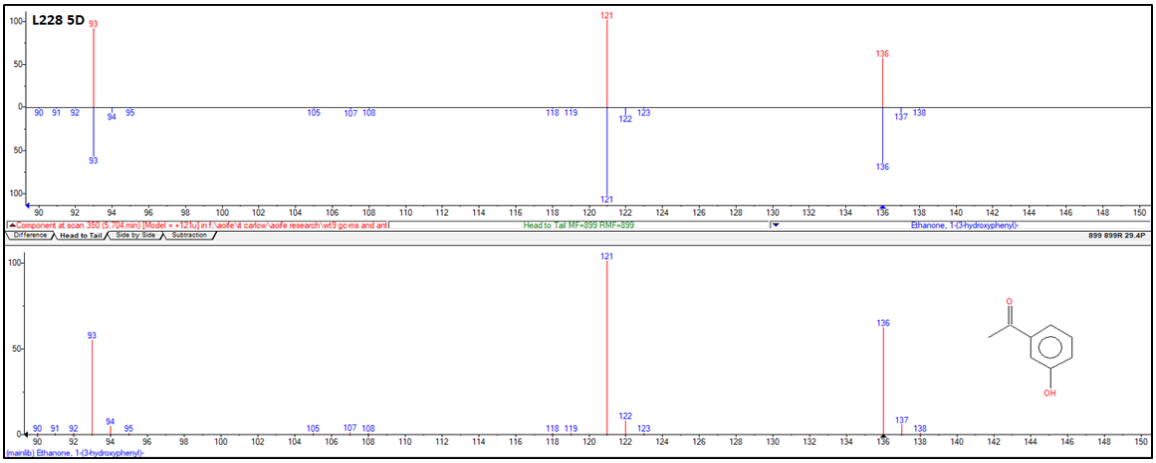

(B)

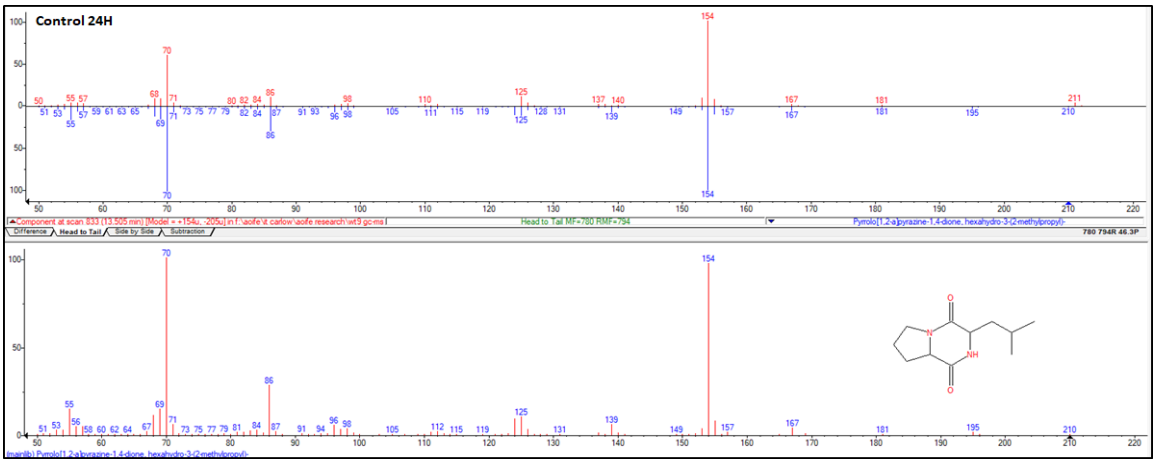

(C)

FIGURE A.8: Mass spectral display of bacterial metabolites identified on NIST library: (A) 2-aminobenzoic acid (Ions: 92, 119, 137 *m/z*. RT = 7.55 and MF = 929) (B) 1-(3hydroxyphenyl)ethanone (Ions: 93, 121, 136 *m/z*. RT = 5.70 and MF = 899) and (C) hexahydro-3(2methylpropyl)-pyrrolo[1,2-a]pyrazine-1,4-dione (Ions: 70, 154 *m/z*. RT = 13.51 and MF = 787). The upper mass spectrum in each figure displays a Head to Tail comparison of the Target (Blue) and the component Hit (Red). The lower mass spectrum displays the Target compound, with ions of interest and compound structure.

Appendix B

Supplementary Information for Chapter 3

B.1 Nematode Attraction to PGP Bacteria and 2,4-DAPG

TABLE B.1: Chemotaxis Index (% CI) statistical analysis.

	4 hours	**24 hours**
	Caenorhabditis elegans	
Kruskal Wallis	χ^2 = 0.96, p = 0.966	χ^2 = 0.64, p = 0.986
Bonferroni [1]	NS	NS
	Meloidogyne javanica	
Kruskal Wallis	χ^2 = 4.37, p = 0.490	χ^2 = 4.37, p = 0.498
Bonferroni	NS	NS
	Globodera pallida	
Kruskal Wallis	χ^2 = 12.52, p = 0.028	χ^2 = 7.22 ,p = 0.205
Bonferroni	L124, p = 0.012	NS

1 Bonferroni significance compares PGP bacterial treatments to the control treatment.
NS = No significance.
Statistical significance at α = 0.05 level.

B.2 Influence of PGP Bacteria and 2,4-DAPG on *Meloidogyne javanica* Development in Tomato Plants

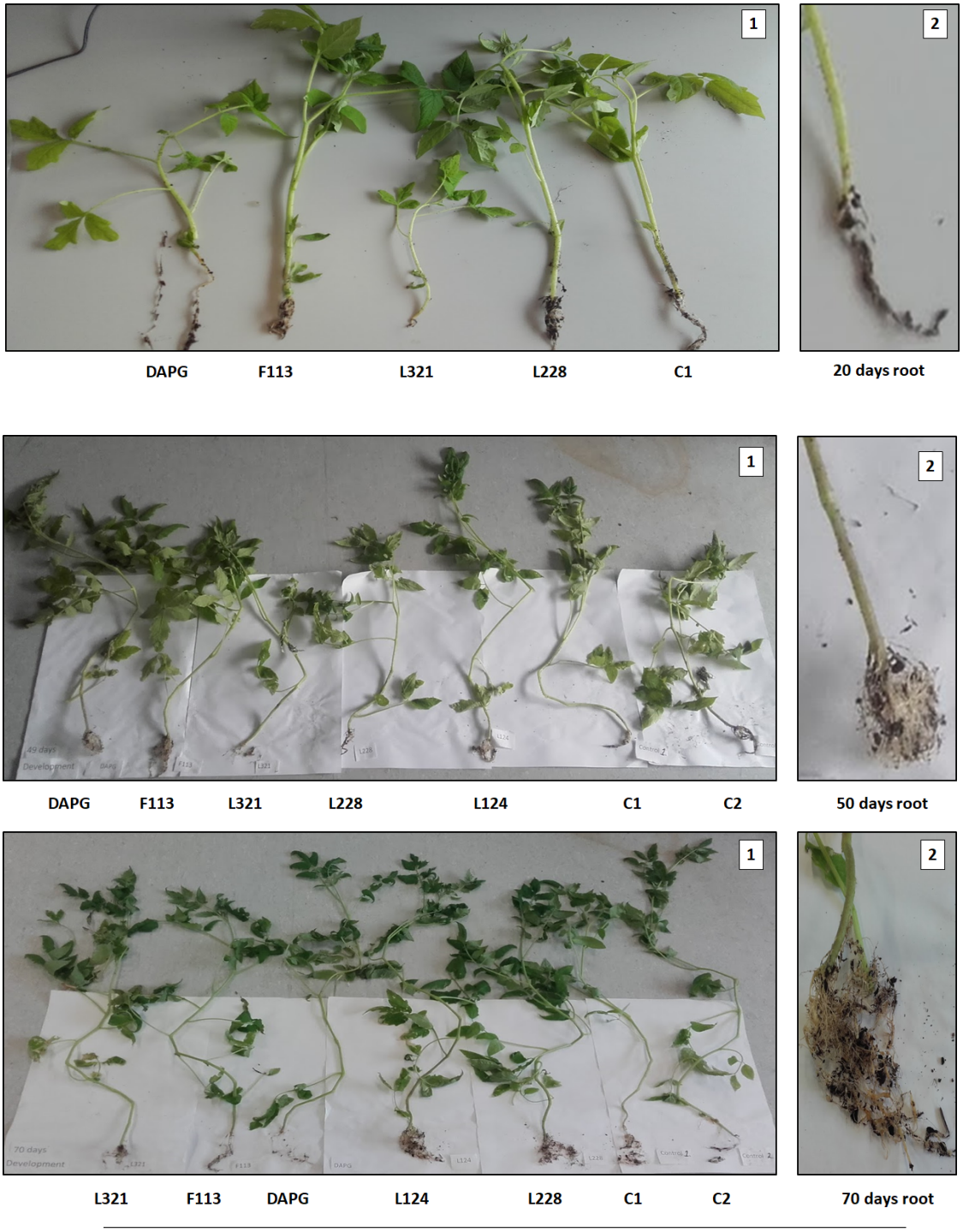

FIGURE B.1: Tomato plants treated with PGP bacterial strains and 2,4-DAPG. The plants were infected with *M. javanica* and plant biomass was assessed after 20, 50 and 70 days. There were 6 replications of each treatment at each time point. Control treatments C1 = Nematodes and no bacteria and C2 = No nematodes and no bacteria. Figure (1) Plants inoculated with bacterial strains after (A) 20 days (B) 50 days and (C) 70 days. Increase in root mass Figure (2) with nematode infection (root galls) evident after 50 and 70 days.

TABLE B.2: Statistical assessment of tomato plant biomass inoculated with bacteria/spiked with 2,4-DAPG and infected with *Meloidogyne javanica*.

Treatment	**Time**		
	20 days	**50 days**	**70 days**
Mean Tomato Plant Height (cm)			
Kruskal Wallis	χ^2 = 18.21, p = 0.006	χ^2 = 12.25, p = 0.057	χ^2 = 18.84, p = 0.004
Bonferroni	F113-C1[1], p = 0.006	NS[1]	NS
Mean Number of Leaves Plant			
Kruskal Wallis	χ^2 = 22.81, p = 0.001	χ^2 = 18.53, p = 0.005	χ^2 = 14.10, p = 0.029
Bonferroni	NS	NS	L124-C1, p = 0.035
Fresh Weight - Stem and Leaf (g)			
Kruskal Wallis	χ^2 = 21.52, p = 0.001	χ^2 = 17.68, p = 0.007	χ^2 = 11.47, p = 0.075
Bonferroni	F113-C1, p = 0.019	NS	NS
Fresh Weight - Roots (g)			
Kruskal Wallis	χ^2 = 26.04, p = 0.000	χ^2 = 12.31, p = 0.055	χ^2 = 9.12, p = 0.167
Bonferroni	F113-C1, p = 0.002 L124-C1, p = 0.002	NS	NS
Dry Weight - Stem and Leaf (g)			
Kruskal Wallis	χ^2 = 18.33, p = 0.005	χ^2 = 18.08, p = 0.006	χ^2 = 17.26, p = 0.008
Bonferroni	NS	NS	NS
Dry Weight - Roots (g)			
Kruskal Wallis	χ^2 = 10.39, p = 0.109	χ^2 = 14.86, p = 0.021	χ^2 = 23.31, p = 0.001
Bonferroni	NS	NS	F113-C1, p = 0.001

1 NS = No significance.

Kruskal Wallis Degrees of Freedom = 6.

Statistical significance at α = 0.05 level.

TABLE B.3: Statistical assessment of the effect of *Meloidogyne javanica* development in tomato plants inoculated with bacteria or spiked with antibiotic treatments, 20, 50 and 70 days post infection (see Figures 3.9a, 3.9b, 3.9c, 3.10a, 3.10b and 3.10c).

Statistical test	**Time**		
	20 days	**50 days**	**70 days**
		J2 Infective Juvenile	
Kruskal Wallis	χ^2 = 6.60, p = 0.359	χ^2 = 10.63, p = 0.101	χ^2 = 19.02, p = 0.004
Bonferroni	NS	NS	F113, p = 0.036
		J3 / J4 Stage	
Kruskal Wallis	χ^2 = 19.42, p = 0.004	χ^2 = 17.81, p = 0.007	χ^2 = 14.28, p = 0.027
Bonferroni	L124, p = 0.012	NS	NS
		Young Adult Female	
Kruskal Wallis	χ^2 = 25.47, p = 0.000	χ^2 = 13.10, p = 0.042	χ^2 = 0.00, p = 1.000
Bonferroni	L321, p = 0.008	F113, p = 0.003 L228, p = 0.002 2,4-DAPG, p = 0.010	NS
		Mature Adult Female	
Kruskal Wallis	χ^2 = 20.60, p = 0.002	χ^2 = 14.59, p = 0.024	χ^2 = 24.89, p = 0.000
Bonferroni	F113, p = 0.043	NS	NS
		Feeding sites	
Kruskal Wallis	χ^2 = 23.13, p = 0.001	χ^2 = 35.76, p = 0.000	χ^2 = 20.44, p = 0.002
Bonferroni	L228, p = 0.004	L124, p = 0.000	NS
		Egg masses	
Kruskal Wallis	χ^2 = 4.43, p = 0.619	χ^2 = 13.47, p = 0.036	χ^2 = 27.76, p = 0.000
Bonferroni	NS	NS	2,4-DAPG, p = 0.015

B.3 Influence of PGP Bacteria and 2,4-DAPG on *Globodera pallida* Development in Potato Plants

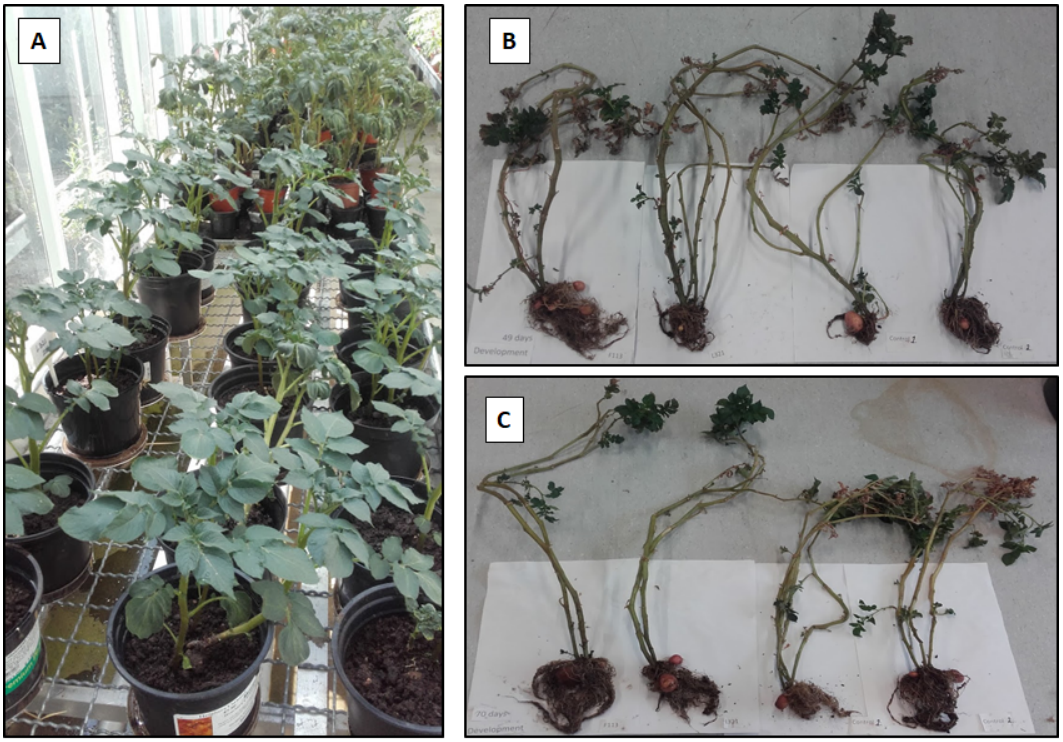

FIGURE B.2: Potato plants treated with PGP bacterial strains and 2,4-DAPG. The plants were infected with *Globodera pallida* and plant biomass was assessed after 20, 50 and 70 days. There were 6 replications of each treatment at each time point. Control treatments C1 = Nematodes and no bacteria and C2 = No nematodes and no bacteria. Plants were inoculated with bacterial strains after (A) 20 days (B) 50 days and (C) 70 days.

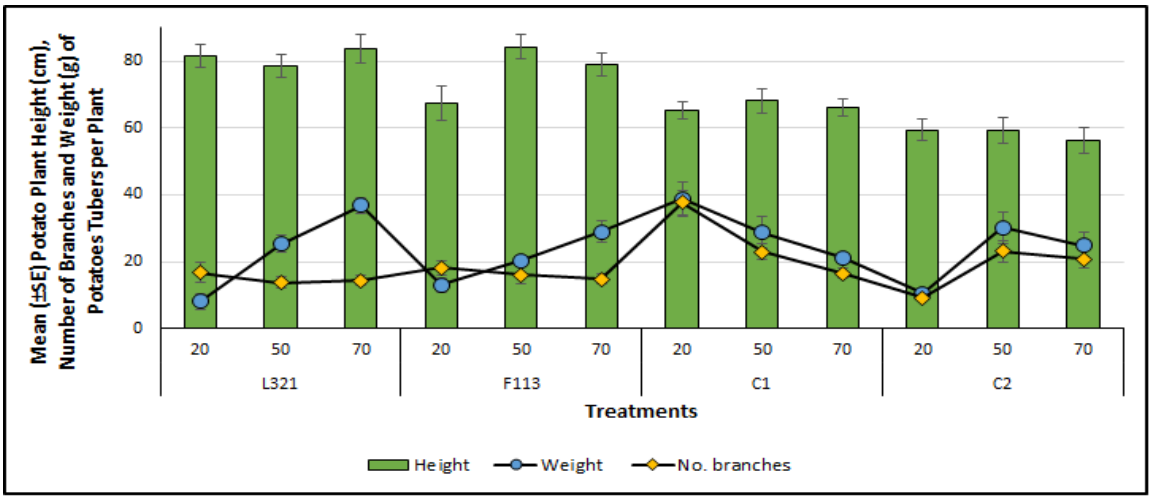

(A)

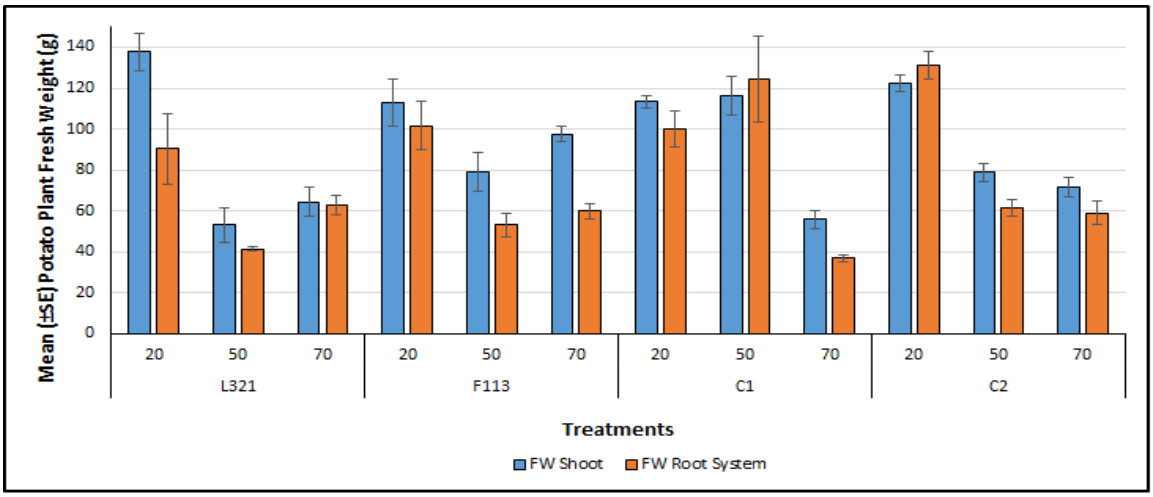

(B)

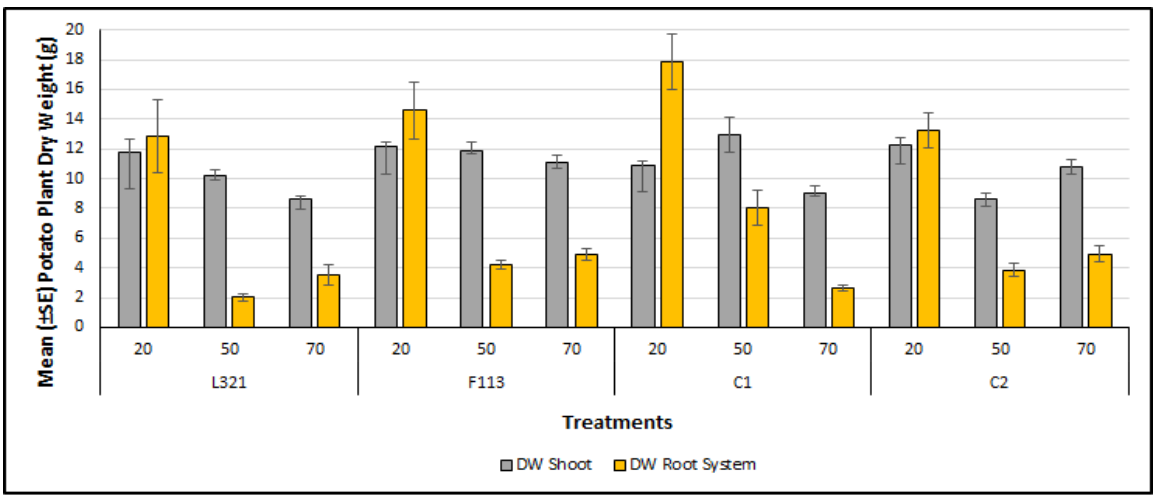

(C)

FIGURE B.3: Biomass of potato plants inoculated with PGP bacteria or spiked with 2,4-DAPG after 20, 50 and 70 days. Figure (A) Mean plant height, number of branches and weight of potatoes produced. Figure (B) FW = fresh weight. Figure (C) DW = dry weight. Error bars = ± SEM, see Appendix B, Table B.4 for statistical assessment.

TABLE B.4: Statistical assessment of potato plant biomass inoculated with bacteria/ spiked with 2,4-DAPG and infected with *Globodera pallida*.

Treatment	20 days	50 days	70 days
Mean Potato Plant Height (cm)			
Kruskal Wallis	$\chi^2 = 4.75$, p = 0.191	$\chi^2 = 4.88$, p = 0.181	$\chi^2 = 4.21$, p = 0.240
Bonferroni	NS[1]	NS	NS
Mean Number of Branches/ Plant			
Kruskal Wallis	$\chi^2 = 9.66$, p = 0.022	$\chi^2 = 5.29$, p = 0.152	$\chi^2 = 12.30$, p = 0.006
Bonferroni	NS	NS	L321, p = 0.028
Mean Weight of Potato Tubers (g)			
Kruskal Wallis	$\chi^2 = 7.29$, p = 0.063	$\chi^2 = 0.71$, p = 0.871	$\chi^2 = 2.82$, p = 0.421
Bonferroni	NS	NS	NS
Fresh Weight - Stem and Leaf (g)			
Kruskal Wallis	$\chi^2 = 1.74$, p = 0.628	$\chi^2 = 3.59$, p = 0.309	$\chi^2 = 8.53$, p = 0.036
Bonferroni	NS	NS	NS
Fresh Weight - Root system (g)			
Kruskal Wallis	$\chi^2 = 2.04$, p = 0.564	$\chi^2 = 4.77$, p = 0.190	$\chi^2 = 5.41$, p = 0.144
Bonferroni	NS	NS	NS
Dry Weight - Stem and Leaf (g)			
Kruskal Wallis	$\chi^2 = 10.15$, p = 0.017	$\chi^2 = 4.26$, p = 0.235	$\chi^2 = 3.68$, p = 0.299
Bonferroni	NS	NS	NS
Dry Weight - Roots system (g)			
Kruskal Wallis	$\chi^2 = 1.03$, p = 0.795	$\chi^2 = 5.37$, p = 0.147	$\chi^2 = 3.35$, p = 0.340
Bonferroni	NS	NS	NS

1 NS = No significance.

Kruskal Wallis Degrees of Freedom = 3.

Statistical significance at $\alpha = 0.05$ level.

B.4 Resistance of Treated Tomato Plants to *Meloidogyne javanica* Infection: Split Root System

TABLE B.5: Statistical assessment of tomato plant biomass in, ISR Part I and Part II. Error bars = ± SEM (see Figures 3.12, 3.13a and 3.13b).

Treatment	ISR Part I	ISR Part II
Mean Tomato Plant Height (cm)		
Control[1]	24.50 ± 1.50	23.42 ± 1.11
Kruskal Wallis	χ^2 = 8.93, p = 0.112	χ^2 = 15.01, p = 0.010
Bonferroni	NS[1]	NS
Mean Number of Leaves/ Plant		
Kruskal Wallis	χ^2 = 2.56, p = 0.767	χ^2 = 14.12, p = 0.015
Bonferroni	NS	NS
Mean Fresh Weight - Stem and Leaf (g)		
Kruskal Wallis	χ^2 = 5.91, p = 0.315	χ^2 = 16.42, p = 0.006
Bonferroni	NS	NS
Mean Fresh Weight - Roots (g)		
Kruskal Wallis	χ^2 = 4.42, p = 0.491	χ^2 = 13.08, p = 0.023
Bonferroni	NS	F113, p = 0.027
Mean Dry Weight - Stem and Leaf (g)		
Kruskal Wallis	χ^2 = 5.38, p = 0.372	χ^2 = 12.39, p = 0.030
Bonferroni	NS	NS
Mean Dry Weight - Roots (g)		
Kruskal Wallis	χ^2 = 22.81, p = 0.000	χ^2 = 14.39, p = 0.013
Bonferroni	2,4-DAPG, p = 0.011 L124, p = 0.046	F113, p = 0.048

1 NS = No significance.
Kruskal Wallis Degrees of Freedom = 5.
Statistical significance at α = 0.05 level.

FIGURE B.4: Statistical assessment of ISR Part I and Part II ($\pm$ SEM) in tomato plants after 30 days (see Figures 3.14a, 3.14b and 3.14c). NS = No significance. Degrees of freedom = 5. Statistical significance at α = 0.05 level.

Statistical test	**ISR I**		**ISR II**	
	Left pot	**Right pot**	**Left pot**	**Right pot**
		Adult Females		
Kruskal Wallis	χ^2 = 0.00, p = 1.000	χ^2 = 11.35, p = 0.045	χ^2 = 6.00, p = 0.306	χ^2 = 7.54, p = 0.183
Bonferroni	NS	NS	NS	NS
		Feeding sites		
Kruskal Wallis	χ^2 = 0.00, p = 1.000	χ^2 = 8.28, p = 0.142	χ^2 = 9.58, p = 0.088	χ^2 = 9.62, p = 0.687
Bonferroni	NS	NS	NS	NS
		Egg masses		
Kruskal Wallis	χ^2 = 0.00, p = 1.000	χ^2 = 0.00, p = 1.000	χ^2 = 7.14, p = 0.211	χ^2 = 9.64, p = 0.086
Bonferroni	NS	NS	NS	NS

B.5 Resistance of Treated Potato Plants to *Globodera pallida* Infection: Split Root System

FIGURE B.5: Resistance of treated potato plants to *G. pallida* infection, 30 days post inoculation. Figure A = Experimental establishment for the split root system of potato plants, Figure B = Potato plants in stacked pots, 20 days post addition of nematodes and Figure C = Potato plant harvest after 30 days.

TABLE B.6: Statistical assessment of potato plant biomass in, ISR Part I and Part II. Error bars = ± SEM (see Figures B.6a, B.6b and B.6c).

Treatment	ISR Part I	ISR Part II
Mean Tomato Plant Height (cm)		
Kruskal Wallis	χ^2 = 0.21, p = 0.975	χ^2 = 4.01, p = 0.260
Bonferroni	NS[1]	NS
Mean Number of Branches/ Plant		
Kruskal Wallis	χ^2 = 0.40, p = 0.940	χ^2 = 11.86, p = 0.008
Bonferroni	NS	NS
Mean Weight of Potato Tubers (g)		
Kruskal Wallis	χ^2 = 2.07, p = 0.557	χ^2 = 5.20, p = 0.158
Bonferroni	NS	NS
Mean Fresh Weight - Stem and Leaf (g)		

Continued on next page

Table B.6 – *Continued from previous page*

Treatment	ISR Part I	ISR Part II
Kruskal Wallis	χ^2 = 2.73, p = 0.435	χ^2 = 1.28, p = 0.733
Bonferroni	NS	NS
Mean Fresh Weight - Roots (g)		
Kruskal Wallis	χ^2 = 4.00, p = 0.262	χ^2 = 4.13, p = 0.248
Bonferroni	NS	NS
Mean Dry Weight - Stem and Leaf (g)		
Kruskal Wallis	χ^2 = 0.76, p = 0.860	χ^2 = 0.57, p = 0.903
Bonferroni	NS	NS
Mean Dry Weight - Roots (g)		
Kruskal Wallis	χ^2 = 5.19, p = 0.158	χ^2 = 0.37, p = 0.947
Bonferroni	NS	NS

1 NS = No significance

Kruskal Wallis Degrees of Freedom = 5.

Statistical significance at α = 0.05 level.

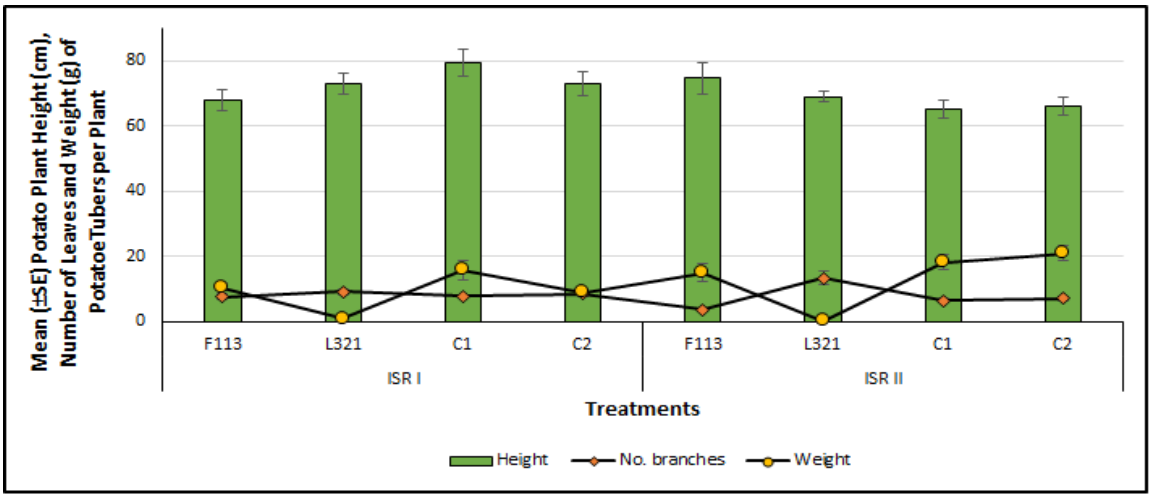

(A)

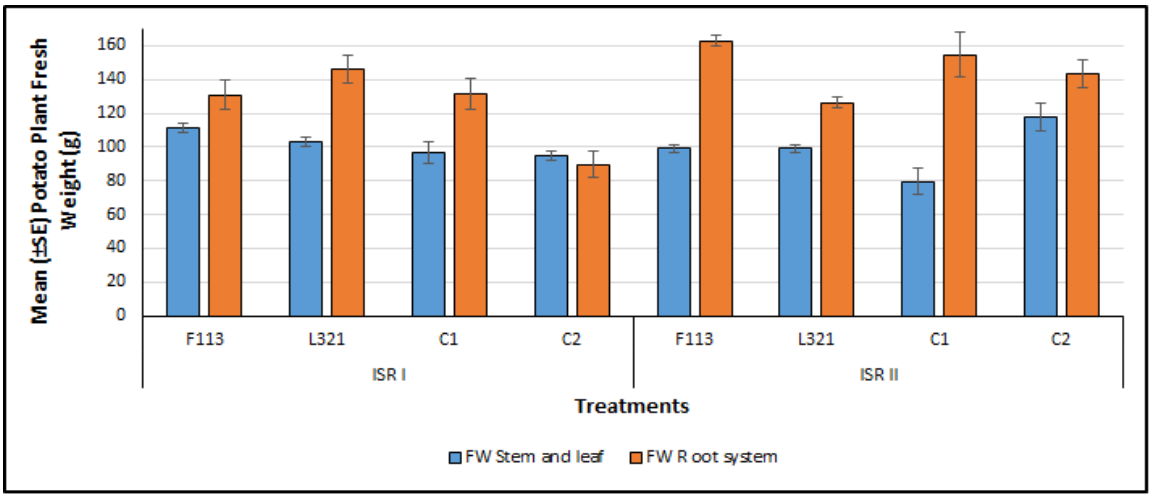

(B)

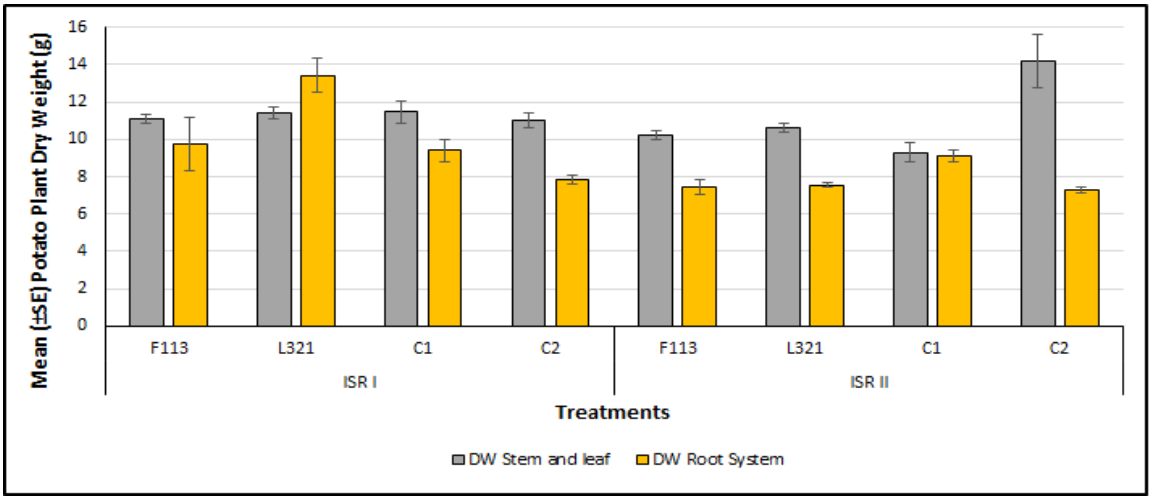

(C)

FIGURE B.6: Biomass of potato plants inoculated with PGP bacteria or spiked with 2,4-DAPG after 30 days *Globodera pallida* infection. Figure (A) Plant height, number of branches and weight of potato tubers. Figure (B) fresh weight (FW) and Figure (C) dry weight (DW) of stem, leaf, and roots were recorded for induced systemic resistance (ISR) experiments, Part I and Part II. Error bars ± SEM, see Appendix B, Table B.5 for statistical assessment.

Appendix C

Supplementary Information for Chapter 4

C.1 Oilseed Rape Microcosm Establishment

C.1.1 Soil Profile Analysis

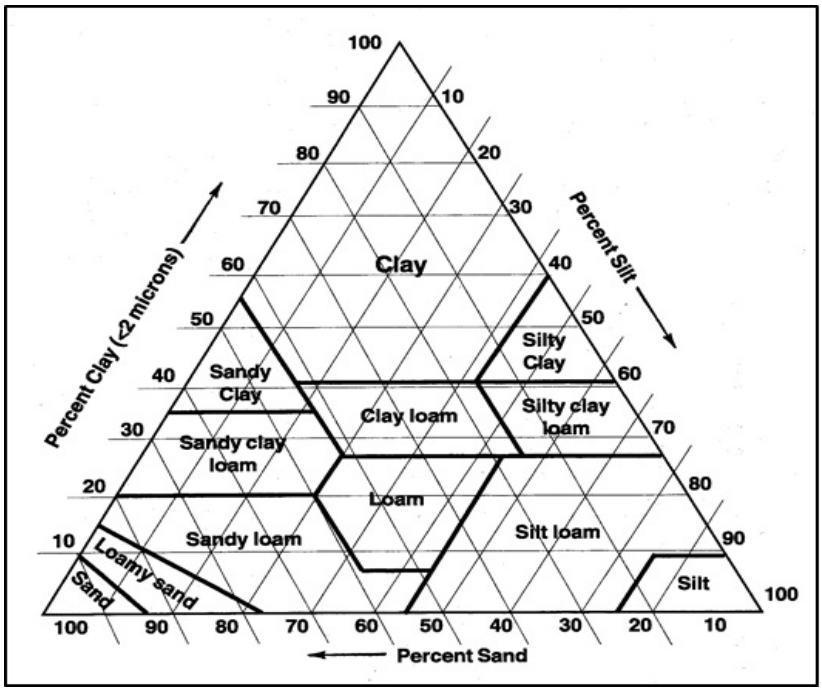

FIGURE C.1: Soil texture triangle for soil profile analysis (Whiting *et al.*, 2014). The direction of the arrows represent the increase of clay, silt or sand from 0-100%.

C.1.2 Bacterial Viability and Ni Bioremediation

TABLE C.1: Statistical analysis of the bacterial viability in OSR and Ni bioremediation potential of OSR after 6 months growth. Data was statistically assessed by non-parametric analysis (see Chapter 4, Table 4.3 for statistical tests and, Figures 4.5, 4.6, 4.7 and 4.8.

	Kruskal Wallis	Bonferroni
Bacterial Viability (log CFU g^{-1})		
Rhizosphere	$\chi^2 = 12.73$, p = 0.013	F113, p = 0.01
Root	$\chi^2 = 6.16$, p = 0.187	
Phyllosphere	$\chi^2 = 4.80$, p = 0.308	
Bioremediation (ppm)		
SPW	$\chi^2 = 11.55$, p = 0.042	NS[1]
Rhizosphere	$\chi^2 = 9.51$, p = 0.147	
OSR	$\chi^2 = 12.96$, p = 0.024	C1, p = 0.040

[1] NS = No significance between the control treatment C2 and the bacterial treatments

Statistical significance at $\alpha = 0.05$ level.

C.1.3 Plant Biomass

TABLE C.2: Statistical assessment of OSR biomass after 3 months and 6 months growth. Data was statistically assessed by non-parametric analysis (see Table 4.3 for statistical tests).

	Kruskal-Wallis	Bonferroni
OSR biomass after 3 months		
FW root	$\chi^2 = 1.72$, p = 0.886	
FW shoot	$\chi^2 = 5.38$, p = 0.371	
FW Total	$\chi^2 = 3.09$, p = 0.686	
DW root	$\chi^2 = 1.79$, p = 0.884	
DW shoot	$\chi^2 = 1.99$, p = 0.851	
DW total	$\chi^2 = 1.97$, p = 0.853	
OSR Biomass after 6 months		
FW root	$\chi^2 = 12.67$, p = 0.027	L321, p = 0.010
FW shoot	$\chi^2 = 17.23$, p = 0.004	L321, p = 0.006
FW Total	$\chi^2 = 17.30$, p = 0.004	L321, p = 0.003
DW root	$\chi^2 = 15.63$, p = 0.008	L321, p = 0.024
DW shoot	$\chi^2 = 13.23$, p = 0.021	L321, p = 0.047
		L111, p = 0.034
DW total	$\chi^2 = 13.59$, p = 0.018	L321, p = 0.027

Post hoc test compares the differences among bacterial treatments and control treatment C2.

Statistical significance at $\alpha = 0.05$ level.

C.2 Nematode Assemblage Characterisation using Morphological Techniques

C.2.1 Morphological Identification of Nematodes

FIGURE C.2: Bacterial feeding nematodes displaying variations in the shape and form of the tail region. The images were captured using Optika Vision Pro software. A = *Achromadora* sp. B = *Rhabditis* sp. C = *Heterocephalobus* sp. D = *Eucephalobus* sp. E = *Acrobeloides*.

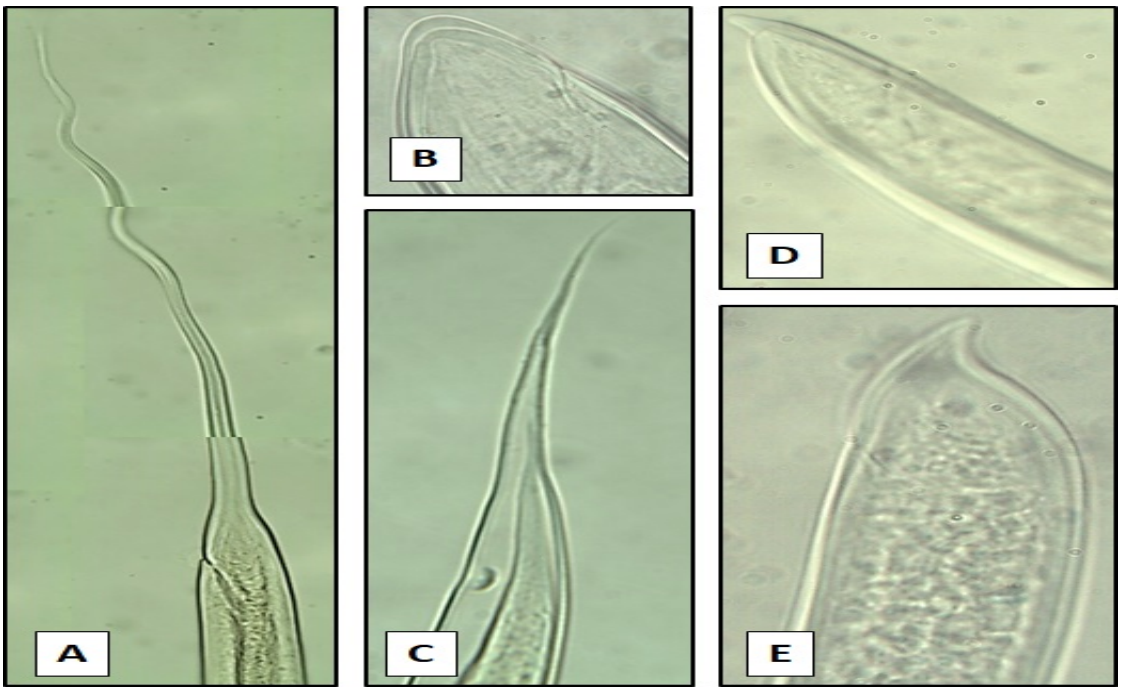

FIGURE C.3: Omnivorous nematodes variations in the shape and form of the tail region. A = *Prodorylaimus sp.* B = *Aporcelaimellus obtusicaudatus* C = *Prodorylaimus* sp., D = *Eudorylaimus* sp. and E = *Eudorylaimus* sp.

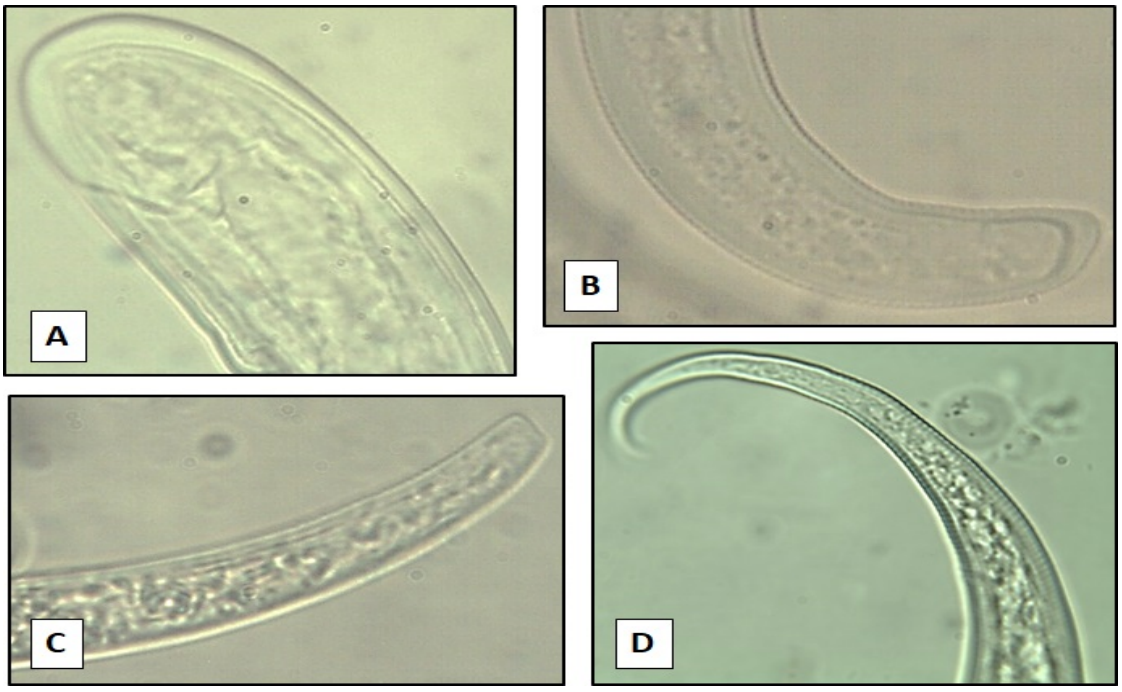

FIGURE C.4: Plant feeding nematodes displaying displaying variations in the shape and form of the tail region. A = *Pungentus* sp. B = *Helicotylenchus* sp. C = *Pratylenchus* sp. D = *Malenchus* sp.

C.2.2 Coloniser-Persister Scale, Trophic Groups and Nematode Biomass

TABLE C.3: Statistical significance assigned to the c-p scale, trophic groups and nematode biomass per trophic groups values for Soil A and Soil B. Trophic groups consist of P = predator, BF = bacterial feeders, FF = fungal feeders, OM = omnivours and PF = plant feeders. Data was statistically assessed by non-parametric analysis (see Chapter 4, Table 4.3 for statistical tests) [a].

	Soil A	Soil B	Post hoc test
c-p scale			
c-p 1	p = 0.003	p = 0.180	
c-p 2	p = 0.175	p = 0.006	NS
c-p 3	p = 0.006	p = 0.005	F113 p = 0.007
			L321 p = 0.031
c-p 4	p = 0.002	p = 0.831	
c-p 5	p = 0.004	p = 0.108	
Trophic groups			
P	p = 0.223	p = 0.232	
BF	p = 0.003	p = 0.006	L321 p = 0.002
			F113 p = 0.007
FF	p = 0.226	p = 0.00	
OM	p = 0.000	p = 0.799	
PF	p = 0.025	p = 0.035	F113 p = 0.013
Biomass per trophic groups			
P	p = 0.007	p = 0.183	
BF	p = 0.948	p = 0.198	
FF	p = 0.463	p = 1.000	
OM	p = 0.009	p = 0.014	NS
PF	p = 0.470	p = 0.040	NS

[a] Statistical significance α= 0.05 level. NS= not significant.

C.2.3 Nematode Abundance

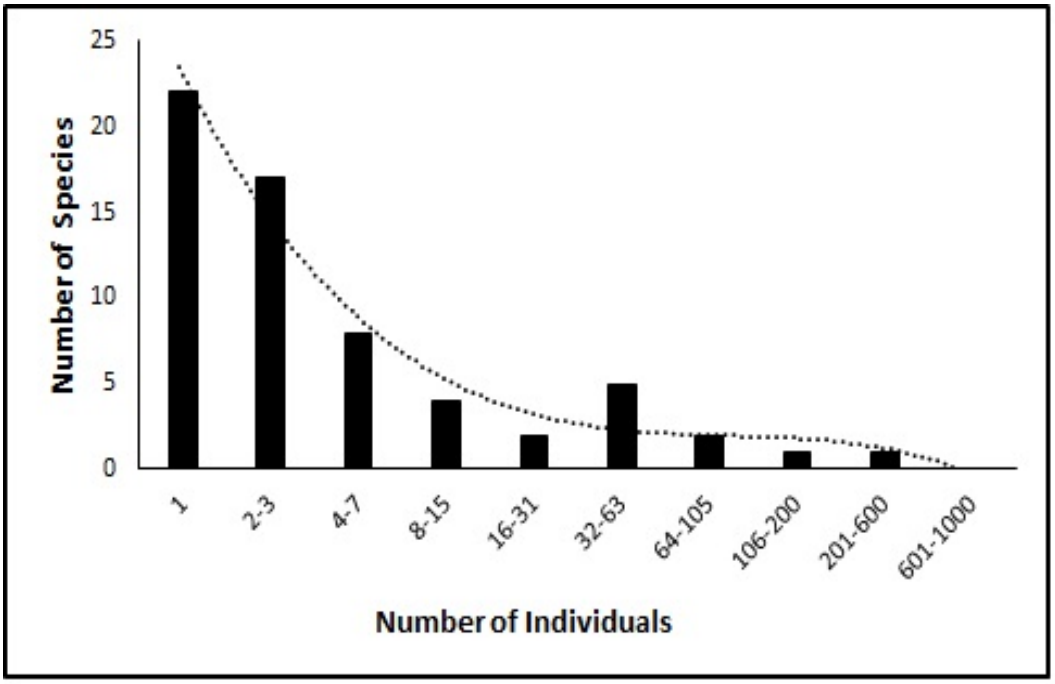

(A)

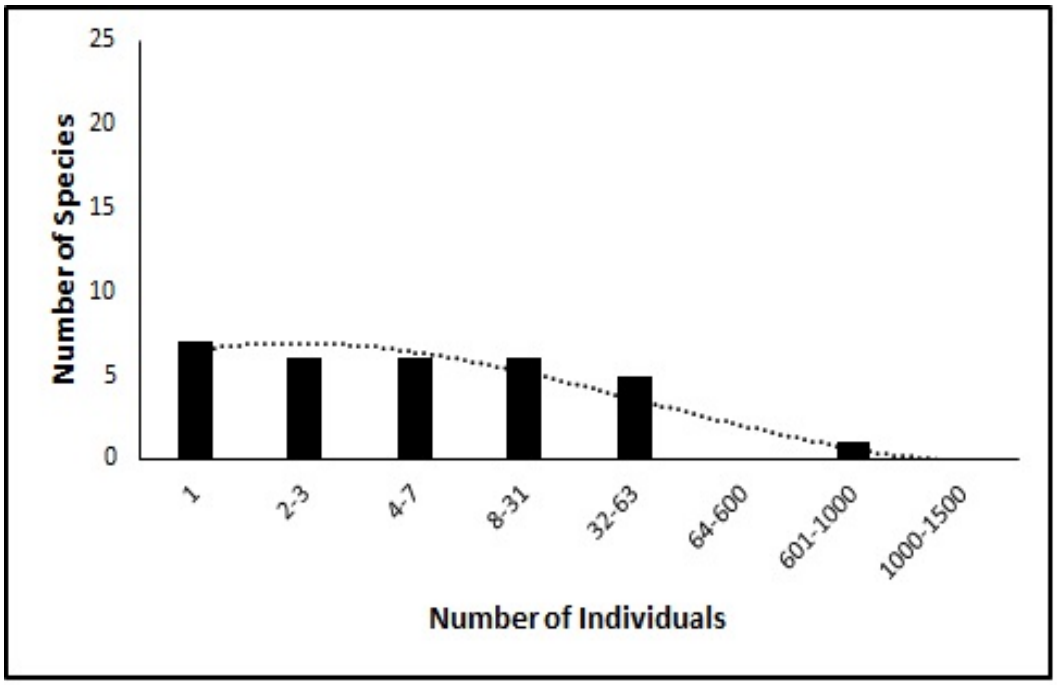

(B)

FIGURE C.5: Species abundance curves represent the number of individual nematodes (x-axis) distribution in relation to the number of nematode species (y-axis) in (A) Soil A and (B) Soil B.

C.2.4 Diversity Indices, Maturity Index Family and Functional Indices

TABLE C.4: Statistical significance assigned to the diversity, maturity and functional indices assigned to Soil A and Soil B in the morphological and molecular assessments. Data was statistically assessed by non-parametric analysis (see Chapter 4, Table 4.3 for statistical tests) [a].

Index	Soil A	Soil B	Post hoc test
Morphological analysis			
J'	U = 0.000, p = 0.000	χ^2 = 11.43, p =0 .022	NS[b]
S_j	U = 0.000, p = 0.002	χ^2 = 7.70, p = 0.103	
H'	U = 0.000, p = 0.002	χ^2 = 10.84, p = 0.028	L321, p = 0.019
MI	U = 0.000, p = 0.002	χ^2 = 1.97, p = 0.740	
PPI	U = 0.000, p = 0.002	χ^2 = 16.51, p = 0.002	L111, p = 0.013
$\sum$MI 2-5	U = 96.00, p = 0.002	χ^2 = 15.57, p = 0.004	F113, p = 0.054
EI	U = 52.050, p = 0.763	χ^2 = 12.60, p = 0.013	NS
SI	U = 96.00, p = 0.001	χ^2 = 18.04, p = 0.001	L111, p = 0.007
BI	U = 92.00, p = 0.004	χ^2 = 9.05, p = 0.06	
Molecular analysis			
J'	U = 352.00, p = 0.211	χ^2 = 17.36, p =0 .002	NS
S_j	U = 3248800, p = 0.863	χ^2 = 3.84, p = 0.428	
H'	U = 370.00, p = 0.310	χ^2 = 7.72, p = 0.102	

[a] Statistical significance α= 0.05 level.

[b] NS= not significant.

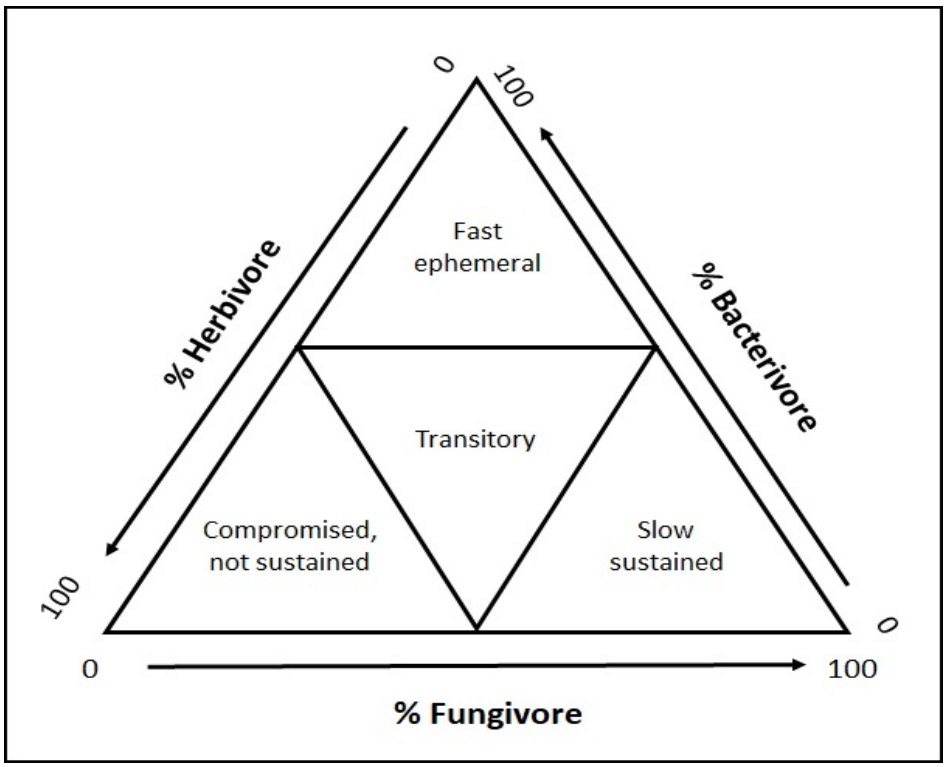

(A)

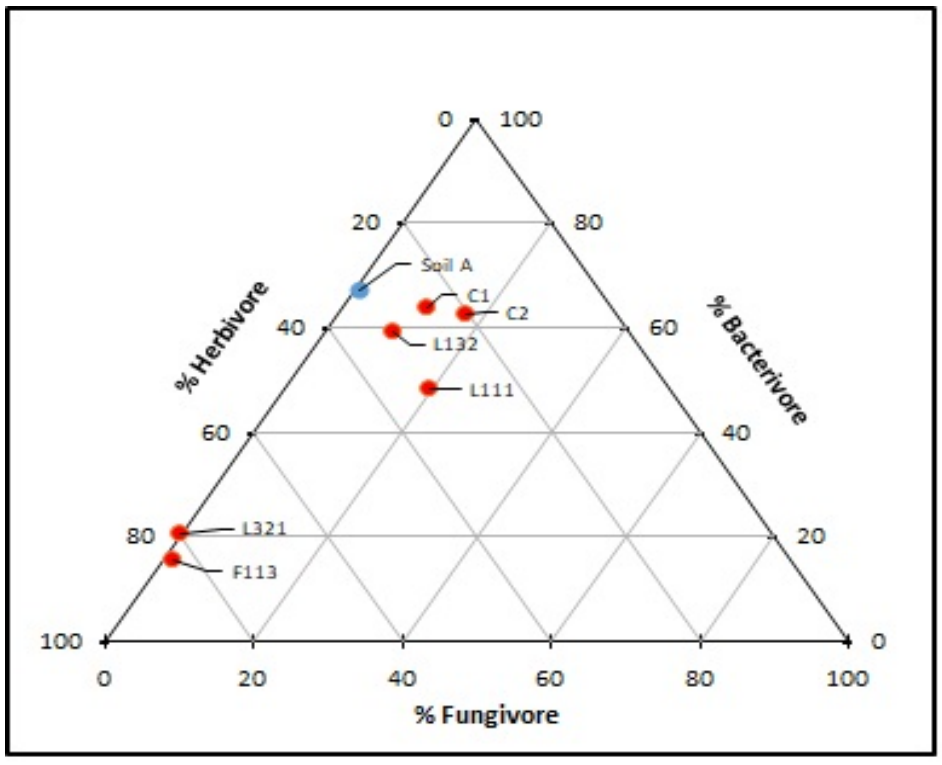

(B)

FIGURE C.6: Enrichment profile assigned to Soil A and Soil B. A = The enrichment profile key. The arrows indicate carbon flow through the food-web and the scale ranges between 0% and 100% (Ferris and Bongers, 2006). B = Nematode enrichment profile represents the mean values assigned to Soil A (blue circle) and Soil B *P. fluorescens* treatments (red circles). Control treatment C1 = Ni and no bacteria, C2 = No Ni and no bacteria.

Appendix D

Supplementary Information for Chapter 5

D.1 Principal Component Analysis

D.1.1 Component Loadings of the Rotated Solution

TABLE D.1: Rotated structure matrix for PCA with varimax rotation of a 5 component FTIR analysis on pure nematode cultures. CE = *C. elegans*, PP = *P. pacificus*, SC = *S. carpocapsae*, HB = *H. bacteriophora*, SFE = *S. feltiae* e-nema, MJ = *M. javanica* and GP = *G. pallida*. The component loadings for each species above a 0.4 limit are highlighted in bold.

Nematode	Component				
	1	2	3	4	5
CE1	**0.656**	0.365	-0.233	**0.537**	-0.142
CE2	**0.639**	0.367	-0.230	**0.567**	-0.150
CE3	**0.597**	0.356	-0.203	**0.650**	-0.144
CE4	**0.646**	0.381	-0.207	**0.567**	-0.149
CE5	**0.574**	0.349	-0.203	**0.683**	-0.163
CE6	**0.642**	0.373	-0.198	**0.580**	-0.149
CE7	**0.405**	0.305	-0.162	**0.778**	-0.167
CE8	**0.531**	0.343	-0.136	**0.734**	-0.161
CE9	**0.471**	0.323	-0.161	**0.764**	-0.158
CE10	**0.562**	0.349	-0.186	**0.696**	-0.152
PP1	**0.801**	-0.188	0.329	0.053	0.046
PP2	**0.887**	-0.170	0.257	-0.010	0.044
PP3	**0.923**	-0.024	0.184	0.196	-0.007
PP4	**0.843**	-0.180	0.311	0.032	0.043
PP5	**0.911**	-0.044	0.206	0.200	-0.003
PP6	**0.884**	-0.055	0.224	0.228	-0.002
PP7	**0.880**	-0.097	0.246	0.169	0.012
PP8	**0.897**	-0.079	0.236	0.151	0.013

Continued on next page

Table D.1 – *Continued from previous page*

Nematode	Component				
	1	2	3	4	5
PP9	**0.868**	0.007	0.179	0.335	-0.031
PP10	**0.832**	-0.150	0.293	0.107	0.032
SFE1	**0.818**	-0.273	-0.209	0.017	0.387
SFE2	**0.640**	**-0.532**	-0.059	0.052	**0.528**
SFE3	**0.794**	-0.345	-0.172	0.043	**0.427**
SFE4	**0.817**	-0.297	-0.200	0.026	**0.409**
SFE5	**0.805**	-0.322	-0.188	0.034	**0.416**
SFE6	**0.813**	-0.291	-0.192	0.033	0.396
SFE7	**0.782**	-0.371	-0.171	0.032	**0.448**
SFE8	**0.789**	-0.349	-0.186	0.011	**0.433**
SFE9	**0.685**	**-0.496**	-0.090	0.041	**0.509**
SFE10	**0.808**	-0.310	-0.205	-0.010	**0.421**
SC1	**0.785**	0.022	-0.201	-0.366	**-0.453**
SC2	**0.798**	0.060	-0.217	-0.341	**-0.415**
SC3	**0.792**	0.070	-0.224	-0.332	**-0.406**
SC4	**0.792**	0.027	-0.190	-0.343	**-0.452**
SC5	**0.794**	0.058	-0.219	-0.341	**-0.416**
SC6	**0.654**	-0.123	-0.084	**-0.430**	**-0.528**
SC7	**0.795**	0.065	-0.221	-0.332	**-0.404**
SC8	**0.795**	0.063	-0.215	-0.333	**-0.411**
SC9	**0.749**	-0.029	-0.170	-0.395	**-0.487**
SC10	**0.744**	-0.034	-0.160	**-0.402**	**-0.490**
HB1	**0.911**	0.024	-0.047	-0.278	0.079
HB2	**0.927**	0.057	-0.054	-0.254	0.067
HB3	**0.721**	-0.282	0.320	-0.296	0.132
HB4	**0.917**	0.044	-0.047	-0.281	0.074
HB5	**0.750**	0.022	-0.001	-0.166	0.069
HB6	**0.910**	0.040	-0.045	-0.253	0.079
HB7	**0.923**	0.052	-0.055	-0.255	0.068
HB8	**0.911**	0.043	-0.048	-0.244	0.075
HB9	**0.920**	0.046	-0.056	-0.267	0.074
HB10	**0.919**	0.048	-0.063	-0.265	0.067
MJ1	0.255	**0.552**	**0.774**	-0.076	0.077
MJ2	0.222	**0.525**	**0.804**	-0.100	0.081
MJ3	0.239	**0.540**	**0.787**	-0.100	0.079
MJ4	0.292	**0.567**	**0.749**	-0.061	0.070
MJ5	0.266	**0.552**	**0.775**	-0.061	0.071
MJ6	0.251	**0.548**	**0.779**	-0.086	0.076
MJ7	0.245	**0.542**	**0.785**	-0.092	0.078
MJ8	0.284	**0.559**	**0.762**	-0.053	0.069
MJ9	0.207	**0.526**	**0.808**	-0.101	0.081
MJ10	0.197	**0.515**	**0.813**	-0.119	0.087
GP1	0.066	**0.811**	**-0.493**	-0.189	0.219
GP2	-0.208	**0.747**	**-0.412**	-0.216	0.260
GP3	0.122	**0.800**	**-0.509**	-0.194	0.211
GP4	-0.179	**0.767**	**-0.419**	-0.212	0.253
GP5	0.031	**0.809**	**-0.487**	-0.190	0.229
GP6	-0.077	**0.791**	**-0.462**	-0.207	0.247
GP7	-0.027	**0.806**	**-0.466**	-0.206	0.240
GP8	0.154	**0.798**	**-0.505**	-0.189	0.205
GP9	-0.204	**0.754**	**-0.408**	-0.221	0.258
GP10	0.175	**0.791**	**-0.517**	-0.183	0.198

TABLE D.2: Rotated structure matrix of each individual nematode group. There were two components for each nematode life strategy investigated: (1) FLBFN CE = *C. elegans* and PP = *P. pacificus*, (2) EPN SC = *S. carpocapsae*, HB = *H. bacteriophora* and SFE = *S. feltiae* e-nema and (3) PPN MJ = *M. javanica* and GP = *G. pallida*. The component loadings for each species above the 0.4 limit are highlighted in bold.

Nematode	**FLBFN Component**		**Nematode**	**EPN Component**		**Nematode**	**PPN Component**	
	1	2		1	2		1	2
CE1	**0.881**	0.054	SFE1	**0.862**	**0.464**	MJ1	**0.994**	0.002
CE2	**0.900**	0.053	SFE2	**0.665**	**0.667**	MJ2	**0.995**	0.000
CE3	**0.912**	0.063	SFE3	**0.829**	**0.529**	MJ3	**0.997**	0.001
CE4	**0.897**	0.061	SFE4	**0.858**	**0.492**	MJ4	**0.989**	0.004
CE5	**0.938**	0.055	SFE5	**0.844**	**0.510**	MJ5	**0.995**	0.002
CE6	**0.893**	0.065	SFE6	**0.851**	**0.484**	MJ6	**0.996**	0.002
CE7	**0.805**	0.041	SFE7	**0.822**	**0.549**	MJ7	**0.997**	0.001
CE8	**0.896**	0.068	SFE8	**0.837**	**0.524**	MJ8	**0.990**	0.003
CE9	**0.872**	0.050	SFE9	**0.717**	**0.639**	MJ9	**0.994**	0.000
CE10	**0.927**	0.056	SFE10	**0.861**	**0.492**	MJ10	**0.989**	0.000
PP1	0.008	**0.982**	SC1	**0.843**	**-0.519**	GP1	0.003	**0.984**
PP2	0.018	**0.959**	SC2	**0.857**	**-0.481**	GP2	0.000	**0.923**
PP3	0.159	**0.828**	SC3	**0.852**	**-0.471**	GP3	0.003	**0.959**
PP4	0.013	**0.982**	SC4	**0.844**	**-0.506**	GP4	0.000	**0.947**
PP5	0.140	**0.856**	SC5	**0.855**	**-0.481**	GP5	0.002	**0.993**
PP6	0.133	**0.865**	SC6	**0.708**	**-0.570**	GP6	0.000	**0.990**
PP7	0.084	**0.914**	SC7	**0.855**	**-0.467**	GP7	0.002	**0.996**
PP8	0.090	**0.907**	SC8	**0.853**	**-0.474**	GP8	0.005	**0.938**
PP9	0.233	**0.759**	SC9	**0.809**	**-0.544**	GP9	0.000	**0.928**
PP10	0.030	**0.960**	SC10	**0.803**	**-0.549**	GP10	0.004	**0.924**
			HB1	**0.954**	-0.022			
			HB2	**0.964**	-0.030			
			HB3	**0.710**	0.095			
			HB4	**0.961**	-0.031			
			HB5	**0.759**	-0.004			
			HB6	**0.945**	-0.020			
			HB7	**0.960**	-0.030			
			HB8	**0.944**	-0.021			
			HB9	**0.960**	-0.028			
			HB10	**0.961**	-0.032			

TABLE D.3: Rotated structure matrix of FTIR 2^{nd} order derivative transformed data analysis on all nematodes and just EPN exposed to soil. CE = *C. elegans*, SFE = *S. feltiae* (e-nema) and SF = *S. feltiae* SB 12(1), HB = *H. bacteriophora*, SC = *S. carpocapsae* and MJ = *M. javanica*. The component loadings for each species above the 0.4 threshold are highlighted in bold.

All nematodes exposed to soil			EPN exposed to soil		
Nematode	Component		Nematode	Component	
	1	2		1	2
CE1	**0.783**	0.005	SF1	**0.752**	0.209
CE2	**0.751**	0.208	SF2	0.379	**0.550**
CE3	**0.683**	0.247	SF3	**0.884**	0.090
SF1	**0.685**	0.261	SFE1	**0.516**	0.096
SF2	0.310	**0.601**	SFE2	0.009	**0.569**
SF3	**0.817**	0.143	SFE3	**0.852**	0.116
SFE1	**0.479**	0.149	SC1	0.259	**0.694**
SFE2	0.003	**0.524**	SC2	**0.829**	0.139
SFE3	**0.793**	0.167	SC3	0.274	**0.690**
SC1	0.201	**0.724**	HB1	**0.434**	**0.518**
SC2	**0.779**	0.191	HB2	0.257	**0.711**
SC3	0.216	**0.722**	HB3	**0.530**	**0.455**
HB1	0.370	**0.565**			
HB2	0.200	**0.746**			
HB3	**0.457**	**0.518**			
MJ1	0.171	**0.612**			
MJ2	0.097	**0.824**			
MJ3	0.195	**0.700**			

D.1.2 Principal Component Analysis Bi-Plots

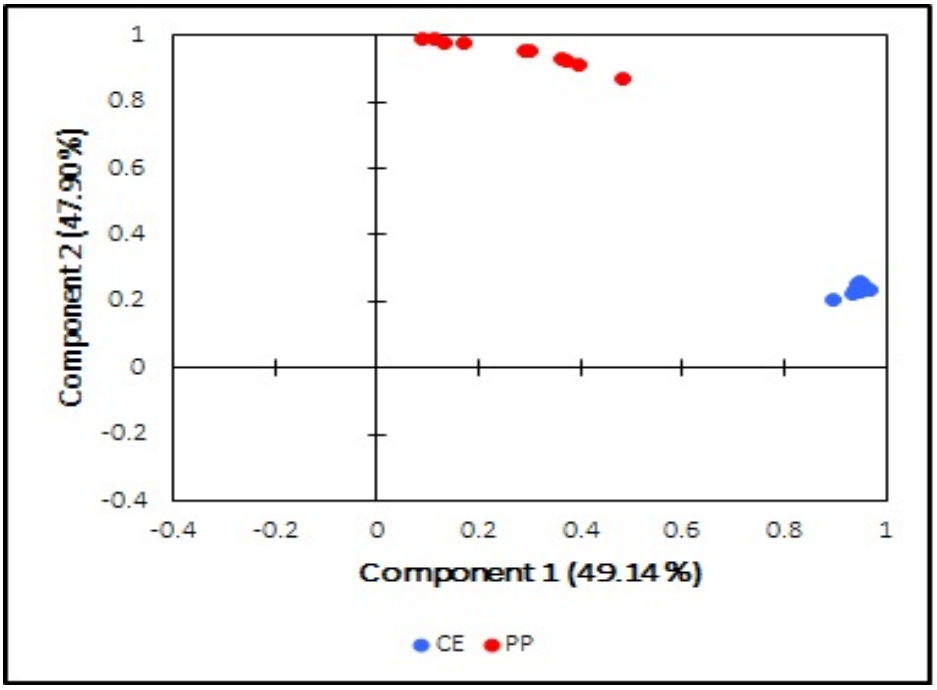

(A)

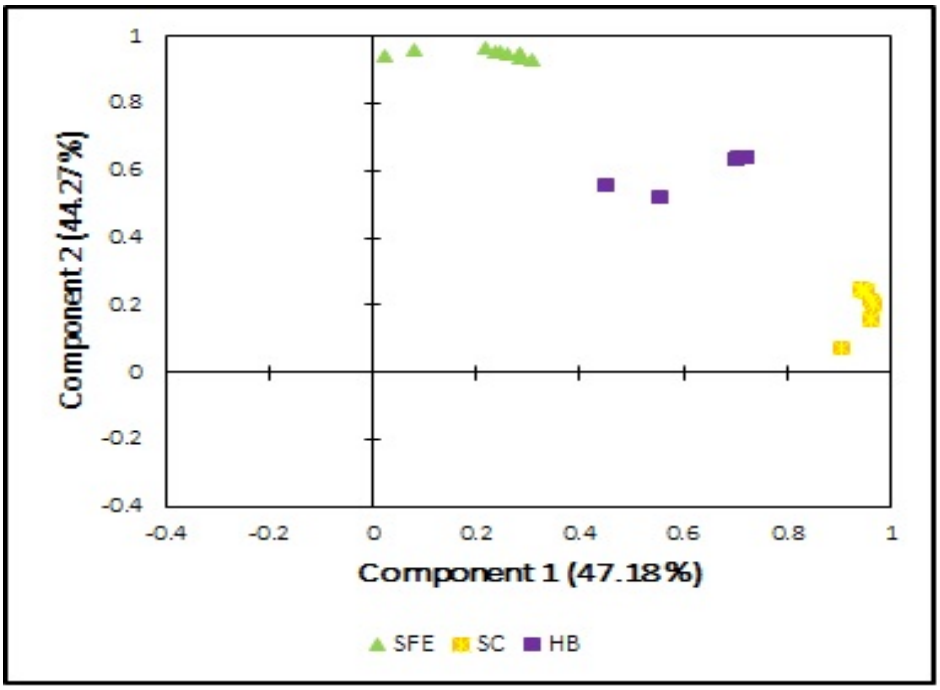

(B)

FIGURE D.1: Principal component analysis of FT-IR spectra of (A) FLBFN *C. elegans* and *P. pacificus* assessed directly from pure cultures, Component 1 describes 49.14% and Component 2 describes 47.90% of the total variance, and (B) EPN *S. feltiae* e-nema, *S. carpocapsae* and *H. bacteriophora*, assessed directly from pure cultures, Component 1 describes 47.18% and component 2 describes 44.27% of the total variance. Component loadings of the rotated solution were presented in, Appendix A (Table D.2). The nematodes are described as CE= *C. elegans*, PP= *P. pacificus*, SFE= *S. feltiae* (e-nema), SC= *S. carpocapsae* and HB= *H. bacteriophora*

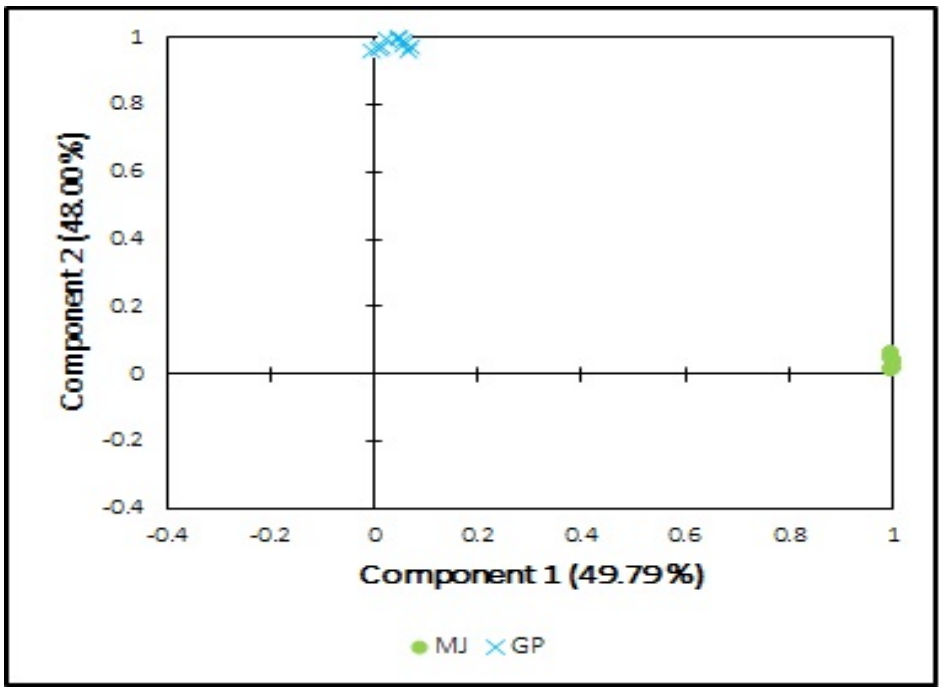

(A)

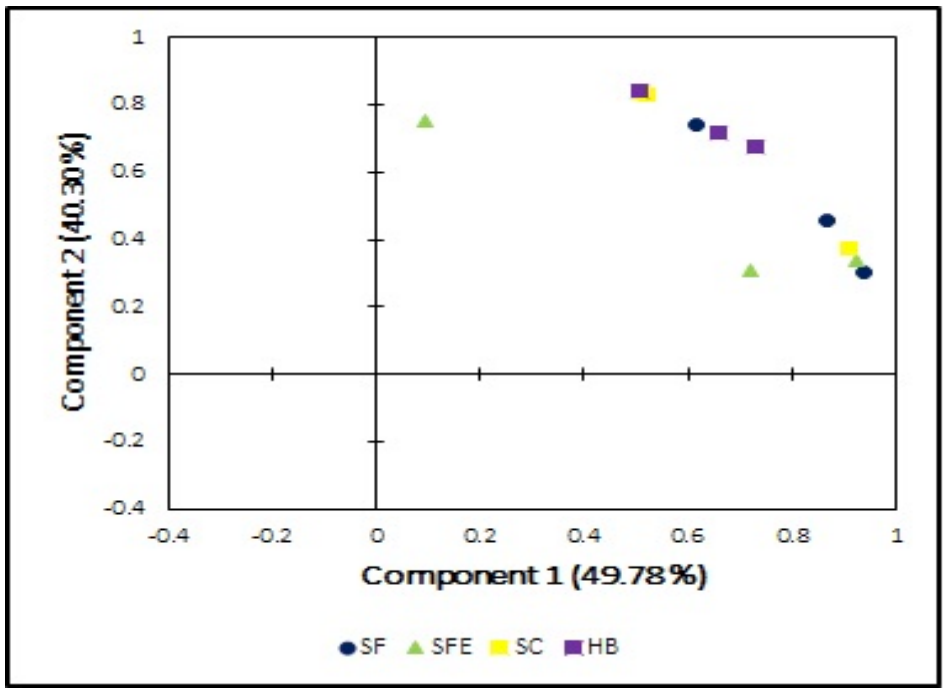

(B)

FIGURE D.2: Principal component analysis of FT-IR spectra of (A) PPN *M. javanica* and *G. pallida*, assessed directly from cultures, Component 1 describes 49.79% and Component 2 describes 48.00% of the total variance, and (B) EPN *S. feltiae* SB 12(1), *S. feltiae* e-nema, *S. carpocapsae* and *H. bacteriophora* that were exposed to soil, Component 1 describes 49.78% and Component 2 describes 40.30% of the total variance. Component loadings of the rotated solution were presented in, Appendix A (Table D.2). The nematodes are described as MJ= *M. javanica*, GP= *G. pallida*, SF = *S. feltiae* SB 12(1), SFE = *S. feltiae* e-nema, SC = *S. carpocapsae* and HB = *H. bacteriophora*.